This electronic thesis or dissertation has been downloaded from the King's Research Portal at https://kclpure.kcl.ac.uk/portal/

Compositional characterisation of human respiratory tract lining fluids for the design of disease specific simulants

Bicer, Elif Melis

Awarding institution:
King's College London

The copyright of this thesis rests with the author and no quotation from it or information derived from it may be published without proper acknowledgement.

END USER LICENCE AGREEMENT

Unless another licence is stated on the immediately following page this work is licensed

under a Creative Commons Attribution-NonCommercial-NoDerivatives 4.0 International

licence. https://creativecommons.org/licenses/by-nc-nd/4.0/

You are free to copy, distribute and transmit the work

Under the following conditions:

- Attribution: You must attribute the work in the manner specified by the author (but not in any way that suggests that they endorse you or your use of the work).
- Non Commercial: You may not use this work for commercial purposes.
- No Derivative Works - You may not alter, transform, or build upon this work.

Any of these conditions can be waived if you receive permission from the author. Your fair dealings and other rights are in no way affected by the above.

Take down policy

If you believe that this document breaches copyright please contact librarypure@kcl.ac.uk providing details, and we will remove access to the work immediately and investigate your claim.

Download date: 05. May. 2023

Compositional characterisation of human respiratory tract lining fluids for the design of disease specific simulants

Elif Melis Bicer

Analytical & Environmental Sciences Division
School of Biomedical & Health Sciences
King's College London

Thesis submitted to the King's College of London
in fulfilment of the requirements for the
degree of Doctor of Philosophy

September 2014

Abstract

The respiratory tract lining fluid (RTLF) is the first physical interface with which inhaled materials and aerosolised drugs come into contact in the airways. Surrounding the underlying epithelial cells, the RTLFs are composed of a thin amphipathic layer, providing crucial physiological and protective roles across the airways. The aim of this thesis was to investigate the composition of this extracellular compartment using human lavage samples from healthy volunteers, asthmatics and patients with Chronic Obstructive Pulmonary Disease (COPD) to guide the development of a series of lung lining fluid simulants for the testing of inhaled drugs. Analysis across nasal, bronchial and alveolar compartments revealed marked compositional differences throughout the respiratory tract in healthy individuals, with significant differences also observed with age, smoking status and the presence of established respiratory disease. Within the asthmatic group I observed evidence of an impaired microbicidal defense network at the air-lung interface, with significant depression of innate immunity proteins in the bronchial RTLFs associated with elevated concentrations of bacterial cell wall components. In the lavage samples obtained from healthy aged populations a general dysregulation of immunity and inflammatory processes was observed, alongside a pro-oxidant shift in the redox balance. In COPD, characteristic pathological changes were identified, from evidence of chronic inflammation, to protease-antiprotease imbalance and oxidative stress. In addition, I obtained preliminary evidence of dysregulated metal homeostasis, superimposed on compositional protein signatures characteristic of normal physiologic ageing. Clear differences in the composition of the RTLF could be attributed to smoking; with the greatest number of proteins identified (234) in the RTLFs of COPD smokers, in stark contrast to only 58 proteins accounted for within the COPD ex-smoking proteome. This extensive characterization of the RTLFs was used to successfully develop a physiologically representative ‘base model’; the suitability of which was assessed in a series of preliminary studies, focusing on particle and cellular interactions (nanoparticle characterization and biocompatibility with in vitro cell lines). These fundamental applications will be significant in evolving both understanding the behaviour of inhaled particles at the surface of the lung and improving the biopharmaceutical screening of aerosolized medicines.

Acknowledgements

First and foremost, I would like to thank Dr. Ian Mudway for his endless enthusiasm, immense knowledge on all topics far and wide, his time, generosity and kindness without whom this thesis just would not have been possible, I could not have imagined a better supervisor. Thank you for everything, particularly in this past year, your patience and understanding has helped me more than you could know.

I would also like to thank my secondary supervisor Dr. Ben Forbes for encouraging a somewhat naive MSc student to apply for a PhD four years ago and for continuing to encourage and advise me throughout my PhD. Similarly I would like to thank Lea Ann Dailey for her support and general loveliness in all matters from the very beginning. Not forgetting my industrial supervisor(s) at GlaxoSmithKline, Dr. Graham Somers and Dr. David Hassall, and all the members of the CSC-Biological Mass Spectrometry Team, thank you for providing the opportunity to work in the beautiful GSK labs in the ever so slightly less beautiful town of Stevenage.

It would be impossible to name everyone else who has supported me throughout the past four years, but to my friends and those members (you know who you are!) of the fourth and fifth floors of the Franklin Wilkins Building, particularly the ever changing members of office 4.131, you've been like family and I cannot thank you enough for the various bits of advice (from the scientific to the completely absurd) and the many shoulders you've provided to cry either hysterically on or to laugh hysterically next to. Throughout all the blood, sweat and tears I have genuinely managed to enjoy almost every minute of my PhD because of you all!

To my family, my Mum, my Dad and my brother who have always had to put up with me, for loving me unconditionally, and supporting me constantly, it's not enough to simply thank you, but thank you, sizi çok seviyorum. Finally to Michal, who made this seemingly impossible past year bearable, for keeping me smiling and always finding me when I felt lost, you I cannot thank enough.

Contributions

Subject recruitment, lavage and plasma sample collection, spirometry and lung function tests, skin prick tests, total and differential cell counts were performed by trained staff at the University of Umea, Sweden.

Members of the CSC-Biological Mass Spectrometry Unit, GlaxoSmithKline, advised on the proteomic analysis methodology outlined.

Members of the Centre of Ultrastructural Imaging at King's College London advised on Transmission Electron Microscopy. ICP-MS was performed at the Centre of Excellence for Mass Spectrometry at King's College London.

I, Elif Melis Bicer, performed the remaining experiments and statistical analyses described in this thesis.

Table of Contents

Abbreviations

1D PAGE: One dimensional polyacrylamide gel electrophoresis

4-HNE: 4-Hydroxy-Trans-2-Nonenal

A1AT: α 1-antitrypsin

A2M: Alpha 2 Macroglobulin

AA: Ascorbate

BAL: Bronchoalveolar lavage

BW: Bronchial Wash

CC16: Clara cell protein

CCM: Cell culture medium

COPD: Chronic Obstructive Pulmonary Disease

DPPC: Dipamitoylphosphatidylcholine

DLS: Dynamic Light Scattering

ELISA: Enzyme-linked immunosorbent assay

FBS: Fetal bovine serum

FEV1: Force Expired Volume in 1 second

FVC: Forced Vital Capacity

GPx: Glutathione peroxidase

GSH: Glutathione

GSSG: Glutathione disulphide

GSx: Total glutathione

HPLC: High Pressure Liquid Chromatography

ICP-MS: Inductively Coupled Plasma Mass Spectrometry

IgA: Immunoglobulin A

IgG: Immunoglobulin G

IgM: Immunoglobulin M

MTT assay: 3-(4,5-dimethylthiazol-2-yl)-2,5-diphenyltetrazolium assay

NAL: Nasal Lavage

Nano LC MS/MS: Nano Liquid Chromatography and Tandem Mass spectrometry

NP: Nanoparticle

PC: Phosphatidycholine

PG: Phosphatidylglycerol

PS 50: Polystyrene 50 nm

PS 200: Polystyrene 200 nm

ROS: Reactive Oxygen Species

RTLF: Respiratory Tract Lining Fluid

SP-A: Surfactant Protein A

SP-B: Surfactant Protein B

SP-C: Surfactant Protein C

SP-D: Surfactant Protein D

UA: Urate

VC: Vital Capacity

List of figures

List of tables

Chapter 1

Introduction

1.1: Introduction

The lung has long been targeted for the localized delivery of pulmonary medicines in the treatment of respiratory diseases, particularly asthma and COPD. However with new pharmaceutical technologies and the development of novel classes of therapeutic agents (e.g. peptides), which are delivered less effectively through common routes of administration, pulmonary drug delivery is an increasingly attractive target for the systemic delivery of medicines (Forbes and Erhadt, 2005; Takizawa, 2009; Agu and Ugwoke, 2011). The various advantages of the inhaled delivery route include the large alveolar surface area for drug absorption, the extensive vascularization, low epithelial barrier thickness, low enzymatic metabolic activity and absence of the first-pass metabolism effect of the liver (Courrier et al., 2002; El-Sherbiny, 2010). Accordingly, the delivery of drugs via the lungs has undergone significant development, both in terms of delivery devices and formulation. Thus there is an urgent need to develop and improve *in vitro* testing systems that reflect the *in vivo* interactions between inhaled drugs and components of the respiratory tract lining fluid that represent the interface between inhaled air and the respiratory epithelium (Forbes et al., 2010).

These *in vitro* investigations are necessary to improve our understanding of the behaviour (aggregation, solubility, chemical modification) of inhaled particles at the air-lung barrier. *In vitro* cell culture systems despite their well-documented limitations, allow investigations into the underlying mechanisms of action of inhaled medicines and particulates at the cellular and molecular level. Several cellular *in vitro* systems of the airways have been developed and are employed in investigations of drug absorption, transport, metabolism and toxicity. These include primary cultures and the 16HBE14o- and Calu-3 bronchial epithelial cell lines, considered to have representative airway barrier properties and commonly used to investigate drug permeability (Forbes, 2000; Mathias et al., 2002; Forbes et al., 2005). Whilst the development of *in vitro* cell culture models is

continuously evolving, models are often too simplistic and fail to replicate the complex interaction and behaviour of inhaled drugs and particles within the airways.

The first physical interactions between materials inhaled into the airways are with the respiratory tract lining fluids (RTLFs) that overlay the underlying epithelial cells. The lungs consist of heterogeneous cell populations, both epithelial and inflammatory, which significantly influence the local composition of the RTLFs, through their secreted products resulting in dramatically differing compositional profiles throughout the respiratory tract, from the nasal to the alveolar regions. In the upper, mucus secreting airways, the RTLF exists as a double layer compartment comprised of an aqueous sol and an overlying gel layer, with the mucus layer promoting the trapping and clearance of microorganisms and particles via the operation of the mucociliary escalator. This contrasts significantly from the alveolar region where surfactant is secreted from Type II pneumocytes to prevent collapse. The composition of human RTLFs has also been shown to vary significantly in different airway pathologies from COPD, asthma, and various interstitial lung diseases, though the available data is often relatively scant due to the difficulty in obtaining lavage samples from patients with chronic airway diseases (Hatch, 1992).

With aerosol particle size used to target drug deposition to specific, therapeutically relevant regions of the airways, an understanding of drug interactions at the air-lung interface requires an appreciation of the variation in RTLF composition both regionally within the respiratory tract and in different target patient groups. Drug particles targeting the respiratory tract are within a narrow size range, typically 0.5-5µm, sufficiently small to pass through the conducting airways (not trapped by the mucus layer as occurs for larger particle sizes), but large enough in aerodynamic diameter to ensure their efficient deposition in the airways without significant losses due to exhalation or swallowing after impaction in the oropharyngeal region (Barnes and Liew, 1995; Bao and Zhao, 2010; Agu and Ugwoke, 2011). Of those particles depositing, the mucociliary escalator is the dominant mechanism of clearance in the upper respiratory tract. Those that deposit deeper within the distal airways may be cleared by the process of dissolution in addition to other processes, including clearance by alveolar macrophages (Ahsan et al., 2002; Davies and Feddah, 2003; Makino et al., 2003). In addition to particle characteristics, patient variables such as airway morphometry, breathing pattern, age and disease will also influence the deposition and effectiveness of inhaled medicines (Fischer et al., 2009; Agu and Ugwoke, 2011).

In vitro methods to establish the fate and interactions of inhaled particles depositing within the airways are therefore vital to an improved understanding of their likely therapeutic or toxicological impacts upon the lung. It is consequently important that *in vitro* models of the airways are truly reflective of what occurs *in vivo*, focusing on interactions with the lung lining fluids, as well as the subsequent cellular interactions to permit the most accurate and realistic testing of particulate behavior. The complexity and regional heterogeneity of the lung however presents challenges to both *in vitro* and *in vivo* testing methods (Agu and Ugwoke, 2011). Currently no single standardized *in vitro* test for inhaled formulations simulating the interactions with human RTLFs has been put into place (Son and McConville, 2009).

Interestingly, in the research fields of medical geochemistry and environmental sciences, the use of simulated extracellular lung fluids has become an integral part of *in vitro* investigations (Plumlee et al., 2006). The importance of using simulated lung fluids for the *in vitro* testing of dust soils, earth materials, metals, uranium, silica and asbestos to assess particulate behaviour - dissolution, solubility, bioavailability and influence on oxidative rate in the lung, have been well described in the literature (De Meringo et al., 1994; Herting et al., 2006; Sdraulig et al., 2007). Although the majority of studies have used a relatively simplistic model for the simulated lung fluid, they also illustrate the importance of the use of biorelevant *in vitro* models in assessing inhaled particulate behaviour (De Meringo et al., 1994).

In addition, the development of simulated intestinal fluids to evaluate the disintegration, dissolution and solids transfer of orally administered drugs *in vitro*, has demonstrated the importance of biorelevant media use throughout the drug development process. If such tests are not performed under appropriate conditions the drug release profiles obtained are often erroneous (Dressman et al., 1998). With *in vitro* testing methods required as part of the development of new formulations, quality control purposes and, in determining bioequivalence, the more physiologically relevant the media, the more likely *in vitro in vivo* correlation can be achieved. There is therefore an urgent need to develop simulant models better able to predict the *in vivo* performance of inhaled medicines and inform the development of pharmaceutical preparations. The great complexity and regional variation of the human RTLFs present many challenges to the design of such simulant models, requiring a detailed characterisation of RTLF components in both health and disease. This is the main objective of the work described in this thesis; with the ultimate aim of providing information relevant to the design of

disease specific simulated models for the testing of inhaled drug behavior at the surface of the lung.

The specific aims of this study are therefore three-fold:

- First to investigate the composition of the major components of the RTLFs, across the nasal, bronchial and alveolar compartments of the respiratory tract, to inform the production of realistic simulants for the screening of drug behaviour at the surface of the lung.
- Further, to investigate compositional differences in the RTLF between patient groups likely to be the end users of inhaled medicines: aged individuals, asthmatics, and patients with COPD.
- Finally, to construct a base RTLF simulant and assess both its impact on particulate behaviour and biocompatibility with commonly used pulmonary cell lines

2: The respiratory tract lining fluids

2.1: Sampling methods:

A considerable body of information on RTLF composition has been published since the 1970s. However, to fully evaluate these data it is both necessary to understand the methodologies employed to obtain these samples from the human lung, as well as the conventions employed in expressing the measured concentrations of RTLF constituents. By the use of various catheters and bronchoscopes (Jackson, 1904; Carlens, 1942; Ikeda, 1968), washings to obtain various secretions and cellular components of the airways have been performed for many decades. Retrieving samples and washings of RTLFs continues to be routinely performed in the clinical setting as a therapeutic tool, as part of the diagnosis and monitoring of airway disorders. Early studies described the use of large volume saline instillations and segmental washing of the airways as a means to remove ‘material’ from the lungs as part of the therapeutic strategy for respiratory failure (Ramirez et al., 1963; Rogers et al., 1972; Reynolds, 2011). In addition, sampling procedures have also provided researchers a way in which to investigate the various extracellular (and the cellular) components of the RTLF, and consequently develop a more comprehensive understanding of its composition (Reynolds, 2011). The assumption

being that fluid instilled into the airways interacts with the fluid compartment overlaying the respiratory epithelium, such that the retrieved aspirate effectively represents a dilute sample of these fluids (Walters and Gardiner, 1991).

2.2: Bronchoalveolar lavage and bronchial wash

The method of bronchoalveolar lavage (BAL) was first used in the treatment of several airway diseases (including alveolar proteinosis, cystic fibrosis and bronchitis) to 'wash out' purulent secretions accumulated within the lung with large volumes of saline. Subsequently it has become the most common approach used to sample the RTLF samples from the distal lung. Samples obtained with this method were used to achieve the first real descriptions of the cellular and non cellular composition of the lower respiratory tract (Finley et al., 1967; Reynolds and Newball, 1974; Reynolds, 2008). The most common BAL procedure routinely employs a fiber-optic bronchoscope gently wedged, into a subsegmental bronchus, through which a volume of buffered saline (37^{o}C) is instilled into the airway and recovered by aspiration and suction (Walters and Gardiner, 1991). Large volume lavages (150-180 mL) to sample distal airway secretions are usually achieved by consecutive instillations of 50-60 mLs of buffered saline, with aspiration after each aliquot and the consecutive returns pooled to provide a single highly dilute sample. The procedural factors that are considered to cause most significant variability in the concentration of lavage cellular and non-cellular components include lavage dwell time, the volume of saline instilled, the number of instilled aliquots and the inclusion/exclusion of the first lavage instillment (Shields and Riedler, 2000). Notably lavage methods vary noticeably between research groups (as **Table 1.1** illustrates) and a standardised procedure for BAL and the reporting of solute concentrations has yet to be put in place (Merrill et al., 1982; Walters and Gardiner, 1991; Reynolds, 2000).

Bronchial airway lining fluid samples may also be sampled using small fixed volume aliquots (Kelly et al., 1987). Alternatively the first aliquot of saline recovered during the BAL procedure can be collected as a separate sample to reflect more proximal airway secretions (Shields and Riedler, 2000). The subsequent mixing of instilled saline during the lavage procedure within the respiratory compartments has been described as a complicating factor worth consideration, with the majority of research groups using BAL pooling aspirated aliquots (Duddridge et al., 1988; Walters and Gardiner, 1991). It has

been suggested that cellular indicators (ciliated bronchial cells vs. squamous cells) can be used to separate aspirated aliquots on the basis of region of the airway sampled (Haslam and Baughman, 1999), with samples retrieved from bronchial wash typically displaying a low total cell count and a high percentage ratio of neutrophils to macrophages (Shields, 2000).

2.3: Lavage dilution correction methods – determining and reporting ELF concentrations

Despite the wealth of information that has been provided using lavage-based techniques, the considerable dilution of the sampled RTLF remains a great problem. The instillation of large volume aliquots of saline results in what is essentially a dilution of an unknown volume of RTLFs, preventing the accurate quantification of soluble components. In addition, poor lavage recoveries, 20-60%, present an additional cause for uncertainty (Baughman, 1997; Shields and Riedler, 2000). Consequently, there is the need to implement an appropriate marker to correct for the dilution produced by lavage. The use of a reliable markers would greatly increase the quantitative robustness of data gathered (Feng et al., 1992), however as of yet no standardized inter-laboratory method for doing so has been implemented (Haslam and Baughman, 1999). Previously proposed and investigated markers of dilution have included external compounds: methylene blue, helium, radioactively labelled markers - 99mTc-diethylenetriaminepentaacetic acid, 51Cr-ETDA, introduced into the instilled saline into the lung; or endogenous compounds including urea, albumin, or total protein. The use of such ‘internal’ markers requires prior knowledge of marker concentrations; both in the blood and lavage aspirate, and require that the marker in question should be freely permeable between the blood plasma and extra-vascular spaces with equivalent concentrations in these two fluids (Baughman, 1997).

The use of methylene blue as an exogenous marker for lavage correction was short lived, on account of its loss via diffusion from the airway surface and it’s binding to airway cells (Baughman, 1997; Rennard et al., 1986). To date no other external marker has been demonstrated to have the required characteristics for an effective dilution marker: safety, resistance to degradation, or uptake by calls, as well as displaying an even

distribution throughout the airway (Haslam and Baughman, 1999). Whilst various corrections for lavage dilution have been implemented, the use of the small molecular weight molecule urea has been the most commonly and widely adopted approach.

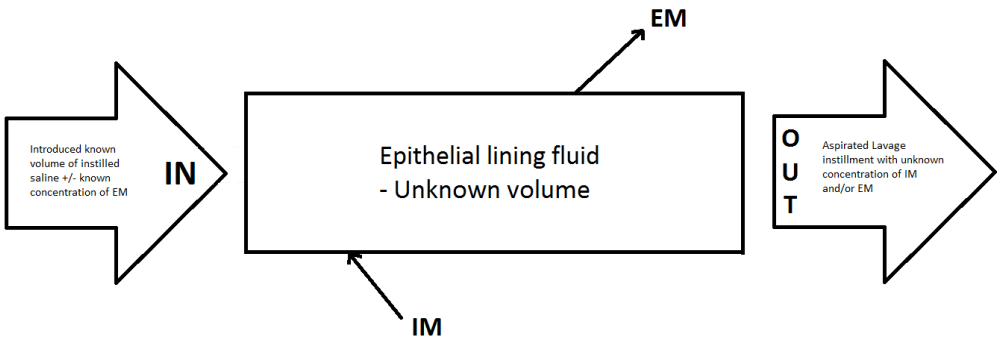

Figure 1.1: *A schematic illustration of lavage procedure and the use of external (EM) and internal markers (IM) in correcting for lavage dilution*. This figure illustrates how the introduction of an external marker with saline instilled as part of the lavage process can thus be analysed from within aspirated fluid collected to determine the resulting dilution. Additionally the figure describes how the measurement of an internal marker present within RTLF of known concentration can be analysed in aspirated fluid as an alternative way in which to determine and correct for the lavage dilution.

2.3.1: The Urea correction method

Rennard et al (1986) were the first group to suggest the use of urea as an effective marker for the correction of lavage dilution. With no net charge at physiological pH, urea is neither used, nor produced by the cells of the respiratory tract and on account of the high permeability of the blood-air barrier, this 60Da molecule would in theory have equivalent concentrations in the RTLF and blood plasma. Thus, Rennard et al (1986) proposed that by the comparison of both plasma and lavage urea concentrations and the application of basic principles of dilution, one could determine with reasonable accuracy the dilution of the RTLF produced by airway lavage, which could then be used to estimate the concentrations of solutes within the RTLF.

Since the use of urea as a marker of dilution was originally suggested, this relatively convenient method has become the most extensively applied for nornalising lavage solute concentrations. However it's use in this manner relies heavily on the assumption that the concentrations of urea in plasma and the RTLF remain equivalent with no source of urea influx throughout the lavage procedure. Several studies have

however demonstrated the rapid influx of urea from blood plasma into the air-spaces, due to the combination of solute flux, passive diffusion and the increased epithelial and endothelial permeability created as a result of the lavage procedure itself (Marcy et al., 1987; Duddridge et al., 1988; Effros et al., 1990; van de Graaf et al, 1991; Feng et al., 1992). The reliability of the urea method of correcting for lavage dilution has therefore come into question, as urea influx into the lavage fluid complicates the interpretation of solute concentrations resulting in the underestimation of RTLF solute concentrations (Marcy et al., 1987; Walters and Gardiner, 1991). Clearly, therefore the length of time between saline instillation and aspiration, the 'dwell' time will strongly influence lavage urea concentrations. The consensus view however is that using urea to normalise lavage dilutions is valid as long as dwell time is kept minimal (van de Graaf et al, 1991). Studies performed by van der Vliet et al (1999) further demonstrated increasing urea concentrations in successive saline instillations when a sequential lavage procedure was employed, and they proposed the use of a single-cycle lavage procedure to minimize urea influx to obtain more accurate and reliable determinations of RTLF solute concentrations. The reliability of urea correction has also been investigated with nasal lavage methods. Kaulbach et al (1993) have suggested it a reliable approach as a result of the minimal dwell time (30-60 seconds) associated with the procedure. However few investigators explicitly describe the lavage procedure followed when using this method or the RTLF dilution determined (as illustrated in **Table 1.1**). This time dependence in the diffusion of urea in lavage and the lack of a standardized procedure ultimately results in the wide range of RTLF solute concentrations that have been reported in the literature.

2.3.2: Other correction methods

In addition to the significant dilution problem associated with lavage, the varying methods for reporting RTLF solute concentrations often hinders the interpretation and understanding of the composition of the RTLF, both at baseline and in response to an acute insult. Reports of the cellular data retrieved from sampling methods have been remarkably consistent; however the concentrations of acellular components are greatly affected by variable dilutions produced by lavage (Haslam and Baughman, 1999). An approach for the standardised reporting of RTLF solute concentrations has often been proposed (Dargaville et al., 1999; Ward et al., 1993; Walters and Gardiner, 1991), but to date the reporting of lavage data in the literature remains inconsistent.

The presentation of lavage data using RTLF volume as a denominator has been much discussed, however direct methods (including the urea method) used to determine

RTLF volume have tended to overestimate it considerably, for the reasons outlined previously (Rennard et al., 1986). A report carried out by the ERS task force suggested that concentrations per volume of lavage fluid cannot be correctly extrapolated to *in vivo* concentrations found in RTLF (Haslam and Baughman, 1999). Surface area and lining thickness measurements of each section of the airways via morphometric methods (Weibel, 1963; Crapo et al., 1983; Hatch, 1992) have been made and it has been suggested the calculation of morphological volumes using this data may allow for superior interpretation of RTLF solute concentration, though the data on which this is based on is rather limited (Hatch, 1992) and this approach requires an appreciation of the total area of the airway sampled. It is also likely to be limited due to unknown differences in RTLF volumes in disease, as well as simply in relation to inter-individual variation in airway structure and volume.

The use of albumin, or total protein (predominately albumin in RTLFs) as denominators to which RTLF solute concentrations are expressed has also been proposed. As with urea, albumin diffuses into the lung lining fluid from the blood plasma (although less rapidly, due to its size) and is easily measurable (Baughman, 1997; Ward et al., 1993). However the use of albumin has a number of limitations, as similar to urea, its use as a marker of sample dilution is based on its equilibrium across the blood-air barrier. With many pulmonary diseases associated with altered epithelial permeability, the use of albumin becomes questionable (Walters and Gardiner, 1991; Ward et al., 1993; Baughman, 1997; Dargaville et al, 1999; Haslam and Baughman, 1999). It has also been recommended that lavage solute concentrations could be exprerssed relative to another component, e.g. individual protein concentrations relative to the total protein measurements. This semi quantitative method may provide the best way to sensibly compare the concentrations of RTLF solute concentrations as it's unaffected by dilution (Haslam and Baughman, 1999). It is noteworthy that very little has been published since the ERS task force lead by Haslam and Baughman (1999) fifteen years ago, probably reflecting the change in direction from invasive RTLF sampling procedures to a variety of less invasive ones, as discussed in the next section.

2.4: Nasal lavage, exhaled breath condensate and induced sputum collection

Historically sampling of the distal airways required the use of invasive lavage procedures; however more recently less invasive methods have become more widely employed. In addition to being less expensive, both in absolute personal and equipment

costs, these methods are more amenable to volunteers and patients and also permit for more detailed time course investigations to be performed (Kelly and Mudway, 2003). Nasal lavage has been routinely employed in studies wishing to selectively sample the nasal airways. Similarly induced sputum has also become popular as a relatively non-invasive method for obtaining bronchial airway lining fluids (Mutlu et al., 2001; Ratto et al., 2006). In addition the collection of exhaled breath condensate (EBC) to provide samples derived from the distal RTLFs has also become widespread. Critically, bronchoscopy-based lavage remains the gold standard of sampling methods and newer methods such as bronchoscopic microsampling have been developed that aim to sample the RTLFs directly.

Non-invasive techniques to sample the RTLFs have been developed to counteract problems faced with lavage procedures. The collection of EBC has been developed as an inexpensive sampling procedure, as a potential substitute for BAL (in the research and clinical settings) based on the collection of 'respiratory fluid droplets' in exhaled air. Condensate samples are typically collected through exhalation into commercially available condensators, cooled with ice water and then dripped into polycarbonate tubes, with approximately one hour required to collect ~ 10ml (Effros et al., 2002; Effros et al., 2003). Measured parameters from condensate samples have included: pH, total protein and phospholipid components of the airway lining fluids (Mutlu et al., 2001; Jackson et al., 2007).

Limitations of this technique have however come to light. Concentrations of solutes found within EBC are greatly influenced by their physical properties (solubility, hydrophobicity etc.), in addition to their relative concentrations in the RTLFs. The site of origin of components recovered from these 'respiratory droplets' is also not fully clear, and it has been suggested that this approach provides a sample reflective of the whole of the respiratory tract from the mouth to the alveoli. With EBC said to sample a much larger area of the lung than BAL, the relative contributions of different regions of the lung to solute concentrations can therefore not be specified using this technique. EBC may also be contaminated by salivary components since it is collected orally, but to what extent this occurs is unclear and has lead to much contention within the published literature (Mutlu et al., 2001; Hunt, 2007; Jackson et al., 2007; Effros, 2010).

Table 1.1: *Procedural differences in BAL sampling procedures used across different studies*

Author	Sampling Procedure used	Volume instilled	Dwell time described?	Dilution marker investigated	Calculated ELF dilution
Rennard et al., 1986	BAL	5x20ml for 3 sites	30-45 seconds	Urea	100 fold
				Albumin	8 fold
Ward et al., 1993	BAL	3x60ml	-	Albumin	n/d
van de Graaf et al., 1991	BAL	7x20ml	-	Urea	n/d
van der Vliet et al., 1999	BAL	5x20ml	2-3 minutes each	Urea	100 fold in initial fraction ~30-40 fold in final
	BAL	1x60ml	<1 minute		100 fold in initial fraction ~30-40 fold in final
Baldwin et al., 1991	BAL	1x20ml	20 seconds	Urea and Total Protein	n/d
		4x50ml	4 minutes total	Urea and Total Protein	n/d
Dargaville et al., 1999	BAL	3x1ml/kg	60-90 seconds	Albumin, Total Protein, Urea	n/d
Sutinen et al., 1995	BAL	4x50ml	-	Urea	n/d

To fully assess the potential of EBC, investigations comparing measured components to those obtained using bronchoscopy-based lavage are required. Jackson et al (2007) compared several biomarkers between EBC and BAL fluids, including various markers of inflammation (eNO, NOx and pH), as well as total protein, cytokine and phospholipid concentrations. They found no correlation, before or after dilution corrections were applied. Total protein concentrations were found to be much higher in BAL whereas phospholipid content was higher in EBC suggesting that solutes measured in EBC could not be directly compared to BAL samples. The potential application of EBC is also seriously hindered by the dilution of respiratory droplets by water vapour. The dilution created by this process has been estimated to vary from 5,000 to 25,000 fold (Effros et al., 2002; Effros et al., 2003; Dwyer, 2003). As with BAL a dilution marker would therefore also be required in the quantification of RTLF solutes from retrieved condensate samples (Effros, 2010).

Urea has therefore also been investigated as a marker to correct for EBC dilution.Since no fluid is instilled into the airways with this technique the issue of urea movement from the blood into the RTLF down an artificial concentration gradient is no longer a complicating factor and yet the results obtained demonstrated great variability (Effros et al., 2003). Conversly in a study performed by Esther et al. (2009) investigating urea as a dilution marker for this procedure, the authors were able to demonstrate correlation between EBC urea and EBC electrolyte concentrations and thus concluded that a biomarker to urea ratio may be effective to control for condensate dilution. The use of electrolytes (K^+, Cl^-, Na^+ and NH_4^+) to correct for dilution in condensate samples has also been investigated (Effros et al., 2002; Effros et al., 2003; Esther et al., 2009), but as with lavage based methods a standardized reporting approach is absent.

Bronchoscopic microsampling (BMS) has been described in recent years as a novel procedure to tackle the problems outlined above, permitting the direct measurement of molecules in the RTLF. This approach makes use of the flexible fibreoptic bronchoscope, through which a bronchoscopic microsampling probe is inserted. This probe first described by Ishizaka et al (2001), consists of a polyester fibre rod (1.2mm diameter) attached to a stainless steel wire for guidance, covered by a polyethylene sheath (2.5mm outer diameter). The probe is placed gently onto the surface of the central or peripheral airways for approximately 10 seconds, sampling the RTLF directly by adsorption. The protocol for this procedure requires the inner probe to be cut and frozen at -80^{o}C, prior to subsequent dilution into 1ml of saline, to produce a solution for the purpose of solute measurement (Ishizika et al., 2001; Yamazaki et al., 2003; Kodama et al., 2009). Bypassing the problems encountered with lavage dilution, this method has

been suggested to provide a more reliable method by which to sample and quantify RTLF components (Kodama et al., 2009). To date this technique has been employed in studies investigating the pharmacokinetics of antimicrobials and their concentrations in the respiratory tract (Yamazaki et al., 2003) and investigations into pulmonary biochemical markers in pathological conditions of the airways (Ishizaka et al., 2001; Watanabe et al., 2003; Kodama et al., 2009). Yamazaki et al. (2003) compared BAL (using the urea correction) and BMS RTLF sampling procedures in the pharmacokinetic determination of levofloxacin concentrations, demonstrating significantly different concentrations between the two methods. Nevertheless, the use of this relatively non invasive technique could potentially solve one of the major issues faced by RTLF sampling procedures and futher investigations are require to assess its use in vivo.

2.5: Compositional differences along the respiratory passages: nasal passages, tracheobronchial and bronchoalveolar compartments

When considering the deposition pattern of inhaled particles in the lung and their interaction with the RTLFs, the regional variation in airway morphology and cell populations, from the nasal passages to the terminal alveolar region is of great importance (Chen et al., 2004; Darquenne et al., 2009). With the size and shape of medicinal particles determining their deposition site within the respiratory tract (Heyder, 2004), there is a need to understand how they interact with the RTLFs at various levels of the respiratory tree. The respiratory tract is often divided into three distinctive morphological areas: the nasal passages, the tracheobronchial airways and finally the bronchoalveolar regions. Investigations making use of airway casting techniques have reported the alveolar surface area to be 890,000 cm^2, approximately 5,000 fold greater than that reported for the nasopharyngeal regions (178 cm^2) (Hatch, 1992). Light and electron microscopic studies have been used to determine thickness of the RTLF along the respiratory tract; with the thickness in the upper airways estimated to be between 5-20 µM (Yoneda, 1976; Wanner; 1994; Widdicombe and Widdicombe, 1995). Rapid freeze techniques have also been applied in determinations of RTLF depth in more distal airways, resulting in estimated depth of 1.8 µM in the bronchioles (Mercer et al., 1992). Overall the available evidence suggestes that RTLF depth decreases from the nasal airways (5-10µM), contrasting with a thickness of approximately only 0.2-0.5µM in the distal alveolar regions (Sleigh et al., 1988; Hatch, 1992; Kelly and Mudway, 2003). Using this quantitative information regarding the relative thickness of the RTLF in each respiratory tract compartment together with the

information on airway area, ‘morphological volumes’ of the RTLF surrounding these compartments have been estimated to be 142 µl in the nasal airways compared with 8.9 ml in the alveoli (Hatch, 1992; Mercer et al., 1992).

The progressive increase in RTLF thickness from the distal to the proximal airways reflects changes in epithelial cell ion transport, as well as a number of passive factors, including evaporation and osmotic water flow (Widdicombe and Widdicombe, 1995). In the upper airways ciliated cells appear to determine the depth of the aqueous layer, and it has been suggested there may be some mechanical regulation via surface tension forces created by the presence of the cilia themselves (Widdicombe, 1997; Widdicombe and Widdicombe, 1995). Many of the epithelial cells of the upper airways, particularly submucosal glands, serous, goblet and Clara cells are secretory in nature and significantly contribute to RTLF composition, though their contribution is greatest in respiratory conditions associated with expansion of secretory cell populations, such as asthma and chronic obstructive pulmonary disease (COPD) (Widdicombe and Widdicombe, 1995; Finkbeiner, 1999). The variation in RTLF depth and composition throughout the respiratory tree is illustrated in **Figure 1.2**.

In addition to changes in epithelial cell populations along the respiratory tract, the general composition of the RTLF varies in composition reflecting its different roles in the upper and lower airways. In the upper airways it is well established that the RTLF is composed of two layers: a perciliary watery sol layer covered and surrounded by a gel like mucous layer. The appearance of these two layers has been clearly demonstrated by electron microscopic studies of rapidly fixed tissues (Widdicombe and Widdicombe, 1995), see **Figure 1.3**. This mucus layer, secreted by underlying sub-mucosal glands allows the entrapment of inhaled particles, including microorganisms, and their subsequent removal by the mucociliary escalator. The alveoli responsible for the majority of gaseous exchange that occurs in the lung does not contain mucus, but the RTLF in this region is enriched with surfactant secreted by alveolar type II cells, preventing alveolar collapse during expiration.

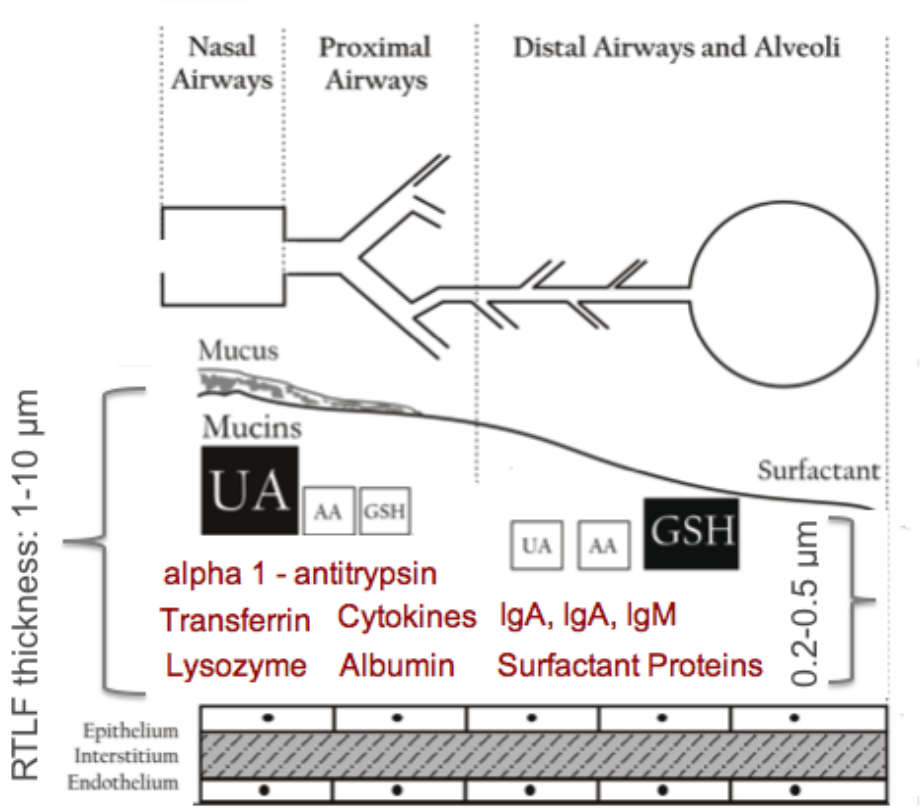

Figure 1.2: *An illustration highlighting the differences in RTLF composition and thickness throughout the respiratory tract*. RTLF thickness alters dramatically from 1-10 µm in the upper airways to 0.2-0.5 µm in the distal airspaces. Additionally both the antioxidants (UA – urate, AA – ascorbate, GSH - glutathione), proteins (as named) and lipids present within the RTLFs alter in composition and concentration between different compartments of the airways, as is highlighted in the image, depending on their relative functional roles.

Figure 1.3: *The two layers (mucus gel and aqueous sol) of the RTLF as seen in rapidly frozen preparations from rabbit tracheal culture*. Reproduced from Sanderson and Sleigh, 1981

2.6: Major components of the respiratory tract lining fluids

Having discussed and described the methods used to sample human RTLFs; the changes in its relative thickness and the roles it plays throughpout the respiratory tract, the proceeding section will focus on a detailed descriprion of its composition. Whilst the main focus of this section will be on the soluble components of the sol layer, attention is also paid to the gel phase. It should be noted up front that the great variability in the reporting of RTLF solute concentrations between different research groups, as well as the variety of sampling methods employed complicates such a discussion.

2.6.1: Mucus gel layer

Mucus is pivotal in airway disease, the major function of the mucus gel phase is protective, trapping microorganisms and large particles which have been inhaled. Allied to mucociliary transport of this layer this provides an effective clearance mechanism, limiting the interaction of inhaled xenobiotics with the underlying epithelial cells. Within the tracheobronchial region of the airways, particles are said to be cleared within twenty four hours of deposition by this mechanism (Kreyling et al., 2002). As a result, the mucus layer is continually being turned over. The velocity of mucus transport in the human trachea is approximately 4mm/min (Sleigh et al., 1988), with the maximal submucosal gland secretion rate estimated at 60µl per cm^2 per hour (Widdicombe and Widdicombe, 1995). The importance of this mucus barrier function is illustrated in the diseases of asthma and chronic bronchitis, in which mucus hypersecretion occurs (Fletcher and Peto, 1977; Vestbo et al., 1996; Vestbo et al., 2002;) in paralell to decreased cilia beat frequency (Agius et al., 1998; Dalhamn, 1958), resulting in airway obstruction and increased airway infections.

A basic description of the mucous layer is one of a high molecular weight glycoconjugate (molecular weights up to 15MDa) polymer matrix with a high affinity for water, various ions and proteins, varying in thickness between 2-20µM (Widdicombe and Widdicombe, 1995). The high molecular weight glycoconjugates can be split into two groups: mucous glycoproteins (mucin) and proteoglycans, providing the characteristic mucoid properties of high viscosity and stringy gel like appearance (Hatch, 1992). They are secreted predominately from the submucosal glands of the upper airways, estimated to occur at a density of 1 per mm^2 in an adult human trachea; as well as by goblet and serous cells (Reid, 1960; Quinton, 1979). Ciliated cells are also responsible for the control of ionic and water

concentrations and for mucous secretions, as are alveolar macrophages and lymphocytes (Hatch, 1992).

Mucous glycoproteins have great inherent polydispersity. These acidic polyanionic mucins are composed of oligosaccharide chains attached to a core peptide region via o-glycosidic linkages. Principle mucin glycoproteins, MUC5AC and MUC5B, are required for both mucociliary clearance and airway defence, with MUC5b found to be crucial in maintining the immune homeostasis of the airways (Roy et al., 2014). The thiol content of mucins is reported to be between 1-2% with disulphide bridge formations playing an important role in the polymerization between cysteine rich regions of chains (Allen, 1983; Hatch, 1992). Proteoglycans in contrast are mainly composed of linear unbranched glycosaminoglycans (Reid, 1978).

2.6.2: Low molecular weight antioxidants

The lung, due to its anatomy and physiological function is exposed to a high oxidant burden both from the inhalation of environmental oxidants/pro-oxidants (tobacco smoke, ambient air pollution, pesticides etc.), or arising from the release of reactive oxygen species from activated phagocytic cells associated with acute respiratory insults or chronic inflammatory disease (Macnee, 2001). The antioxidant content of the RTLFs has therefore received much attention, due to their role in maintaining the reducing environment at the air-lung interface (Skoza et al., 1983; Cross et al., 1994), limiting oxidative injury to the lung (Cantin et al., 1987; Gutteridge et al., 1996; Hernandez et al., 2009). It has therefore been argued that the capacity of the respiratory tract epithelium to transport and maintain the RTLF antioxidant pool represents a critical determinant of the protective ability of this compartment (Nel et al., 2006; Stone and Donaldson, 2006; Behndig et al., 2009).

The antioxidant milieu of the RTLFs includes a variety of components; the high molecular weight glycoproteins of mucus (described in the previous subsection), metal chelating proteins, antioxidant enzyme systems (including extracellular glutathione peroxidase and superoxide dismutase) and low molecular weight soluble antioxidants, which will be the focus of this sub-section.

2.6.2.1: Urate

Urate (UA), an oxidized purine base, is a major low molecular weight antioxidant found throughout the RTLFs, with particularly high concentrations within the nasal lining fluids,

where it represents the predominant sacrificial antioxidant, present at concentrations equivalent to those in plasma, see Table 1.2 (Peden et al., 1990; Kaliner, 1991; Cross et al., 1998). Urate has been implicated as a highly potent scavenger of a variety of radicals and gaseous pollutants, particularly ozone in the nasal passages, and it has thus been speculated that its high concentrations within the upper airways may act as a mechanism to protect the distal airways from oxidative stress (Kaliner, 1991; Peden et al., 1993; Crosset al., 1992; Meadows and Smith, 1986). Due to the high concentrations of urate observed within upper airway secretions and the apparent correlation with plasma concentrations, its presence within the RTLF is thought to occur as a result of passive transudation from the plasma pool (Kelly and Mudway, 2003). Additionally, it has been proposed that epithelial submucosal glands take up plasma or interstitial UA, concentrating and subsequently co-secreting this antioxidant alongside mucin in the nasal and upper RTLFs (Peden et al., 1990; Peden et al, 1993; Cross et al., 1994).

2.6.2.2: Ascorbate

The highly water-soluble, reactive oxygen species scavenger ascorbic acid (ascorbate, AA) is distributed throughout the RTLF, present in both its reduced (L-ascorbic acid) and oxidized form (dehydroascorbic acid). Humans lack the ability to synthesize AA due to the lack of the enzyme gulonolactone oxidase, consequently its presence is entirely dietary dependent (Frei et al., 1989). RTLF AA concentrations have been attributed to passive pericellular diffusion from the plasma pool due to the similar concentrations observed between plasma and lavage dilution corrected nasal lavage samples (van der Vliet et al., 1999). However no association between AA concentrations in lavage and plasma samples has ever been clearly demonstrated (Blomberg et al., 1999; Mudway et al., 2004). Studies investigating the supplementation of Vitamin C (L-ascorbate) on RTLF concentrations have shown rapid movement of ascorbate into the RTLF, that is either rapidly lost from the airway surface by oxidation, or taken up into airway cells (Behndig et al., 2009). Whilst, the former would support the relatively high concentrations of dehydroascorbate that have been measured in the airway, such continual oxidative losses from the airway surface would present a significant drain on bodily vitamin C reserves. Consequently, some form of recycling or cellular salvaging system would be required, but to date none has been identified. A number of reports have demonstrated significantly reduced, or even absent AA concentrations within the RTLFs of asthmatic patients which have been related to the presence of airway inflammation and oxidative stress in their airways (Olusi et al., 1979; Cluzel et al, 1987; Kelly et al., 1999).

Table 1.2: *RTLF antioxidant concentrations as determined from BAL and NL, with plasma concentrations of these antioxidants presented for comparative purposes*.

	ELF Concentrations		
	BAL	NL	Plasma
Antioxidant (μM)			
Ascorbate	40[1],100.0[2], 200[3]	28[1], 40[5]	67[1], 40[6]
Urate	207[1], 90[2], 200[3]	225[1], 160[5]	387[1], 300[7]
Glutathione	109[1], 100[2],129[4]	<0.05[1]	1[1], 1.5[6]
References	[1]van der Vliet et al., 1999; [2] Hatch, 1992; [3]Slade et al., 1993; [4]Cantin et al., 1987; [5]Peden et al., 1990; [6]Frei et al., 1992; [7]Svardal et al., 1990		

2.6.2.3: Glutathione

L-y-glutamyl-L-cysteinyl-glycine, or glutathione, is a sufhydryl containing tripeptide constituting the major component of the antioxidant network in the distal RTLFs (Cantin et al., 1987; Kelly et al., 1999). Under normal physiological conditions > 95% is found in its reduced form (GSH), with the remainder present as glutathione disulfide (GSSG) (Meister and Anderson, 1983; Cantin et al., 1987; Kelly et al., 1999). GSH is found in all cells at mM concentrations, with reported RTLF concentrations approximately one hundred times (100-300 μM) that found in the plasma pool (1-10 μM) in normal healthy RTLFs – see **Table 1.2** (Van der Vliet et al., 1999). The increased GSH concentration in RTLF strongly suggest that the local concentrations do not arise by passive diffusion from the plasma pool, but suggest local synthesis, recycling and export from airway cells. The majority of extracellular GSH is catabolized by y-glutamyl-transpeptidase, an enzyme expressed by type II epithelial cells, clara cells, mononuclear phagocytes, lymphocytes and fibroblasts, and is believed to play an important role in determining RTLF GSH concentrations (Griffith and Meister, 1979; Rahman and MacNee, 2000; Kelly and Mudway, 2003; Reynaert, 2011). Elevated GSSG concentrations are a clear marker of oxidative stress, and have been reported in asthmatic RTLFs (Reynaert, 2011; Kelly et al, 2003; Kelly et al, 1999). Higher total glutathione concentrations have also been observed within the RTLFs of asthma sufferers (Smith et al, 1993; Kelly et al., 1999), whilst decreased concentrations have been reported in sufferers of idiopathic pulmonary fibrosis and cystic fibrosis (Cantin et al., 1989; Roum et al., 1993).

2.6.2.3: α-tocopherol

This lipid soluble antioxidant is found integrated within biological membranes where it acts as a direct free radical scavenger terminating lipid peroxidation reactions at relatively low concentrations (Davis and Pacht, 1991; Rustow et al., 1993; Burton et al., 1983). In the lung it is believed to be secreted alongside surfactant by type II alveolar cells. Investigations have demonstrated the important oxidant protection this antioxidant provides to the airways, with lower concentrations demonstrated to result in increased lung injury (Pryor, 1991). Significantly lower concentrations of this antioxidant have been observed in the RTLFs sampled from asthmatic patients. A similar deficiency has been reported in the RTLFs of current smokers (Kelly et al., 1999; Pacht et al., 1986).

2.6.3: Major protein components of human RTLFs

The protein constituents of the RTLF are important when considering the potential biophysicochemical interactions occurring when inhaled particles deposit in the lung. Particularly the likely impact of the protein corona formed around particles interacting with biofluids has attracted considerable attention, as this is likely to modify surface properties, including charge, propensity to aggregate and hydrodynamic diameter, altering particle behaviour *in vivo* (Nel et al., 2009; Monopoli et al., 2011).

The presence of protein within the RTLFs was first demonstrated electrophoretically by Warfvinge et al. (1955), since this initial study the protein components found within this extra-cellular compartment have been extensively studied through the use of various techniques. The great complexity of the RTLF proteome is in part due to the large number of distinct individual proteins present but also a result of the variety in their source of origin (Noel-Georis et al., 2002). Proteins may be derived from plasma transudation (e.g. albumin), or synthesized locally (e.g. surfactant protein A), with certain proteins unique to the airways (Stockley, 1984; Kim et al., 2002; Hermans et al., 1998). As described previously uncertainties regarding the interpretation of BAL solute concentration data, in addition to differences as a result of pathological airway conditions, complicate the quantitative description and interpretation of the RTLF proteome. The clearance of proteins from the airways also plays an important role in determining concentrations within this compartment. Protein clearance has been studied in both animal models and human participants, with protein tracers the most common procedure employed (Folkesson et al., 1996). Clearance mechanisms include elimination via the

mucociliarly escalator followed by swallowing, endocytosis by alveolar macrophages, degradation of proteins by peptidases within the airways or absorption across the airway epithelial cells into the circulation (Hastings et al., 1992; Phipps and Richardson, 1976; Matthay et al., 1996). To date RTLF proteome comparisons have only observed small differences across gender, age and ethnic groups (Hatch, 1992).

Serum proteins found present in the RTLF generally have molecular weights <200, 000 Da, corresponding to the significantly lower protein concentrations found within this compartment compared to plasma, and indicating a size dependent diffusional process at play (Bell et al., 1981; Feng et al., 1992). Of those proteins derived by transudative mechanisms, the most dominant plasma protein is albumin. Early experiments in which radiolabelled albumin was injected into the peripheral circulation, later to be detected within airway lavage samples, clearly demonstrated this process (Bonomo, 1964).

Clear regional differences in protein concentrations have become apparent throughout the airway. Alveolar lining fluids have been reported to have higher total protein concentrations compared with bronchial and nasal compartments and it has been speculated that this might reflect difference in the relative leakiness of the blood-air barrier at various levels of the respiratory tree (Hatch, 1992). Additionally, surfactant-associated proteins were also reported to have their highest concentrations within the distal airways, a result of the selective secretion of surfactant by type II cells (Serrano and Perez-gil, 2006). Conversely, bronchial and nasal airways have been reported to contain higher concentrations of several secretory proteins, including proteoglycans found within mucin, lysozyme and lactoferrin, reflecting secretions from submucosal glands located in the upper airways (Kelly et al., 2003; Raphael et al., 1989).

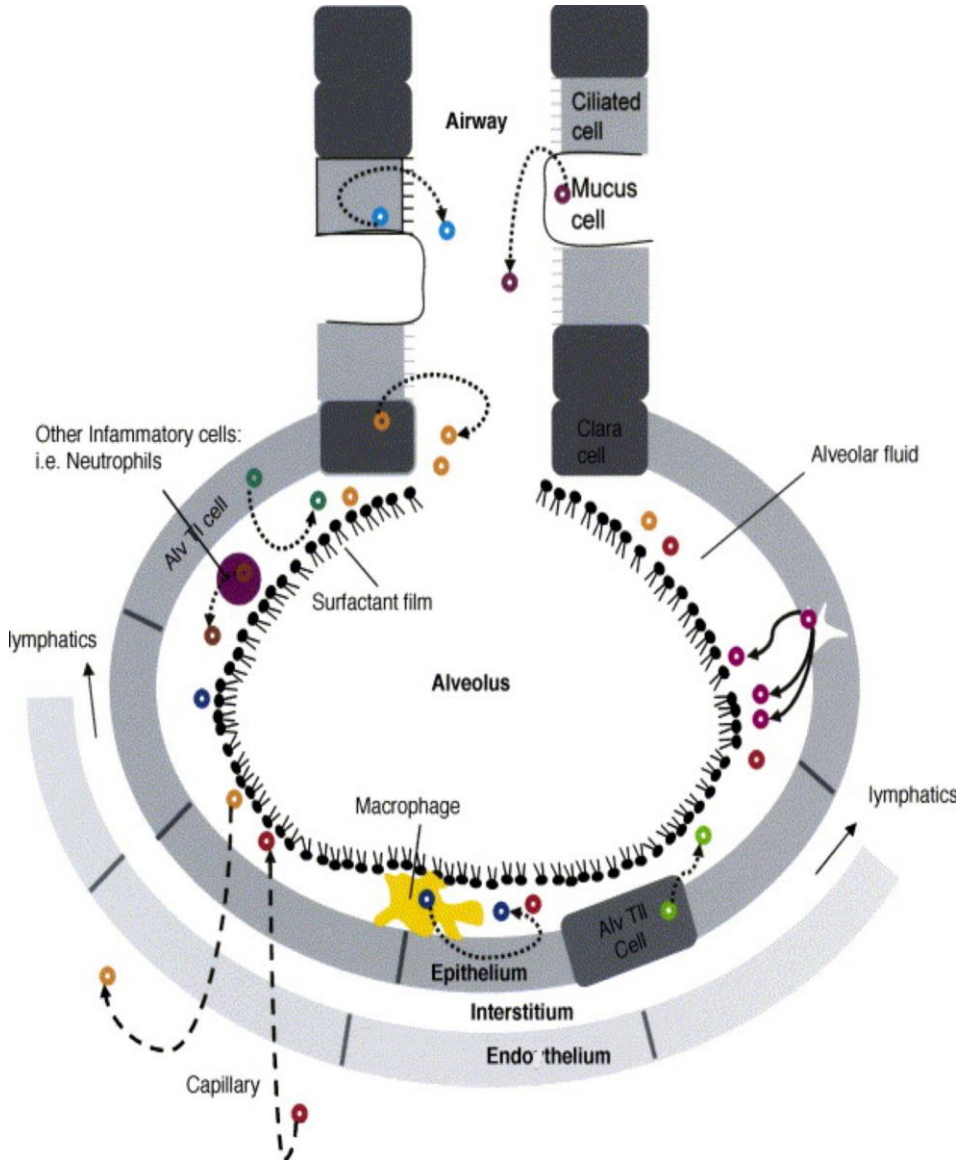

Figure 1.4. *An overview of the various sources of origin of proteins found within BAL samples.* Proteins identified within BAL may be derived from plasma following transudation across the air-blood barrier, secreted within the airways by inflammatory cells, and secretory cells composing the epithelium including Clara cells and serous cells. Reproduced from Wattiez et al., 2005.

While the quantification of lavage total protein content is relatively straight forward using common methods (Lowry et al., 1951; Bradford, 1976; Smith et al., 1985), the quantification of individual protein components requires more sensive immunological or mass spectroscopy-based techniques, due to the low concentrations present in dilute RTLF samples (Boutten et al., 1998; Wattiez et al., 1999). High resolution techniques have been applied to 'map' the RTLF proteome and to build up a detailed picture of the protein composition of this compartment in a variety of clinical conditions. Electrophoretic methods in particular, 2-dimensional electrophoresis (2-DE), in which polypeptides are separated by both their

isoelectric point and molecular weight, are employed in the analysis of complex protein mixtures and have thus provided a vast wealth of information regarding the protein composition of various body fluids including those obtained from the respiratory tract (Wattiez et al., 1999; Magi et al., 2006), see **Figure 1.4**.With the first 2-DE map of proteins identified from a lung lavage sample published in 1979 by Bell and colleagues (1981). The popularity of 2-DE techniques for the analysis of BAL fluid resulted in the production of a reference protein map, which currently comprises of over 1,200 silver stained spots (Noel-Georis et al., 2002). The comparison of 2-DE BAL protein maps to the human reference plasma protein 2-DE map and macrophage-like cell line maps have also helped identifying the source of origin of proteins present within human RTLFs (Wattiez et al., 1999).

However many factors complicate 2-DE techniques, from the range in the magnitude of protein concentrations within human RTLFs, protein pIs, charge, molecular weight, relative hydrophobicity; all of which make the effective separation of all proteins within this compartment extremely challenging (Magi et al., 2006). Many alternative approaches are often used or combined with 2-DE techniques to maximize the number of identifiable spots, their accuracy, recovery, speed and separation (Magi et al., 2006). Currently, 1,500 different proteins have been identified in human BAL fluid using the combination of these approaches: affinity depletion of the most abundant BAL proteins, SDS PAGE fractionation, and protein in-gel digestion followed by nano-LC-MS/MS (Wu et al., 2005).

Such techniques have identified the major soluble protein components of human RTLFs; in addition to permitting biomarker identification in relation to early airway disease and progression. The following section will discuss the major proteins identified within the RTLF, focusing on their concentrations, origins, and functions, in addition to differences observed between various disease states.

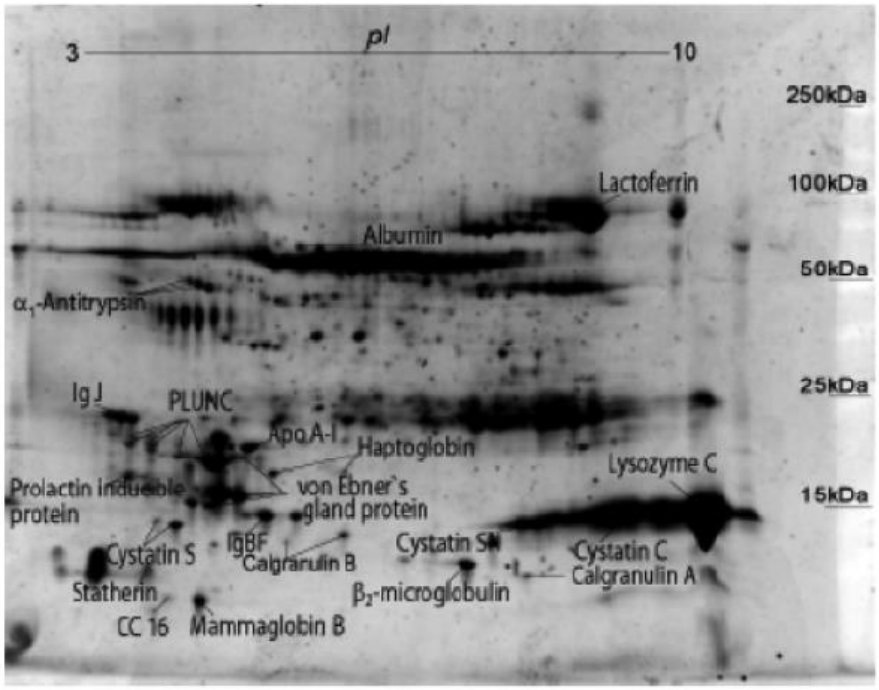

Figure 1.5: *A 2D-gel map of a lavage sample retrieved from a healthy human airway. Proteins (100 μg) were separated on pI 3-10 nonlinear IPG strips (first dimension) and on 11-18%T SDS polyacrylamide gels (second dimension).* The gel was stained with SYPRO Ruby, with a detection limit of about 10 ng protein. The proteins were identified by 2-DE and MALDI-TOF MS after tryptic cleavage and are indicated). Albumin has been removed from the sample prior to analysis. Reproduced from Gharfouri et al., 2005. * PLUNC- palate lung nasal epithelial clone

2.6.3.1: Albumin

Albumin is a single 585 amino acid polypeptide chain of 66.5 kDa molecular weight and represents the most abundant plasma protein (35-50 mg/mL). In addition to its role as an acute phase protein, it has also been proposed as the major antioxidant protein within plasma by virtue of its free thiol group. The majority of albumin synthesis occurs in the hepatocytes of the liver. It is a major protein component of the RTLF, found at concentrations approximately 10 fold lower than plasma, accounting for approximately half of total protein content (with concentrations of 2-5 mg/mL reported, **See Table 1.3**). Derived from passive plasma transudation across the airway epithelium it is a well established marker of vascular permeability (Webber and Widdicombe, 1989; Hatch, 1992; Greiff et al., 2003). Concentrations of albumin have been shown to be increased in lavages obtained from patients with a range of acute and chronic inflammatory airway disease, including interstitial lung disease (Noel-Goeris et al., 2001); asthma (Nocker et al., 1999) and seasonal allergic rhinitis (Ghafouri et al., 2006).

Table 1.3: *Major RTLF protein concentrations (mg/mL) as determined by the urea method for lavage dilution correction.*

	RTLF protein concentrations (mg/mL)	% contribution to total protein
Total Protein	5.7[1],9.0[14], 9.5[15], 10.9[4],11.7[12]	
IgA	0.026[1]*,0.032[1]*, 0.057[4]*, 0.64[2], 1.42[3]	5-10[7], 6-12[13]
IgG	0.64[2],0.65[3], 0.89[4]	15.6[7], 5.5[13]
IgM	0.028[4]	
Albumin	2.0[1],3.8[4], ,4.6[14], 5.35[2]	35[1], 30-45[13], 51[14], 50[16], 55.8[7], 40-50[11]
Transferrin	0.3[2],0.16[3]	4-5.6[7]
Lysozyme	0.031[5], 0.070[6]	15[8] □,35[9]□
α 1- antitrypsin		3.2[7]
CC16		7[10]

[1]Dargaville et al, 1999 (NL/BAL); [2]Rennard et al, 1990 (BAL); [3]Rennard et al, 1990 (BW); [4] Sutinen et al, 1995 (BAL); [5] Thompson, 1990 (BAL); [6] Thompson et al, 1990 (BW); [7] Bell, 1981 (BAL); [8] Kaliner, 1991; [9] Raphael et al, 1989; [10] Bernard et al, 1992; [11]Peterson et al, 1993 (BAL); [12]Koren et al, 1989 (BAL); [13] Hatch, 1992, [14] Holter et al, 1986, [15]van der Vliet et al, 1999, [16]Lenz et al, 1993. * denotes values are derived from a secretory component, □denotes values are obtained from nasal

2.6.3.2: Transferrin

Transferrin is an 80kDa glycoprotein found abundantly within human RTLFs. It is predominately derived from the plasma, with additional local production by alveolar macrophages and lymphocytes. Transferrin represents a greater proportion of total protein within the RTLF (4-5.6% see **Table 1.3**) than it does within the plasma pool on account of local synthesis within the airways (Wesselius et al., 1994; Mateos et al., 1998). Transferrin is responsible for the transport of free iron by the reversible binding of two ferric ions. In this manner it has important antioxidant properties at the air-lung interface, preventing iron catalysed free radical production, as well as limiting iron availability to bacteria within the airway (Romero et al., 1993; Mateos et al., 1998). The greatest transferrin concentrations have been observed within the more distal airway compartments in healthy samples (Lindahl et al., 1998). For patients with acute respiratory distress syndrome, a twenty fold increase in transferrin RTLF concentrations has been reported; related to its role in the removal of excess free iron following cell death (Holter et al., 1986; Pacht and Davis, 1988). Greater

concentrations have also been demonstrated in sarcoidiosis patients, likely due to increased transudation of protein from the plasma pool (Wattiez et al., 2000).

2.6.3.3: Immunoglobulins: A, G, M

The lungs have been described as one of the major 'immunological organs' in the body, reflecting their position as the first line of defence against inhaled xenobiotics. The production of immunoglobulins is central to this role, being involved in the recognition and binding to specific antigens and the activation of various immunological responses (Burnett, 1986). In contrast to plasma, in which IgG is the most predominant immunoglobulin, IgA forms the major class of immunoglobulin within RTLF (Daniele, 1990). The plasma form of this immunoglobulin exists as a 150kDa protein, and is found within the RTLF, a result of passive plasma transudative forces, the secretory form (sIgA), a dimer of 400kDa is synthesized by serous cells and submucosal glands of the respiratory epithelium of the upper airways (Hatch; 1992; Raphael et al., 1989). The secretory form represents approximately 80% of IgA in secretions found of the nasal airways, as confirmed by 2D-gel work examining concentrations in NL versus BAL fluids (Hatch, 1992; Lindahl, et al. 1995; Lindahl et al., 1998), highlighting the extensive local synthesis that occurs. IgA producing plasma cells are most prominent within the major bronchioles of the airways, corresponding with the higher concentrations observed in samples obtained from the upper airways, at concentrations reported between 0.05-1.42 mg/mL (see **Table 1.3**), (Burnett, 1986).

Whilst immunoglobulin G does not form the major immunoglobulin present within this compartment, its concentration remains considerable (concentrations of 0.64-0.89 mg/mL have been reported see **Table 1.3**), being derived from plasma via transduction, as well as by local production of specific subclasses, with IgG secreting plasma cells located in the bronchial mucosa (Burnett, 1986; Nijhuis-Heddes et al., 1982).

Immunoglobulin M is the largest class of immunoglobulins with a molecular weight of 900kDa, implying that movement from the plasma pool is limited, and as such is much less abundant than IgA and IgG: 0.028mg/mL (**Table 1.3**). Some local production is possible due to the presence of IgM plasma cells in the bronchial mucosa (Burnett, 1986; Nijhuis-Heddes et al., 1982; Stockley et al., 1979).

Concentrations of immunoglobulins are altered in several diseases of the airways; with interstitial diseases (sarcoidiosis, alveolitis, idiopathic pulmonary fibrosis) all associated with significant increases in IgG and IgA RTLF concentrations, presumably reflecting both increased local synthesis (increased T helper cells have been observed in BAL samples) and increased

permeability of the air blood barrier (Stockley and Burnett, 1980; Bauer et al., 1985; Rankin et al., 1983; Reynolds et al., 1977). Chronic bronchitis sufferers have also been observed to have significantly greater concentrations of IgA; however conflicting results have been reported suggesting that bronchitic patients are deficient in IgA plasma cells (Stockley and Burnett, 1980; Soutar, 1977).

2.6.3.4: Lysozyme

This small 14kDa secretory antimicrobial protein is a hydrolytic enzyme which acts to degrade bacterial cell walls. It has been found in greater concentrations (approximately three to four fold greater according to 2-DE maps) in the proximal airways compared with the more distal alveolar airway (concentrations of 0.16-0.3mg/mL observed in BAL samples – **Table 1.3**), as determined by NL versus BAL sampling techniques (Lindahl et al., 1998). The high levels of lysozyme in samples from nasal airways are presumably due to the secretion of this protein from the submucosal glands, specifically serous cells that constitute the bronchus and nasal epithelium (Raphael et al., 1989). Another possible, but minor source of this enzyme might occur through its release from neutrophils and alveolar macrophages. Increased lavage concentrations of lysozyme have been reported in allergic rhinitis and allergic extrinsic alveolitis (Ghafouri et al, 2006; Raphael et al., 1989; Perez-Arellano et al., 1996). Interestingly, lysozyme is often secreted alongside the bacteriostatic and bacteriocidal lactoferrin by serous cells (Revenis and Kaliner, 1992), an iron binding protein found particularly in glandular secretions of the upper airways and nasal passages (Mateos et al., 1998). The highest concentrations of both these proteins are observed within external secretions including tears and mucus, on account of their antimicrobial actions (Raphael et al., 1989).

2.6.3.4: α-2-macroglobulin

α-2-macroglobulin is one of the major protease inhibitors found within plasma, with its main action the inhibition of endopeptidase enzymes. The main site of synthesis in the body of this protein is the liver and due to its high molecular weight,700kDa its passive transudation onto the surface of the lung is unlikely. It's presence in the RTLF is likely a result of its secretion by alveolar macrophages (White et al., 1980). Through the formation of complexes with serine proteases or metalloproteinase, these enzymes are recognized by macrophage α-2-macroglobulin receptors, internalized and degraded (Moestrup et al., 1993). Its presence in RTLFs has been shown to increase in a variety of lung diseases, including asthma, pneumonia,

acute respiratory distress syndrome, sarcoidiosis and tuberculosis (Nocker et al., 1999; Holter et al., 1986; Titanian et al., 1987).

2.6.3.5: α 1-antitrypsin

This serine proteinase inhibitor is responsible for inactivating proteolytic enzymes, particularly neutrophil elastase, providing an important defence mechanism within the airways against uncontrolled enzyme mediated tissue injury (Ghafouri et al, 2006). The presence of α 1-antitrypsin in RTLF is accordingly increased in inflammatory diseases of the lung (pneumonia, tuberculosis, sarcoidiosis, interstitial pulmonary fibrosis and allergic rhinitis) presumably a result of increased protease release from activated inflammatory cells within the airways (Gadek et al., 1981; Titaninan et al., 1987; Wattiez et al., 2000; Ghafouri et al., 2006). It has also been linked with a protective role in atopic asthma and deficiency of this enzyme has been associated with the development of emphysema (Boutten et al., 1998). The major source of this enzyme is from plasma, with hepatocytes being the major site of production. In addition pulmonary alveolar macrophages and alveolar epithelial cells are believed to be sources of this protein within the RTLFs (Takemura et al., 1986; Boutten et al., 1998).

2.6.3.6: Clara cell secretory protein (CC16)

CC16 is a 16kDa low molecular weight protein, uniquely synthesized in the airways by the Clara cells of the bronchial and alveolar epithelium, and reported to be a major protein constituent within BAL fluids (Bernard et al., 1992; Singh et al., 1988; Hermans and Bernard, 1999). This protein is however also found in plasma, relefecting its retrograde diffusion across the air blood barrier from the airway surface. Consequently the plasma concentrations of CC16 have been proposed as a sensitive biomarker of altered blood-air barrier permeability (Bernard et al., 1992; Hermans and Bernard, 1999; Broeckaert et al., 2000) and plasma concentrations have been shown to be elevated in a variety of respiratory diseases, (Bernard et al., 1992; Hermans and Bernard, 1996). Transient increases in serum CC16 concentration have been observed in response to several airway irritants such as ozone (Blomberg, et al. 2003), lipopolysaccharide (LPS) (Michel, et al. 2005) and smoke (Bernard, et al. 1997). Altered concentrations of this protein have been demonstrated in tobacco smokers (decrease in BAL) and patients with interstitial lung disease (increase in serum levels) (Bernard et al., 1992; Hermans and Bernard, 1996). Lower concentrations of CC16 have also been demonstrated in nasal lavage samples from children with allergic asthma and rhinitis (Lindahl et al., 1995;

Lindahl et al., 2001), as well as in severe COPD patients compared to those with moderate COPD or healthy controls (Braido et al., 2007). CC16 is believed to have anti-inflammatory actions in the airways. It is a potent inhibitor of PLA2 activity (Levin et al., 1986) and monocyte, neutrophil and fibroblast chemotaxis (Vasanthakumar et al., 1988; Lesur et al., 1995). Higher susceptibility to airway inflammation and injury in response to irritants including ozone (Mango et al., 1998) and hyperoxia (Johnston et al., 1997) has been observed in CC16-deficient mouse strains compared to wild type.

2.6.4: Surfactant

Secreted by type II alveolar cells, surfactant forms a crucial physiological component of RTLFs by reducing the surface tension of the alveoli, preventing their collapse during breathing (Hills, 1988; Creuwels et al., 1997). Investigations by Von Neergaard et. al (1929) initiated the research into this unique material, identifying a surface active substance which lowered the tension of the air water interface. Later studies by Pattle (1955) suggested a 'surfactant' was responsible for the maintenance and stability of low surface tension within the fluid lining the lung; with Macklin et al (1954, 1955) demonstrating that the material was specifically secreted by the epithelial cells lining the alveoli. Investigations carried out by Clements et al. (1972) were the first to identify the presence of phospholipids with surface tension lowering properties, with the actions of proteins in this surface active material later identified in studies performed by King et al. (1973). Since these initial investigations, the composition of surfactant has been extensively studied. Approximately 90% of surfactant is composed of lipid, wih the remaining fraction accounted for by the four surfactant associated proteins (A-D), with surfactant protein A the predominant form, representing approximately 5% of surfactant.

Neutral lipids including cholesterol, triglycerides and free fatty acids contribute to the lipid fraction of surfactant; however it is phospholipids that comprise the major fraction, with phospathidycholine (PC) the predominant form. Approximately half (41-70%) of PC is in the form of dipamitoylphosphatidylcholine (DPPC), with the remainder including phosphotidylglycerol (~8-10%), phosphatidylethonanolamine (~5%), phosphatidylinositol (~3%), with sphingomyelin and phosphatidylserine also providing minor contributions. The analysis of these lipid fractions has predominantly involved the use of HPLC techniques (Creuwels et al., 1997; Goerke, 1998; Kahn et al., 1995). These lipids account for the main surface active properties of surfactant, DPPC is considered the chief tensoactive component responsible for lowering surface tension (Perez-Gil and Keough, 1998).

Proir to its secretion from type II alveolar cells surfactant is packaged and assembled into densely packed bilayers by lamellar bodies located within these cells. Following secretion, surfactant must cross the aqueous lining fluid surrounding cells, during which time it assumes a structure known as tubular myelin and finally, in order to transfer into the interface, where it must adsorb rapidly forming a monolayer film, it is compressed to facilitate its tensoactive properties (Sanders et al., 1980; Perez-Gil and Keough, 1998; Goerke; 1998). *In vitro* studies have suggested the continuous removal of subphase surfactant from the interface (Gross et al., 1988; Putman et al., 1996), either by phagocytosis by alveolar macrophages or recycling by type II cells (Wright and Clements, 1987).

2.6.4.1: Surfactant Proteins

It is important to note that despite surfactant associated proteins (A, B, C and D) providing only a modest percentage contribution to surfactant (8-10%), they impart critical dynamic properties to surfactant, without which its full functionality could not be achieved (Perez-Gil and Keough, 1998). Surfactant protein A (SP-A), is the predominant form, representing approximately 5% of surfactant. It was the first of the surfactant proteins identified and is a hydrophilic 26-38kDa mannose binding glycoprotein member of the collectin family (King et al., 1973; White et al., 1985; Weaver and Whitsett, 1991), with a high affinity for DPPC over other lipid components. Secreted in lamellar bodies of type II alveolar cells, it has an essential role in the formation of tubular myelin structures due to its ability to aggregate lipid vesicles in a calcium dependent manner, promoting movement of materials to surface films (Veldhuizen et al., 1996; Perez-Gil and Keough, 1998). It is also believed to be involved in the interfacial properties of surfactant, though the precise contribution of SP-A to the tensoactive properties of surfactant have yet to be fully clarified (Perez-Gil, 2008). In addition to its role in the modulation of phospholipid uptake and secretion by type II cells, it has also been implemented in immunological defense through the activation and chemotactic stimulation of alveolar macrophages, as well as in the binding and clearance of microorganisms (Kalina et al., 1995; Van Iwaarden et al., 1992; Van Iwaarden et al., 1994; Creuwels et al., 1997). Whilst surfactant protein A is predominately found within the distal airways it has also been identified in lavages from the proximal conducting airways (Kuroki and Akino, 1991; Casals et al., 1993; Khoor et al., 1993).

The 43Kda surfactant protein D (SP-D), a hydrophilic member of the collectin family of proteins, also plays a role in host defence, binding to both bacteria and alveolar macrophages

(Kuan et al., 1992; Lim et al., 1994). This protein only accounts for ~0.5% of surfactant; with only 10% associated with surfactant phosphilipids, binding to phosphatidylinositol in a calcium dependent manner (Serrano, 2006; Persson, 1989; Persson, 1992; Ogasawara, 1992). Similiar to SP-A, SP-D contains a collagenous region and C-type lectin domain providing them the structural characteristics necessary to bind numerous ligands (inhaled particles and pathogens) within the alveolar RTLF permitting their function as part of the innate immune system (Serrano and Perez-Gil, 2006; Crouch and Wright, 2001).

The hydrophobic anionic surfactant proteins B and C, with molecular weights 8.7kDa and 4.2kDa respectively, contribute approximately 1-1.5% to surfactant. They are both secreted by type II pneumocytes and are implicated in independently promoting the interfacial adsorption of surfactant lipids and stabilizing the films formed, vital for the full functionality of surfactant (Wang et al., 1996; Perez-Gil et al., 1992; Weaver and Conkright, 2001). It has been reported that only surfactant protein C can really be considered a specific surfactant associated protein, being found uniquely present within the alveolar compartment (Serrano and Perez-Gil, 2006).

Conflicting results of the behaviour of surfactant proteins have been reported in asthmatics. Increased expression of surfactant proteins has been observed in allergic asthma (Magi et al., 2006; Noel-Goeris et al., 2002; Lenz et al., 1993; McCormack et al., 1991; Cheng et al., 2000), whilst van de Graaf et al (1992) reported a decrease in SP-A and Wright et al (2000) observed no apparent changes in SP-A concentration in asthmatic RTLFs. In IPF patients lower concentrations of surfactant proteins have been reported, possibly related to decreased synthesis from damaged alveolar type II cells (Magi et al., 2006; Noel-Goeris et al., 2002; Lenz et al., 1993; McCormack et al., 1991). As with CC16, the circulating plasma concentrations of SP-A, SP-B and SP-D have been employed as retrograde biomarkers of air-blood barrier dysfunction, and have been shown to be elevated in several lung disorders (Hermans et al., 1999; Hermans et al., 1998; Kuroki et al., 1993; Doyle et al., 1997).

3: The evaluation of inhaled particles in vitro

3.1: Dissolution, solubility and bioavailability testing of inhaled particulates

Only a small percentage of inhaled materials are deposited within the respiratory system, with a proportion exhaled immediately and others cleared through mechanical processes. Furthermore, the lung contains different location specific clearance mechanisms, the mucociliary escalator of the upper airways to alveolar macrophage clearance in the distal lung. Particle elimination by macrophages is believed to be slow within the human airways (Snipes et

al., 1989). Those inhaled particles/materials that evade these defenses accumulate, degrade or undergo dissolution within the RTLF (Borm et al., 2006). The deposition of inhaled particles and drugs within the RTLFs is therefore influenced by a variety of factors: deposition rate, clearance, retention, translocation and dissolution within this compartment. Thus the 'retained dose' may be quite different to the initial inhaled dose into the lung and this is greatly influenced by its physical properties of the inhaled material itself (Oberdorster et al., 1994; Sdraulig et al., 2008). The regional deposition of inhaled materials within the respiratory tract is also dependent on its aerodynamic diameter. For example, particulate materials deposited within the distal airways encounter large surface-to-volume ratios, in which even effectively insoluble particles can be cleared by the process of dissolution (Lippmann et al., 1980). Size, shape, composition and other physiochemical characteristics help determine the level of interaction between inhaled materials with the RTLF and underlying airway epithelial cells. The precise nature of these interactions remains somewhat undefined and there is therefore the need for the development of physiologically relevant *in vitro* models that permit these interactions to be examined. The development of simulated lung lining fluids to model these initial interactions *in vitro* has therefore been identified as a critical requirement (Taunton et al., 2010).

In vitro dissolution studies investigate the process by which a solid enters into a solvent, yielding a solution. The kinetics of this process are dependent on the affinity of the interaction between solutes and the solvent in question, including both physiochemical particle properties and the dissolution media (or solvent) that mediate this process. Dissolution profiles (a cumulative description of dissolved drug over time) and parameters which provide a summary of the process (the dissolution rate constant or dissolution rate coefficient) are determined to deliver predictive estimates of this process *in vivo* (Aulton, 2007). Dissolution studies are used as part of the characterization of inhaled materials, determining the rate of dispersion and the retention time in the body, major determinants of bioavailability (and therapeutic potential in the case of pharmaceutical compounds). The process of drug dissolution is dynamic and highly influenced by the properties of the solvent used, from pH, ionic strength and concentration (Borm et al., 2006). As this determines the dose of an inhaled material that can be absorbed into the systemic blood circulation, it is often considered the critical step in determining the fate of drugs. 'Simulated lung lining fluids' have been used in investigations as a proxy for the RTLF surrounding the respiratory tract cells, with this the primary dissolution environment of inhaled particulate materials. The use of such simulated lung fluids to assess the fraction of inhaled material made soluble and thus available for absorption has been employed in the assessment of a variety of inhaled materials. With dissolution described as an important element for the

characterization of inhaled materials, the use of representative dissolution media is an important part of this approach (Takaya et al., 2006).

From a pharmaceutical perspective, there is a real need for the development of methods that accurately assess inhaled drug solubility and dissolution *in vitro*, since the proportion of inhaled drug that undergo the process of dissolution determines its therapeutic effect (Wiedmann et al., 2000). With *in vitro* testing providing crucial information at several stages of the drug development process; to the formulation scientist in the choice of appropriate formulation excipient; to the clinical scientist in helping determine *in vitro in vivo correlation* and to the regulatory scientist to ensure the product meets appropriate requirements. If dissolution testing is not performed under relevant and meaningful conditions, results from such studies will be invalid, increasing both the time and cost of product development (Dressman et al., 1998). Pharmacopoeias describe the official *in vitro* dissolution testing methods for conventional solid and semi solid drug delivery methods, specifying factors from the apparatus, solvent and volume used, since dissolution is an important predictor of the behaviour and bioavailiability of drugs *in vivo*. However no accepted dissolution method is currently available for inhaled medicines (Agu and Ugwoke, 2011). As has been described by Forbes et al (2010) in order for this to be achieved the RTLFs must be fully characterized prior to the development of biological relevant simulant fluids and to establish appropriate modeling parameters.

3.2: Composition and design of simulated lung fluids

As the inclusion of complex biomolecules in simulant RTLFs provides a greater number of potential particle interactions, the majority of particle behaviour studies have limited the complexity of their simulant models to reflect only the electrolyte composition of this compartment. The complexity and variability in composition of lung lining fluids has also been used as justification for the use of simple *in vitro* fluids in these studies (Midander et al., 2007). Gambles solution, often referred to as simulated epithelial lung fluid (sELF) has been routinely employed for over 30 years as a simulant lung fluid. Originally this solvent comprised solely of inorganic salts, chlorides, carbonates, various phosphates, citrate and acetate, kept at 37^{o}C, with a 5% CO_2-air mixture bubbled through it (see **Table 1.4**). Whilst Gambles fluid has been used most often to mimic lung lining fluid in the study of inhaled particle dissolution,it is considered an acceptable simulant. Various different modifications/adaptations are often applied (see **Table 1.5**), though these have not resulted in significant differences in the solubility data obtained (de Meringo et al., 1994). Additionally, fluid simulating the acidic (pH 4.5-5) lysozymal

environment following particle ingestion by alveolar macrophages has also been used in similar investigations (Sebastien et al., 1990; Thelohan et al., 1993; Herting et al., 2006).

Studies by Midander,et al. (2007) compared simpler models, including PBS to both Gambles solution and simulated lysosymal fluids and demonstrated clear differences between the magnitude and kinetics of particle dissolution. A more representative simulant model based on Hatch's (1992) description of RTLF composition has also been used to evaluate particle solubility (Berlinger et al., 2008). The main difference in these simulant models is the inclusion of various physiologically relevant proteins and enzymes. Investigations by Harrington et al. (2012) studying the effects of Survanta on pyrite oxidative dissolution found marked effect. Other groups have considered the addition of RTLF antioxidants to create more realistic simulant models. Charrier and Anastasio (2010) demonstrated the significant effect the inclusion of ascorbate, citrate, glutathione and uric acid at physiological concentrations, on metal catalysed hydroxyl radical generation.

However these approaches do not realistically mimic the complexity of *in vivo* RTLFS and whilst a simulant model should be relatively simple it should also aim to account for the major constituents present in the lung lining fluids in order to provide more accurate interpretations of particle behaviour from *in vitro* testing systems. The extent to which simulated lung fluids and *in vitro* testing systems are able to model the epithelial lining fluids of the airways would perhaps be best evaluated by *in vitro in vivo* correlations. Taunton et al (2010) concluded that the limited knowledge on the aqueous composition of RTLFs and their replenishment rates, limit our understanding of the fate of inhaled drugs. However this is not wholly the case, with a great wealth of information available regarding the composition of human RTLFs it is therefore feasible to create more detailed and realistic simulant models to allow for the realistic *in vitro* testing of particles in the airways.

The influence of biorelevant *in vitro* simulants, were explored in investigations by Berlinger et al (2008) into the dissolution of welding fume particulates. In this study the authors employed both Gambles and Hatch's solution (with the addition of defined protein and low molecular weight components – see **Table 5.1**) to study the *in vitro* behavioural characteristics of welding fumes, concluding that the latter was the most appropriate choice as an in vitro dissolution media, producing the most biorelevant results. From the pharmaceutical perspective *in vitro* tissue culture models integrating inhaled particle deposition alongside particle dissolution in the sRTLFs (Simulated Respiratory Tract Lining Fluid) have attempted to mimic *in vivo* interactions at the lung surface following drug inhalation. *In vitro* dissolution studies of pharmaceutical compounds have utilised a sRTLF modified by the addition of DPPC (0.02%

w/v), based on the contention that surfactant phospholipids components of surfactant would enhance wettability, preventing the aggregation of hydrophobic drugs, resulting in an increased rate of dissolution (Sinswat et al., 2008; Agu and Ugwoke, 2011). Davies and Feddah (2003) investigated the effects of increasing DPPC concentrations (0.01, 0.02 and 0.05%) in simulant models and found increased solubility of the glucocorticoids under investigation with increasing lipid concentration. The results observed *in vitro* for the glucorticoid drug flutacisone propionate, correlated with data obtained in *in vivo* clinical studies (Davies and Feddah, 2003; Esmailpour et al., 1997). Wiedmann et al (2000) focused on the use of an artificial surfactant (Survanta) in their investigations into drug solubilization, observing that the addition of this commercial bovine lung surfactant increased glutocorticoid drug solubilization. These such examples from the literature further demonstrate the importance of using biorelevant simulant fluids with *in vitro* studies investigating inhaled particle behaviour, for the purposes of understanding inhaled drug and xenobiotic interaction at the surface of the human lung.

Table 1.4: *The composition of RTLFs previously employed in in vitro studies.*

	Simulated RTLF	**Simulated alveolar RTLF**
Gamble's solution	Concentration (g/L)	Concentration (g/L)
$MgCl_2$	0.095[1], 0.203[2], 0.212[3]	0.05[4,5]
NaCl	6.019[1,2], 6.415[3]	3.21[4,5]
$NaHCO_3$	2.604[1,2], 2.703[3]	
NaH_2PO_4	0.126[1], 0.358[2],0.148[3]	0.071[4,5]
Na_2SO_4	0.063[1], 0.071[2], 0.079[3]	0.039[4]
Na_3 citrate	0.097[1,2], 0.153[3]	0.077[4,5]
$CaCl_2$	0.368[1,2], 0.255[3]	0.128[4,5]
Glycine		0.059[4,5]
KCl	0.298[1,2]	
Na_2 tartrate		0.09[4,5]
Na lactate		0.085[4,5]
Na pyruvate		0.086[4,5]
Citric Acid		20.8[4,5]
pH	7.4[1,2],7.6[3]	4.5[4,5]

References: [1]Midander et al, 2007; [2]Sdraulig et al, 2008; [3]Takaya et al, 2006; [4]Herting et al, 2006; [5]Midander et al, 2006.

3.3: Work plan

The three major aims of my thesis are decribed in **Section 1.1.** These are addressed in the proceeding four experimental chapters (**3**, **4**, **5** and **6**). **Chapters 3-4** present a detailed assessment of RTLF composition in healthy adults and mild asthmatics (**Chapter 3**), in aged healthy populations (**Chapter 4**) and in patients with COPD, including ex- and current smokers (**Chapter 5**). The data within these chapters represent the most up to date summary of RTLF composition in these conditions. In addition, data on the proteome of the bronchial RTLFs are presented for the first time. Based on this information I have designed a base model of human RTLFs, which can be modified to reflect regional and disease specific compositional profiles. In the final chapter, I present data characterizing particle behavior within this simulant model and assessing its biocompatibility with commonly used cell lines.

Table 1.5: *Various simulated RTLF variants described in the literature*

sELF Variant	Material investigated	Author
Gambles solution	Welding fumes	Berlinger et al., 2008; Ansoborlo et al., 1990; Midlander et al., 2007; Sdraulig et al., 2008
Gambles + 0.02% DPPC	Micronised hydrocortisone gelatin capsule dissolution	Son and McConville, 2009
Gambles + 0.02% DPPC	Amorphous or crystalline nanoparticles of tacrolimus	Sinswat et al., 2008
Gambles + 0.01, 0.02 and 0.05% DPPC	Various glucocorticoids	Davies and Feddah, 2003
Gambles - pH3 and pH9	Various glucocorticoids	Davies and Feddah, 2003
PBS + 100uM urate, 200uM ascorbate, 100uM reduced glutathione, 300uM citrate	Mixed Transition metals	Charrier and Anastasio, 2010
Gambles + aluminium (320uM), K+ (0.004M)	Mineral particles	Taunton et al., 2010
Gambles - proteins	Rare earth oxide dissolution rates	Takaya et al., 2006
PBS + Survanta	Cationic drugs e.g. Amitriptylline, Imipramine	Liao and Wiedmann, 2003
Hatches solution (glucose, DPPC, alpha tocopherol, uric acid, serum albumin, lysosyme, apo-transferrin, ascorbate, glutathione)	Welding fumes (manual metal arc, metal inert gas and tungsten inert gas)	Berlinger et al., 2008

Chapter 2

General Materials and Methods

2.1: Subjects and study design

All subjects were recruited following advertisement at the Umea University campus and in the local newspapers. Informed written consent was obtained from all subjects prior to inclusion into the studies outlined in Chapters 3, 4 and 5. The studies described in this thesis were approved by the local ethics committee at the University Hospital, Umea, Sweden, in accordance with the Declaration of Helsinki.

2.2: Sample Collection

2.2.1: Plasma collection

In all of the clinical studies reported in this thesis peripheral blood was collected into heparinized tubes and centrifuged at 2,000 g for 10 min at 4 ^{o}C. An aliquot of the plasma (450 μL) was treated with 50 μL of 50% metaphosphoric acid (MPA) and centrifuged at 13,000 rpm for 5 minutes (4^{o}C) to remove protein, with the resultant supernatant stored at -80 $^{\circ}$C within 30 minutes of blood collection until required for analysis. This sample was subsequently used for the determination of plasma ascorbate and urate concentrations. Further aliquots of unacidified plasma (~1ml) were frozen and stored at -80 $^{\circ}$C for analysis of other markers (urea). All procedures and sample pre-treatment steps were performed by laboratory personal at Umea University.

2.2.1: Nasal lavage

Nasal lavage samples (**Chapter 3**) were collected using the metered nasal spray method, as previously described (Mudway et al., 1999). Briefly, five 1 ml volumes of 0.9% saline were sprayed into each nostril, with the recovered material pooled and transferred into a sterile plastic receptacle maintained on wet ice. The lavage was self administered by the subject after demonstration of the procedure, with the aspirates collected after each 1-ml instillation to limit the instilled volume and dwell time of the saline in the nose. In total the protocol took approximately 2 minutes per nostril, with a total instilled volume of 10 ml. The recovered

aspirate was filtered through a sterile 100-μm pore nylon filter to remove mucus aggregates before centrifugation at 400g for 15 minutes (4◦C) to isolate the cell free fraction. Nasal lavage samples were then similarly acidified with MPA for ascorbate and urate analysis as described for the plasma samples and the de-proteinated supernatant stored at −80◦C prior to analysis. The pH (5.4) of the saline used for the lavage procedure was slightly acidic, which acts to limit the extent of ascorbate auto-oxidation, during the lavage procedure. As with plasma, further 1ml aliquots of cell free nasal lavage were stored for protein and urea determinations.

2.2.2: Bronchial wash and Broncholaveolar Lavage

Bronchoscopy was performed, following an overnight fast. A flexible video bronchoscope (Olympus BF IT240, Tokyo, Japan) was inserted through the mouth with the subject in the supine position. Pre-medication with atropine (1 mg) was given subcutaneously 30 minutes prior to bronchoscopy to reduce airway mucous secretion, with Lidocaine (5% and 1%) sprayed onto the airways to achieve topical anaesthesia. Bronchial wash (BW) was performed by infusing two aliquots of 20 mL sterile sodium chloride (NaCl), pH 7.3 at 37^{o}C into the lingular or middle lobe, which was gently aspirated after each infusion. These recovered aspirates were kept as separate aliquots on wet ice. Bronchoalveolar lavage (BAL) was performed immediately after these small volume infusions by the instillation and immediate aspiration of 3 consecutive aliquots of 60 mL saline. The recovered aspirates were pooled and placed on wet ice prior to transport to the laboratory for processing. All lavage samples were passed through a nylon filter (pore diameter 100μm) and centrifuged at 400g for 15 minutes at 4˚C. The BW and BAL supernatants for vitamin C and urate determinations were treated as previously outlined for the nasal lavage samples. Samples for GSH and GSSG determination were treated with the metal chelator desferoxamine mesylate and the synthetic antioxidant butylated hydroxytoluene both at 2 mM, 5 ml of each to 490 ml of lavage, prior to storage at -80°. The remaining lavage was untreated, but immediately aliquoted and stored at -80°.

2.3: Total and differential cell counts

BW and BAL fluid cell pellets were suspended in saline at a concentration of 10^6 cells/ml, for total and differential cell counts. Total leukocyte numbers were determined using a Bürker chamber. Cyto-centrifuged specimens were prepared with $5x10^4$ non-epithelial cells per slide using a Cytospin 3® (Shandon Southern Instruments Inc., Sewikly, PA, USA) at 1,000 rpm (96g) for 5 min. Differential cell counts were performed on slides stained with May-Grünwald Giemsa, with 500 cells counted per slide using a light microscope at 100 x magnification and

the proportion of non-epithelial cells including macrophages, neutrophils, eosinophils and lymphocytes was established. Cells were analyzed on slides stained with acid toluidine blue and counterstained with Mayer´s acid haematoxylin, counting a minimum of 12 visual fields at 20x magnification. Mast cells were counted in at least 10 visual fields at a magnification of x160 on slides stained with acid toluidine blue and counter stained with Mayer's acid haematoxylin. Based on the total cell concentration and the differential cell counts, the concentration of each cell type was determined as cell/ml. Cell count data are expressed throughout as absolute cell numbers, to avoid artifacts related to proportional changes in cell populations, e.g. apparent increases in neutrophils due to a fall in lavage macrophages. Thus, absolute total cell counts are vital for the adequate interpretation of differential cell counts, avoiding interlaboratory variations and underestimations, as there is no evidence they are influenced by dilution, variability in total lavage volume or number of aliquots, permitting more accurate comparison across studies.

2.4: Antioxidant and oxidative damage markers determination

2.4.1: Vitamin C and urate analysis

The concentrations of Vitamin C (ascorbate (AA), plus dehydroascorbate (DHA)) and uric acid (UA) were determined simultaneously in NL, BW and BAL samples via reverse phase HPLC with electrochemical detection (Iriyama et al., 1984). After thawing on ice the pre-acidifed deproteinated samples were then lipid extracted by addition of 200µl of ice cold heptane, followed by vortexing for 60 seconds and centrifuging at 13,000 rpm for 5 minutes (4^{o}C) (Behndig et al., 2009). The resultant lower layer was then carefully decanted into amber HPLC vials for analysis. All sample processing was performed on wet ice with care taken to protect the samples from light at all times. A Gilson 234 auto-sampler was used to inject 20µl aliquots of each sample for analysis onto a 5µm C18 column (4.6 x 150mm, Phenomenex) eluted with a 0.2mM K_2HPO_4-H_3PO_4 mobile phase (pH 2.1) containing 0.25mM octanesulphonic acid (pH 2.1) at a flow rate of 1.5 ml/min. An E&EG amperometric electrochemical detector (Jones Chromatography, Hengoed, Wales) was used for detection set at 800mV and a sensitivity of 0.2µA for lavage samples and 0.5 µA for plasma samples. Ascorbate and urate concentrations were determined against appropriate standards. Typical standard curves for both compounds are shown in **Figure 2.1**.

Total vitamin C was measured in all samples by pre-treating 400 µl aliquots of the acidified sample with 50 µl 50 mM Tris(2-carboxylethyl)phosphine (TCEP) in 5% MPA (Molecular Probes, Eugene, Oregon USA) for 15 minutes and then performing the lipid

extraction and HPLC analysis as described above. The DHA concentration was then calculated by subtracting the measured ascorbate concentration from the total vitamin C concentration.

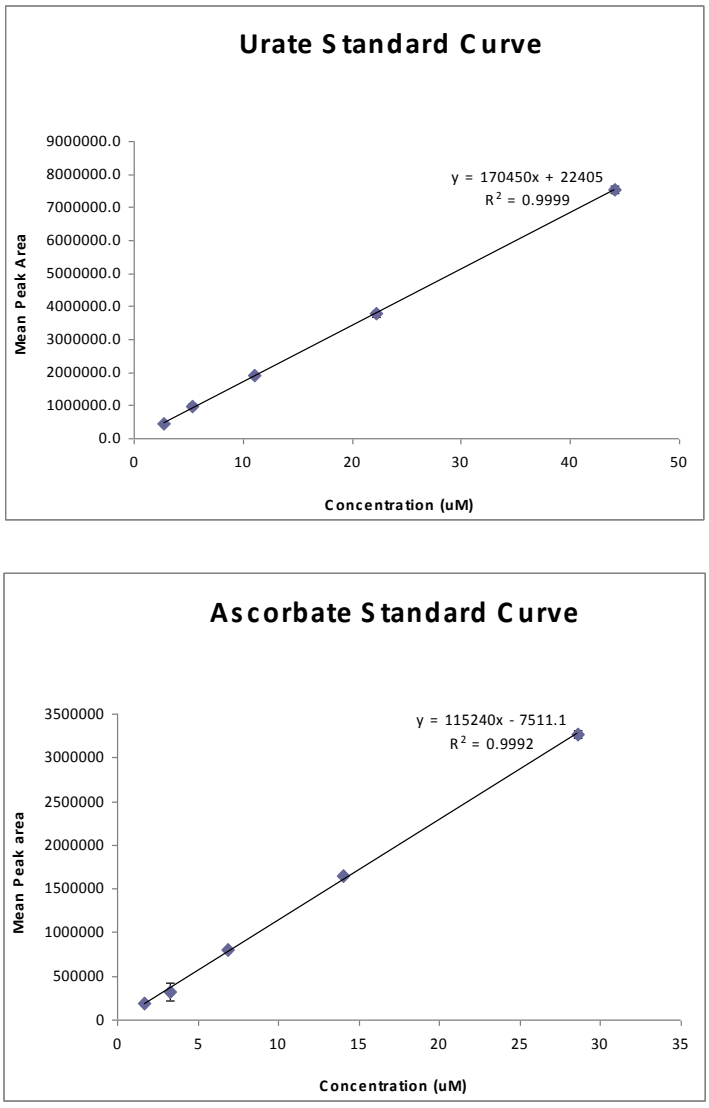

Figure 2.1: *Example ascorbate and urate calibration curves*

2.4.2: Glutathione determinations

Glutathione and glutathione disulfide (GSSG) concentrations were measured spectrophotometrically in NL, BW and BAL samples using the GSSG-reductase recycling assay (Baker et al.,1990), a kinetic assay in which glutathione causes a continuous reduction of 5,5'-dithiobis-(2-nitrobenzoic) acid (DTNB) to TNB. The samples used for this assay were those stored in BHT/DES. Fifty µl aliquots of samples were transferred to a 96 well plate and 100µl of a DTNB-reaction mixture added to give final concentrations of 0.15mM DTNB, 0.2mM

NADPH and 1U glutathione reductase in each well. Immediately following addition of the reaction mixture the plate was analysed on a plate reader (SpectraMAX 190; Molecular Devices) with the rate of change in absorbance at 405 nm followed for two minutes at 30 °C, with absorbance read every 10 seconds with mixing between measurements. Glutathione concentrations in samples were measured by comparison with a set of standards (GSSG: 0-6.6 µM). A typical standard curve for total glutathione is illustrated in Figure 2.2.This assay measures total glutathione (GSx). The concentration of GSSG was determined by combining 2-vinyl pyridine (5 µL) and 130 µL of samples or controls in 2 mL micro-centrifuge tubes. This solution was vortexed for 5 seconds and incubated for 1 hour at room temperature. This reagent forms a conjugate with reduced glutathione (GSH) and prevents it from reacting with the DTNB. Once plated out, glutathione disulfide (GSSG) was measured using the same procedure as outlined for GSx. GSSG produces two molecules of TNB when it reacts with DTNB whereas reduced GSH produces only one, consequently the reduced GSH concentration was calculated as:

Total glutathione – (2 x GSSG)

GSSG concentrations in samples were again measured by comparison with a set of standards (GSSG: 0-3.3 µM) also treated with 2-vinyl pyridine. A typical standard curve for GSSG ran with and without 2-vinyl pyridine treatment is shown in **Figure 2.2**.

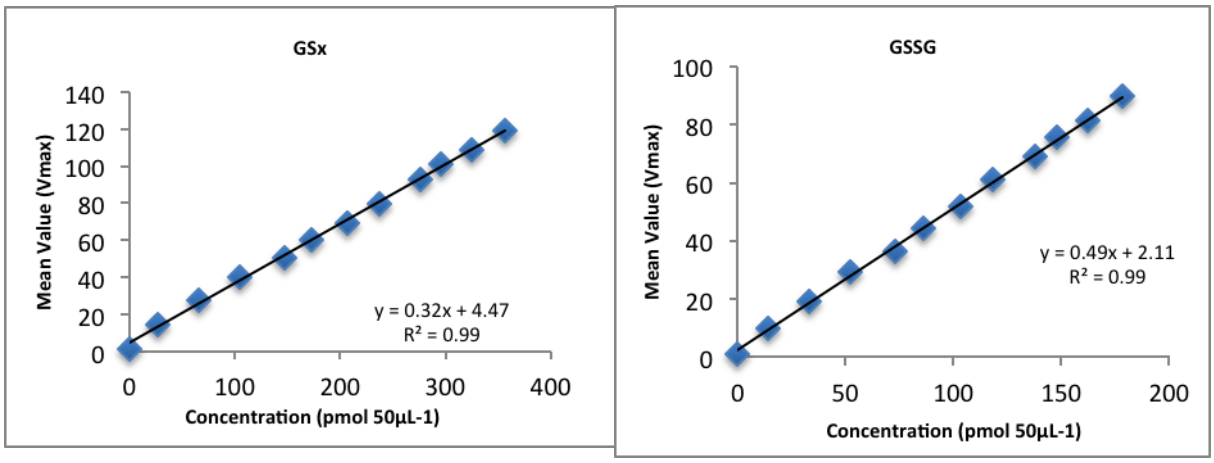

Figure 2.2: *Typical standard curves of total glutathione.* Total glutathione concentrations: 0, 30, 60, 90, 120, 150, 180, 210, 240, 270, 300 and 330 ρmol/50 µl; n = 2) and glutathione disulphide concentrations: 0, 15, 30, 45, 60, 75, 90, 105, 120, 135, 150 and 165 ρmol/50 µl).

2.4.3:Protein carbonyl and 4HNE adduct formation

Oxidized protein concentrations were determined quantitatively using commercially available protein carbonyl and 4-HNE-HIS protein adduct ELISA kits. Protein carbonyl formation was measured spectrophotometrically using OxiSelect protein carbonyl spectrophotometric kit (Cell Biolabs, Inc., USA). The measurement is based on derivitization of protein carbonyl groups with 2,4-dinitrophenylhydrazine (DNPH). BSA standards (mixture of oxidized/reduced BSA) and samples (10 µg/mL) were adsorbed in duplicate onto a 96-well plate for 2 hrs at 37ºC. After DNPH derivatization of the protein carbonyls present, the protein samples were incubated with an anti-DNP antibody and a horseradish peroxidase–conjugated secondary antibody according to the manufacturer's instructions. The protein carbonyl contents were determined by colorimetric analysis at 450 nm using a standard curve prepared from predetermined reduced and oxidized BSA standards. Carbonyl levels are expressed as nmol/mg of protein.

The level of 4-HNE protein adducts was determined using the OxiSelect HNE Adduct ELISA Kit (Cell Biolabs, San Diego, CA, USA). BSA standards (mixture of oxidized/reduced BSA) and samples (10 µg/mL) were adsorbed in duplicate onto a 96-well plate for 2 hrs at 37ºC. 4-HNE adducts were detected at 450 nm after incubation with a mouse monoclonal anti-HNE–His antibody followed by HRP-conjugated secondary anti-mouse antibody. HNE protein adduct concentration was then determined using a standard curve containing known amounts of HNE–BSA (0-10 µg/ml).

2.5: Urea: Lavage dilution factor

RTLF concentrations of each component were determined using the urea correction for lavage dilution. Urea was measured with the QuantiChrom urea assay kit (BioAssay Systems, Hayward) a spectrophotometric assay based on the complexation of urea with a chromogenic reagent, with a linear detection range of 0.00006 mg/mL (1µM) to 1 mg/mL (17mM) urea. For plasma, samples (5 µl) were incubated with 200 µl reagent for 20 minutes and for lavage fluid (200 µl), incubations with 200 µl reagent for 50 minutes, after which the absorbance was measured at at 520 nm. Concentrations were determined with reference to a standard curve (8 standards of 0, 0.0025,0.005,0.01,0.025,0.05,0.1, 0.125 mg/ml urea were used) made up in a supplied buffer.

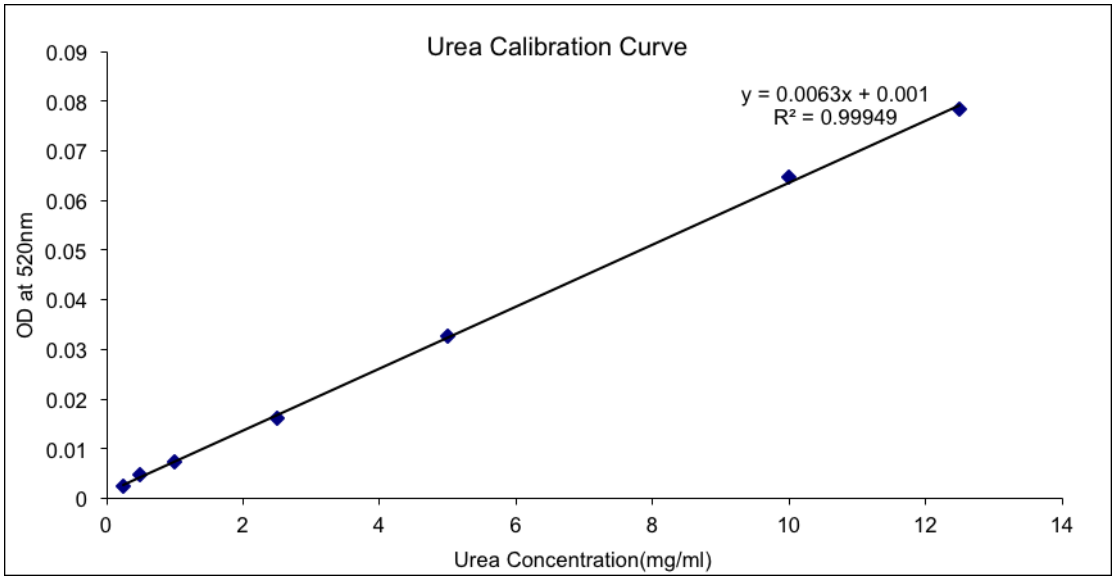

Figure 2.3: *Example of a typical Urea calibration curve.*

The dilution of RTLF fluids obtained from lavage procedures was estimated for a given individual from the ratio between the determined urea concentrations in parallel lavage and plasma samples obtained from the same subject:

Dilution factor= ([urea]plasma/[urea]lavage)

The RTLF concentration of each solute was calculated by multiplying the values determined in the lavage returns by the dilution factors calculated in this manner for each subject. The urea concentrations determined in each sample compartment together with the calculated dilution factor for each patient group included in this thesis are summarised in **Table 2.2a** (nasal lavage and bronchial wash**) and 2.2b** (bronchoalveolar lavage). No significant differences were observed between the groups. The results presented from this point forward will only discuss these urea corrected RTLF concentrations. Both urea concentrations and dilution factors determined are consistent with those reported in the literature for NL and BAL samples (van der Vliet, 1999; Marcy; 1986). Interestingly the dilution factors determined for BW were much greater than those seen with BAL.

Table 2.1: *Dilution factors determined in upper airway (nasal lavage and bronchial wash) lavage samples retrieved across all subject groups investigated in this thesis*. Concentrations are presented as medians and the 25th and 75th percentiles.

	Nasal Lavage		**Bronchial Wash**					
	Healthy Control	***Mild asthmatic***	***Healthy Control***	***Mild asthmatic***	***Healthy Aged Control***	***Healthy Smoker***	***COPD Smoker***	***COPD Ex-Smoker***
	(n=16)	*(n=16)*	*(n=16)*	*(n=16)*	*(n=14)*	*(n=11)*	*(n=14)*	*(n=18)*
Lavage Urea (mg/ml)	0.043 (0.029-0.054)	0.0503 (0.042-0.058)	0.0018 (0.0014-0.0024)	0.0016 (0.0012-0.0023)	0.0021 (0.0017-0.0025)	0.003 (0.0028-0.0032)	0.0017 (0.0013-0.0029)	0.0028 (0.0023-0.0036)
Plasma Urea (mg/ml)	0.705 (0.603-0.779)	0.7256 (0.613-0.831)	0.705 (0.603-0.779)	0.7256 (0.613-0.831)	0.7629 (0.543-0.878)	0.8366 (0.715-0.931)	0.6914 (0.546-0.762)	0.7021 (0.647-0.895)
Dilution Factor	15.5 (11.2-24.5)	11.1 (9.5-13.3)	417.7 (307.6-572.2)	364.4 (275.9-510.3)	348.4 (245.1-427.8)	277.5 (251.9-299.6)	397.1 (158.1-524.9)	269.7 (220.7-335.3)

Table 2.2: *Dilution factors determined in bronchoalveolar lavage samples retrieved across all subject groups investigated in this thesis*. Concentrations are presented as medians and the 25th and 75th percentiles.

	Bronchoalveolar lavage					
	Healthy Control	***Mild asthmatic***	***Healthy Aged Control***	***Healthy Smoker***	***COPD Smoker***	***COPD Ex-Smoker***
	(n=16)	*(n=16)*	*(n=14)*	*(n=11)*	*(n=14)*	*(n=18)*
Lavage Urea (mg/ml)	0.0039 (0.004-0.006)	0.0029 (000.23-0.0046)	0.005 (0.0045-0.0057)	0.0051 (0.0044-0.0077)	0.0059 (0.0054-0.0068)	0.0038 (0.003-0.004)
Plasma Urea (mg/ml)	0.7256 (0.613-0.831)	0.7629 (0.543-0.878)	0.8366 (0.715-0.931)	0.6914 (0.546-0.762)	0.7021 (0.647-0.895)	0.705 (0.603-0.779)
Dilution Factor	181.3 (119.7-239.6)	233.9 (133.4-336.9)	184.6 (145.2-259.8)	136.1 (89.1-160.3)	131.8 (116.0-171.1)	197.1 (155.5-216.9)

2.6: Total protein determination

Total protein was measured by reaction with bicinchoninic acid (BCA) and 4% copper (II) sulphate, against a set of bovine serum albumin (BSA) standards (0-1 mg/mL) (Smith *et al.*, 1985) in NL, BAL and BW samples. This method is based on the reduction of Cu^{2+} by proteins in an alkaline medium, with the highly sensitive and selective colourimetric detection of Cu^{+} using BCA. The chelation of two molecules of BCA with each Cu^{1+} ion forms a purple coloured product that exhibits a strong absorbance at 562 nm, linear with protein concentration. A typical standard curve is illustrated in **Figure 2.4**. It should be noted that all measurements from the various samples fell within the range of the standard curve generated for each biomarker of interest.

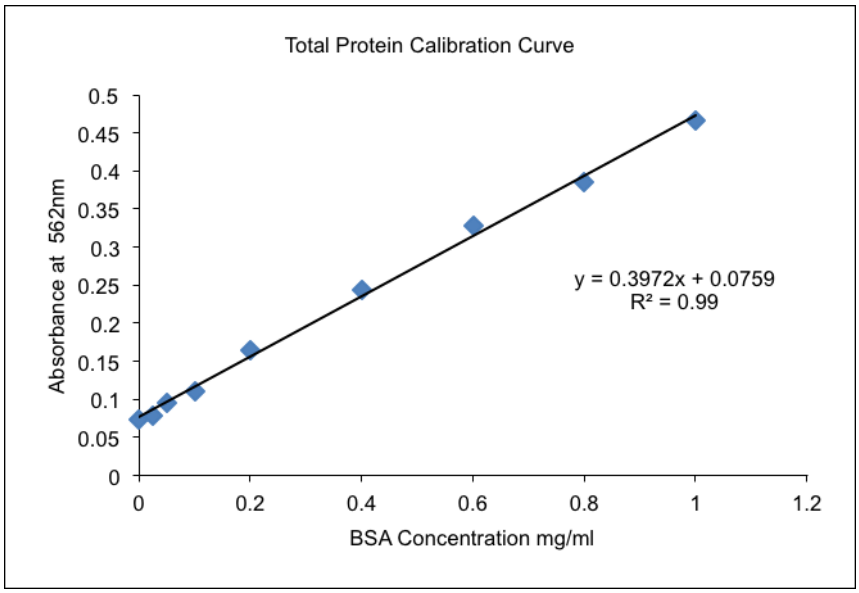

Figure 2.4: *Typical standard curve of total protein concentration with BSA standard concentrations of 0, 0.025, 0.05, 0.1, 0.2, 0.4, 0.6, 0.8 and 1.0 mg/mL.*

2.7: Quantification of individual proteins

2.7.1: Albumin determination

BAL and BW samples were assayed for albumin concentration using the bromocresol green assay (Alpha Diagnostics, San Antonio). The absorbance was then read on a spectrophotometer set at a wavelength of 628 nm. Albumin binds to the dye bromocresol green at pH 4.3 to form a blue-green colored complex, directly proportional to albumin concentration.

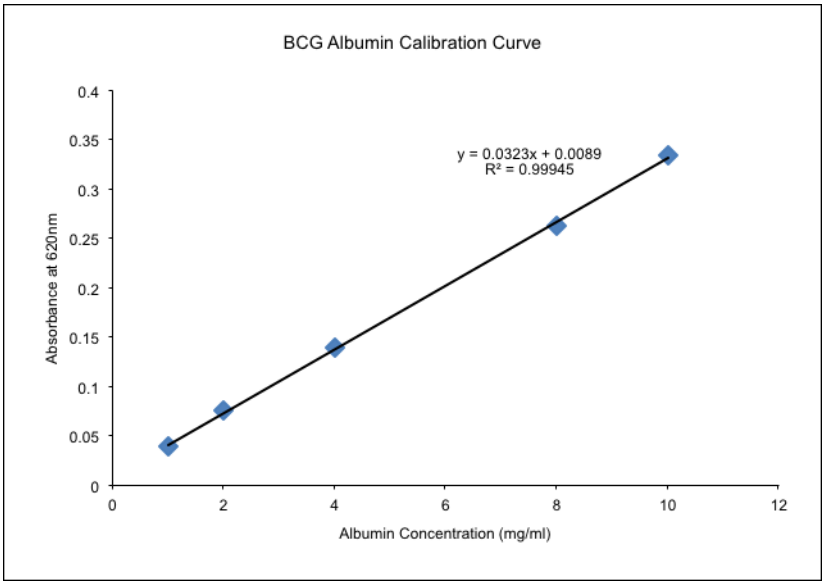

Figure 2.5:. *Example of a typical BCG calibration curve for albumin determination.*

2.7.2: Antibody based quantification

Individual Enzyme-Linked Immunosorbent Assays (ELISAs) were performed according to the manufacturers instructions. The proteins asayed in each sample type and subject groups, together with all other relevant information are presented in **Table 2.2**. Representative standard curves from 4 of the 15 proteins assayed by ELISA (lactoferrin, IgA, IgG and α1-antitrypsin (A1AT)) are presented in **Figure 2.6**.

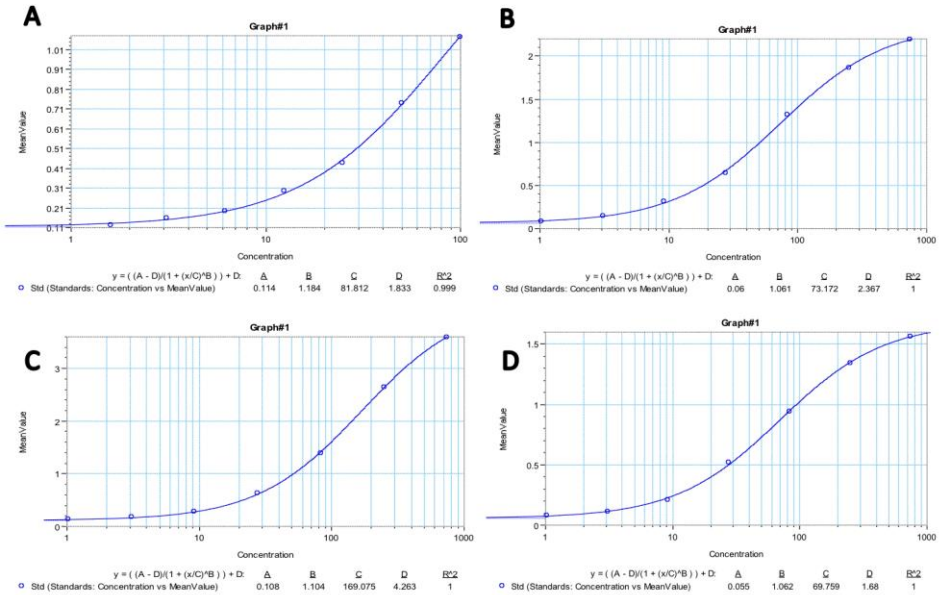

Figure 2.6: *Examples of typical standard curves obtained from ELISAs performed across samples.(A) Lactoferrin, (B) IgA, (C) IgM and (D) A1AT.*

Table 2.3: *List of ELISAs performed across different subject groups and sample types detailing the Vendor, the range of the standard curve and dilution factor used as part of the assay.*

Protein	Samples investigated	Subject groups investigated	Vendor	Standard curve range	Dilution used (fold)
Lysozyme	BAL and BW	HC, MA	Immunodiagnostik	0-30 ng/ml	100
Lactoferrin	BW	HC, MA	Merck	0-100 ng/ml	100
Lactoperoxidase	BW	HC, MA	Gentaur	0-10 ng/ml	50
A1AT	BAL and BW	HC, MA, HAC, HS, CS, CES	Bethyl Laboratories	0-250 ng/ml	100
IgA	BAL and BW	HC, MA, HAC, HS, CS, CES	Bethyl Laboratories	0-250 ng/ml	100
IgG	BAL and BW	HC, MA, HAC, HS, CS, CES	Bethyl Laboratories	0-250 ng/ml	100
IgM	BAL and BW	HC, MA	Bethyl Laboratories	0-250 ng/ml	100
SP-A	BAL and BW	HC, MA, HAC, HS, CS, CES	Biovendor	0-100 ng/ml	100
SP-B	BAL and BW	HC, HAC, HS, CS, CES	CusaBio	0-10 ng/ml	50
Transferrin	BAL and BW	HC, MA, HAC, HS, CS, CES	Alpha Diagnostic	0-200 ng/ml	50
Haptoglobin	BAL and BW	HC, HAC, HS, CS, CES	Immunology Consultants Lab, Inc.	0-200 ng/ml	100
α 2 Macrogloblin	BAL and BW	HC, HAC, HS, CS, CES	Assaypro	0-320 ng/ml	50
Caeruloplasmin	BAL and BW	HC, HAC, HS, CS, CES	Assaypro	0-320 ng/ml	100
Ferritin	BAL and BW	HC, HAC, HS, CS, CES	Biovendor	0-800ng/ml	n/a
CC16	BAL and BW	HC, HAC, HS, CS, CES	Abnova	0-50 ng/ml	200

Key: A1AT - alpha-1-antitrypsin; SP-A - surfactant protein A; SP-B - surfactant protein B; CC16 - Clara Cell secretory protein 16; BAL - bronchoalveolar lavage; BW - bronchial wash; HC - healthy controls; MA - mild asthmatics; HAC - healthy aged controls; HS - healthy aged smokers; CS - COPD current smokers; CES - COPD ex-smokers. (HC *n= 16*, MA *n=16*, HAC *n=14*, HS *n=11*, CS *n=14*, CES *n=18*).

2.8: Proteomic analysis

2.8.1 Desalting and lavage concentration

To overcome the large dilution and high salinity of the airway lavages (150mM NaCl), samples were concentrated using 9K MWCO iCON Pierce concentrators (Thermo Scientific). Twenty ml of each BAL sample was loaded into iCON concentrators prior to centrifugation at 4,000 rpm at 4^{o}C, for 15 minute cycles until complete. This results in a filter retentate, corresponding to lavage components in excess of 9kDa, which was then resuspended in HBSS. The supernatant was retained to study components of the low molecular weight pool. This step was necessary as the high salt concentration of the saline used is incompatible with the downstream 1D PAGE and MS applications. It also helps reduce the great analytical complexity of the RTLF proteome, removing the low molecular weight proteome (> 9kDa). This large dynamic range of molecular weights creates a challenge for both the successful detection and relative quantification of BAL proteins, limiting the number of proteins successfully identified. The concentration protocol also increased the likelihood of detecting relatively low abundance proteins within the lavage samples.

2.8.2: Albumin Depletion

The highly abundant plasma protein albumin was removed from the concentrated BAL samples, using SwellGel Blue Albumin Removal Discs (Pierce) according to the manufacturer's instructions. Each disc has a reported binding capacity of <2mg of albumin. The removal of albumin is necessary to identify proteins within a similar mass range, which would overwise be masked by the high concentration of this RTLF protein, allowing for improved separation in the subsequent 1D-PAGE analysis.

2.8.3: 1D-PAGE

Volumes equivalent to 100 µg protein per sample were lyophilized in a SpeedVac (Eppendorf), resuspended in sample loading buffer (63 mM Tris HCl, 10% glycerol, 2% SDS, 0.0025% bromophenol blue, pH 6.8) in 50mM DTT (Sigma) and denatured at 87^{o}C for 5 minutes prior to SDS-PAGE. Samples were loaded into 4-12% Precast Bis Tris gels (NuPAGE, life technologies) using MOPS SDS running buffer (NuPAGE, life technologies) in an XCell sure lock gel electrophoresis chamber (Life Technologies). HiMark™ Pre-Stained HMW Protein Standards were used as a molecular weight markers. A potential of 50v was applied for 15 minutes, increased to 150v and run for 1 hour. Gels

were removed and bands stained using InstantBlue Coomassie stain (Expedeon) on a rocker for one hour, finally gels were left to rinse with water overnight.

2.8.4: Trypsin digestion and protein extraction

Protein bands were excised from the polyacrylamide gel, reduced with DTT and the cysteine residues carboxyamidated prior to digestion in situ with Trypsin according to a modification of the method of Shevchenko et al. (1996), as described below.

Ten protein bands were excised per sample, and washed sequentially with dH_2O. Excised bands were cut into cubes (ca $1mm^3$), transferred into LoBind eppendorff tubes and centrifuged for 5 minutes on a bench top microcentrifuge. Fifty µl of Acetonitrile was then added to shrink the gel pieces and the samples dried in a Speed-Vac. To reduce the protein, gel pieces were subsequently swollen with 50 µl ul DTT, 0.1M ammonium bicarbonate for 30 minutes at 56 ^oC. Following this, in order to derivatise cysteine resides in the protein, 50 µl iodoacetamide, 0.1M ammonium bicarbonate was added and samples incubated at room temperature for 20 minutes in the dark. All steps were performed on an orbital shaking platform. In order to destain gel pieces, residual liquid was removed and gel pieces washed with 200ul 0.1M ammonium bicarbonate for 15 minutes on an orbital shaker (Benchmark). Residual liquid was then removed and acetonitrile added to shrink gel pieces for ten minutes. Samples were then dried for 30 minutes by Speed-Vac.

Dried gel pieces were then saturated with Trypsin digestion buffer (13 ng/ml Trypsin (Promega), 50mM ammonium bicarbonate) for 45 minutes on ice. Finally 10µl of this digestion buffer was added to samples and they were incubated at 37^oC overnight. In order to ensure optimal protein extraction, digested samples were centrifuged and incubated with acetonitrile at 30 ^oC for 30 minutes. The supernatant then transferred to a new LoBind ependorff tube, whilst 50 µl of 1% formic acid was added to the digested gel pieces and incubated for a further 20 minutes. This supernatant was then transferred to the lobind ependorff tube described above and the process repeated. One-hundred and fifty µl of Acetonitrile was then added to shrink gel pieces and the supernatant again transferred. The supernatants were lyophilized in a SpeedVac and resuspended in 1% formic acid,

2.8.5: Nano LC MS/MS

Following the steps described (in **2:8.3** and **2.8.4**): 1D PAGE separation, band excision, trypsin digestion and protein extraction, samples were analysed with an automated nanoLC MS/MS system. Samples were first separated using an easy nano-LC

1000 system (Thermo) with a 75um x 2cm reverse phase column (C18 3um 100 Å). Injection volumes of 2 µl were used with a flow rate of 300nl/min. The mobile phase consisted of solvents A (water with 0.1% formic acid) and B (ACN with 0.1% formic acid), and a linear gradient of 5% Solvent A to 40% Solvent B in 70 min then to 95% B in 5 min which remained for 15 min prior to column re-equilibration at 5%. This was coupled to an LTQ Orbitrap XL mass spectrometer equipped with a nanoelectrospray ionization source (ThermoFinnigan, San Jose, CA). The mass spectrometer was set up in a data-dependent mode for which every MS scan (**m**/**z** acquisition range from 300-1800) was followed by tandem (Collision induced dissociation (CID)) mass spectra scans (**m**/**z** acquisition range from 350-5000 Da) for the five most intense peaks in any full scan.

2.8.6: Protein identification and database searching

Tandem mass spectra were extracted by Proteome Discoverer version 1.3.0.339. Charge state deconvolution and deisotoping were not performed. All MS/MS samples were analyzed using Mascot (Matrix Science, London, UK; version 1.3.0.339) and X! Tandem (The GPM, thegpm.org; version CYCLONE (2010.12.01.1)). Mascot was set up to search Mascot5_swissprot_Homo sapiens (human) assuming the digestion enzyme trypsin. X! Tandem was set up to search a subset of the HUMAN database also assuming trypsin. Mascot and X! Tandem were searched with a fragment ion mass tolerance of 0.80 Da and a parent ion tolerance of 10.0 PPM. Trypsin/P was set as the protease, allowing for one missed cleavage cysteine, oxidation of methionine, carbamidomethylaltion of cysteine and phosphorylation of serine, threonine and tyrosine were specified in Mascot and X! Tandem as variable modifications.The false discovery rate for automated interpretation of the MS/MS spectra was set between 0.01-0.05 when searched against a decoy database (a comparable database with all of the protein sequences reversed).

Scaffold (version Scaffold_3.6.3, Proteome Software Inc., Portland, OR) was used to validate MS/MS based peptide and protein identifications. Stringent criteria were used for protein identification. Peptide identifications were accepted if they could be established at greater than 90.0% probability as specified by the Peptide Prophet algorithm (Keller et al., 2002). Protein identifications were accepted if they could be established at greater than 99.0% probability and contained at least 2 identified peptides. Protein probabilities were assigned by the Protein Prophet algorithm (Nesvizhskii, et al., 2003). Proteins that

contained similar peptides and could not be differentiated based on MS/MS analysis alone were grouped to satisfy the principles of parsimony.

The abundance of an individual protein was calculated as the sum of the three most intense peptide precursor ions derived from that protein. The normalization of peak areas was achieved by correcting values for total protein concentrations (see **Section 2.6**) determined for individual BAL samples, and further corrected for the lavage dilution using the urea method (**Section 2.5**). The annotation of protein cellular localization and biological function were mapped to Gene Ontology (GO) biological process terms. Further to this, proteins were further excluded if not found present in at least 3 out of 5 subjects. The full proteomic analytical protocol is summarised in **Figure 2.7**.

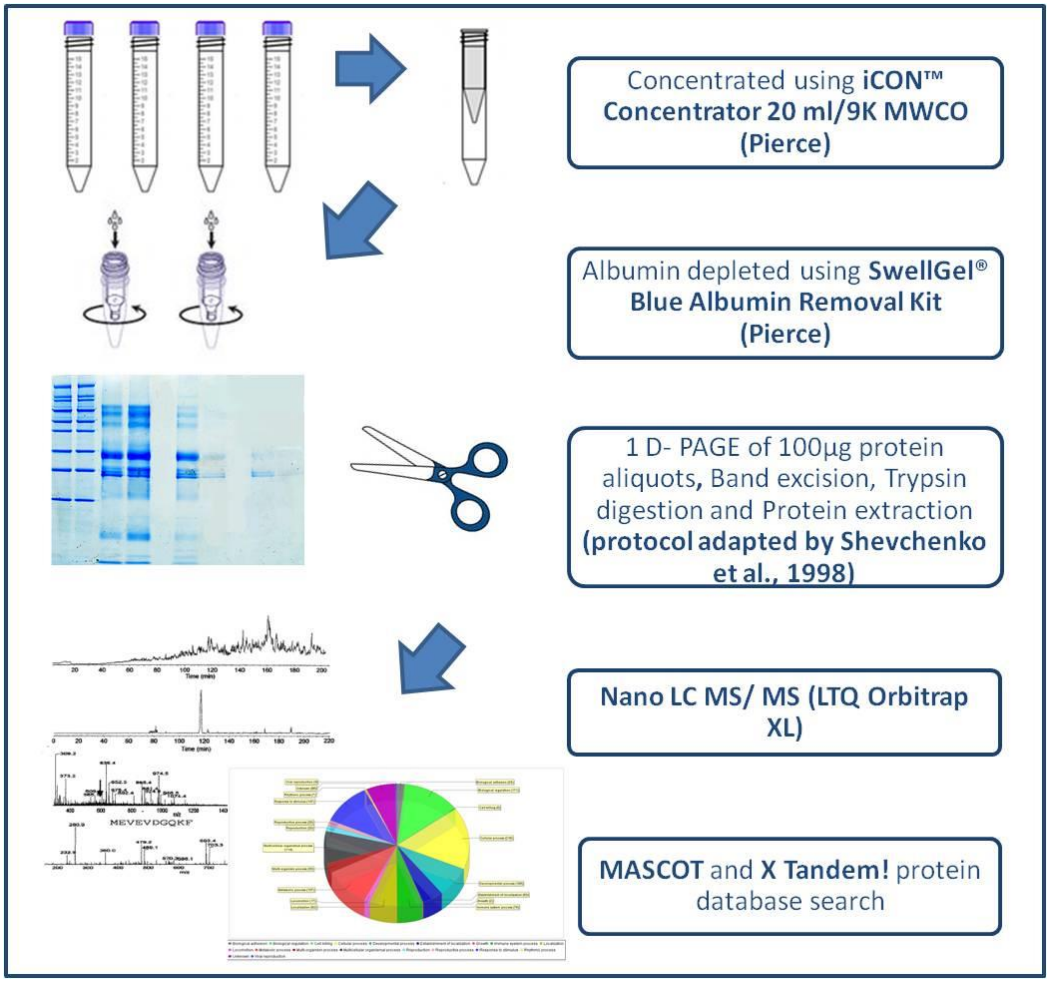

Figure 2.7: *Scheme of the overall proteomics strategy*. This approach permitted for both the idenitification and comparative semi-quantification of proteins using an ion peak based method.

2.9: Assessment of bacterial load within the airways

2.9.1: Limulus Amebocyte Lysate (LAL) assay

In order to quantify the endotoxin content of BW and BAL fluid samples, as a biomarker of Gram-negative bacterial load, the kinetic *Limulus Amebocyte Lysate* (LAL) assay from *Lonza* (Walkersville, MD, USA) was performed according to manufacturer's instructions. Endotoxin catalyzes the activation of the propeptide contained in LAL, within the provided *Kinetic-QCL Reagent*^{R} (*Lonza*). The activated enzyme cleaves a peptide to yield a colored substrate, with the rate of proenzyme activation dependent on endotoxin concentration. Thus the rate of color change is dependent on sample endotoxin concentration. One-hundred µl of Kinetic-QCL^{R} Reagent (*Lonza*) was added to all wells per 96 well plate, and incubated for 1 hour at 37^{o}C in a spectrophotometer (*Spectra Max 190 Molecular Devices*) set for a kinetic assay with readings every 30 seconds at 405 nm. *SoftMax Pro 3.1.2* was used to determine Endotoxin concentrations in samples determined against known endotoxin standards (0.005- 5 EU from 50 EU endotoxin stock: *E. Coli O55:B5 Endotoxin, Lonza*). A representative standard curve is illustrated below (**Figure 2.8**).

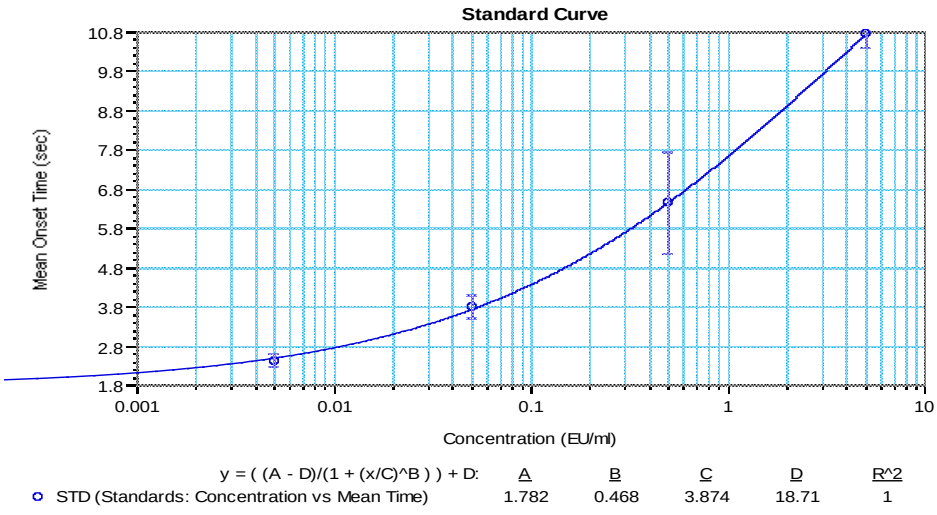

Figure 2.8: *Example of a typical LAL calibration curves*

2.9.1: Assessment of lipoteichoic acid

Lipoteichoic acid (LTA) was employed as a marker of Gram-positive bacterial load. LTA concentrations within BW samples were determined quantitatively using a commercially available ELISA (UscnLife Science Inc., Wuhan, PR China), according to manufacturers

instructions. One hundred ul of standards and samples were added to a precoated 96 well plate with an antibody specific to LTA. Next a biotin-conjugated polyclonal antibody preparation specific for LTA and Avidin conjugated to Horseradish Peroxidase (HRP) was added to each well and incubated for 1 hour. Following this a TMB substrate solution was added to each well, with only those wells containing LTA, biotin-conjugated antibody and enzyme-conjugated Avidin exhibiting a change in color. The enzyme-substrate reaction was terminated by the addition of a sulphuric acid stop solution and measured spectrophotometrically at 450 nm. The concentration of LTA in the samples could then be determined by comparing samples to the standard curve (0-20 ng/ml), see **Figure 2.9**.

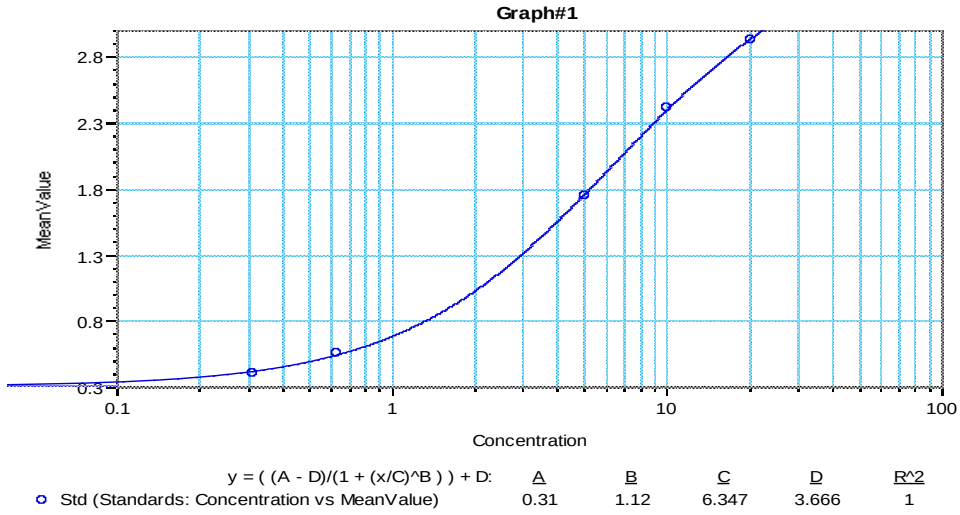

Figure 2.9: *Example of a typical LTA calibration curves.*

2.10: Determination of lavage elemental composition by Inductively Coupled Plasma Mass Spectrometry (ICP-MS)

Trace concentrations of biometals (^{44}Ca, ^{52}Cr, ^{65}Cu, ^{57}Fe, ^{39}K, ^{24}Mg, ^{55}Mn, ^{95}Mo, ^{60}Ni, ^{31}P, ^{48}S, ^{82}Se and ^{66}Zn) in BAL fluid samples were established using inductively coupled plasma mass spectroscopy (ICP-MS) following an acid digestion in a solution prepared with 60% HNO_3 and 30% HCl combined in a 1:3 ratio (in dH_2O). Fifty □L aliquots of lavage were added to 450 µL of this digesting medium in acid washed (2% HNO_3) Teflon vials. Each sample was additionally spiked with Yttrium (to a final concentration of 10 ppb), which was used as an internal standard to correct for any sample volume losses during the digestion process. Acidified samples were vortexed for

two minutes prior to heating in a hot water bath at 90 °C for 90 minutes. The resultant digests were then allowed to cool to room temperature overnight in a fume cupboard prior to centrifugation at 4,000 rpm for 10 minutes. Acid extracted solutions were stored at 4 °C until analysis using an ICP-MS (ELAN DRC, MSF008) housed within the King's College London mass spectrometry facility. The selected isotopes were chosen to avoid known potential isotopic interferences, with the instruments dynamic reaction cell (based on the reaction with ammonia) employed for ^{44}Ca, ^{52}Cr, ^{39}K, ^{24}Mg, ^{55}Mn and ^{48}SO. Digestion blanks (using 150mM NaCl) were also ran at regular intervals throughout the analytical runs with the mean concentrations substracted from those measured in the lavage samples. Trace metal calibrations were conducted using dilutions of a certified multi-elemental standard solution (VI CertiPUR Merck, Lot. No.OC529648). Typical 7 point standard curves are illustrated in **Figure 2.10**.

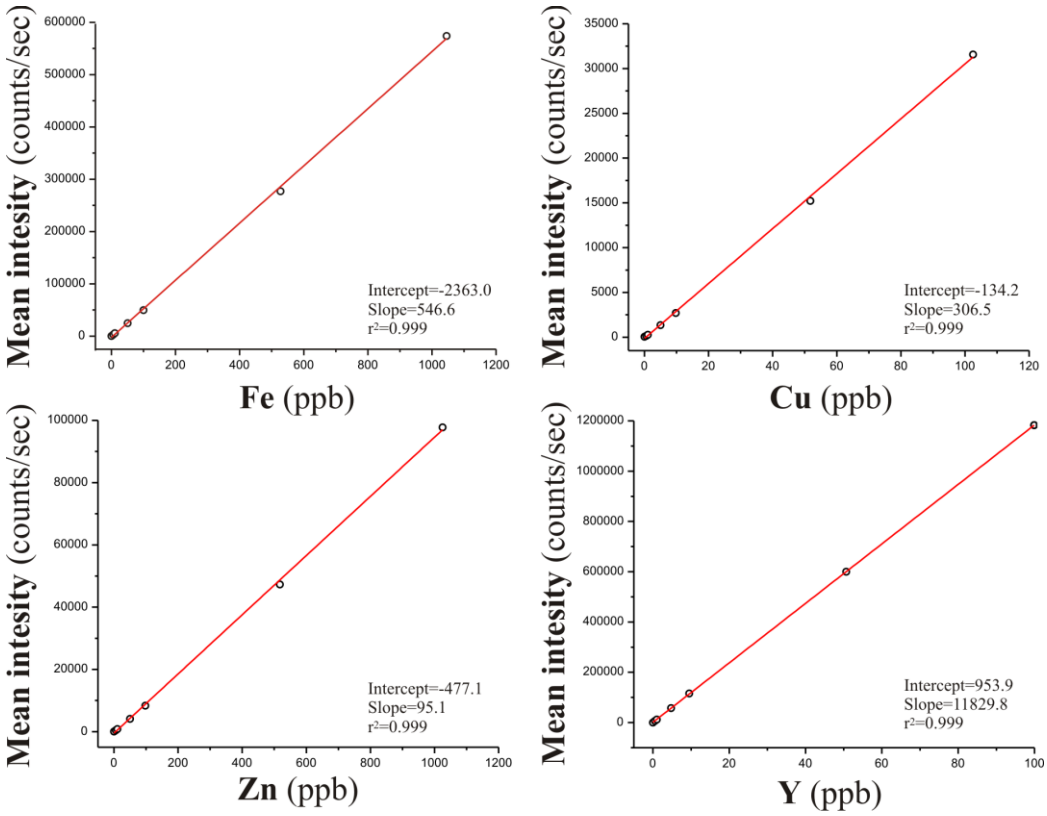

Figure 2.10: *Typical elemental standard curves. Data points represent the mean intensity from triplicate readings*. Y represents the digestion internal standard.

2.11: Statistical analysis

All statistical analysis was performed using SPSS statistical program for Mac version 22 (SPSS Inc., Chicago, IL, USA). Data were normally distributed (Shapiro-Wilks test) and are therefore expressed throughout as medians with the 25^{th} and 75^{th} percentiles (except when stated otherwise). Analysis between subjects was performed using a Kruskal-Wallis test with post-hoc Mann-Whitney U tests with the Bonferroni correction or using the Mann-Whitney U test with significance assumed at the 5% level.

Chapter 3

Characterising the composition of the respiratory tract lining fluids in the young, healthy and mild asthmatics

3.1: Introduction

The RTLFs provide the first physical interface within the airways, surrounding the human respiratory tract from the proximal airways to the distal airspaces, playing an active and vital role as the first line of defence; possessing a robust antioxidant network, metal chelation proteins; as well as proteins with innate immune functions (Hatch, 1992; O'Neil et al., 2011). The composition of this extracellular compartment reflects both macromolecules derived by transduction from the plasma pool, as well as local secretory products arising from the various epithelial and resident inflammatory cells within the airways (reviewed in **Chapter 1**). Hence, any condition that alters the permeability of the air-blood barrier, stimulates secretory cells, or changes the cellular milieu of the airway is likely to have a profound impact on RTLF composition. In this chapter I have therefore investigated the compositional difference between the RTLF in healthy young adults with that observed in patients with mild atopic asthma, the latter group reflecting a major pharmaceutical market for inhaled drugs: anti-inflammatories and bronchodilators. The rationale for this approach is that when testing drug interactions and behaviors within airway lining fluids, it is necessary that any developed simulant is reflective of the underlying condition targeted for treatment.

Asthma is a highly variable disease clinically, with multiple overlapping phenotypes associated with differing underlying mechanisms (Lötvall et al., 2011; Lin et al., 2013; Wenzel, 2013). Despite this heterogeneity, some pathophysiological features are characteristic of this disease including reversible airway obstruction, increased responsiveness of the airway to irritant stimuli, airway remodeling with expansion in mucus secreting cells (serous and goblet cells) smooth muscle in the conducting airways (Bai and Knight, 2005), the presence of allergic inflammation and impaired innate

immunity (Holgate, 2012) and evidence of elevated oxidative stress in the airways (Dozor, 2010).

These characteristic features of asthma are all inter-related, with the presence of episodes of allergic and neutrophilic inflammation associated with oxidative stress; evidenced by increased production of reactive oxygen species (Ranguelova et al., 2012; Murata et al., 2014), depressed antioxidant defenses (Smith et al., 1997; De Raeve et al., 1997; Kelly et al., 1999) and the formation of oxidative damage markers (Aldridge et al., 2002; Schock et al., 2003; Montuschi et al., 2004; Fitzpatrick et al., 2011). In turn the oxidative stress induced in the airway, causes the activation of redox sensitive signaling pathways, triggering either antioxidant adaptations to protect the airway (Roth and Black, 2006; Reynaert et al., 2011), or the upregulation of pro-inflammatory mediators via the transcription factor nuclear factor kappa-light-chain-enhancer of activated B cells (NF□B) (Abdulamir et al., 2009), with balance dependent on the clinical severity of the subjects asthma. In the latter scenario, induction of NF□B further amplifies the cycle of inflammation and oxidative stress, causing tissue injury, resulting in adaptive remodelling of the respiratory epithelium (Manuyakorn et al., 2013) and stimulating mucus hypersecretion (Voynow and Kummarapurugu, 2011).

In addition it is now clear that asthma is not only a disease of the adaptive immune system but is associated with dysregulation of innate immunity (Hansel et al., 2013), characterised by: neutrophilia in severe asthma (Fahy, 2009), impaired phagocytosis (Simpson et al., 2013; Brugha et al., 2014); decreased mucociliary clearence (Daviskas et al., 2005; Fahy and Dickey, 2010); impaired barrier function (Hansel et al., 2013); the presence of alternatively activated macrophages (Byers and Holtzman et al., 2011); and evidence of decreased innate immunity proteins (Balzar et al., 2006). These features of the asthmatic airway reflect the disordered airway microbial communities that have been reported in asthmatics (Hilty et al., 2010), as well their reported increased sensitivity to bacterial (Papadopoulos et al., 2011) and viral infections (Folkerts et al., 1998; Rosenthal et al., 2010).

All of the asthma phenotypes outlined above are likely to have profound effects on the composition of the RTLF, altering the behavior of inhaled materials at the air-lung interface, and their subsequent interaction with the underlying epithelial cells. In this study I therefore performed a detailed compositional analysis of both upper and lower RTLFs, sampled by bronchial wash (BW) and bronchoalveolar lavage (BAL) respectively, in mild atopic asthmatic and non-allergic healthy controls. This analysis consisted of a detailed proteomic analysis (with antibody-based validation of selected

proteins), as well as an assessment of the antioxidant, elemental and lipid profile in the recovered aspirates. While the aim was simply to characterize the dominant RTLF components to permit the design of representative simulants of the upper and lower airways, representing the healthy and asthmatic lung, the data obtained also allowed an investigation into the underlying biology of the asthmatic RTLF, especially in relation to defective innate immunity.

3.2: Methods

3.2.1: Subjects:

Healthy and asthmatic subjects were invited to participate in the study through advertisement. Inclusion criteria were: age 18-40 years, no history of smoking, normal lung function (forced expiratory volume in 1 second (FEV_1) and forced vital capacity (FVC) of at least 80% of predicted and a normal FEV_1/FVC ratio) and absence of concomitant diseases, apart from allergy in the asthmatic group. All asthmatics had a positive history of allergy together with at least one positive skin prick test against a standard panel of common aeroallergens. In the asthmatic group, increased bronchial hyper-responsiveness to methacholine with a provocative concentration causing a 20% fall in FEV1 < 8 mg/mL was required. In total, 16 healthy and 16 age-matched asthmatics were included in the study. All participants were free of chest infection within 6 weeks prior to and during the study. No antioxidant supplementation or anti-inflammatory medication was allowed within 2 weeks prior to or during the study. Asthma severity was classified as intermittent according to GINA guidelines (GINA, 2006) with short-acting inhaled β2-agonists on demand as sole medication. Inhaled or nasal corticosteroids were terminated at least three months prior to the study. Informed consent was obtained from all volunteers after verbal and written information. The study was approved by the local ethical review board at Umeå University, and performed according to the declaration of Helsinki. Subject demographics are presented in **Table 3.1**.

3.2.2: Lung function

Lung function was measured using a Vitalograph spirometer (Vitalograph Ltd. Buckingham, UK). At least three satisfactorily performed and well-co-operated measurements of each variable were carried out, according to recommendations of the American Thoracic Society (1995). Methacholine challenge was carried out using the method described by Juniper *et al*. (1994).

3.2.3: Nasal and Bronchoscopy-based lavages

All airway sampling was performed outside the pollen season in Northern Sweden. Prior to the study visit, subjects fasted from midnight. All lavage procedures were performed in the morning and healthy and asthmatic participants were examined in a randomized order. Prior to pre-medication for the bronchoscopy procedures patients

provided a blood sample (see **Section 2.2.1**) and performed a self-administered nasal lavage; as outlined in **Section 2.2.2**. Pre-medication with 1.0 mg of atropine was given subcutaneously 30 minutes before the bronchoscopy procedure. Subjects with asthma inhaled 0.2 mg of salbutamol. Lidocaine was used for topical anesthesia. A flexible video bronchoscope (Olympus BF-1T160, Tokyo, Japan) was inserted through the mouth with the subject in the supine position. Bronchial wash (BW, 2x20 mL) and bronchoalveolar lavage (BAL, 3x60 mL) were carried out on the contralateral side using sterile sodium chloride. The aspirates were collected into separate siliconised containers and immediately placed on ice, with the three separate BAL aspirates pooled to provide a combined sample. All lavage samples were filtered through nylon (pore diameter 100 □m) and centrifuged at 400xg for 15 min to separate the cell pellet from the supernatant. Cell pellets derived from the BW (first aspirate) and the combined BAL aspirates were re-suspended in phosphate buffered saline (PBS) at a cell concentration of 10^6 cells/mL. Differential cell counts were performed on cytocentrifuge preparations stained with May-Grünwald Giemsa and 400 cells per slide were counted. Information on BW and BAL differential cell counts are presented in **Table 3.2**. Lavage supernatants for vitamin C (900 □L) were treated with 100 uL of 50% metaphosphoric acid prior the centrifugation at 13,000 rpm for 5 minutes (4^oC). The resultant, deproteinated sample was then transferred into a new tube for storage at -80^oC. This acidification protocol has previously been shown to prevent sample auto-oxidation during storage (Lykkesfeldt, 2007). The remaining cell free lavage was stored untreated as 1 mL aliquots. The second BW return was employed for all analysis of soluble mediators, according to previous convention (Blomberg et al., 1999; Mudway et al., 1999; Mudway et al., 2006). For the BAL fluid samples large volume aliquots were also stored (30-50 mL) to provide material for subsequent concentration.

3.2.4: Antioxidant analysis

Vitamin C, ascorbate, dehydroascorbate, total glutathione (GSx), glutathione (GSH), and glutathione disulphide (GSSG) concentrations were determined in nasal lavage, BW and BAL as previously described,(Mudway et al., 2001; Behndig et al., 2009); further details are provided in Chapter 2 (**Section 2.4**). Glutathione, total protein and urea determinations were performed in untreated lavage samples. Lavage and plasma urea concentrations were determined using the QuantiChrom urea assay kit (BioAssay Systems, Hayward). Urea dilution factors for BW and BAL for each subject were

calculated as [urea]plasma/[urea]lavage. Each subject's lavage measurements were multiplied by his/her unique dilution factors to correct for dilution to derive bronchial and alveolar RTLF concentrations. Total protein was determined using the bicinchoninic acid (BCA) method described by Smith et al (1985) in NL, BAL and BW samples (**Section 2.6**). Acidified and deproteinated lavage samples for ascorbate determinations underwent lipid extraction with heptane prior to analysis by reverse phase HPLC, with electrochemical detection (500mV, 100nA). An identical protocol was followed for the determination of vitamin C (ascorbate plus dehydroascorbate), with the exception that the samples underwent a reduction step with Tris (2-carboxylethyl) phosphine (TCEP) (Molecular Probes, Eugene, Oregon USA) (Lykkesfeldt, 2000).The dehydroascorbate concentration was determined by subtracting the measured ascorbate from the vitamin C concentration. Glutathione and glutathione disulphide concentrations were determined using the glutathione disulphide reductase–dithiobisnitrobenzoic acid recycling assay (Baker et al., 1990; Mudway et al., 2006).

Table 3.1: *Demographics and clinical characteristics of the study population.*

Characteristics	**Healthy controls** n = 16	**Asthmatics** n = 16
Male/female	5F / 11M	10F / 6M
Age (years)	25 (2)	26 (6)
Methacholine PC_{20} (mg/mL)	-	1.1 (0.7-4.4)
Skin Prick Test (SPT)	Neg	Pos
Lung Function (mean, SD)		
FEV_1	4.09 (0.77)	3.61 (0.69)
FEV_1 %pred	105 (8)	98 (10)*
FVC	4.81 (1.05)	4.48 (1.22)
FVC %pred	106 (9)	101 (13)

BMI=body mass index; FEV_1=forced expiratory volume in one second; PC_{20}=provocative concentration causing a 20% fall in FEV_1. * p=0.043

3.2.5: Proteomic analysis

Five representative large volume cell free lavage sample from both the healthy and asthmatic groups were selected for concentration using 9K MWCO iCON Pierce concentrators (Thermo Scientific), as described in **Section 2.8.1**. This analysis was restricted to the bronchoalveolar lavage samples, as insufficient volume was available from the BW and nasal lavage procedures. The demographics of these two subgroups were as follows: for the healthy control population (n=5), 27±2 years, 4 females/1 male, with no significant differences noted in basal lung function, or differential cell counts relative to the full group (summarized in **Tables 3.1** and **3.2**). The mild asthmatic group was of a similar age (26±6 years) and gender distribution (4F/1M), again with no significant difference apparent in basal lung function and airway inflammatory status relative to the full group.

Following sample concentration, albumin removal was achieved using SwellGel Blue Albumin Removal Discs (Pierce) prior to sample separation using 1D-page (**Section 2.8.2**, with equal protein loadings), with the subsequent protein bands excised (10 per sample) prior to trypsin digestion (**Section 2.8.4**) and analysis by nanoLC MS/MS (**Section 2.8.5**). A description of the protein identification and the bioinformatic strategies adopted in the analysis of the resulting spectra are provided in **Section 2.8.6**. Comparison of relative protein concentrations within each group and for specific proteins between groups was based on a semi-quantitative analysis using the area of the three major ion peaks as a proxy for protein concentration. Having identified the most abundant proteins, these concentrations were confirmed using commercially available ELISAs (see **Section 2.7.2, Table 2.3**) in BW and BAL fluid samples from all 16 subjects in each group. All final protein concentrations were adjusted for the total protein concentration within the original concentrated lavage sample, as well as for the lavage dilution.

3.2.6: Determination of bacterial lipopolysaccharide and lipoteichoic acid

BAL fluid LPS concentrations were determined using the kinetic Limulus Amebocyte Lysate (LAL) assay from Lonza (Walkersville, MD, USA) according to manufacturer's instructions. Lipoteichoic acid (LTA) concentrations were determined using a commercially available ELISA (UscnLife Science Inc., Wuhan, PR China).

3.2.7: Elemental analysis

Trace concentrations of biometals (^{44}Ca, ^{52}Cr, ^{65}Cu, ^{57}Fe, ^{39}K, ^{24}Mg, ^{55}Mn, ^{95}Mo, ^{60}Ni, ^{31}P, ^{48}S, ^{82}Se and ^{66}Zn) in BAL fluid were established using inductively coupled plasma mass spectroscopy (ELAN DRC, MSF008) following an acid digestion in a solution prepared with 60% HNO_3 and 30% HCl combined in a 1:3 ratio. Full details of the protocol are provided in **Section 2.10**. The instruments dynamic reaction cell was employed for the determination of ^{44}Ca, ^{52}Cr, ^{39}K, ^{24}Mg, ^{55}Mn and ^{48}SO to avoid common isotopic interferences.

3.2.8: Statistics

Antioxidant, inflammatory cell and immunohistochemistry data were not normally distributed and are therefore described as medians with 25th and 75th percentiles. Mann-Whitney U tests were employed to compare healthy and asthmatic data, with Spearman's rank correlation employed for analysis of association. Statistical analyses were performed using the IBM SPSS software, version 20 (SPSS, Armonk, NY, USA). A p-value <0.05 was regarded as significant.

3.3: Results

3.3.1: Baseline characteristics

BW and BAL were performed in all subjects. Median BW and BAL recoveries were 42% and 72%, with no significant differences between the two groups. In the asthmatic group, predicted FEV_1 was significantly lower than in the healthy controls (**Table 3.1**). Consistent with their allergic status, asthmatic subjects had increased eosinophil and mast cell numbers in their BW (**Table 3.2**).

***Table 3.2**: Inflammatory cell counts in bronchial wash (BW) and bronchoalveolar lavage (BAL) fluid, obtained from mild asthmatic and healthy individuals.*

Cell type and location	**Healthy controls** n = 16	**Asthmatics** n = 16	**p value**
Bronchial Wash			
($\times 10^4$ cells·mL^{-1})			
Macrophages	7.2 (5.2–12.3)	5.3 (4.6–9.2)	NS
Neutrophils	0.7 (0.3–1.0)	0.2 (0.1–0.6)	NS (P=0.06)
Lymphocytes	0.3 (0.2–0.7)	0.6 (0.3–0.9)	NS
Eosinophils	0.0 (0.0–0.1)	0.1 (0.0–0.3)	*
Mast cells	0.01 (0.00–0.02)	0.03 (0.01–0.04)	*
Bronchoalveolar Lavage			
($\times 10^4$ cells·mL^{-1})			
Macrophages	13.9 (8.9–17.6)	12.0 (10.6–16.1)	NS
Neutrophils	0.1 (0.0–0.2)	0.1 (0.0–0.2)	NS
Lymphocytes	0.7 (0.5–1.0)	1.1 (0.6–1.4)	NS
Eosinophils	0.0 (0.0–0.1)	0.1 (0.0–0.2)	NS
Mast cells	0.01 (0.00–0.03)	0.02 (0.01–0.04)	NS

[a] = Data given as medians (interquartile range). Statistical comparisons between groups performed using the Mann-Whitney U-test. NS indicates results were not significant, * indicates significance at the 5% level.

3.3.2: Low molecular weight antioxidants

Lavage samples were analysed for the low molecular weight antioxidants ascorbate, urate, and glutathione (total, reduced and glutathione disulphide). Individual lavage correction factors based on the urea method were used to derive undiluted RTLF

concentrations, as illustrated in **Table 3.1**, overall no significant differences were observed between the concentrations of these antioxidants between the two groups, however analyses revealed clear regional differences in antioxidant concentrations between the alveolar, bronchial and nasal lining fluids sampled. For both healthy subjects and mild asthmatics, ascorbate concentrations were significantly greater within the alveolar RTLFs (122.1 (97.7-154.3) μM and 79.4 (62.2-144.6) μM respectively) compared with those of the bronchial and nasal passages ($p<0.001$) – **Table 3.1**. Conversely for urate, significantly ($p<0.001$) higher concentrations were observed in the nasal lining fluids (compared with the concentrations determined in the bronchial, or alveolar RTLFs (**Table 3.1**). Glutathione concentrations appeared greatest in the bronchial conducting airways, in both the healthy and mild asthmatic subjects ($p<0.001$), being approximately four fold greater than alveolar and ten-fold greater than concentrations measured in the nasal compartment.

3.3.3: The RTLF Proteome

1D PAGE and Nano LC MS/MS analysis of the mild asthmatic and healthy BAL RTLF proteomes identified 217 and 199 proteins respectively, 140 of which were common across both groups (**Figure 3.1**). Of the 77 proteins unique to the mild asthmatic proteome, CD151 antigen, a cell adhesion molecule implicated in the proliferation of T cells; Caveolin-1, essential in T-cell receptor mediated T-cell activation and HLA class II histocompatibility antigens, which have a responsibility in the binding of antigens for recognition by CD4 T-cells, in a Th1 specific response were identified. Ferritin, an intracellular iron storage protein and Protein AMBP, a protease inhibitor found which forms a complex with tryptase in mast cells were also found uniquely in the mild asthmatic proteome.

Many of the proteins 'missing' from the asthmatic RTLFs, compared with the healthy controls, were related to antioxidant defense or innate immunity. Glutathione-S-Transferase omega, glutathione peroxidase and thioredoxin like proteins were all absent from the RTLFs. With LPLUNC1, neutrophil gelatinase associated lipocalin and CD59 glycoprotein; all secreted, with roles in innate immune defense also absent in mild asthmatic RTLFs.

Table 3.3: *Dilution factors determined in nasal lavage, bronchial wash and bronchoalveolar samples retrieved. Values are Medians and IQR, n=16 for both healthy controls and mild asthmatics*

	Nasal Lavage		**Bronchial Wash**		**Bronchoalveolar lavage**	
	Healthy Control	*Mild asthmatic*	*Healthy Control*	*Mild asthmatic*	*Healthy Control*	*Mild asthmatic*
Lavage Urea (mg/dl)	4.3 (2.9-5.4)	5.03 (4.2-5.8)	0.18 (0.14-0.24)	0.16 (0.12-0.23)	0.38 (0.3-0.4)	0.39 (0.4-0.6)
Plasma Urea (mg/dl)	70.5 (60.3-77.9)	72.56 (61.3-83.1)	70.5 (60.3-77.9)	72.56 (61.3-83.1)	70.5 (60.3-77.9)	72.56 (61.3-83.1)
Dilution Factor	15.5 (11.2-24.5)	11.1 (9.5-13.3)	417.7 (307.6-572.2)	364.4 (275.9-510.3)	197.1 (155.5-216.89)	181.3 (119.7-239.6)

Table 3.4: *RTLF Antioxidant and total protein concentrations determined from parallel BAL, BW, NL and Plasma samples obtained from both healthy and mild asthmatic subjects. Data are Medians with IQR values, n=16 for both asthmatics and healthy controls*

	Healthy RTLF				**Asthmatic RTLF**			
	Alveolar	*Bronchial*	*Nasal*	*Plasma*	*Alveolar*	*Bronchial*	*Nasal*	*Plasma*
Vitamin C (□M)	141.5 (110.7-198.5)	52.5 (37.6-114.0)	-		96.1 (79.8-155.4)	49.0 (32.4-137.5)	-	
Ascorbic acid □□M)	122.1 (97.7-154.3)	10.5 (0.0-63.8)	55.6 (33.5-68.7)	93.7 (68.5-136.5)	79.4 (62.2-144.6)	6.4 (0.0-79.6)	57.4 (30.2-117.8)	77.1 (59.1-100.4)
Dehydroascorbic acid (□M)	17.2 (11.2-154.3)	40.7 (33.1-55.1)	-		13.1(9.3-24.2)	38.5 (27.0-50.3)	-	
Uric acid (□M)	95.5 (59.0-107.7)	127.9 (97.0-175.3)	291.0 (193.2-351.3)	325.4 (250.9-379.8)	108.9 (85.3-145.6)	112.6 (87.6-201.9)	263.7 (166.5-373.5)	320.5 (258.0-387.4)
GSx (□M)	161.6 (128.0-243.9)	508.0 (350.8-744.8)	22.2 (8.2-40.8)	n/d	176.9 (127.0-225.6)	464.6 (337.0-604.6)	23.0 (0.85-4.6)	n/d
GSH (□M)	137.2 (114.3-184.7)	323.3 (281.4-559.3)	21.1 (8.2-32.1)	n/d	129.1 (104.3-205.3)	348.1 (217.5-430.9)	23.0 (14.6-35.6)	n/d
GSSG (□M)	3.4 (0-25.9)	52.3 (34.1-75.2)	0.87 (0.0-2.8)	n/d	11.6 (6.1-25.4)	45.4 (30.3-86.0)	0.25 (0.0-0.77)	n/d
Total protein (mg/mL)	14.3 (11.8-24.6)	40.4 (28.9-51.4)	n/d	n/d	17.5 (12.4-21.5)	28.0 (24.1-40.8)	n/d	n/d

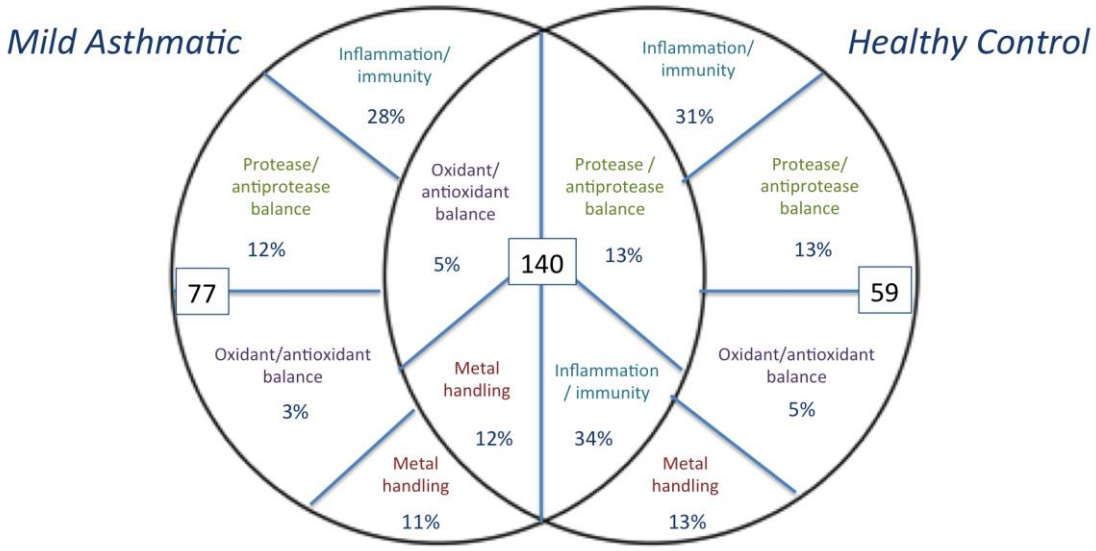

Figure 3.1: *A venn diagram illustrating the proteins shared and specific to mild asthmatic and healthy control subjects*. (Data is based on data derived from five subjects for both mild asthmatics and healthy controls).

Across both groups the identified proteins were predominantly classified, based on their gene ontological definitions as being related to five major categories: immunity and inflammation, metal handling, protease-antiprotease balance, transport and the oxidant-antioxidant balance of the airways. The largest category in both groups were proteins involved in immunity and inflammation, with 62 and 61 proteins identified in the healthy controls and mild asthmatics respectively (**Figure 3.4**). This was followed by proteins related to protease/antiprotease balance (24 and 25 proteins respectively) and metal handling (25 and 23 proteins respectively). Only 9 and 7 proteins were identified that were classified as being involved in oxidant-antioxidant balance within the young and asthmatic RTLFs (see **Appendix A** for the full protein lists classified by ontology).

Additionally the source of each protein was annotated, with the majority of proteins classified as being extracellularly derived (101 and 94 for healthy controls and mild asthmatics respectively), but with the most abundant proteins largely of plasma origin: Serotransferrin, Serum albumin, Ig gamma chains, alpha-1-antrypsin and Haptoglobin, (see **Table 3.4**). Proteins were then ranked by relative abundance, based on the three most abundant ion peaks identified for each protein. **Table.3.4** displays the top fifteen most abundant proteins from both the healthy controls and mild asthmatics, with additional annotation concerning their source of origin, ontological definition and the

relative fold difference between healthy and asthmatic RTLFs. The proteins listed were limited to those present within at least 3 out of 5 subjects investigated in each group. Considering these most abundant proteins, a general decline in expression of the majority of these proteins was observed within the mild asthmatic proteome with the exception of Haptoglobin, which demonstrated an increase (2.9 fold) in the mild asthmatics.

Considering the full protein list a few prominent fold differences were noted between the healthy and asthmatic RTLFs, highlighted in **Tables 3.5** and **3.6**. The immunoglobulin chains (Ig lambda chain V region 4A, Ig lambda chain V-III region LOI, Ig kappa chain C region) were 10.6, 7.4, 5.9 lower, respectively in mild asthmatics. Lysozyme a key secretory protein involved in innate immunity, demonstrated a six fold decrease in asthmatic RTLFs. Whilst relatively few proteins were identified contributing to the oxidant/antioxidant balance, of the 6 proteins identified, Glutathione S-Transferase P and Protein DJ-1 were found 3.6 and 2.3 fold lower in mild asthmatics respectively. Of the proteins with roles in metal handling serotransferrin and the ferroxidase caeruloplasmin were found to have lower expression in the mild asthmatics subjects (2.8 fold and 4.4 fold lower respectively). Interestingly only two proteins, Haptoglobin and Leucine rich alpha 2 glycoprotein were found to be increased in the asthmatic proteome, 3 and 6-fold respectively. Neither has previously been implicated in the pathology of asthma.

3.3.4: Protein quantification

Analyses of urea corrected total protein in BAL, showed no significant differences between groups with values of 14.34 (11.8-24.6) and 17.46 (12.4-21.5) mg/mL in healthy controls and mild asthmatics respectively. Total protein concentrations determined in BW were 40.38 (28.9-51.4) and 27.99 (24.1-40.8) mg/mL for HC and MA groups respectively (no significant differences between the groups), approximately two fold greater than concentrations in alveolar samples ($p<0.001$). However prior to the application of the urea correction for lavage dilution, total protein values measured in BW (0.09 (0.06-0.12) and 0.09 (0.07-0.10) mg/mL) were broadly similar to those of BAL (0.08 (0.06-0.11) and 0.09 (0.07-0.12) mg/mL) in both HC and MA subgroups.

Table 3.5: *The most abundant alveolar proteins identified in healthy and mild asthmatic RTLFs*. The 15 most abundant proteins common to both young and aged subjects identified (out of 140) are listed alongside their source of origin, their ontological classification and their relative fold differences. In all cases the proteins listed were identified in all five of the concentrated BAL fluid samples.

Protein	Source	Ontology	Healthy Control (n=5)	Mild Asthmatic (n=5)	Fold difference (healthy vs asthma)
Serotransferrin	Extracellular, Secreted	Metal Handling and Transport	1.28E+10	4.55E+09	2.8 ↓ with asthma
Serum albumin	Extracellular, Secreted	Metal Handling and Transport	3.97E+09	3.32E+09	1.19 ↓ with asthma
Ig gamma-1 chain C region	Extracellular, Secreted	Immunity and Inflammation	1.23E+10	3.04E+09	4.1 ↓ with asthma
Ig gamma-3 chain C region	Extracellular, Secreted	Immunity and Inflammation	9.36E+09	2.52E+09	3.7 ↓ with asthma
Ig gamma-2 chain C region	Extracellular, Secreted	Immunity and Inflammation	9.10E+09	2.20E+09	4.1 ↓ with asthma
Ig kappa chain C region	Extracellular, Secreted	Immunity and Inflammation	5.90E+09	1.00E+09	5.9 ↓ with asthma
Uncharacterized protein C3orf38	Unknown	Unknown	4.10E+09	2.18E+09	1.9 ↓ with asthma
α-1-antitrypsin	Extracellular, Secreted	Protease/antiprotease	2.69E+09	7.42E+08	3.6 ↓ with asthma
Ig alpha-1 chain C region	Extracellular, Secreted	Immunity and Inflammation	2.81E+09	1.24E+09	2.3 ↓ with asthma
Haptoglobin	Extracellular, Secreted	Immunity and Inflammation	3.82E+08	1.13E+09	3.0↑ with asthma
Ig lambda-2 chain C	Extracellular, Secreted	Immunity and Inflammation	3.07E+09	7.00E+08	4.4 ↓ with asthma
Ig alpha-2 chain C region	Extracellular, Secreted	Immunity and Inflammation	2.05E+09	8.46E+08	2.4 ↓ with asthma
Ig heavy chain V-III region HIL	Extracellular, Secreted	Immunity and Inflammation	1.66E+09	6.93E+08	2.5 ↓ with asthma
Ig heavy chain V-III region VH26	Extracellular, Secreted	Immunity and Inflammation	1.25E+09	5.29E+08	2.4 ↓ with asthma
Lactotransferrin	Extracellular, Secreted	Metal Handling and Transport	1.38E+09	7.34E+08	1.9 ↓ with asthma

Table 3.6: *Alveolar proteins demonstrating the largest relative fold decreases with Asthma*. The proteins of the common 134 identified showing the greatest fold decrease with asthma are listed alongside their source of origin, their ontological classification and their relative fold differences. Data shown is a comparison of the mean of the three most abundant ion peaks of each protein identified, with an arbitrary fold change cut off threshold of 2.5 used. In all cases the proteins listed were identified in all five of the concentrated BAL fluid samples. References are indicated for those proteins identified that have previously been implicated in asthma.

Protein	Source	Ontology	Healthy Control (n=5)	Mild Asthmatic (n=5)	Fold difference (healthy vs asthma)
Rho GDP-dissociation inhibitor 2 [1]	Intracellular	Cell morphology / interaction; signalling	1.36E+09	6.99E+06	194 ↓ with Asthma
Ig lambda chain V-IV region Bau [2,3]	Extracellular	Immunity and Inflammation	4.40E+08	4.15E+07	10.6 ↓ with Asthma
Ig lambda chain V region 4A [2,3]	Extracellular	Immunity and Inflammation	1.06E+08	9.96E+06	10.6 ↓ with Asthma
14-3-3 protein epsilon	Intracellular	Signalling, Apoptosis	9.02E+07	1.49E+07	6.1 ↓ with Asthma
Ig kappa chain C region [2,3]	Extracellular	Immunity and Inflammation	5.90E+09	1.00E+09	5.9 ↓ with Asthma
Lysozyme C	Extracellular	Immunity and Inflammation	2.75E+06	4.75E+05	5.8 ↓ with Asthma
Alpha-1-antichymotrypsin [4]	Extracellular	Protease/antiprotease	1.49E+08	3.86E+07	3.9 ↓ with Asthma
Alpha-1B-glycoprotein	Extracellular	Unknown	1.36E+08	3.46E+07	3.9 ↓ with Asthma
Angiotensinogen	Extracellular	Regulation of Renin-angiotensin-aldosterone system	9.61E+07	1.95E+07	4.9 ↓ with Asthma
Glutathione S-transferase P [5,6,7]	Intracellular	Antioxidant/oxidant balance	3.42E+07	9.57E+06	3.6 ↓ with Asthma
Serpin B3	Intracellular	Protease/antiprotease	3.01E+07	7.74E+06	3.9 ↓ with Asthma
Antithrombin-III [8,9]	Extracellular	Blood coagulation cascade regulation	2.92E+07	7.80E+06	3.8 ↓ with Asthma
Afamin	Extracellular	Vitamin E binding	2.55E+07	7.98E+06	3.2 ↓ with Asthma

References: 1. Jeong et al., 2005, 2. Stockley and Burnett, 1980, 3. Soutar, 1977, 4. Lindmark et al., 1990, 5. Hoskins et al., 2013, 6. Fruth et al., 2011; 7. Schroer, 2010, 8. Gabazza et al., 1999, 9. Kawada et al., 2003

Table 3.7: *Alveolar proteins demonstrating the largest relative fold increases with Asthma.* The proteins of the common 124 identified showing the greatest fold increases with asthma are listed alongside their source of origin, their ontological classification and their relative fold differences. In all cases the proteins listed were identified in all five of the concentrated BAL fluid samples

Protein	**Source**	**Ontology**	**Healthy Control** (n=5)	**Mild Asthmatic** (n=5)	**Fold difference** (healthy vs. asthma)
Leucine-rich alpha-2-glycoprotein	Extracellular	Cell morphology / interaction; signalling	3.79E+06	2.36E+07	6.2 ↑ with Asthma
Haptoglobin	Extracellular and Secreted	Immunity and Inflammation	3.82E+08	1.13E+09	3.0 ↑ with Asthma

The contribution of albumin to the measured total protein content of the healthy and asthmatic alveolar RTLFs were equivalent, 49.19 (36.3-62.6) and 47.4 (36.0-61.3)% respectively (**Figure 3.2**): 8.16 (6.49-9.37) and 7.77 (5.34-10.04) mg/mL (**Figure 3.3A**), the greatest contribution of any individual protein. In the bronchial RTLF, albumin represented a significantly greater ($p<0.001$) proportion of the total protein pool, 54.54 (49.6-85.5) and 71.70 (57.6-90.8)% (**Figure 3.4**) in both healthy volunteers and asthmatics: 24.09 (18.25-30.00) and 22.03 (14.73-30.60) mg/mL (**Figure 3.5A**).

Following albumin the combined immunoglobulin contribution to the total protein pool was the second most dominant, with the total immunoglobulin (G, A and M) contribution to the alveolar RTLF protein pool being 15.7 and 17.9% in the healthy and asthmatic subjects, with IgG being the major contributor (**Figure 3.2**). No significant differences were observed between the two groups (**Figure 3.3B**). In the bronchial samples the combined immunoglobulin contribution to the protein pool was similar, representing 15.3% (healthy) and 13.5% (asthmatic) of total protein (**Figure 3.4**), although IgA was the major immunoglobulin. IgM was the least abundant of the three immunoglobulin classes investigated in all samples, both BAL and BW, with no significant differences observed between HC and MA (**Figure 3.3C** and **3.5C**).

The protease inhibitor α-1 antitrypsin (A1AT) represented the third most abundant protein in the alveolar RTLFs, contributing 6.87 (5.05-16) and 10.44 (7.7-14.0)% to the total protein pool in the healthy and asthmatic subjects (**Figure 3.2**), with absolute concentrations of 0.94 (0.55-2.16) and 1.55 (1.37-21) mg/mL (**Figure 3.3F**). This contribution was significantly lower in the bronchial samples ($P<0.05$), in which A1AT comprised 2.66 (1.19-3.39) (healthy) and 2.40 (0.9-3.8)% (asthmatic) of the measured total protein (**Figure 3.4**), with absolute concentrations of 0.60 (0.38-1.07) and 0.68 (0.26-1.43) mg/mL. No significant differences in A1AT concentration were observed between the two groups in either compartment (**Figure 3.3F** and **3.5G**).

Surfactant protein A, the only of the four surfactant proteins investigated, contributed 5.11 (3.7-8.1) and 3.39 (2.5-4.9)% to the alveolar RTLFs (**Figure 3.2**); 1.00 (0.6-1.3) and 0.64 (0.5-0.8) mg/mL in the healthy and asthmatic subjects respectively (**Figure 3.3H**). A similar contribution was seen to the bronchial protein pool, representing 2.87 (1.6-6.5) and 2.07 (1.3-4.0)% (**Figure 3.4**): 1.30 (0.7-3.1) and 0.99 (0.4-1.6) mg/mL in healthy and asthmatic samples respectively. No significant differences in protein concentration were noted between the two groups (**Figure 3.3H** and **3.5H**).

Transferrin comprised 6.65 (4.4-10.4)% of alveolar lining fluid total protein in the healthy and 8.94 (6.0-11.3) % in the asthmatics (**Figure 3.2**): 1.09(0.6-1.7) and 1.5 (1.2-1.9) mg/mL, respectively, representing the fourth most abundant protein (**Figure 3.3E**). In the bronchial RTLFs transferrin represented 5.26 (3.6-8.1) and 3.06 (2.2-4.4)% of total protein (**Figure 3.4**): 1.91(1.3-3.0) and 1.22 (0.7-1.5) mg/mL, in the healthy and asthmatic subjects respectively, with the measured concentration significantly lower ($P<0.05$) in the asthmatic group (**Figure 3.5E**).

The antimicrobial protein lysozyme comprised a smaller proportion of the total protein content in the alveolar compartment, 0.22 (0.14-0.4) (healthy) and 0.27 (0.15-0.50)% (asthmatic), **Figure 3.2**: 0.03(0.02-0.06) and 0.05 (0.03-0.07) mg/mL, respectively (**Figure 3.3G**). It's contribution to total protein in the bronchial lining fluids was significantly greater ($P<0.001$) in both healthy and asthmatic subjects, 0.74 (0.21-1.53) and 0.35 (0.23-0.52)% (**Figure 3.4**): 0.22 (0.11-0.46) and 0.13 (0.08-0.15) mg/mL, in controls and asthmatics. In addition bronchial RTLF lysozyme concentrations were significantly greater ($P<0.05$) in the healthy subjects compared with the mild asthmatics (**Figure 3.5J**).

Having established the significantly depressed concentrations of two proteins of related to innate airway immunity in the asthmatic bronchial RTLFs: transferrin and lysozyme, two further proteins involved in limiting Fe availability (lactoferrin) and maintaining airway sterility (lactoperoxidase) were also investigated. Neither of these proteins were significantly reduced in the asthmatic bronchial RTLFs, though there was a trend ($P=0.054$) suggestive of lower lactoperoxidase concentrations in the asthmatics: 1.37 (0.58-2.72) versus 0.51 (0.34-1.28) mg/mL (**Figure 3.5I**).

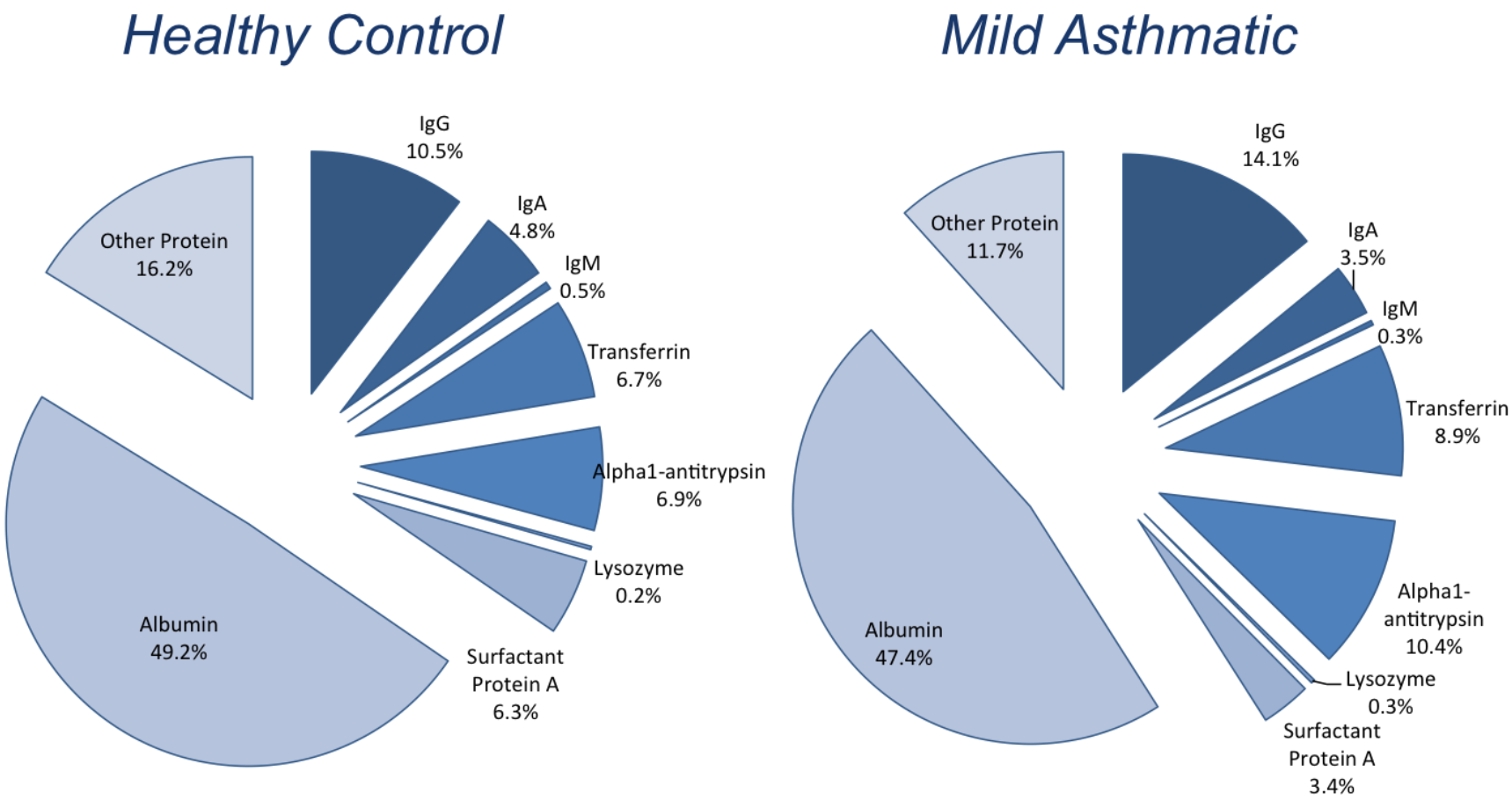

Figure 3.2: *Percentage contributions of individual alveolar protein components relative to total alveolar RTLF protein.* Values are represented as median values. Healthy controls n=16, 25.0±2.6 years, 6M/10F, Mild asthmatics n=16, 26.7±6.2 years, 5M/11F.

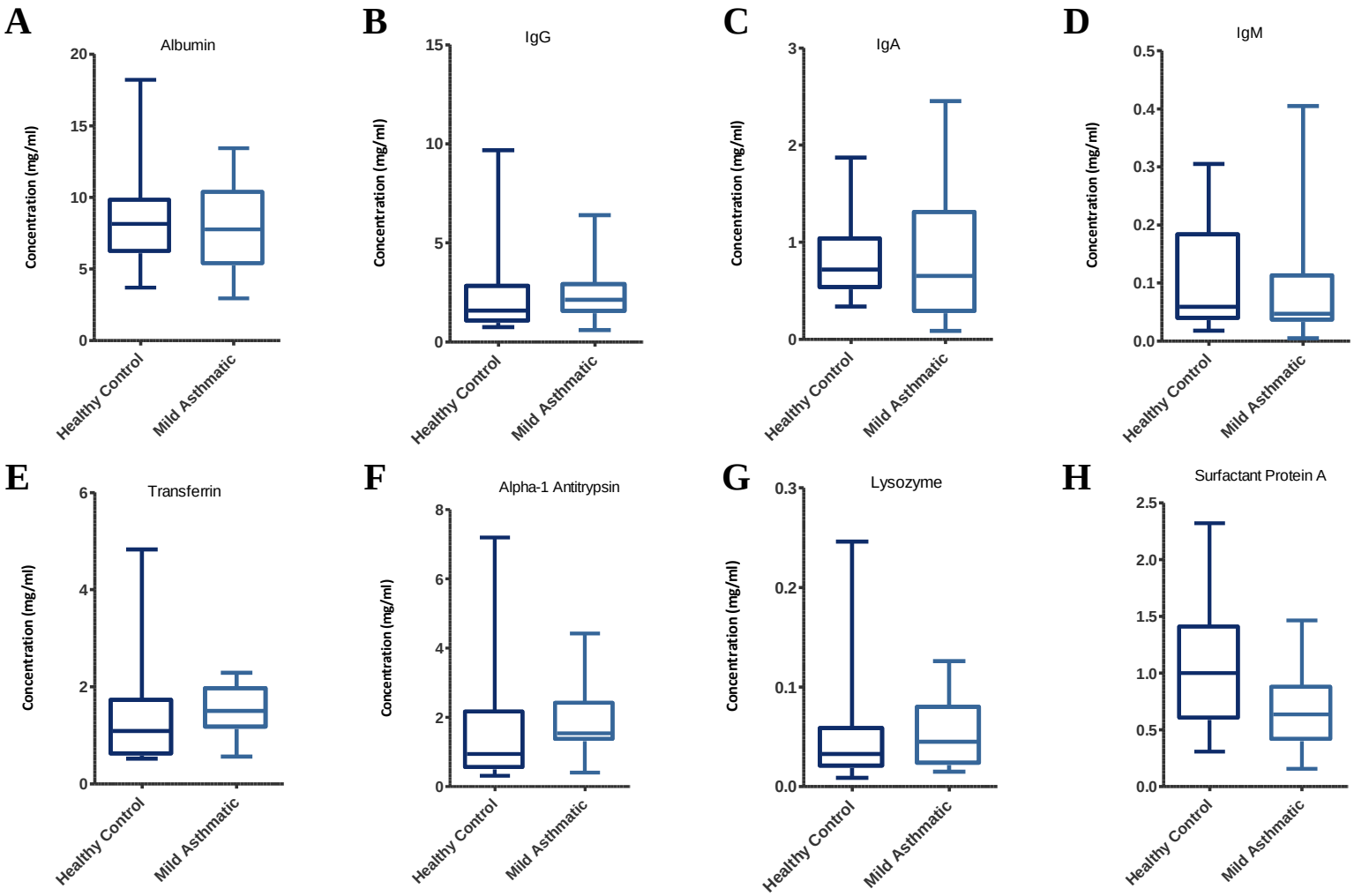

Figure 3.3: *The proteins of the alveolar RTLF in mild asthmatics and healthy controls*. Values Corrected for dilution using the urea method. First row from left to right: Albumin (**A**) , IgA (**B**), IgG (**C**), IgM **(D);** Second row: Transferrin (**E**), A1AT (**F**), Lysozyme (**G**) and Surfactant Protein A (**H).** Healthy controls n=16, 25.0±2.6 years, 6M/10F , Mild asthmatics n=16, 26.7±6.2 years, 5M/11F. * denotes a statistical difference where $p<0.05$.

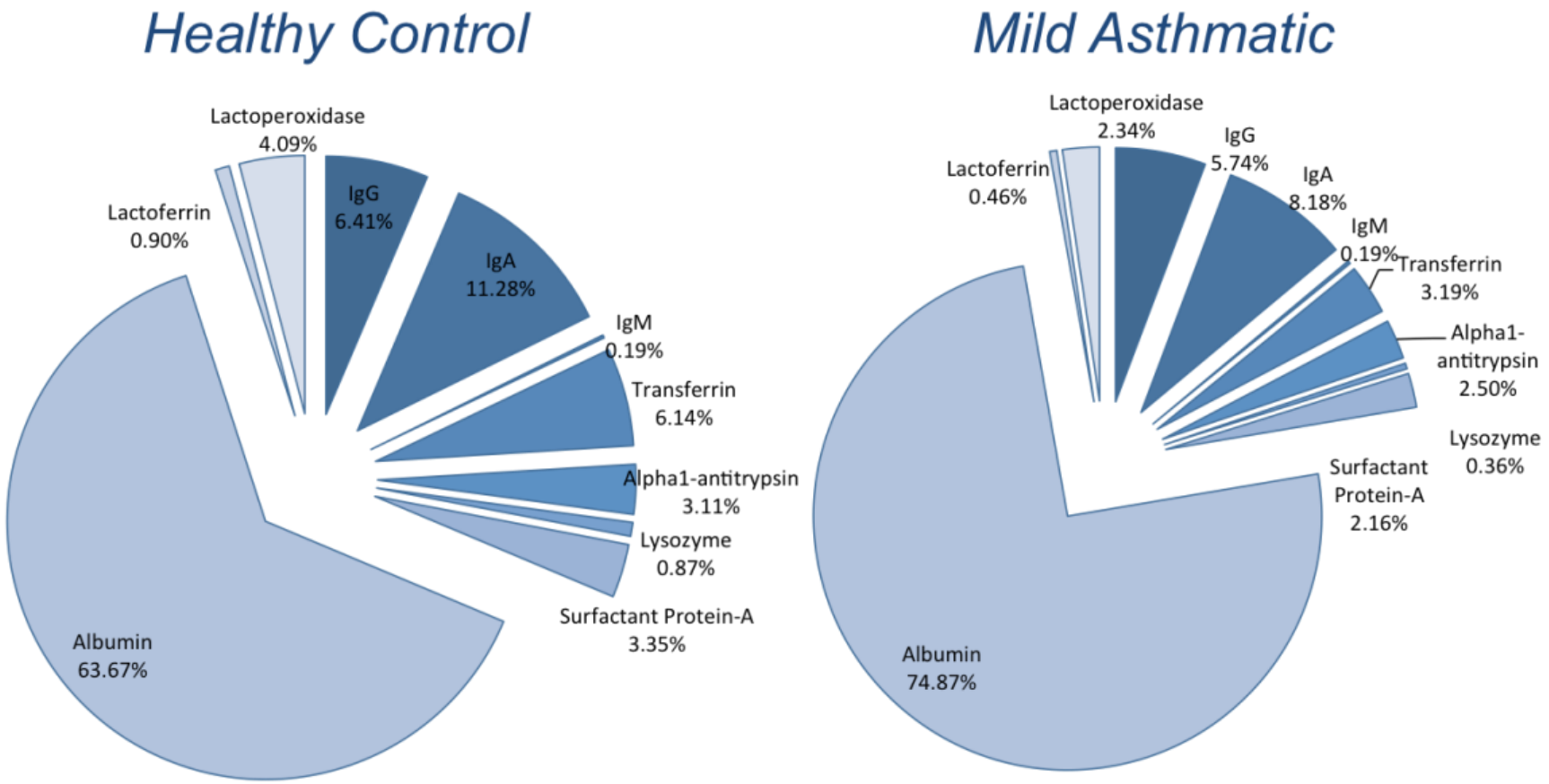

Figure 3.4*: Percentage contributions of individual bronchial protein components relative to total bronchial RTLF protein***.** Proportions are represented as median values.

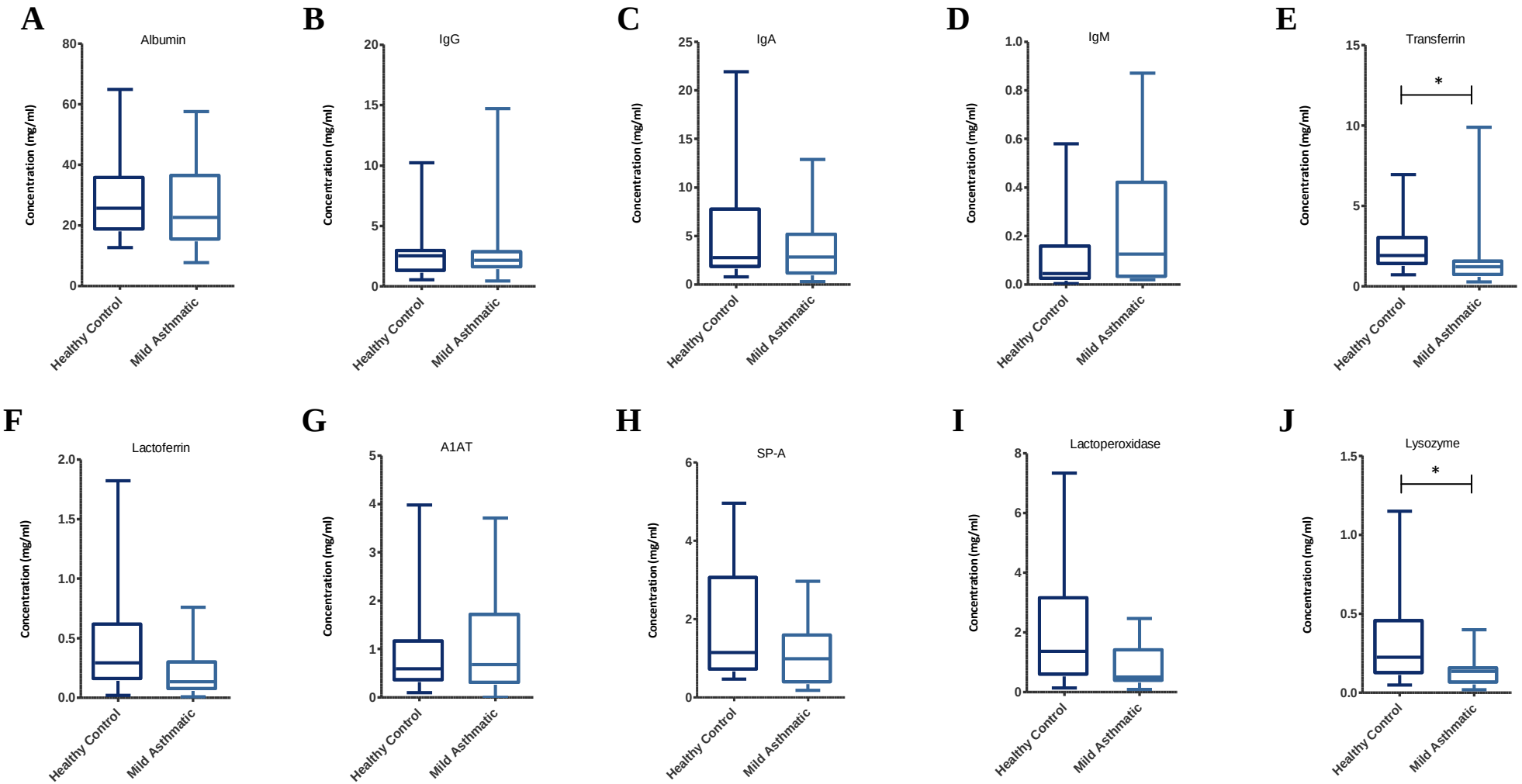

Figure 3.5: *The proteins of the bronchial RTLF in mild asthmatics and healthy controls*. Values corrected for lavage dilution using the urea approach. First row from left to right: Albumin (A) , IgA (B), IgG (C), IgM (D) Transferrin (E) Second row: A1AT (E), Surfactant Protein A (G), Lactoferrin (H), Lactoperoxidase (I) and Lysozyme (J) . * denotes a statistical difference where $p<0.05$

3.3.5: Bacterial Load

Concentrations of the Gram negative bacterial cell wall component LPS were significantly elevated ($p<0.05$) in the bronchial RTLFs of mild asthmatic patients (27.12 (8.7-125.9) EU/ml) relative to healthy controls (4.1(1.6-13.3) EU/ml) – **Figure 3.6**. A quantitatively similar difference was also noted between both groups in the BAL RTLF (28.3 (9.2-76.0) and 14.3(5.5-40.4) in MA and HC respectively). The gram positive cell wall component of bacteria LTA was additionally investigated within bronchial samples only (0.27 (0.15-0.36) and 0.19 (0.15-0.29) mg/mL in MA and HC respectively). However, no significant difference was observed between the two groups.

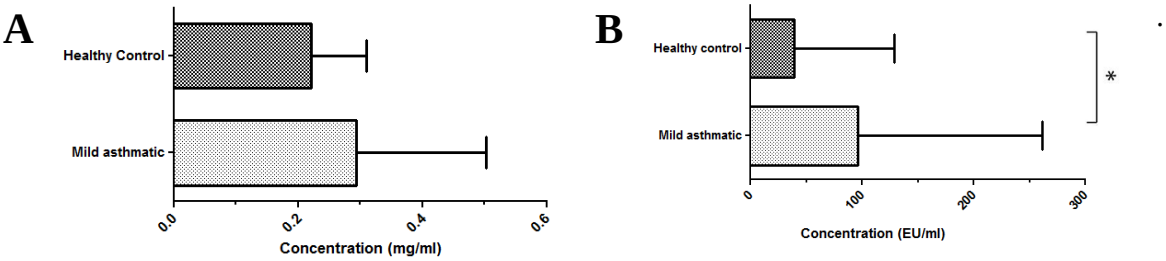

Figure 3.6: ***LTA (A) and LPS (B) concentrations in healthy and mild asthmatic bronchial wash samples***. Values corrected for lavage dilution using the urea approach. Healthy controls n=16, 25.0±2.6 years, 6M/10F; Mild asthmatics n=16, 26.7±6.2 years, 5M/11F. * denotes a statistical difference where $p<0.05$

3.3.6: Elemental analysis of BAL fluid

Phosphorous (P), calcium (Ca) and potassium (K) were the most abundant elements within the digested BAL fluid samples in both groups. Of the 14 elements investigated significantly higher ($p<0.05$) concentrations of the following metals were found within the asthmatic samples: Zn, 2.0 (1.1-2.5) [*asthmatics*] vs. 1.3 (0.7-17) µM [*healthy*]; Fe, 2.4 (2.3-2.6) vs. 2.3 (2.3-2.4) µM); S, 7.3 (7.1-8.4) vs. 6.7 (6.4-7.0) µM; Ca, 66.7 (63.8-77.5) vs. 60.9 (56.3-64.4) µM and K, 114.1 (90.5-132.9) vs. 91.3 (56.4-100.6) µM. Correlation analysis (Spearman's rank order correlation for non-parametric data) was performed to examine the relationships between individual elements, with several significant positive correlations ($P<0.05$) observed including: Zn and S (□□Spearman's rho□=0.714), S and Ca (□=0.922), Ca and Mg (□=0.639), S and Mg (□=0.647) and Cu and Zn (□=0.543).

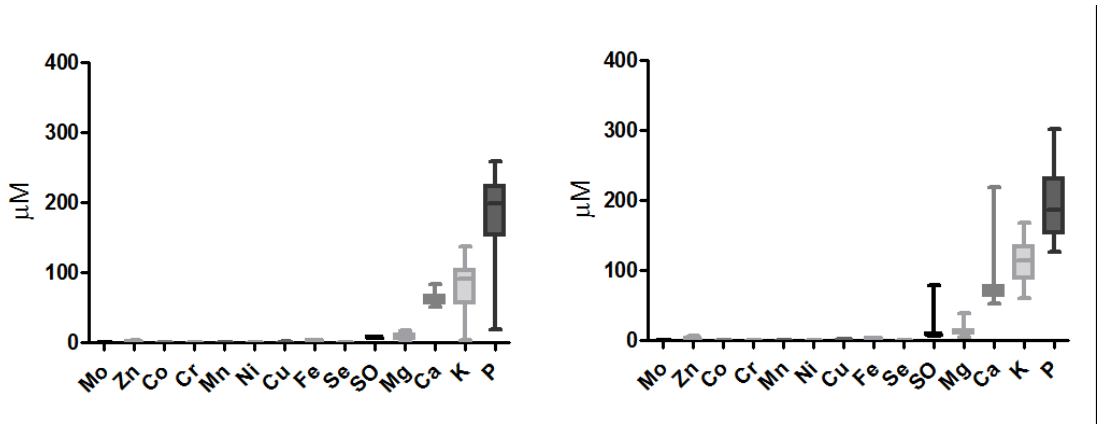

Figure 3.7: ***ICP-MS results from healthy controls (A) and mild asthmatic (B) in bronchoalveolar lavage samples.*** Healthy controls n=16, 25.0±2.6 years, 6M/10F , Mild asthmatics n=16, 26.7±6.2 years, 5M/11F . * denotes a statistical difference where $p<0.05$

3.3.6: Lipids of the RTLF

Measurements of the most abundant surfactant phospholipid, phosphatidylcholine (PC) revealed no significant differences between mild asthmatic (3.8 (3.0-6.1) mg/mL) and healthy (4.8 (3.1-5.4) mg/mL) alveolar RTLFs. Using the previously determined phosphorous concentrations (186.4 (152.9-227.1) and 198.9 (159.6-219.4) µM) in the asthmatic and healthy subjects as an approximate of total RTLF phospholipid, the % contribution of PC was 17.74 (15.1-21.2)% and 17.28 (14.4-19.3)% in the asthmatics and healthy controls respectively. Alveolar RTLF cholesterol concentrations of 0.09 (0.07-0.12) mg/mL (asthmatic) and 0.10 (0.09-0.14) mg/mL (control) were determined, with the Phospholipid to Cholesterol concentrations calculated at a % ratio of 4.2 (3.8-5.1) and 4.5 (3.9-5.4) for MA and HC respectively. No significant differences were observed between groups.

3.4: Discussion

The aim of this study was to characterise the composition of the healthy and mild asthmatics RTLFs, with the objective of using this information as a basis for the construction of disease-specific lung lining fluid simulants for the *in vitro* testing of drug interactions at the air lung interface (described in **Chapter 6**). To achieve this aim I focused on quantifying the key components of this physiologically important extracellular compartment; including a detailed description of the RTLF proteome, as well as the lipid, low molecular weight antioxidant and elemental composition.

The RTLF represents the first line of defense at the air-lung interface, protecting the underlying airway epithelium from inhaled xenobiotics, in part through its robust extra-cellular antioxidant network (Skoza, 1983; Cross et al., 1994; Mudway and Kelly, 2000; van der Vliet and Cross, 2001). The antioxidant concentrations established in this study and adjusted for sample dilution using the urea method are generally consistent with previously published results (Cantin et al., 1987; Kelly et al., 1999; van der Vliet et al., 1999). This pre-existing literature has demonstrated significant regional differences in RTLF antioxidant composition throughout the human airway, with glutathione concentrations highest within the alveolar region (Hatch, 1992; Cross et al., 1994; van der Vliet et al., 1999), whilst urate concentrations dominate within the nasal passages and conducting airways (Peden et al., 1990; Davis and Pacht, 1991; Peterson et al., 1993; Housley et al., 1995; Blomberg, et al., 1998). This study confirmed these previously reported regional variations.

Alveolar RTLF ascorbate concentrations were similar to plasma levels, with lower concentrations determined in the nasal RTLFs, consistent with previous observations (van der Vliet et al., 1999). As outlined in previous studies there is still a great deal of uncertainty regarding the source and regulation of ascorbate within the RTLFs and the view that this simply reflects passive diffusion from the plasma pool is not strongly supported in the literature (Kelly and Mudway, 2003; van der Vliet et al., 1999). It was also notable that a significant proportion of the RTLF vitamin C pool was present as its oxidised product, dehydroascorbate, especially within the bronchial airways. As the samples used for vitamin C analysis were acidified and deproteinated to prevent erroneous sample oxidation, this is unlikely to reflect a storage artefact. In addition, GSSG concentrations in the bronchial wash samples were not similarly increased, relative to the levels seen in the alveolar samples. This suggests that the ascorbate moving onto the surface of the lung is subject to oxidation, partly explaining the absence of a clear association between plasma and RTLF pools previously reported (Blomberg et al., 1999; Mudway et al,

2001). Previous supplementation studies have shown a rapid flux of ascorbate into the airways (Schock et al., 2004; Behndig et al., 2009), which is subsequently lost over a 24-hour period (Behndig et al., 2009). Schock and colleagues demonstrated that ascorbate in induced sputum is rapidly oxidised in an azide-inhibitable manner, suggesting that endogenous peroxidases contribute to the oxidative losses observed (Schock et al., 2004). The RTLF has also been shown to contain appreciable concentrations of non-transferrin-bound iron (NTBI), (Gutteridge et al., 1996) consistent with a pro-oxidant environment.

I found no significant differences in antioxidant concentrations between the two groups, despite reports of lower concentrations of ascorbate in bronchial wash, bronchoalveolar lavage and induced sputum obtained from asthmatic subjects (Chanez et al., 1988; Blomberg et al., 1998; Kongerud et al., 2003). This discrepancy could reflect differences in airway neutrophilia between this and the earlier studies. In the former study, (Mudway et al., 2001) a pronounced airway neutrophilia was present in the asthmatics compared to healthy controls, which was absent here. Indeed in the present study there was a trend (P=0.06) suggestive of reduced neutrophil numbers in the bronchial compartment of asthmatic subjects. Given that there was clear evidence of allergic inflammation in the asthmatic airways in this study, this suggests that the previous observation of low ascorbate concentrations in asthmatics may in fact, more accurately, be interpreted as a function of on-going airway neutrophilia, rather than that of asthma or allergic inflammation per se. The difference in the inflammatory profile between the current and previous studies, likely reflects the clinical heterogeneity of asthma endotypes (Lötvall et al., 2011), with increasing evidence of different underlying pathophysiologies in asthma. Thus, whilst the current study failed to show evidence of enhanced oxidative stress in the asthmatic airway, this should be framed more accurately as mild allergic asthma, without concomitant neutrophilia. This caveat is applicable to all of the subsequent discussion of asthma RTLF composition, as the results can only reflect patients with mild disease and one of many potential underlying disease processes, not all asthma.

Having established that the antioxidant composition of the healthy and asthmatic RTLFs was broadly equivalent, I next examined the proteome of this compartment in subsets (n=5) of the two groups. 2D-gel maps examining the protein composition of bronchoalveolar lavage fluids have existed for over 30 years ago (Bell and Hook, 1979), with approximately 900 protein spots (not corresponding to individual proteins) identified in previous investigations (Noel-Georis et al., 2001). In this study using the combination of 1D PAGE and nano-LC MS/MS I was able to resolve 353 unique proteins in both subsets of healthy control (n=5) and mild asthmatic subjects (n=5), using stringent identification algorithms (see **Section 2.8.5**). In order to assign broad functional classes to the proteins identified, gene ontologies were employed. This identified 5

major functional groups related to: (**1**) immunity and inflammation, (**2**) metal handling, (**3**) transport, (**4**) antioxidant-oxidant balance, and (**5**) antiprotease- protease balance; consistent with the requirement of the surface of the airway to maintain a sterile, anti-inflammatory and reducing environment. In general, based on the proteomic data alone, the majority of proteins identified in the alveolar lining fluids from mild asthmatics were found to be decreased relative to the control group (**Tables 3.4** and **3.5**), though these differences were not statistically significant, reflecting the small group sizes and the semi-quantitative analysis employed, based on the area of the three major ion peaks as a proxy of concentration. The proteomic analysis was therefore used as a guide to identify the most abundant proteins, perceived as being the most important in terms of simulant design, with validation of protein concentrations performed using ELISAs on all the subjects within each group (n=16). As my aim was to account for the major protein components a quasi-mass balance approach was adopted, with individual protein concentrations related to the total measured concentration. My overall aim was to account for >70% of the total protein pool. Previous studies using a similar approach have only accounted for approximately 30-50% of total protein (Hatch, 1992; Sutinen et al., 1995; Dargaville et al., 1999); whilst in the present study I was able to account for 88.3% and 83.8% of the measured total protein in the asthmatic and healthy control alveolar lining fluids, based on quantification of the 8 most abundant proteins (**Figure 3.2**). This figure was inflated to account for the all of the measured 'total' protein pool, 104.3 and 111.7%, when the bronchial RTLFs were considered, based on the 10 determined proteins within this compartment (**Figure 3.4**).

The RTLF total protein measurements, following urea correction (14.3 [healthy] and 17.5 mg/mL [asthmatic]), were considerably in excess of previously published concentrations: 6 to 11 mg/mL (Hatch, 1992; Cross et al., 1994; van der Vliet et al., 1999). Albumin represented the greatest contributor to the protein pool, consistent with numerous previous reports (Bell, 1981; Peterson, 1993; Rennard et al., 1990), accounting for approximately 50% of total protein, with the concentrations, approximately 1.5 to 2 fold greater than previously quoted values: 8.2 and 7.8 mg/mL in asthmatics and healthy alveolar RTLFs, respectively (Hatch, 1992; Cross et al., 1994; van der Vliet et al., 1999). Total protein concentrations in the bronchial RTLFs were significantly greater than those in the alveolar compartment: 40.4 (healthy) and 28 mg/mL (asthma) respectively, representing the first published estimates of urea corrected total protein concentrations in this compartment.

Immunoglobulins provided the second greatest contribution to the alveolar lining fluid proteome, with the most abundant: IgG, IgA and IgM combined accounting for 15.7% and 17.9% of the total protein pool in healthy and asthmatic RTLFs respectively (Note: the least abundant

immunoglobulin IgE was not included on account of it's low contribution to total RTLF protein). Previous reports of the immunoglobulin contribution to the RTLF proteome have been variable with both higher (30% of total protein) (Hatch, 1992; Lenz et al., 1993) and lower (5-10 fold) contributions reported (Rennard et al., 1990; Sutinen et al., 1995; Dargaville et al., 1999). As immunoglobin concentrations within the RTLFs are largely derived from plasma cells found within the airways, they are much more likely to vary in concentration across study populations, especially in conditions with a known inflammatory component, than albumin, which is derived exclusively from the plasma pool by transduction (Burnett, 1986; Raphael et al., 1988; Daniele, 1990; Hatch, 1992).

The immunoglobulin composition of the bronchial RTLFs was characterized by a significantly greater proportion of IgA relative to the alveolar compartment, corresponding to the higher density of IgA secreting plasma cells within the conducting bronchioles (Burnett, 1986). The concentration of the secretory protein lysozyme was also significantly greater in the bronchial lining fluids, consistent with a previous report by Rogan et al. (2006) who demonstrated lysozyme to be ten times more abundant in the aspirate from the first BAL aliquot instilled. They further noted the absence of a correlation with neutrophil numbers and suggested that this implied that bronchial airway submucosal glands were the likely source (Rogan et al., 2006). A similar regional pattern of lactoperoxidase enrichment in the upper airways was also observed, with this secretory protein responsible for catalysing the production of the biocidal compound hypothiocynate (Gerson et al., 2000; Wijkstrom-Frei et al., 2003), however this failed to attain statistical significance (P=0.054). In contrast, concentrations of the 80kDa glycoprotein transferrin were greatest in the distal airway. This was consistent with previous reports in airway lavages from healthy subjects (Lindahl et al., 1998), where transferin concentrations constituted a greater proportion of RTLF protein (4-5.6%) than within the plasma pool, implying local synthesis within the airways themselves, from alveolar macrophages and lymphocytes (Wesselius et al., 1994; Mateos et al., 1998). This emphasizes the importance of Fe homeostasis at the air lung interface, both to limit metal catalyzed reactive oxygen species generation (Ghio, 2009; Vlasic et al., 2009; Quinlan et al., 2002), but also to limit metal availability to bacterial populations (Dehner et al., 2013).

Proteins related to the innate immune system were strongly represented within the extracellular RTLFs, posessing intrinsic microbicidal, bacteriostatic, antiviral and antifungal properties, as has previously been shown (Bals and Hiemstra, 2004; Martin et al., 2005; Rogan et al., 2006). Fleming was the first to demonstrate the bactericidal effects of airway secretions in 1922, with many of the above proteins actively secreted into the RTLF by serous cells of the upper airways, as well as by activated plasma cells, Clara cells and type II pneumocytes of the

more distal airspaces (Travis et al., 1999). The current data demonstrate that in the bronchial airways in particular, the RTLF provides a powerful 'microbicidal barrier', providing a relatively broad spectrum protection against gram positive and negative bacteria. In addition to the independent antimicrobial activities of these proteins, many have been shown to act in a synergistic manner. Lysozyme a hydrolytic enzyme, is secreted alongside lactoferrin (Revenis and Kaliner, 1992), which acts to destabilize bacterial membranes, increasing the penetration of lysozyme into the gram negative bacteria where the enzyme can then disrupt the glycosidic linkages of the cell wall (Ellison and Giehl, 1991; Baveye et al., 1999; Rogan et al., 2006). Additionally lactoferrin acts as an iron binding protein, depriving bacteria of this essential nutrient (Ellison and Giehl, 1991).

Considerable inter-individual variability was observed for all the determined proteins within both the alveolar and upper airway RTLFs. Overall no significant differences were noted between the determined protein concentrations in the alveolar RTLFs between the healthy and asthmatic subjects. In contrast antimicrobial proteins lysozyme and transferrin were both significantly lower in bronchial RTLFs of the asthmatic subjects, with a trend for reduced lactoperoxidase, consistent with an overall impairment of the microbicidal defense network at the air-lung interface of mild asthmatics. The low transferrin concentration was consistent with reduced synthesis within the airway, and contrasted with previous reports of increased airway concentrations under conditions of acute inflammation and airway injury. In patients suffering from acute respiratory distress syndrome a twenty fold increase in transferrin RTLF concentration has been reported, likely reflective of both the breakdown in the air blood barrier and a protective response to the release of excess free iron from dying airway cells (Holter et al., 1986; Pacht and Davis, 1988). Greater concentrations have also been demonstrated in sarcoidiosis patients, likely due to the increased transduction of protein from the plasma pool (Wattiez et al., 2000). This data is therefore consistent with the absence of active inflammation in asthmatic subjects, but infers a basal reduction in innate immune defense.

Before discussing this aspect of the results in detail it is worth noting that whilst the determined concentrations of RTLF proteins in this study varied from those in the literature, their relative contributions to the total protein pool appeared broadly similar. This implies that the higher concentrations likely reflect the application of different lavage dilution correction factors. Due to the scarcity of data on dilution factors in the published literature it is difficult to make meaningful comparisons between individual protein concentrations across studies. It should however be stated that in the present study we employed a high sensitivity urea method, as the implied dilution factors from the pre-existing literature suggested that the lavage urea concentrations were near the detection limit of the commercially available kits at the time of their

publication. It is therefore likely that these previous dilution estimates underestimated the true dilution of human RTLF during airway lavages and hence the RTLF protein concentration.

It is now recognized that the airways of humans are not completely sterile environments (Huang et al., 2011), reflecting the presence of commensal bacterial populations (Beck et al., 2012; Hansel et al., 2013; Huang, 2013), as well as the contribution from the large number of microbes inhaled every day. It is thus increasingly clear, that whilst asthma has often been framed as a disease of adaptive immune dysregulation, the innate immune system of the lung may play an important role in disease etiology and symptom exacerbation (Bals and Hiemstra, 2004; Holgate, 2012; Hansel et al., 2013; Huang, 2013). In light of the evidence of depressed immune defenses within the asthmatics RTLFs in the present study I hypothesized that their airways were likely to contain increased and potentially more diverse bacterial populations. In addition to such basal differences one would also expect an increased susceptibility to microbial infection in the asthmatic airway (Singh et al. 2000). I therefore investigated whether there was evidence of increased gram negative and gram positive bacterial loads within the airway lining fluids of the mild asthmatics, employing lipopolysaccharide (LPS) and lipoteichoic acid (LTA) as indicative biomarkers. Consistent with this view I observed an approximate 7-fold increase in the concentration of the soluble gram negative bacterial cell wall component LPS in asthmatic bronchial wash. In agreement with these findings, a previous investigation demonstrated increased bacterial populations within the bronchial airways of asthmatics compared with healthy controls, with the most diverse microbial populations found in the most hyperresponsive asthmatics (Huang et al., 2011). In contrast, Dubin et al (1996) found similar concentrations of LPS in BAL fluid recovered from subjects with and without mild asthma, but reported that the asthmatic airway had increased sensitivity to LPS (bronchial hyperresponsiveness, neutrophilia and increased airway obstruction) compared with healthy controls. LPS has also been linked to the pathogenesis of asthma, with short exposures at high concentrations heavily implicated in the development of acute respiratory illnesses (Rylander and Haglind, 1984; Mamolen et al., 1993; Schwartz et al., 1995), and early exposure apparently protective against the development of allergic diseases (Michel, 2003). Chronic exposures to LPS have been reported to contribute to the development of chronic airway conditions, including asthma (Castellan et al, 1987; Niven et al., 1997; Pal et al, 1997). Specific bacterial infections have also been linked to asthmatic exacerbations, although the incidence of this has yet to be fully elucidated (Toews, 2005), to date no association between indoor LPS exposure and the clinical severity of asthma has been demonstrated (Michel et al., 1991). A similar increase in bronchial RTLF lipoteichoic acid, reflecting the presence of gram positive bacteria was also noted but this did not attain statistical significance.

In addition to the low molecular weight antioxidant and protein components of the RTLF, I also examined the concentrations of the most abundant surfactant phospholipid, phosphatidylcholine (PC) and cholesterol in the alveolar RTLFs. It is only relatively recently that surfactant dysfunction has been implicated in asthma; with Wright et al (2000) suggesting that it may predispose the development and severity of the condition, and a report by Kurashima et al (1997) having described the successful treatment of asthma by exogenous surfactant treatment, also implicating its dysfunction in this disease. Further evidence comes from the exudation of plasma proteins into the airway lumen during inflammatory events in asthma, which has been shown to inhibit the action of surfactant, impairing its surface tension lowering ability (Van de Graaf et al., 1991). Reported differences observed in surfactant composition between the relative ratios of phospholipids within asthmatic RTLFs, including significant increases in phosphatidylcholine - phosphatidylglycerol ratio, were later identified to be the result of specifically increased levels of plasma derived PC after allergen induced inflammation and thus increased plasma infiltration into the airways (Heeley et al., 2000). Analyses of sputum samples from asthmatics have further revealed changes in % ratios of dipalmitoyl phosphatidylcholine in surfactant (Wright et al., 2000) with Kurashima et al. (1997) reporting that sputum samples obtained from asthmatics displayed lower surface activity, although these same studies revealed no such changes in BAL surfactant composition (Kurashima et al., 1997; Wright et al, 2000). In the present study the concentrations of both PC and cholesterol in the alveolar lining fluids were equivalent in asthmatic and healthy populations.

Elemental analysis was performed predominately as a means of obtaining a measurement of total phosphourous as a proxy for total lipid in the alveolar RTLFs. In addition a panel of 13 elements were also considered: Mo (reflective of xanthine oxidase in the RTLF (Pinamonti et al., 1998)), Zn (extra-cellular superoxide dismutase, plus other Zn containing proteins, including matrix metalloproteinases and S100 proteins (Heizmann and Cox et al., 1998; Mudway et al., 2001; Ko et al., 2005)), Co (marker of smoking or environmental tobacco smoke (ETS) exposure), Cr (smoking, ETS), Mn (Mn-SOD as a marker of cell lysis in the absence of other known extracellular Mn containing protein in the lung), Ni (smoking, ETS), Cu (extra-cellular superoxide dismutase, caeruloplasmin (Schoonbrood et al., 1994; Mudway et al., 2001)), Fe (lactoferrin, ferritin and transferrin (Ghio et al., 2007)), Se (glutathione peroxidase (Fitzpatrick et al., 2009)), S (predominately glutathione and cysteine rich proteins (Mudway et al., 2001)), Mg (to inform ionic RTLF composition), Ca (ionic composition and concentration of Ca-binding proteins, such as Calgranulin B (Bargagli et al., 2008) and K (ionic composition). Fe, Zn, Ca, K and S were all significantly elevated in asthmatic alveolar lining fluids. Whilst Fe was

significantly elevated in asthmatic RTLFs, the actual quantitative difference was negligible. Nevertheless this is the first observation of increased total iron (Fe) in the RTLFs of asthmatic subjects, with previous studies in plasma demonstrating conflicting results, with evidence of both enhanced plasma concentrations of total Fe in asthmatics (Kocyigit et al., 2004), or no overall difference compared with controls (Vural et al., 2000). This observation gains greater relevance when coupled with the significant decrease of transferrin observed within the mild asthmatic RTLFs, suggesting that Iron uptake and sequestration into cells might be impaired. Furthermore, significant correlations between BAL total Fe measurements and both bronchial and alveolar LPS concentrations that were restricted to the mild asthmatics only, suggest that the enhanced Iron pool might play a role in providing a favorable microbial growth environment. Whether this exists in a redox active form would require further investigation, but it would be consistent with previous reports (Gutteridge et al., 1996), as well as the evidence of extensive ascorbate oxidation within this compartment (Behndig et al., 2009).

Increased concentrations of Cu have been previously reported in the plasma of asthmatics (Kadrabova et al., 1996; Vural et al., 2000; Ermis et al., 2004), where it has been argued to reflect the presence of acute or chronic inflammation within the airways. This is the first report of a similar increase within actual RTLFs; though attributing the elevated concentrations in asthmatics to the presence of inflammation is far too simplistic. The fact that this increase in Cu occurred in parallel to increased Zn concentrations in the asthmatic RTLFs, strongly implicates a possible upregulation of extra-cellular superoxide dismutase (EC-SOD), supported by the positive correlation between Cu and Zn. It should be noted however that previous studies have reported decreased Zn concentrations in the plasma of asthmatics (el-Kholy et al., 1990; Kadrabova et al., 1996; Soutar et al., 1997; Vural et al., 2000; Ermis et al., 2004) and there are no published reports demonstrating increased EC-SOD concentrations in the asthmatic RTLFs. Rather, there are a number of studies demonstrating SOD inactivation in asthma (De Raeve et al., 1997; Comhair et al., 2000; Comhair et al., 2005), though which isoform of this enzyme is implicated remains an area of contention. Assuming the upregulation of Cu and Zn to reflect an increase in EC-SOD, though the Cu:Zn stoichiometry was not 1:1, this would imply a response to oxidative stress. One would thus expect a general upregulation of antioxidant enzyme expression in the asthmatic airway, with a parallel increase in plasma glutathione peroxidase to catalyze the reduction of the hydrogen peroxide formed by EC-SOD to water; as well as glutathione, which is an essential co-factor for this enzymatic function. The elemental data however fails to provide a wholly coherent picture as Se, the catalytic metal at the active site of glutathione peroxidase was not increased, whilst S (used as a proxy for GSH due to its high concentrations in the RTLF) was. Previous

reports have actually associated low Se concentrations in airway lavages as a potential biomarker for asthma severity (Flatt et al., 1990; Misso et al., 1996; Hoffmann, 2008; Jacobson et al., 2007). In addition the concentration of sulphur within the RTLFs did not correlate with the actual measured glutathione concentrations, which was also not found to increase in the mild asthmatics, suggesting that the S measurement was strongly influenced by contributions from other thiol containing proteins.

Calcium is essential in many cellular processes, with numerous Ca-binding or utilizing proteins identified within the RTLF during the proteomic analysis, including the S100 calgranulin proteins, surfactant proteins A and D, as well as the high molecular weight glycoconjugate mucin. However no differences in these proteins were observed within asthmatic RTLFs, based on the proteomic data, and no correlation could be established between calcium and surfactant protein-A, which was measured in all 32 subjects by ELISA.. The basis for the increase in RTLF potassium in asthma remains similarly oblique.

Summary and conclusions

The aim of this study was to explore the major compositional features of the RTLFs, across the respiratory tract in both healthy subjects and mild asthmatics, with the aim of identifying the major components for inclusion in lung lining fluid simulants. Using a mass balance approach I was able to show that the proteome in both healthy and asthmatic subjects could be accounted for by a relatively small panel of abundant proteins identified by the proteomic screen; 8 for the alveolar RTLF and 10 for the lining fluids of the bronchial airways. This does not infer that these proteins are the most significant to the clinical phenotype, or the underlying disease process, only that they should be included within a designed simulant for it to be representative of RTLF composition *in vivo*. In the alveolar compartment there was little difference in the composition of the RTLF between the healthy and asthmatic subjects, when the low molecular weight antioxidant pool, proteins and lipids were considered, indicating that a common simulant could be designed for asthmatics and controls if drug delivery was to be targeted to this compartment. The situation was somewhat different in the bronchial lining fluids, where there was an enrichment of proteins related to innate immunity relative to the alveolar compartment with evidence that these defences were somewhat degraded in the asthmatic subjects. Following this result I was able to demonstrate that this depression in innate immune proteins in the asthmatics was associated with increased LPS concentrations in the recovered lavage fluids, consistent with increased basal bacterial populations in the lung and a potential heightened susceptibility to infection. This observation has to be placed in the context that the

mild asthmatics examined in this study were stable, with well controlled asthma symptoms, consistent with the absence of overt oxidative stress in their airways, or neutrophilia. Hence, these observations likely reflect an underlying deficiency related to the disease, rather than as a response to disease exacerbation.

Chapter 4

Age-related changes in the composition of human respiratory tract lining fluids

4.1:Introduction

Currently over a third of the UK population is over 50 years of age, with the number of people aged over 65 expected to rise by 65% in the next 25 years to over 16.4 million in 2033 (age, UK London). Despite the shift toward a more aged population surprisingly little information is known regarding the normal biochemical changes that accompany the established age related decline in lung function (Sharma and Goodwin, 2006; Ito and Barnes, 2009), see **Figure 4.1**. This is a critical issue for inhaled drug development, as the aged population represents the single largest market for drugs worldwide and yet the *in vitro* models employed to evaluate drug efficacy and toxicity make no allowance for the affect of normal physiological ageing. The underlying causes for the observed changes in lung structure and function are likely multifactorial, from the presence of oxidative stress, an imbalance in protease-antiprotease regulation, the glycosylation of collagen and connective tissue supporting structures, to the presence of low grade chronic inflammation. All of these age-related declines likely contribute to the physiological loss of adaptability, making the aged lung not only more susceptible to infection, but also to other environmental stressors. This is reflected by the high prevalence of chronic and obstructive respiratory diseases and acute infections within the aged population where airway diseases constitute the second largest cause of severe disability (Dyer et al, 2012). As argued previously, these changes to the lung are likely to have a profound impact on the composition of airway RTLFs. In this chapter I used a similar strategy to that employed previously to investigate the RTLF composition in a healthy aged population. ‘Healthy’ in this context inferring the absence of repiratory disease and predicted lung function within the normal range.

Ageing is an inevitable process defined by four basic principles; it is intrinsic, universal, progressive and ultimately detrimental to the host .The mechanisms driving ageing, remain fairly poorly understood, with numerous (over 300) theories proposed to explain the ageing process. Hayflick’s (1987) theory of cell senescence, Bjorkstens Cross-linking Theory (1968), the role of

changing immunity (Walford, 1969), the mitochondrial- lysosomal axis theory of ageing (Brunk and Terman, 1989) and the 'free radical hypothesis' proposed by Harman (1956), describe events on both the cellular and molecular levels, all of which have greatly evolved our understanding into the phenomenon of ageing; however no one theory is generally accepted (Medvedev, 1990; Weinert and Timiras, 2003).

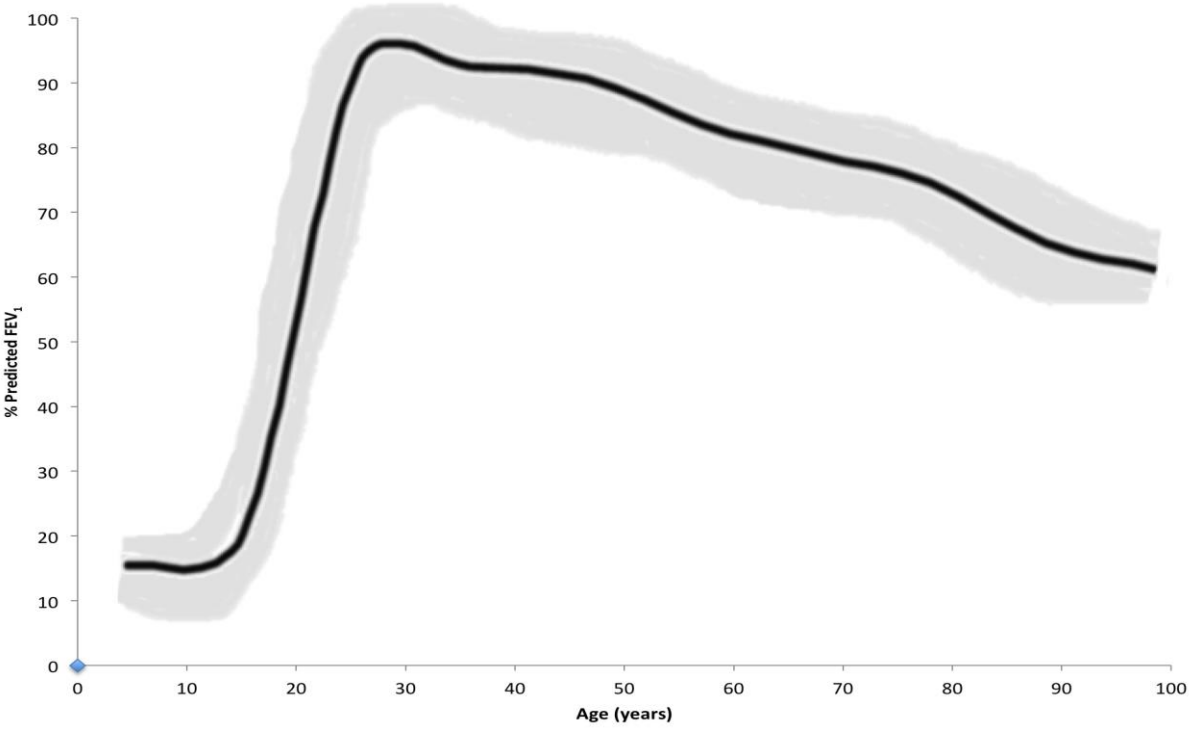

Figure 4.1: *Age-related decline in forced expiratory volume in one second (FEV_1) with increasing age.* Adapted from Sharman and Goodwin and Ware JH, Dockery DW, Louis TA, et al. 1990.

The gradual functional deterioration in lung function with age (decreases in lung volume, maximum rates of airflow, forced vital capacity (FVC), FEV_1 and diffusing lung capacity) reflect underlying structural and anatomical changes of the airways (Rode and Shephard, 1994; Brandli et al., 1996; Ito and Barnes 2009). The dilatation of the ageing alveolus, increasing alveolar dead space and reducing parenchymal support to the small airways is known as known as 'senile emphysema'; with onset reported to occur after 50 years of age (Sobin et al., 1988; Gillooly and Lamb, 1993; Janssens et al., 1999). Changes in structural elastic fibers and collagen also contribute to the loss of elastic recoil, effectively resulting in non-uniform ventilation/blood flow ratios in the aged lung (John and Thomas, 1972). This deterioration in lung function is exacerbated by osteoporosis and age-related declines in diaphragmatic strength (McClaran et al., 1995; Sharma

and Goodwin, 2006). The decline in respiratory muscle strength may have a particularly important impact on cough, essential for airway clearance, resulting in an increased risk of airway infection (Dyer et al, 2012). Finally, detrimental effects of ageing have also been reported on the respiratory centre and peripheral chemoreceptors of the respiratory system, which become increasingly unresponsive to stimuli including hypoxia, increasing the vulnerability of the lungs in conditions such as pneumonia, heart failure and ventilatory failure (Kronenberg et al., 1973).

Animal models including the senescence associated mouse (SAM), developed from an AKR/J strain (Takeda et al., 1981), have been used to study 'normal' physiological ageing, in the absence of complicating environmental factors. These animals have shown to develop the morphological and mechanical changes consistent with senile lung with increasing age, including airspace enlargement (without the alveolar destruction as seen in emphysema), and loss of elastic recoil, in the absence of extrinsic factors (Verbeken et al., 1992). In addition, minor but nevertheless statistically significant impairments of important physiological and protective functions of the airways have been observed: immunity, protease-antiprotease and oxidant-antioxidant balance in these mouse models (Takeda et al., 1981). The normal physiological changes as seen in these models were further identified to be exacerbated by exposure to extrinsic factors such as inducers of inflammation, including tobacco smoke and LPS, suggesting that they accelerate the normal ageing process (Shock, 1962; Thurlbeck, 1967; Takeda et al., 1981).

Sustained low-grade inflammation alongside dysregulation of respiratory immune systems may provide for a mechanism explaining the structural and functional changes occurring with age (Ito and Barnes, 2009). A study by Thompson et al (1992) demonstrated a considerable increase in the number of neutrophils in the airways with increasing age, associated with fewer, but still functionally active alveolar macrophages. The presence of chronic inflammation would contribute to the ageing associated changes occurring in the lung, through oxidant mediated and enhanced proteolytic damage to the airways (Ito and Barnes, 2009). Two further important components of innate immune defence in the airways, mucociliary clearance and bronchial secretions into the RTLFs, have both been shown to decline in the aged lung (Goodman et al., 1978; Gyetko and Toews, 1993), consistent with an increased age-related susceptibility to acute respiratory infections, particularly pneumonia, the second most prevalent cause of death in the elderly. This would be further exacerbated by the reduction in neutrophil phagocytic activity observed in the very elderly (Meyer, 2004). Whilst this depression in innate immunity is well established in aged individuals (Shaw et al., 2013), there is a paucity of information regarding how this impacts the composition of human RTLFs. There is also evidence of changes to the adaptive immune system in aged populations, with T helper (CD4+) cells, essential in the activity of other immune cells of the airways (antibody secreting B cell class switching and the activation

and maturation of cytotoxic T cells), reported to increase relative to CD8+ lymphocytes. The accumulation of CD4+ cells within the distal alveolar airspaces, suggests a heightened presence of primed T cells in aged healthy RTLFs, which may be reflective of the large number of insults and repeated antigenic exposure occcuring over time. Immunoglobulin concentrations have been shown to increase in age, alongside increased levels of various cytokines (including IL-6 and IL-8) across central and distal RTLFs (Meyer et al., 1998; Meyer, 2001).

The role of oxidative damage has been implicated in the pathogenesis of ageing, with advanced glycation end products (Simm, 2013), DNA oxidation (Evans et al., 2004; Siomek et al., 2007), protein oxidation (Levine, 2002; Stadtman et al., 2005; Baraibar et al., 2013) and lipid peroxidation (Barreiro, 2005; Cruz et al., 2009; Benlloch-Navarro et al., 2013) products all observed to increase with age (Jacob et al., 2013). In many organs ageing is accompanied with increased concentrations of oxidatively modified proteins, reflected by the carbonylation of amino acids, tyrosine nitration and oxidation of cysteine residues, all of which have been shown to mark proteins for degradation, as well as alter protein function (Umstead et al., 2009; Oettl and Stauber, 2007). Importantly, ageing has also been shown to be associated with impaired lysomal and proteosomal function (Höhn et al. 2013), promoting the accumulation and aggregation of these oxidation products (Jung et al., 2007). These changes have been related to both increased reactive oxygen species production (Ma et al., 2009; Wang et al., 2013), as well as diminished endogenous antioxidant defences (Teramoto et al., 1994; Kumawat et al., 2012; Currais and Maher, 2013), with evidence that antioxidant enzyme activites are significantly reduced with airway leukocytes from aged subjects (Behndig et al., 2009). This increased oxidative imbalance is further exacerbated by poorer diets deficient in antioxidants, in the aged population (Kelly and Mudway, 2003; Schwartz and Weiss, 1990). **Table 4.1** highlights the types and consequence of the oxidative modifications that have been shown to occur in ageing.

These intrinsic factors are however also exacerbated across the life course by exposure to external 'insults'. The respiratory tract, and the respiratory tract lining fluids surrounding them are exposed to a huge array of lung 'insults' from environmental/occupational pollutants, tobacco smoke and exposure to infectious agents all of which elicit inflammation and injury to the airway which effectively accelerate age-related functional declines (Ito and Barnes, 2009). Thus the literature examining age related changes in the airways is often complicated by factors such as smoking status or the presence of concomitant disease (Nicholas et al. 2010; Merkel et al., 2005; Ohlmeier et al., 2008). This consequently has blurred our understanding of the biochemical processes underpinning the age-related declines in lung function. Therefore in this study I have selected only healthy aged subjects; never smokers, with no significant lifetime exposures to

occupational dust and fumes, to focus on the underlying normal ageing process.

Aims

In this chapter I have investigated the composition of the aged RTLF, comparing BW and BAL samples obtained from non-smoking healthy aged subjects to their non-smoking younger counterparts; this latter group reflecting the control group from the previous chapter. The primary aim was to provide an understanding of the compositional changes occuring at the surface of the lung, attributable to 'healthy' ageing, to permit the design of simulants representative of the aged RTLF. In addition, I aimed to gain a greater insight into the biochemical changes associated with the aged lung, with a specific focus on impacts on the antioxidant and innate immune networks present within this extra-cellular compartment.

Table 4.1: *Evidence of oxidative modifications occurring during ageing.*

Type of Oxidative modification		Evidence of oxidative stress with ageing and functional significance	Reference
DNA	8-oxo-7,8-dihydro-2′-deoxyguanosine(8-oxodG) adducts	Influences protein synthesis, has mutagenic portential and interfers with gene expression and epigentic processes. Age related changes in proteins are regulated both at the transcriptional and translational levels, as well as post translational modifications and physiological cellular clearance mechanisms, that together determine the concentration, activity and stability of proteins	Cheng et al., 1992; Evans et al., 2004; Rattan, 1996
Lipid	Products inclusing (4-HNE and MDA) are capable of forming stable protein adducts	HNE protein adduct formation, has been correlated with respiratory muscle function	Barreiro et al., 2005
		MDA and HNE adducts of apolipoproteins B-100 lys residues implicated in atherosclerotic lesions	Martinez-Vicente et al., 2005
	Oxidative modification of LDL	Resulting in their aggregation and uptake by mactophages has been crucially implicated in the development of atherosclerotic plaques	Martinez-Vicente et al., 2005; Shacter et al., 2000
Protein	Protein oxidation: carbonyl, 4-HNE and MDA adducts	Protein carbonyl derivatives are used as a marker of the free radical mediated effects on proteins, with carbonyl adducts added on to proteins either by reacting with aldehyde groups (4-hydroxy-2-nonenal, malondialdehyde), products of lipid peroxidation, or reacting with reactive carbonyl derivatives, the products of glycation and glycoloxidation reactions. The presence of carbonyl groups has been used to establish the association between oxidatively damaged proteins with ageing. Oxidative modifications have been said to serve to either inactivate proteins or mark them for clearance. These modifications are typically irreversible and thought to be relatively nonspecific. Accumulation of oxidised and glycated proteins, could be attributed to defective autophagy, a consequence of age related alterations in proteolytic systems	Berlett and Stadtman, 1997; Levine, 2002; Bader and Grune, 2006; Cecarini et al., 2007; Levine and Stadtman, 2006; Bito et al, 2005
	Formation of intra- or inter-molecular protein cross-linked derivatives.	Ageing has been associated with the decreased efficiency of cellular protein degradation. The degradative processes, both lysosomal and proteasomal, impaired with ageing resulting in the accumulation of oxidised protein aggregates.	Kirkwood, 2005; Terman and Brunk, 2004; Ward et al., 2002; Szweda et al., 2003; Cuervo and Dice, 2000
	The susceptibility of specific proteins in the RTLFs to oxidation has previously been reported (Starosta and Griese, 2006).	Oxidation of the most abundant plasma derived protein within RTLF, albumin, has been demonstrated to both inhibit its functional binding capacity and increase its degradation. Conformational changes to albumin also modify in its biological antioxidant functions.	Oettl and Stauber., 2007; Iwao et al., 2006; Nagai et al., 2006
		Oxidation of fibrinogen, results in loss of function, clotting, correlates with carbonyl formation	Shacter et al., 2000
		Oxidation of immunoglobulins, has been shown to result in aggregation observed in Rheumatoid arthritis	Shacter et al., 2000
		Oxidation of alpha-1 antitrypsin, results in loss of function that can have severe physiological consequences contributing to tissue destruction	Shacter et al., 2000; Beatty et al., 1980
		Positive correlation between loss of biological function and elevation of level of oxidised protein in brain in specific regions controlling cognitive function	Carney et al., 1994; Forster et al., 1996
		Actin carbonylation, which has structural consequences	Dalle-Donne et al., 2003
	Amino acid oxidation: tyrosine nitration and oxidation of cysteine residues	Influences many signal transduction pathways. Oxidation of sulfide groups and the phosphorylation of tyrosine is crucual in many signalling pathways. Oxidation of signalling proteins causes structural modifications, which in turn affects redox-sensitive signalling pathways. Oxidative modification of sulfhydryls has been observed in Altzhiemers disease.	Dalle-Donne et al., 2003; Halliwell and Chirico, 1993.
	Oxidation of methionine residues	Carbonic anydrase III oxidation implicated in ageing	Dalle-Donne et al., 2003

4.2: Methods

4.2.1: Subjects:

Selection criteria for the healthy young controls are as outlined in **Section 3.2.1**. Inclusion criteria for the aged healthy controls were: being between 50-75 years, never smokers with normal lung function. Subjects underwent a detailed medical consultation with ECG and chest X-ray prior to inclusion. Exclusion criteria for all groups were the use of any medications other than those specifically stated in the inclusion criteria and any use of antioxidant supplementation. All participants gave their informed consent and the local Ethics Committee of Umeå University approved the study, in accordance with the declaration of Helsinki. Subject demographics are presented in **Table 4.2**, showing the age related decline in absolute lung volumes, though the aged subjects test results were within the predicted range for their sex and age.

Table 4.2: *Demographics and clinical characteristics of the young and aged study populations.*

Characteristics	Healthy controls (n=16)	Aged Controls (n=13)
Male/female	5F / 11M	6F / 7M
Age (years)	25 (2)	67 (5)***
Lung Function (mean SD)		
FEV_1	4.09 (0.77)	2.95 (0.80)***
FEV_1 %	85 (7)	78 (4)
FEV_1 %pred	105 (8)	100 (18.5)
FVC	4.81 (1.05)	4.07 (0.97)***
FVC %pred	106 (9)	104 (12)

Data presented as mean values with standard deviation, BMI=body mass index; FEV_1=forced expiratory volume in one second. FVC- forced vital capacity. ***P<0.001.

4.2.2: Experimental proceedure:

Spirometry was performed as outlined in **Section 3.2.2.** Bronchoscopy with bronchial wash and bronchoalveolar lavage was performed as described in **Section 3.2.3**. Nasal lavage was not performed on the aged subjects. Details of the total and differential cell counts have been decribed previously (**Section 3.2.3**).

4.2.3: Antioxidant, total protein and urea determinations

Vitamin C, (ascorbate and dehydroascorbate), urate, total glutathione (GSx), glutathione (GSH), and glutathione disulphide (GSSG) concentrations were determined in BW and BAL as previously described, (Mudway et al., 2001; Behndig et al., 2009); further details are provided in Chapter 2 (**Section 2.4**). Total protein determinations were made using the BCA assay (Smith et al., 1985), with paired plasma and lavage urea concentration assessed using the high sensitivity QuantiChrom urea assay kit (BioAssay Systems, Hayward). Protein carbonyl formation was measured spectrophotometrically using OxiSelect protein carbonyl spectrophotometric kit (Cell Biolabs, Inc., USA), with 4-HNE protein adducts determined using the OxiSelect HNE Adduct ELISA Kit (Cell Biolabs, San Diego, CA, USA).

4.2.4: Proteomic analysis

The strategy employed was identical to that outlined in the previous chapter (**Section 3.2.5**), with analysis performed on a subset of 5 individuals drawn from each of the young and aged groups. For the young group, (n=5), 27±2 years 1M/4F; and for the aged population, (n=5) ,67±9 years, 3M/2F.

4.2.5: Elemental analysis

ICP-MS was performed on acid digested BAL fluid samples by inductively coupled plasma mass spectroscopy (ELAN DRC, MSF008) as described previously in Section 3.2.7 with the amendment that consideration was limited to ^{65}Cu, ^{57}Fe and ^{66}Zn.

4.2.6: Statistics

Inflammatory cell numbers, plus urea adjusted protein, elemental and antioxidant concentration data were not normally distributed and are therefore described as medians with 25th and 75th percentiles throughout. Mann-Whitney U tests were employed to compare data derived from the healthy and aged populations, with Spearman's rank correlation employed for analysis of association. Statistical analyses were performed using the IBM SPSS software, version 20 (SPSS, Armonk, NY, USA). A p-value <0.05 was regarded as significant

4.3: Results

4.3.1: Baseline characteristics

All subjects tolerated the lavage procedure well with mean returns for the young population of 17.2/40mL and 132.4/180mL for the bronchial wash and bronchoalveolar lavage respectively. These returns were significantly decreased within the aged population (lavage return thus appears to be associated with airflow limitation): 9.8/40mL (bronchial wash) and 86.4/180mL (bronchoalveolar lavage). No evidence of increased inflammation was seen in either the upper or lower airway lavages from the aged individuals (**Table 4.3**).

Table 4.3: *Inflammatory cell counts in bronchial wash (BW) and bronchoalveolar lavage (BAL) fluid, obtained from young and aged populations.*

Cell type and location	**Young** n = 16	**Aged** n = 13	**Significance**
Bronchial Wash			
(×10^4 cells·mL^{-1})			
Macrophages	7.2 (5.2–12.3)	6.2 (3.4–9.3)	NS
Neutrophils	0.7 (0.3–1.0)	1.1 (0.3–1.4)	NS
Lymphocytes	0.3 (0.2–0.7)	0.6 (0.3–0.8)	NS
Eosinophils	0.0 (0.0–0.1)	0.0 (0.0–0.1)	NS
Mast cells	0.01 (0.00–0.02)	0.00 (0.00–0.01)	NS
BAL-fluid			
(×10^4 cells·mL^{-1})			
Macrophages	13.9 (8.9–17.6)	14.1 (9.8–16.6)	NS
Neutrophils	0.1 (0.0–0.2)	0.1 (0.1–0.2)	NS
Lymphocytes	0.7 (0.5–1.0)	1.7 (0.9–3.9)	NS
Eosinophils	0.0 (0.0–0.1)	0.0 (0.0–0.1)	NS
Mast cells	0.01 (0.00–0.03)	0.01 (0.01–0.02)	NS

[a] = Data given as medians (interquartile range). Statistical comparisons between groups performed using the Mann-Whitney U-test. NS indicates results were not significant

4.3.2: The Ageing RTLF Proteome: 1D PAGE and nano -LC MS/MS

1D PAGE and nano LC MS/MS proteomic analysis identified 199 and 163 proteins within young and aged RTLFs respectively. One hundred and twenty-four were common to both proteomes, (**Figure 4.2**, see **Appendix B** for a detailed description of all the proteins identified), with the majority, 63 and 78 % of the total proteome in young and aged RTLFs, respectively, being of extra-cellular, or secretory origin. Only 38 proteins were attributed an intra-cellular designation.

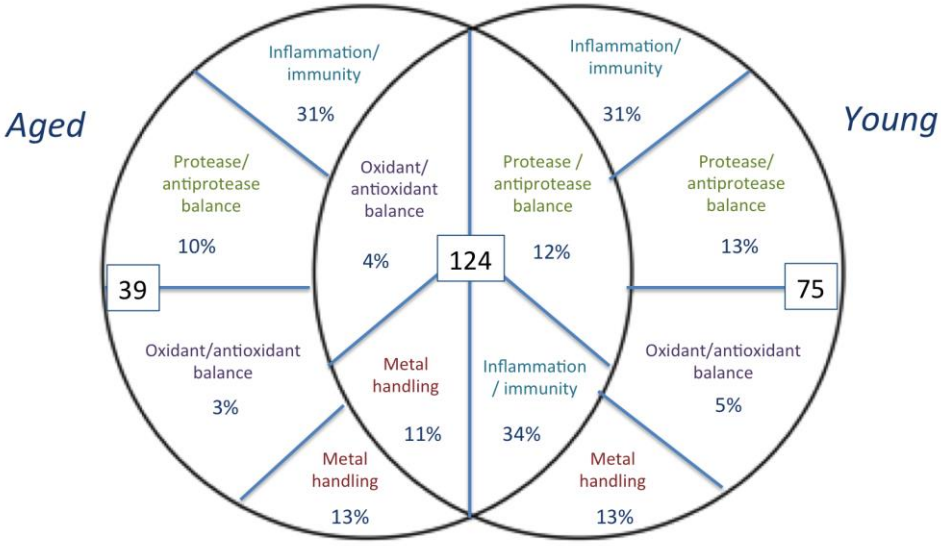

Figure 4.2: *Venn diagram illustrating the proteins common and unique to healthy young and aged alveolar RTLFs, as organised by the most common ontological classifications*. Classifications include: Inflammation and immunity, metal handling, oxidant/antioxidant balance and protease/antiprotease balance, alongside their respective % contributions to the total protein pool. Data is representative of n=5 for both subject groups.

Approximately two thirds of proteins common to young and aged RTLFs were extracellularly derived, either secreted into the RTLFs, or derived from the plasma. Proteins secreted within the airways, i.e. pneumoproteins, contributed only 10% to the identified proteome in both groups; with the proportion of intracellular proteins also similar; 32 and 26% in the young and aged RTLFs respectively.

Proteins uniquely identified in the aged RTLFs included CD166 antigen, a cell adhesion molecule implicated in the priming of T and B cells (Degen et al., 1998) and

ferritin, a large (450 kDa) intracellular Fe storage protein, which has often, been used to signify cellular damage. Further by examining those proteins 'missing' in the aged RTLF (i.e. those unique to 'young' RTLFs), we identified proteins contributing to the antioxidant defence, including SOD (Cu-Zn) and the peroxiredoxins, indicative of a compromised antioxidant network at the air-lung interface. The low molecular weight innate immune peptide defensins were also found absent in aged RTLFs. Proteins responsible for the protease-antiprotease balance of the airways also appeared to be affected by age, with both leucocyte elastase inhibitor and plasma protease C1 inhibitor absent. Cathepsin D an intracellular secreted protease was also absent in aged RTLFs. Interestingly this lysosomal protein is believed to be involved in the induction of autophagy and has previously been implicated in the pathogenesis of age-related diseases (Papassotiropoulos et al., 2000; Steinfeld et al., 2006). Napsin A secreted locally by type II alveolar cells, which has been shown to be important in the processing of surfactant precursors (Woischnik et al., 2008; Chuman et al., 1999), was also absent in the aged RTLF proteome.

Proteins were classified according to their gene ontological definitions. As highlighted in **Figure 4.1**, the largest functional grouping was for proteins involved in inflammation and the immune response at the surface of the lung: 62 and 51 proteins in young and aged RTLFs respectively. This was followed by those with roles in the protease/antiprotease balance (25 (young) and 16 (aged) proteins) and metal handling (25 and 22 proteins respectively). Only 9 and 5 proteins were identified as contributing to the oxidant-antioxidant balance within young and aged RTLFs (see **Appendix B** for full protein lists grouped by ontological definition).

Based on a semi-quantitative comparison of the three most intense precursor ion peaks for the proteins identified, it was clear that the majority of common alveolar proteins decreased with age. **Table 4.4** highlights the fifteen most abundant of the 124 communal proteins (the full list is provided in **Appendix B**), further annotated by their source of origin, ontological definition and the relative fold difference between young and aged RTLFs. All, with the exception of uncharacterized protein C3orf38, a protein of unknown function and origin, are derived from extracellular sources.

Table 4.4: *The most abundant alveolar proteins identified in RTLF samples from young and aged subjects***.** The 15 most abundant proteins common to both young and aged subjects identified (out of 125) are listed alongside their source of origin, ontological classification and relative fold differences. In all cases the proteins listed were identidied in all five of the concentrated BAL fluid samples.

Protein	**Source**	**Ontology**	**Young** (n=5)	**Aged** (n=5)	**Fold difference (Aged v Young)**
Serotransferrin	Extracellular, Secreted	Metal Handling and Transport	1.28E+10	7.62E+09	0.6 ↓ with age
Ig gamma-1 chain C region	Extracellular, Secreted	Immunity and Inflammation	1.23E+10	8.92E+09	0.7 ↓ with age
Ig gamma-3 chain C region	Extracellular, Secreted	Immunity and Inflammation	9.36E+09	6.71E+09	0.7 ↓ with age
Ig gamma-2 chain C region	Extracellular, Secreted	Immunity and Inflammation	9.10E+09	5.60E+09	0.6 ↓ with age
Ig gamma-4 chain C region	Extracellular, Secreted	Immunity and Inflammation	9.10E+09	5.60E+09	0.6 ↓ with age
Ig kappa chain C region	Extracellular, Secreted	Immunity and Inflammation	5.90E+09	3.47E+09	0.6 ↓ with age
Uncharacterized protein C3orf38	Unknown	Unknown	4.10E+09	2.73E+09	0.7 ↓ with age
Serum albumin	Extracellular, Secreted	Metal Handling and Transport	3.97E+09	2.77E+09	0.7 ↓ with age
Ig lambda-2 chain C regions	Extracellular, Secreted	Immunity and Inflammation	3.07E+09	2.31E+09	0.8 ↓ with age
Ig alpha-1 chain C region	Extracellular, Secreted	Immunity and Inflammation	2.81E+09	2.42E+09	0.9 ↓ with age
Alpha-1-antitrypsin	Extracellular, Secreted	Protease/antiprotease	2.69E+09	3.20E+09	0.8 ↑ with age
Ig alpha-2 chain C region	Extracellular, Secreted	Immunity and Inflammation	2.05E+09	1.79E+09	0.9 ↓ with age
Immunoglobulin lambda-like polypeptide 5	Extracellular, Secreted	Immunity and Inflammation	1.96E+09	1.44E+09	0.7 ↓ with age
Ig heavy chain V-III region HIL	Extracellular, Secreted	Immunity and Inflammation	1.66E+09	1.47E+09	0.9 ↓ with age
Ig heavy chain V-III region CAM	Extracellular, Secreted	Immunity and Inflammation	1.22E+09	1.05E+09	0.9 ↓ with age

Table 4.5: *Alveolar proteins demonstrating the largest relative fold decreases with increasing age.* The proteins of the common 125 identified showing the greatest fold decreae with age are listed alongside their source of origin, ontological classification and relative fold differences. Data shown reflects the mean intensity of the three most abundant ion peaks of each protein identified, with an arbitrary fold change cut off threshold of 2.5 used. The number of samples, out of five, in which the proteins were identified, is illustrated.

Protein	Source	Ontology	Young	Aged	Fold difference (Aged v Young)
Annexin A5	Intracellular	Blood coagulation, signalling	6.60E+07 (n=3/5)	1.36E+06 (n=3/5)	48.4 ↓ with age
Pulmonary surfactant-associated protein B	Extracellular, Secreted	Surfactant, Immunity	2.54E+07 (n=4/5)	3.26E+06 (n=5/5)	7.8 ↓ with age
14-3-3 protein beta/alpha	Intracellular	Signalling, Apoptosis	1.07E+08 (n=5/5)	1.46E+07 (n=3/5)	7.3 ↓ with age
Coactosin-like protein	Intracellular	Cell morphology / interaction	3.46E+07 (n=3/5)	5.15E+06 (n=3/5)	6.7 ↓ with age
Carbonic anhydrase 1	Intracellular	Metabolic process	2.36E+07 (n=5/5)	3.91E+06 (n=5/5)	6.1 ↓ with age
Pulmonary surfactant-associated protein A2	Extracellular, Secreted	Surfactant, Immunity	1.95E+08 (n=4/5)	3.74E+07 (n=5/5)	5.2 ↓ with age
Glutathione S-transferase P	Intracellular	Antioxidant/oxidant balance	3.42E+07 (n=3/5)	8.51E+06 (n=3/5)	4.0 ↓ with age
Epididymal secretory protein E1	Secreted and Lysosomal	Lipid transport	5.26E+07 (n=5/5)	1.37E+07 (n=5/5)	3.8 ↓ with age
CC16	Extracellular, Secreted	Immunity and Inflammation	6.27E+08 (n=5/5)	1.74E+08 (n=5/5)	3.6 ↓ with age
Glutathione peroxidase 3	Extracellular	Antioxidant/oxidant balance	1.13E+07 (n=5/5)	3.66E+06 (n=3/5)	3.1 ↓ with age
Haptoglobin	Extracellular, Secreted	Immunity and Inflammation	3.82E+08 (n=5/5)	1.26E+08 (n=5/5)	3.0 ↓ with age

Table 4.6: *Alveolar proteins demonstrating the largest relative fold increases with age.* The proteins of the common 125 identified showing the greatest fold increases with asthma are listed alongside their source of origin, ontological classification and relative fold differences. The number of samples, out of five, in which the proteins were identified, is illustrated.

Protein	Source	Ontology	Young	Aged	Fold difference (Aged v Young)
Dipeptidyl peptidase 4	Extracellular, Secreted	Protease/antiprotease , signalling, apoptosis	1.64E+07 (n=3/5)	6.17E+07 (n=3/5)	3.8 ↑ with age
Alpha-2-macroglobulin	Extracellular, Secreted	Protease/antiprotease	6.75E+07 (n=5/5)	1.66E+08 (n=5/5)	2.5 ↑ with age

Focusing on age-related differences across the entire proteome, the greatest fold differences were noted for intracellular signalling proteins annexin a5 and 14-3-3 protein beta/alpha, decreasing 48 and 7 fold in the aged population, **Table 4.5**. A similar pattern was observed with coactosin like protein, an F-actin binding intracellular protein predominantly expressed in the lungs. Glutathione-S-Transferase and glutathione peroxidase 3, two key proteins involved in the phase II xenobiotic metabolism (Ketterer, 1982) and antioxidant defense (Erzurum et al., 1993; Cross et al., 1994)) exhibited a 4 and 3 fold decrease respectively; with haptoglobin concentrations, a protein with both antioxidant and antimicrobial properties (Yang et al., 1995; Verrills et al., 1994), also observed to decrease with age, **Table 4.5**. Proteins unique to the airways, including SP-A, SP-B, secreted by type II pneumocytes and CC16, secreted by bronchial Clara cells (Hermans and Bernard, 1999) were also reduced within the aged RTLFs (8, 5 and 4-fold respectively), **Table 4.5**. Only two proteins were found to be elevated within the aged RTLFs: dipetidyl peptidase 4 and alpha 2 Macrogobulin (**Table 4.6**).

Using the proteomic data as a guide, a more quantitative analysis of the most abundant proteins was performed across all samples in each group. Again, as with the previous analysis in Chapter 3 the objective was to account for in excess of 70% of the total RTLF protein pool, which was the arbitrary cut off we employed for simulant design. Total alveolar protein concentrations were significantly elevated in the aged alveolar RTLFs: 35.3 (21.0-52.1) versus 13.8 (11.6-24.0) mg/mL, P=0.001. Correspondingly concentrations of albumin were also significantly elevated within the aged airways, approximately 3.5 fold greater than within young alveolar RTLFs: 28.1 (23.1-35.9 and 7.8 (5.9-9.0) mg/mL P=0.0001, **Figure 4.3**. In contrast, although total bronchial protein concentrations were increased in the aged population, the approximate 2-fold increase failed to attain statistical significance: 0.07 (0.04-0.1) and 0.035 (0.03-0.05) mg/mL, with equivalent albumin concentration in the two groups: 23.6 (19.9-32.7) and 24.1 (16.0-30.0) mg/mL, **Figure 4.4**.

Alveolar transferrin concentrations were equivalent in the aged and young groups: 1.2 (0.5-1.6) [*aged*] and 0.9 (0.6-1.7) mg/mL [*young*] (**Figure 4.2**), but were significantly lower in the bronchial RTLFs in the aged group: 0.89 (0.5-1.2) mg/mL versus 1.91 (1.3-2.8) mg/mL, P=0.01, **Figure 4.4**. In contrast, alpha-2 macroglobulin was significantly elevated in the alveolar RTLF within the aged group only: 0.07 (0.04-0.23) versus 0.01 (0.005-0.02) mg/mL, P= 0.008, **Figure 4.5**. Both alveolar and bronchial RTLF alpha-1 antitrypsin concentrations were equivalent in the aged and young groups, **Figure 4.5** and **4.6**.

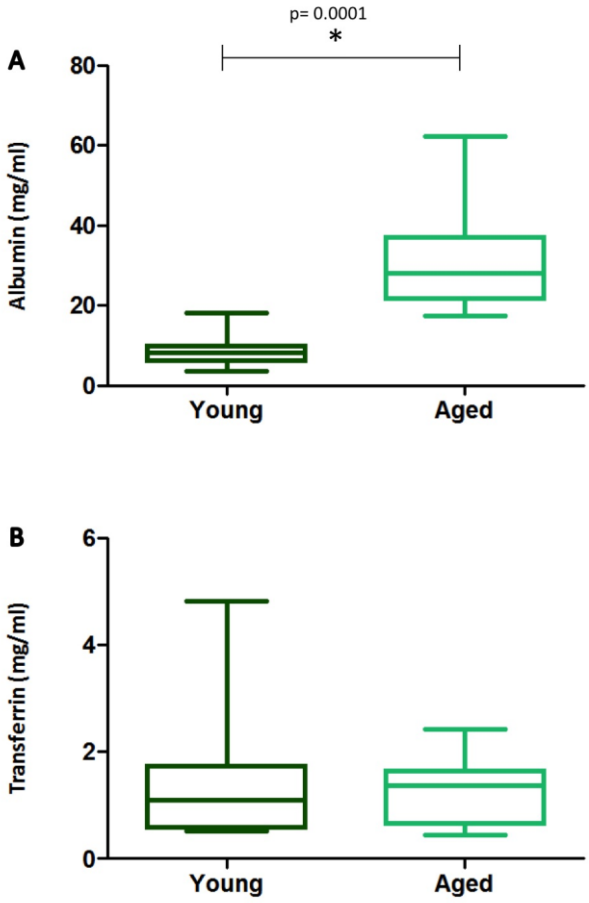

Figure 4.3: *Transport and metal handling proteins of the alveolar RTLFs.* Alveolar protein concentrations as determined by ELISA, with values corrected for lavage dilution using the urea method. **(A)** Albumin and **(B)** Transferrin. Data are illustrated as box plots, with the central line indicating the median concentration, the lower and upper boundaries of the box, the 25th and 75 percentiles, respectively, and the whiskers the 95% confidence interval. Healthy young non-smoker n=16, healthy aged non-smoker n=14, * denotes a statistical difference where $p<0.05$.

Of the RTLF innate immunity proteins only IgA was significantly higher in the aged alveolar proteome: 1.5 (0.9-2.1) versus (0.7(0.5-0.9) mg/mL, P= 0.0001, with

equivalent concentrations of IgG: 2.2 (1.0-3.6) and 1.5 (0.9-2.5) mg/mL and haptoglobin; 0.05 (0.02-0.07) and (0.08 (0.07-0.1) mg/mL, **Figure 4.7.** In contrast within the bronchial RTLFs, no aged related differences were noted in either IgA or IgG, but a significant age-related decrease in haptoglobin was noted: 2.2 (1.0-3.6) and 1.5 (0.9-2.5), P=0.003 (**Figure 4.8**).

Surfactant proteins A and B were both observed to decrease significantly in alveolar RTLFs of the aged group: 0.3 (0.2-0.5) versus 1.04 (0.5-1.3) mg/mL and 0.0045 (0.003-0.006) versus 0.009 (0.008-0.01) mg/mL, P=0.0001 and 0.021 in the aged and young respectively, **Figure 4.9**, with the age related decline in SP-A also evident in the bronchial RTLFs: 0.17 (0.13-0.45) and 1.15 (0.86-1.5) mg/mL, P=0.0001, **Figure 4.10**. A similar trend for an age-related decrease in SP-B was also observed in the bronchial RTLFs, but this failed to attain statistical significance: 0.007(0.004-0.01) and 0.61 (0. 4-1.1) mg/mL. CC16 revealed no such significant declines with age in either the alveolar: 0.07 (0.04-0.1) and 0.035 (0.03-0.05) mg/mL; or bronchial RTLFs: 0.003 (0.002-0.005) and 0.06 (0.04-0.01) mg/mL in aged and young samples respectively, **Figures 4.9** and **4.10**.

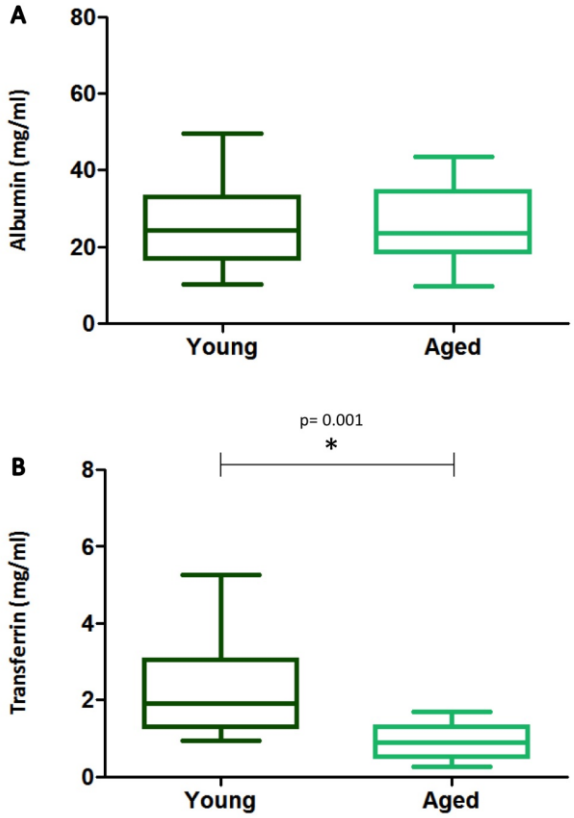

Figure 4.4: *Transport and metal handling proteins of the Bronchial RTLF.* Details as outlined in the legend to **Figure 4.3**.

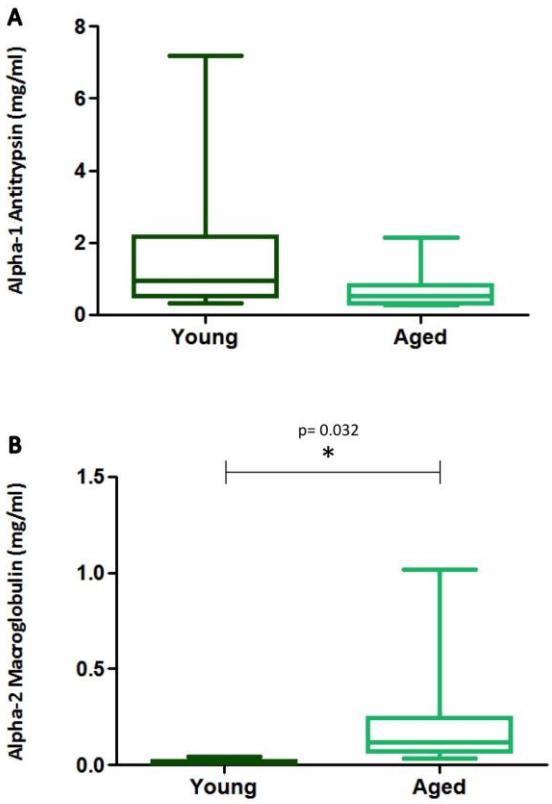

Figure 4.5: *Airway antiproteases in the alveolar RTLFs.* Panel **(A)** alpha-1 Antitrypsin and **(B)** alpha-2 Macroglobulin. All other details as outlined in the legend to **Figure 4.3**.

Considering the relative contributions of the individual proteins to the total protein pool, only albumin was noted to increase markedly within aged alveolar RTLFs: 85 (82–90) versus 48 (33–62) %, see **Figure 4.11**. With the exception of IgA: 5.6 (1.4–7.7) versus 4.8 (3.3–5.6)%, and alpha-2 macroglobulin: 0.1 (0.09–0.15) versus 0.09 (0.04–0.13)%, which represented similar proportions in both the aged and young proteomes, the remaining proteins contributed markedly lower proportions in the alveolar RTLF. Considering the bronchial RTLFs, again the proportion of albumin: 65 (40-77) and 55 (47-89) %, alongside alpha 2-macroglobulin: 0.27 (0.0-0.65) and 0.08 (0.07-0.1)%, were increased within the aged proteome, with lower % contributions from the remaining measured proteins, **Figure 4.12**.

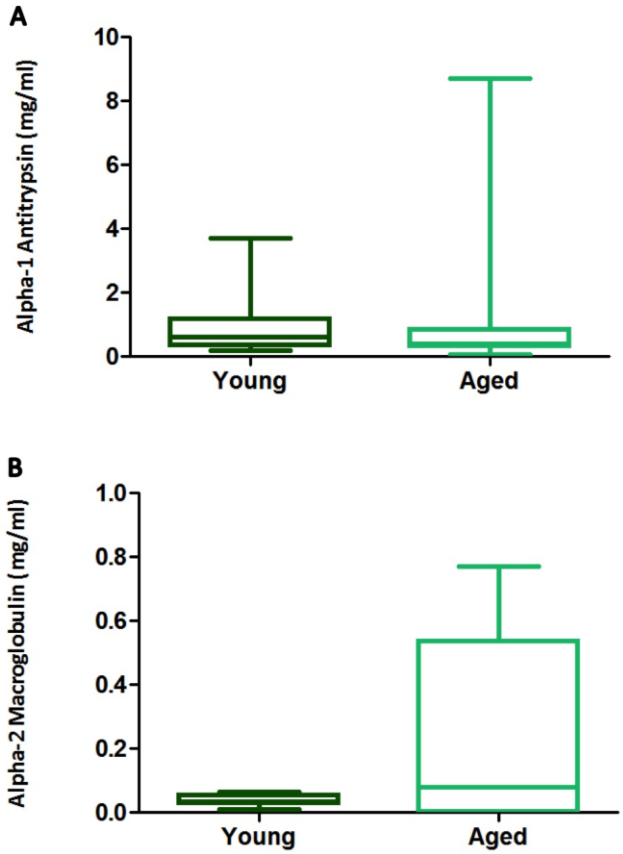

Figure 4.6: *Airway antiproteases in the bronchial RTLFs.* Panel **(A)** alpha-1 Antitrypsin and **(B)** alpha-2 Macroglobulin. All other details as outlined in the legend to **Figure 4.3**.

To fully explore the impact of a potential imbalance of the oxidant-antioxidant handling within the ageing RTLFs, aged and young bronchoalveolar lavage samples were analysed for a panel of low molecular weight antioxidants (ascorbate, urate, and glutathione), together with markers of oxidative injury: protein carbonyls, 4-hydroxynonenal protein adducts and glutathione disulphide. Insufficent material was available to perform these analyses in the bronchial compartment. Individual lavage urea corrections factors were determined (**Section 2.5, Tables 2.2a and 2.2b)** and applied to the antioxidant concentrations measured in the lavage samples, to derive undiluted RTLF antioxidant concentrations, as illustrated in **Table.4.7.**

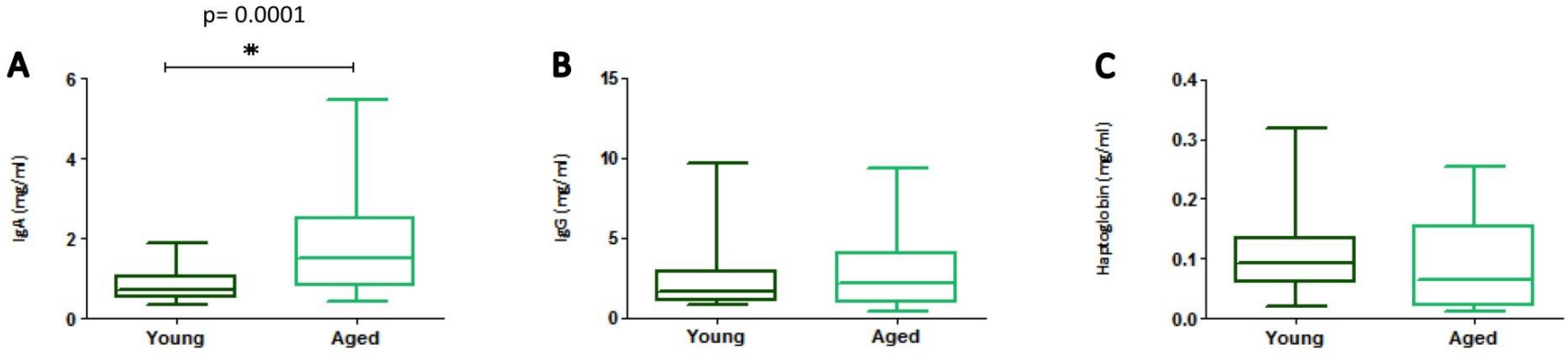

Figure 4.7: *Innate immunity proteins of the alveolar RTLFs.* Panel **(A)** IgA, **(B)** IgG and **(C)** haptoglobin. All other details as outlined in the legend to **Figure 4.3**.

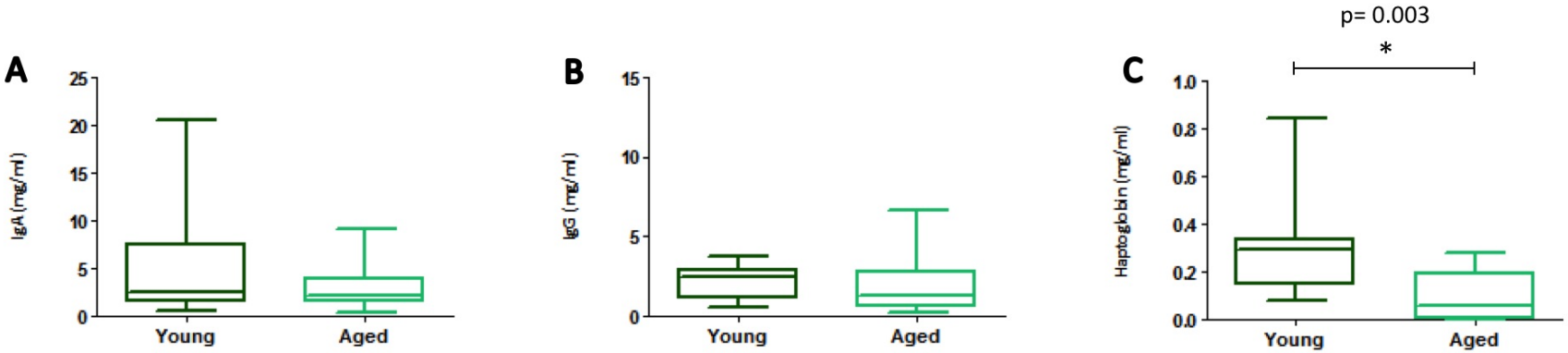

Figure 4.8: *Innate immunity proteins of the bronchial RTLFs.* Panel **(A)** IgA, **(B)** IgG and **(C)** haptoglobin. All other details as outlined in the legend to **Figure 4.3**.

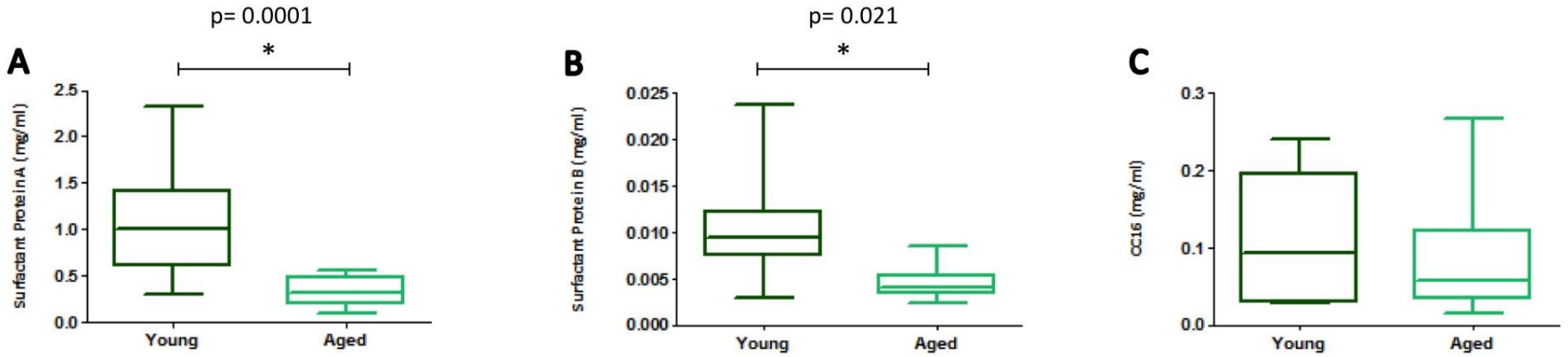

Figure 4.9: *Alveolar RTLF pneumoproteins.* Panel **(A)** surfactant protein-A, **(B)** surfcatant protein-B and **(C)** CC16. All other details as outlined in the legend to **Figure 4.3.**

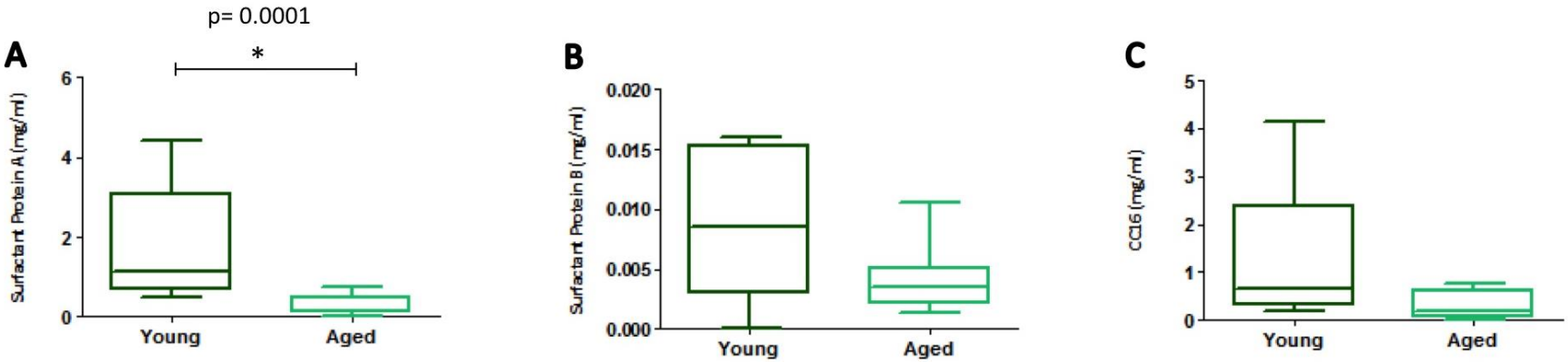

Figure 4.10: *Bronchial RTLF pneumoproteins.* Panel **(A)** surfactant protein-A, **(B)** surfcatant protein-B and **(C)** CC16. All other details as outlined in the legend to **Figure 4.3.**

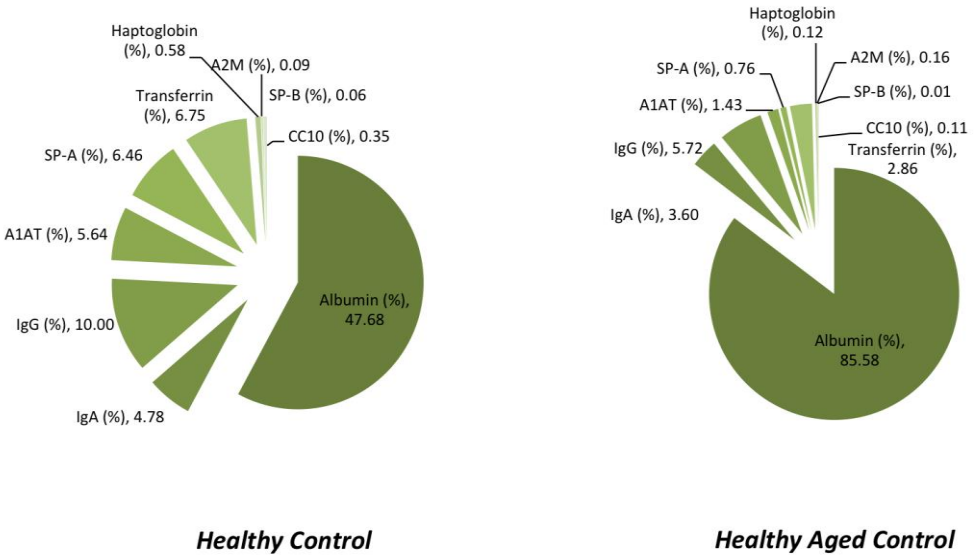

Figure 4.11: *Percentage contributions of individual alveolar protein components relative to the total RTLF protein***.** Proportions are represented as median values.

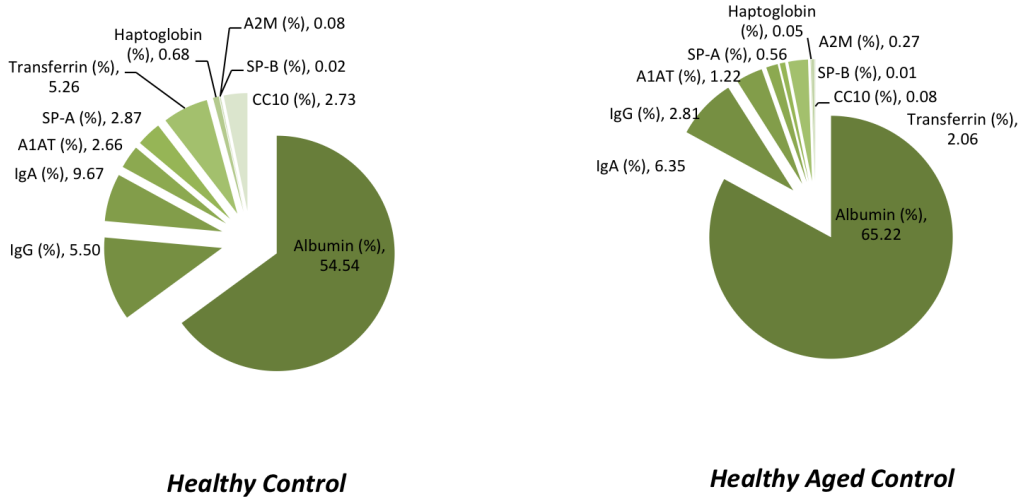

Figure 4.12: *Percentage contributions of individual bronchial protein components relative to the total RTLF protein***.** Proportions are represented as median values.

Table 4.7. *Low molecular weight antioxidants in alveolar RTLFs fron young and aged subjects.*

	Young	Aged
Vitamin C (□M)	141.5 (110.7-198)	80.4(46.0-119.3)
Ascorbate (□M)	122.1 (97.7-154.3)	0.00 (0.00-2.54)**
Dehydroascorbate(□M)	1.22 (1.12-1.30)	66.7 (35.5-94.3)
Urate (□M)	95.5 (59.0-107.7)	86.2 (64.1-184.8)
GSx (□M)	161.6 (128.0-243.9)	141.1 (128.9-190.1)
GSH (□M)	137.2 (114.3-184.7)	118.9 (82.8-154.5)
GSSG (□M)	3.4 (0-25.9)	11.1 (0-39.5)
GSSG:GSH	0.15 (0.09-0.22)	2.75 (2.26-3.31)**

Data represents median values and the interquartile range, where n=16 for healthy young subjects, n=13 for healthy aged subjects. * denotes a statistical difference where $p<0.05$, ** denotes a statistical difference where $p<0.001$.

4.3.3: The oxidant-antioxidant imbalance in ageing RTLFs

Vitamin C concentrations were lower within the aged alveolar RTLFs: 80.4 (46.0-119.3) versus 141.5 (110.7-198) □M, see **Table 4.7**. This difference was highly significant when ascorbate concentrations were considered (P=0.001) with non-detectable levels observed in the majority of the aged subjects. This was associated with a corresponding increase in the concentration of dehydroascorbate, though this failed to attain statisitical significance due to the large inter-individual variation in concentration. No other statistically significant differences in the antioxidants measured were observed, though the concentrations of glutathione disulphide were increased within the aged RTLFs (non-significantly), and the ratio of the oxidised to reduced form of glutathione was significantly increased with age: 2.75 (2.26-3.31) versus 0.15 (0.09-0.22) respectively, P=0.0001, consistent with oxidative stress within the aged RTLF, **Table 4.7**.

These changes in ascorbate concentration and glutathione disulphide/glutathione ratio occurred parallel to an increase in the total protein carbonyl concentration in the aged group: 69.8 (66.0-89.7) nmol (aged) versus 26.3 (18.7-33.5) nmol (young). However when the data was expressed per unit of concentration of RTLF protein, this increase in carbonyl protein adduct was no longer significant: 367.5(280.3-471.4) versus 267.5 (169.3-355.9) nmol/mg protein, **Figure 4.13**. Within the ageing bronchial RTLFs no significant change in carbonyl adduct formation was observed: 859.1(192.33-2492.9) and 1346.8 (1065.6-1759.7) nmol/mg RTLF protein, between young and aged RTLFs

respectively, **Figure 4.14**. It was notable however that when protein carbonyl concentrations in the bronchial RTLFs were compared against those in the alveolar compartment there was a significant elevation in concentration in the former compartment, **Figures 4.13** and **4.14**, consistent with a more oxidizing environment in the upper airways, though this regional difference was most marked in the young group. Consistent with evidence of oxidative stress in the aged group, concentrations of 4-HNE protein adducts were significantly elevated, 4.5 fold, in the aged alveolar RTLFs: 425.0 (384.0-489.0) versus 94.2 (54.9-116.4) □g/ml per mg of protein. Unfortunately insufficient bronchial wash was available for 4-HNE measurements to be made in this compartment.

Finally, based on the results obtained in **Chapter 3**, I decided to examine age dependent changes in transition metals concentrations within the RTLF. This analysis was restricted to the determination of BAL fluid Cu, Zn and Fe concentrations. Whilst no statistical difference was noted in Cu or Zn concentrations with age, total Fe concentrations appeared significantly elevated in the aged alveolar RTLFs: 5.14 (4.8-5.4) □M versus 2.34 (2.3-2.4) □M, **Figure 4.15**. No statistically significant correlations were observed between transition metals with markers of protein oxidation (protein carbonyl or 4-HNE adducts) or RTLF antioxidant concentrations.

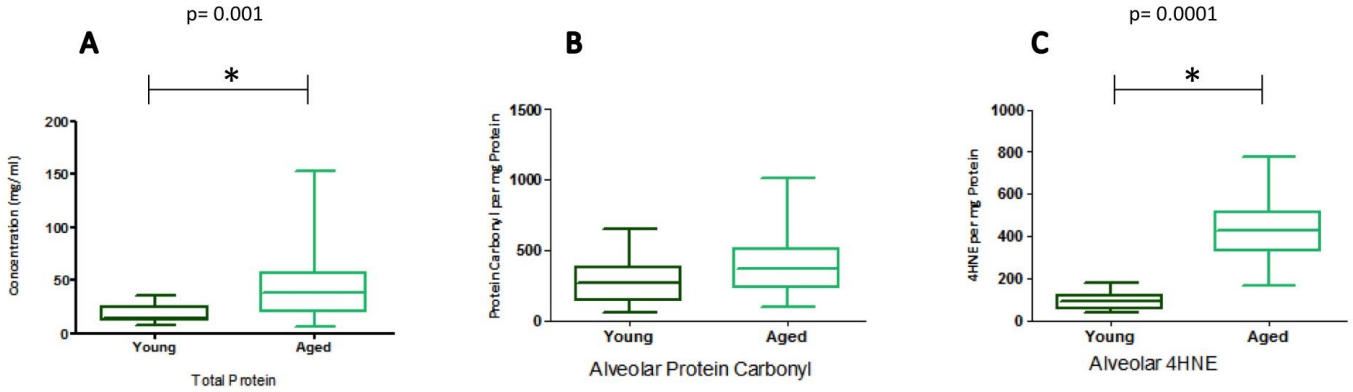

Figure 4.13: *Total alveolar RTLF protein (A) , protein carbonyl (per mg protein) (B) and 4-HNE adduct (per mg protein) concentrations (C) in young and aged subjects.* * denotes a statistical difference where $p<0.05$.

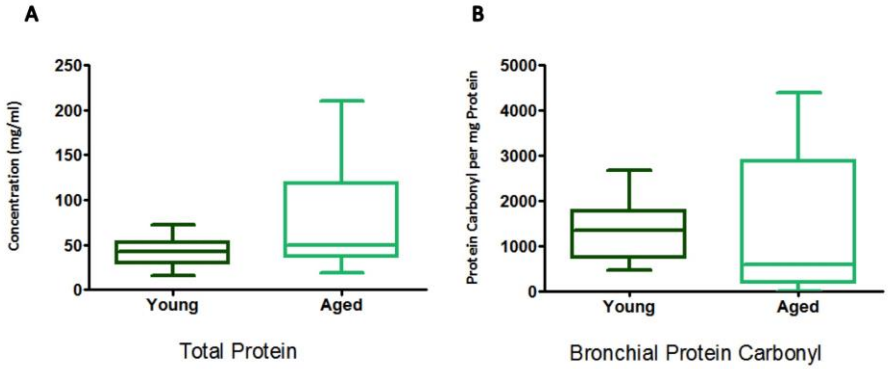

Figure 4.14: *Total bronchial RTLF protein (A) , protein carbonyl (per mg protein) (B) and 4-HNE adduct (per mg protein) concentrations (C) in young and aged subjects.* * denotes a statistical difference where $p<0.05$.

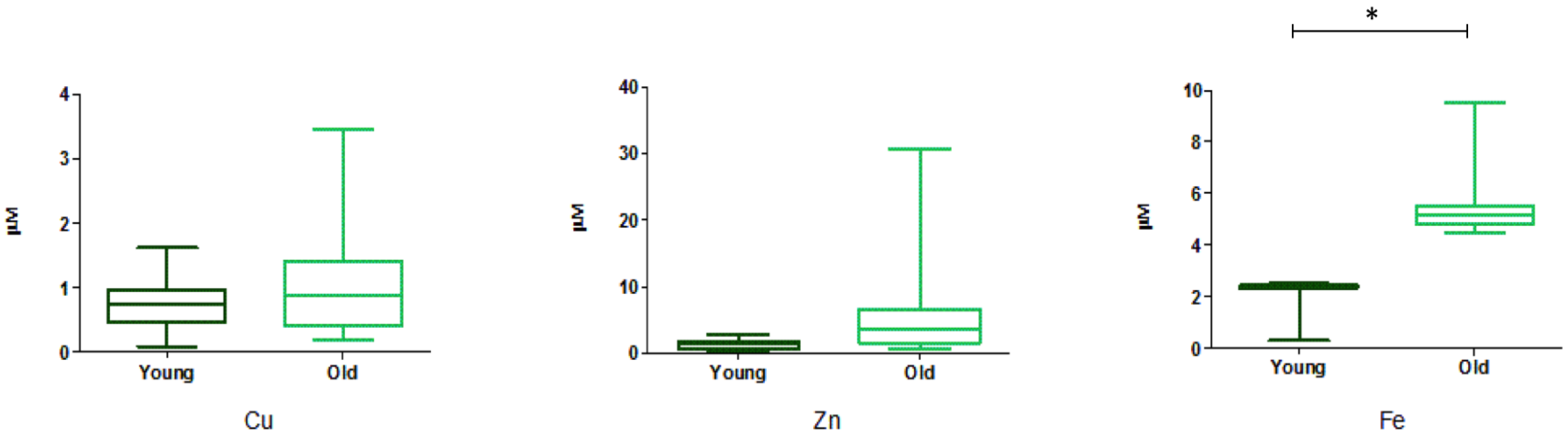

Figure 4.15: *The concentrations of metals: Cu, Zn and Fe, in aged and young bronchoalveolar lavage samples.* Healthy young non-Smoker n=16, healthy aged non-smoker n=13, * denotes a statistical difference where $p<0.05$.

4.4: Discussion

The primary aim of this analysis was to characterize the composition of the RTLFs in healthy aged individuals, reflective of the normal ageing process, independent of disease. In light of the previous literature demonstrating both deterioration of antioxidant and innate immune defences with age in other organs (Mahbub et al., 2011;Vida et al., 2011; Fernandez-Real and Pickup, 2012; Solana et al., 2012; Shaw et al., 2013; Vitale et al., 2013) I hypothesised that similar changes would occur in the lung, altering the composition of the RTLFs and increasingly pulmonary susceptibility to various extrinsic and intrinsic factors.

The ageing lung is characterized by a well defined decline in lung function (Anthonisen et al., 1986), associated with low grade chronic inflammation (Ito and Barnes, 2009; Okamoto et al., 2012), and the imposition of oxidative stress, reflecting increased ROS generation against a background of deteriorating antioxidant defences. Together these progressive changes result in the formation of the 'senile lung', increasing the lungs susceptability to respiratory infections and other inhaled xenobiotics. Despite the importance of respiratory infections in the aged population surprising little is known concerning age-related changes to the composition of the RTLFs during normal physiological ageing, with the majority of studies focusing on respiratory disease. In this study I attempted to fill this data gap by performing a detailed compositional analysis in healthy and aged adults. The key observations were as follows:

1. There were no differences in the ontological classes of proteins identified across age groups, or their source of origin.
2. A general dysregulation of the immune and inflammatory processes within the ageing RTLFs was evident.
3. An age-related dysregulation of protease-antiprotease was not seen.
4. A pro-oxidant shift in the RTLF redox balance was seen in the aged population.

While numerous previous studies have employed MS based proteomics to assess the nature of the airways under disease conditions, only two such studies have investigated healthy ageing in the airways (Merkel et al., 2005 and Ohlmeier et al., 2008). As with this investigation, Merkel utilized BAL fluid samples, though without pre-concentration, combining a nano LC MS/MS method with Surface-Enhanced Laser

Desorption/Ionization (SELDI) MS for identification. In contrast to the present study where individual samples within each group were analysed separately, in their analysis the 5 samples investigated were pooled to provide a single representative sample, with only 60 individual proteins identified, across all of the investigated groups; COPD smokers and healthy smoking subjects were also included. Ohlmeier et al (2008) focused their analysis on lung tissue and induced sputum retrieved from subjects, preventing simple comparisons with our investigation, in addition, in this study they limited themselves to a 2-D approach, quantifying and comparing specific proteins identified by western blot anlaysis

In this context, the current investigation is unique in that it directly addresses the impact of normal physiological ageing, without the presence of concomitant age-related disease. It employs a more stringent analytical approach, with panels of individual samples (n=5 per group) analysed after pre-concentration, to both encompass normal inter-individual variability and optimize the detection of relatively low abundance proteins, that would otherwise not be detectable within dilute lavage samples. The majority of early investigations into the RTLF proteome utilized a 2-DE approach, however the nanoLC MS/MS methodology employed in this investigation not only allows for the identification of a larger number of proteins, with a higher degree of certainty, it also permits a semiquantitative comparison of relative changes in MS signal intensities. Here, in line with good analytical practice the semiquantitive MS based approach was employed as an exploratory tool, alongside an antibody based approach, to validate any changes oberved (Bodarenko et al., 2002; Chelius et al., 2003; Wang et al., 2003; Liao et al, 2004; Wu et al., 2005).

As with **Chapter 3** we focused our attention on the high abundance proteins of the RTLFs to guide the design of lung lining fluid simulants. Using this approach I was again able to account for in excess of 70% of the total alveolar and bronchial RTLF protein pool. My investigation also demonstrated significantly elevated total protein and albumin concentrations within the alveolar RTLFs of the aged group. To date only a single investigation has examined RTLF albumin concentrations during ageing, demonstrating significantly elevated albumin concentration across both bronchial and distal airway lavage samples, consistent with the present result (Thompson et al., 1992). Intriguingly this major plasma protein has previously been reported to decline in serum with age and has been used as a predictor of subclinical disease in otherwise healthy elderly patients (Campion et al., 1988; Salive et al., 1992). However a more recent study

has ruled this out, revealing no age related changes in the synthesis or concentration of this protein, associated with declining health status (Schalk et al., 2004).

Proteins related to immunity and inflammatory responses represented the greatest proportion of the proteome by number, in both groups. IgA, a key component of mucosal immunity, often regarded as a bridge between innate and adaptive responses was observed to increase in the alveolar RTLF with age, with a similar trend evident in the bronchial RTLFs. IgA, within the upper respiratory tract, is produced locally by B cells within the mucosa, the airway epithelium plays a vital role in maintaining concentrations of the secreted form within the RTLF, through expression of the polymeric immunoglobulin receptor (PigR). The pIgR is considered an essential part of airway antibody immunity, restricted to mucosal and glandular epithelia, where it is responsible for binding polymeric IgA at the basolateral surface of the lung epithelium, transporting the secreted complex to the airway lumen and thus into the RTLFs (Kuhn and Kraehenbuhl, 1981; Jaffar et al., 2009). In the present study despite PIgR's significant role in the transycotis of secretory IgA, it was actually found to decrease three fold, based upon our semiquantitative proteomic analysis, with age.

During the transcytosis of dimeric IgA onto the apical surface by pIgR, a cleavage occurs separating what is known as the extracellular secretory component from the transmembrane receptor segment as part of the secretory form of IgA. Unfortunately the antibody based ELISA used in this study is unable to distinguish the form (serum or secretory) of IgA within the RTLFs sampled. Interestingly however the J chain, responsible for linking IgA dimers of the secretory phenotype, was absent in the proteomic investigation of aged RTLFs. IgG, the most abundant plasma derived immunoglobulin, demonstrated no such difference in either the bronchial or alveolar regions of the airways with age.

In line with our observations, previous studies have also demonstrated the production of immunoglobulins by bronchial lymph nodes to be more efficient within the airways of aged individuals. The BAL cooperative study (1990), a multicenter study involving 198 volunteers, demonstrated increased IgA and IgG in the aged airways, however the subjects recruited included both smokers and non-smokers making interpretation of the findings difficult. Meyer et al. (1996) similarly reported significantly increased concentrations of IgA in RTLFs from non-smoking aged individuals (in addition to IgM), in the absence of a similar increase in IgG. A study by Thompson et al (1992) however was unable to demonstrate consistent differences for IgA, in aged

bronchial and alveolar RTLFs, and in contrast to our study reported significantly increased IgG concentrations with age.

Whilst lysozyme was also elevated within the aged alveolar RTLFs, beta2 microglobulin, lactotransferrin, galectin-3 and complement c3 and complement factor B were all diminished within the aged airways, according to the proteomic analysis. These proteins also form an important component of immune defences of the mucosal airways. Further, the major family of antimicrobial peptides, defensins, associated with mucosal immunity undetected in aged RTLFs using MS/MS methodology, yet consistently present across all healthy young control samples analyzed. Thus the overall picture that emerges is one of innate immune dysregulation with age, rather than a simple global downregulation of innate immunity proteins. This may reflect a general drift towards cellular senescence in the aged airway. As the number of senescent cells increases with age, there is evidence of a senescence associated secretory phenotype that promotes the secretion of a series of proinflammatory cytokines, chemokines, growth factors and remodeling factors, which together may contribute to the presence of a low level chronic inflammation in age, furthermore altering local tissue structure and function (Campisi, 2003; Campisi, 2005; Ohtani and Hara, 2013; Kuilman et al., 2010; Rodier and Campisi, 2011). The presence of chronic BAL inflammation in the ageing airways may however also be beneficial, by permitting a natural, non-injurious and efficient exit of pro-inflammatory cells through apoptotic and phagocytic pathways (Persson and Uller, 2010).

The reduced concentrations of haptoglobin within the aged alveolar RTLF identified by the semi-quantitative proteomic analysis were confirmed in the full panel of subjects using ELISA in both the bronchial and alveolar samples. This plasma protein synthesized predominately by hepatocytes, but also by lung epithelial cells and in alveolar macrophages (Yang et al., 1995; Sung-Min Kang et al., 2011), possesses antimicrobial, antibacterial and antioxidant properties by sequestering haem iron. Whilst no previous studies have reported changes in the expression of this protein with age, the presence of chronic inflammation within the ageing lungs may play a role in modifying the expression of this protein. Haptoglobin is part of the acute phase response, during acute inflammation and infection, with its expression regulated by several cytokines associated with the response (IL1, IL-6, TNF alpha). It is therefore tempting to speculate that the decreased concentrations in the aged RTLF may imply the altered expression of these regulatory inflammatory cytokines under chronic inflammation of the ageing airways

(Okamoto et al., 2012), though it should be noted that in the present study no evidence of chronic inflammation was observed in our aged population.

This investigation also revealed that SP-A, a member of the collectin family of glycoproteins, secreted by alveolar type II cells and non ciliated bronchial cells was significantly decreased in the bronchial and alveolar RTLF of aged individuals. An investigation by Betsuyaku et al. (2004) also reported bronchial concentrations of surfactant protein A to be decreased in older (non-smoking) subjects, however the bronchoalveolar concentrations in their investigation demonstrated no such age-dependence. While SP-A plays an important role in surfactant stabilization, it also confers innate immunity to the distal airspaces (Wright, 1997; Crouch, 1998; Eggleton and Reid, 1999; Lawson and Reid, 2000), facilitating the clearance of microorganisms by the opsonization and agglutination of a broad range of pathogens and particles, enhancing phagocytosis (Tenner et al., 1989; Van Iwaarden et al., 1990). No previous studies have examined altered surfactant protein expression as a result of normal physiological ageing, unassociated with extrinsic factors such as smoking or COPD. A decline in the function of alveolar type II pneumocytes has however been reported, associated with the remodeling of the lung parenchyma with age, this may contribute to the decrease in SP-A secretion observed in this study (Janssens et al., 1999). It has also been suggested SP-A may serve as an indicator of epithelial integrity, with the decrease in RTLF SP-A concentrations possibly reflecting its retrograde diffusion from the surface of the lung into the plasma pool (Betsuyaku et al., 2004). To date however no such changes in alveolar epithelial permeability have been shown to occur with age.

SP-B was also observed to decline in the ageing alveolar RTLFs. This surfactant protein is also secreted by type II pneumocytes, but has no function in immunity, with its predominant role being the maintenance of alveolar stability by lowering surface tension at the air-liquid interface (Revak et al., 1988; Suzuki et al., 1989; Williams et al., 1991). Given the similar response to SP-A, it seems likely that the reduced concentrations of both of these proteins may reflect a similar underlying mechanism and suggests an age related impairement in the function of type II cells.

The final pneumoprotein investigated in detail was CC16; a major secretory protein within the airways. The precise function of this protein remains unknown, however its role in inflammatory processes within the airways has long been hypothesized (Evans et al. 1978, Plopper et al. 1992). Secreted by the nonciliated bronchiolar Clara cells, it is perhaps unsurprising that CC16 was significantly elevated in the conducting young bronchial RTLFs. Concentrations of CC16 were not altered

between the aged and young groups in either the upper or lower airway. As CC16 has been used extensively as a marker of lung epithelial/endothelial barrier permeability (Hermans and Bernard, 1996; Blomberg et al, 2003), the fact that it did not behave in the same manner as SP-A or SP-B further supports the contention that the decreased concentrations of these two proteins reflect defective production by type II pneumocytes.

The protease/antiprotease balance of the aged airway is particularly important in the understanding of the structural changes occurring within the aging airway. Interestingly the present data failed to show any age-related change in the major antiprotease of the airways, alpha-1 antitrypsin (α1AT). Whilst inherited deficiencies of this antiprotease are associated with the development of early onset emphysema (Eriksson, 1965; Kueppers and Black, 1974), Meyer et al. (1998) previously reported increased levels of α1AT /neutrophil elastase complex in older subjects, in contrast to our observations. This was related to the presence of infiltrating neutrophils, routinely observed in older airways, though not in our present study. Our MS/MS proteomic analysis was unable to detect neutrophil elastase or other degradative enzymes including the Cathepsin family of lysosomal proteases, implicated in diseases of the aged airways such as emphysema (Papassotiropoulos et al., 2000; Steinfeld et al., 2006). Our results suggest the protease-antiprotease balance of the airways does not appear to be dysregulated in healthy ageing in the absence of overt inflammation.

In contrast to α1AT, our study demonstrated significantly elevated concentrations of alpha 2 Macroglobulin (A2M), another major antiprotease in both the bronchial and alveolar RTLFs in aged subjects (based upon both MS/MS and antibody quantification). A2M has been heavily linked to diseases of ageing: genetically with Alzheimers disease, as a result of its role in the clearance and degradation of amyloid beta (Blacker et al., 1998) and with diabetes, where it has been observed to be found significantly elevated with age (James, 1990). A2M has the capacity to recognize and bind a broad spectrum of proteinases, forming complexes that are subsequently recognized and cleared by alveolar macrophages (Marchandise et al., 1988; Starkey et al., 1977; Strauss et al., 1999; Armstrong and Quigley, 2001). It also has a key immunoregulatory role, with the A2M receptors of the alveolar macrophage presenting an important clearance mechanism for the pro-inflammatory cytokine IL-8, and with A2M having also been demonstrated to modulate inflammatory T cell responses (Kurdowska et al., 2000). A2M has also been implicated as a marker of airway plasma exudation (Cucullo et al., 2003; Hye et al., 2006), as it increases rapidly following acute lung injury (Jorens, 1995; Out, 1987). In the

absence of significant increases in the permeability of the epithelial/endothelial barrier as a consequence of ageing in the present study (based on the equivalent urea ratios), the increases in A2M observed cannot be explained by this phenomenon.

As stated previously the RTLF possesses a robust antioxidant network under normal conditions that protects the underlying epithelium from oxidant injury from inhaled xenobiotics and acute inflammatory episodes. Ascorbate concentrations within the alveolar RTLFs were significantly reduced, often to non-detectable levels in the aged subjects, with a corresponding increase in its oxidation product dehydroascorbate. Whilst such deficiencies at the air lung interface have been reported previously, associated with asthma (Kelly et al., 1999), the inhalation of oxidants (Kelly et al., 1996; Mudway et al., 2001) and inflammation (McGrath et al., 1999), the presence of active neutrophilia is usually a cardinal feacture of these conditions. In the current study, in the absence of clear inflammation in the aged subjects, the deficiency may simply reflect low vitamin C intakes in the elderly (Kelly and Mudway, 2003), though the fact that this was seen in parallel to increased GSSG/GSH ratios and evidence of protein oxidation (4-HNE adducts) suggests an increased oxidative burden in the lung, independent of neutrophilic inflammation. Investigations using the Senescence-accelerated mouse model of ageing have also reported similar changes in GSSG/GSH ratio, in both BAL fluid and lung tissue with age (Teramoto et al., 1994).

The increase in 4-HNE adducts, together with the increased total protein and albumin observed in the aged RTLF, suggest the accumulation of oxidatively modified proteins within the normal aged airway, which may therefore impair normal clearance mechanisms. A study by Umstead et al. (2009) investigating proteins associated with healthy ageing in rat airways, has demonstrated that in addition to changes in protein concentration, specific proteins possess a higher potential to from adducts during periods of oxidative stress. The importance of these oxidative post-translational modifications depends on whether they cause functional consequences. For example, oxidation of a critical Met residue in alpha-1 antirtypsin, results in its loss of function (Taggart et al., 2000), actin carbonylation results in functional impairment of filament formation (Conrad et al., 2001) and albumin oxidation reduces its binding capacity (Iwao et al., 2006; Oettl and, Stauber, 2007). Unfortunately due to experimental limitations, this investigation was unable to determine which proteins, if any, were more sensitive to adduct formation and the role this may play within the ageing process still requires clarification.

I also examined the concentration of transition metals within the RTLFs as a potential cause for the observed oxidative imbalance within the aged airways. The maintenance of metal ions within strict physiological limits as a result of their great catalytic and redox potential is essential, and thus proteins directly involved in the 'handling' (storage, transport and sequestration) of metals possess crucial antioxidant roles (Bertini and Cavallaro, 2008; Jomova and Valko, 2011). In this study we observed significantly elevated total Fe concentrations within the aged RTLFs. This is consistent with previous reports demonstrating increased free non-haem bound iron in infection, fibrosis and neoplasms (Munro and Linder, 1978; Worwood, 1982; Erbaycu et al., 2007). Similarly studies in the ageing non-smoking airways of both humans and animals have also demonstrated elevated free iron, with extrinsic factors, such as smoking, only serving to further elevate these concentrations (Ghio et al.,1997).

The majority of biological Fe is not however 'free', with approximately two thirds bound to hemoglobin, 10% reserved for cellular processes through myoglobin, cytochromes, and iron-containing enzymes, with the remainder found in iron storage proteins such as ferritin (Cheng and Li, 2007). Iron concentrations are maintained in the RTLFs by their high affinity for Transferrin and Lactoferrin (Young and Woodside, 2001), and MS/MS proteomic analysis revealed both these proteins to be significantly diminished in the ageing alveolar RTLFs, with transferrin additionally decreased in the bronchial compartment, as determined by the antibody based approach. MS/MS results further revealed both heavy and light chains of Ferritin, were completely absent in young healthy RTLFs, their presence thus unique to the ageing RTLFs. Elevated concentrations of ferritin are typically associated with tissue necrosis, with high alveolar concentrations most likely the result of cell death. Ferritin concentrations have been reported to increase in the lower respiratory tracts of smokers, sufferers of chronic bronchitis, cystic fibrosis, pneumonia and lung transplant patients, with its synthesis potentially regulated by factors including hypoxia, NO, oxidative stress and various cytokines, all extrinsic factors the ageing lungs are likely to be exposed to (Mateos et al., 1998; Brewer et al., 2007; Erbaycu et al., 2008).

Altered iron homeostasis is well established as a consequence of ageing, with total iron content (both free and protein bound) shown to increase with age in various species (Cook and Yu, 1998). Such an age related disturbance in iron homeostasis is particularly important because of the capacity of iron to catalyze the production of damaging ROS, including the toxic hydroxyl radical (Brewer, 2007). In addition

increased iron has been associated with various diseases of ageing, including atherosclerosis and Alzheimers Disease (Ong and Haliwell, 2004; Brewer, 2007).

Summary and conclusions

This is the first study to investigate changes in the RTLF proteome associated with healthy ageing, combining a stringent semi-quantitative MS analytical approach with validation using antibody based methods. It is also the first study to examine age-related changes in the bronchial airways. My data revealed clear differences between the healthy young and aged RTLFs, with increased alveolar total protein, albumin and alpha-2-macroglobulin, consistent with an age-related increase in the permeability of the endothelial/epithelial barrier. Despite this, in the absence of differing blood to lavage urea ratios, it appeared more likely that the accumulation of vascular proteins in aged RTLFs, was attributable to a failure of clearance mechanisms. I also observed a general dysregulation of innate immunity proteins within the aged RTLFs, characterized by elevated IgA, alongside significant declines in the concentrations of transferrin, SP-A and haptoglobin. This occurred in parallel to a more oxidizing environment present within the RTLFs, as demonstrated by the significant decline in ascorbate and the corresponding increase in oxidized protein adducts. The increased concentration of Fe within the alveolar RTLF, associated with the reduced transferrin concentrations also suggests defective metal handling at the air-lung interface, the first time this has been observed in the aged lung. This would not only potentially contribute to the more oxidizing environment within aged RTLFs by catalyzing reactive oxygen species generation, but also promote bacterial growth. In general, the changes observed within the aged RTLFs are consistent with the increasing sensitivity of the aged lung to the detrimental effects of extrinsic factors such as inhaled pathogens and oxidants.

Chapter 5

Chronic Obstructive Pulmonary Disease changes in the composition of human respiratory tract lining fluids

5.1: Introduction

Chronic obstructive pulmonary disease (COPD) is a progressive and debilitating disease of the airway, estimated to affect over 65 million people worldwide (although it should be noted that physician based diagnosis has been suggested to underestimate true COPD prevalence), and to rank as the 3rd leading cause of death by 2030 (WHO). However the Global initiative for chronic obstructive lung disease (GOLD) defines COPD as a health challenge that is both preventable and treatable, but with no treatments currently able to prevent disease progression and at best able to reduce symptoms of breathlessness, or exacerbations of this disease, new insights into the pathogenesis of COPD are urgently required (Macnee, 2000; Alexandre and Penque, 2012).

The GOLD classification system, describes COPD as a disease 'characterized by airflow limitation that is not fully reversible', assessing the severity of the disease by lung function, FEV_1 (forced expiratory volume in 1 second). With airflow limitation (reduction in FEV_1) usually progressive in COPD, the disease can be further categorized into rapid and slow declining subjects. Rapid decliners are defined by a FEV_1 loss of more than 63 ml per year while slow decliners display losses in FEV_1 of approximately 31 ml per year (Vestbo et al., 2011; Nishimura et al., 2012). It should be noted however that age itself is an important factor in this decline and even in the absence of disease, the decline in FEV_1 in healthy non-smokers is approximately 20-30 ml per year (Tager et al., 1988); therefore the use of lung function alone appears inappropriate in classifying COPD (Burgel et al., 2010). COPD has further been described as a disease of accelerated ageing, with markers of cell senescence observed in lung cells and circulating leukocytes in COPD and marked reductions in anti-ageing molecules (SIRT1), potentially providing compelling evidence

that underlying ageing processes are accelerated in the pathogenesis of this disease (Ito and Barnes, 2009; Macnee, 2009).

Epidemiological studies have firmly established that cigarette smoking is the major risk factor for the development of COPD, with as many as 20–30% of smokers going on to develop this disease (Fletcher and Peto, 1977; Snider, 1989; Doll et al., 2004). Further, the cessation of smoking has been demonstrated to prevent disease progression (Anthonisen et al., 1994). Age is another leading factor determining the incidence of COPD, with life expectancy further increasing in the western world, the incidence of COPD is thus likely to continue to remain a leading cause of death (Lokke et al., 2006). The morbidity, mortality and social impact is expected to increase as both smoking frequencies rise and the population ages (Mannino and Buist, 2007; Macnee, 2009). Whilst cigarette smoking remains the leading environmental risk factor for this disease, other risk factors include occupational and environmental exposures to dusts, fumes and biomass burning (Blanc et al., 2009). Furthermore an inherited Alpha-1 antitrypsin deficiency is present in 1-2% of people with COPD (Tuder et al., 2010).

It is the interaction of these various environmental and host factors that contribute to the highly variable histopathology of COPD, which ultimately result in the main pathophysiological features of this disease: the progressive destruction of the small airways and lung parenchyma and the chronic inflammation present in the central and peripheral airways, as inferred by its two major clinical manifestations: emphysema and chronic bronchitis (Ito and Barnes, 2009).

Several underlying and interactive processes have been implicated in disease progression:

- Oxidative stress
- Protease-antiprotease imbalance
- Chronic inflammation

These interactions have previously been described as the ‘pathogenic triad’ of COPD, not separate independent entities on their own but integrally related with one another (Fischer et al., 2011). The resulting changing environment of the diseased airways, from hyperplasia of seromucousal and goblet cells, mucous hypersecretion, fibrosis and parenchymal destruction, correspondingly reflected in the composition of the RTLFs (Churg and Wright, 2006; Rahman and Adcock, 2006), see **Figure 5.1**.

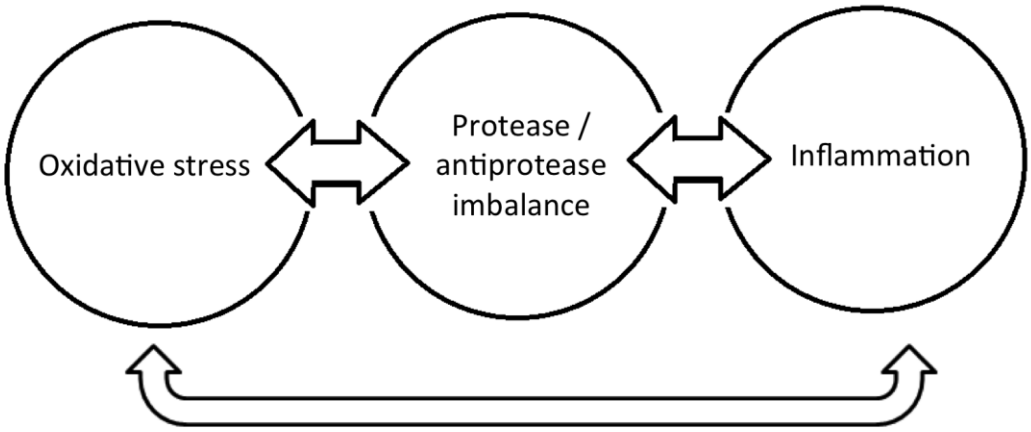

Figure 5.1: *The interactivity of the classical 'pathogenic triad' of COPD*

COPD is a complex chronic inflammatory disease resulting in the airway remodeling and obstruction of the peripheral airways, as well as the destruction of the lung parenchyma. COPD patients also demonstrate further extra-pulmonary complications as a result of the 'overspill' of inflammatory mediators from the lung into the systemic circulation (Agusti et al., 2003; Barnes, 2004). Mediators that have been shown to play a critical role in the airflow obstruction observed in COPD, include leukotriene (LT) B_4, interleukins (IL)-1, 6 and 8 and tumour necrosis factor alpha (TNFa) (Keatings et al., 1996; Chung, 2005; Profita et al., 2005; Sinden and Stockley, 2010), with multiple inflammatory and structural cells involved in the chronic inflammation of the airway, with characteristic infiltration of neutrophils, macrophages and T cells (Keatings et al., 1996; Di Stefano et al., 1998; Pesci et al., 1998; Saetta et al., 1998; Barnes et al., 2003; Retamales et al., 2001).

Neutrophils, have historically been the most investigated inflammatory cell in COPD, on account of their ability to cause deleterious tissue injury through secretion of a range of serine proteases including: neutrophil elastase, cathepsin G, and proteinase-3, as well as matrix metalloproteinase (MMP)-8 and MMP-9, highly implicated in the tissue destruction observed as COPD progresses. The increased presence of primed neutrophils in the COPD airway has been inferred from the increased concentrations of granule proteins myeloperoxidase and human neutrophil lipocalin, enhanced chemotaxis and increased extracellular proteolysis (Burnett et al., 1987; Keatings and Barnes, 1997; Yamamoto et al., 1997; Peleman et al., 1999).

The presence of activated neutrophils has been observed in sputum and BAL retrieved from COPD airways, (Thompson et al., 1989; Lacoste et al., 1993; Linden et al., 1993; Keatings et al., 1996; O'Shaughnessy et al., 1996; Di Stefano et al., 1998), with a correlation between the number of circulating neutrophils and airway obstruction, as measured by a fall in FEV_1 (Sparrow et al., 1984). Smoking has been shown to directly stimulate the subsequent production of granulocytes such as neutrophils from the bone marrow (Terashima et al., 1997), and may further increase the retention of neutrophils within the airways (MacNee et al., 1989).

Macrophages are also markedly increased within the COPD airways (Shapiro, 1999; Retamales et al., 2001; Barnes, 2004). Emphysematous patients have been shown to have a twenty-five-fold increase in the number of macrophages in both alveolar tissue and BAL fluid, with a clear correlation between the number of airway macrophages and the severity of COPD (Di Stefano et al., 1998). The increased alveolar macrophage populations seen in COPD have been associated with increased elastolytic activity, alongside augmented secretions of inflammatory proteins, which are only further exacerbated by smoking (Lim et al., 2000; Russell et al., 2002).

An increase in total T cell numbers across the airways, from the conducting airways to the alveolar region, as well as within the pulmonary arteries has been reported (Finkelstein et al., 1995; O'Shaughnessy et al., 1997; Saetta et al., 1999; Majo et al., 2001; Retamales et al., 2001). This predominately reflects an expansion in cytotoxic CD8+ T cells (de Jong et al., 1997; Kim et al., 2002).

The changing nature of the inflammatory cell profile in COPD RTLFs is likely part of an overall increase in the innate and adaptive immune response associated with the progression of the disease (Hogg et al., 2004; Curtis et al., 2007). These altered responses are all also likely to have an important role in regulating the frequency, severity and duration of acute exacerbations, which further contribute to the decline in lung function. Cigarette smoke in particular has been shown to exacerbate immune and inflammatory mechanisms, reported to activate both innate and adaptive immune responses, influencing anti-microbial defense mechanisms (Nikota and Stampfli, 2012).

The presence of chronic inflammation, and recurrent episodes of acute inflammation during exacerbations, is associated with evidence of pulmonary and systemic oxidative stress (Repine et al., 1997; MacNee, 2001), with increased concentrations of H_2O_2, 8-isoprostane, and ethane, measured in exhaled breath concentrate, correlated with disease severity (Dekhuijzen et al., 1996; Nowak et al., 1999; Paredi et al., 2000; Montuschi et al., 2000). Increased 4-HNE protein adducts have also

been observed in the alveolar epithelium of COPD subjects, with malondialdehyde (MDA), another end product of lipid peroxidation observed to increase in the plasma of COPD subjects (Rahman et al., 2002; Demedts et al., 2006; Wright et al., 2008). Consistent with oxidative damage degraded antioxidant defences have also been reported in COPD. Rahman et al., (1996) observed a significant decrease in the total antioxidant capacity and thus a shift in the oxidant-antioxidant balance, in smokers and subjects with acute exacerbations of COPD. Superoxide dismutase is also reportedly lower in COPD patients (Kirkil et al., 2008), with antioxidant proteins responsible for iron homeostasis such as caeruloplasmin, reported to decline in COPD, correlating positively with airway obstruction (Ito and Barnes, 2009).

The imposition of oxidative stress in the airway, also acts to amplify the ongoing chronic inflammatory responses in COPD through the activation of pro-inflammatory signaling cascades, particularly via NF□B mediated transcription (Di Stefano et al., 2002). Oxidative stress and inflammation have also both been implicated in shifting the protease antiprotease balance of the COPD airways. Reactive oxygen species released from activated phagocytes promote the release of proteases from activated inflammatory cells, including cathepsins, MMPs, and neutrophil elastase, thus contributing to the airway tissue destruction observed in COPD (Shapiro, 2002; Churg and Wright, 2003). Additionally oxidative modifications act to impair the anti-protease activity of crucial enzymes found in RTLFs responsible for normal airway homeostasis, the most heavily implicated of which is alpha-1 antitrypsin (Taggart et al., 2000). Patients with an inherited alpha-1 antitrypsin deficiency have been shown to develop early-onset emphysema, and an increase in complexes of this enzyme with neutrophil elastase have been observed in BAL retrieved from COPD patients, correlating positively with the rate of FEV_1 decline (Yoshioka et al., 1995; Betsuyaku et al., 2000).

With several underlying mechanisms believed to contribute to disease pathogenesis: oxidative stress, chronic inflammation of the airways, an imbalance between proteolytic and anti-proteolytic activity, as well as alpha-1-antitrypsin deficiency (Demedts et al., 2006), it becomes interesting to note that the interaction of these self propagating processes have also been proposed to increase ageing associated events, including apoptosis, autophagy, and senescence, all of which have been reported in the progression of COPD (Fischer et al., 2009; Hogg and Timens, 2009). Ultimately it is the great heterogeneity of this disease, which has complicated our understanding into the underlying cellular and molecular mechanisms involved in COPD.

Aims

With the mechanisms that govern COPD initiation and progression still poorly understood, the primary aim of the work described in this chapter was to characterize the changing composition of the RTLFs across the COPD airway, investigating this important extracellular compartment in both the smoking and non-smoking COPD airways using appropriate smoking and non-smoking aged matched controls. Secondly, with this disease affecting >10% of the world population over the age of 40 years, and with large clinical trials of current therapies showing limited effects on reducing morbidity and mortality, this data will be used to inform the development of physiologically relevant simulants representative of COPD airways, to aid future drug development in this challenging group of diseases.

5.2: Methods

5.2.1: Subject demographics

Subjects for all groups were invited to participate in the present study through advertisements in the local media. COPD patients (aged 50-75 years) had moderate to severe disease according to the GOLD criteria (FEV1 30-80% of predicted, FEV1/FVC less than 0.7) with a smoking history of at least ten pack-years and no evidence of other concomitant disease. All patients were required to be non-atopic and clinically stable, i.e. without any respiratory tract infection within a six-week period prior to and during the study, along with no history of frequent exacerbations during a period of at least 3 months prior to inclusion. The only medication permitted were short-acting β2-agonists and/or anti-cholinergic drugs. Neither long-acting bronchodilators nor inhaled corticosteroids were allowed. All subjects were also required to undergo a detailed medical consultation with an ECG and chest X-rays prior to inclusion. Healthy never-smoking volunteers were age-matched (50-75 years), had normal lung function (>80 FEV_1 % of predicted) and were all non-atopic. Similarly, aged 'healthy' smokers were required to have normal lung function, as previously defined, were age-matched (50-75 years) and had a smoking history of more than ten pack-years. All subjects were non-atopic and clinically stable. A total of 62 subjects were recruited; 19 healthy aged controls (all ex-, or never smokers); 11 aged smokers (with no evidence of chronic respiratory disease); 18 COPD patients (ex-smokers) and 14 patients who had continued to smoke following their diagnosis of COPD. All subjects participated following submission of formal consent with study approval awarded by the local Ethics Committee of the University of Umeå, in accordance with the declaration of Helsinki. A summary of the subject demographics is provided in **Table 5.1.**

5.2.2: Pulmonary function test

Dynamic spirometry variables (Vital capacity (VC), FVC and FEV_1) were measured pre and 15-20 minutes post-bronchodilation with 1mg of terbutalin (Bricanyl® Turbuhaler® AstraZeneca, Södertälje, Sweden) using a Vitalograph spirometer (Buckingham, UK) and reversibility calculated. At least three satisfactorily performed and well-cooperated measurements of each variable were carried out according to the recommendations of the American Thoracic Society.

5.2.3: Bronchoscopy-based lavage

Bronchoscopy with bronchial wash and bronchoalveolar lavage was performed as described in **Section 3.2.3**. Nasal lavage was not performed on the aged subjects. Details of the total and differential cell counts have been described previously (**Section 3.2.3**).

5.2.4: Antioxidant, total protein and urea determinations

Vitamin C, (ascorbate and dehydroascorbate), urate, total glutathione (GSx), glutathione (GSH), and glutathione disulphide (GSSG) concentrations were determined in BW and BAL as previously described, (Mudway et al., 2001; Behndig et al., 2009); further details are provided in Chapter 2 (**Section 2.4**). Total protein determinations were made using the BCA assay (Smith et al., 1985), with paired plasma and lavage urea concentrations assessed using the high sensitivity QuantiChrom urea assay kit (BioAssay Systems, Hayward). Protein carbonyl formation was measured spectrophotometrically using OxiSelect protein carbonyl spectrophotometric kit (Cell Biolabs, Inc., USA), with 4-HNE protein adducts determined using the OxiSelect HNE Adduct ELISA Kit (Cell Biolabs, San Diego, CA, USA).

5.2.5: Proteomic analysis

The strategy employed was identical to that outlined in the previous chapter (**Section 3.2.5**), with analysis performed on a subset of 5 individual's drawn from the each of the four groups. For the healthy aged group, (n=5), 67±6 years, 3 male/ 2 female; aged smokers (n=5), 61±6 years 1M/4F; COPD ex-smokers, 66±7 years, 6M/4F; and for the current COPD smokers, 64±7 years, 2M/3F. A larger number of COPD ex-smokers were included as a validation of the original results obtained in the first 5 subjects tested.

Table 5.1: ***Subject demographics for the subject groups employed in the current investigation.***

	Age Control Never smoker *(n=19)*	**Aged Control Current smoker** *(n=11)*	**COPD patients Ex-smokers** *(n=18)*	**COPD patients Current smokers** *(n=14)*	**KW-test**
Age (*mean + range*)	67.8 (57-77)	61.7 (50-76)*a*	67.7 (53-77)	63.1 (55-75)	$P = 0.014$
Gender (*m/f*)	11/8	4/7	13/5	9/5	
Pack years (*mean + range*)	0	36.9 (18-95)*a*	33.5 (5-68)*c*	35.2 (13-80)	$P < 0.001$
FVC (median, IQR, L)	4.1 (3.6-4.7)	4.0 (3.1-4.9)	2.9 (2.3-3.0)*c*	2.4 (2.2-2.6)*b*	$P < 0.001$
FVC % of predicted (*%*)	104.0 (95.0-116.0)	114.5 (107.0-122.3)	73.0 (66.0-77.5)*c*	85.0 (67.5-91.0)*b*	$P < 0.001$
FEV_1 (*median, IQR, L*)	3.0 (2.2-3.4)	3.2 (2.6-3.8)	1.4 (1.0-1.9)*c*	1.3 (1.1-1.6)b	$P < 0.001$
FEV_1 % of predicted (*%*)	100.0 (91.0-118.0)	113.0 (104.0-115.8)	51.0 (42.0-64.0)*c*	60.0 (39.0-69.0)*b*	$P < 0.001$
Reversibility (*%*)	1.0 (-0.5-4.4)	2.7 (1.2-4.9)	17.1 (12.0-24.4)*c*	6.2 (1.9-15.1)*d*	$P < 0.001$
TLC (*median, IQR, L*)	nd	6.8 (5.4-8.1)	7.0 (6.1-7.6)	6.0 (5.3-6.5)	NS
IC (*median, IQR, L*)	nd	3.1 (2.7-3.6)	2.6 (2.2-3.0)	2.0 (1.7-2.5)b	$P = 0.006$
MEF_{50} (*median, IQR, L s^{-1}*)	nd	2.76 (2.15-3.64)	0.37 (0.28-0.70)	0.72 (0.40-0.79)*b*	$P < 0.001$
TL_{CO}^{SB} (*median, IQR, mmol min^{-1} kPa^{-1}*)	nd	7.4 (6.1-7.8)	5.7 (3.9-6.3)	5.2 (4.8-5.7)*b*	$P < 0.001$
BAL recovery (*%*)	50.0 (44.0-56.0)	53.0 (48.8-63.8)	36.0 (29.0-48.0)*c*	39.0 (29.0-48.0)	$P = 0.025$

All data are expressed as medians with either the inter-quartile or full range, as indicated. Significant differences across groups were assumed at the 5% level using the Kruskal–Wallis one-way analysis of variance by ranks (significance illustrated in the far right hand column), with post-hoc testing between specified groups performed using the Mann Whitney U Test. Comparison of individual groups were restricted to healthy smokers versus never smokers (a, $P < 0.05$), healthy smokers and COPD current smokers (b, $P < 0.05$), never smokers versus COPD ex-smokers (c, $P < 0.05$) and COPD current and ex-smokers (d, $P < 0.05$). Lung function measurements are based on post bronchodilator values, with evidence of % airway reversibility indicated. Pack years were calculated by multiplying the number of packs of cigarettes smoked per day by the number of years the person had smoked. FVC = Forced Vital Capacity; FEV1 = Forced Expiratory Volume in 1 second; TLC = Total Lung Capacity; IC = Inspiratory Capacity; MEF50 = Maximum Expiratory Flow when 50% of the FVC has been exhaled; TLCOSB, lung carbon monoxide diffusing capacity in a Single Breath; % BAL recovery, based on a total instilled saline volume of 180 mLs.

5.2.6: Statistics

Data were not normally distributed (Shapiro-Wilks test) and are therefore expressed throughout as medians with the 25th and 75th percentiles. Comparison of inflammatory cell numbers, antioxidant and oxidative damage markers and protein concentrations across the various subject groups were performed using the Kruskal–Wallis one-way analysis of variance by ranks, with post-hoc testing between specific groups performed using the Mann-Whitney U test. In all cases significant differences were assumed at the 5% level. Correlation analysis for each individual group, plus compiled groups of COPD patients (current and ex-smokers) and smokers (both aged 'healthy' smokers and COPD smokers) were performed using the Spearman Rank Order Correlation. Statistical analyses were performed using the IBM SPSS software, version 20 (SPSS, Armonk, NY, USA). Significance was assumed at the 5% level.

.

5.3: Results

5.3.1: Baseline characteristics

BAL was tolerated well by all subjects, with recovery being significantly lower (36%) in the COPD ex-smoking group relative to the aged never-smokers (50%, $p<0.05$) – **Table 5.2**. Increased leukocyte numbers were seen in smokers versus never-smokers, reflecting a 2.6 and 2.1-fold expansion in BAL macrophages in aged healthy and COPD smokers compared with their corresponding never-smoking or ex-smoking controls ($p<0.001$ in both cases – **Table 5.2**). No increase in macrophage numbers were observed in the COPD patients, current or ex-smokers, compared with their relevant control groups. Further there was no evidence of increased neutrophil numbers in the COPD smokers and non-smokers compared with their respective controls (**Table 5.2**). Increases in BAL mast cell numbers were observed in the aged smoking group (0.06 (0.03-0.10) cell/mL*10^4) relative to the aged non-smokers (0.01 (0.01-0.02) cell/mL*10^4, $p=0.002$), with a similar increase also apparent in the more proximal BW sample ($p=0.017$). Equivalent increases were not observed in the COPD smokers.

5.3.2: The RTLF proteome in COPD: 1D PAGE and nano LC MS/MS

As previously described, the 1D PAGE and nano LC MS/MS proteomic analysis examined individual concentrated BAL samples, with protein concentrations approximated, based on the mean of the three most intense precursor ions, back corrected for the total protein concentration in the samples and the lavage dilution using the urea ratio method. Furthermore proteins identified were limited to those present within at least 3 out of 5 subjects investigated, except in the case of COPD ex-smokers where 10 subjects underwent proteomic analysis (on account of the low number of protein identifications made in this group, and the repeat analysis performed to confirm this unexpected result), in which case proteins identified had to be present within at least 7 out of the 10 subjects.

Table 5.2: *Differential white blood cell counts in BW and BAL fluids from COPD patients and aged and smoking matched controls. Cell numbers are presented as cell/mL*10^4.*

	Age Control Never smoker (n=19)	**Aged Control Current smoker** (n=11)	**COPD patients Ex-smokers** (n=18)	**COPD patients Current smokers** (n=14)	**KW-test**
Bronchial wash					
Total Cells	7.0 (5.6-11.2)	9.7 (7.9-19.9)	3.8 (2.1-10.2)	9.7 (3.4-14.5)	NS
Macrophages	6.2 (3.4-9.3)	8.7 (6.5-17.0)	2.0 (1.6-6.6)*c*	8.9 (3.2-13.0)	$P = 0.031$
Neutrophils	1.2 (0.3-1.4)	0.4 (0.2-0.7)	0.6 (0.2-1.4)	0.5 (0.2-0.6)	NS
Lymphocytes	0.6 (0.3-0.8)	0.7 (0.4-0.9)	0.3 (0.1-0.5)*c*	0.2 (0.1-0.4)*b*	$P = 0.016$
Eosinophils	0.0 (0.0-0.1)	0.1 (0.0-0.1)	0.0 (0.0-0.1)	0.0 (0.0-0.2)	NS
Mast cells	0.00 (0.00-0.01)	0.03 (0.01-0.04)*a*	0.00 (0.00-0.01)	0.00 (0.00-0.01)	$P = 0.027$
Bronchoalveolar lavage fluid					
Total Cells	17.1 (11.1-26.9)	39.7 (34.0-48.3)*a*	17.7 (14.7-23.8)	29.7 (27.4-45.6)*d*	$P < 0.001$
Macrophages	14.1 (9.8-16.6)	36.6 (30.7-45.5)*a*	14.0 (11.3-20.7)	29.0 (26.1-39.3)*d*	$P < 0.001$
Neutrophils	0.1 (0.1-0.2)	0.5 (0.3-0.8)*a*	0.3 (0.1-0.4)	0.1 (0.1-0.6)	NS
Lymphocytes	1.7 (0.9-3.9)	2.3 (1.5-3.2)	2.3 (1.1-3.2)	1.3 (0.6-1.5)	NS
Eosinophils	0.0 (0.0-0.1)	0.1 (0.0-0.1)	0.1 (0.0-0.2)	0.2 (0.1-0.3)	NS
Mast cells	0.01 (0.01-0.02)	0.06 (0.03-0.10)*a*	0.01 (0.00-0.02)	0.03 (0.03-0.07)	$P = 0.013$

All data are expressed as medians with either the inter-quartile or full range, as indicated. Significant differences across groups were assumed at the 5% level using the Kruskal–Wallis one-way analysis of variance by ranks (significance illustrated in the far right hand column), with post-hoc testing between specified groups performed using the Mann Whitney U Test. Comparison of individual groups were restricted to healthy smokers versus never smokers (*a*, $P < 0.05$), healthy smokers and COPD current smokers (*b*, $P < 0.05$), never smokers versus COPD ex-smokers (*c*, $P < 0.05$) and COPD current and ex-smokers (*d*, $P < 0.05$). Subject numbers given in parenthesis represent the subjects recruited, plus the number of subjects from which BW (≠) or BAL (§) was recovered for differential cell counts.

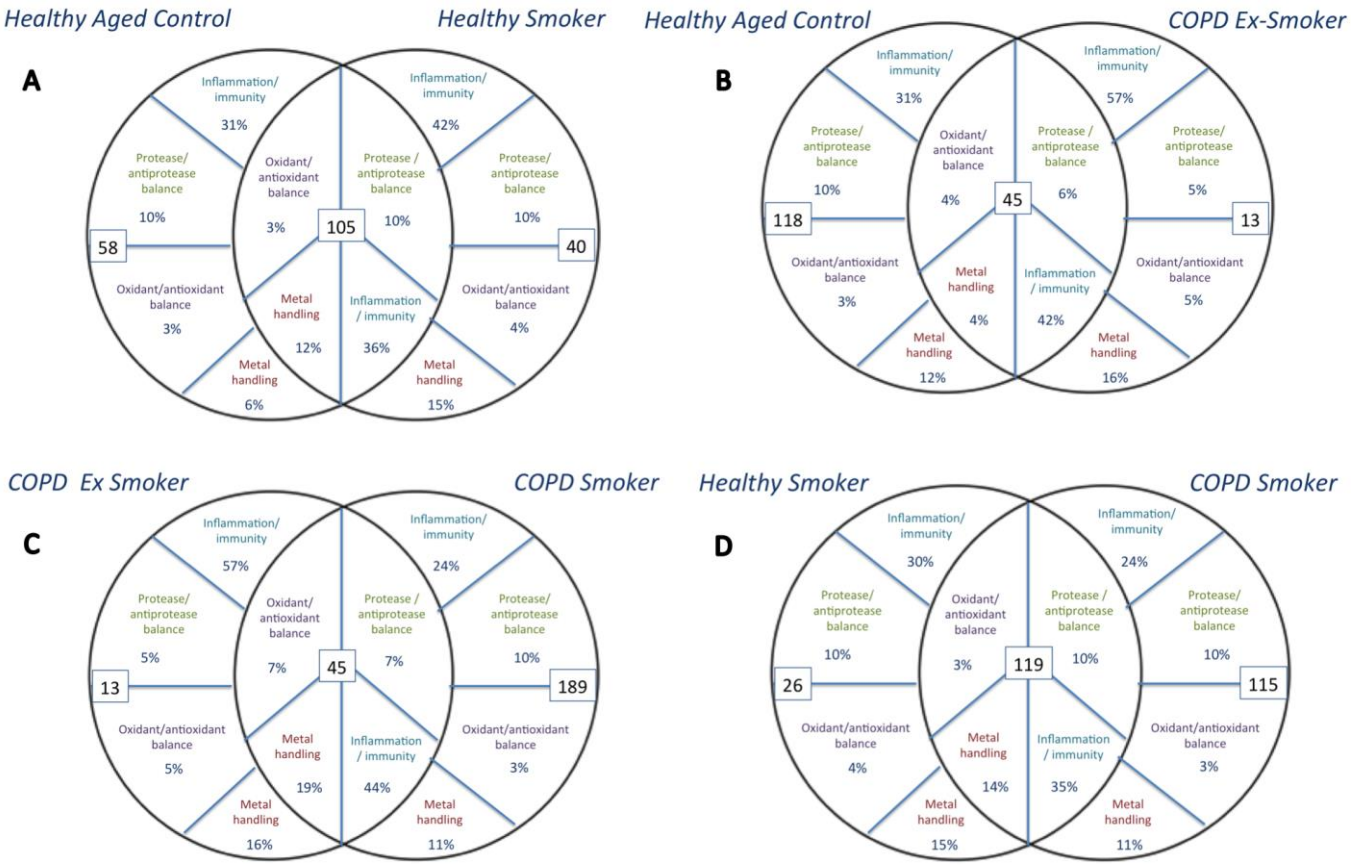

Figure 5.2: *Venn diagrams illustrating the proteins common and unique to (A) aged non-smoking and aged smoking alveolar RTLFs; (B) aged smoking and COPD ex-smoking alveolar RTLFs (C) COPD ex-smoking and COPD smoking alveolar RTLFs; and (D) aged smoking and COPD smoking alveolar RTLFs, as organized by the most common ontological classifications*. Classifications include: inflammation and immunity, metal handling, oxidant/antioxidant balance, protease/antiprotease balance, alongside their respective % contributions to the total protein pool. Data is representative of n=5 for healthy aged controls, healthy smokers and COPD smokers, n=10 for COPD ex-smokers.

Table 5.3 highlights the fifteen most abundant communal proteins across all four subject groups (The full list is provided in **Appendix C**), further annotated by their source of origin, ontological definition. All, with the exception of uncharacterized protein C3orf38, a protein of unknown function and origin, and actin, an intracellular protein integral to cell motility, are derived from extracellular sources.

Thirty-two proteins were identified as being common to all four proteomes investigated: healthy aged non-smokers, healthy aged smokers, COPD smokers and COPD ex-smokers (see **Appendix C** for full list of all proteins identified across and between groups). A total of 163 proteins were identified in healthy aged controls, with a similar number, 145 proteins identified in healthy smoking proteomes. The COPD smoking proteome had the highest number of protein identifications, 234, in contrast to the COPD ex-smoking proteome that had only 58 identifiable proteins. The non-smoking proteomes demonstrated a higher percentage of proteins of extracellular origin 72 and 74 % in healthy aged and COPD ex-smoking RTLFs respectively. Only 61% of the smoking proteomes (healthy and COPD) were classified as extra-cellular or secretory, indicative of a greater contribution from intra-cellular sources, potentially inferring cell injury.

If we first compare the healthy aged RTLF with that of the healthy smokers, the majority of the identified proteins (105), were common to both proteomes. Of these, only the calgranulin proteins A and B were found upregulated within the aged smoking RTLFs, 47 and 24 fold respectively (see **Table 5.4**). Of the 40 proteins uniquely identified in the smoking RTLFs, intracellular proteins contributing to the oxidant-antioxidant balance at the air-lung interface: SOD (Cu-Zn), peroxiredoxin and glutathione-S transferase, were identified. Further intracellular proteins involved in protease-antiprotease balance within the airways were identified, including the protease inhibitors serpin B4, cystatin, leucocyte elastase inhibitor and cathepsin S. Absent from the smoking proteome were a variety of proteins involved in innate immunity, from secreted proteins of the upper airways, such as mucin-1 and galectin-3, to proteins involved in innate immune responses such as CD59, which has a role in signaling for T-cell activation, cell adhesion molecule 2 and complement proteins C2 and C3.

Table 5.3: *Abundant alveolar proteins common across the four subject groups.* The 15 most abundant common proteins (out of 32) listed with their source of origin and their ontological classification. The number of samples in which the protein was identified in each group is indicated.

Protein	Source	Ontology	Healthy Smoker	COPD smoker	Healthy Aged Control	COPD ex-smoker
Serotransferrin	Extracellular, Secreted	Metal Handling and Transport	3.42E+09 (n=5/5)	4.56E+09 (n=5/5)	7.62E+09 (n=5/5)	1.10E+09 (n=9/10)
Ig gamma-1 chain C region	Extracellular, Secreted	Immunity and Inflammation	3.30E+09 (n=5/5)	5.79E+09 (n=5/5)	8.92E+09 (n=5/5)	3.55E+09 (n=10/10)
Ig gamma-2 chain C region	Extracellular, Secreted	Immunity and Inflammation	2.57E+09 (n=5/5)	4.65E+09 (n=5/5)	5.60E+09 (n=5/5)	5.64E+07 (n=10/10)
Uncharacterized protein C3orf38	Unknown	Unknown	1.62E+09 (n=5/5)	1.83E+09 (n=5/5)	2.73E+09 (n=5/5)	5.97E+08 (n=9/10)
Serum albumin	Extracellular, Secreted	Metal Handling and Transport	1.54E+09 (n=5/5)	3.86E+09 (n=5/5)	2.77E+09 (n=5/5)	5.49E+08 (n=10/10)
Ig kappa chain C region	Extracellular, Secreted	Immunity and Inflammation	1.07E+09 (n=5/5)	2.92E+09 (n=5/5)	3.47E+09 (n=5/5)	9.25E+09 (n=9/10)
Ig lambda-2 chain C regions	Extracellular, Secreted	Immunity and Inflammation	7.91E+08 (n=5/5)	1.09E+09 (n=5/5)	2.31E+09 (n=5/5)	8.59E+06 (n=8/10)
Ig alpha-1 chain C region	Extracellular, Secreted	Immunity and Inflammation	6.14E+08 (n=5/5)	1.56E+09 (n=5/5)	2.42E+09 (n=5/5)	6.04E+09 (n=7/10)
Alpha-1-antitrypsin	Extracellular, Secreted	Protease/antiprotease	2.75E+08 (n=5/5)	1.61E+09 (n=5/5)	3.20E+09 (n=5/5)	3.86E+07 (n=7/10)
Hemopexin	Extracellular, Secreted	Metal Handling and Transport	1.89E+08 (n=5/5)	3.48E+08 (n=5/5)	2.71E+08 (n=5/5)	1.75E+08 (n=7/10)
Polymeric immunoglobulin receptor	Cell Membrane	Immunity and Inflammation	1.54E+08 (n=5/5)	2.83E+08 (n=5/5)	1.94E+08 (n=5/5)	2.37E+09 (n=7/10)
Actin, cytoplasmic 1	Intracellular	Cell morphology / interaction	1.38E+08 (n=5/5)	5.36E+07 (n=5/5)	6.89E+07 (n=5/5)	4.06E+08 (n=7/10)
Alpha-1-acid glycoprotein 1	Extracellular, Secreted	Immunity and Inflammation	1.29E+08 (n=5/5)	2.76E+08 (n=5/5)	3.39E+08 (n=5/5)	2.88E+06 (n=7/10)
Ig kappa chain V-III region SIE	Extracellular, Secreted	Immunity and Inflammation	1.24E+08 (n=5/5)	2.67E+08 (n=5/5)	2.40E+08 (n=5/5)	1.85E+06 (n=7/10)
Caeruloplasmin	Extracellular, Secreted	Metal Handling and Transport	1.15E+08 (n=5/5)	2.38E+08 (n=5/5)	3.67E+08 (n=5/5)	2.73E+06 (n=7/10)

Table 5.4: *Alveolar proteins demonstrating the largest relative fold increases between healthy aged controls and healthy smokers.* The proteins of the common 105 identified showing the greatest fold increase are listed alongside their source of origin, their ontological classification and their relative fold differences. The number of samples in which the protein was identified in each group is indicated.

Protein	**Source**	**Ontology**	**Healthy Aged Control**	**Healthy Smoker**	**Fold difference** (Healthy Smoker v Healthy Aged Control)
Calgranulin B	Extracellular, Secreted	Immunity and Inflammation	1.13E+07 (n=4/5)	5.29E+08 (n=5/5)	46.9↑
Calgranulin A	Extracellular, Secreted	Immunity and Inflammation	3.59E+07 (n=4/5)	8.57E+08 (n=5/5)	23.8 ↑

Comparing the healthy aged RTLF proteome to that of COPD ex-smokers provided an insight into the effect of COPD on the nature of this extra-cellular compartment, in the absence of smoking. Forty-five proteins were common to both RTLFs, with only 13 unique to the RTLF of COPD ex-smokers: mucin and SP-D, the immunoglobulin chains, kappa chain C and gamma-3 chain C, as well as the highly abundant plasma proteins: A2M, alpha-1-antichymotrypsin and haemoglobin were all absent. Of the communal RTLF proteins, large fold differences were noted, with a decreased expression of caeruloplasmin (134.6-fold), A1AT (82.9-fold), haptoglobin (13.3-fold) and SP-A (20.2-fold), see **Table 5.5.** Proteins demonstrating large fold increases in the COPD ex-smokers included, PIGR and lysozyme with 12.3 and 754-fold increases respectively, with CC16 secreted by bronchial Clara cells also demonstrating a 25.8 fold increase. Furthermore the intracellular proteins ferritin and actin were increased in COPD ex-smokers (31.9 and 5.9-fold) as highlighted in **Table 5.6**.

Focusing down on the COPD RTLFs, 45 proteins were identified as common between smokers and ex-smokers. Mucin and SP-D were once more absent in the ex-smokers, as was SP-B, immunoglobulin kappa C and gamma- 3 chains, A2M and alpha-1-antichymotrypsin. Various proteins contributing to the protease-antiprotease balance of the airway; including serpins B6 and B12, pro-cathepsin H, cathepsins B, D, S and Z, were absent from the RTLF of COPD ex-smokers. Of the communal proteins, concentrations of SP-A and calgranulin A were depressed (15.6 and 10.5-fold respectively) in the COPD ex-smokers, as were the plasma proteins, caeruloplasmin, haptoglobin (87.2 and 27.8-fold), with the intracellular protein ferritin also decreased (2.6-fold), see **Table 5.7**. Of the proteins demonstrating the largest fold increases in the RTLF of COPD ex-smokers both PIGR and Lysozyme demonstrated an increase (8.4 and 78.8 fold respectively), with this also the case for CC16 (22.6 fold). Finally once more, the intracellular protein actin was found elevated (7.6 fold) in the ex-smoking COPD subjects, **Table 5.8**.

Table 5.5: *Alveolar proteins demonstrating the largest relative fold decrease between healthy aged controls and COPD ex-smokers.* All detail as in the legend to **Table 5.4**.

Protein	**Source**	**Ontology**	**Healthy Aged Control**	**COPD Ex-Smoker**	**Fold difference** (COPD Ex-Smoker v Healthy Aged Control)
SP-A	Extracellular, Secreted	Immunity and Inflammation,	3.74E+07 (n=5/5)	1.85E+06 (n=9/10)	20.2 ↓
Ig kappa chain C region	Extracellular, Secreted	Immunity and Inflammation	3.47E+09 (n=5/5)	1.60E+07 (n=7/10)	67.1 ↓
Ig gamma-3 chain C region	Extracellular, Secreted	Immunity and Inflammation	6.71E+09 (n=5/5)	5.64E+07 (n=7/10)	50.9 ↓
Caeruloplasmin	Extracellular, Secreted	Metal Handling and Transport	3.67E+08 (n=5/5)	2.73E+06 (n=7/10)	134.6 ↓
Alpha-1-antitrypsin	Extracellular, Secreted	Protease/antiprotease	3.20E+09 (n=5/5)	3.86E+07 (n=7/10)	82.9 ↓
Leucine-rich alpha-2-glycoprotein	Extracellular, Secreted	Cell morphology / interaction	4.46E+07 (n=5/5)	7.23E+05 (n=7/10)	61.7 ↓
Haptoglobin	Extracellular, Secreted	Immunity and Inflammation	1.26E+08 (n=5/5)	9.50E+06 (n=9/10)	13.3↓

Table 5.6: *Alveolar proteins demonstrating the largest relative fold increases between healthy aged controls and COPD ex-smokers*.

Protein	**Source**	**Ontology**	**Healthy Aged Control**	**COPD Ex-Smoker**	**Fold difference** (COPD Ex-Smoker v Healthy Aged Control)
Thioredoxin	Intracellular	Oxidant/antioxidant balance,	8.21E+06 (n=4/5)	1.54E+08 (n=7/10)	18.7 ↑
Beta-2-microglobulin	Extracellular, Secreted	Immunity and Inflammation	2.59E+07 (n=5/5)	5.86E+08 (n=7/10)	22.7 ↑
Hemoglobin subunit beta	Plasma	Metal Handling and Transport	1.28E+08 (n=5/5)	1.66E+09 (n=10/10)	13.0 ↑
Ferritin light chain	Intracellular	Metal Handling and Transport	4.73E+06 (n=5/5)	1.51E+08 (n=8/10)	31.9↑
Annexin A5	Intracellular	Blood coagulation, signaling	1.36E+06 (n=5/5)	9.47E+07 (n=7/10)	69.4↑
Complement C3	Extracellular, Secreted	Immunity and Inflammation	2.66E+06 (n=5/5)	2.06E+08 (n=8/10)	77.3↑
CC16	Extracellular, Secreted	Unknown	1.74E+08 (n=5/5)	4.49E+09 (n=10/10)	25.8 ↑
Polymeric immunoglobulin receptor	Extracellular, Secreted	Immunity and Inflammation	1.94E+08 (n=5/5)	2.37E+09 (n=7/10)	12.3↑
Peptidyl-prolyl cis-trans isomerase A	Intracellular	Immunity and Inflammation	6.43E+06 (n=5/5)	7.51E+07 (n=9/10)	11.7 ↑
Lysozyme	Extracellular, Secreted	Immunity and Inflammation	3.69E+07 (n=5/5)	5.31E+08 (n=7/10)	754↑
Actin, cytoplasmic 1	Intracellular	Cell morphology / interaction	6.89E+07 (n=5/5)	4.06E+08 (n=7/10)	5.9 ↑

Finally by comparing the RTLF proteomes of smokers, with and without COPD, we were able to explore the impact of current smoking, superimposed on the underlying disease. Of the 155 proteins unique to the COPD smokers airways, proteins involved in the protease-antiprotease balance were identified: cathepsin D, serpin B6 and B12; with glutathione synthetase and transferases also uniquely within this proteome, together with the innate immune proteins HLA class II histocompatibility antigen, CD59, CAM2, and complement C2 and C3. Interestingly, fewer (119) of the identified proteins were common to both proteomes. Of these proteins, lysozyme was elevated; as was locally secreted protein SP-D (2.6 and 5- fold respectively) in the COPD smokers. Abundant plasma proteins: A2M, A1AT and haptoglobin (2.7, 5.9 and 2.5 fold) were also elevated in the smoking COPD patents, but the greatest fold differences were for both chains of the intracellular protein ferritin (19.4 and 27.7-fold increase), **Figure 5.9**. In contrast the secretory protein calgranulin A was significantly depressed in the COPD smokers, 386-fold compared with the healthy smoking group, as was the case for intracellular protein actin (2.6-fold), **Table 5.10**.

All proteins identified with the alveolar RTLFs were classified based on their gene ontological definitions, with the largest classification being proteins involved in inflammation and immune responses, representing 57% of the identified COPD ex-smoking proteome, but only 24% in the COPD smoker RTLF. Proteins annotated as being involved in metal handling represented the second greatest grouping within the healthy smoker, COPD smoker, and COPD ex-smoker (22, 26 and 9 proteins respectively) proteomes. The second largest grouping in the healthy aged population was those proteins involved in the protease-antiprotease balance (16 proteins). Only 5, 6, 3 and 7 proteins were identified to contribute to the oxidant-antioxidant balance within healthy aged controls, healthy smokers, COPD ex-smokers and COPD smokers, respectively (See **Appendix C** for full list of proteins according to ontological classifications).

Table 5.7: *Alveolar proteins demonstrating the largest relative fold decreases between COPD smokers and ex-smokers.*

Protein	**Source**	**Ontology**	**COPD Smoker**	**COPD Ex-Smoker**	**Fold difference** (COPD Ex-Smoker v COPD Smoker)
Ig kappa chain C region	Extracellular, Secreted	Immunity and Inflammation	2.92E+09 (n=5/5)	1.60E+07 (n=9/10)	182.5 ↓
Ig gamma-3 chain C region	Extracellular, Secreted	Immunity and Inflammation	5.04E+09 (n=4/5)	5.64E+07 (n=7/10)	89.36 ↓
Caeruloplasmin	Extracellular, Secreted	Metal Handling and Transport	2.38E+08 (n=5/5)	2.73E+06 (n=7/10)	87.18 ↓
Alpha-1-antitrypsin	Extracellular, Secreted	Protease/antiprotease	1.61E+09 (n=5/5)	3.86E+07 (n=7/10)	41.71 ↓
Leucine-rich alpha-2-glycoprotein	Extracellular, Secreted	Cell morphology / interaction	3.29E+07 (n=5/5)	7.23E+05 (n=7/10)	45.50 ↓
Haptoglobin	Extracellular, Secreted	Immunity and Inflammation	2.64E+08 (n=5/5)	9.50E+06 (n=9/10)	27.79 ↓
Calgranulin A	Extracellular, Secreted	Immunity and Inflammation	2.22E+06 (n=5/5)	2.33E+07 (n=7/10)	10.50 ↓
SP-A	Extracellular, Secreted	Immunity and Inflammation,	2.89E+07 (n=5/5)	1.85E+06 (n=9/10)	15.62 ↓
Ferritin light chain	Intracellular	Metal Handling and Transport	3.93E+08 (n=5/5)	1.51E+08 (n=8/10)	2.60 ↓

Table 5.8: *Alveolar proteins demonstrating the largest relative fold increases between COPD smokers and ex-smokers.*

Protein	**Source**	**Ontology**	**COPD Smoker**	**COPD Ex-Smoker**	**Fold difference** (COPD Ex-Smoker v COPD Smoker)
Hemoglobin subunit alpha	Intracellular, Plasma	Metal Handling and Transport	8.29E+07 (n=4/5)	5.24E+08 (n=7/10)	6.32 ↑
Thioredoxin	Intracellular	Oxidant/antioxidant balance,	2.98E+07 (n=5/5)	1.54E+08 (n=7/10)	5.17 ↑
Beta-2-microglobulin	Extracellular, Secreted	Immunity and Inflammation	3.80E+07 (n=5/5)	5.86E+08 (n=7/10)	15.42 ↑
CC16	Extracellular, Secreted	Unknown	1.99E+08 (n=5/5)	4.49E+09 (n=9/10)	22.56 ↑
Polymeric immunoglobulin receptor	Extracellular, Secreted	Immunity and Inflammation	2.83E+08 (n=5/5)	2.37E+09 (n=7/10)	8.37 ↑
Peptidyl-prolyl cis-trans isomerase A	Intracellular	Immunity and Inflammation	7.32E+06 (n=5/5)	7.51E+07 (n=9/10)	10.26 ↑
Lysozyme	Extracellular, Secreted	Immunity and Inflammation	6.74E+06 (n=5/5)	5.31E+08 (n=7/10)	78.78 ↑
Actin, cytoplasmic 1	Intracellular	Cell morphology / interaction	5.36E+07 (n=5/5)	4.06E+08 (n=7/10)	7.57 ↑
Complement C3	Extracellular, Secreted	Immunity and Inflammation	7.33E+07 (n=5/5)	2.06E+08 (n=8/10)	2.81 ↑

Table 5.9: *Alveolar proteins demonstrating the largest relative fold decreases between COPD smokers and healthy smokers*

Protein	**Source**	**Ontology**	**Healthy Smoker**	**COPD Smoker**	**Fold difference** (COPD Smoker v Healthy Smoker)
Beta-2-microglobulin	Extracellular, Secreted	Immunity and Inflammation	1.03E+07 (n=5/5)	3.80E+07 (n=5/5)	3.69 ↑
Angiotensinogen	Extracellular, Secreted	Blood coagulation, signaling	1.41E+06 (n=5/5)	5.39E+07 (n=5/5)	38.23 ↑
Hemoglobin subunit beta	Plasma	Metal Handling and Transport	2.04E+07 (n=5/5)	7.32E+07 (n=5/5)	3.59 ↑
Ferritin light chain	Intracellular	Metal Handling and Transport	2.03E+07 (n=5/5)	3.93E+08 (n=5/5)	19.36 ↑
Ferritin heavy chain	Intracellular	Metal Handling and Transport	5.09E+06 (n=5/5)	1.41E+08 (n=5/5)	27.70 ↑
Lysozyme	Extracellular, Secreted	Immunity and Inflammation	2.61E+06 (n=5/5)	6.74E+06 (n=5/5)	2.58 ↑
Cathepsin S	Intracellular	Protease/antiprotease	3.74E+06 (n=5/5)	3.07E+07 (n=5/5)	8.21 ↑
Calmodulin	Intracellular	Signaling	2.84E+06 (n=4/5)	2.48E+07 (n=4/5)	8.73 ↑
Apolipoprotein A-I	Plasma	Lipid Metabolism	7.56E+06 (n=4/5)	5.68E+07 (n=4/5)	7.51 ↑
Dipeptidyl peptidase 4	Secreted, plasma	Protease/antiprotease , signaling, apoptosis	3.08E+06 (n=4/5)	1.99E+07 (n=3/5)	6.46 ↑
Proactivator polypeptide	Intracellular	Not known	1.35E+06 (n=4/5)	6.97E+06 (n=4/5)	5.16 ↑
Coactosin-like protein	Intracellular	Cell morphology / interaction	6.78E+06 (n=4/5)	3.50E+07 (n=4/5)	5.16 ↑
Pulmonary surfactant-associated protein D	Secreted	Immunity and Inflammation	5.11E+06 (n=5/5)	2.63E+07 (n=5/5)	5.15 ↑
Ig kappa chain C region	Extracellular, Secreted	Immunity and Inflammation	1.07E+09 (n=5/5)	2.92E+09 (n=5/5)	2.73 ↑
Alpha-1-antitrypsin	Extracellular, Secreted	Protease/antiprotease	2.75E+08 (n=5/5)	1.61E+09 (n=5/5)	5.85 ↑
Haptoglobin	Extracellular, Secreted	Immunity and Inflammation	1.04E+08 (n=5/5)	2.64E+08 (n=5/5)	2.54 ↑
Alpha-2-macroglobulin	Extracellular, Secreted	Protease/antiprotease	4.14E+06 (n=5/5)	1.01E+07 (n=5/5)	2.65 ↑

Table 5.10: *Alveolar proteins demonstrating the largest relative fold decreases between COPD smokers and healthy smokers.*

Protein	**Source**	**Ontology**	**Healthy Smoker**	**COPD Smoker**	**Fold difference** (COPD Smoker v Healthy Smoker)
Calgranulin A	Extracellular, Secreted	Immunity and Inflammation	8.57E+08 (n=5/5)	2.22E+06 (n=5/5)	386.12 ↓
Actin, cytoplasmic 1	Intracellular	Cell morphology / interaction	1.38E+08 (n=5/5)	5.36E+07 (n=5/5)	2.57 ↓

Dilution factors for the lavage samples were calculated based on the urea method. These were similar across all four groups for the alveolar compartment: healthy aged, 191.56 (166.1-300.1); healthy smokers, 172.4 (131.7-248.5); COPD ex smokers, 128.6 (112.1-172.3) and COPD smokers 138.0 (89.3- 162.5). The urea-based lavage correction factors for the bronchial samples, although higher with respect to alveolar values, were also similar across the groups: 322.1 (221.3-466.2), 288.4 (254.3-330.4), 359.6 (265.6-437.4) and 338.5 (164.5-439.5), respectively. It should be noted that these differences in Bronchial and Alveolar urea levels and thus the corresponding basal correction factors determined will directly influence all subsequently lavage corrected values. Whilst previous investigations have expressed specific proteins allowing for the numbers of cells determined, particularly those of an inflammatory nature, for the purpose of this study this was not performed in this investigation (Hatch, 1992).

Based on the quantitative analysis of all the lavage samples, the total alveolar RTLF protein concentrations across the 4 groups were equivalent: 38.6 (21.7-56.0) and 23.6 (16.7-35.9) mg/mL in healthy aged and smoking subjects, and 22.2 (14.2-59.2) and 14.3 (8.5-22.7) mg/mL in COPD ex smokers and smokers. Focusing first on the selected proteins involved in transport and metal handling, ferritin was found to be significantly elevated in healthy smokers versus non-smoking controls (**Figure 5.3**). This was also the case for COPD smokers compared with the non-smoking controls, supporting the results of the semi-quantitative proteomic analysis. No other significant differences were noted in the concentration of the remaining proteins in this grouping: caeruloplasmin, transferrin and albumin, **(see Figure 5.3).**

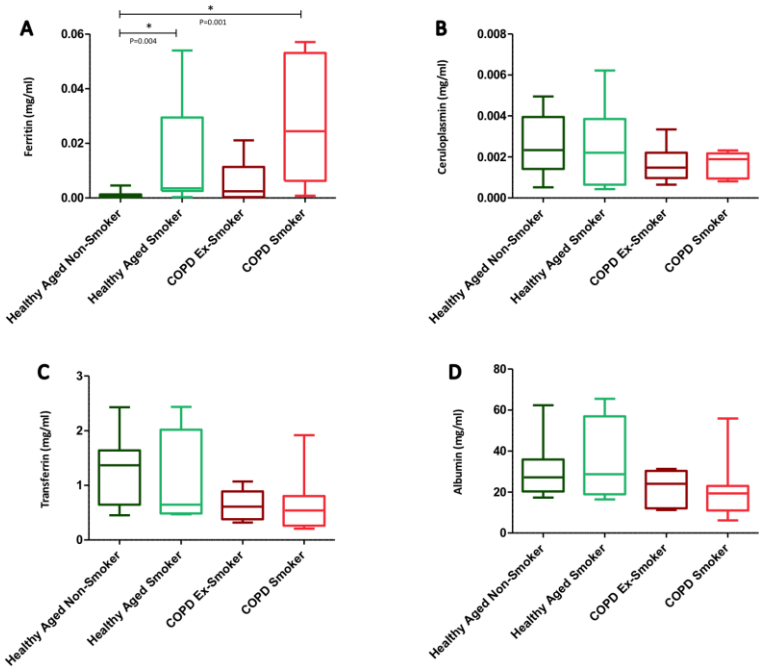

Figure 5.3: *Transport and metal handling proteins of the alveolar RTLFs.* Alveolar protein concentrations as determined by ELISA; values corrected for lavage dilution using the urea method. **(A)** Ferritin, **(B)** Caeruloplasmin , **(C)** Transferrin and **(D)** Albumin. Healthy Aged Non-Smoker n=19, Healthy Aged Smoker n=11, COPD Ex-Smoker n = 18, COPD Smoker n = 14, * denotes a statistical difference where $p<0.05$.

Examining the selected proteins involved in inflammation and immunity within the airways, IgA was found to be significantly decreased in COPD smokers (0.34 (0.2-0.6mg/mL) compared to healthy smokers (2.1 (0.1-4.0), P=0.02 and healthy aged controls (1.4 (0.8-1.9) mg/mL), P=0.01, **Figure 5.4**. IgG appeared to follow a similar pattern, although no significant differences were observed. Haptoglobin concentrations were equivalent across the four subject groups, **Figure 5.4**.

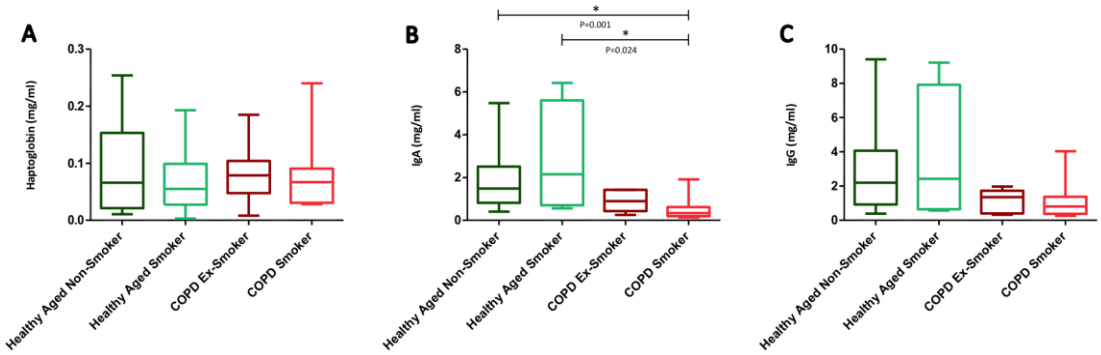

Figure 5.4: *Immunity and inflammatory process proteins of the alveolar RTLFs.* All other details as outlined in the legend to **Figure 5.3**.

Proteins involved in protease-antiprotease balance in the airways are summarised in **Figure 5.5**. The acute phase protein A2M, was significantly decreased in COPD ex-smokers (0.00008 (0.00002-0.0001) mg/mL) versus healthy aged (0.12 (0.08-0.2) mg/mL), p=0.001, and healthy smoking (0.23 (0.17-0.67) mg/mL) controls, P=0.001. A2M was also decreased in the RTLFs of COPD smokers (0.017 (0.004-0.06) mg/mL) versus both healthy smokers, P=0.025, and healthy aged controls, P=0.005. No significant differences were observed in A1AT in the quantitative analysis, contrasting with the results of the semi-quantitative analysis, which suggested 82.0-fold decreases between COPD ex-smokers and healthy aged control, and a 5.9-fold increase between COPD smokers and healthy smokers.

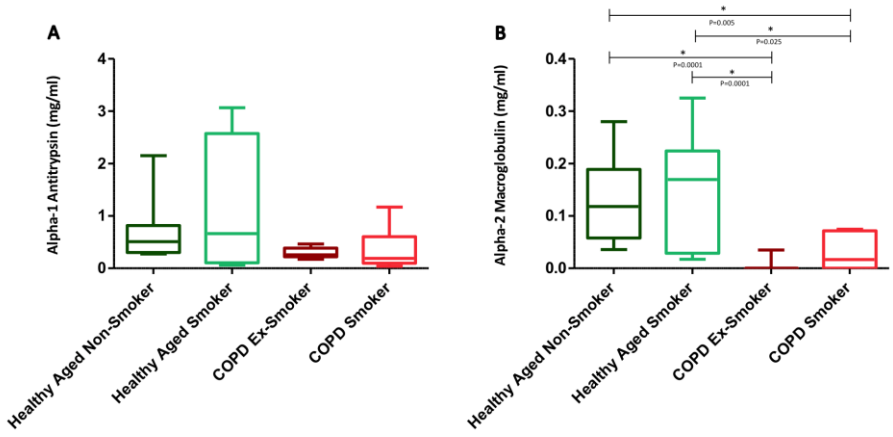

Figure 5.5:._Airway antiprotease-protease balance proteins of the alveolar RTLFs._ All other details as outlined in the legend to **Figure 5.3**.

Focusing on those proteins uniquely secreted by the airway epithelium itself (see **Figure 5.6**), Surfactant protein A, was observed to decline significantly in both COPD ex smokers (0.09 (0.01-0.14) mg/mL), P=0.003, and COPD smokers (0.09 (0.05-0.19) mg/mL), P=0.01 compared to the healthy aged controls (0.32 (0.2-0.5) mg/mL). This concurred with the results of the more limited semi-quantitative analysis, which inferred a 20-fold decrease in SP-A in COPD ex-smokers versus healthy aged controls. Surfactant protein B was signicantly elevated in smoking, without disease; healthy aged smokers (0.0076 (0.005-0.01) mg/mL) versus their non smoking counterparts (0.0038 (0.003-0.05) mg/mL), P=0.004, **Figure 5.6**. In the RTLFs of patients with COPD surfactant protein B was found to decline significantly: COPD ex-smokers (0.002 (0.001-0.003) mg/mL) compared to healthy smoking controls (0.0076 (0.005-0.01) mg/mL), P=0.002.

Furthermore, SP-B was observed to decrease in the RTLFs of COPD smokers (0.0018 (0.0016-0.004) mg/mL) relative to the concentrations within the RTLFs of the healthy smoker, P=0.002. Similar differences were not apparent from the semi-quantitative proteomic analysis. No significant differences were observed for CC16 in the alveolar RTLFs, again contrasting the semi-quantitative proteomic analysis, which inferred a 25.8-fold increase in COPD ex-smokers versus healthy aged controls, and a 22.6-fold increase between the COPD ex-smokers and the COPD smokers, in the subgroup analysis.

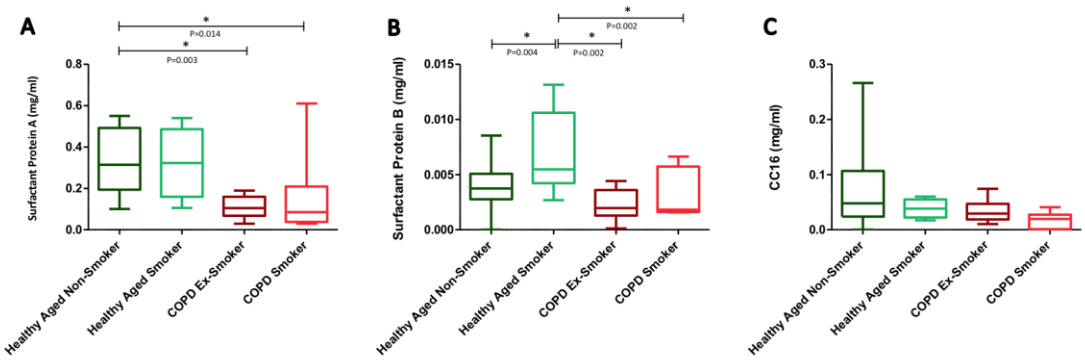

Figure 5.6: *Lung specific proteins of the alveolar RTLFs.* All other details as outlined in the legend to **Figure 5.3**.

Within the bronchial RTLFs only transferrin, of the proteins involved in metal handling and transport, displayed significant differences in COPD, being lower in the COPD smokers (0.45(0.3-0.8) mg/mL) versus healthy smokers (1.21(1.1-2.1) mg/mL), P=0.004, and the healthy aged controls (0.87(0.5-1.2) mg/mL), P=0.02. Ferritin no longer demonstrated a smoking dependent effect in bronchial RTLFs, with caeruloplasmin and albumin equivalent across all groups, see **Figure 5.7**.

Considering the bronchial RTLFs proteins, classified within the immune and inflammatory grouping (see **Figure 5.8**), the concentration of IgA was again found to be significantly lower in COPD smokers (0.68 (0.5-1.2) mg/mL), versus both the healthy smokers (3.6 (2.6-4.6) mg/mL), P=0.01, and the healthy aged controls (2.2 (1.5-3.8) mg/mL), P=0.02. IgG in the bronchial RTLF reflected this pattern, with reduced concentrations in COPD smokers (0.62 (0.45-0.89) mg/mL), versus both healthy smoking (2.4 (1.1-3.9) mg/mL), P=0.008, and non-smoking controls (1.05 (0.47-1.7) mg/mL), P=0.025. Haptoglobin concentrations were equivalent across all four groups.

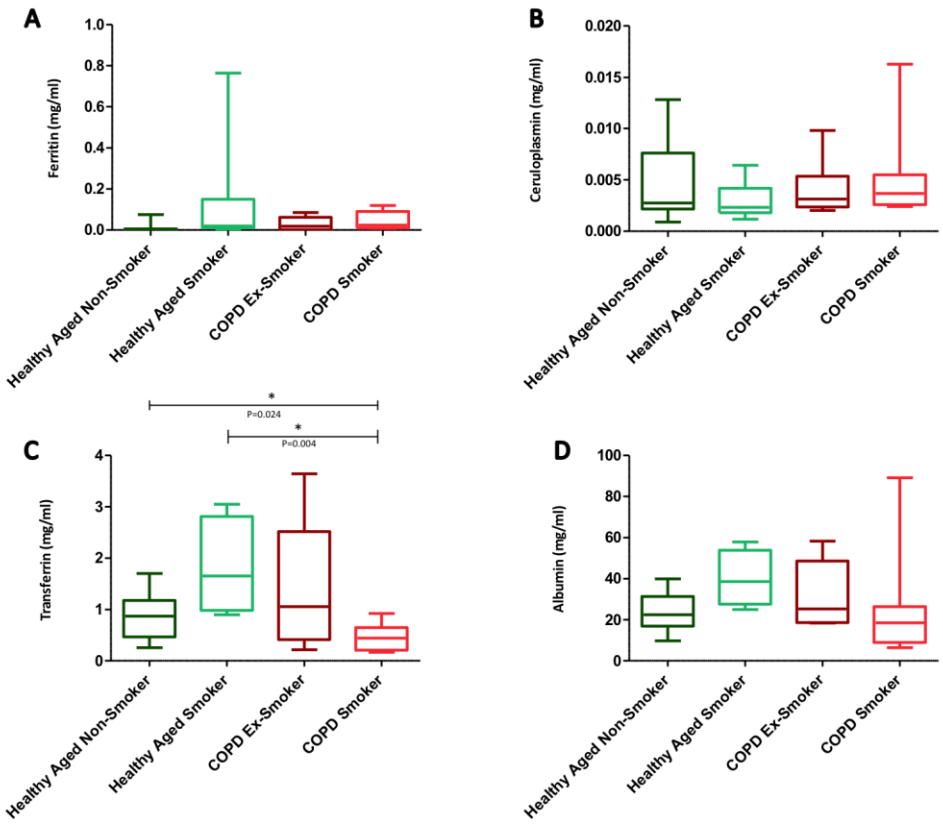

Figure 5.7: *Transport and metal handling proteins of the bronchial RTLF.* All other details as outlined in the legend to **Figure 5.3**.

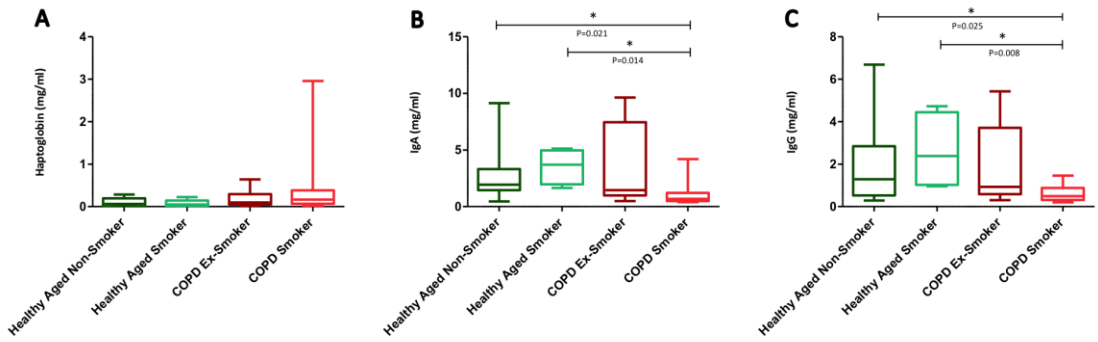

Figure 5.8: *Immunity and inflammatory process proteins of the bronchial RTLF.* All other details as outlined in the legend to **Figure 5.3**.

No significant differences in either A2M or A1AT concentrations were observed within the bronchial RTLFs (**Figure 5.9**). Of the pneumoproteins, bronchial SP-A concentrations, as observed in the alveolar compartment, were significantly lower in the patients with COPD: In COPD smokers (0.05 (0.02-0.07) mg/mL), compared with both

healthy smokers (0.40 (0.30-0.54) mg/mL), P=0.003, and healthy non-smokers (0.17 (0.13-0.46) mg/mL), P=0.002; and significantly lower in COPD ex-smokers (0.06 (0.04-0.19) mg/mL) versus the healthy smokers, P=0.016. SP-A was also found to be significantly elevated in the bronchial RTLFs of healthy smokers compared to their non-smoking healthy counterparts, P=0.04. SP-B in contrast no longer demonstrated any differences across subject groups in bronchial RTLFs, and CC16 concentrations were equivalent across all 4 groups (see **Figure 5.10**).

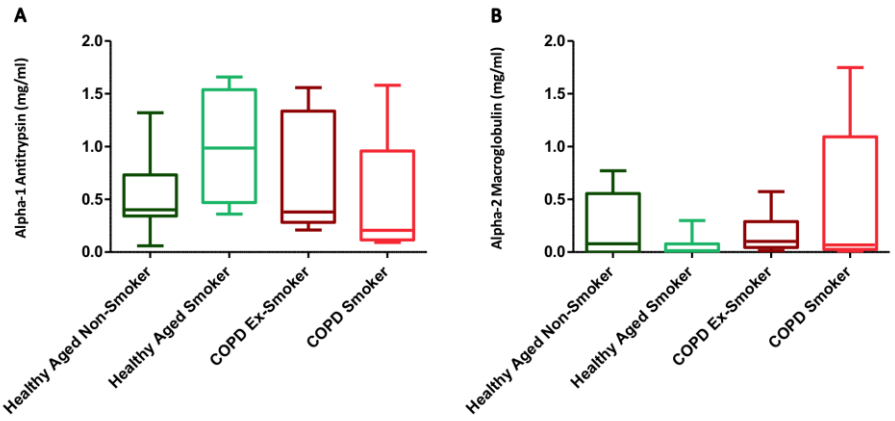

Figure 5.9: *Airway antiprotease-protease balance proteins of the Bronchial RTLFs.* All other details as outlined in the legend to **Figure 5.3**.

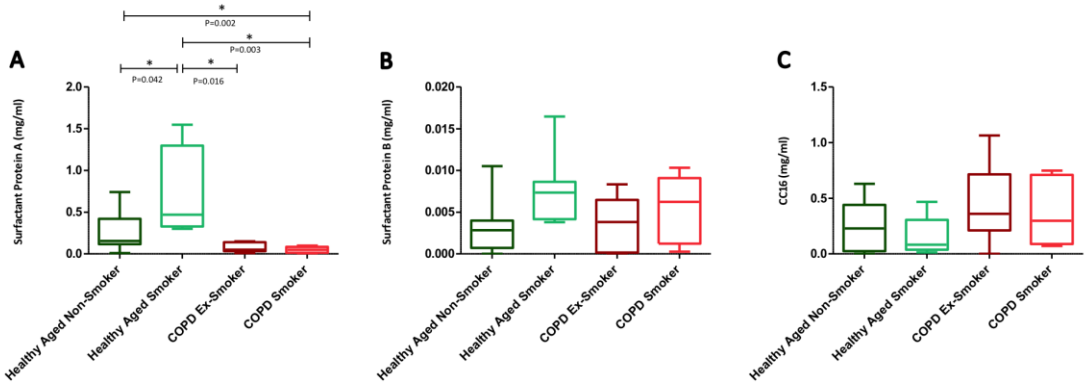

Figure 5.10: *Lung specific proteins of the bronchial RTLFs.* All other details as outlined in the legend to **Figure 5.3**.

Considering the relative contributions of individual proteins to the total alveolar protein pool, Smoking was observed to have a profound effect on RTLF protein composition (see **Figure 5.11** panels **A** and **B)**. Comparing healthy aged smoking and

healthy aged non-smoking RTLFs, albumin, was observed to increase markedly with smoking (from 56.1 (32.8-83.2) to 82.0 (79.9-86.2)% respectively). This was also the case for other plasma proteins; including haptoglobin, A2M, and caeruloplasmin, the latter demonstrating a ~40 fold increase (0.005 (0.002-0.01) to 0.5 (0.008-1.1)%). Of the locally secreted proteins, CC16, displayed a similar ~ 40 fold increase (0.16(0.04-0.2) to 12.7(2.2-47.3)%) and SP-B a ~100 fold increase (0.07(0.004-0.014) to 1.3(0.4-3.3)%) in the smoking RTLFs. The most significant increase in % contribution (~400 fold) was however noted for ferritin, increasing from 0.0013 (0.007-0.003)% of total protein in healthy aged controls, to 9.5 (0.07-12.5)% in the healthy smokers.

Within the bronchial airways (see **Figure 5.12**, panels **A** and **B**), the contribution of albumin was again observed to increase with smoking in the non-COPD population: from 68.8 (55.7-84.9) in the non-smokers to 81.7 (74.4-88.8)% in the healthy smokers. A similar smoking related increase was also noted in haptoglobin (0.15 (0.03-0.2) to 17.0 (0.1-30.1)%) and A2M (.13 (0.001-0.5) to 19.7 (1.1-49.8)%, ~100 fold) concentrations. Of the locally secreted proteins SP-B contributions increased from 0.006 (0.002-0.008)% of total protein to 1.1 (0.01-4.1)% with smoking, 130 fold; with a similar increase in CC16: 0.33 (0.04-0.6) to 7.0 (0.1-17.2)%, 40 fold, As with the alveolar RTLFs smoking in the healthy population was associated with a significant increase in the proportion of ferrtitin within the bronchial RTLF proteome: 0.005 (0.001-0.008) to 0.87 (0.07-6.2)%, ~170 fold).

Focusing on the alveolar RTLF composition in COPD in ex-smokers (**Figure 5.11,** panels **A** and **C**) I found the % contributions of albumin to the total proteome to decrease relative to aged non-smoking controls: 31.4 (27.4-39.5) compared with 56.1 (32.8-83.2)%, with a similar decrease in A2M (0.0002 (0.0001-0.0007) versus 0.14 (0.1-0.5%). Haptoglobin proved an exception, with its proportion increasing 2.5 fold in the COPD ex-smokers relative to the aged controls: 0.3 (0.15-0.42) and 0.12 (0.08-0.16)%. The proportion of CC16 was also observed to decrease, 2 fold, in COPD ex-smokers, with a similar 3-fold decrease in SP-A. Of the remaining panel of proteins investigated only ferritin was shown to differ markedly in the COPD ex-smokers relative to the aged controls, increasing 10 fold: 0.02 (0.003-0.06) versus 0.0013 (0.0007-0.003)%). A similar reduction of the contribution of albumin to bronchial RTLFs was seen in the COPD ex-smokers, but the proportions of haptoglobin, a2M and SP-B were equivalent in the COPD ex and control non-smoking groups. The contribution of SP-A was however once again

decreased in COPD: 0.12 (0.06-0.13) versus 0.56 (0.3-1.3)%), **Figure 5.12**, panels **A** and **C**.

A comparison of the impact of current smoking on the proportion of major proteins within the COPD alveolar proteome is illustrated in **Figure 15.11**, panels **C** and **D.** A large proportion of the alveolar RTLF proteome in the COPD ex-smoking smoking alveolar protein pool appears unaccounted for (~60%). Consequently the relative proportions of these major proteins were significantly increased with current smoking in COPD; with marked increases in albumin (75.7 (73.7-81.6) versus 31.4 (27.4-39.5)%), A1AT (0.74 (0.3-1.0) versus 0.4 (0.2-0.6)%) and IgG (3.1 (1.5-7.8) versus 1.9 (1.2-2.8)%). Transferrin was also observed to increase in COPD smokers versus ex-smokers (4.5 (1.2-7.3) versus 1.2 (0.6-1.6)), as did caeruloplasmin (0.009 (0.005-0.01) versus 0.004 (0.003-0.01)%), and A2M (0.1 (0.03-0.2) versus 0.0002 (0.0001-0.007)%). The proportion of ferritin was also increased in COPD smoking RTLFs (0.15 (0.06-0.2) versus 0.02 (0.003-0.06)%), as was SP-A, (0.63(0.6-0.7) versus 0.14 (0.1-0.2)%). In contrast, few changes were evident in the protein proportions within the bronchial COPD RTLF, with only albumin shown to have increased in the smoking COPD patients: 85.8 (62.7-101.8) versus 57.7 (44.9-85.0)%), see **Figure 5.12**, panels **C** and **D**.

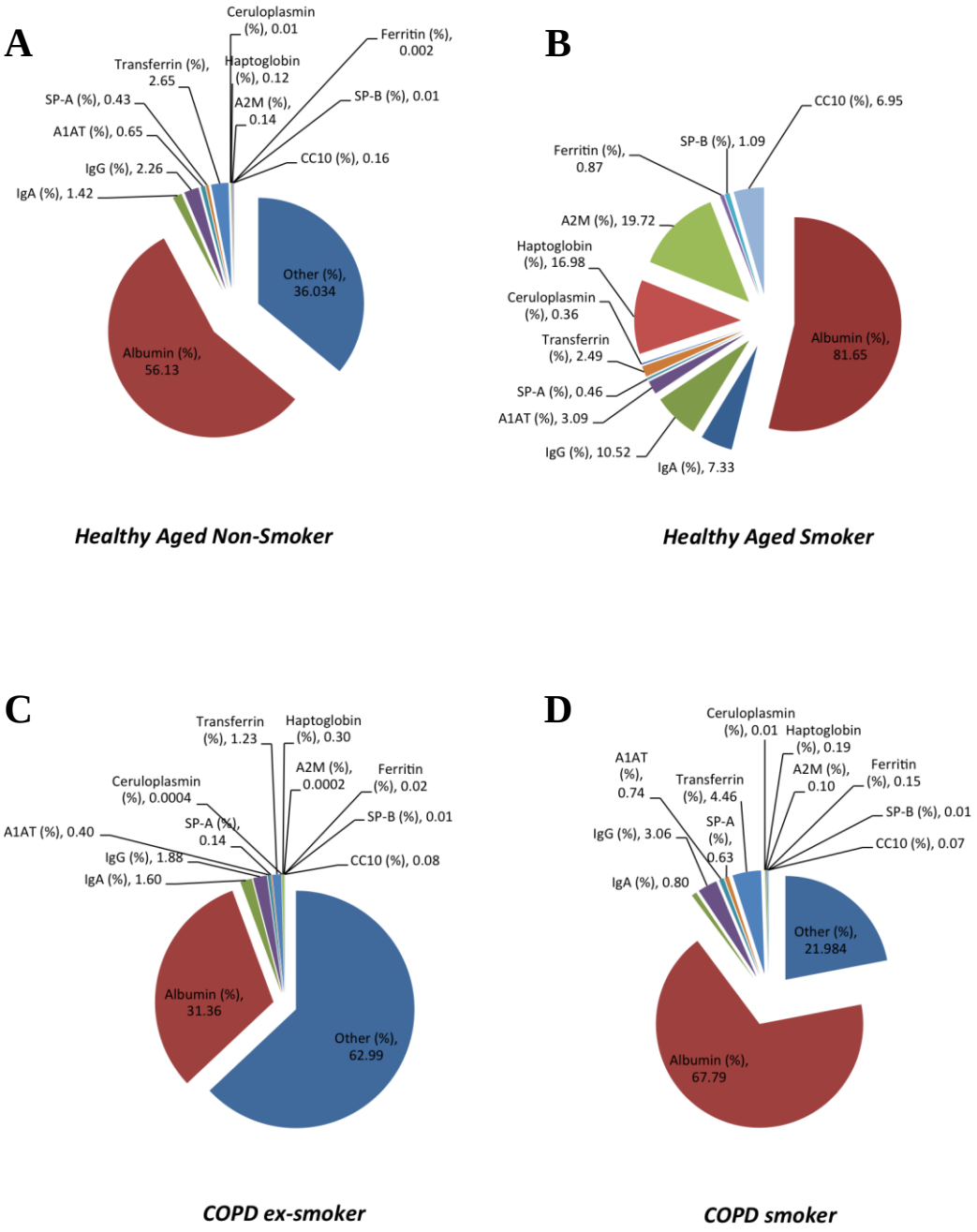

Figure 5.11: *Percentage contributions of individual alveolar protein components relative to total alveolar RTLF protein.*

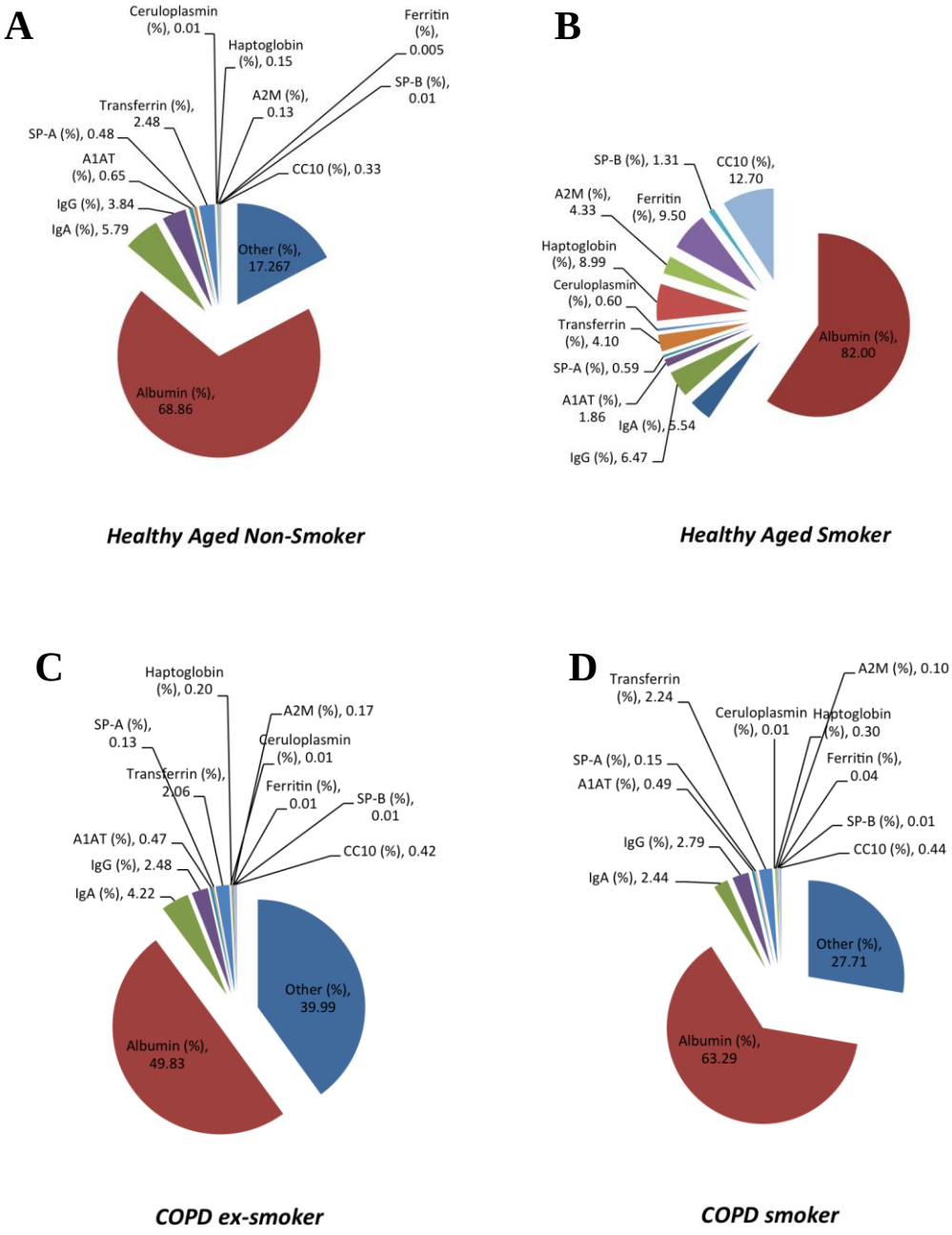

Figure 5.12: *Percentage contributions of individual bronchial protein components relative to total bronchial RTLF protein.*

5.3.3: The RTLF oxidant-antioxidant imbalance in COPD

To explore the impact of a potential oxidant-antioxidant imbalance, bronchoalveolar lavage samples were analysed for the low molecular weight antioxidants: vitamin C (ascorbate and dehydroascorbate), urate, and glutathione (total, reduced and glutathione disulphide). Individual lavage urea correction factors determined were applied to the antioxidant concentrations measured in order to yield alveolar RTLF concentrations, as illustrated in **Table 5.11**. Ascorbate was significantly increased in the RTLFs of COPD smokers (28.7 (7.5-48.9) μM) versus the healthy aged controls (0.00 (0.0-11.0) μM). Within the COPD RTLFs, significantly elevated RTLF ascorbate was also observed in the COPD smokers versus the ex-smoking subjects (2.66 (0.0-11.9) μM). No significant differences were however noted in dehydroascorbate concentrations, or total vitamin C concentrations across subject groups. Conversely, glutathione was significantly decreased in the RTLFs of COPD smokers (29.7 (89.2-296.5) μM) versus, healthy smoking controls (400.5 (257.5-499.6) μM). However, the RTLF glutathione of COPD smokers was found to be significantly elevated versus that observed in ex-smokers (96.0 (45.0-123.2) μM). Healthy aged smokers displayed significantly elevated concentrations of GSH compared with both healthy non-smokers (118.9 (82.8-154.5) μM) and COPD ex-smokers (96.0 (45.0-123.2) μM). No significant differences in total glutathione or glutathione disulphide were observed across groups investigated. Despite the significant changes in RTLF antioxidant concentrations, no evidence of protein oxidation was apparent; either in terms of protein carbonyl (**Figure 5.13**) or 4-HNE adduct (**Figure 5.14**) concentrations across the four groups.

Table 5.11: *Low molecular weight antioxidants*

	Healthy Aged Non-Smoker	Healthy Aged Smoker	COPD Ex-Smoker	COPD Smoker
Vitamin C (□M)	82.5(67.6-123.4)	116.7 (68.7-141.7)	45.7 (35.0-66.1)	74.57(46.13-98.5)
Ascorbic acid (□M)	0.00 (0.0-11.0) ♯	19.2 (1.5-40.4)	2.66 (0.0-11.9) §	28.7 (7.5-48.9) § ♯
Dehydroascorbic acid (□M)	73.6 (35.5-101.3)	58.6 (42.5-111.4)	34.3 (26.6-59.7)	58.1(34.0-65.9
Uric acid (□M)	86.6 (84.4-190.4)	81.1 (50.7-119.8)	70.8 (61.4-99.4)	72.3 (42.3-96.0)
GSx (□M)	141.1 (128.9-190.4)	473.8 (312.7-658.3)	110.3 (67.5-307.6)	286.4 (237.3-404.1)
GSH (□M)	118.9 (82.8-154.5) £	400.5 (257.5-499.6) £	96.0 (45.0-123.2) §**	229.7 (89.2-296.5) §*
GSSG (□M)	11.14 (0.0-39.5)	43.1 (13.3-72.3)	4.0 (0.0-102.0)	29.0 (20.7-41.3)
GSSG:GSH	30.8 (0.0-113.9)	12.4 (5.0-28.4)	10.6 (0.0-68.9)	20.5 (18.1-38.4)

Data represents urea corrected values for all subjects: Healthy aged non-smoker (n=19), healthy aged smoker (n=11), COPD ex-smoker (n = 18), COPD smoker (n = 14). Concentrations are expressed median values with interquartile range. Statistical differences where $p<0.05$, are represented by the following symbols: * CS vs HS, ♯ CS vs HAC, ** CES vs HS,♯♯ CES vs HAC, £ HS vs HAC, § CS vs CES.

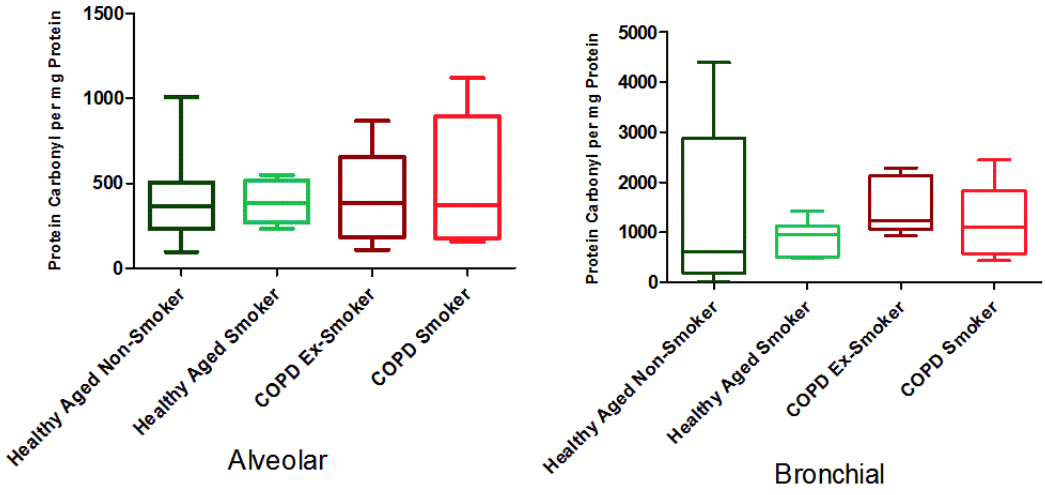

Figure 5.13: *Protein carbonyl (per mg protein) in (A) alveolar and (B) bronchial RTLFs of aged smoking, non-smoking healthy and smoking, non-smoking COPD airways.* All other details as outlined in the legend to **Figure 5.2**.

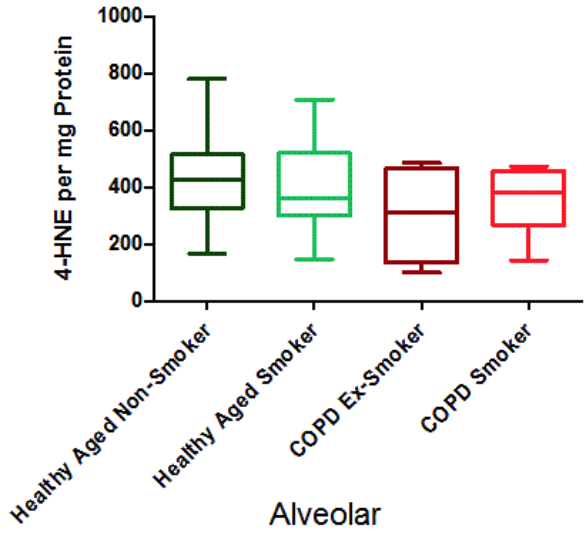

Figure 5.14: *Protein HNE adducts (per mg protein) in alveolar RTLFs of aged smoking, non-smoking healthy and smoking, non-smoking COPD airways.* All other details as outlined in the legend to **Figure 5.2**.

5.4: Discussion

The principal aim of this chapter was to characterize the composition of the RTLFs across the bronchial and alveolar compartments of the COPD airway. To achieve this I employed age and smoking history matched controls, including a group of aged healthy smokers, i.e. with normal lung function and no evidence of respiratory or cardiovascular disease, to fully isolate the effects of COPD itself from those of smoking. I hypothesized that the changes observed would be reflective not only of the key pathological changes occurring within the airway of COPD patients: oxidative stress, chronic inflammation and protease/anti-protease imbalance, but also features typical of the normal ageing processes of the airways (as outlined in **Chapter 4**). The investigation focused on the RTLF proteome, with identified proteins classified according to their role in the underlying pathology of the disease: grouped by the immune/inflammatory response, proteolytic/anti-proteolytic balance, and those with antioxidant properties. Furthermore, I identified that a large proportion of the proteins identified were related to metal handling processes; the second largest grouping in three of the four groups examined. This grouping was therefore included in my classification of alveolar proteins.

Examining the existing literature regarding proteomic investigations into COPD, using a PubMed search for COPD and proteomics identified 84 papers. The majority of these previous investigations in COPD focused on the identification of biomarkers for diagnostic purposes, and thus plasma samples were routinely used to assess the systematic effects of this disease (Rana et al., 2010; York et al., 2010; Verrills et al., 2011; Merali et al., 2014). Other proteomic investigations have employed induced sputum as a means of non-invasively sampling the central airways (Ohlmeier et al., 2012), with further studies examining lung tissue (Ohlmeier et al., 2008; Ishikawa et al., 2010; Ohlmeier et al., 2010; Barreiro et al., 2014) or the proteome associated with exhaled breath condensate (Chhabra and Gupta, 2012). Only four have specifically investigated the RTLF composition of the diseased airway itself (Merkel et al., 2005; Franciosi et al., 2013; Pastor et al., 2013; Tu et al., 2013); these studies are summarized in **Table 5.11**, which summarizes the cited papers major findings, analysis platform and the manner of protein quantification performed.

In this study I have utilized the same stringent analytical approach adopted in **Chapters 3** and **4**; analyzing five representative samples individually from each of the 4 groups analysed, as opposed to pooling. In all cases lavage samples were analysed after

pre-concentration and the final data adjusted, both for the total protein concentration in the original sample, but also the lavage dilution. Of the 4 proteomic studies performed specifically addressing the RTLF, Merkel et al., (2005) concentrated samples, but did not attempt to quantify their results, whilst Tu et al., (2013) employed an ion-current-area-based label-free quantification method, based on samples that had undergone a soft precipitation. The present investigation is therefore the first proteomic study that has attempted to go one step further and derive semi-quantitative estimates of RTLF protein concentrations, based on the MS data after adjustment for the lavage dilution. It is also important to state that the MS data has been employed only as an indicative guide for the identification of the major common proteins across the 4 proteomes and for the generation of novel hypotheses, and as with previous proteomic investigations I have used conventional antibody based techniques to follow-up and validate interesting results (Bondarenko et al., 2002; Chelius et al., 2003; Wang et al., 2003; Liao et al, 2004; Wu et al., 2005).

Finally, this investigation arises out of a wider program of work aimed at characterizing RTLFs to permit the informed design of disease specific simulants for the improvement in the delivery of inhaled medicines. With COPD now believed to affect >10% of the world population over 40, COPD patients are clearly a key patient group and market for inhaled medicines. Whilst it could be argued that the use of a COPD patient population not taking medication, such as inhaled corticosteroids, cannot be wholly considered a 'real world' population, however the focus of this investigation was to characterise changes in the RTLF attributed to COPD and not the likely significant influence of corticosteroids on disease progression. In choosing to focus on the most abundant proteins of the RTLF in this analysis, we were able to determine over ~65% of the total RTLF protein pool across all subject groups to inform the development of physiologically representative simulant lung lining fluids. It should be noted that within the COPD ex-smoking groups only 40% of the proteome was accounted for, with only 58 proteins identified in the MS proteomic analysis.

The key observations arising out of these investigations can be defined as those informing our understanding of the impact of cigarette smoking on the composition of the RTLF in the healthy (non and current smokers) and COPD lung (ex and current smokers); as well as changes related to the presence of COPD, either basally, i.e. through comparison of healthy aged non-smokers with COPD ex-smokers; or in relation to the response of the COPD airway to oxidative stress, related to cigarette smoke inhalation;

comparing healthy aged smokers to COPD active smokers. With this in mind the key observations arising out of this study were as follows:

(**1**) Equivalent total protein concentrations were seen in the bronchial and alveolar RTLF across all four groups, though the concentrations were higher in the bronchial compartment. Despite this, the relative proportions of the most abundant proteins identified in the proteomic pre-screen varied markedly between groups. Significantly, within both RTLF compartments a significant proportion of the total protein was not accounted for, with the exception of the healthy aged smokers.

(**2**) The proteomic analysis highlighted the importance of metal handling proteins at the air-lung interface, particularly iron related proteins, representing the second largest functional classification in three of the four groups.

(3) The proteome in COPD ex-smokers lacked the complexity of that in healthy non smokers and smokers. This result was confirmed in two separate sub groups of COPD ex-smokers. The complexity of the COPD RTLF proteome was increased in the COPD current smokers, though there was a larger contribution of protein of intra-cellular origin.

(**4**) Smoking induced a significant increase in alveolar RTLF ferritin, indicative of cellular injury and the release of this intra-cellular protein in healthy aged subjects and COPD patients, a similar response was not evident in the bronchial compartment.

(**5**) Smoking was associated with an increase of SP-B in alveolar RTLFs, but this response was restricted to the healthy aged population. A similar increase in SP-B was also seen in the bronchial compartment of healthy smokers, through this failed to attain statistical significance. In contrast SP-A was increased with smoking in the aged healthy population, with the response again absent in the COPD patients.

(6) Patients with COPD had significant reductions in alveolar RTLF innate immunity proteins (IgA, A2M and SP-A) compared with their age-matched controls, irrespective of smoking status. Similar deficiencies were observed within the bronchial RTLFs, with reduced concentrations of IgA, IgG, transferrin and SP-A.

(**7**) Smoking was associated with an increase in transferrin concentrations in the bronchial RTLFs of healthy subjects. This response was absent in the COPD smokers.

Table 5.12: *Summary of previous proteomic studies addressing the RTLF composition in COPD*

Reference	Sample	Subject groups	Analysis platform	Sample treatment	Quantification?	Key results
Merkel et al., 2005	BAL	CS, n=10 HS, n=8 NS, n=8	RP HPLC and MALDI-TOF nanoLC MS/MS Concentrated SELDI MS	Concentrated (using centricon MW cutoff 10kDa) for SELDI samples Samples pooled from5 donors for RP-HPLC and MALDI-TOF	no	60 proteins identified using all methods 100 distinct protein/peptide mass peaks were constantly detected Defensins 1 and 2, s100A8 and A9 increased in CS vs HS
Tu et al., 2014	BAL	Patients with stable COPD (n = 10, 67.8 ± 8.5) and healthy non smoking subjects (n = 10, 63.4 ± 11.73)	nanoLC MS/MS Western Blot	Precipitation/On-Pellet-Digestion	Ion-current-area-based label-free quantification method that provides high quantitative precision.	423 identified and quantified proteins, 167 (39.5%) were designated as secreted proteins. 50 proteins were significantly elevated ($p<0.05$) and 26 were significantly decreased in COPD ($p<0.05$). 38 proteins, 50% were located in extracellular region and 25, 32.9% in plasma membrane Significantly altered proteins identified to have a role in lung inflammatory responses, gluconeogenesis/glycolysis include: cathepsin D, galectin 3, ADH1B, transgelin 2, fibronogen β , SAP, ALDH2, and ALDH3A1
Pastor et al., 2013	BAL	COPD, n=15 COPD+LC, n=15 LC, n=15	2D-PAGE and MALDI TOF/TOF Western blot	Samples were then depleted of the two most abundant BAL proteins (albumin and immunoglobulin G) to allow an adequate identification of the less abundant ones. This was accomplished by the use of SpinTrap columns	Western blotting only	40 differentially expressed (greater than 2 fold difference) Four proteins appeared up-regulated in the COPD and LC/COPD groups. These proteins are enzymatic antioxidants, and represent the first line of defence against oxidative stress. Proteins up-regulated in the LC and/or LC/COPD groups in our comparative proteomic study included TKT, FBP1, ALDOA, PYGM and PKM2. All these proteins are involved in the regulation of glycolysis,
Franciosi et al., 2011	ELF	COPD (current and ex-smokers), n=4 Control (current and ex-smokers), n=4	1D PAGE and Chip LC MS/MS	Samples were taaken using the BMP smapling probe, to avoidlarge and variable saline with lavage procedures	iTRAQ labelling between COPD and non COPD controls	300 proteins identified Lactoferrin, HMGB-1, alpha-1 antichymotrypsina nd cofilin significantly increased in COPD

(**8**) These changes in RTLF composition were seen within the context of an expansion of macrophages numbers in the distal lung of healthy and COPD smokers, relative to their non-smoking control groups. This was seen in the absence of neutrophilia, either related to smoking or disease status, suggesting that the COPD patients were well controlled. There was also an absence of overt oxidative stress in the COPD airway, with GSH concentrations significantly increased with smoking in both healthy control and COPD patients.

The smoking related increase in macrophage number in the distal lung of both healthy subjects and COPD patients in the present study accord with other published studies showing an increase in total leukocytes in the airways of smokers with normal lung function (Wallace et al. 1992; Barcelo et al. 2008); with a similar expansion in airway macrophage numbers reported in the lungs of young smokers (Ohnishi et al. 1998). No increase in macrophage numbers was observed in the COPD patients, current or ex-smokers compared with their relevant control groups. This result is somewhat at odds with the literature reports of increased macrophage numbers in the bronchial sub-mucosa (Saetta et al. 1993; Di Stefano et al. 1996; Rutgers et al. 2000), bronchial glands (Saetta et al. 1997) and airway epithelium (Turato et al. 2002) of COPD patients. Furthermore, there is some evidence supporting a positive association between alveolar macrophage numbers and the severity of COPD (Finkelstein et al. 1995; Gorska et al. 2008).

In addition I observed no evidence of neutrophilia in COPD smokers and non-smokers relative to their control groups. This observation differs markedly from the published literature where increased BAL neutrophils have been reported in both smoking and ex-smoking COPD patients (Babusyte et al. 2007). Moreover, this increase in neutrophil numbers has been reported to persist even after smoking cessation (Louhelainen et al. 2009). The basis for this cellular recruitment to the airways has been associated with the increased release of chemotactic factors such as interleukin 8 (IL-8) and leukotriene B4 (LTB4), which have been shown to be elevated in the airways of patients with COPD (Corhay et al. 2009). It is important to state that the COPD patients in the current study were all clinically stable, with no airway infection for a period of 3 months prior to the bronchoscopy, no recent exacerbations and were not taking anti-inflammatory medications. These tight recruitment criteria were adopted to minimise the influence of recent exacerbations and medication usage. Other studies examining airway inflammation in COPD have often provided limited information on the patient's recent

history of infection, medication usage or smoking history, which makes a simple comparison of observations between studies difficult.

The observation of an increase in respiratory tract lining fluid GSH concentrations in the smoker groups, accords with previous observations (Cantin et al 1987; MacNee, 2000). Whether this reflects an adaptive response to oxidative stress or the consequence of the release of intra-cellular GSH into the extra-cellular spaces from dying cells is not clear. Notably this increase occurred in parallel to increased alveolar RTLF ascorbate and ferritin concentration. As ascorbate is exclusively derived from the diet in humans and ferritin is a large intra-cellular protein, these parallel increases are supportive of GSH leakage from injured or dying cells. It is long established that cells induced to undergo apoptosis demonstrate a rapid and specific efflux of GSH (van den Dobbelsteen et al. 1996). Beyond these smoking related impacts on the RTLF antioxidant network, no affect of COPD itself was seen. Further, no increases in markers of protein oxidation, or indeed, increased concentrations of either dehydroascorbate or glutathione disulphide were observed in the distal lung in relation to either smoking status, or the presence of COPD. Thus in contrast to previous studies (Nowak et al., 1999; Montuschi et al. 2000; Beeh et al. 2004; Di Stefano et al. 2002; Rahman et al. 2002; Ricciardolo et al. 2005), we saw no overt evidence of oxidative stress in our COPD subjects.

Despite the absence of active neutrophilia, or oxidative stress within the alveolar or bronchial RTLF proteomes clear smoking related responses were observed. Ferritin concentrations were increased in the alveolar RTLFs of both healthy and COPD smokers, in the absence of a similar response in the bronchial compartment. Elevated concentrations of ferritin have previously been associated with necrosis in the RTLFs of smokers (Mateos et al, 1998; Erbaycu et al., 2007). Dying alveolar macrophages have also been shown to release ferritin, with a significant association observed between ferritin and LDH concentrations, which is significant given the increase in alveolar macrophage numbers associated with smoking (McGowan and Henley, 1988; Wesselius et al., 1994). Evidence was also observed for smoking related increases in surfactant proteins in bronchial and alveolar compartments, though the responses were restricted to the healthy aged controls. The presence of surfactant proteins within the bronchial compartment indicates a certain degree of admixture between the proximal and distal airway lavages. Consequently here I will discuss the smoking related increases in SP-A and SP-B in general across the airway, rather than focus on a given compartment. With regard to the smoking related increase in SP-A seen in the healthy aged subjects in the

present study the existing literature presents conflicting evidence, with some in line with our findings (Behera et al., 2005; Ohlmeier et al., 2008; Mazur et al., 2011), whilst others reported decreased concentrations (Honda et al., 1996; Hermans et al., 1999; Betsuyaku et al., 2004). Vlachaki et al, (2010) suggested that SP-A may play a protective effect role against effects of smoking, due to its anti-inflammatory properties. SP-B was similarly increased with smoking in the healthy aged subjects, though the effect was most marked in the alveolar RTLFs. No previous reports have identified a similar cigarette smoke induced increase in this protein in the lung. Significantly no such response was seen in the COPD smokers, despite previous evidence of increased concentrations of SP-A in the sputum of COPD smokers (Ishikawa et al., 2011). In contrast Betsuyaku et al., (2004) observed a reduction in both SP-A and SP-D, in aged smokers with emphysema.

Under the chronic inflammatory conditions such as those observed within the COPD airway, phenotypic changes in resident alveolar cells, from type II pneumocytes into the non surfactant secreting type I pneumocytes has been observed (Wirtz and Schmidt, 1996; Subramaniam et al., 1996; Barnes et al., 2003; Bernhard et al., 2004; Milic-Emili, 2004). It is therefore plausible that the absence of a smoking related increase in surfactant proteins in COPD patients may reflect an underlying remodelling of the alveolar epithelium.

One of the key observations of the current study was the decrease in a number of key innate immunity proteins within the RTLFs of COPD patients, which was observed irrespective of the patients smoking status (IgA, IgG, SP-A and A2M). The lower concentrations of SP-A in both lower and upper airway COPD RTLFs likely reflected a reduction in the number of type II pneumocytes in COPD due to squamous cell metaplasia, as described above. The reduced concentration of IgA may reflect isotype switching of immunoglobulin secreting plasma cells of the airways (from IgA to IgG) in COPD patients, which has been proposed to occur in response to bacterial or viral infections, and as a specific response induced by long term smoking (Soutar, 1977; Bell, 1981; Stockley, 1980; Brandsma et al., 2012). However the fact that IgG was also depressed suggests a more fundamental dysregulation of antibody production within the COPD airway (Pauwels, 2001). Similarly, in the absence of a clear signal indicative or altered airway permeability, the decreased concentrations of both A2M and haptoglobin suggest a reduction in the local production within the lung, from epithelial cells and alveolar macrophages (Yang et al., 1995). Smoking was associated with increased transferrin concentrations in the healthy bronchial RTLF, which was absent in the COPD smokers. The available literature on airway transferrin concentrations in relation to

smoking is varied and restricted to healthy controls, with evidence of both decreased concentrations (Stites et al., 1995; Ghio et al., 2008), or no overall change (Mateos et al., 1998). Transferrin however is also secreted locally within the airways and thus the remodelling of the airway epithelium in COPD might impact on basal rate of production, explaining the current result (Bell et al., 1981; Wesselius et al., 1992; Stites et al., 1995; Mateos et al., 1998).

Conclusions

In the present study I sought to investigate the composition of the RTLFs in COPD patients, an important group for the development of inhaled medications. In order to isolate disease specific signatures it was necessary to include both age and cigarette smoking matched controls groups. Consequently, the subsequent analysis revealed information not only on COPD itself, but also on the impact of smoking on the RTLF proteome. Using the approaches adopted in the previous two chapters I first identified the most abundant proteins common across the four groups in subsets of subjects, before analyzing these within the full groups. Whereas previously using this approach I had been able to account for the majority of the total protein within both the bronchial and alveolar RTLFs (>70%), in the current investigation, a significant proportion of the total protein pool remained unaccounted for, in all groups, with the exception of the COPD smokers. Also, whilst total protein concentrations were equivalent across the 4 groups, the relative proportion of individual proteins varied considerably, suggesting that COPD RTLF simulants would need to differ significantly from the base model identified in Chapter 3.

The relative paucity of the RTLF proteome in the COPD ex-smokers was an unexpected result. When it was initially observed in the first subset of subjects, the decision was made to repeat the analysis in a further 5 COPD ex-smokers, which confirmed the original result. At this time there is no simple explanation for this finding and further work will be required to assess whether this is a function of decreased basal secretion from airways cells, attributable to increased levels of senescence, or increased proteolysis. The result is further complicated by the observation that the COPD smokers had the most abundant proteome, though many of the identified protein were of intra-cellular origin and may therefore reflect augmented injury, rather than an enhanced secretory response. Finally, perhaps the most significant ancillary observation arising from this study was clear evidence of reduced innate immunity protein concentrations within the airway of COPD subjects, which was apparent throughout the respiratory tract,

irrespective of the subjects smoking status. Such an underlying change would confer an increased sensitivity to the COPD airway to both infection and other inhaled irritants, in line with the formal definition of the disease. A key question going forward will be whether this reflects a remodeling of the airways, or precedes it, and hence contributes to the underlying pathological changes observed in COPD.

Chapter 6

The design and evaluation of simulated epithelial lining fluids

6.1: Introduction

The overall aim of this thesis was to develop a series of standardised lung lining fluid simulants reflective of the different regions of the airways and compositional alterations characteristic of asthmatic and chronic obstructive pulmonary disease. Lung lining fluid stimulants, designed to represent different lung regions and disease conditions, will be used for the *in vitro* biopharmaceutical screening of inhaled particulate drugs, and therefore must not only be physiologically representative of RTLF composition, but also optimised for cost, convenience and reproducibility, as well as stability upon storage.

The approach was first to design a 'base' model simulant based on the major protein, lipid and low molecular weight constituents, referencing this against human RTLF composition. As described in detail throughout **Chapters 3, 4 and 5**, the composition of the RTLF varied significantly across the proximal conducting bronchial airways down to the distal alveolar regions, reflective of the physiological requirements of these airway compartments. **Table 6.1** highlights the variations in concentrations determined in healthy RTLFs compared to those previously reported within the literature. Furthermore, significant compositional changes within this crucial extracellular compartment were established in relationship to age, airway disease and smoking status, presumably reflective of ongoing processes. The focus on these subgroups is believed to be a necessary consideration in the design of simulated epithelial lining fluids, with the majority of the key demographic user groups of inhaled medicines consisting of individuals in both the disease and age groups.

Table 6.1: *The RTLF components of healthy alveolar and bronchial airways, determined within this investigation and the existing literature.*

RTLF components		Alveolar RTLF Concentrations	Alveolar RTLF Concentrations from the literature	Bronchial RTLF Concentrations	Bronchial RTLF Concentrations from the literature
Antioxidants	Ascorbic Acid µM	122.1	40[1], 100[2], 200[3], 100[5], 283.9[10]	40.7	
	Uric Acid µM	95.5	207[1],90[2],200[3],90[5], 148.7[10]	127.9	
	GSH µM	161.6	109[1], 100[2], 129[4], 100[5], 162.7[10]	323.3	
	Catalase U/mL		410		
	Glutathione Peroxidase U/mL		0.051		
	Superoxide dismutase U/mL		4010		
	Alpha tocopherol µM		0.1-1.7[2], 2.3[10]		
Proteins	Albumin mg/mL	8.8	3-5[2], 5.35[6], 3.8[7], 7.4[10]	24.2	
	Transferrin mg/mL	1.5	0.4	2.3	0.2[6]
	IgG mg/mL	2.6	0.7[2], 0.6[6], 0.9[7]	2.6	0.7[6]
	IgA mg/mL	0.8	0.6-1.4[2], 0.6[6], 0.06[7]	6.2	1.4[6]
	IgM mg/mL	0.1	0.03	0.1	
	Lysozyme mg/mL	0.06	1-3[2], 0.03[9], 2.5[10]	0.4	0.08[9]
	Alpha 1-antitrypsin mg/mL	2.0		1.2	
	Lactoferrin mg/mL		0.21		
Surfactant	Phospholipids mg/mL	4.8	0.4 ± 0.1[8], 0.4[11]		
	Phosphatidylcholine (DPPC) mg/mL	4.6	0.007 ± 0.0008[8], 10[10]		
	Phosphatidylglycerol mg/mL		0.002 ± 0.0003[8]		
	Neutral lipids mg/mL	0.1	0.02 ± 0.006[14]		
	SP-A mg/mL	1.0	0.005 ± 0.0002[8], 6.4±0.7[11], 0.004 ± 0.0003[13]	1.5	
	SP-B mg/mL		0.0007 ± 0.00009[15]		
	SP-C mg/mL		0.0006 ± 0.00005[16]		
	SP-D mg/mL		0.5±0.07[11], 0.00007 ± 0.000003[12]		

1. Van der Vliet et al., (1999); 2. Hatch (1992); 3.. Slade et al.,(1993); 4. Cantin et al.,(1987); 5. Cross et al., (1994); 6. Rennard et al., (1990); 7. Sutinen et al., (1995); 8. Meyer et al., (2000); 9. Thompson et al., (1990); 10. Sun et al., (2001); 11. Cheng et al., (2000); 12. Honda et al., (1996); 13 Hamm et al., (1994); 14 Ito et al., (2006); 15 Kramer et al., (1995); 16 Schmidt et al., (2002).

First, it must be recognized why the design and development of physiologically representative simulants is necessary. As discussed in detail (see **Chapter 1**) RTLFs form the first physical interface inhaled particles encounter following their delivery into the airways. In the fields of geochemistry and environmental studies simulated extracellular lung fluids are an integral part of *in vitro* investigations, despite their relative simplicity they nevertheless illustrate the importance of biorelevant models in the analysis of inhaled materials (de Meringo et al., 1994; Herting et al., 2006; Sdraulig et al., 2008). In contrast however, fluids representative of this extracellular compartment have not been incorporated into the majority of *in vitro* studies investigating the fate of inhaled medicines (Eixarch et al., 2010; Agu and Ugwoke, 2011).

The advantages of delivering drugs through the inhalatory route are extensive: the large surface area for drug absorption alongside the extensive alveolar capillary network result in both rapid clearance and rapid onset of drug action, suitable for small molecules to large molecular weight proteins. Furthermore, low extracellular and intracellular enzymatic activity and the absence of first pass metabolism have made inhalation an attractive and established route for both local and systemic drug delivery (Dolovich, 1989; Newman et al., 1991; Liu et al., 1993). Nevertheless gaps remain in our understanding of the fate of inhaled medicines, and with emerging developments in pulmonary medicine (particularly in the development of nanoparticulate formulations) the need for physiologically representative *in vitro* methods to evaluate the behaviour and thus ultimately bioavailability of inhaled drugs is apparent (Forbes and Ehrhardt, 2005; Sadler et al., 2011).

In the case of orally delivered compounds the use of bio relevant media, FASSIF and FESSIF, have demonstrated clear improvements in establishing *in vitro- in vivo* correlations of drug behaviour (versus that of compendial media) (Sunesen et al., 2005; Wei and Lobenberg et al., 2006; Lue et al., 2008; Okumu et al., 2008; Jantratid et al., 2009; Shono et al., 2009). However the complexity in modeling the various unique features of the respiratory system *in vitro*, i.e. the large surface area (human alveolar surface area alone is ~100 m^2), anatomical diversity, the relatively low volume and the static nature of the RTLFs, have limited the use of physiologically relevant media in *in vitro* models of inhaled drugs, in contrast to use of biorelevant media to represent the fluid in the gastro-intestinal tract (Patton, 1996; Gray et al., 2008; Son and McConville, 2009).

Preliminary studies incorporating RTLF components, into simulated fluids, although mainly limited to DPPC, have already demonstrated significant effects in the relative solubilization of drug compounds, particularly those hydrophobic in nature, by increasing both wettability and preventing aggregation of drug particles (Wiedmann et al., 2000; Sinswat et al., 2008). Similarly with investigations into the dissolution of inhaled drug particulates, buffer systems incorporating varying concentrations of DPPC have been investigated in attempts to mimic the *in vivo* situation. The addition of DPPC has been demonstrated to enhance the dissolution profiles of poorly soluble compounds, predictably following the trend observed in solubility studies (Wiedmann et al., 2000; Pham and Wiedmann, 2001; Davies and Feddah, 2003; Son and McConville, 2009). Obtaining accurate *in vitro* dissolution profiles of drugs is a necessary parameter in estimating the bioavailability of drugs *in vivo* (and thus establishing *in vitro-in vivo* correlation), however, no pharmacopoeial standard for the dissolution media or apparatus required for the testing of inhaled drugs is available (Davies and Feddah, 2003).

The use of *in vitro* cell-culture techniques (A549, Calu-3, 16HBE14o-, hAEpC primary cell cultures) are also employed in investigations to screen the behaviour of inhaled medicines. Cell culture studies are typically useful for examining aspects of drug delivery such as absorption, permeability, transport, metabolism and toxicity, crucial factors in evolving our understanding of the underlying mechanisms at the cellular level (Forbes, 2000; Forbes et al., 2003; Cooney et al., 2004; Rothen-Rutishauser et al., 2005; Sporty et al., 2008; Agu and Ugwoke, 2011). These techniques have undergone significant developments, incorporating particle deposition, dissolution and absorption in immortalized cell culture models (Tee et al., 2001; Fiegel et al., 2003; Forbes et al., 2003; Cooney et al., 2004; Buttini et al., 2008; Bur et al., 2009; Grainger et al., 2009; Hein et al., 2011). Also, fully differentiated models of primary nasal, bronchial and trachea cells cultured at the air liquid interface are commercially available (PneumaCult™-ALI and MucilAir™) and have been reported to be capable of mimicking aspects of airway epithelium from ion transport, metabolic activity, chemokine and cytokine release to mucus production and ciliary beating. However, these models are less robust and less economically viable compared to immortalized cell lines and thus have not become a routine part of biopharmaceutical screening of inhaled drugs (Forbes and Ehrhardt, 2005).

An international workshop held by the Academy of Pharmaceutical Sciences Great Britain in 2010, was convened to discuss the challenges in the development of inhaled

medicines, one of the main summary objectives reached describes the necessity for the development of physiologically relevant simulated fluids based upon the characterization of RTLFs to improve these current *in vitro* methods for assessing inhaled drug behaviour (Forbes et al., 2010). The incorporation of simulated RTLFs in such models would be of great significance in guiding the formulation, development and design of inhaled drugs particularly from a biopharmaceutical perspective, improving prediction of the *in vivo* behaviour of inhaled medicines.

However, not all inhaled particles dissolve within the RTLFs. Mucociliary clearance mechanisms dominate the larger ciliated airways whilst phagocytic and endocytic clearance mechanisms are crucial in the clearance of slowly dissolving and insoluble particles in the distal alveolar regions (Sibille and Reynolds., 1990; Yang et al., 2008). Nanoparticles deposit optimally within the distal alveolar RTLFS and make use of non-absorptive clearance mechanisms, with the ability to translocate across the respiratory epithelium (approximately only 0.2 μm thick in the alveoli) to the systemic circulation (Weibel, 1973; Borm et al., 2006). Nanoparticles have exceptional and unique properties on account of their size and increased particle surface-to-volume ratio. It is these properties that have thus been exploited for drug delivery purposes (Shargel and Yu, 1999; Oberdorster et al., 2005; Jones and Grainger, 2009; Nel et al., 2006; Sung et al., 2007).

For the inhaled drug delivery of nanomedicines (it should be noted that 1 to 1000 nm diameter sized particles are encompassed by this term for drug delivery purposes) formulations have been developed using polymeric or liposomal materials (Sun et al., 2004; Yokoyama, 2005; Medina et al., 2007; Braeckmans, 2010). Once deposited within the RTLFs the physiochemical properties of nanoparticles (size, composition material, surface charge, hydrophobicity) determine their degree of interaction with protein and lipid components of RTLF and thus the nature of the dynamic 'corona' that forms on their surface (Vranic et al., 2013). The formation of these protein-lipid complexes on the surface of nanoparticles has the capability of modifying particle behaviour, from influencing the rate of particle aggregation to cellular interactions including macrophage phagocytosis and endocytosis, or increasing their recognition by surface receptors and uptake into cells (Oberdorster et al., 2005; Borm et al., 2006; Nel et al., 2006; Yang et al., 2008). Therefore it comes as a surprise that physiologically relevant RTLF simulants have not become an established or integrated component of *in vitro* work concerning nanoparticulates (Schleh et al., 2013).

Whilst particles can be characterized in simple media at the time of preparation to provide useful information regarding the physiochemical properties of nanoparticles, these do not take into account constituents of the RTLFs, and it is the characterization of nanoparticles in biologically relevant media that is essential in providing the basis for understanding the properties of nanoparticles that go on to determine their biological fate and effects (Powers et al., 2006).

The commercially available, surfactant preparations for treatment of respiratory distress syndrome of neonates are the only physiologically relevant epithelial lung lining fluid simulants in use both clinically and additionally in the *in vitro* investigations of inhaled particle behaviour. These commercial preparations consist of natural, modified or synthetic surfactants, with six out of the nine surfactant replacements available today being natural surfactants (Wrobel, 2004; Lopez et al., 2013; Polin et al., 2014). The animal derived surfactants, isolated from porcine or bovine lungs (lavage or minced) by organic solvent extraction, with saturated phospholipids particularly DPPC and the hydrophobic surfactant proteins B and C form the major active components of these clinical formulations (Sun et al., 1997; Lal and Sinha, 2008). Commonly used animal surfactants include, Curosurf® (a porcine surfactant extract) purified after extraction from porcine lungs by liquid-gel chromatography, Infasurf® (a bovine surfactant) an unmodified suspension obtained from bovine lung lavage and Survanta®, also a bovine surfactant extract, fortified with additional synthetic lipids (Bloom et al., 1997; Soll and Fermin, 2001; Nguyen et al., 2003; Ramanathan et al., 2004; Bloom and Clark, 2005; Kim and Shim, 2013; Do et al., 2014). However individual natural surfactant preparations demonstrate significant variation 'batch to batch' in the concentrations of phospholipid and protein components (Lal and Sinha, 2008). Synthetic surfactant preparations such as Exosurf® (which lacks protein) have also been developed (Jobe et al., 1993; Corcoran et al., 1994), and Surfaxin®, a synthetic formulation containing a novel synthetic peptide, KL4, designed to mimic surfactant protein B. Clinical trials have demonstrated the safety and efficacy of this preparation (Curstedt and Johansson, 2006).

These commercially available preparations have been used in investigations assessing the influence surfactant has on the dispersion, toxicity and bioavailability of particles *in vitro*. Those investigations included carbon walled nanotubes in Survanta® and SiO_2 and TiO_2 nanoparticles in Curosurf® (Keane et al., 1991; Kendall et al., 2004; Foucaud et al., 2007; Schleh et al., 2009; Wang et al., 2010; Vranic et al., 2013). Whilst the majority

of these studies come from an environmental and occupational exposure perspective, they nevertheless demonstrate the necessity to mimic a more physiologically representative media representative of the RTLFs. The commercially available preparations are limited to representing the surfactant component of distal RTLFs, the highly abundant proteins composing the aqueous component of this fluid is absent. Thus, in the development of a 'fit for purpose' simulant, an ideal model would possess physiological relevance and biocompatibility, but must also be able to be manufactured in a standardised, cost effective manner.

Aims and objectives

A physiologically-relevant simulated lung fluid 'base model' representative of the alveolar RTLFs will be developed and optimized incorporating the objectives summarized below, and evaluated in preliminary investigations for the assessment of its suitability for the biopharmaceutical screening of inhaled particles.

1. Physiologically relevant: unlike generic ionic solutions, which are supplemented with arbitrarily chosen protein and/or DPPC concentrations, the base model must incorporate the major protein, lipid and low molecular weight components at concentrations determined to be representative of the RTLF. Whilst compositional differences attributed to region, disease and age have all been characterised, as a 'first step' a base model will be designed to represent the healthy alveolar RTLF.
2. Cost: It must be appreciated that the components chosen for the base model should be readily and commercially available.
3. Ease of manufacture: The stimulant preparation procedure must be reproducible, and the time to manufacture simulant must be realistic.
4. Stability: Both optimal temperature upon storage, the length of time that the simulant remains viable, and remains within acceptable limits of microbial growth must be considered and assessed.
5. Incorporation into existing *in vitro* investigations: This base model will be used in the physiochemical characterisation of reference drug delivery particles.
6. Biocompatibility - How readily can simulants be incorporated into currently employed *in vitro* cell models used to investigate the behaviour of inhaled drug particles within the respiratory tract

6.2: Methods

6.2.1: Simulant development and preparation

The formulation of simulant was based upon measured RTLF concentrations of protein, lipid and antioxidant components of healthy human lavage samples, corrected for dilution by the urea method, as detailed in **Chapter 3**, referencing data obtained from the literature. **Table 6.2** outlines the concentrations of the major protein, lipid and antioxidant constituents of the base model of stimulant.

Table 6.2: Components of 'base' simulated lung epithelial lining fluid

Base model components	**Concentration**
Albumin	8.8 mg/mL
IgG	2.6 mg/mL
Transferrin	1.5 mg/mL
DPPC	4.8 mg/mL
DPPG	0.5 mg/mL
Cholesterol	0.1 mg/mL
Ascorbate	140 µM
Urate	95 µM
Glutathione	170 µM

6.2.2: Protocol for preparation of 10 mL of base alveolar simulant

First liposome variants were manufactured by the two methods described below:

1. DPPC only
    a. 0.048 g DPPC weighed into small glass round bottomed flask containing 1 mL chloroform which was evaporated under nitrogen in waterbath at 55 ^{o}C for ~15 mins
    b. 2 mL resuspending solution (HBSS) pre-warmed to 55 ^{o}C was added
    c. This was then mixed vigorously on a vortex for 15-30 min
    d. Finally sonicated for ~ 1 h in waterbath at 55 ^{o}C

2. DPPC with PG and cholesterol
    a. 0.048 g DPPC, 0.005 g PG, 0.001 g cholesterol weighed into small glass round bottomed flask containing 1 mL chloroform and evaporated under nitrogen in waterbath at 55 ^{o}C for ~15 min
    b. 2 mL resuspending solution (HBSS) pre-warmed to 55 ^{o}C was added
    c. This was then mixed vigorously on a vortex for 15-30 min
    d. Finally sonicated for ~ 1 h in waterbath at 55 ^{o}C

To this mixture of lipids, a solution of proteins was added slowly (0.0816 g of albumin, 0.0158 g IgG, 0.01904 g transferrin, to make up to 3 mL with buffer) Finally, UA, AA and GSH were added from concentrated 100mL stock solutions for AA, GSH and UA. For AA 81.43 µl were added, for GSH 85.87 µl added and finally 85.39 µl of UA was added. HBSS was added to a final volume of 10mL. The pH of simulant was checked to be between 7.2 and 7.4 and stored at 4^{o}C.

6.2.3: Dynamic Viscosity

The viscosity of simulants, RTLF, BAL and cell culture medium (supplemented with 2% fetal bovine serum (FBS)) was measured at 37°C using an AMVn Automated Micro Viscometer (Anton Parr). Briefly the samples were loaded onto the microcapillary and the viscosity was determined in triplicate according to Höpplers falling ball principle. The following viscosity values were obtained, CCM FBS2%= 0.734x10-3 Pa s, simulant (DPPC)= 0.738x10-3 Pa s and simulant (DPPC, PG, cholesterol)= = 0.789x10-3 Pa s.

6.2.4: DLS measurements

All DLS sizing was performed using a Zetasizer Nano ZS (Malvern, Worcestershire, UK). Size was measured at 37 °C and measurements were taken at a scattering angle of 173° and a refractive index of 1.337 (176). Viscosity values were adjusted for each medium: CCM FBS2%= 0.734x10-3 Pa s, simulant (DPPC)= 0.738x10-3 Pa s and simulant (DPPC, PG, Cholesterol)= = 0.789x10-3 Pa s. Three batches of each simulant formulation were analysed for size in triplicate.

6.2.5: Particle sizing in simulant and concentrated BAL

50 nm (2.62% w/v) and 200 nm (2.5% w/v) non-functionalized polystyrene microsphere aqueous suspensions and 50 nm (2.5% w/v) carboxylated polystyrene microsphere aqueous suspensions were used (Duke Scientific, Palo Alto, CA). For particle size analysis, particles were prepared at a concentration of 2.5 mg/mL in the respective medium. Three batches of each nanoparticle investigated were analysed for size in triplicate for 4 h periods, measurements were made every 15 min.

6.2.6: Culture of A549 cells

Human alveolar epithelial cells (A549, ATCC, USA) were cultured in cell culture medium supplemented with 10% FBS (CCMFBS10%) in a humidified incubator at 37°C and 95% air and 5% CO2. All experiments were performed on cells seeded at a density of 10,000 cells/cm2 in cell culture medium supplemented with 2% fetal bovine serum (CCMFBS2%), unless stated otherwise.

6.2.7: Cell viability assay using MTT

The MTT assay is a colorimetric assay used to measure the metabolic activity of cells. The mitochondrial reductase enzyme reduces the yellow tetrazole, MTT (3-(4,5-dimethylthiazol-2-yl)-2,5-diphenyltetrazolium bromide), to a formazan dye, which has a purple colour, thus allowing the investigator to assess the viability and/or death of cells. Sodium dodecyl sulphate (SDS), a solubilising agent, is then used to dissolve the insoluble purple formazan, which yields a coloured solution. A spectrophotometer is then used to measure the absorbance of this coloured solution at 570 nm.

Cell viability as assessed by the MTT assay, was used as a proxy to determine the bicompatibilty of simulants with cells *in vitro*, by assessing the effects of the exogenously applied simulants on cell layer metabolism. Cells were seeded in a 96-well plate (see **Figure 6.1** below) and, after 24 h, were treated with 100 μL concentrations of simulant species (Protein and DPPC and Protein DPPC, PG and Cholesterol) (at concentrations of 1.1, 2.2, 4.3, 6.5, 8.7, 10.8 mg/mL protein respectively) CCM FBS2% alone (negative control) and incubated at for 1, 2, 4 and 12 h. After the exposure period, the particle suspensions were aspirated and replaced by 200 μL fresh CCMFBS2%. 50 μL MTT (5 mg/mL) was then

added to the wells and the plate was incubated for a further 4 h. The medium was then removed and the resulting intracellular formazan crystals were dissolved over 24 h in 100 µL of 10% SDS prepared in 1:1 water:DMF, after which the absorbance from the solubilized formazan was measured spectrophotometrically (SpectraMax UK) at an absorbance wavelength of 560 nm.

The relative viability of cells was calculated as follows:

$$Cell\ viability\ (\%) = \frac{A - S}{CM - S} \times 100$$

Where A is the absorbance obtained for each concentration of the simulant, S is the absorbance obtained for positive control (1% v/v Triton-X) and CM is the absorbance obtained for untreated cells (incubated with CCM FBS2% alone). The latter reading is defined as 100% cell proliferation (fully viable cells).

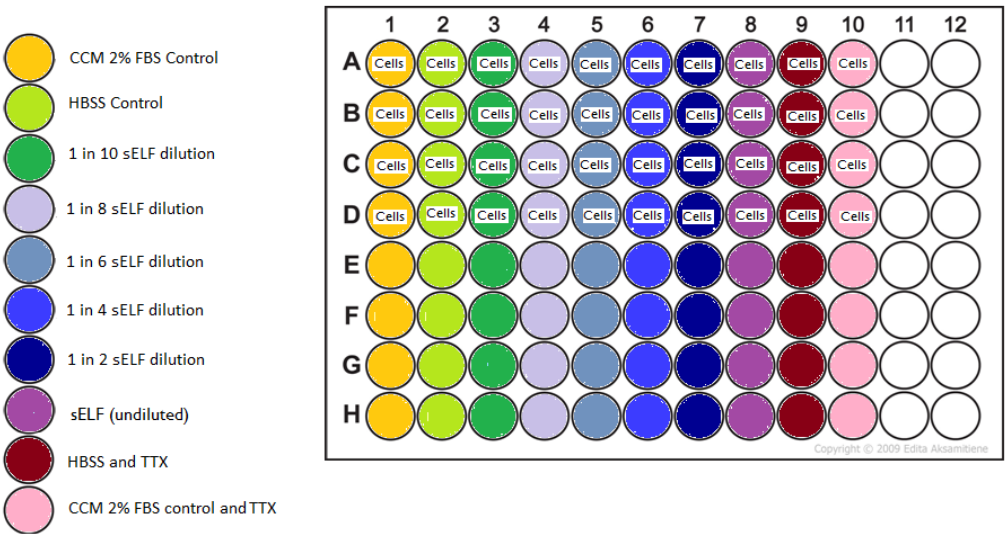

Figure 6.1: *Template of the 96-well plate used in MTT investigation assessing the biocompatibility of A549 cell lines with simulant. Dilutions and negative controls are highlighted on the left.*

6.2.8: Transmission Electron Microscopy

Morphological examination of simulant and of NPs in simulant were conducted by transmission electron microscopy (TEM). The samples were negatively stained with 2% (w/v) phosphotungstic acid pH 6.5 and 0.1% trehalose and placed on 150 mesh Formvar copper grids prior to TEM observation. Samples were examined on a FEI Tecnai 12

transmission microscope operated at 120 kV. Images were acquired with an AMT 16000M camera, with a minimum of 10 images per condition acquired.

A549 cells were grown to confluence inside a 6 well plate and treated with or without simulated epithelial lining fluids suspended in cell culture medium (2% FBS) for 4 hs. After treatment with simulant for TEM, cells were fixed by removing the medium and replacing it immediately with 2.5% (v/v) glutaraldehyde in 0.15 M cacodylate (pH 7.3). The cells were fixed for 1 h at room temperature. The cells were then scraped from wells using a cell scraper (BD Falcon), transferred into ependorff tubes and spun for 5 minutes at 3,000 rpm in a microcentrifuge. Cells were then resuspended in fresh 2.5% (v/v) glutaraldehyde in 0.15 M cacodylate buffer and further fixed overnight at 4°C. After fixation, cells were washed with 0.15M cacodylate buffer and post-fixed in 1% (w/v) osmium tetroxide in 0.15M cacodylate buffer (pH 7.3) for 1 h at 4°C. Samples were then dehydrated through a graded ethanol series, equilibrated with propylene oxide before infiltration with TAAB epoxy resin and polymerised at 70°C for 24 hs. Ultrathin sections (50-70 nm) were prepared using a Reichert-Jung Ultracut E ultramicrotome, mounted on 150 mesh Formvar copper grids and contrasted using uranyl acetate and lead citrate. Samples were examined on a FEI Tecnai 12 transmission microscope operated at 120 kV. Images were acquired with an AMT 16000M camera. At least 10 images from each condition were acquired, cellular changes were assessed by visual inspection of the representative TEM images, and quantitative estimates of cell morphology made. using ImageJ 1.47 software (http://rsb.info.nih.gov/ij).

6.2.9: Statistical analysis

All statistical analysis was performed using the student's t-test. All analyses were performed using SPSS statistical program for Mac version 22 (SPSS Inc., Chicago, IL, USA).

6.3: Results

6.3.1: Base model development

Table 6.3: *Protein, lipid and antioxidant concentrations in RTLF, Simulant and CCM (supplemented with 2% FBS).*

	RTLF (urea corrected)	Simulant	CCM 2% FBS
Ionic constituent	Concentration (mg/mL)		
Inorganic salts			
Calcium Chloride (CaCl2) anhydrous		0.14	0.2
Magnesium Chloride (MgCl2-6H2O)		0.1	
Magnesium Sulfate (MgSO4-7H2O)		0.1	0.098
Potassium Chloride (KCl)		0.4	0.4
Potassium Phosphate monobasic (KH2PO4)		0.06	
Sodium Bicarbonate (NaHCO3)		0.35	0.85
Sodium Chloride (NaCl)		8	6.8
Sodium Phosphate dibasic (Na2HPO4) anhydrous		0.048	0.12
Other			
Glucose		1	1
Amino acids			
L-glutamine			0.292
Proteins			
Albumin	8.8±3.6	8.8	0.4
IgG	2.6±2.4	2.6	
IgA	0.79±0.4		
Transferrin	1.50±1.2	1.5	
alpha globulins	1.03±0.5		0.3
beta globulins	1.99±1.9		0.1
Lipids			
PL	6.55 ± 3.9	6.6	-
PC	4.84±2.22	4.8	-
Cholesterol	0.11±0.04	0.1	-
Antioxidants (μM)			
Ascorbate	137.1±75.5	140	
Urate	92.6±39.4	95	
GSH	171.4±111.7	170	
pH		7.2-7.4	7.4

The formulation of simulants, whilst different to BAL, were based upon measured RTLF concentrations, as detailed in **Chapter 3**, additionally referencing data obtained from the literature. Urea corrected total protein concentrations were determined to be 17.9±8.6 mg/mL however only 12.9 mg/mL total protein could be used within the developed simulants (due to commercial unavailability of RTLF human protein components: SP-A, IgA, A1AT), approximately 15-fold greater than frequently used cell culture media supplemented with FBS (0.8 mg/mL total protein). The major protein, lipid and antioxidant constituents of the base model of simulant relative to RTLF and CCM 2%FBS are described in **Table 6.3** above.

Due to the inherent limitations of DLS sizing techniques in media with high protein content, significant background scattering occurs as a result of the formation of bimolecular protein agglomerates (Felipe et al., 2010). It should therefore be noted that the Z-average size is calculated using the intensity weighted distribution, and thus is shifted in the presence of light scattering non uniform solutions such as concentrated BAL and simulant. It can be more informative to focus on the intensity distribution graphs as opposed to the calculated Z-average values alone. Consequently as part of the characterization of the developed base models, intensity distribution profiles obtained using DLS were used also in conjunction with TEM imaging, to provide more accurate insights regarding the size and behaviour of simulant protein and lipid components.

It should be noted that two "buffers" were used in simulant development, Hanks balanced salt solution) HBSS and 2-[4-(2-hydroxyethyl)piperazin-1-yl]ethane sulfonic acid (HEPES). HBSS, a commercially available chemically defined, balanced salt solution (see **Appendix D** for formulation and product no.) was chosen for physiologically relevance, however high salt concentrations interfered with TEM imaging and thus simulant prepared in both HBSS and the zwitterionic chemical buffer HEPES**.** DLS measurements shown below are representative of n=3 at t=0 h, however each sample was measured for 4 h with measurements taken automatically every 15 min.

Despite the limitations in DLS, size based on intensity was able to provide a clear picture of the protein and lipid particle agglomeration in the fluids investigated. Interesting differences in the relative intensity profiles were observed across fluids investigated, concentrated BAL samples demonstrate a single highly intense peak at ~5000 nm (see **Figure 6.2 E**), representative of large protein and lipid aggregates, as confirmed by TEM (see **Figure 6.2 F**, see **Appendix D** for more images). In simulant containing proteins and

liposomes made of DPPC only, DLS measurements obtained revealed a predominant peak (according to both volume and intensity) between ~150-250 nm, representative of liposomes of corresponding size, as confirmed by TEM (see **Figure 6.2 A and B**). The DPPC liposomes manufactured appear to be broadly uniform across images obtained from simulant in HEPES (see Appendix D). A low intensity peak at ~30nm was indicative of the presence of non-agglomerated simulant-protein, with a second intensity peak observed at ~5000 nm representative of low levels of simulant protein agglomeration (see **Figure 6.2 E and F)**. Within simulant in HBSS the high salt concentration appears to influence the formation of protein agglomerates, with the large peaks of ~5000nm at an almost 10X greater intensity compared to simulant manufactured in HEPES (see **Appendix D**).

Previous investigations have focused solely upon DPPC as the representative surfactant component in simulated lung lining fluids, with DPPC responsible for 40-70% of phosphatidlycholines present in surfactant, in turn contributing to 80% of surfactant phospholipids. The analysis previously performed in this investigation (see **Chapter 3**) determined the RTLF concentration of PC. With physiological relevance a key objective in the design and development of simulants however, the other major lipid species of surfactant were also incorporated in base model simulant development. Of the lipids included in this second variation of simulant, Phosphatidylglycerol (PG) was chosen, the second most abundant component of surfactant after DPPC, reported to represent approximately 10% of total phospholipids and observed to increase the dynamic properties of surfactant alongside DPPC *in vitro* and cholesterol a neutral lipid, reported to account for up to 5-10% of surfactant (Yu et al., 1992; Holm et al., 1996; Karagiorga, 2006; Perez-gil et al., 1998; Perez-gil, 2006). Furthermore, cholesterol, known to have a stabilizing role in bilayer structures (such as the plasma membrane), 'filling in the gaps', often included to increase the rigidity of bilayers improving liposome stability (Tseng, 2007), was incorporated into the developed simulants. Cholesterol concentrations used in the simulant were based upon measurements outlined in **Chapter 3** and representative of 2.8 mol% phospholipid.

Within this 'second' simulant developed using liposomes made of DPPC, PG with cholesterol in HEPES, DLS intensity profiles revealed low intensity peaks representative of lipid formations at ~2000-8000 nm (see **Figure 6.2 C and** D). Peaks observed at ~10 nm and ~100 nm (of the greatest intensity) were attributed to the presence of non-agglomerated and agglomerated protein respectively. In HBSS the high salt concentration once again

influences the formation of protein agglomerates, with intensity peaks only observed at~100-200 nm (see **Appendix D**).

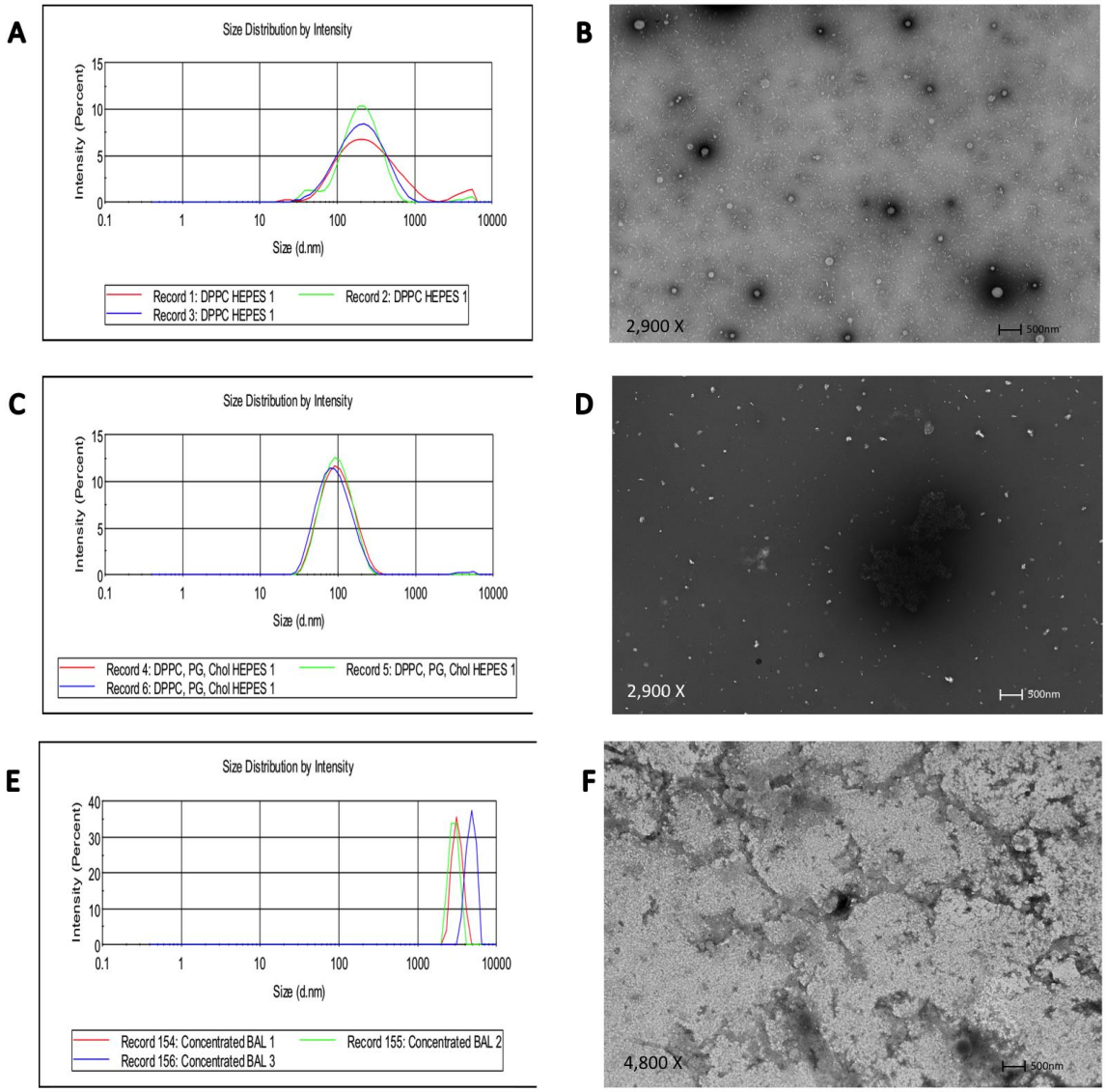

Figure 6.2: *Intensity distribution measurements and corresponding TEM images acquired for simulant variants and concentrated BAL fluids investigated. Representative DLS and TEM images of (A) and (B) simulant: Protein and DPPC in HEPES; (B) and (C) simulant: Protein and DPPC, PG, Cholesterol in HEPES; (D) and (E) Concentrated BAL, respectively. Individual distribution curves as measured by DLS are representative of at n = 3 at 37 °C at t=0 h, TEM images were acquired with an AMT 16000M camera using a FEI Tecnai 12 transmission microscope operated at 120 kV, Negative staining of liposomes with 2% PTA pH 6.5 and 0.1% trehalosewas employed.*

6.3.2: Simulant- Particle interactions

Commercially available polystyrene particles are well-defined with regards to their shape, size and chemical composition and have been investigated in a variety of studies

(Brown et al., 2001; Kato et al., 2003; Xia et al., 2007; Monopoli et al., 2011; Jones et al., 2014). For these reasons, they were chosen as the reference nanoparticles to investigate the interaction of drug delivery like particles within simulant fluid, as part of a series of fundamental investigations into the applications of simulant. With the physicochemical properties particularly hydrophobicity, size and surface chemistry implicated to play a crucial role in both the behaviour and biocompatibility of nanoparticles (McNeil, 2009; Nel et al., 2009), the three model polystyrene nanoparticles chosen for this investigation into particle sizing in simulant were: unmodified 50 nm, 200 nm and carboxyl surface modified 50 nm polystyrene particles.

The size of PS 50 nm increased two and five-fold to 90.9±1.4 nm and 250.5±157.0 nm in HEPES and HBSS respectively, remaining stable over the 4 h time course investigated. Sizes based on intensity distribution as opposed to the hydrodynamic diameter calculated, have been used in the following discussion into particle behaviour in simulant and BAL solutions. In simulant (DPPC HEPES), peaks observed at 379.8±6.81 nm were the result of the formation of PS50 nm particle plus liposome interactions, see **Figure 6.3.A and B**. Low intensity peaks between 60-100 nm were confirmed by TEM to be the result of non aggregated particles and/or non agglomerated simulant protein. Within simulant (DPPC, PG, cholesterol in HEPES) investigated, TEM analysis (see **Figure 6.3 C and D**) similarly confirmed the presence of particle plus lipid interactions, responsible for peaks observed at 151.27±31.41 nm. The presence of few but large particle, protein and lipid aggregate formations were also observed, with the presence of low intensity peaks between ~3000-5000 nm. In concentrated BAL however, PS50 nm particles demonstrated a large degree of aggregation, the presence of particle plus protein and lipid aggregates, were seen between 1056±87 nm and 4752±1840.1 nm. Particle aggregates however remained stable at sizes measured over the time course investigated.

In contrast to PS50 nm particles, ps200nm particles investigated demonstrated only minor increases in diameter to 305.6±66.3 nm and 315.3±95.39 nm in HEPES and HBSS respectively, again remaining stable over the 4 h time course investigated. In simulant (DPPC HEPES), the intensity profiles obtained revealed few PS200 nm particles remained unassociated with simulant components- the lowest intensity peak was observed ~200 nm, see **Figure 6.3 A and B**. It should be noted that the DPPC liposomes themselves however were also of this size (150-200 nm) (Figure 6.2 A and B). The most intense peak observed at 2104±1856.05 nm represents the formation of large agglomerates, the result of interactions between particles and lipid or protein, with few but larger aggregates observed around ~4000 nm (see **Figure 6.4 A and B**). In contrast, the majority

of PS200 nm in simulant (DPPC, PG, Cholesterol HEPES) did not aggregate to the extent observed in simulant (DPPC), with the most intense peak observed at 363.55±62.5 nm, the result of low-

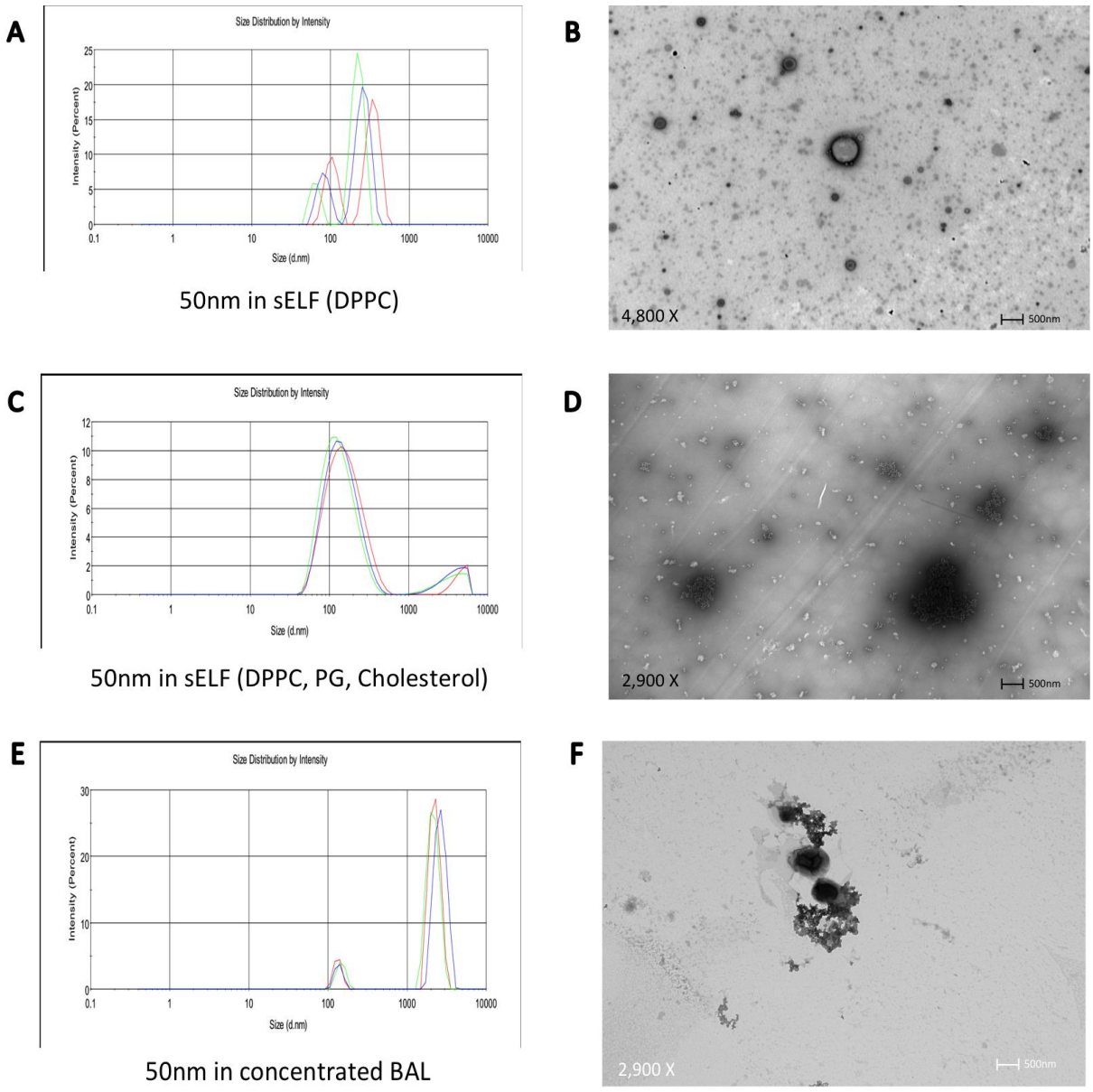

Figure 6.3: *The average intensity distribution measurements and respective TEM images acquired for 50nm polystyrene particles in simulant variants and concentrated BAL fluids investigated. (A) and (B) simulant: Protein and DPPC in HEPES; (B) and (C) simulant: Protein and DPPC, PG, Cholesterol in HEPES; (D) and (E) Concentrated BAL, respectively. Individual distribution curves as measured by DLS are representative of at n = 3 at 37 °C at t=0 h, TEM images wereacquired with an AMT 16000M camera using a FEI Tecnai 12 transmission microscope operated at 120 kV, Negative staining of liposomes with 2% PTA pH 6.5 and 0.1% trehalosewas employed.*

levels of protein interaction on the surface of particles. Low intensity 4862±894 nm peaks observed were the result of the larger lipid formations within the simulant (DPPC, PG, cholesterol) formulation (see Figure 6.2 C and D). In concentrated BAL, TEM work confirms the presence of

particle plus protein and lipid aggregates, in accordance with peaks observed at 446.6±89 nm and 988.35±395.48 nm. The third peak observed at 3022.0±387 nm was attributed to the protein lipid aggregates within BAL samples themselves. In general, PS200 nm particles demonstrated a much lower degree of aggregation compared to PS 50 nm particles.

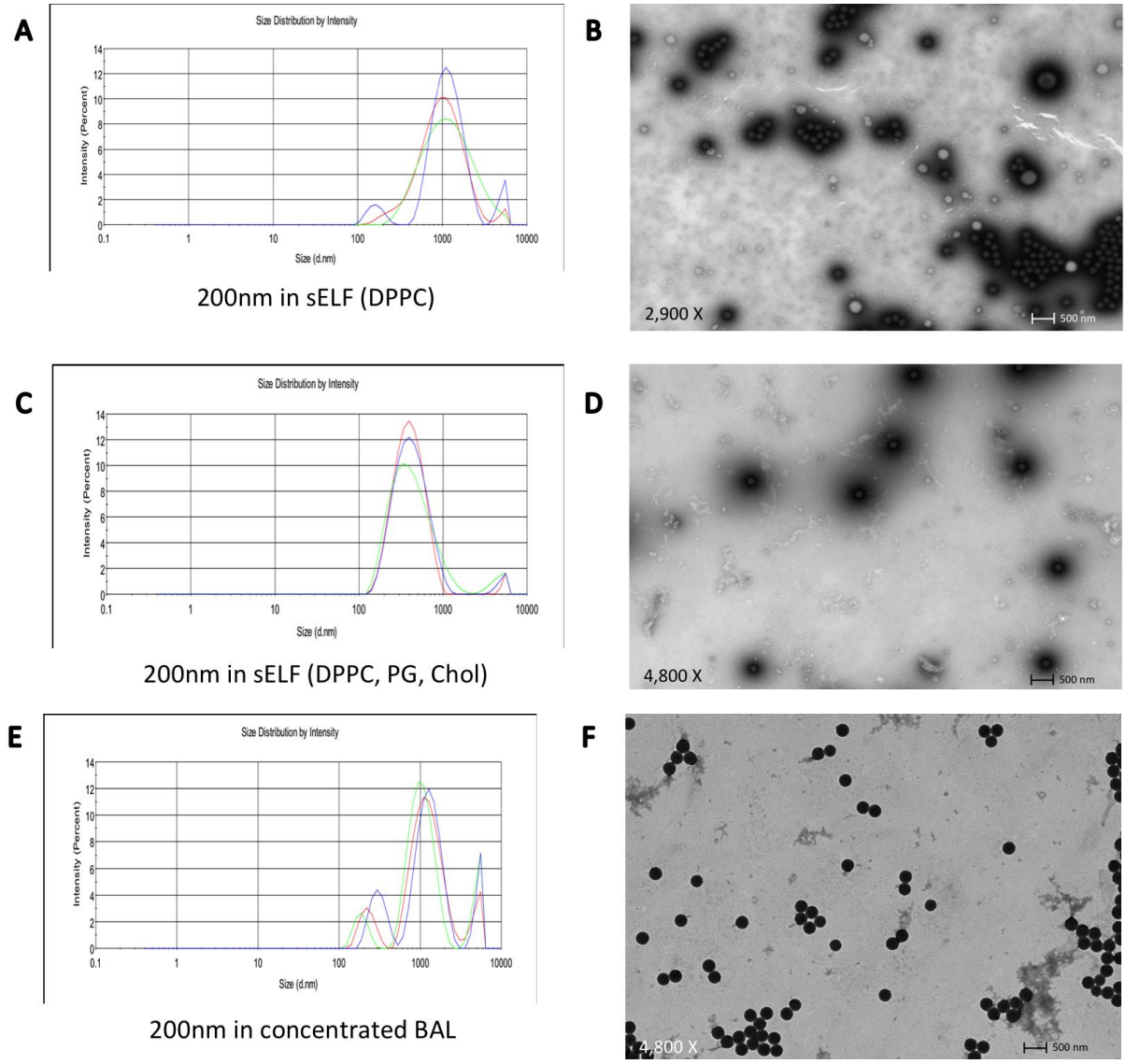

Figure 6.4: *The average intensity distribution measurements and respective TEM images acquired for 200nm polystyrene particles in simulant variants and concentrated BAL fluids investigated. (A) and (B) simulant: Protein and DPPC in HEPES; (B) and (C) simulant: Protein and DPPC, PG, Cholesterol in HEPES; (D) and (E) Concentrated BAL, respectively. Individual distribution curves as measured by DLS are representative of at n = 3 at 37 °C at t=0 h, TEM images wereacquired with an AMT 16000M camera using a FEI Tecnai 12 transmission microscope operated at 120 kV, Negative staining of liposomes with 2% PTA pH 6.5 and 0.1% trehalosewas employed.*

PS50 nm carboxyl-modified particles demonstrated an increase in size to 73.28±6.97 nm and 90.6±27.9 nm in HEPES and HBSS respectively. With respect to unmodified 50 nm particles, the carboxylate anion appeared to have an immediate stabilizing effect, preventing the aggregation observed in the non-functionalized particles which remained stable over the 4 h time course investigated. In simulant (DPPC HEPES), peaks observed at 96.3±69.9 nm were the result of visible particle surface interactions with both proteins and lipids of simulant, see **Figure 6.5 A and B**. TEM and DLS analysis together also confirmed the presence of a peak of similar intensity at 2104±129 nm, due to the formation of larger such aggregates (see **Appendix D**).

In the DPPC, PG, Cholesterol in HEPES simulant broad intensity peaks were observed between 84.4±14.0 and 282.15±96.8 nm. TEM images revealed the presence of fairly well dispersed particles, with minimal particle aggregation, see **Figure 6.5 B and C**. The negatively charged particles appear to interact with both protein and lipids in solution, resulting in the broad peak size measured. The lower intensity peaks observed at ~5000 nm were the result of few but large particle protein aggregates, as confirmed by TEM. In concentrated BAL, the carboxylated PS50 nm particles continued to demonstrate a relatively greater degree of interaction with protein and lipid components (compared to unmodified particles), TEM work confirmed the presence of particle plus protein and lipid aggregates of 1043±218.8 nm. Aggregates appear well dispersed and remained stable over the time course investigated.

Ultimately it appeared the carboxylated surface of PS50 nm particles limited the formation of larger particle-only aggregates in simulant versus non surface modified particles. The formation of the ‘dynamic’ corona at the surface interface of particles with biomolecules, such as proteins and lipids that are found within physiologically relevant systems, such as the simulants developed for this investigation, have been described in the literature for over ten years (Kendall et al., 2004; Nel et al., 2009; Braeckmans et al., 2010; Monopoli et al., 2011). The modification of particle surface, in this case through functionalization of carboxyl groups, appears to have altered the nature of these biomolecular surface interactions. Increased particle size (PS200 nm) has also resulted in clear changes in particle stability and behaviour within the physiologically relevant simulant solutions. DLS measurements were performed over a four h period to monitor any changes in these ‘dynamic interactions’ and thus the behaviour of nanoparticles over an extended

period of time. However particles either demonstrated immediate aggregation (in the case of PS50 nm particles) or stayed at the same or similar sizes for the four h period investigated (PS200 nm and PS50 nm carboxylated).

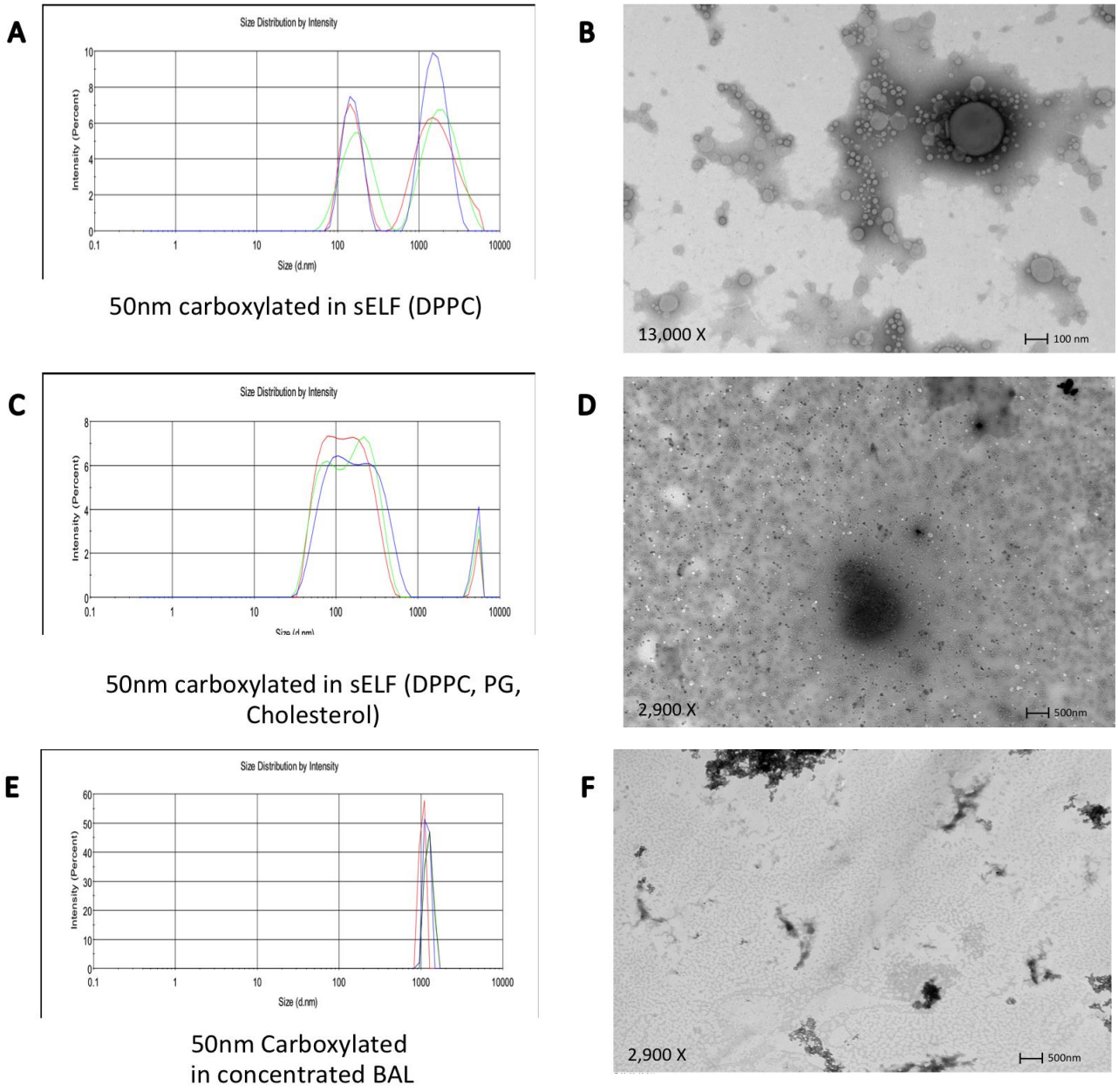

Figure 6.5: *The average intensity distribution measurements and respective TEM images acquired for 50 nm carboxylated polystyrene particles in simulant variants and concentrated BAL fluids investigated. (A) and (B) simulant: Protein and DPPC in HEPES; (B) and (C) simulant: Protein and DPPC, PG, Cholesterol in HEPES; (D) and (E) Concentrated BAL, respectively. Individual distribution curves as measured by DLS are representative of at n = 3 at 37 °C at t=0 h, TEM images were acquired with an AMT 16000M camera using a FEI Tecnai 12 transmission microscope operated at 120 kV, Negative staining of liposomes with 2% PTA pH 6.5 and 0.1% trehalose was employed.*

6.3.3: Simulant - Cell interactions

The biocompatibility of the alveolar base simulant (HBSS) model developed was investigated using the A549 alveolar epithelial cell line *in vitro*, the MTT assay was used to assess mitochondrial activity and thus the proliferation of cells following simulant incubation over 2, 4 and 12 h periods respectively.

For simulant (DPPC only), no significant differences in A549 cell proliferation were observed. The lowest % cell proliferation (compared to CCM FBS 2% only controls, in which cells were observed to proliferate 'normally') was calculated after the longest, 12 h, incubation with simulant DPPC. In which cell proliferation was observed to decrease by ~30%, see **Figure 6.7**. However, no significant differences in cell proliferation were observed for either 4 and 12 h incubations (see **Figure 6.7 A**) At the shortest incubation time of 2 h, cell proliferation demonstrated no measurable difference in proliferation versus control cells incubated in CCM FBS 2%.

Similarly for A549 cells incubated in the presence of simulant (DPPC, PG, cholesterol), the lowest % cell proliferation was determined after 12 h. Interestingly a concentration dependent trend was observed for cells incubated for this time point, with cell proliferation found to increase alongside increasing concentrations of the lipid and protein simulant components, see **Figure 6.3. B**.

The biocompatibility of concentrated BAL samples with A549 cells monolayers was also assessed to complement simulant-investigations, with a statistically significant time dependent effect in % proliferation observed. Significantly lower mitochondrial viability was determined after 12 h versus both 2 and 4 h incubation periods ($p=0.02$). Furthermore, a protein concentration dependent effect was observed across all time points, with % proliferation increasing alongside increasing protein and lipid concentration of BAL.

After the 4 h incubation time point, cell proliferation was significantly decreased ($p=0.02$) versus the 2 h simulant incubation period, with no demonstrable change in mitochondrial viability calculated for 2 h long incubations

No measurable detrimental effects on mitochondrial viability (as assessed by MTT) were determined for A549 cells incubated with base simulant models. The data suggests that simulant and thus the physiologically relevant protein and liposome concentrations within simulant are compatible with A549 cell monolayers *in vitro*. In order to fully

ascertain the compatibility of simulant models *in vitro*, cell morphology was assessed post-simulant incubation.

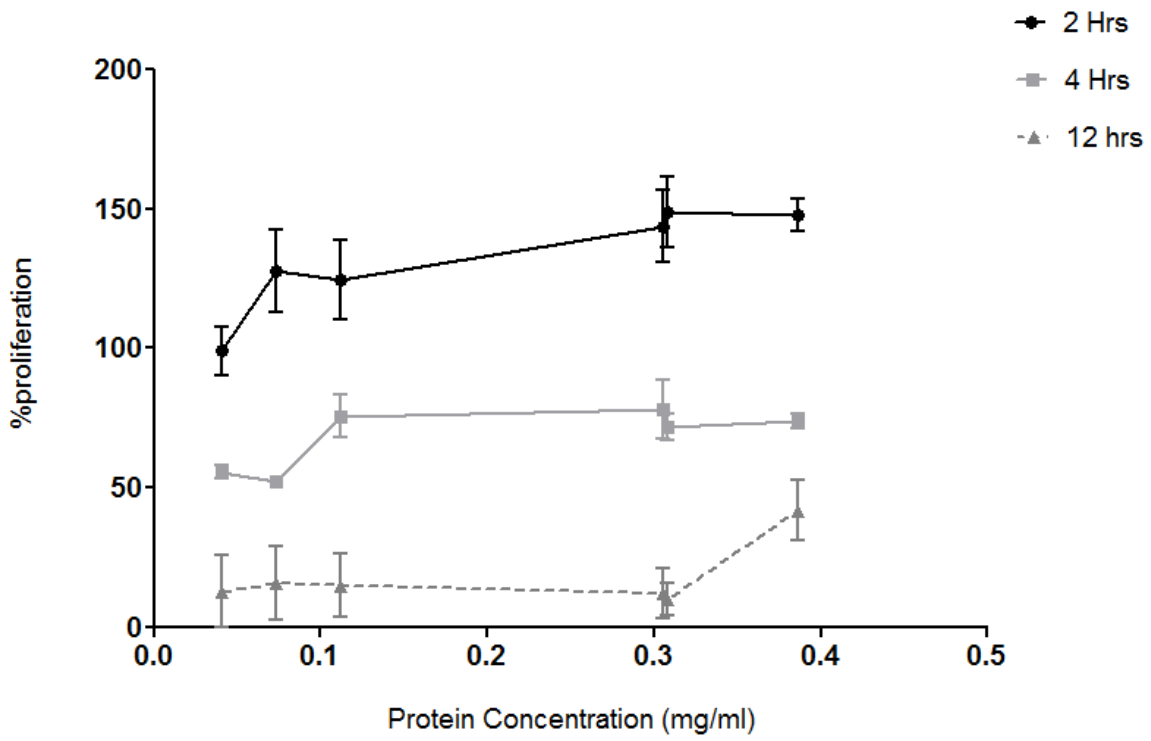

Figure 6.6: *The effect of concentrated BAL on the proliferation of A549 cell monolayers. The influence of BAL on cell proliferation was calculated as a percentage of the control (CCM FBS2%). The effect of simulant (at protein concentrations of 0.04, 0.07, 0.3, 0.4 mg/mL protein respectively) was assessed over 2, 4 and 12 h periods of incubation with cells respectively. Cellular metabolic activity was measured spectrophotometrically at 570 nm, data represents the mean±SD, n = 3 experiments, four replicates per experiment at each dilution.*

Morphometric analysis following a 4-h incubation of simulant (simulant DPPC) with A549 cells revealed no major differences versus controls (CCM FBS 2% treated), see **Figure 6.5.** The average cellular, nuclear and mitochondrial areas of A549 cells incubated with simulant versus control cells, demonstrated no significant differences, see **Figure 6.9**.

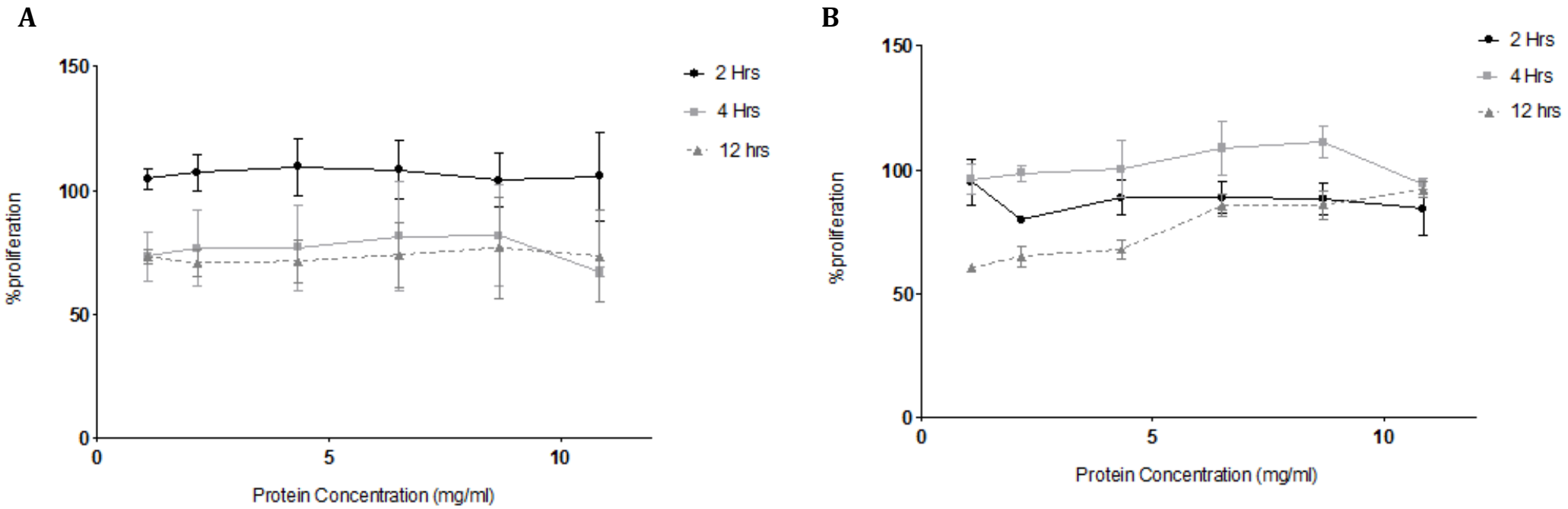

Figure 6.7: *The effect of (A) simulant (Protein and DPPC) and (B) simulant (Protein and DPPC, PG, cholesterol) on the proliferation of A549 cell monolayers. The influence of simulant on cell proliferation was calculated as a percentage of the control (CCM FBS2%). The effect of simulant (at different protein concentrations of 1.1, 2.2, 4.3, 6.5, 8.7, 10.8 mg/mL respectively) was assessed over 2, 4 and 12 h periods of incubation with cells respectively. Cellular metabolic activity was measured spectrophotometrically at 570nm, data represents the mean±SD, , n = 3 experiments, four replicates per experiment at each dilution.*

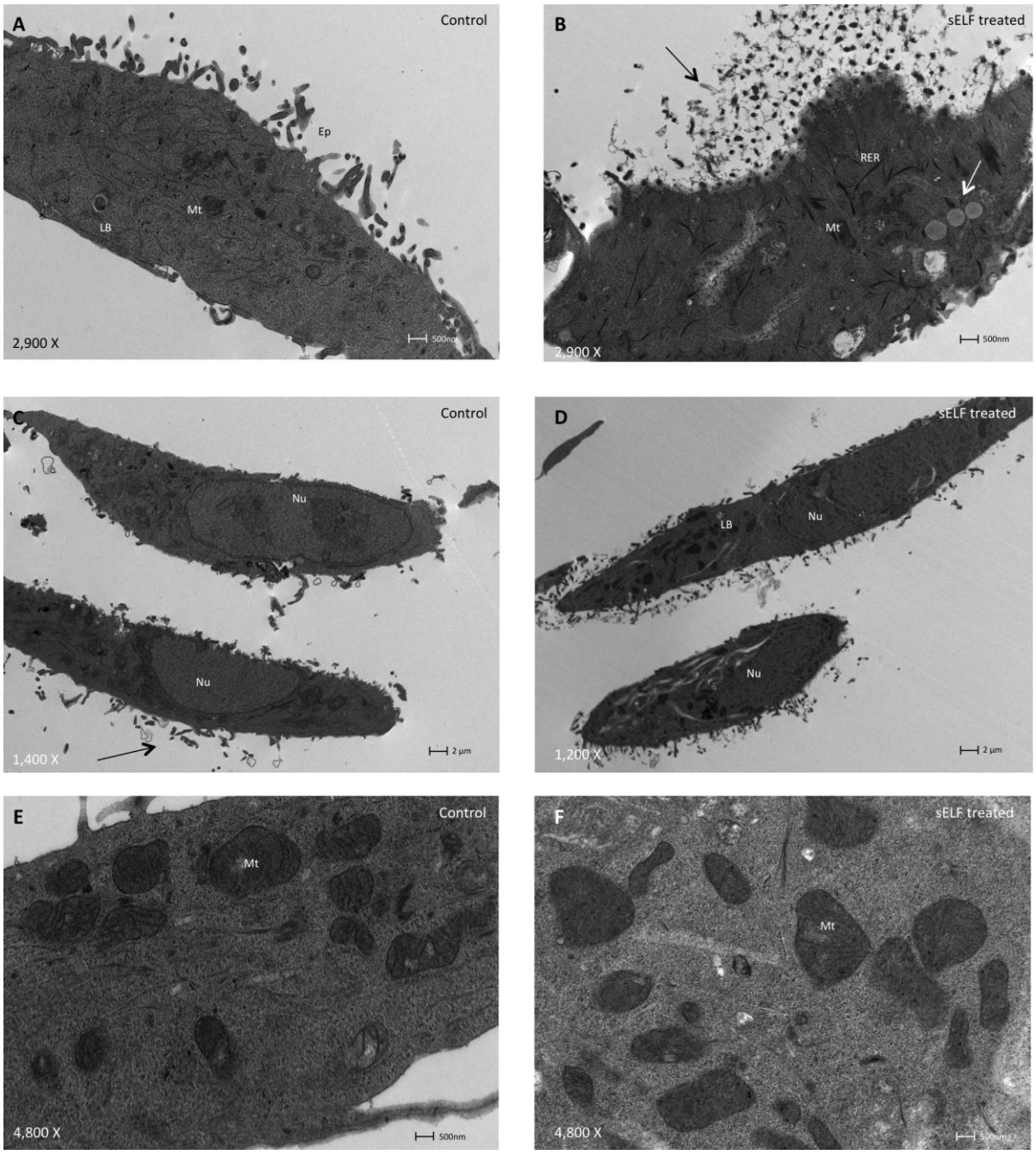

Figure 6.8: *Morphology of A549 epithelial cells treated with or without simulated epithelial lining fluids (simulant). TEM images are representative of (A), (C) and (E) A549 control cells incubated with CCM 2%, (B), (D) and (F) A549 cells incubated with simulant for 4 hs. Interactions of simulant with A549 cells are indicated with arrows, cellular organelles are also indicated: mitochondria (Mt), Lamellar bodies (LB), epithelial projections (Ep), Nuclei (Nu) and rough endoplasmic reticulum (RER), no differences in cellular morphology were observed between groups. Samples were examined on a FEI Tecnai 12 transmission microscope operated at 120 kV. Images were acquired with an AMT 16000M camera.*

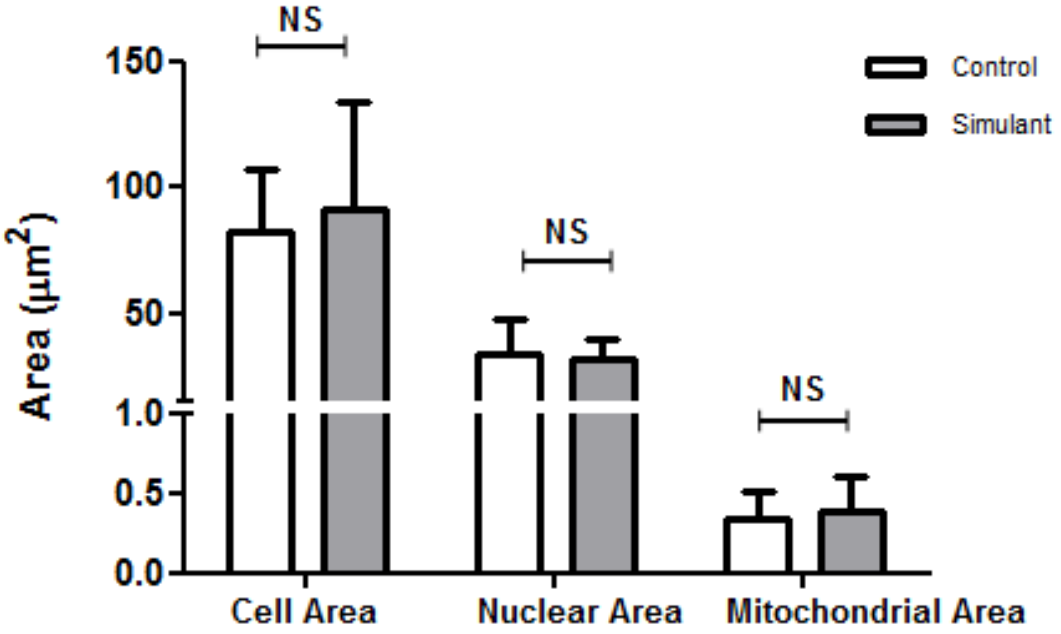

Figure 6.9: *Morphometric analysis of A549 epithelial ells following 4 h incubation with simulated epithelial lining fluids versus control. The overall morphologies of control versus simulant incubated cells were equivalent, the average cellular, nuclear and mitochondrial areas of A549 cells demonstrated no significant differences. Data calculated represent the mean ± sd of n=10 images*.

Furthermore, no differences in the presence of other morphological cell features (lamellar bodies, and epithelial projections) characteristic of A549 cells were observed between treated and non-treated cells see **Figure 6.8**. No signs of cellular distress (nuclear condensation or evidence of crescent shaped condensed chromatin) were noted upon visual inspection either. However TEM analysis of simulant treated cells revealed what appeared to be the internalization of DPPC liposomes in the majority of cells examined. **Figure 6.10** highlights the presence of these inclusions following simulant incubation. Membrane bound liposome containing vacuoles were particularly prominent at the apical surface of the plasma membrane. Additionally, the epithelial microvilli like projections characteristic of A549 cells, appear to have interacted with lipid or protein components following simulant incubation, see **Figure 6.10** It should be noted however that these may also be potential artefacts attributed to the fixing process prior to TEM imaging (note: cell area measurements were absent on TEM preps).

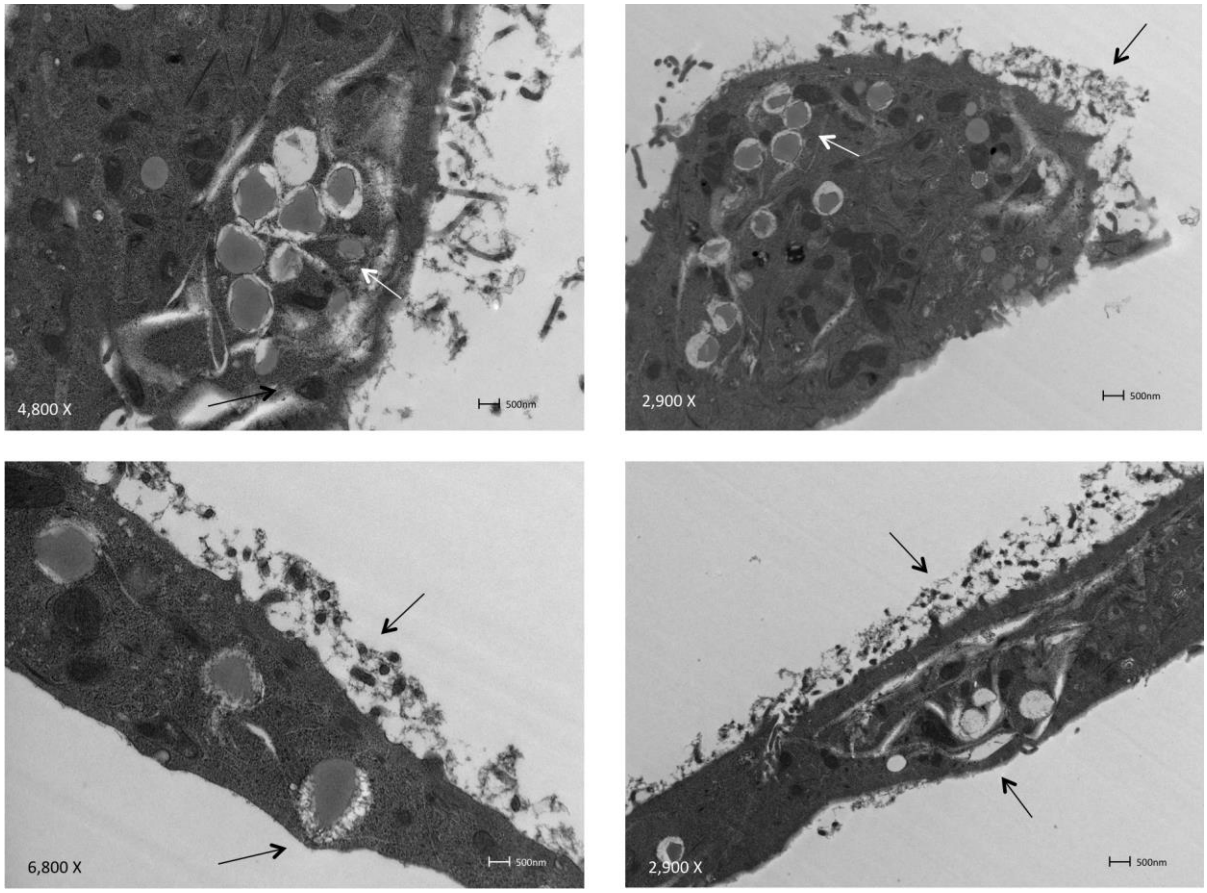

Figure 6.10: *Morphology of A549 epithelial cells treated with simulated epithelial lining fluids (simulant).TEM images are representative of A549 cells incubated with simulant for 4 hs, the presence of phospholipid inclusions and lipid interactions on the cell surface are indicated with arrows. Samples were examined on a FEI Tecnai 12 transmission microscope operated at 120 kV. Images were acquired with an AMT 16000M camera.*

6.4: Discussion

The first steps in the design of a simulated epithelial lining fluid as a physiologically relevant base model for the investigation of inhaled materials *in vitro* were performed in this investigation.

In the objectives outlined for the development of the base model, the major protein, lipid and low molecular weight components representative of healthy alveolar RTLFs were incorporated into the simulant. Components within the base model were commercially available: Synthetic antioxidants (Sigma Chemical Company Ltd. Poole, U.K.) and phospholipids were purchased from Avanti lipids, lyophilized human proteins: albumin, transferrin and Immunoglobulin G were all obtained from Sigma Aldrich, and sourced from human serum. The inclusion of other RTLF human protein components such as SP-A however proved impractical, their inclusion in previous studies either the result of extraction and isolation from human alveolar proteinosis patients (Ruge et al., 2012) or recombinant forms, expressed in SF21 cells, the cDNA of SP-A contained in the plasmids pMTE HS10/5 and pMTE HS10/4 subcloned into the EcoRI site of the baculovirus expression vector pVL1393Th (Sanchez-Barbero et al., 2007). Furthermore the biocompatibility requirements and need to incorporate simulants into existing *in vitro* studies has resulted in the use of two buffering systems: HBSS and HEPES, one a physiologically balanced salt solution, microbiologically tested, containing glucose was deemed necessary for *in vitro* cell culture investigations, whereas the zwitterionic chemical buffer, HEPES was considered most suitable for TEM and DLS analysis.

Using the successfully developed base alveolar model in a series of preliminary investigations it's suitability for the biopharmaceutical screening of inhaled particles in the fundamental applications of particle and cellular interactions were assessed for the first time.

6.4.1: Particle behaviour in simulant

Dynamic light scattering has become the most established method to obtain particle sizing data as part of the physiocochemical characterisation of particles in solution. DLS determines the Z-average by calculating the intensity weighted distribution or the intensity weighted harmonic mean size (by the method of cumulants), and has become the standard way in which to present DLS sizing data. However the suitability of this

technique in obtaining sizing data from particles within biological fluids has been questioned. Biologically relevant solutions generally already consist of particles, in the case of simulant, in the form of its protein and lipid components. It is the presence of such particles in solution which results in background light scattering that influence the calculation of the Z-average value (Braeckmans et al., 2010; van Gaal et al., 2010). The difficulty in assigning peak intensity profiles obtained from DLS in non 'simple' media as the developed simulants, necessitated the use of TEM methodology in conjunction with this sizing technique. Whilst TEM provides limited statistical power, and the preparation and fixation of cells for microscopy has the potential to result in morphological changes, the use of TEM provided a clearer insight into the previously unreported behaviour of particles within physiologically relevant lung simulants.

A study by van Gaal et al (2010) attempted to resolve the significant background scattering observed in particle sizing within biological solutions (CCM supplemented with FBS) by labelling and subsequently measuring particle fluorescence intensity, in an attempt to subtract 'background noise', distinguishing the particles of interest from background signals of equivalent intensity. Whilst this has the additional complication of changing the nature of the particles surface, it may also simply not be relevant for use in biological solutions including the developed simulants, where as observed in this investigation the interaction of particles with protein and lipid components of simulant did not result in the formation of a simple corona at the particle surface, but in its place, large agglomerates of particle, protein and lipid composition.

The formation of the biomolecular corona at the surface of particles in biological fluids has been heavily investigated in the literature, with particle-plasma interactions in particular the focus of recent work (Kobzik et al., 1990; Bihari et al., 2008; Nel et al., 2009; Braeckmans et al., 2010; Doshi and Mitragotri, 2010; Monopoli et al., 2011). However, whilst the influence of inhaled particle opsonisation on the receptor mediated endocytosis of particles in cells has been demonstrated *in vivo* and *in vitro*, no previous studies have investigated this in physiologically-relevant lung lining fluids until now. The significant levels of particle agglomeration and the high degree of interaction observed between simulant components are likely to have a greater impact than simple protein opsinization on the final particle size 'seen' by cells, and thus ultimately the bioavailability and potential toxicity of these particles (Brown et al., 1997; Furumoto et al., 2001; Oberdorster et al., 2005; Chithrani et al., 2006; Kanno et al., 2007; Powers et al., 2007; Muhlfeld et al., 2008; Doshi and Mitragotri, 2010).

Nanoparticle uptake mechanisms exhibit clear size dependence (Doshi and Mitragotri, 2010). For particles less than 200 nm clathrin-dependent and caveolae-mediated modes of endocytosis are thought to dominate, clathrin-dependent endocytosis have a reported maximum uptake size of 200 nm, attributed to the size limit of endocytotic compartments within cells (Zauner et al., 2001; Rejman et al., 2004). Pinocytotic mechanisms are believed to play an important role in the uptake of smaller nanoparticles, limited to less than 100 nm since this cellular mechanism is responsible for the uptake of soluble material (Rejman et al., 2004; Nel et al., 2009). Phagocytic mediated uptake by macrophages has also demonstrated size dependence, preferentially internalizing particle sizes greater that 500 nm (Nel et al., 2009).

The physicochemical aspects of size and surface charge were targeted in this study, with both properties highly implicated in influencing the formation of the macromolecular corona at the surface of particles (Braeckmans et al., 2010; Monopoli et al., 2011). It is well established that particle size determines the surface area of particles and thus the area available for interaction with proteins or lipids in solution, the reduced uptake of 200 nm polystyrene versus 50 nm polystyrene particles by the human hepatocyte cell lines (C3A and HepG2) has been reported and attributed to the reduced surface area available for adsorption of biological components (Renwick et al. 2001; Borm et al. 2006; Choi et al. 2007; Nel et al., 2009; Johnston et al., 2010). The surface charge of particles is also believed to play a significant role in determining the degree of surface interactions with the components of biological solutions and cells, particularly charged phospholipid heads or protein domains. For example changing the surface charge of gold nanorods was shown to dramatically modify the nature of the biomolecular surface of gold nanorods decreasing their uptake into cells (Gratton et al., 2008; Nel et al., 2009). In contrast the carboxylated negatively charged surface of polystyrene particles, has previously been reported to enhance cellular uptake as a consequence of improved dispersion of negative charged particles, a lower extent of aggregation and thus smaller size for uptake (Johnston et al., 2010)

The interaction between protein and lipid components of simulant and the formation of large agglomerates across all particle sizes investigated, and whilst differences attributed to surface charge in particular were apparent, future work must focus on the impact of particle incubation within the physiologically-relevant simulant solutions in order to establish how these interactions may then influence underlying cellular uptake mechanisms which ultimately determine the fate of these inhaled particles.

Whilst simulants and reference RTLFs (concentrated BAL solutions) revealed similar levels of particle agglomeration and protein/lipid interactivity (particularly evident when compared to sizing perfomed in HBSS, HEPES and CCM FBS 2%), differences were observed in sizing perfomed within concentrated BAL, with larger agglomerates of <5000 nm observed. This could be attributed to the presence of surfactant proteins within BAL samples, absent within the developed simulants. The role of both hydrophilic surfactant proteins A and D in influencing the bimolecular nature at the surface of inhaled nanoparticulates, promoting the interaction of particles with macrophages and particle agglomeration has previously been reported (Wright, 2005; Ruge et al., 2012). Surfactant protein A, the most abundant of the surfactant proteins possesses a quaternary structure consisting of a 'hexamer of trimers', each of which possess a globular head containing a carbohydrate-recognition domain (CRD domain) (Casals, 2001; Hawgood and Poulain, 2001; Haagsman, 2002; Heinrich et al., 2006). It is these CRD domains that enable the association of SP-A with pulmonary surfactant lipid membranes (Palaniyar et al., 1998; Palaniyar et al., 2001). SP-A has been observed to both promote and maintain the aggregation of surfactant (Ruano et al., 1996; Veldhuizen et al., 1996; Worthman et al., 2000; Sanchez-Barbero et al., 2005), *in vitro* investigations have revealed SP-A induced aggregation of lipids occurs in a Ca2+ dependent manner and is observed at physiological Ca2+ concentrations (Ruano et al., 1996; Ruano et al., 2000; Casals, 2001). This SP-A dependent phospholipid aggregation is dependent on the intact CRD domain, it has been proposed that through these domains SP-A is able to recognise ordered lipid patterns, in both a hydrophobic and polar manner (Casals, 2001; Palaniyar et al., 2001), which may in turn be responsible for the lattice architecture of TM *in vivo*.

6.4.2: Biocompatibility of simulant

The A549 cells used as part of the vitro assessment of the biocompatibility of the healthy alveolar base model are representative of type II alveolar epithelial cells, originating from a lung carcinoma (PubMed 4357758), they have been used extensively since their initiation by D.J. Giard et al (1972). The A549 cell line has most often been used to assess the toxicity of inhaled materials alongside standard cellular metabolic assays including the MTT assay as performed in this study (Wilson et al., 2000; Kawasaki et al., 2001; Laan et al., 2004; Forbes and Ehrhardt, 2005).

This investigation revealed no adverse impact of the physiologically relevant protein and liposome concentrations within simulant on the proliferation of A549 cell

monolayers. The observations obtained were somewhat unexpected with *in vitro* models described to possess a higher susceptibility to toxicity than *in vivo*, for example the toxicity of plasma on vascular endothelial cells *in vitro* is well established despite this being the physiologically occurring interface *in vivo*, the toxicity observed has been attributed to various physiological limitations including the absence of innate defence mechanisms (Kleberg et al., 2010). The compatibility of simulated intestinal fluid (SIF) with *in vitro* cell models have similarly been investigated, both fasted, FaSSIF and fed, FeSSIF, formulations have been assessed on the apical surface of the intestinal Caco-2 cell line *in vitro* (Kataoka et al., 2006; Patel et al., 2006). With the Caco-2 cell line widely used in studies of oral drug permeability, the incorporation and tissue compatibility of biorelevant SIFs with cellular models, as with this investigation, were viewed as a step forward in improving the predictability of these *in vitro* assays, to avoid the over or under estimation of drug solubility or permeability (Kleberg et al., 2010; Marques et al., 2011). Ingels et al (2002) reported the high toxicity of FeSSiF on Caco-2 cells, the conversion of MTT was even reduced in the mitochondria of cells and the absorbance of the purple formazan extremely low following FeSSIF incubation. The high toxicity of this SIF formulation has also been observed to result in the collapse of transepithelial resistance in monolayers (Patel, et al. 2006). However, Caco-2 cells demonstrated increased viability following incubation with a modified formulation of this simulant, with the observed toxicity of FeSSIF determined to be the combination of high concentrations of sodium tacrocholate (15 mM), low pH of 5.0 and high osmalilty (Ingels et al., 2002; Lind et al., 2007). Furthermore, cells treated with FASSIF, have demonstrated normal cell viability using the MTT assay, with no significant differences observed for this formulation, in fact incorporating FASSIF into the Caco-2 model was used to successfully determine the *in vitro-in vivo* correlation (IVIVC) of six oral solid drug formulations (Buch et al., 2009; Kleberg, 2010). The modification of simulants to enable tissue compatibility whilst remaining biorelevant is necessary, accordingly this investigation tried to ensure the compatibility of developed simulants, and achieved it by incorporating HBSS with physiologically relevant pH and electrolytes and glucose concentrations.

Although previous investigations with SIFs, suggest the relative concentrations and interactions of individual components within the simulant may influence biocompatibility, the different lipid compositions investigated revealed no quantifiable differences in biocompatibility versus CCM controls. It was only the concentrated BAL preparations, which lack glucose, prepared in 150 mM saline solution that proved incapable of maintaining A549 cell viability. Whilst the vacuolisation of phospholipid liposomes was

observed within A549 cells, this did not appear to influence cell viability. Type II cells possess well characterized endocytic properties with the endocytosis of various particles; nanoparticles (50 nm TiO2) cationic liposomes, previously reported (Ito et al., 1992; Ryan et al., 1994; Friend et al., 1996; Foster et al., 1998; Stearns et al 2001). Type II cells additionally play a role in the 'recycling' of surfactant components, which may in turn explain the endocytosis of liposomes observed following simulant incubation. It has been proposed that the cleared surfactant lipids either end up in lamellar bodies or are degraded to then be reused in the synthesis of new surfactant lipids (Wright et al., 1984; Wright, 1990).

As has already been achieved with SIF formulations, the incorporation of physiologically relevant yet biocompatible media, such as the simulant developed in this investigation, must be the gold standard reached for the *in vitro* cellular studies investigating the behaviour of inhaled drugs and particles. Ultimately this must be attained if we are to develop a better understanding of the interaction of inhaled materials and will serve to evolve our understanding of their subsequent behaviour within the airways.

Conclusions

In conclusion, this thesis describes the first steps in the development of a standardised epithelial lining fluid simulant from which the following conclusions were reached :

1. Particle sizing with DLS alongside TEM revealed the interaction of particles investigated with both the protein and lipid components of developed simulants. The large agglomerates observed may provide a more realistic reflection of the *in vivo* situation following particle deposition, and thus may be significant in evolving our interpretation and understanding of inhaled particle bioavailability and toxicity.

2. Broad biocompatibility of the base alveolar simulant was established across commonly used *in vitro* cell line representative of the alveolar airways, at time points relevant for commonly used *in vitro* pharmaceutical assays.

Future and ongoing studies

The extensive characterization of healthy human RTLFs as described in **Chapter 3**, was the foundation behind the design of the base simulant model, representing the major protein, lipid and antioxidant components of this extracellular compartment, the results described here in **Chapter 6** detailing the first few steps undertaken in assessing the applicability of the base model, as illustrated in **Figure 6.11** below.

Figure 6.11: *Requirements for the development of a validated, disease and region specific lung lining fluid simulant.*

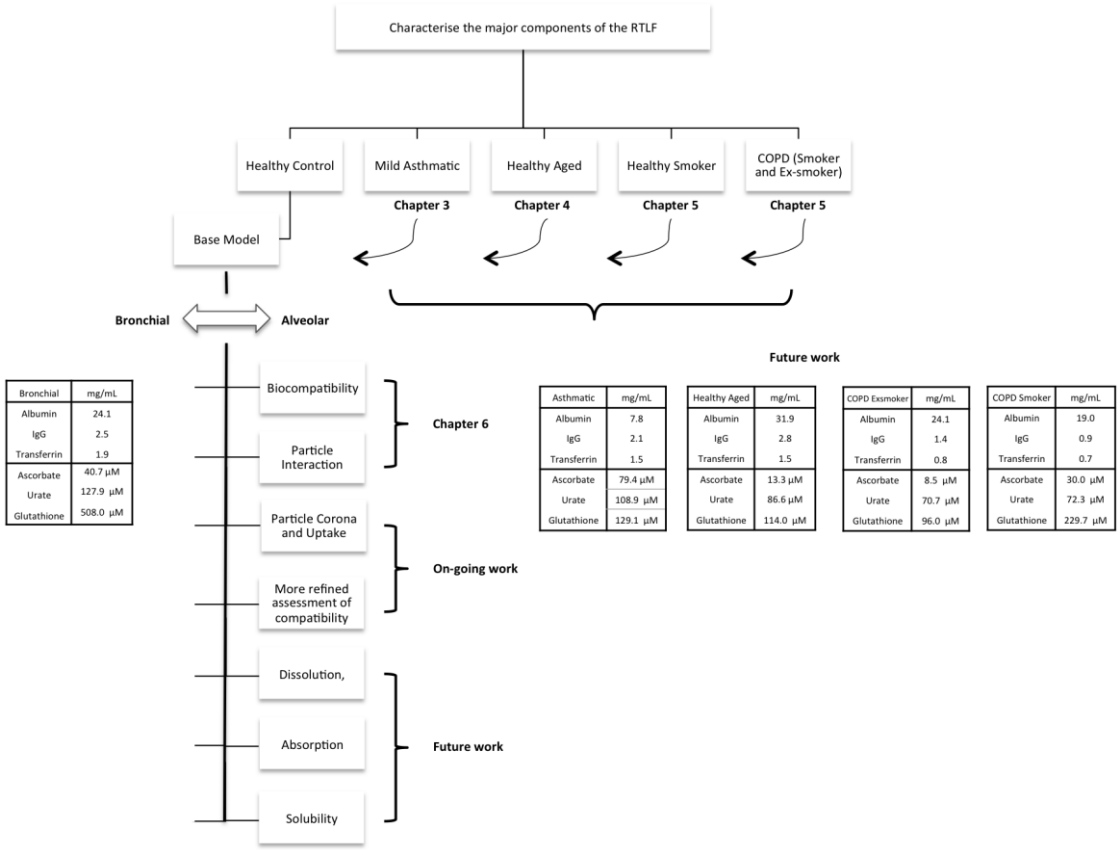

However whilst one of the strengths of the developed model is its physiological relevance, the implementation of a primary base model also created several practical limitations, these were resolved by the decision to focus the design of simulant, in this initial phase of its development, on the alveolar RTLFs alone. The assessment of the biocompatibility of this model was thus focused on the human alveolar epithelial A549 cell line, however future work must incorporate the characterization of different regions of the airways, the composition of which has already been examined and outlined within this thesis (**Chapters 3, 4 and 5**). Not only is the development of 'bespoke' regionally specific

models: bronchial or nasal RTLF simulants, an important next step, these regionally specific simulants must also be evaluated for their compatibility with the most relevant cell lines employed *in vitro*. This is a crucial step in fully integrating simulants with models used in screens for drug dissolution-absorption, biocompatibility and particle uptake. In addition to investigations determining cell proliferation (such as the MTT assay employed within this thesis) more refined markers of cellular dysfunction from cytokine and chemokine release, cell metabolism to tight junction formation must be employed in the assessment of simulant compatibility. It must be highlighted that one of the critical limitations of the A549 cell line is it's unsuitability for use in drug absorption and permeability assays, on account of the lack of tight junction formation and their inherent leakiness (Elbert et al., 1999; Kim et al., 2001). Thus more relevant barrier forming cell lines including the Calu-3, 16HBE14o- or primary cells may be more relevant in determining simulant integration into commonly used *in vitro* models for drug development. Future work must also refine models in order to effectively reflect diseased (asthma and COPD) and aged RTLFs, with the current base model only representative of the healthy young airways, not only are these key user groups of inhaled medicines, but as established throughout **Chapters 3, 4 and 5** the composition of this extracellular compartment is significantly altered in these conditions. Whether suitable *in vitro* cell lines are currently available for which modified simulants can then be incorporated may however be an important limitation in exploring this next step.

Whilst *in vitro* cell culture models have proven useful in the study of drug absorption and transport, the integration of region and disease specific simulants with the currently available *in vitro* cell models would ultimately provide the greatest relevance to the *in vivo* situation. If integrated cell culture models are developed in the future they would not only permit for the rapid screening, establishing the pharmacokinetics and pharmacodynamic effects of inhaled particulates, but become an essential part of mechanistic investigations concerning drug permeability and metabolism. The incorporation of simulants in *in vitro* dissolution tests which are are often used to guide the early development of drugs and their formulation, as well as to ensure quality assurance (QA) and IVIVC of drugs (Davies, 2003; Agu, 2011), as well as to predict the solubilization process of inhaled formulations (Wiedmann, 2000; Pham and Wiedmann, 2001) is another key point for future studies to address, with no current standardized method available for the evaluation of dissolution of inhaled drugs.

In addition to these future pharmaceutical challenges that must be explored throughout the continued development of lung lining fluid simulants, the integration of physiologically relevant simulants within the various toxicity screening methods used for inhaled environmental particulates will also be an important next step. Ultimately the impact the pre-incubation of particulate formulations within the developed simulant models and their subsequent uptake into pulmonary cells, i.e. 'the particle –cell interaction' must be established. Studies evaluating the incubation of nanoparticles within the developed base models (and concentrated human BAL samples as a reference) are currently underway. The aim of these experiments is to explore the nature of the macromolecular 'corona' that forms on the surface of nanoparticles following their deposition in the RTLFs. Since it is this corona that ultimately represents the biological identity of particles, only by understanding the nature of this interaction can we begin to elucidate just how this biomolecular interface influences the cellular interactions of particles *in vitro* and in vivo. 200nm SiO_2 and polyvinyl acetate (PVA) particles (particles of varying degrees of hydrophobicity) have been chosen for this investigation. Focusing on, the proteomic identity and thus the nature of the 'protein corona' formed, the number and classification of proteins bound to the surface of particles is being evaluated using a semi-quantitive nanoLC-MS/MS approach, as previously explored in this thesis. No previous studies have investigated the nature of this interaction using a physiologically relevant model, however as highlighted earlier in this chapter, TEM imaging obtained following particle incubation within the base model has already demonstrated the interaction between protein and lipid components of simulant. The data obtained will be the first to elucidate the protein corona profile of particles within RTLF models.

Whatever the next steps are in the continuing development of the lung lining fluid simulant, more detailed and informative measures regarding the compatibility of simulated lung lining fluids with the many various assays in use must be considered. Whether it is the incorporation of components such as growth factors, which may become necessary if primary cells are in use, or if lipid analysis is an important component of the assay in question, surfactant proteins may be a necessary addition. What exact refinements are necessary will ultimately depend on the experimental objective in question.

However future studies must ultimately provide greater insight into the 'real world' applicability of the developed simulants in order for them become successfully and easily incorporated into *in vitro* investigations guiding and improving the drug development process of inhaled medicines. The development of a standardised simulant

model must consider the requirements of pharmacopoeial or ISO standards, information regarding appearance, sterility and endotoxin content, purity, buffer capacity, ionic strength, osmolality and viscosity must be accounted for, with defined limits and acceptance criteria based on an observed range of variation. However in physiological solutions such as simulant practical considerations must also include colloidal stability and aggregation, criteria must account for the acceptable limits for liposome size distribution and a validated sizing method (DLS, TEM), to assure a consistent particle distribution.

This study investigated both the reproducibility of manufactured simulants and the stability of formulations with TEM and DLS techniques in order to fulfill the criteria described above. Simulants were stored at 4° C, and stability assessed over 3 and 6 month periods. How this influences the physicochemical interactions of simulants with particles or cells must however be established in more detail if they are to incorporated in standardised *in vitro* testing of inhaled drugs in future studies. Furthermore, volume, temperature and pH requirements for individual assay purposes must also be tailored to physiological features of the airways as well as the practical limits of the test apparatus. As of yet the preliminary investigations performed have utilised the physiological temperature of $37^{O}C$ at volumes suited to cell culture and particle sizing requirements. But with a wide range of inhaled and nasal pharmaceutical products, flexibility in testing methodology will be required. These criteria must be an important component of future work in the continued development of the simulant model established.

Appendix A

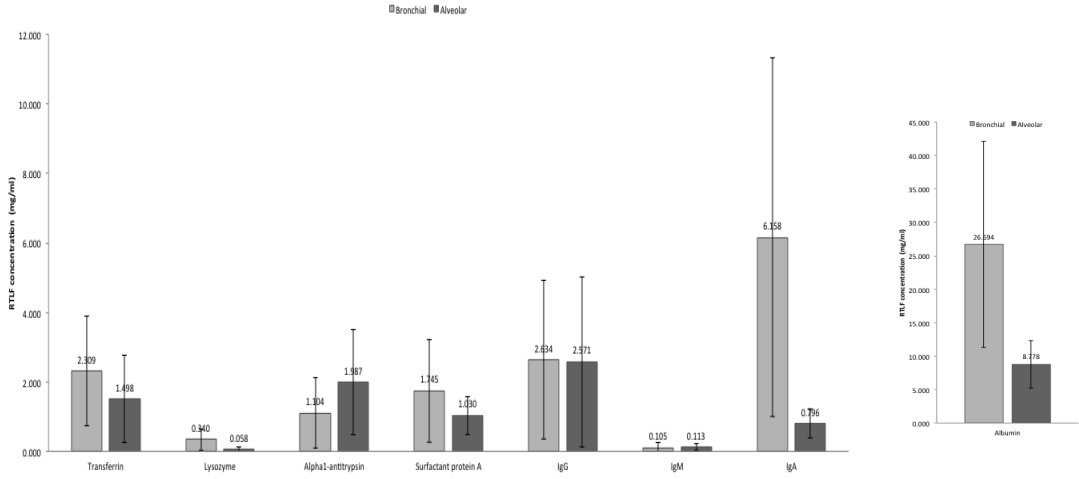

Figure A.1: *<u>The bronchial versus alveolar airway RTLF protein components in healthy controls</u>: Transferrin, Lysozyme, Alpha-1 Antitrypsin, SP-A, IgG, IgM, IgA and Albumin. Healthy controls n=16, 25.0±2.6 years, 6M/10F, * denotes a statistical difference where p<0.05.*

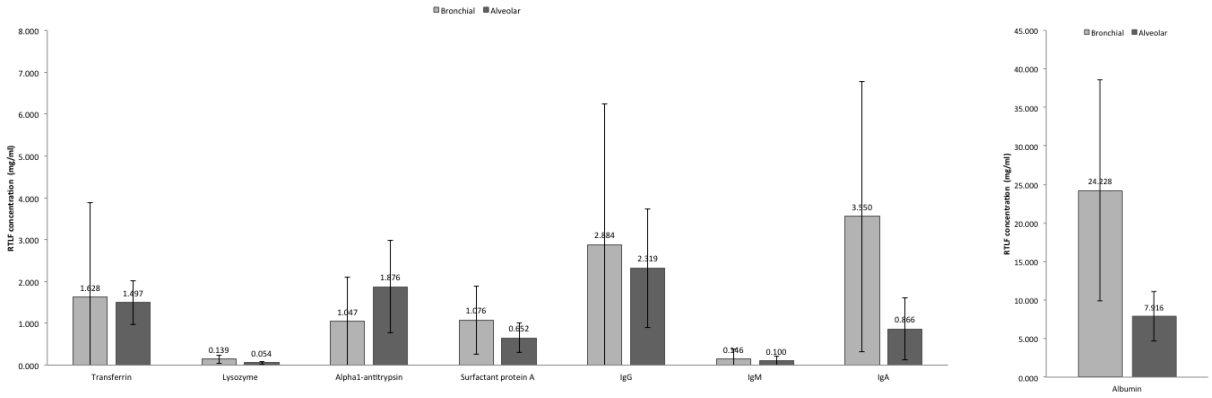

Figure A.2: *<u>The bronchial versus alveolar airway RTLF protein components in mild asthmatics</u>: Transferrin, Lysozyme, Alpha-1 Antitrypsin, SP-A, IgG, IgM, IgA and Albumin, in mild asthmatic. Mild asthmatics n=16, 26.7±6.2 years, 5M/11F. * denotes a statistical difference where p<0.05.*

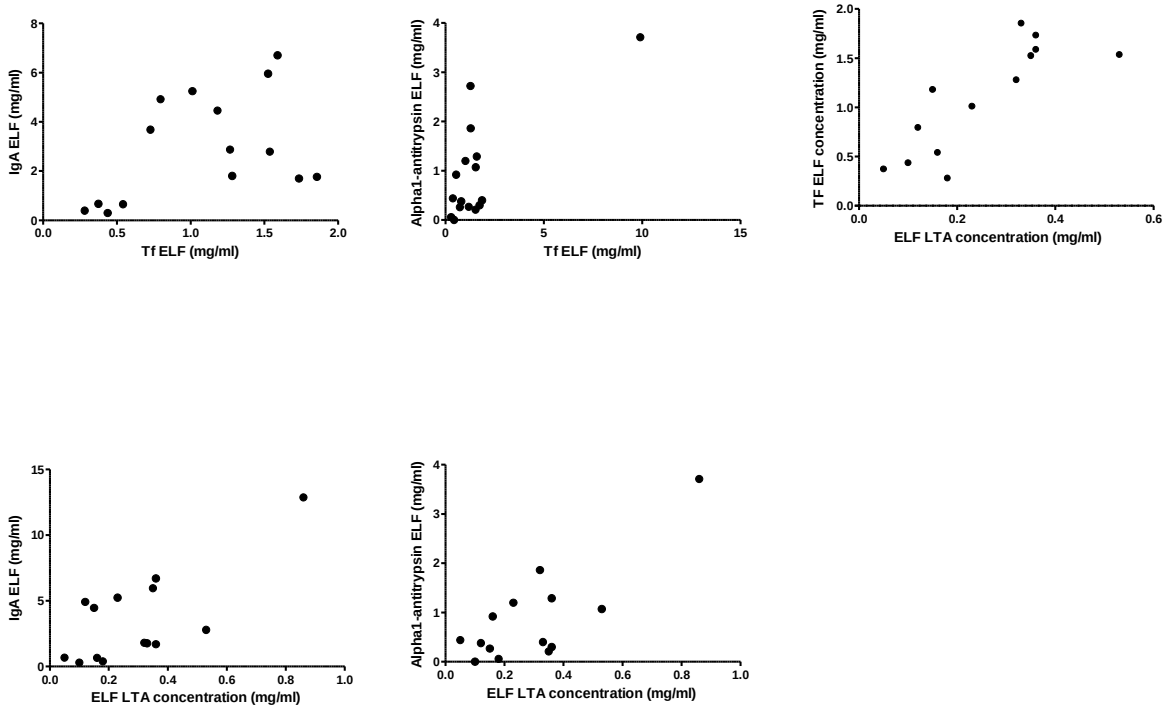

Figure A.3: *Correlation of proteins of innate immunity (IgA, Alpha-1 Antitrypsin, Transferrin) and LTA concentrations in asthmatic Bronchial Wash . Mild asthmatics n=16, 26.7±6.2 years, 5M/11F. * denotes a statistical difference where p<0.05.*

Table A.1: *All alveolar proteins identified by 1D PAGE and nano LC MS/MS in healthy control RTLFs. The 199 proteins identified in healthy control subjects investigated, (n=5), alongside the mean of the three most abundant ion peaks of each respective protein identified. Accession numbers included according to entries in UniProtKB/Swiss-Prot.*

Healthy Control	
Serotransferrin OS=Homo sapiens GN=TF PE=1 SV=3	1.28E+10
Ig gamma-1 chain C region; [Homo sapiens (Human)] - [IGHG1_HUMAN]	1.23E+10
Ig gamma-3 chain C region OS=Homo sapiens GN=IGHG3 PE=1 SV=2	9.36E+09
Ig gamma-2 chain C region OS=Homo sapiens GN=IGHG2 PE=1 SV=2	9.10E+09
Ig gamma-4 chain C region OS=Homo sapiens GN=IGHG4 PE=1 SV=1	9.10E+09
Ig kappa chain C region OS=Homo sapiens GN=IGKC PE=1 SV=1	5.90E+09
Uncharacterized protein C3orf38; [Homo sapiens (Human)] - [CC038_HUMAN]	4.10E+09
Serum albumin OS=Homo sapiens GN=ALB PE=1 SV=2	3.97E+09

Ig lambda-2 chain C regions OS=Homo sapiens GN=IGLC2 PE=1 SV=1	3.07E+09
Ig alpha-1 chain C region OS=Homo sapiens GN=IGHA1 PE=1 SV=2	2.81E+09
Alpha-1-antitrypsin OS=Homo sapiens GN=SERPINA1 PE=1 SV=3	2.69E+09
Ig alpha-2 chain C region OS=Homo sapiens GN=IGHA2 PE=1 SV=3	2.05E+09
Immunoglobulin lambda-like polypeptide 5; AltName: Full=G lambda-1; AltName: Full=Germline immunoglobulin lambda 1; Flags: Precursor; [Homo sapiens (Human)] - [IGLL5_HUMAN]	1.96E+09
Ig heavy chain V-III region HIL; [Homo sapiens (Human)] - [HV310_HUMAN]	1.66E+09
Lactotransferrin OS=Homo sapiens GN=LTF PE=1 SV=6	1.38E+09
Rho GDP-dissociation inhibitor 2 OS=Homo sapiens GN=ARHGDIB PE=1 SV=3	1.36E+09
Ig heavy chain V-III region VH26 OS=Homo sapiens PE=1 SV=1	1.25E+09
Ig heavy chain V-III region CAM OS=Homo sapiens PE=1 SV=1	1.22E+09
Ig heavy chain V-III region BRO; [Homo sapiens (Human)] - [HV305_HUMAN]	1.19E+09
Ig heavy chain V-III region TUR; [Homo sapiens (Human)] - [HV318_HUMAN]	1.18E+09
Ig heavy chain V-III region GAL OS=Homo sapiens PE=1 SV=1	1.17E+09
Ig heavy chain V-III region BUT OS=Homo sapiens PE=1 SV=1	1.16E+09
Cathepsin D OS=Homo sapiens GN=CTSD PE=1 SV=1	1.10E+09
Probable E3 ubiquitin-protein ligase HERC6; EC=6.3.2.-; AltName: Full=HECT domain and RCC1-like domain-containing protein 6; [Homo sapiens (Human)] - [HERC6_HUMAN]	8.68E+08
Hemopexin OS=Homo sapiens GN=HPX PE=1 SV=2	7.70E+08
Uteroglobin OS=Homo sapiens GN=SCGB1A1 PE=1 SV=1	6.27E+08
Ceruloplasmin OS=Homo sapiens GN=CP PE=1 SV=1	5.37E+08
Polymeric immunoglobulin receptor OS=Homo sapiens GN=PIGR PE=1 SV=4	5.24E+08
Ig kappa chain V-I region Wes; [Homo sapiens (Human)] - [KV119_HUMAN]	5.03E+08
Ig kappa chain V-I region DEE OS=Homo sapiens PE=1 SV=1	4.84E+08
Ig kappa chain V-I region WAT; [Homo sapiens (Human)] - [KV125_HUMAN]	4.74E+08

Ig lambda chain V-IV region Bau; [Homo sapiens (Human)] - [LV401_HUMAN]	4.40E+08
Ig kappa chain V-I region EU OS=Homo sapiens PE=1 SV=1	4.22E+08
Xin actin-binding repeat-containing protein 2 OS=Homo sapiens GN=XIRP2 PE=1 SV=2	4.22E+08
Haptoglobin OS=Homo sapiens GN=HP PE=1 SV=1	3.82E+08
Ig kappa chain V-III region VG; Flags: Precursor; Fragment; [Homo sapiens (Human)] - [KV309_HUMAN]	3.81E+08
Ig kappa chain V-III region SIE OS=Homo sapiens PE=1 SV=1	3.17E+08
Ig kappa chain V-III region POM OS=Homo sapiens PE=1 SV=1	3.13E+08
Ig kappa chain V-II region GM607; Flags: Precursor; Fragment; [Homo sapiens (Human)] - [KV205_HUMAN]	2.91E+08
Ig lambda chain V-IV region Hil; [Homo sapiens (Human)] - [LV403_HUMAN]	2.91E+08
Ig heavy chain V-III region GAR; [Homo sapiens (Human)] - [HV322_HUMAN]	2.84E+08
Ig lambda chain V-III region LOI OS=Homo sapiens PE=1 SV=1	2.61E+08
Ig kappa chain V-I region Scw; [Homo sapiens (Human)] - [KV117_HUMAN]	2.48E+08
Caspase recruitment domain-containing protein 6; [Homo sapiens (Human)] - [CARD6_HUMAN]	2.40E+08
Ig kappa chain V-III region Ti; [Homo sapiens (Human)] - [KV304_HUMAN]	2.35E+08
Putative V-set and immunoglobulin domain-containing protein 6 OS=Homo sapiens GN=VSIG6 PE=5 SV=2	2.22E+08
FAS-associated factor 1; Short=hFAF1; AltName: Full=UBX domain-containing protein 12; AltName: Full=UBX domain-containing protein 3A; [Homo sapiens (Human)] - [FAF1_HUMAN]	2.21E+08
Vitamin D-binding protein OS=Homo sapiens GN=GC PE=1 SV=1	2.19E+08
Ig lambda chain V-I region HA OS=Homo sapiens PE=1 SV=1	2.17E+08
Ig heavy chain V-I region HG3; Flags: Precursor; [Homo sapiens (Human)] - [HV102_HUMAN]	2.14E+08
Hemoglobin subunit alpha; AltName: Full=Alpha-globin; AltName: Full=Hemoglobin alpha chain; [Homo sapiens (Human)] - [HBA_HUMAN]	2.06E+08
Hemoglobin subunit beta OS=Homo sapiens GN=HBB PE=1 SV=2	2.06E+08
Alpha-1-acid glycoprotein 1 OS=Homo sapiens GN=ORM1 PE=1 SV=1	2.04E+08

Ig kappa chain V-I region Roy; [Homo sapiens (Human)] - [KV116_HUMAN]	1.96E+08
Pulmonary surfactant-associated protein A2 OS=Homo sapiens GN=SFTPA2 PE=1 SV=1	1.95E+08
Alpha-1-acid glycoprotein 2 OS=Homo sapiens GN=ORM2 PE=1 SV=2	1.81E+08
Ig kappa chain V-III region NG9; Flags: Precursor; Fragment; [Homo sapiens (Human)] - [KV303_HUMAN]	1.74E+08
Hemoglobin subunit delta OS=Homo sapiens GN=HBD PE=1 SV=2	1.66E+08
Ig kappa chain V-IV region Len OS=Homo sapiens PE=1 SV=2	1.66E+08
Desmoplakin OS=Homo sapiens GN=DSP PE=1 SV=3	1.60E+08
Alpha-1-antichymotrypsin OS=Homo sapiens GN=SERPINA3 PE=1 SV=2	1.49E+08
Ribonuclease P protein subunit p40; Short=RNaseP protein p40; EC=3.1.26.5; AltName: Full=RNase P subunit 1; [Homo sapiens (Human)] - [RPP40_HUMAN]	1.42E+08
Phosphatidylinositol 3,4,5-trisphosphate-dependent Rac exchanger 1 protein; Short=P-Rex1; Short=PtdIns(3,4,5)-dependent Rac exchanger 1; [Homo sapiens (Human)] - [PREX1_HUMAN]	1.41E+08
Alpha-1B-glycoprotein OS=Homo sapiens GN=A1BG PE=1 SV=4	1.36E+08
Ig lambda chain V-I region WAH OS=Homo sapiens PE=1 SV=1	1.26E+08
cGMP-specific 3',5'-cyclic phosphodiesterase; EC=3.1.4.35; AltName: Full=cGMP-binding cGMP-specific phosphodiesterase; Short=CGB-PDE; [Homo sapiens (Human)] - [PDE5A_HUMAN]	1.22E+08
Beta-2-microglobulin OS=Homo sapiens GN=B2M PE=1 SV=1	1.20E+08
Zinc-alpha-2-glycoprotein OS=Homo sapiens GN=AZGP1 PE=1 SV=2	1.16E+08
Ig kappa chain V-I region Ni; [Homo sapiens (Human)] - [KV121_HUMAN]	1.15E+08
Ig heavy chain V-II region NEWM; [Homo sapiens (Human)] - [HV207_HUMAN]	1.14E+08
LIM domain only protein 7; Short=LMO-7; AltName: Full=F-box only protein 20; AltName: Full=LOMP; [Homo sapiens (Human)] - [LMO7_HUMAN]	1.14E+08
Transthyretin OS=Homo sapiens GN=TTR PE=1 SV=1	1.12E+08
14-3-3 protein beta/alpha OS=Homo sapiens GN=YWHAB PE=1 SV=3	1.07E+08
14-3-3 protein gamma OS=Homo sapiens GN=YWHAG PE=1 SV=2	1.07E+08
14-3-3 protein zeta/delta OS=Homo sapiens GN=YWHAZ PE=1 SV=1	1.07E+08

Ig lambda chain V region 4A OS=Homo sapiens PE=4 SV=1	1.06E+08
Angiotensinogen OS=Homo sapiens GN=AGT PE=1 SV=1	9.61E+07
Apolipoprotein A-I OS=Homo sapiens GN=APOA1 PE=1 SV=1	9.59E+07
Protein S100-A6 OS=Homo sapiens GN=S100A6 PE=1 SV=1	9.49E+07
Ig kappa chain V-IV region JI; Flags: Precursor; [Homo sapiens (Human)] - [KV403_HUMAN]	9.06E+07
14-3-3 protein epsilon OS=Homo sapiens GN=YWHAE PE=1 SV=1	9.02E+07
Protein Shroom3; AltName: Full=Shroom-related protein; Short=hShrmL; [Homo sapiens (Human)] - [SHRM3_HUMAN]	8.34E+07
Immunoglobulin J chain OS=Homo sapiens GN=IGJ PE=1 SV=4	8.29E+07
Histone-lysine N-methyltransferase MLL3 OS=Homo sapiens GN=MLL3 PE=1 SV=3	7.98E+07
Pre-mRNA cleavage complex 2 protein Pcf11; AltName: Full=Pre-mRNA cleavage complex II protein Pcf11; [Homo sapiens (Human)] - [PCF11_HUMAN]	7.88E+07
CD44 antigen OS=Homo sapiens GN=CD44 PE=1 SV=3	7.78E+07
Ig heavy chain V-II region ARH-77 OS=Homo sapiens PE=4 SV=1	7.57E+07
Alpha-2-HS-glycoprotein OS=Homo sapiens GN=AHSG PE=1 SV=1	7.52E+07
Ig lambda chain V-I region NIG-64 OS=Homo sapiens PE=1 SV=1	6.96E+07
ATP-binding cassette sub-family C member 8; AltName: Full=Sulfonylurea receptor 1; [Homo sapiens (Human)] - [ABCC8_HUMAN]	6.85E+07
Coiled-coil domain-containing protein 37; [Homo sapiens (Human)] - [CCD37_HUMAN]	6.84E+07
Ig heavy chain V-II region OU; [Homo sapiens (Human)] - [HV201_HUMAN]	6.80E+07
Alpha-2-macroglobulin OS=Homo sapiens GN=A2M PE=1 SV=3	6.75E+07
Annexin A5 OS=Homo sapiens GN=ANXA5 PE=1 SV=2	6.60E+07
Ig mu chain C region OS=Homo sapiens GN=IGHM PE=1 SV=3	6.47E+07
Ig heavy chain V-I region V35 OS=Homo sapiens PE=1 SV=1	6.05E+07
Glucosamine--fructose-6-phosphate aminotransferase [isomerizing] 2; EC=2.6.1.16; AltName: Full=D-fructose-6-phosphate amidotransferase 2; AltName: Full=Glutamine:fructose 6 phosphate amidotransferase 2; Short=GFAT 2; Short=GFAT2; AltName: Full=Hexosephosphate aminotransferase 2; [Homo sapiens (Human)] - [GFPT2_HUMAN]	5.95E+07

Glutathione S-transferase A2 OS=Homo sapiens GN=GSTA2 PE=1 SV=4	5.83E+07
Beta-microseminoprotein; AltName: Full=Immunoglobulin-binding factor; Short=IGBF; AltName: Full=PN44; AltName: Full=Prostate secreted seminal plasma protein; AltName: Full=Prostate secretory protein of 94 amino acids; Short=PSP-94; Short=PSP94; AltName: Full=Seminal plasma beta-inhibin; Flags: Precursor; [Homo sapiens (Human)] - [MSMB_HUMAN]	5.82E+07
Deleted in malignant brain tumors 1 protein OS=Homo sapiens GN=DMBT1 PE=1 SV=2	5.59E+07
Actin, cytoplasmic 1 OS=Homo sapiens GN=ACTB PE=1 SV=1	5.55E+07
Epididymal secretory protein E1 OS=Homo sapiens GN=NPC2 PE=1 SV=1	5.26E+07
Corticosteroid-binding globulin OS=Homo sapiens GN=SERPINA6 PE=1 SV=1	5.17E+07
28S ribosomal protein S26, mitochondrial; Short=MRP-S26; Short=S26mt; AltName: Full=28S ribosomal protein S13, mitochondrial; Short=MRP-S13; Short=S13mt; Flags: Precursor; [Homo sapiens (Human)] - [RT26_HUMAN]	4.89E+07
Transmembrane protein 198; [Homo sapiens (Human)] - [TM198_HUMAN]	4.77E+07
Histone H4 OS=Homo sapiens GN=HIST1H4A PE=1 SV=2	4.75E+07
Pulmonary surfactant-associated protein D OS=Homo sapiens GN=SFTPD PE=1 SV=3	4.71E+07
G antigen family D member 2; AltName: Full=Cancer/testis antigen 12.1; Short=CT12.1; AltName: Full=Protein XAGE-1; [Homo sapiens (Human)] - [GAGD2_HUMAN]	4.41E+07
Intercellular adhesion molecule 1 OS=Homo sapiens GN=ICAM1 PE=1 SV=2	4.01E+07
Protein DJ-1 OS=Homo sapiens GN=PARK7 PE=1 SV=2	3.98E+07
Triosephosphate isomerase OS=Homo sapiens GN=TPI1 PE=1 SV=3	3.83E+07
Calmodulin OS=Homo sapiens GN=CALM1 PE=1 SV=2	3.58E+07
Coactosin-like protein OS=Homo sapiens GN=COTL1 PE=1 SV=3	3.46E+07
Glutathione S-transferase P OS=Homo sapiens GN=GSTP1 PE=1 SV=2	3.42E+07
Serpin B3 OS=Homo sapiens GN=SERPINB3 PE=1 SV=2	3.01E+07
Antithrombin-III OS=Homo sapiens GN=SERPINC1 PE=1 SV=1	2.92E+07
Angiotensin-converting enzyme OS=Homo sapiens GN=ACE PE=1 SV=1	2.86E+07
Ig lambda chain V-III region SH; [Homo sapiens (Human)] - [LV301_HUMAN]	2.83E+07
Pro-cathepsin H OS=Homo sapiens GN=CTSH PE=1 SV=4	2.79E+07

Apolipoprotein A-II OS=Homo sapiens GN=APOA2 PE=1 SV=1	2.59E+07
Afamin OS=Homo sapiens GN=AFM PE=1 SV=1	2.55E+07
Pulmonary surfactant-associated protein B OS=Homo sapiens GN=SFTPB PE=1 SV=3	2.54E+07
Annexin A4 OS=Homo sapiens GN=ANXA4 PE=1 SV=4	2.52E+07
Selenium-binding protein 1 OS=Homo sapiens GN=SELENBP1 PE=1 SV=2	2.43E+07
Carbonic anhydrase 1 OS=Homo sapiens GN=CA1 PE=1 SV=2	2.36E+07
Transaldolase OS=Homo sapiens GN=TALDO1 PE=1 SV=2	2.33E+07
Scavenger receptor cysteine-rich type 1 protein M130 OS=Homo sapiens GN=CD163 PE=1 SV=2	2.29E+07
CD9 antigen OS=Homo sapiens GN=CD9 PE=1 SV=4	2.20E+07
Complement C4-A; AltName: Full=Acidic complement C4; AltName: Full=C3 and PZP-like alpha-2-macroglobulin domain-containing protein 2; Contains: RecName: Full=Complement C4 beta chain; Contains: RecName: Full=Complement C4-A alpha chain; Contains: RecName: Full=C4a anaphylatoxin; Contains: RecName: Full=C4b-A; Contains: RecName: Full=C4d-A; Contains: RecName: Full=Complement C4 gamma chain; Flags: Precursor; [Homo sapiens (Human)] - [CO4A_HUMAN]	1.80E+07
Delta-like protein 4; AltName: Full=Drosophila Delta homolog 4; Short=Delta4; Flags: Precursor; [Homo sapiens (Human)] - [DLL4_HUMAN]	1.80E+07
Mesothelin OS=Homo sapiens GN=MSLN PE=1 SV=2	1.78E+07
Dipeptidyl peptidase 4 OS=Homo sapiens GN=DPP4 PE=1 SV=2	1.64E+07
Actin-related protein 2; AltName: Full=Actin-like protein 2; [Homo sapiens (Human)] - [ARP2_HUMAN]	1.56E+07
Uncharacterized protein KIAA0947; [Homo sapiens (Human)] - [K0947_HUMAN]	1.56E+07
Thyroxine-binding globulin OS=Homo sapiens GN=SERPINA7 PE=1 SV=2	1.56E+07
Complement decay-accelerating factor OS=Homo sapiens GN=CD55 PE=1 SV=4	1.49E+07
Aldo-keto reductase family 1 member C3; EC=1.-.-.-; AltName: Full=17-beta-hydroxysteroid dehydrogenase type 5; Short=17-beta-HSD 5; AltName: Full=3-alpha-HSD type II, brain; AltName: Full=3-alpha-hydroxysteroid dehydrogenase type 2; Short=3-alpha-HSD type 2; EC=1.1.1.213; AltName: Full=Chlordecone reductase homolog HAKRb; AltName: Full=Dihydrodiol dehydrogenase 3; Short=DD-3; Short=DD3; AltName: Full=Dihydrodiol dehydrogenase type I; AltName: Full=HA1753; AltName: Full=Indanol dehydrogenase; EC=1.1.1.112; AltName: Full=Prostaglandin F synthase; Short=PGFS; EC=1.1.1.188; AltName: Full=Testosterone 17-beta-dehydrogenase 5; EC=1.1.1.63; EC=1.1.1.64; AltName: Full=Trans-1,2-	1.46E+07

dihydrobenzene-1,2-diol dehydrogenase; EC=1.3.1.20; [Homo sapiens (Human)] - [AK1C3_HUMAN]	
Protein kinase-like protein SgK196; AltName: Full=Sugen kinase 196; [Homo sapiens (Human)] - [SG196_HUMAN]	1.39E+07
Mucin-1 OS=Homo sapiens GN=MUC1 PE=1 SV=3	1.31E+07
Thioredoxin; Short=Trx; AltName: Full=ATL-derived factor; Short=ADF; AltName: Full=Surface-associated sulphydryl protein; Short=SASP; [Homo sapiens (Human)] - [THIO_HUMAN]	1.30E+07
Retinoic acid-induced protein 3 OS=Homo sapiens GN=GPRC5A PE=1 SV=2	1.29E+07
Complement C3 OS=Homo sapiens GN=C3 PE=1 SV=2	1.25E+07
Peptidyl-prolyl cis-trans isomerase A OS=Homo sapiens GN=PPIA PE=1 SV=2	1.19E+07
Biotinidase OS=Homo sapiens GN=BTD PE=1 SV=2	1.19E+07
Xaa-Pro dipeptidase; Short=X-Pro dipeptidase; EC=3.4.13.9; AltName: Full=Imidodipeptidase; AltName: Full=Peptidase D; AltName: Full=Proline dipeptidase; Short=Prolidase; [Homo sapiens (Human)] - [PEPD_HUMAN]	1.18E+07
Galectin-3-binding protein OS=Homo sapiens GN=LGALS3BP PE=1 SV=1	1.14E+07
Puromycin-sensitive aminopeptidase; Short=PSA; EC=3.4.11.14; AltName: Full=Cytosol alanyl aminopeptidase; Short=AAP-S; [Homo sapiens (Human)] - [PSA_HUMAN]	1.13E+07
SH3 domain-binding glutamic acid-rich-like protein 3; AltName: Full=SH3 domain-binding protein 1; Short=SH3BP-1; [Homo sapiens (Human)] - [SH3L3_HUMAN]	1.13E+07
Attractin OS=Homo sapiens GN=ATRN PE=1 SV=2	1.13E+07
Histone H3.3C; [Homo sapiens (Human)] - [H3C_HUMAN]	1.08E+07
Apolipoprotein A-IV OS=Homo sapiens GN=APOA4 PE=1 SV=3	1.04E+07
Gelsolin OS=Homo sapiens GN=GSN PE=1 SV=1	9.95E+06
Plasma protease C1 inhibitor OS=Homo sapiens GN=SERPING1 PE=1 SV=2	9.83E+06
Fatty acid-binding protein, adipocyte OS=Homo sapiens GN=FABP4 PE=1 SV=3	9.73E+06
Ig lambda chain V-V region DEL; [Homo sapiens (Human)] - [LV501_HUMAN]	9.50E+06
Carbonic anhydrase 2 OS=Homo sapiens GN=CA2 PE=1 SV=2	9.50E+06
Superoxide dismutase [Cu-Zn] OS=Homo sapiens GN=SOD1 PE=1 SV=2	9.13E+06
Transcriptional adapter 2-beta; AltName: Full=ADA2-like protein beta;	8.54E+06

Short=ADA2-beta; [Homo sapiens (Human)] - [TAD2B_HUMAN]	
Leukocyte elastase inhibitor OS=Homo sapiens GN=SERPINB1 PE=1 SV=1	8.21E+06
V-set and immunoglobulin domain-containing protein 4; AltName: Full=Protein Z39Ig; Flags: Precursor; [Homo sapiens (Human)] - [VSIG4_HUMAN]	8.17E+06
Protein S100-A11 OS=Homo sapiens GN=S100A11 PE=1 SV=2	7.59E+06
Cystatin-B OS=Homo sapiens GN=CSTB PE=1 SV=2	7.58E+06
Cell adhesion molecule 1; AltName: Full=Immunoglobulin superfamily member 4; Short=IgSF4; AltName: Full=Nectin-like protein 2; Short=NECL-2; AltName: Full=Spermatogenic immunoglobulin superfamily; Short=SgIgSF; AltName: Full=Synaptic cell adhesion molecule; Short=SynCAM; AltName: Full=Tumor suppressor in lung cancer 1; Short=TSLC-1; Flags: Precursor; [Homo sapiens (Human)] - [CADM1_HUMAN]	7.37E+06
Long palate, lung and nasal epithelium carcinoma-associated protein 1; AltName: Full=Von Ebner minor salivary gland protein; Short=VEMSGP; Flags: Precursor; [Homo sapiens (Human)] - [LPLC1_HUMAN]	7.16E+06
Glutathione S-transferase omega-1 OS=Homo sapiens GN=GSTO1 PE=1 SV=2	6.98E+06
Complement C2 OS=Homo sapiens GN=C2 PE=1 SV=2	6.82E+06
Ig delta chain C region; [Homo sapiens (Human)] - [IGHD_HUMAN]	6.39E+06
Dermcidin OS=Homo sapiens GN=DCD PE=1 SV=2	6.20E+06
Peroxiredoxin-5, mitochondrial OS=Homo sapiens GN=PRDX5 PE=1 SV=4	6.12E+06
Vitamin K-dependent protein S; Flags: Precursor; [Homo sapiens (Human)] - [PROS_HUMAN]	6.05E+06
Junctional adhesion molecule A OS=Homo sapiens GN=F11R PE=1 SV=1	5.60E+06
Heme-binding protein 2; AltName: Full=Placental protein 23; Short=PP23; AltName: Full=Protein SOUL; [Homo sapiens (Human)] - [HEBP2_HUMAN]	5.28E+06
Glyoxalase domain-containing protein 4 OS=Homo sapiens GN=GLOD4 PE=1 SV=1	5.28E+06
Kininogen-1 OS=Homo sapiens GN=KNG1 PE=1 SV=2	5.17E+06
Prostaglandin-H2 D-isomerase; EC=5.3.99.2; AltName: Full=Beta-trace protein; AltName: Full=Cerebrin-28; AltName: Full=Glutathione-independent PGD synthase; AltName: Full=Lipocalin-type prostaglandin-D synthase; AltName: Full=Prostaglandin-D2 synthase; Short=PGD2 synthase; Short=PGDS; Short=PGDS2; Flags: Precursor; [Homo sapiens (Human)] - [PTGDS_HUMAN]	4.69E+06

Hornerin OS=Homo sapiens GN=HRNR PE=1 SV=2	4.56E+06
Myoglobin; [Homo sapiens (Human)] - [MYG_HUMAN]	4.44E+06
Putative inactive carboxylesterase 4; AltName: Full=Inactive carboxylesterase 1 pseudogene 1; AltName: Full=Placental carboxylesterase 3; Short=PCE-3; Flags: Precursor; [Homo sapiens (Human)] - [CES1P_HUMAN]	4.34E+06
Neutrophil gelatinase-associated lipocalin; Short=NGAL; AltName: Full=25 kDa alpha-2-microglobulin-related subunit of MMP-9; AltName: Full=Lipocalin-2; AltName: Full=Oncogene 24p3; AltName: Full=p25; Flags: Precursor; [Homo sapiens (Human)] - [NGAL_HUMAN]	4.22E+06
Glutathione peroxidase 3 OS=Homo sapiens GN=GPX3 PE=1 SV=2	4.07E+06
CD59 glycoprotein OS=Homo sapiens GN=CD59 PE=1 SV=1	4.04E+06
Phosphatidylethanolamine-binding protein 1; Short=PEBP-1; AltName: Full=HCNPpp; AltName: Full=Neuropolypeptide h3; AltName: Full=Prostatic-binding protein; AltName: Full=Raf kinase inhibitor protein; Short=RKIP; Contains: RecName: Full=Hippocampal cholinergic neurostimulating peptide; Short=HCNP; [Homo sapiens (Human)] - [PEBP1_HUMAN]	4.01E+06
Phosphoglycerate mutase 1 OS=Homo sapiens GN=PGAM1 PE=1 SV=2	3.87E+06
Leucine-rich alpha-2-glycoprotein OS=Homo sapiens GN=LRG1 PE=1 SV=2	3.79E+06
Thioredoxin domain-containing protein 17; AltName: Full=14 kDa thioredoxin-related protein; Short=TRP14; AltName: Full=Protein 42-9-9; AltName: Full=Thioredoxin-like protein 5; [Homo sapiens (Human)] - [TXD17_HUMAN]	3.64E+06
Serpin B6; AltName: Full=Cytoplasmic antiproteinase; Short=CAP; AltName: Full=Peptidase inhibitor 6; Short=PI-6; AltName: Full=Placental thrombin inhibitor; [Homo sapiens (Human)] - [SPB6_HUMAN]	3.30E+06
Eosinophil lysophospholipase; EC=3.1.1.5; AltName: Full=Charcot-Leyden crystal protein; Short=CLC; AltName: Full=Galectin-10; Short=Gal-10; AltName: Full=Lysolecithin acylhydrolase; [Homo sapiens (Human)] - [LPPL_HUMAN]	3.22E+06
Folate receptor alpha OS=Homo sapiens GN=FOLR1 PE=1 SV=3	3.11E+06
Transmembrane protein 200C; AltName: Full=Transmembrane protein TTMA; AltName: Full=Two transmembrane domain-containing family member A; [Homo sapiens (Human)] - [T200C_HUMAN]	2.87E+06
SH3 domain-binding glutamic acid-rich-like protein OS=Homo sapiens GN=SH3BGRL PE=1 SV=1	2.80E+06
Aldose 1-epimerase OS=Homo sapiens GN=GALM PE=1 SV=1	2.77E+06
Lysozyme C OS=Homo sapiens GN=LYZ PE=1 SV=1	2.75E+06

Matrix metalloproteinase-23; Short=MMP-23; EC=3.4.24.-; AltName: Full=Femalysin; AltName: Full=MIFR-1; AltName: Full=Matrix metalloproteinase-21; Short=MMP-21; AltName: Full=Matrix metalloproteinase-22; Short=MMP-22; Contains: RecName: Full=Matrix metalloproteinase-23, soluble form; Flags: Precursor; [Homo sapiens (Human)] - [MMP23_HUMAN]	2.66E+06
Napsin-A OS=Homo sapiens GN=NAPSA PE=1 SV=1	2.37E+06
Peroxiredoxin-6 OS=Homo sapiens GN=PRDX6 PE=1 SV=3	2.13E+06
Protein S100-P; AltName: Full=Protein S100-E; AltName: Full=S100 calcium-binding protein P; [Homo sapiens (Human)] - [S100P_HUMAN]	2.12E+06
Neutrophil defensin 1 OS=Homo sapiens GN=DEFA1 PE=1 SV=1	1.79E+06
Gamma-glutamylcyclotransferase; EC=2.3.2.4; AltName: Full=Cytochrome c-releasing factor 21; [Homo sapiens (Human)] - [GGCT_HUMAN]	1.29E+06
Sodium-dependent phosphate transport protein 2B; Short=Sodium-phosphate transport protein 2B; AltName: Full=Na(+)-dependent phosphate cotransporter 2B; AltName: Full=NaPi3b; AltName: Full=Sodium/phosphate cotransporter 2B; Short=Na(+)/Pi cotransporter 2B; Short=NaPi-2b; AltName: Full=Solute carrier family 34 member 2; [Homo sapiens (Human)] - [NPT2B_HUMAN]	1.14E+06

Table A.2: *All alveolar proteins identified by 1D PAGE and nano LC MS/MS in mild asthmatic RTLFs. The 217 proteins identified in mild asthmatic subjects investigated, (n=5), alongside the mean of the three most abundant ion peaks of each respective protein identified. Accession numbers included according to entries in UniProtKB/Swiss-Prot.*

Mild asthmatic	
14-3-3 protein beta/alpha; AltName: Full=Protein 1054; AltName: Full=Protein kinase C inhibitor protein 1; Short=KCIP-1; Contains: RecName: Full=14-3-3 protein beta/alpha, N-terminally processed; [Homo sapiens (Human)] - [1433B_HUMAN]	1.82E+07
14-3-3 protein epsilon OS=Homo sapiens GN=YWHAE PE=1 SV=1	1.49E+07
14-3-3 protein zeta/delta OS=Homo sapiens GN=YWHAZ PE=1 SV=1	1.82E+07
28S ribosomal protein S26, mitochondrial; Short=MRP-S26; Short=S26mt; AltName: Full=28S ribosomal protein S13, mitochondrial; Short=MRP-S13; Short=S13mt; Flags: Precursor; [Homo sapiens (Human)] - [RT26_HUMAN]	2.80E+07
Actin, cytoplasmic 1 OS=Homo sapiens GN=ACTB PE=1 SV=1	3.03E+07
ADP-ribosyl cyclase 2 OS=Homo sapiens GN=BST1 PE=1 SV=2	1.38E+06
Afamin OS=Homo sapiens GN=AFM PE=1 SV=1	7.98E+06
Aldo-keto reductase family 1 member C2; EC=1.-.-.-; AltName: Full=3-alpha-HSD3; AltName: Full=Chlordecone reductase homolog HAKRD; AltName: Full=Dihydrodiol dehydrogenase 2; Short=DD-2; Short=DD2; AltName: Full=Dihydrodiol dehydrogenase/bile acid-binding protein; Short=DD/BABP; AltName: Full=Trans-1,2-dihydrobenzene-1,2-diol dehydrogenase; EC=1.3.1.20; AltName: Full=Type III 3-alpha-hydroxysteroid dehydrogenase; EC=1.1.1.213; [Homo sapiens (Human)] - [AK1C2_HUMAN]	2.09E+06
Aldose 1-epimerase OS=Homo sapiens GN=GALM PE=1 SV=1	3.53E+06
Alpha-1-acid glycoprotein 1 OS=Homo sapiens GN=ORM1 PE=1 SV=1	2.89E+08

Alpha-1-acid glycoprotein 2 OS=Homo sapiens GN=ORM2 PE=1 SV=2	2.60E+08
Alpha-1-antichymotrypsin OS=Homo sapiens GN=SERPINA3 PE=1 SV=2	3.86E+07
Alpha-1-antitrypsin OS=Homo sapiens GN=SERPINA1 PE=1 SV=3	7.42E+08
Alpha-1B-glycoprotein OS=Homo sapiens GN=A1BG PE=1 SV=4	3.46E+07
Alpha-2-HS-glycoprotein OS=Homo sapiens GN=AHSG PE=1 SV=1	1.13E+08
Alpha-2-macroglobulin OS=Homo sapiens GN=A2M PE=1 SV=3	6.40E+07
Alpha-N-acetylglucosaminidase OS=Homo sapiens GN=NAGLU PE=1 SV=2	1.61E+06
Angiotensinogen OS=Homo sapiens GN=AGT PE=1 SV=1	1.95E+07
Annexin A2 OS=Homo sapiens GN=ANXA2 PE=1 SV=2	7.67E+06
Annexin A3 OS=Homo sapiens GN=ANXA3 PE=1 SV=3	1.29E+07
Annexin A5 OS=Homo sapiens GN=ANXA5 PE=1 SV=2	1.83E+07
Antithrombin-III OS=Homo sapiens GN=SERPINC1 PE=1 SV=1	7.80E+06
Apolipoprotein A-I OS=Homo sapiens GN=APOA1 PE=1 SV=1	1.55E+08
Apolipoprotein A-II OS=Homo sapiens GN=APOA2 PE=1 SV=1	1.84E+07
Apolipoprotein A-IV OS=Homo sapiens GN=APOA4 PE=1 SV=3	7.77E+06
Aspartate aminotransferase, cytoplasmic OS=Homo sapiens GN=GOT1 PE=1 SV=3	3.43E+06
ATP-binding cassette sub-family C member 8; AltName: Full=Sulfonylurea receptor 1; [Homo sapiens (Human)] - [ABCC8_HUMAN]	2.80E+07
ATP-sensitive inward rectifier potassium channel 10; AltName: Full=ATP-dependent inwardly rectifying potassium channel Kir4.1; AltName: Full=Inward rectifier K(+) channel Kir1.2; AltName: Full=Potassium channel, inwardly rectifying subfamily J member 10; [Homo sapiens (Human)] - [IRK10_HUMAN]	2.14E+06
Attractin OS=Homo sapiens GN=ATRN PE=1 SV=2	9.79E+06
Beta-2-microglobulin OS=Homo sapiens GN=B2M PE=1 SV=1	6.95E+07
Biotinidase OS=Homo sapiens GN=BTD PE=1 SV=2	6.35E+06
BTB/POZ domain-containing protein 8; [Homo sapiens (Human)] - [BTBD8_HUMAN]	4.21E+05
C-type natriuretic peptide; Contains: RecName: Full=CNP-22; Contains: RecName: Full=CNP-29; Contains: RecName: Full=CNP-53; Flags: Precursor; [Homo sapiens (Human)] - [ANFC_HUMAN]	2.75E+08
Calcyphosin OS=Homo sapiens GN=CAPS PE=1 SV=1	2.67E+06
Calmodulin OS=Homo sapiens GN=CALM1 PE=1 SV=2	1.93E+07
Carbonic anhydrase 1 OS=Homo sapiens GN=CA1 PE=1 SV=2	2.40E+07
Carbonic anhydrase 2 OS=Homo sapiens GN=CA2 PE=1 SV=2	6.78E+06
CASP8-associated protein 2; AltName: Full=FLICE-associated huge protein; [Homo sapiens (Human)] - [C8AP2_HUMAN]	2.44E+07
Caspase recruitment domain-containing protein 6; [Homo sapiens (Human)] - [CARD6_HUMAN]	1.40E+08
Cathepsin D OS=Homo sapiens GN=CTSD PE=1 SV=1	4.60E+08
Caveolin-1; [Homo sapiens (Human)] - [CAV1_HUMAN]	2.23E+06
CD151 antigen; AltName: Full=GP27; AltName: Full=Membrane glycoprotein SFA-1; AltName: Full=Platelet-endothelial tetraspan antigen 3; Short=PETA-3; AltName: Full=Tetraspanin-24; Short=Tspan-24; AltName: CD_antigen=CD151; [Homo sapiens (Human)] - [CD151_HUMAN]	1.17E+06
CD166 antigen OS=Homo sapiens GN=ALCAM PE=1 SV=2	3.45E+06
CD44 antigen OS=Homo sapiens GN=CD44 PE=1 SV=3	5.58E+07
CD63 antigen; AltName: Full=Granulophysin; AltName: Full=Lysosomal-associated membrane protein 3; Short=LAMP-3; AltName: Full=Melanoma-associated antigen ME491; AltName: Full=OMA81H; AltName: Full=Ocular melanoma-associated antigen; AltName: Full=Tetraspanin-30; Short=Tspan-30; AltName: CD_antigen=CD63; [Homo sapiens (Human)] - [CD63_HUMAN]	3.91E+06

CD9 antigen OS=Homo sapiens GN=CD9 PE=1 SV=4	1.45E+07
Cell adhesion molecule 1 OS=Homo sapiens GN=CADM1 PE=1 SV=2	3.41E+06
Cell adhesion molecule 2; AltName: Full=Immunoglobulin superfamily member 4D; Short=IgSF4D; AltName: Full=Nectin-like protein 3; Short=NECL-3; Flags: Precursor; [Homo sapiens (Human)] - [CADM2_HUMAN]	4.06E+06
Ceruloplasmin OS=Homo sapiens GN=CP PE=1 SV=1	1.23E+08
cGMP-specific 3',5'-cyclic phosphodiesterase; EC=3.1.4.35; AltName: Full=cGMP-binding cGMP-specific phosphodiesterase; Short=CGB-PDE; [Homo sapiens (Human)] - [PDE5A_HUMAN]	5.00E+07
Choline transporter-like protein 2 OS=Homo sapiens GN=SLC44A2 PE=1 SV=3	1.09E+06
Choline transporter-like protein 4; AltName: Full=Solute carrier family 44 member 4; [Homo sapiens (Human)] - [CTL4_HUMAN]	9.70E+05
Coactosin-like protein OS=Homo sapiens GN=COTL1 PE=1 SV=3	1.15E+07
Coiled-coil and C2 domain-containing protein 1B; [Homo sapiens (Human)] - [C2D1B_HUMAN]	2.00E+07
Complement C2 OS=Homo sapiens GN=C2 PE=1 SV=2	6.38E+06
Complement C3 OS=Homo sapiens GN=C3 PE=1 SV=2	2.94E+07
Complement decay-accelerating factor OS=Homo sapiens GN=CD55 PE=1 SV=4	1.63E+07
COP9 signalosome complex subunit 1; Short=SGN1; Short=Signalosome subunit 1; AltName: Full=G protein pathway suppressor 1; Short=GPS-1; AltName: Full=JAB1-containing signalosome subunit 1; AltName: Full=Protein MFH; [Homo sapiens (Human)] - [CSN1_HUMAN]	7.47E+08
Corticosteroid-binding globulin OS=Homo sapiens GN=SERPINA6 PE=1 SV=1	1.39E+07
Cystatin-B OS=Homo sapiens GN=CSTB PE=1 SV=2	6.67E+06
Deleted in malignant brain tumors 1 protein OS=Homo sapiens GN=DMBT1 PE=1 SV=2	3.56E+07
Delta-like protein 4; AltName: Full=Drosophila Delta homolog 4; Short=Delta4; Flags: Precursor; [Homo sapiens (Human)] - [DLL4_HUMAN]	1.73E+07
Dermcidin OS=Homo sapiens GN=DCD PE=1 SV=2	3.67E+06
Desmoglein-1 OS=Homo sapiens GN=DSG1 PE=1 SV=2	6.95E+06
Desmoplakin OS=Homo sapiens GN=DSP PE=1 SV=3	2.67E+07
Dipeptidyl peptidase 4 OS=Homo sapiens GN=DPP4 PE=1 SV=2	1.11E+07
DNA mismatch repair protein Msh3; Short=hMSH3; AltName: Full=Divergent upstream protein; Short=DUP; AltName: Full=Mismatch repair protein 1; Short=MRP1; [Homo sapiens (Human)] - [MSH3_HUMAN]	5.91E+06
Dynein heavy chain 10, axonemal; AltName: Full=Axonemal beta dynein heavy chain 10; AltName: Full=Ciliary dynein heavy chain 10; [Homo sapiens (Human)] - [DYH10_HUMAN]	1.80E+08
Ecto-ADP-ribosyltransferase 4; EC=2.4.2.31; AltName: Full=Dombrock blood group carrier molecule; AltName: Full=Mono(ADP-ribosyl)transferase 4; AltName: Full=NAD(P)(+)--arginine ADP-ribosyltransferase 4; AltName: CD_antigen=CD297; Flags: Precursor; [Homo sapiens (Human)] - [NAR4_HUMAN]	5.37E+07
Epididymal secretory protein E1 OS=Homo sapiens GN=NPC2 PE=1 SV=1	1.26E+08
Erythrocyte band 7 integral membrane protein OS=Homo sapiens GN=STOM PE=1 SV=3	1.60E+08
Ezrin OS=Homo sapiens GN=EZR PE=1 SV=4	3.09E+06
FAS-associated factor 1; Short=hFAF1; AltName: Full=UBX domain-containing protein 12; AltName: Full=UBX domain-containing protein 3A; [Homo sapiens (Human)] - [FAF1_HUMAN]	1.03E+08
Fatty acid-binding protein, adipocyte; AltName: Full=Adipocyte lipid-binding	1.31E+07

protein; Short=ALBP; AltName: Full=Adipocyte-type fatty acid-binding protein; Short=A-FABP; Short=AFABP; AltName: Full=Fatty acid-binding protein 4; [Homo sapiens (Human)] - [FABP4_HUMAN]	
Ferritin heavy chain; Short=Ferritin H subunit; EC=1.16.3.1; AltName: Full=Cell proliferation-inducing gene 15 protein; [Homo sapiens (Human)] - [FRIH_HUMAN]	2.76E+06
Fibrocystin-L; AltName: Full=Polycystic kidney and hepatic disease 1-like protein 1; Short=PKHD1-like protein 1; Flags: Precursor; [Homo sapiens (Human)] - [PKHL1_HUMAN]	2.62E+06
Folate receptor alpha OS=Homo sapiens GN=FOLR1 PE=1 SV=3	2.79E+06
Galectin-3-binding protein OS=Homo sapiens GN=LGALS3BP PE=1 SV=1	3.89E+06
Ganglioside GM2 activator; AltName: Full=Cerebroside sulfate activator protein; AltName: Full=GM2-AP; AltName: Full=Shingolipid activator protein 3; Short=SAP-3; Contains: RecName: Full=Ganglioside GM2 activator isoform short; Flags: Precursor; [Homo sapiens (Human)] - [SAP3_HUMAN]	3.20E+06
Gastricsin OS=Homo sapiens GN=PGC PE=1 SV=1	1.71E+07
Glutathione S-transferase A1 OS=Homo sapiens GN=GSTA1 PE=1 SV=3	1.83E+07
Glutathione S-transferase P OS=Homo sapiens GN=GSTP1 PE=1 SV=2	9.57E+06
Haptoglobin OS=Homo sapiens GN=HP PE=1 SV=1	1.13E+09
HEAT repeat-containing protein 1; AltName: Full=Protein BAP28; [Homo sapiens (Human)] - [HEAT1_HUMAN]	9.00E+06
Heme-binding protein 2; AltName: Full=Placental protein 23; Short=PP23; AltName: Full=Protein SOUL; [Homo sapiens (Human)] - [HEBP2_HUMAN]	2.71E+06
Hemoglobin subunit alpha OS=Homo sapiens GN=HBA1 PE=1 SV=2	6.04E+08
Hemoglobin subunit beta OS=Homo sapiens GN=HBB PE=1 SV=2	4.82E+08
Hemoglobin subunit delta OS=Homo sapiens GN=HBD PE=1 SV=2	3.78E+08
Hemopexin OS=Homo sapiens GN=HPX PE=1 SV=2	4.44E+08
Histone-lysine N-methyltransferase MLL3; EC=2.1.1.43; AltName: Full=Homologous to ALR protein; AltName: Full=Lysine N-methyltransferase 2C; Short=KMT2C; AltName: Full=Myeloid/lymphoid or mixed-lineage leukemia protein 3; [Homo sapiens (Human)] - [MLL3_HUMAN]	8.05E+07
HLA class II histocompatibility antigen, DP beta 1 chain; AltName: Full=HLA class II histocompatibility antigen, DP(W4) beta chain; AltName: Full=MHC class II antigen DPB1; Flags: Precursor; [Homo sapiens (Human)] - [DPB1_HUMAN]	1.03E+07
HLA class II histocompatibility antigen, DR alpha chain OS=Homo sapiens GN=HLA-DRA PE=1 SV=1	3.67E+06
HLA class II histocompatibility antigen, DRB1-15 beta chain OS=Homo sapiens GN=HLA-DRB1 PE=1 SV=2	9.93E+06
HLA class II histocompatibility antigen, DRB1-4 beta chain; AltName: Full=MHC class II antigen DRB1*4; Short=DR-4; Short=DR4; Flags: Precursor; [Homo sapiens (Human)] - [2B14_HUMAN]	4.70E+06
Homeobox protein Nkx-3.2; AltName: Full=Bagpipe homeobox protein homolog 1; AltName: Full=Homeobox protein NK-3 homolog B; [Homo sapiens (Human)] - [NKX32_HUMAN]	5.43E+06
Ig alpha-1 chain C region OS=Homo sapiens GN=IGHA1 PE=1 SV=2	1.24E+09
Ig alpha-2 chain C region OS=Homo sapiens GN=IGHA2 PE=1 SV=3	8.46E+08
Ig delta chain C region; [Homo sapiens (Human)] - [IGHD_HUMAN]	8.04E+06
Ig gamma-1 chain C region OS=Homo sapiens GN=IGHG1 PE=1 SV=1	3.04E+09
Ig gamma-2 chain C region OS=Homo sapiens GN=IGHG2 PE=1 SV=2	2.20E+09
Ig gamma-3 chain C region OS=Homo sapiens GN=IGHG3 PE=1 SV=2	2.52E+09
Ig heavy chain V-I region HG3 OS=Homo sapiens PE=4 SV=1	5.87E+07
Ig heavy chain V-I region V35; Flags: Precursor; [Homo sapiens (Human)] -	1.96E+07

[HV103_HUMAN]	
Ig heavy chain V-II region ARH-77 OS=Homo sapiens PE=4 SV=1	1.73E+08
Ig heavy chain V-II region NEWM; [Homo sapiens (Human)] - [HV207_HUMAN]	6.76E+07
Ig heavy chain V-II region OU; [Homo sapiens (Human)] - [HV201_HUMAN]	2.46E+07
Ig heavy chain V-III region BUR; [Homo sapiens (Human)] - [HV312_HUMAN]	6.85E+08
Ig heavy chain V-III region BUT; [Homo sapiens (Human)] - [HV306_HUMAN]	5.55E+08
Ig heavy chain V-III region CAM OS=Homo sapiens PE=1 SV=1	5.71E+08
Ig heavy chain V-III region GAL OS=Homo sapiens PE=1 SV=1	4.86E+08
Ig heavy chain V-III region GAR; [Homo sapiens (Human)] - [HV322_HUMAN]	7.31E+07
Ig heavy chain V-III region HIL; [Homo sapiens (Human)] - [HV310_HUMAN]	6.93E+08
Ig heavy chain V-III region TUR OS=Homo sapiens PE=1 SV=1	4.62E+08
Ig heavy chain V-III region VH26 OS=Homo sapiens PE=1 SV=1	5.29E+08
Ig kappa chain C region OS=Homo sapiens GN=IGKC PE=1 SV=1	1.00E+09
Ig kappa chain V-I region DEE; [Homo sapiens (Human)] - [KV105_HUMAN]	3.48E+08
Ig kappa chain V-I region EU OS=Homo sapiens PE=1 SV=1	1.95E+08
Ig kappa chain V-I region Kue; [Homo sapiens (Human)] - [KV112_HUMAN]	1.92E+08
Ig kappa chain V-I region Roy; [Homo sapiens (Human)] - [KV116_HUMAN]	1.45E+08
Ig kappa chain V-I region Wes; [Homo sapiens (Human)] - [KV119_HUMAN]	2.28E+08
Ig kappa chain V-II region TEW OS=Homo sapiens PE=1 SV=1	1.29E+08
Ig kappa chain V-III region NG9 (Fragment) OS=Homo sapiens PE=1 SV=1	1.00E+08
Ig kappa chain V-III region POM OS=Homo sapiens PE=1 SV=1	1.01E+08
Ig kappa chain V-III region SIE OS=Homo sapiens PE=1 SV=1	1.59E+08
Ig kappa chain V-III region VG; Flags: Precursor; Fragment; [Homo sapiens (Human)] - [KV309_HUMAN]	1.06E+08
Ig kappa chain V-IV region JI OS=Homo sapiens PE=4 SV=1	6.13E+07
Ig lambda chain V region 4A; Flags: Precursor; [Homo sapiens (Human)] - [LV001_HUMAN]	6.04E+07
Ig lambda chain V-I region HA OS=Homo sapiens PE=1 SV=1	3.45E+07
Ig lambda chain V-I region NIG-64 OS=Homo sapiens PE=1 SV=1	2.39E+07
Ig lambda chain V-II region NEI; [Homo sapiens (Human)] - [LV202_HUMAN]	2.39E+07
Ig lambda chain V-III region LOI OS=Homo sapiens PE=1 SV=1	3.54E+07
Ig lambda chain V-III region SH; [Homo sapiens (Human)] - [LV301_HUMAN]	1.90E+07
Ig lambda chain V-III region SH; [Homo sapiens (Human)] - [LV301_HUMAN]	3.54E+07
Ig lambda chain V-IV region Bau; [Homo sapiens (Human)] - [LV401_HUMAN]	4.15E+07
Ig lambda chain V-IV region Hil; [Homo sapiens (Human)] - [LV403_HUMAN]	3.39E+07
Ig lambda-2 chain C regions OS=Homo sapiens GN=IGLC2 PE=1 SV=1	7.00E+08
Ig mu chain C region OS=Homo sapiens GN=IGHM PE=1 SV=3	7.42E+07
Immunoglobulin J chain OS=Homo sapiens GN=IGJ PE=1 SV=4	8.35E+07
Immunoglobulin lambda-like polypeptide 5 OS=Homo sapiens GN=IGLL5 PE=2 SV=2	4.17E+08
Intercellular adhesion molecule 1 OS=Homo sapiens GN=ICAM1 PE=1 SV=2	1.77E+07
Junctional adhesion molecule A OS=Homo sapiens GN=F11R PE=1 SV=1	9.69E+06
Lactotransferrin; Short=Lactoferrin; EC=3.4.21.-; AltName: Full=Talalactoferrin; Contains: RecName: Full=Kaliocin-1; Contains: RecName: Full=Lactoferroxin-A; Contains: RecName: Full=Lactoferroxin-B; Contains: RecName: Full=Lactoferroxin-C; Flags: Precursor; [Homo sapiens (Human)] - [TRFL_HUMAN]	7.34E+08
Latexin; AltName: Full=Endogenous carboxypeptidase inhibitor; Short=ECI; AltName: Full=Protein MUM; AltName: Full=Tissue carboxypeptidase inhibitor; Short=TCI; [Homo sapiens (Human)] - [LXN_HUMAN]	2.49E+08
Lethal(3)malignant brain tumor-like protein 4; Short=H-l(3)mbt-like protein 4;	9.09E+06

Short=L(3)mbt-like protein 4; [Homo sapiens (Human)] - [LMBL4_HUMAN]	
Leucine-rich alpha-2-glycoprotein OS=Homo sapiens GN=LRG1 PE=1 SV=2	2.36E+07
Leukocyte elastase inhibitor OS=Homo sapiens GN=SERPINB1 PE=1 SV=1	9.09E+06
Liprin-beta-2; AltName: Full=Protein tyrosine phosphatase receptor type f polypeptide-interacting protein-binding protein 2; Short=PTPRF-interacting protein-binding protein 2; [Homo sapiens (Human)] - [LIPB2_HUMAN]	8.52E+06
Lysozyme C; EC=3.2.1.17; AltName: Full=1,4-beta-N-acetylmuramidase C; Flags: Precursor; [Homo sapiens (Human)] - [LYSC_HUMAN]	4.75E+05
Mesothelin OS=Homo sapiens GN=MSLN PE=1 SV=2	1.74E+07
Mucin-1 OS=Homo sapiens GN=MUC1 PE=1 SV=3	8.52E+06
NADH dehydrogenase [ubiquinone] 1 beta subcomplex subunit 2, mitochondrial; AltName: Full=Complex I-AGGG; Short=CI-AGGG; AltName: Full=NADH-ubiquinone oxidoreductase AGGG subunit; Flags: Precursor; [Homo sapiens (Human)] - [NDUB2_HUMAN]	1.75E+07
Napsin-A; EC=3.4.23.-; AltName: Full=Aspartyl protease 4; Short=ASP4; Short=Asp 4; AltName: Full=Napsin-1; AltName: Full=TA01/TA02; Flags: Precursor; [Homo sapiens (Human)] - [NAPSA_HUMAN]	1.75E+07
Neuron navigator 1; AltName: Full=Pore membrane and/or filament-interacting-like protein 3; AltName: Full=Steerin-1; AltName: Full=Unc-53 homolog 1; Short=unc53H1; [Homo sapiens (Human)] - [NAV1_HUMAN]	9.10E+06
Neutrophil defensin 1; AltName: Full=Defensin, alpha 1; AltName: Full=HNP-1; Short=HP-1; Short=HP1; Contains: RecName: Full=HP 1-56; Contains: RecName: Full=Neutrophil defensin 2; AltName: Full=HNP-2; Short=HP-2; Short=HP2; Flags: Precursor; [Homo sapiens (Human)] - [DEF1_HUMAN]	3.60E+06
Olfactory receptor 4K5 OS=Homo sapiens GN=OR4K5 PE=2 SV=1	3.84E+08
Pancreatic alpha-amylase; Short=PA; EC=3.2.1.1; AltName: Full=1,4-alpha-D-glucan glucanohydrolase; Flags: Precursor; [Homo sapiens (Human)] - [AMYP_HUMAN]	7.36E+06
Peroxiredoxin-5, mitochondrial OS=Homo sapiens GN=PRDX5 PE=1 SV=4	3.31E+06
Peroxiredoxin-6 OS=Homo sapiens GN=PRDX6 PE=1 SV=3	4.96E+06
Phosphatidylethanolamine-binding protein 1; Short=PEBP-1; AltName: Full=HCNPpp; AltName: Full=Neuropolypeptide h3; AltName: Full=Prostatic-binding protein; AltName: Full=Raf kinase inhibitor protein; Short=RKIP; Contains: RecName: Full=Hippocampal cholinergic neurostimulating peptide; Short=HCNP; [Homo sapiens (Human)] - [PEBP1_HUMAN]	8.97E+05
Phosphoglycerate mutase 1 OS=Homo sapiens GN=PGAM1 PE=1 SV=2	1.88E+06
Plasma protease C1 inhibitor OS=Homo sapiens GN=SERPING1 PE=1 SV=2	6.56E+06
Polymeric immunoglobulin receptor OS=Homo sapiens GN=PIGR PE=1 SV=4	3.32E+08
Pro-cathepsin H OS=Homo sapiens GN=CTSH PE=1 SV=4	2.12E+07
Proactivator polypeptide OS=Homo sapiens GN=PSAP PE=1 SV=2	4.34E+06
Probable G-protein coupled receptor 116; Flags: Precursor; [Homo sapiens (Human)] - [GP116_HUMAN]	2.77E+07
Prostasin; EC=3.4.21.-; AltName: Full=Serine protease 8; Contains: RecName: Full=Prostasin light chain; Contains: RecName: Full=Prostasin heavy chain; Flags: Precursor; [Homo sapiens (Human)] - [PRSS8_HUMAN]	2.35E+06
Proteasome subunit alpha type-1; EC=3.4.25.1; AltName: Full=30 kDa prosomal protein; Short=PROS-30; AltName: Full=Macropain subunit C2; AltName: Full=Multicatalytic endopeptidase complex subunit C2; AltName: Full=Proteasome component C2; AltName: Full=Proteasome nu chain; [Homo sapiens (Human)] - [PSA1_HUMAN]	3.32E+07
Protein AMBP OS=Homo sapiens GN=AMBP PE=1 SV=1	2.31E+06

Protein DJ-1 OS=Homo sapiens GN=PARK7 PE=1 SV=2	1.75E+07
Protein S100-A11 OS=Homo sapiens GN=S100A11 PE=1 SV=2	4.68E+06
Protein S100-A6 OS=Homo sapiens GN=S100A6 PE=1 SV=1	8.46E+07
Protein Shroom3; AltName: Full=Shroom-related protein; Short=hShrmL; [Homo sapiens (Human)] - [SHRM3_HUMAN]	7.90E+07
Pulmonary surfactant-associated protein A2 OS=Homo sapiens GN=SFTPA2 PE=1 SV=1	5.87E+07
Pulmonary surfactant-associated protein B OS=Homo sapiens GN=SFTPB PE=1 SV=3	2.53E+07
Pulmonary surfactant-associated protein D OS=Homo sapiens GN=SFTPD PE=1 SV=3	2.06E+07
Puromycin-sensitive aminopeptidase; Short=PSA; EC=3.4.11.14; AltName: Full=Cytosol alanyl aminopeptidase; Short=AAP-S; [Homo sapiens (Human)] - [PSA_HUMAN]	1.43E+07
Putative inactive carboxylesterase 4; AltName: Full=Inactive carboxylesterase 1 pseudogene 1; AltName: Full=Placental carboxylesterase 3; Short=PCE-3; Flags: Precursor; [Homo sapiens (Human)] - [CES1P_HUMAN]	3.62E+06
Putative uncharacterized protein HUG-1; AltName: Full=HOX11 upstream gene 1 protein; [Homo sapiens (Human)] - [HUG1_HUMAN]	3.05E+06
Putative V-set and immunoglobulin domain-containing protein 6 OS=Homo sapiens GN=VSIG6 PE=5 SV=2	7.72E+07
Retinoic acid-induced protein 3 OS=Homo sapiens GN=GPRC5A PE=1 SV=2	3.24E+07
Retinol-binding protein 4; AltName: Full=Plasma retinol-binding protein; Short=PRBP; Short=RBP; Contains: RecName: Full=Plasma retinol-binding protein(1-182); Contains: RecName: Full=Plasma retinol-binding protein(1-181); Contains: RecName: Full=Plasma retinol-binding protein(1-179); Contains: RecName: Full=Plasma retinol-binding protein(1-176); Flags: Precursor; [Homo sapiens (Human)] - [RET4_HUMAN]	3.11E+07
Rho GDP-dissociation inhibitor 2 OS=Homo sapiens GN=ARHGDIB PE=1 SV=3	6.99E+06
Rho guanine nucleotide exchange factor 17; AltName: Full=164 kDa Rho-specific guanine-nucleotide exchange factor; Short=p164-RhoGEF; Short=p164RhoGEF; AltName: Full=Tumor endothelial marker 4; [Homo sapiens (Human)] - [ARHGH_HUMAN]	1.03E+08
Ribonuclease P protein subunit p40; Short=RNaseP protein p40; EC=3.1.26.5; AltName: Full=RNase P subunit 1; [Homo sapiens (Human)] - [RPP40_HUMAN]	9.04E+07
RNA-binding protein MEX3A; AltName: Full=RING finger and KH domain-containing protein 4; [Homo sapiens (Human)] - [MEX3A_HUMAN]	5.43E+08
Scavenger receptor cysteine-rich type 1 protein M130 OS=Homo sapiens GN=CD163 PE=1 SV=2	1.28E+07
Selenium-binding protein 1 OS=Homo sapiens GN=SELENBP1 PE=1 SV=2	2.55E+07
Serine/threonine-protein phosphatase 6 regulatory ankyrin repeat subunit A; Short=PP6-ARS-A; Short=Serine/threonine-protein phosphatase 6 regulatory subunit ARS-A; AltName: Full=Ankyrin repeat domain-containing protein 28; AltName: Full=Phosphatase interactor targeting protein hnRNP K; Short=PITK; [Homo sapiens (Human)] - [ANR28_HUMAN]	3.40E+06
Serotransferrin OS=Homo sapiens GN=TF PE=1 SV=3	4.55E+09
Serpin B3 OS=Homo sapiens GN=SERPINB3 PE=1 SV=2	7.74E+06
Serpin B6; AltName: Full=Cytoplasmic antiproteinase; Short=CAP; AltName: Full=Peptidase inhibitor 6; Short=PI-6; AltName: Full=Placental thrombin inhibitor; [Homo sapiens (Human)] - [SPB6_HUMAN]	1.37E+06
Serum albumin OS=Homo sapiens GN=ALB PE=1 SV=2	3.32E+09

Sodium-dependent phosphate transport protein 2B; Short=Sodium-phosphate transport protein 2B; AltName: Full=Na(+)-dependent phosphate cotransporter 2B; AltName: Full=NaPi3b; AltName: Full=Sodium/phosphate cotransporter 2B; Short=Na(+)/Pi cotransporter 2B; Short=NaPi-2b; AltName: Full=Solute carrier family 34 member 2; [Homo sapiens (Human)] - [NPT2B_HUMAN]	2.12E+06
Spectrin beta chain, brain 2; AltName: Full=Beta-III spectrin; AltName: Full=Spectrin, non-erythroid beta chain 2; [Homo sapiens (Human)] - [SPTN2_HUMAN]	2.24E+07
Superoxide dismutase [Cu-Zn] OS=Homo sapiens GN=SOD1 PE=1 SV=2	6.94E+06
Sushi domain-containing protein 2 OS=Homo sapiens GN=SUSD2 PE=1 SV=1	9.38E+06
Tetraspanin-1; Short=Tspan-1; AltName: Full=Tetraspan NET-1; AltName: Full=Tetraspanin TM4-C; [Homo sapiens (Human)] - [TSN1_HUMAN]	2.59E+06
Thioredoxin OS=Homo sapiens GN=TXN PE=1 SV=3	1.15E+07
Thyroxine-binding globulin OS=Homo sapiens GN=SERPINA7 PE=1 SV=2	8.96E+06
Transaldolase OS=Homo sapiens GN=TALDO1 PE=1 SV=2	2.30E+07
Transcriptional adapter 2-beta; AltName: Full=ADA2-like protein beta; Short=ADA2-beta; [Homo sapiens (Human)] - [TAD2B_HUMAN]	3.36E+06
Transmembrane protease serine 13; EC=3.4.21.-; AltName: Full=Membrane-type mosaic serine protease; Short=Mosaic serine protease; [Homo sapiens (Human)] - [TMPSD_HUMAN]	2.98E+07
Transmembrane protein 198; [Homo sapiens (Human)] - [TM198_HUMAN]	1.29E+07
Transmembrane protein 200C; AltName: Full=Transmembrane protein TTMA; AltName: Full=Two transmembrane domain-containing family member A; [Homo sapiens (Human)] - [T200C_HUMAN]	2.80E+06
Triosephosphate isomerase OS=Homo sapiens GN=TPI1 PE=1 SV=3	2.05E+07
Trypsin-3; EC=3.4.21.4; AltName: Full=Brain trypsinogen; AltName: Full=Mesotrypsinogen; AltName: Full=Serine protease 3; AltName: Full=Serine protease 4; AltName: Full=Trypsin III; AltName: Full=Trypsin IV; Flags: Precursor; [Homo sapiens (Human)] - [TRY3_HUMAN]	2.49E+06
Uncharacterized protein C19orf68; [Homo sapiens (Human)] - [CS068_HUMAN]	1.26E+07
Uncharacterized protein C3orf38; [Homo sapiens (Human)] - [CC038_HUMAN]	2.18E+09
UPF0556 protein C19orf10; AltName: Full=Interleukin-25; Short=IL-25; AltName: Full=Stromal cell-derived growth factor SF20; Flags: Precursor; [Homo sapiens (Human)] - [CS010_HUMAN]	3.69E+06
Uteroglobin OS=Homo sapiens GN=SCGB1A1 PE=1 SV=1	4.14E+08
V-set and immunoglobulin domain-containing protein 4; AltName: Full=Protein Z39Ig; Flags: Precursor; [Homo sapiens (Human)] - [VSIG4_HUMAN]	1.67E+06
Vitamin D-binding protein OS=Homo sapiens GN=GC PE=1 SV=1	2.16E+08
Vitamin D-binding protein OS=Homo sapiens GN=GC PE=1 SV=1	2.16E+08
Voltage-gated potassium channel subunit beta-1; AltName: Full=K(+) channel subunit beta-1; AltName: Full=Kv-beta-1; [Homo sapiens (Human)] - [KCAB1_HUMAN]	9.03E+07
Xin actin-binding repeat-containing protein 2; AltName: Full=Beta-xin; AltName: Full=Cardiomyopathy-associated protein 3; AltName: Full=Xeplin; [Homo sapiens (Human)] - [XIRP2_HUMAN]	1.92E+08
Zinc finger protein 784; [Homo sapiens (Human)] - [ZN784_HUMAN]	9.62E+05
Zinc-alpha-2-glycoprotein OS=Homo sapiens GN=AZGP1 PE=1 SV=2	1.08E+08

Table A.3: *Alveolar proteins identified by 1D PAGE and nano LC MS/MS in healthy and mild asthmatic RTLFs. The 140 proteins common to both healthy and mild asthmatic subjects investigated, n=5 for both subject groups, alongside the mean of the three most abundant ion peaks of each respective protein identified,.Accession numbers included are according to entries in UniProtKB/Swiss-Prot.*

Healthy Control		Mild asthmatic	
14-3-3 protein beta/alpha OS=Homo sapiens GN=YWHAB PE=1 SV=3	1.07E+08	14-3-3 protein beta/alpha; AltName: Full=Protein 1054; AltName: Full=Protein kinase C inhibitor protein 1; Short=KCIP-1; Contains: RecName: Full=14-3-3 protein beta/alpha, N-terminally processed; [Homo sapiens (Human)] - [1433B_HUMAN]	1.82E+07
14-3-3 protein epsilon OS=Homo sapiens GN=YWHAE PE=1 SV=1	9.02E+07	14-3-3 protein epsilon OS=Homo sapiens GN=YWHAE PE=1 SV=1	1.49E+07
14-3-3 protein zeta/delta OS=Homo sapiens GN=YWHAZ PE=1 SV=1	1.07E+08	14-3-3 protein zeta/delta OS=Homo sapiens GN=YWHAZ PE=1 SV=1	1.82E+07
28S ribosomal protein S26, mitochondrial; Short=MRP-S26; Short=S26mt; AltName: Full=28S ribosomal protein S13, mitochondrial; Short=MRP-S13; Short=S13mt; Flags: Precursor; [Homo sapiens (Human)] - [RT26_HUMAN]	4.89E+07	28S ribosomal protein S26, mitochondrial; Short=MRP-S26; Short=S26mt; AltName: Full=28S ribosomal protein S13, mitochondrial; Short=MRP-S13; Short=S13mt; Flags: Precursor; [Homo sapiens (Human)] - [RT26_HUMAN]	2.80E+07
Actin, cytoplasmic 1 OS=Homo sapiens GN=ACTB PE=1 SV=1	5.55E+07	Actin, cytoplasmic 1 OS=Homo sapiens GN=ACTB PE=1 SV=1	3.03E+07
Afamin OS=Homo sapiens GN=AFM PE=1 SV=1	2.55E+07	Afamin OS=Homo sapiens GN=AFM PE=1 SV=1	7.98E+06
Aldose 1-epimerase OS=Homo sapiens GN=GALM PE=1 SV=1	2.77E+06	Aldose 1-epimerase OS=Homo sapiens GN=GALM PE=1 SV=1	3.53E+06
Alpha-1-acid glycoprotein 1 OS=Homo sapiens GN=ORM1 PE=1 SV=1	2.04E+08	Alpha-1-acid glycoprotein 1 OS=Homo sapiens GN=ORM1 PE=1 SV=1	2.89E+08
Alpha-1-acid glycoprotein 2 OS=Homo sapiens GN=ORM2 PE=1 SV=2	1.81E+08	Alpha-1-acid glycoprotein 2 OS=Homo sapiens GN=ORM2 PE=1 SV=2	2.60E+08
Alpha-1-antichymotrypsin OS=Homo sapiens GN=SERPINA3 PE=1 SV=2	1.49E+08	Alpha-1-antichymotrypsin OS=Homo sapiens GN=SERPINA3 PE=1 SV=2	3.86E+07
Alpha-1-antitrypsin OS=Homo sapiens GN=SERPINA1 PE=1 SV=3	2.69E+09	Alpha-1-antitrypsin OS=Homo sapiens GN=SERPINA1 PE=1 SV=3	7.42E+08
Alpha-1B-glycoprotein OS=Homo sapiens GN=A1BG PE=1 SV=4	1.36E+08	Alpha-1B-glycoprotein OS=Homo sapiens GN=A1BG PE=1 SV=4	3.46E+07
Alpha-2-HS-glycoprotein OS=Homo sapiens GN=AHSG PE=1 SV=1	7.52E+07	Alpha-2-HS-glycoprotein OS=Homo sapiens GN=AHSG PE=1 SV=1	1.13E+08
Alpha-2-macroglobulin OS=Homo sapiens GN=A2M PE=1 SV=3	6.75E+07	Alpha-2-macroglobulin OS=Homo sapiens GN=A2M PE=1 SV=3	6.40E+07

Angiotensinogen OS=Homo sapiens GN=AGT PE=1 SV=1	9.61E+07	Angiotensinogen OS=Homo sapiens GN=AGT PE=1 SV=1	1.95E+07
Annexin A5 OS=Homo sapiens GN=ANXA5 PE=1 SV=2	6.60E+07	Annexin A5 OS=Homo sapiens GN=ANXA5 PE=1 SV=2	1.83E+07
Antithrombin-III OS=Homo sapiens GN=SERPINC1 PE=1 SV=1	2.92E+07	Antithrombin-III OS=Homo sapiens GN=SERPINC1 PE=1 SV=1	7.80E+06
Apolipoprotein A-I OS=Homo sapiens GN=APOA1 PE=1 SV=1	9.59E+07	Apolipoprotein A-I OS=Homo sapiens GN=APOA1 PE=1 SV=1	1.55E+08
Apolipoprotein A-II OS=Homo sapiens GN=APOA2 PE=1 SV=1	2.59E+07	Apolipoprotein A-II OS=Homo sapiens GN=APOA2 PE=1 SV=1	1.84E+07
Apolipoprotein A-IV OS=Homo sapiens GN=APOA4 PE=1 SV=3	1.04E+07	Apolipoprotein A-IV OS=Homo sapiens GN=APOA4 PE=1 SV=3	7.77E+06
ATP-binding cassette sub-family C member 8; AltName: Full=Sulfonylurea receptor 1; [Homo sapiens (Human)] - [ABCC8_HUMAN]	6.85E+07	ATP-binding cassette sub-family C member 8; AltName: Full=Sulfonylurea receptor 1; [Homo sapiens (Human)] - [ABCC8_HUMAN]	2.80E+07
Attractin OS=Homo sapiens GN=ATRN PE=1 SV=2	1.13E+07	Attractin OS=Homo sapiens GN=ATRN PE=1 SV=2	9.79E+06
Beta-2-microglobulin OS=Homo sapiens GN=B2M PE=1 SV=1	1.20E+08	Beta-2-microglobulin OS=Homo sapiens GN=B2M PE=1 SV=1	6.95E+07
Biotinidase OS=Homo sapiens GN=BTD PE=1 SV=2	1.19E+07	Biotinidase OS=Homo sapiens GN=BTD PE=1 SV=2	6.35E+06
Calmodulin OS=Homo sapiens GN=CALM1 PE=1 SV=2	3.58E+07	Calmodulin OS=Homo sapiens GN=CALM1 PE=1 SV=2	1.93E+07
Carbonic anhydrase 1 OS=Homo sapiens GN=CA1 PE=1 SV=2	2.36E+07	Carbonic anhydrase 1 OS=Homo sapiens GN=CA1 PE=1 SV=2	2.40E+07
Carbonic anhydrase 2 OS=Homo sapiens GN=CA2 PE=1 SV=2	9.50E+06	Carbonic anhydrase 2 OS=Homo sapiens GN=CA2 PE=1 SV=2	6.78E+06
Caspase recruitment domain-containing protein 6; [Homo sapiens (Human)] - [CARD6_HUMAN]	2.40E+08	Caspase recruitment domain-containing protein 6; [Homo sapiens (Human)] - [CARD6_HUMAN]	1.40E+08
Cathepsin D OS=Homo sapiens GN=CTSD PE=1 SV=1	1.10E+09	Cathepsin D OS=Homo sapiens GN=CTSD PE=1 SV=1	4.60E+08
CD44 antigen OS=Homo sapiens GN=CD44 PE=1 SV=3	7.78E+07	CD44 antigen OS=Homo sapiens GN=CD44 PE=1 SV=3	5.58E+07
CD9 antigen OS=Homo sapiens GN=CD9 PE=1 SV=4	2.20E+07	CD9 antigen OS=Homo sapiens GN=CD9 PE=1 SV=4	1.45E+07
Cell adhesion molecule 1; AltName: Full=Immunoglobulin superfamily member 4; Short=IgSF4; AltName: Full=Nectin-like protein 2; Short=NECL-2; AltName: Full=Spermatogenic immunoglobulin superfamily; Short=SgIgSF; AltName: Full=Synaptic cell adhesion molecule; Short=SynCAM; AltName: Full=Tumor suppressor	7.37E+06	Cell adhesion molecule 1 OS=Homo sapiens GN=CADM1 PE=1 SV=2	3.41E+06

in lung cancer 1; Short=TSLC-1; Flags: Precursor; [Homo sapiens (Human)] - [CADM1_HUMAN]			
Ceruloplasmin OS=Homo sapiens GN=CP PE=1 SV=1	5.37E+08	Ceruloplasmin OS=Homo sapiens GN=CP PE=1 SV=1	1.23E+08
cGMP-specific 3',5'-cyclic phosphodiesterase; EC=3.1.4.35; AltName: Full=cGMP-binding cGMP-specific phosphodiesterase; Short=CGB-PDE; [Homo sapiens (Human)] - [PDE5A_HUMAN]	1.22E+08	cGMP-specific 3',5'-cyclic phosphodiesterase; EC=3.1.4.35; AltName: Full=cGMP-binding cGMP-specific phosphodiesterase; Short=CGB-PDE; [Homo sapiens (Human)] - [PDE5A_HUMAN]	5.00E+07
Coactosin-like protein OS=Homo sapiens GN=COTL1 PE=1 SV=3	3.46E+07	Coactosin-like protein OS=Homo sapiens GN=COTL1 PE=1 SV=3	1.15E+07
Complement C2 OS=Homo sapiens GN=C2 PE=1 SV=2	6.82E+06	Complement C2 OS=Homo sapiens GN=C2 PE=1 SV=2	6.38E+06
Complement C3 OS=Homo sapiens GN=C3 PE=1 SV=2	1.25E+07	Complement C3 OS=Homo sapiens GN=C3 PE=1 SV=2	2.94E+07
Complement decay-accelerating factor OS=Homo sapiens GN=CD55 PE=1 SV=4	1.49E+07	Complement decay-accelerating factor OS=Homo sapiens GN=CD55 PE=1 SV=4	1.63E+07
Corticosteroid-binding globulin OS=Homo sapiens GN=SERPINA6 PE=1 SV=1	5.17E+07	Corticosteroid-binding globulin OS=Homo sapiens GN=SERPINA6 PE=1 SV=1	1.39E+07
Cystatin-B OS=Homo sapiens GN=CSTB PE=1 SV=2	7.58E+06	Cystatin-B OS=Homo sapiens GN=CSTB PE=1 SV=2	6.67E+06
Deleted in malignant brain tumors 1 protein OS=Homo sapiens GN=DMBT1 PE=1 SV=2	5.59E+07	Deleted in malignant brain tumors 1 protein OS=Homo sapiens GN=DMBT1 PE=1 SV=2	3.56E+07
Delta-like protein 4; AltName: Full=Drosophila Delta homolog 4; Short=Delta4; Flags: Precursor; [Homo sapiens (Human)] - [DLL4_HUMAN]	1.80E+07	Delta-like protein 4; AltName: Full=Drosophila Delta homolog 4; Short=Delta4; Flags: Precursor; [Homo sapiens (Human)] - [DLL4_HUMAN]	1.73E+07
Dermcidin OS=Homo sapiens GN=DCD PE=1 SV=2	6.20E+06	Dermcidin OS=Homo sapiens GN=DCD PE=1 SV=2	3.67E+06
Desmoplakin OS=Homo sapiens GN=DSP PE=1 SV=3	1.60E+08	Desmoplakin OS=Homo sapiens GN=DSP PE=1 SV=3	2.67E+07
Dipeptidyl peptidase 4 OS=Homo sapiens GN=DPP4 PE=1 SV=2	1.64E+07	Dipeptidyl peptidase 4 OS=Homo sapiens GN=DPP4 PE=1 SV=2	1.11E+07
Epididymal secretory protein E1 OS=Homo sapiens GN=NPC2 PE=1 SV=1	5.26E+07	Epididymal secretory protein E1 OS=Homo sapiens GN=NPC2 PE=1 SV=1	1.26E+08
FAS-associated factor 1; Short=hFAF1; AltName: Full=UBX domain-containing protein 12; AltName: Full=UBX domain-containing protein 3A; [Homo sapiens (Human)] - [FAF1_HUMAN]	2.21E+08	FAS-associated factor 1; Short=hFAF1; AltName: Full=UBX domain-containing protein 12; AltName: Full=UBX domain-containing protein 3A; [Homo sapiens (Human)] - [FAF1_HUMAN]	1.03E+08
Fatty acid-binding protein, adipocyte OS=Homo sapiens GN=FABP4 PE=1 SV=3	9.73E+06	Fatty acid-binding protein, adipocyte; AltName: Full=Adipocyte lipid-binding protein; Short=ALBP;	1.31E+07

		AltName: Full=Adipocyte-type fatty acid-binding protein; Short=A-FABP; Short=AFABP; AltName: Full=Fatty acid-binding protein 4; [Homo sapiens (Human)] - [FABP4_HUMAN]	
Folate receptor alpha OS=Homo sapiens GN=FOLR1 PE=1 SV=3	3.11E+06	Folate receptor alpha OS=Homo sapiens GN=FOLR1 PE=1 SV=3	2.79E+06
Galectin-3-binding protein OS=Homo sapiens GN=LGALS3BP PE=1 SV=1	1.14E+07	Galectin-3-binding protein OS=Homo sapiens GN=LGALS3BP PE=1 SV=1	3.89E+06
Glutathione S-transferase P OS=Homo sapiens GN=GSTP1 PE=1 SV=2	3.42E+07	Glutathione S-transferase P OS=Homo sapiens GN=GSTP1 PE=1 SV=2	9.57E+06
Haptoglobin OS=Homo sapiens GN=HP PE=1 SV=1	3.82E+08	Haptoglobin OS=Homo sapiens GN=HP PE=1 SV=1	1.13E+09
Heme-binding protein 2; AltName: Full=Placental protein 23; Short=PP23; AltName: Full=Protein SOUL; [Homo sapiens (Human)] - [HEBP2_HUMAN]	5.28E+06	Heme-binding protein 2; AltName: Full=Placental protein 23; Short=PP23; AltName: Full=Protein SOUL; [Homo sapiens (Human)] - [HEBP2_HUMAN]	2.71E+06
Hemoglobin subunit alpha; AltName: Full=Alpha-globin; AltName: Full=Hemoglobin alpha chain; [Homo sapiens (Human)] - [HBA_HUMAN]	2.06E+08	Hemoglobin subunit alpha OS=Homo sapiens GN=HBA1 PE=1 SV=2	6.04E+08
Hemoglobin subunit beta OS=Homo sapiens GN=HBB PE=1 SV=2	2.06E+08	Hemoglobin subunit beta OS=Homo sapiens GN=HBB PE=1 SV=2	4.82E+08
Hemoglobin subunit delta OS=Homo sapiens GN=HBD PE=1 SV=2	1.66E+08	Hemoglobin subunit delta OS=Homo sapiens GN=HBD PE=1 SV=2	3.78E+08
Hemopexin OS=Homo sapiens GN=HPX PE=1 SV=2	7.70E+08	Hemopexin OS=Homo sapiens GN=HPX PE=1 SV=2	4.44E+08
Ig alpha-1 chain C region OS=Homo sapiens GN=IGHA1 PE=1 SV=2	2.81E+09	Ig alpha-1 chain C region OS=Homo sapiens GN=IGHA1 PE=1 SV=2	1.24E+09
Ig alpha-2 chain C region OS=Homo sapiens GN=IGHA2 PE=1 SV=3	2.05E+09	Ig alpha-2 chain C region OS=Homo sapiens GN=IGHA2 PE=1 SV=3	8.46E+08
Ig delta chain C region; [Homo sapiens (Human)] - [IGHD_HUMAN]	6.39E+06	Ig delta chain C region; [Homo sapiens (Human)] - [IGHD_HUMAN]	8.04E+06
Ig gamma-1 chain C region; [Homo sapiens (Human)] - [IGHG1_HUMAN]	1.23E+10	Ig gamma-1 chain C region OS=Homo sapiens GN=IGHG1 PE=1 SV=1	3.04E+09
Ig gamma-2 chain C region OS=Homo sapiens GN=IGHG2 PE=1 SV=2	9.10E+09	Ig gamma-2 chain C region OS=Homo sapiens GN=IGHG2 PE=1 SV=2	2.20E+09
Ig gamma-3 chain C region OS=Homo sapiens GN=IGHG3 PE=1 SV=2	9.36E+09	Ig gamma-3 chain C region OS=Homo sapiens GN=IGHG3 PE=1 SV=2	2.52E+09

Ig heavy chain V-II region ARH-77 OS=Homo sapiens PE=4 SV=1	7.57E+07	Ig heavy chain V-II region ARH-77 OS=Homo sapiens PE=4 SV=1	1.73E+08
Ig heavy chain V-II region NEWM; [Homo sapiens (Human)] - [HV207_HUMAN]	1.14E+08	Ig heavy chain V-II region NEWM; [Homo sapiens (Human)] - [HV207_HUMAN]	6.76E+07
Ig heavy chain V-II region OU; [Homo sapiens (Human)] - [HV201_HUMAN]	6.80E+07	Ig heavy chain V-II region OU; [Homo sapiens (Human)] - [HV201_HUMAN]	2.46E+07
Ig heavy chain V-III region BUT OS=Homo sapiens PE=1 SV=1	1.16E+09	Ig heavy chain V-III region BUT; [Homo sapiens (Human)] - [HV306_HUMAN]	5.55E+08
Ig heavy chain V-III region CAM OS=Homo sapiens PE=1 SV=1	1.22E+09	Ig heavy chain V-III region CAM OS=Homo sapiens PE=1 SV=1	5.71E+08
Ig heavy chain V-III region GAL OS=Homo sapiens PE=1 SV=1	1.17E+09	Ig heavy chain V-III region GAL OS=Homo sapiens PE=1 SV=1	4.86E+08
Ig heavy chain V-III region GAR; [Homo sapiens (Human)] - [HV322_HUMAN]	2.84E+08	Ig heavy chain V-III region GAR; [Homo sapiens (Human)] - [HV322_HUMAN]	7.31E+07
Ig heavy chain V-III region HIL; [Homo sapiens (Human)] - [HV310_HUMAN]	1.66E+09	Ig heavy chain V-III region HIL; [Homo sapiens (Human)] - [HV310_HUMAN]	6.93E+08
Ig heavy chain V-III region VH26 OS=Homo sapiens PE=1 SV=1	1.25E+09	Ig heavy chain V-III region VH26 OS=Homo sapiens PE=1 SV=1	5.29E+08
Ig kappa chain C region OS=Homo sapiens GN=IGKC PE=1 SV=1	5.90E+09	Ig kappa chain C region OS=Homo sapiens GN=IGKC PE=1 SV=1	1.00E+09
Ig kappa chain V-I region EU OS=Homo sapiens PE=1 SV=1	4.22E+08	Ig kappa chain V-I region EU OS=Homo sapiens PE=1 SV=1	1.95E+08
Ig kappa chain V-I region Roy; [Homo sapiens (Human)] - [KV116_HUMAN]	1.96E+08	Ig kappa chain V-I region Roy; [Homo sapiens (Human)] - [KV116_HUMAN]	1.45E+08
Ig kappa chain V-I region Wes; [Homo sapiens (Human)] - [KV119_HUMAN]	5.03E+08	Ig kappa chain V-I region Wes; [Homo sapiens (Human)] - [KV119_HUMAN]	2.28E+08
Ig kappa chain V-III region POM OS=Homo sapiens PE=1 SV=1	3.13E+08	Ig kappa chain V-III region POM OS=Homo sapiens PE=1 SV=1	1.01E+08
Ig kappa chain V-III region SIE OS=Homo sapiens PE=1 SV=1	3.17E+08	Ig kappa chain V-III region SIE OS=Homo sapiens PE=1 SV=1	1.59E+08
Ig kappa chain V-III region VG; Flags: Precursor; Fragment; [Homo sapiens (Human)] - [KV309_HUMAN]	3.81E+08	Ig kappa chain V-III region VG; Flags: Precursor; Fragment; [Homo sapiens (Human)] - [KV309_HUMAN]	1.06E+08
Ig lambda chain V-I region HA OS=Homo sapiens PE=1 SV=1	2.17E+08	Ig lambda chain V-I region HA OS=Homo sapiens PE=1 SV=1	3.45E+07
Ig lambda chain V-I region NIG-64 OS=Homo sapiens PE=1 SV=1	6.96E+07	Ig lambda chain V-I region NIG-64 OS=Homo sapiens PE=1 SV=1	2.39E+07
Ig lambda chain V-III region LOI OS=Homo sapiens PE=1 SV=1	2.61E+08	Ig lambda chain V-III region LOI OS=Homo sapiens PE=1 SV=1	3.54E+07
Ig lambda chain V-III region SH; [Homo sapiens (Human)] - [LV301_HUMAN]	2.83E+07	Ig lambda chain V-III region SH; [Homo sapiens (Human)] - [LV301_HUMAN]	1.90E+07
Ig lambda chain V-IV region Bau;	4.40E+08	Ig lambda chain V-IV region Bau;	4.15E+0

[Homo sapiens (Human)] - [LV401_HUMAN]		[Homo sapiens (Human)] - [LV401_HUMAN]	7
Ig lambda chain V-IV region Hil; [Homo sapiens (Human)] - [LV403_HUMAN]	2.91E+08	Ig lambda chain V-IV region Hil; [Homo sapiens (Human)] - [LV403_HUMAN]	3.39E+07
Ig lambda-2 chain C regions OS=Homo sapiens GN=IGLC2 PE=1 SV=1	3.07E+09	Ig lambda-2 chain C regions OS=Homo sapiens GN=IGLC2 PE=1 SV=1	7.00E+08
Ig mu chain C region OS=Homo sapiens GN=IGHM PE=1 SV=3	6.47E+07	Ig mu chain C region OS=Homo sapiens GN=IGHM PE=1 SV=3	7.42E+07
Immunoglobulin J chain OS=Homo sapiens GN=IGJ PE=1 SV=4	8.29E+07	Immunoglobulin J chain OS=Homo sapiens GN=IGJ PE=1 SV=4	8.35E+07
Immunoglobulin lambda-like polypeptide 5; AltName: Full=G lambda-1; AltName: Full=Germline immunoglobulin lambda 1; Flags: Precursor; [Homo sapiens (Human)] - [IGLL5_HUMAN]	1.96E+09	Immunoglobulin lambda-like polypeptide 5 OS=Homo sapiens GN=IGLL5 PE=2 SV=2	4.17E+08
Intercellular adhesion molecule 1 OS=Homo sapiens GN=ICAM1 PE=1 SV=2	4.01E+07	Intercellular adhesion molecule 1 OS=Homo sapiens GN=ICAM1 PE=1 SV=2	1.77E+07
Junctional adhesion molecule A OS=Homo sapiens GN=F11R PE=1 SV=1	5.60E+06	Junctional adhesion molecule A OS=Homo sapiens GN=F11R PE=1 SV=1	9.69E+06
Lactotransferrin OS=Homo sapiens GN=LTF PE=1 SV=6	1.38E+09	Lactotransferrin; Short=Lactoferrin; EC=3.4.21.-; AltName: Full=Talalactoferrin; Contains: RecName: Full=Kaliocin-1; Contains: RecName: Full=Lactoferroxin-A; Contains: RecName: Full=Lactoferroxin-B; Contains: RecName: Full=Lactoferroxin-C; Flags: Precursor; [Homo sapiens (Human)] - [TRFL_HUMAN]	7.34E+08
Leucine-rich alpha-2-glycoprotein OS=Homo sapiens GN=LRG1 PE=1 SV=2	3.79E+06	Leucine-rich alpha-2-glycoprotein OS=Homo sapiens GN=LRG1 PE=1 SV=2	2.36E+07
Leukocyte elastase inhibitor OS=Homo sapiens GN=SERPINB1 PE=1 SV=1	8.21E+06	Leukocyte elastase inhibitor OS=Homo sapiens GN=SERPINB1 PE=1 SV=1	9.09E+06
Lysozyme C OS=Homo sapiens GN=LYZ PE=1 SV=1	2.75E+06	Lysozyme C; EC=3.2.1.17; AltName: Full=1,4-beta-N-acetylmuramidase C; Flags: Precursor; [Homo sapiens (Human)] - [LYSC_HUMAN]	4.75E+05
Mesothelin OS=Homo sapiens GN=MSLN PE=1 SV=2	1.78E+07	Mesothelin OS=Homo sapiens GN=MSLN PE=1 SV=2	1.74E+07
Mucin-1 OS=Homo sapiens GN=MUC1 PE=1 SV=3	1.31E+07	Mucin-1 OS=Homo sapiens GN=MUC1 PE=1 SV=3	8.52E+06
Napsin-A OS=Homo sapiens GN=NAPSA PE=1 SV=1	2.37E+06	Napsin-A; EC=3.4.23.-; AltName: Full=Aspartyl protease 4;	1.75E+07

		Short=ASP4; Short=Asp 4; AltName: Full=Napsin-1; AltName: Full=TA01/TA02; Flags: Precursor; [Homo sapiens (Human)] - [NAPSA_HUMAN]	
Neutrophil defensin 1 OS=Homo sapiens GN=DEFA1 PE=1 SV=1	1.79E+06	Neutrophil defensin 1; AltName: Full=Defensin, alpha 1; AltName: Full=HNP-1; Short=HP-1; Short=HP1; Contains: RecName: Full=HP 1-56; Contains: RecName: Full=Neutrophil defensin 2; AltName: Full=HNP-2; Short=HP-2; Short=HP2; Flags: Precursor; [Homo sapiens (Human)] - [DEF1_HUMAN]	3.60E+06
Peroxiredoxin-5, mitochondrial OS=Homo sapiens GN=PRDX5 PE=1 SV=4	6.12E+06	Peroxiredoxin-5, mitochondrial OS=Homo sapiens GN=PRDX5 PE=1 SV=4	3.31E+06
Peroxiredoxin-6 OS=Homo sapiens GN=PRDX6 PE=1 SV=3	2.13E+06	Peroxiredoxin-6 OS=Homo sapiens GN=PRDX6 PE=1 SV=3	4.96E+06
Phosphatidylethanolamine-binding protein 1; Short=PEBP-1; AltName: Full=HCNPpp; AltName: Full=Neuropolypeptide h3; AltName: Full=Prostatic-binding protein; AltName: Full=Raf kinase inhibitor protein; Short=RKIP; Contains: RecName: Full=Hippocampal cholinergic neurostimulating peptide; Short=HCNP; [Homo sapiens (Human)] - [PEBP1_HUMAN]	4.01E+06	Phosphatidylethanolamine-binding protein 1; Short=PEBP-1; AltName: Full=HCNPpp; AltName: Full=Neuropolypeptide h3; AltName: Full=Prostatic-binding protein; AltName: Full=Raf kinase inhibitor protein; Short=RKIP; Contains: RecName: Full=Hippocampal cholinergic neurostimulating peptide; Short=HCNP; [Homo sapiens (Human)] - [PEBP1_HUMAN]	8.97E+05
Phosphoglycerate mutase 1 OS=Homo sapiens GN=PGAM1 PE=1 SV=2	3.87E+06	Phosphoglycerate mutase 1 OS=Homo sapiens GN=PGAM1 PE=1 SV=2	1.88E+06
Plasma protease C1 inhibitor OS=Homo sapiens GN=SERPING1 PE=1 SV=2	9.83E+06	Plasma protease C1 inhibitor OS=Homo sapiens GN=SERPING1 PE=1 SV=2	6.56E+06
Polymeric immunoglobulin receptor OS=Homo sapiens GN=PIGR PE=1 SV=4	5.24E+08	Polymeric immunoglobulin receptor OS=Homo sapiens GN=PIGR PE=1 SV=4	3.32E+08
Pro-cathepsin H OS=Homo sapiens GN=CTSH PE=1 SV=4	2.79E+07	Pro-cathepsin H OS=Homo sapiens GN=CTSH PE=1 SV=4	2.12E+07
Protein DJ-1 OS=Homo sapiens GN=PARK7 PE=1 SV=2	3.98E+07	Protein DJ-1 OS=Homo sapiens GN=PARK7 PE=1 SV=2	1.75E+07
Protein S100-A11 OS=Homo sapiens GN=S100A11 PE=1 SV=2	7.59E+06	Protein S100-A11 OS=Homo sapiens GN=S100A11 PE=1 SV=2	4.68E+06
Protein S100-A6 OS=Homo sapiens GN=S100A6 PE=1 SV=1	9.49E+07	Protein S100-A6 OS=Homo sapiens GN=S100A6 PE=1 SV=1	8.46E+07
Protein Shroom3; AltName: Full=Shroom-related protein; Short=hShrmL; [Homo sapiens	8.34E+07	Protein Shroom3; AltName: Full=Shroom-related protein; Short=hShrmL; [Homo sapiens	7.90E+07

(Human)] - [SHRM3_HUMAN]		(Human)] - [SHRM3_HUMAN]	
Pulmonary surfactant-associated protein A2 OS=Homo sapiens GN=SFTPA2 PE=1 SV=1	1.95E+08	Pulmonary surfactant-associated protein A2 OS=Homo sapiens GN=SFTPA2 PE=1 SV=1	5.87E+07
Pulmonary surfactant-associated protein B OS=Homo sapiens GN=SFTPB PE=1 SV=3	2.54E+07	Pulmonary surfactant-associated protein B OS=Homo sapiens GN=SFTPB PE=1 SV=3	2.53E+07
Pulmonary surfactant-associated protein D OS=Homo sapiens GN=SFTPD PE=1 SV=3	4.71E+07	Pulmonary surfactant-associated protein D OS=Homo sapiens GN=SFTPD PE=1 SV=3	2.06E+07
Puromycin-sensitive aminopeptidase; Short=PSA; EC=3.4.11.14; AltName: Full=Cytosol alanyl aminopeptidase; Short=AAP-S; [Homo sapiens (Human)] - [PSA_HUMAN]	1.13E+07	Puromycin-sensitive aminopeptidase; Short=PSA; EC=3.4.11.14; AltName: Full=Cytosol alanyl aminopeptidase; Short=AAP-S; [Homo sapiens (Human)] - [PSA_HUMAN]	1.43E+07
Putative inactive carboxylesterase 4; AltName: Full=Inactive carboxylesterase 1 pseudogene 1; AltName: Full=Placental carboxylesterase 3; Short=PCE-3; Flags: Precursor; [Homo sapiens (Human)] - [CES1P_HUMAN]	4.34E+06	Putative inactive carboxylesterase 4; AltName: Full=Inactive carboxylesterase 1 pseudogene 1; AltName: Full=Placental carboxylesterase 3; Short=PCE-3; Flags: Precursor; [Homo sapiens (Human)] - [CES1P_HUMAN]	3.62E+06
Putative V-set and immunoglobulin domain-containing protein 6 OS=Homo sapiens GN=VSIG6 PE=5 SV=2	2.22E+08	Putative V-set and immunoglobulin domain-containing protein 6 OS=Homo sapiens GN=VSIG6 PE=5 SV=2	7.72E+07
Retinoic acid-induced protein 3 OS=Homo sapiens GN=GPRC5A PE=1 SV=2	1.29E+07	Retinoic acid-induced protein 3 OS=Homo sapiens GN=GPRC5A PE=1 SV=2	3.24E+07
Rho GDP-dissociation inhibitor 2 OS=Homo sapiens GN=ARHGDIB PE=1 SV=3	1.36E+09	Rho GDP-dissociation inhibitor 2 OS=Homo sapiens GN=ARHGDIB PE=1 SV=3	6.99E+06
Ribonuclease P protein subunit p40; Short=RNaseP protein p40; EC=3.1.26.5; AltName: Full=RNase P subunit 1; [Homo sapiens (Human)] - [RPP40_HUMAN]	1.42E+08	Ribonuclease P protein subunit p40; Short=RNaseP protein p40; EC=3.1.26.5; AltName: Full=RNase P subunit 1; [Homo sapiens (Human)] - [RPP40_HUMAN]	9.04E+07
Scavenger receptor cysteine-rich type 1 protein M130 OS=Homo sapiens GN=CD163 PE=1 SV=2	2.29E+07	Scavenger receptor cysteine-rich type 1 protein M130 OS=Homo sapiens GN=CD163 PE=1 SV=2	1.28E+07
Selenium-binding protein 1 OS=Homo sapiens GN=SELENBP1 PE=1 SV=2	2.43E+07	Selenium-binding protein 1 OS=Homo sapiens GN=SELENBP1 PE=1 SV=2	2.55E+07
Serotransferrin OS=Homo sapiens GN=TF PE=1 SV=3	1.28E+10	Serotransferrin OS=Homo sapiens GN=TF PE=1 SV=3	4.55E+09
Serpin B3 OS=Homo sapiens GN=SERPINB3 PE=1 SV=2	3.01E+07	Serpin B3 OS=Homo sapiens GN=SERPINB3 PE=1 SV=2	7.74E+06
Serpin B6; AltName: Full=Cytoplasmic antiproteinase;	3.30E+06	Serpin B6; AltName: Full=Cytoplasmic antiproteinase;	1.37E+06

Short=CAP; AltName: Full=Peptidase inhibitor 6; Short=PI-6; AltName: Full=Placental thrombin inhibitor; [Homo sapiens (Human)] - [SPB6_HUMAN]		Short=CAP; AltName: Full=Peptidase inhibitor 6; Short=PI-6; AltName: Full=Placental thrombin inhibitor; [Homo sapiens (Human)] - [SPB6_HUMAN]	
Serum albumin OS=Homo sapiens GN=ALB PE=1 SV=2	3.97E+09	Serum albumin OS=Homo sapiens GN=ALB PE=1 SV=2	3.32E+09
Sodium-dependent phosphate transport protein 2B; Short=Sodium-phosphate transport protein 2B; AltName: Full=Na(+)-dependent phosphate cotransporter 2B; AltName: Full=NaPi3b; AltName: Full=Sodium/phosphate cotransporter 2B; Short=Na(+)/Pi cotransporter 2B; Short=NaPi-2b; AltName: Full=Solute carrier family 34 member 2; [Homo sapiens (Human)] - [NPT2B_HUMAN]	1.14E+06	Sodium-dependent phosphate transport protein 2B; Short=Sodium-phosphate transport protein 2B; AltName: Full=Na(+)-dependent phosphate cotransporter 2B; AltName: Full=NaPi3b; AltName: Full=Sodium/phosphate cotransporter 2B; Short=Na(+)/Pi cotransporter 2B; Short=NaPi-2b; AltName: Full=Solute carrier family 34 member 2; [Homo sapiens (Human)] - [NPT2B_HUMAN]	2.12E+06
Superoxide dismutase [Cu-Zn] OS=Homo sapiens GN=SOD1 PE=1 SV=2	9.13E+06	Superoxide dismutase [Cu-Zn] OS=Homo sapiens GN=SOD1 PE=1 SV=2	6.94E+06
Thioredoxin; Short=Trx; AltName: Full=ATL-derived factor; Short=ADF; AltName: Full=Surface-associated sulphydryl protein; Short=SASP; [Homo sapiens (Human)] - [THIO_HUMAN]	1.30E+07	Thioredoxin OS=Homo sapiens GN=TXN PE=1 SV=3	1.15E+07
Thyroxine-binding globulin OS=Homo sapiens GN=SERPINA7 PE=1 SV=2	1.56E+07	Thyroxine-binding globulin OS=Homo sapiens GN=SERPINA7 PE=1 SV=2	8.96E+06
Transaldolase OS=Homo sapiens GN=TALDO1 PE=1 SV=2	2.33E+07	Transaldolase OS=Homo sapiens GN=TALDO1 PE=1 SV=2	2.30E+07
Transcriptional adapter 2-beta; AltName: Full=ADA2-like protein beta; Short=ADA2-beta; [Homo sapiens (Human)] - [TAD2B_HUMAN]	8.54E+06	Transcriptional adapter 2-beta; AltName: Full=ADA2-like protein beta; Short=ADA2-beta; [Homo sapiens (Human)] - [TAD2B_HUMAN]	3.36E+06
Transmembrane protein 198; [Homo sapiens (Human)] - [TM198_HUMAN]	4.77E+07	Transmembrane protein 198; [Homo sapiens (Human)] - [TM198_HUMAN]	1.29E+07
Transmembrane protein 200C; AltName: Full=Transmembrane protein TTMA; AltName: Full=Two transmembrane domain-containing family member A; [Homo sapiens (Human)] - [T200C_HUMAN]	2.87E+06	Transmembrane protein 200C; AltName: Full=Transmembrane protein TTMA; AltName: Full=Two transmembrane domain-containing family member A; [Homo sapiens (Human)] - [T200C_HUMAN]	2.80E+06
Triosephosphate isomerase	3.83E+07	Triosephosphate isomerase	2.05E+0

OS=Homo sapiens GN=TPI1 PE=1 SV=3		OS=Homo sapiens GN=TPI1 PE=1 SV=3	7
Uncharacterized protein C3orf38; [Homo sapiens (Human)] - [CC038_HUMAN]	4.10E+09	Uncharacterized protein C3orf38; [Homo sapiens (Human)] - [CC038_HUMAN]	2.18E+09
Uteroglobin OS=Homo sapiens GN=SCGB1A1 PE=1 SV=1	6.27E+08	Uteroglobin OS=Homo sapiens GN=SCGB1A1 PE=1 SV=1	4.14E+08
V-set and immunoglobulin domain-containing protein 4; AltName: Full=Protein Z39Ig; Flags: Precursor; [Homo sapiens (Human)] - [VSIG4_HUMAN]	8.17E+06	V-set and immunoglobulin domain-containing protein 4; AltName: Full=Protein Z39Ig; Flags: Precursor; [Homo sapiens (Human)] - [VSIG4_HUMAN]	1.67E+06
Vitamin D-binding protein OS=Homo sapiens GN=GC PE=1 SV=1	2.19E+08	Vitamin D-binding protein OS=Homo sapiens GN=GC PE=1 SV=1	2.16E+08
Xin actin-binding repeat-containing protein 2 OS=Homo sapiens GN=XIRP2 PE=1 SV=2	4.22E+08	Xin actin-binding repeat-containing protein 2; AltName: Full=Beta-xin; AltName: Full=Cardiomyopathy-associated protein 3; AltName: Full=Xeplin; [Homo sapiens (Human)] - [XIRP2_HUMAN]	1.92E+08
Zinc-alpha-2-glycoprotein OS=Homo sapiens GN=AZGP1 PE=1 SV=2	1.16E+08	Zinc-alpha-2-glycoprotein OS=Homo sapiens GN=AZGP1 PE=1 SV=2	1.08E+08

Table A.4: *The biological process classification of Metal handling according to Gene Ontology annotation of proteins identified. Data shown is a comparison of the mean of the three most abundant ion peaks of each protein identified, in Healthy Controls and Mild Asthmatics respectively, n=5 for both subject groups.*

Metal handling	Healthy control	Mild Asthmatic
Annexin A2	X	7.67E+06
Annexin A3	X	1.29E+07
Annexin A4	2.52E+07	X
Annexin A5	6.60E+07	1.83E+07
Calcyphosin	X	2.67E+06
Calmodulin	3.58E+07	1.93E+07
Carbonic anhydrase 1	2.36E+07	2.40E+07
Carbonic anhydrase 2	9.50E+06	6.78E+06
Ceruloplasmin	5.37E+08	1.23E+08
Complement decay-accelerating factor	1.49E+07	1.63E+07
Ferritin heavy chain	X	2.76E+06
Gelsolin	9.95E+06	X
Glutathione peroxidase 3	4.07E+06	X
Hemoglobin subunit alpha	2.06E+08	6.04E+08
Hemoglobin subunit beta	2.09E+08	4.82E+08
Hemoglobin subunit delta	1.66E+08	3.78E+08
Hemopexin	7.70E+08	4.44E+08
Hornerin	4.56E+06	X
Kininogen-1	5.17E+06	X
Lactotransferrin	1.38E+09	7.34E+08
Neutrophil gelatinase-associated lipocalin	4.22E+06	X

Probable hydrolase PNKD	1.07E+07	X
Protein S100-A11	7.59E+06	4.68E+06
Protein S100-A3	1.22E+07	X
Protein S100-A6	X	8.46E+07
Retinoic acid-induced protein 3	X	3.24E+07
Selenium-binding protein 1	2.43E+07	2.55E+07
Serotransferrin	1.28E+10	4.55E+09
Serum albumin	3.97E+09	3.32E+09
Superoxide dismutase [Cu-Zn]	9.13E+06	6.94E+06
Zinc-alpha-2-glycoprotein	1.16E+08	1.08E+08

Table A.5: *The biological process classification of Inflammation/immunity according to Gene Ontology annotation of proteins identified. Data shown is a comparison of the mean of the three most abundant ion peaks of each protein identified, in Healthy Controls and Mild Asthmatics respectively, n=5 for both subject groups.*

Inflammation/immunity	Healthy control	Mild Asthmatic
Alpha-1-acid glycoprotein 1	2.04E+08	2.89E+08
Alpha-1-antichymotrypsin	1.49E+08	3.86E+07
Alpha-1-antichymotrypsin	1.49E+08	3.86E+07
Alpha-2-HS-glycoprotein (fetuin A)	7.52E+07	1.13E+08
Annexin A3	X	1.29E+07
Antithrombin-III	2.92E+07	7.80E+06
Beta-2-microglobulin	1.20E+08	6.95E+07
Beta-microseminoprotein	5.82E+07	X
Cell adhesion molecule 1	7.37E+06	3.41E+06
Cell adhesion molecule 2	X	4.06E+06
Complement C2	6.82E+06	6.38E+06
Complement C3	1.25E+07	2.94E+07
Complement C4-A	1.80E+07	X
Complement decay-accelerating factor (CD55)	1.49E+07	1.63E+07
Deleted in malignant brain tumors 1 protein	5.59E+07	3.56E+07
Dipeptidyl peptidase 4	1.64E+07	1.11E+07
Galectin-3 binding protein	1.14E+07	3.89E+06
Haptoglobin	3.82E+08	1.13E+09
HLA class II histocompatibility antigen, DR alpha chain	X	3.67E+06
HLA class II histocompatibility antigen, DRB1-15 beta chain	7.37E+06	9.93E+06
Ig alpha-1 chain C region	2.81E+09	1.24E+09
Ig alpha-2 chain C region	2.05E+09	8.46E+08
Ig delta chain C region	6.39E+06	8.04E+06
Ig gamma-1 chain C region	1.23E+10	3.04E+09
Ig gamma-2 chain C region	9.10E+09	2.20E+09
Ig gamma-3 chain C region	9.36E+09	2.52E+09
Ig gamma-4 chain C region	9.10E+09	X
Ig heavy chain V-I region HG3	2.14E+08	5.87E+07
Ig heavy chain V-I region V35	6.05E+07	1.96E+07
Ig heavy chain V-II region ARH-77	7.57E+07	3.81E+07

Ig heavy chain V-III region CAM	1.22E+09	5.71E+08
Ig heavy chain V-III region GAL	1.17E+09	4.86E+08
Ig kappa chain C region	5.90E+09	1.00E+09
Ig kappa chain V-I region DEE	4.84E+08	X
Ig kappa chain V-I region Kue	X	1.92E+08
Ig kappa chain V-II region TEW	X	1.29E+08
Ig kappa chain V-III region POM	3.13E+08	1.01E+08
Ig kappa chain V-III region SIE	3.17E+08	1.59E+08
Ig kappa chain V-IV region Len	1.66E+08	6.04E+07
Ig lambda chain V region 4A	1.06E+08	9.96E+06
Ig lambda chain V-I region HA	2.17E+08	3.45E+07
Ig lambda chain V-I region NIG-64	6.96E+07	2.39E+07
Ig lambda chain V-III region LOI	2.61E+08	3.54E+07
Ig lambda chain V-III region SH	2.83E+07	1.90E+07
Ig lambda chain V-VI region SUT	2.58E+07	X
Ig lambda-2 chain C regions	3.07E+09	7.00E+08
Ig mu chain C region	6.47E+07	7.42E+07
IgBF	5.82E+07	X
Immunoglobulin J chain	8.29E+07	8.35E+07
Immunoglobulin lambda-like polypeptide 5	1.96E+09	4.17E+08
Intercellular adhesion molecule 1	4.01E+07	1.77E+07
Junctional adhesion molecule A	5.60E+06	9.69E+06
Lactotransferrin	1.38E+09	7.34E+08
Leukocyte elastase inhibitor	8.21E+06	9.09E+06
Lysozyme C	2.75E+06	4.75E+05
Neutrophil defensin 1	1.79E+06	3.60E+06
Neutrophil gelatinase-associated lipocalin	4.22E+06	X
Plasma protease C1 inhibitor	9.83E+06	6.56E+06
Polymeric immunoglobulin receptor	5.24E+08	3.32E+08
Pulmonary surfactant-associated protein A	1.95E+08	5.87E+07
Pulmonary surfactant-associated protein D	4.71E+07	2.06E+07
Sushi domain-containing protein 2	X	9.38E+06
V-set and immunoglobulin domain-containing protein 6	2.22E+08	7.72E+07
V-set and immunoglobulin domain-containing protein 8	3.05E+07	X
Zinc-alpha-2-glycoprotein	1.16E+08	1.08E+08

Table A.6: *The biological process classification of Oxidant/antioxidant balance to Gene Ontology annotation of proteins identified. Data shown is a comparison of the mean of the three most abundant ion peaks of each protein identified, in Healthy Controls and Mild Asthmatics respectively, n=5 for both subject groups.*

Oxidant/antioxidant balance	**Healthy control**	**Mild Asthmatic**
Glutathione peroxidase 3	4.07E+06	X
Glutathione S-transferase A1	X	1.83E+07
Glutathione S-transferase A2	5.83E+07	X
Glutathione S-transferase omega-1	6.98E+06	X
Glutathione S-transferase P	3.42E+07	9.57E+06
Peroxiredoxin-5, mitochondrial	6.12E+06	X
Peroxiredoxin-6	2.13E+06	X
Protein DJ-1	3.98E+07	1.75E+07
Superoxide dismutase [Cu-Zn]	9.13E+06	6.94E+06
Thioredoxin	1.30E+07	1.15E+07

Table A7.: *The biological process classification of Protease/antiprotease balance to Gene Ontology annotation of proteins identified. Data shown is a comparison of the mean of the three most abundant ion peaks of each protein identified, in Healthy Controls and Mild Asthmatics respectively, n=5 for both subject groups.*

Protease/antiprotease balance	**Healthy control**	**Mild Asthmatic**
Alpha-1-antichymotrypsin	1.49E+08	3.86E+07
Alpha-1-antitrypsin	2.69E+09	7.42E+08
Alpha-2-macroglobulin	6.75E+07	6.40E+07
Alpha-N-acetylglucosaminidase	X	1.61E+06
Angiotensin-converting enzyme; Dipeptidyl carboxypeptidase I	2.86E+07	X
Antithrombin-III	2.92E+07	7.80E+06
Cathepsin D	1.10E+09	4.60E+08
Cathepsin Z	4.01E+06	X
Complement C2	6.82E+06	6.38E+06
Cystatin-B	7.58E+06	6.67E+06
Dermcidin	6.20E+06	3.67E+06
Dipeptidyl peptidase 4	1.64E+07	1.11E+07
Gastricsin	7.66E+06	1.71E+07
Haptoglobin	3.82E+08	1.13E+09
Kininogen-1; Alpha-2-thiol proteinase inhibitor	5.17E+06	X
Lactotransferrin	1.38E+09	7.34E+08
Latexin	X	2.49E+08
Leukocyte elastase inhibitor; Monocyte/Neutrophil elastase inhibitor	9.09E+06	8.21E+06
Matrix metalloproteinase-23	2.66E+06	X
Matrix metalloproteinase-28		x
Napsin-A	2.37E+06	1.75E+07
Pancreatic alpha-amylase	X	7.36E+06
Pro-cathepsin H	2.79E+07	2.12E+07

Probable hydrolase PNKD	1.07E+07	X
Prostasin	2.41E+06	2.35E+06
Proteasome subunit alpha type-1	X	3.32E+07
Protein DJ-1	3.98E+07	1.75E+07
Serpin B6	X	1.37E+06
Transmembrane protease serine 13	X	2.98E+07
Trypsin-3	X	2.49E+06
Xaa-Pro dipeptidase	1.18E+07	X

Appendix B

Table. B.1: *All alveolar proteins identified by 1D PAGE and nano LC MS/MS in healthy control RTLFs. The 199 proteins identified in healthy control subjects investigated, (n=5), alongside the mean of the three most abundant ion peaks of each respective protein identified. Accession numbers included according to entries in UniProtKB/Swiss-Prot*

Healthy Control	
Serotransferrin OS=Homo sapiens GN=TF PE=1 SV=3	1.28E+10
Ig gamma-1 chain C region; [Homo sapiens (Human)] - [IGHG1_HUMAN]	1.23E+10
Ig gamma-3 chain C region OS=Homo sapiens GN=IGHG3 PE=1 SV=2	9.36E+09
Ig gamma-2 chain C region OS=Homo sapiens GN=IGHG2 PE=1 SV=2	9.10E+09
Ig gamma-4 chain C region OS=Homo sapiens GN=IGHG4 PE=1 SV=1	9.10E+09
Ig kappa chain C region OS=Homo sapiens GN=IGKC PE=1 SV=1	5.90E+09
Uncharacterized protein C3orf38; [Homo sapiens (Human)] - [CC038_HUMAN]	4.10E+09
Serum albumin OS=Homo sapiens GN=ALB PE=1 SV=2	3.97E+09
Ig lambda-2 chain C regions OS=Homo sapiens GN=IGLC2 PE=1 SV=1	3.07E+09
Ig alpha-1 chain C region OS=Homo sapiens GN=IGHA1 PE=1 SV=2	2.81E+09
Alpha-1-antitrypsin OS=Homo sapiens GN=SERPINA1 PE=1 SV=3	2.69E+09
Ig alpha-2 chain C region OS=Homo sapiens GN=IGHA2 PE=1 SV=3	2.05E+09
Immunoglobulin lambda-like polypeptide 5; AltName: Full=G lambda-1; AltName: Full=Germline immunoglobulin lambda 1; Flags: Precursor; [Homo sapiens (Human)] - [IGLL5_HUMAN]	1.96E+09
Ig heavy chain V-III region HIL; [Homo sapiens (Human)] - [HV310_HUMAN]	1.66E+09
Lactotransferrin OS=Homo sapiens GN=LTF PE=1 SV=6	1.38E+09
Rho GDP-dissociation inhibitor 2 OS=Homo sapiens GN=ARHGDIB PE=1 SV=3	1.36E+09
Ig heavy chain V-III region VH26 OS=Homo sapiens PE=1 SV=1	1.25E+09
Ig heavy chain V-III region CAM OS=Homo sapiens PE=1 SV=1	1.22E+09
Ig heavy chain V-III region BRO; [Homo sapiens (Human)] - [HV305_HUMAN]	1.19E+09
Ig heavy chain V-III region TUR; [Homo sapiens (Human)] - [HV318_HUMAN]	1.18E+09
Ig heavy chain V-III region GAL OS=Homo sapiens PE=1 SV=1	1.17E+09
Ig heavy chain V-III region BUT OS=Homo sapiens PE=1 SV=1	1.16E+09
Cathepsin D OS=Homo sapiens GN=CTSD PE=1 SV=1	1.10E+09
Probable E3 ubiquitin-protein ligase HERC6; EC=6.3.2.-; AltName: Full=HECT domain and RCC1-like domain-containing protein 6; [Homo sapiens (Human)] - [HERC6_HUMAN]	8.68E+08
Hemopexin OS=Homo sapiens GN=HPX PE=1 SV=2	7.70E+08
Uteroglobin OS=Homo sapiens GN=SCGB1A1 PE=1 SV=1	6.27E+08
Ceruloplasmin OS=Homo sapiens GN=CP PE=1 SV=1	5.37E+08
Polymeric immunoglobulin receptor OS=Homo sapiens GN=PIGR PE=1 SV=4	5.24E+08
Ig kappa chain V-I region Wes; [Homo sapiens (Human)] - [KV119_HUMAN]	5.03E+08
Ig kappa chain V-I region DEE OS=Homo sapiens PE=1 SV=1	4.84E+08

Ig kappa chain V-I region WAT; [Homo sapiens (Human)] - [KV125_HUMAN]	4.74E+08
Ig lambda chain V-IV region Bau; [Homo sapiens (Human)] - [LV401_HUMAN]	4.40E+08
Ig kappa chain V-I region EU OS=Homo sapiens PE=1 SV=1	4.22E+08
Xin actin-binding repeat-containing protein 2 OS=Homo sapiens GN=XIRP2 PE=1 SV=2	4.22E+08
Haptoglobin OS=Homo sapiens GN=HP PE=1 SV=1	3.82E+08
Ig kappa chain V-III region VG; Flags: Precursor; Fragment; [Homo sapiens (Human)] - [KV309_HUMAN]	3.81E+08
Ig kappa chain V-III region SIE OS=Homo sapiens PE=1 SV=1	3.17E+08
Ig kappa chain V-III region POM OS=Homo sapiens PE=1 SV=1	3.13E+08
Ig kappa chain V-II region GM607; Flags: Precursor; Fragment; [Homo sapiens (Human)] - [KV205_HUMAN]	2.91E+08
Ig lambda chain V-IV region Hil; [Homo sapiens (Human)] - [LV403_HUMAN]	2.91E+08
Ig heavy chain V-III region GAR; [Homo sapiens (Human)] - [HV322_HUMAN]	2.84E+08
Ig lambda chain V-III region LOI OS=Homo sapiens PE=1 SV=1	2.61E+08
Ig kappa chain V-I region Scw; [Homo sapiens (Human)] - [KV117_HUMAN]	2.48E+08
Caspase recruitment domain-containing protein 6; [Homo sapiens (Human)] - [CARD6_HUMAN]	2.40E+08
Ig kappa chain V-III region Ti; [Homo sapiens (Human)] - [KV304_HUMAN]	2.35E+08
Putative V-set and immunoglobulin domain-containing protein 6 OS=Homo sapiens GN=VSIG6 PE=5 SV=2	2.22E+08
FAS-associated factor 1; Short=hFAF1; AltName: Full=UBX domain-containing protein 12; AltName: Full=UBX domain-containing protein 3A; [Homo sapiens (Human)] - [FAF1_HUMAN]	2.21E+08
Vitamin D-binding protein OS=Homo sapiens GN=GC PE=1 SV=1	2.19E+08
Ig lambda chain V-I region HA OS=Homo sapiens PE=1 SV=1	2.17E+08
Ig heavy chain V-I region HG3; Flags: Precursor; [Homo sapiens (Human)] - [HV102_HUMAN]	2.14E+08
Hemoglobin subunit alpha; AltName: Full=Alpha-globin; AltName: Full=Hemoglobin alpha chain; [Homo sapiens (Human)] - [HBA_HUMAN]	2.06E+08
Hemoglobin subunit beta OS=Homo sapiens GN=HBB PE=1 SV=2	2.06E+08
Alpha-1-acid glycoprotein 1 OS=Homo sapiens GN=ORM1 PE=1 SV=1	2.04E+08
Ig kappa chain V-I region Roy; [Homo sapiens (Human)] - [KV116_HUMAN]	1.96E+08
Pulmonary surfactant-associated protein A2 OS=Homo sapiens GN=SFTPA2 PE=1 SV=1	1.95E+08
Alpha-1-acid glycoprotein 2 OS=Homo sapiens GN=ORM2 PE=1 SV=2	1.81E+08
Ig kappa chain V-III region NG9; Flags: Precursor; Fragment; [Homo sapiens (Human)] - [KV303_HUMAN]	1.74E+08
Hemoglobin subunit delta OS=Homo sapiens GN=HBD PE=1 SV=2	1.66E+08
Ig kappa chain V-IV region Len OS=Homo sapiens PE=1 SV=2	1.66E+08
Desmoplakin OS=Homo sapiens GN=DSP PE=1 SV=3	1.60E+08
Alpha-1-antichymotrypsin OS=Homo sapiens GN=SERPINA3 PE=1 SV=2	1.49E+08
Ribonuclease P protein subunit p40; Short=RNaseP protein p40; EC=3.1.26.5; AltName: Full=RNase P subunit 1; [Homo sapiens (Human)] - [RPP40_HUMAN]	1.42E+08
Phosphatidylinositol 3,4,5-trisphosphate-dependent Rac exchanger 1 protein;	1.41E+08

Short=P-Rex1; Short=PtdIns(3,4,5)-dependent Rac exchanger 1; [Homo sapiens (Human)] - [PREX1_HUMAN]	
Alpha-1B-glycoprotein OS=Homo sapiens GN=A1BG PE=1 SV=4	1.36E+08
Ig lambda chain V-I region WAH OS=Homo sapiens PE=1 SV=1	1.26E+08
cGMP-specific 3',5'-cyclic phosphodiesterase; EC=3.1.4.35; AltName: Full=cGMP-binding cGMP-specific phosphodiesterase; Short=CGB-PDE; [Homo sapiens (Human)] - [PDE5A_HUMAN]	1.22E+08
Beta-2-microglobulin OS=Homo sapiens GN=B2M PE=1 SV=1	1.20E+08
Zinc-alpha-2-glycoprotein OS=Homo sapiens GN=AZGP1 PE=1 SV=2	1.16E+08
Ig kappa chain V-I region Ni; [Homo sapiens (Human)] - [KV121_HUMAN]	1.15E+08
Ig heavy chain V-II region NEWM; [Homo sapiens (Human)] - [HV207_HUMAN]	1.14E+08
LIM domain only protein 7; Short=LMO-7; AltName: Full=F-box only protein 20; AltName: Full=LOMP; [Homo sapiens (Human)] - [LMO7_HUMAN]	1.14E+08
Transthyretin OS=Homo sapiens GN=TTR PE=1 SV=1	1.12E+08
14-3-3 protein beta/alpha OS=Homo sapiens GN=YWHAB PE=1 SV=3	1.07E+08
14-3-3 protein gamma OS=Homo sapiens GN=YWHAG PE=1 SV=2	1.07E+08
14-3-3 protein zeta/delta OS=Homo sapiens GN=YWHAZ PE=1 SV=1	1.07E+08
Ig lambda chain V region 4A OS=Homo sapiens PE=4 SV=1	1.06E+08
Angiotensinogen OS=Homo sapiens GN=AGT PE=1 SV=1	9.61E+07
Apolipoprotein A-I OS=Homo sapiens GN=APOA1 PE=1 SV=1	9.59E+07
Protein S100-A6 OS=Homo sapiens GN=S100A6 PE=1 SV=1	9.49E+07
Ig kappa chain V-IV region JI; Flags: Precursor; [Homo sapiens (Human)] - [KV403_HUMAN]	9.06E+07
14-3-3 protein epsilon OS=Homo sapiens GN=YWHAE PE=1 SV=1	9.02E+07
Protein Shroom3; AltName: Full=Shroom-related protein; Short=hShrmL; [Homo sapiens (Human)] - [SHRM3_HUMAN]	8.34E+07
Immunoglobulin J chain OS=Homo sapiens GN=IGJ PE=1 SV=4	8.29E+07
Histone-lysine N-methyltransferase MLL3 OS=Homo sapiens GN=MLL3 PE=1 SV=3	7.98E+07
Pre-mRNA cleavage complex 2 protein Pcf11; AltName: Full=Pre-mRNA cleavage complex II protein Pcf11; [Homo sapiens (Human)] - [PCF11_HUMAN]	7.88E+07
CD44 antigen OS=Homo sapiens GN=CD44 PE=1 SV=3	7.78E+07
Ig heavy chain V-II region ARH-77 OS=Homo sapiens PE=4 SV=1	7.57E+07
Alpha-2-HS-glycoprotein OS=Homo sapiens GN=AHSG PE=1 SV=1	7.52E+07
Ig lambda chain V-I region NIG-64 OS=Homo sapiens PE=1 SV=1	6.96E+07
ATP-binding cassette sub-family C member 8; AltName: Full=Sulfonylurea receptor 1; [Homo sapiens (Human)] - [ABCC8_HUMAN]	6.85E+07
Coiled-coil domain-containing protein 37; [Homo sapiens (Human)] - [CCD37_HUMAN]	6.84E+07
Ig heavy chain V-II region OU; [Homo sapiens (Human)] - [HV201_HUMAN]	6.80E+07
Alpha-2-macroglobulin OS=Homo sapiens GN=A2M PE=1 SV=3	6.75E+07
Annexin A5 OS=Homo sapiens GN=ANXA5 PE=1 SV=2	6.60E+07
Ig mu chain C region OS=Homo sapiens GN=IGHM PE=1 SV=3	6.47E+07
Ig heavy chain V-I region V35 OS=Homo sapiens PE=1 SV=1	6.05E+07
Glucosamine--fructose-6-phosphate aminotransferase [isomerizing] 2; EC=2.6.1.16; AltName: Full=D-fructose-6-phosphate amidotransferase 2; AltName: Full=Glutamine:fructose 6 phosphate amidotransferase 2; Short=GFAT 2; Short=GFAT2; AltName: Full=Hexosephosphate	5.95E+07

aminotransferase 2; [Homo sapiens (Human)] - [GFPT2_HUMAN]	
Glutathione S-transferase A2 OS=Homo sapiens GN=GSTA2 PE=1 SV=4	5.83E+07
Beta-microseminoprotein; AltName: Full=Immunoglobulin-binding factor; Short=IGBF; AltName: Full=PN44; AltName: Full=Prostate secreted seminal plasma protein; AltName: Full=Prostate secretory protein of 94 amino acids; Short=PSP-94; Short=PSP94; AltName: Full=Seminal plasma beta-inhibin; Flags: Precursor; [Homo sapiens (Human)] - [MSMB_HUMAN]	5.82E+07
Deleted in malignant brain tumors 1 protein OS=Homo sapiens GN=DMBT1 PE=1 SV=2	5.59E+07
Actin, cytoplasmic 1 OS=Homo sapiens GN=ACTB PE=1 SV=1	5.55E+07
Epididymal secretory protein E1 OS=Homo sapiens GN=NPC2 PE=1 SV=1	5.26E+07
Corticosteroid-binding globulin OS=Homo sapiens GN=SERPINA6 PE=1 SV=1	5.17E+07
28S ribosomal protein S26, mitochondrial; Short=MRP-S26; Short=S26mt; AltName: Full=28S ribosomal protein S13, mitochondrial; Short=MRP-S13; Short=S13mt; Flags: Precursor; [Homo sapiens (Human)] - [RT26_HUMAN]	4.89E+07
Transmembrane protein 198; [Homo sapiens (Human)] - [TM198_HUMAN]	4.77E+07
Histone H4 OS=Homo sapiens GN=HIST1H4A PE=1 SV=2	4.75E+07
Pulmonary surfactant-associated protein D OS=Homo sapiens GN=SFTPD PE=1 SV=3	4.71E+07
G antigen family D member 2; AltName: Full=Cancer/testis antigen 12.1; Short=CT12.1; AltName: Full=Protein XAGE-1; [Homo sapiens (Human)] - [GAGD2_HUMAN]	4.41E+07
Intercellular adhesion molecule 1 OS=Homo sapiens GN=ICAM1 PE=1 SV=2	4.01E+07
Protein DJ-1 OS=Homo sapiens GN=PARK7 PE=1 SV=2	3.98E+07
Triosephosphate isomerase OS=Homo sapiens GN=TPI1 PE=1 SV=3	3.83E+07
Calmodulin OS=Homo sapiens GN=CALM1 PE=1 SV=2	3.58E+07
Coactosin-like protein OS=Homo sapiens GN=COTL1 PE=1 SV=3	3.46E+07
Glutathione S-transferase P OS=Homo sapiens GN=GSTP1 PE=1 SV=2	3.42E+07
Serpin B3 OS=Homo sapiens GN=SERPINB3 PE=1 SV=2	3.01E+07
Antithrombin-III OS=Homo sapiens GN=SERPINC1 PE=1 SV=1	2.92E+07
Angiotensin-converting enzyme OS=Homo sapiens GN=ACE PE=1 SV=1	2.86E+07
Ig lambda chain V-III region SH; [Homo sapiens (Human)] - [LV301_HUMAN]	2.83E+07
Pro-cathepsin H OS=Homo sapiens GN=CTSH PE=1 SV=4	2.79E+07
Apolipoprotein A-II OS=Homo sapiens GN=APOA2 PE=1 SV=1	2.59E+07
Afamin OS=Homo sapiens GN=AFM PE=1 SV=1	2.55E+07
Pulmonary surfactant-associated protein B OS=Homo sapiens GN=SFTPB PE=1 SV=3	2.54E+07
Annexin A4 OS=Homo sapiens GN=ANXA4 PE=1 SV=4	2.52E+07
Selenium-binding protein 1 OS=Homo sapiens GN=SELENBP1 PE=1 SV=2	2.43E+07
Carbonic anhydrase 1 OS=Homo sapiens GN=CA1 PE=1 SV=2	2.36E+07
Transaldolase OS=Homo sapiens GN=TALDO1 PE=1 SV=2	2.33E+07
Scavenger receptor cysteine-rich type 1 protein M130 OS=Homo sapiens GN=CD163 PE=1 SV=2	2.29E+07
CD9 antigen OS=Homo sapiens GN=CD9 PE=1 SV=4	2.20E+07
Complement C4-A; AltName: Full=Acidic complement C4; AltName: Full=C3 and PZP-like alpha-2-macroglobulin domain-containing protein 2; Contains: RecName: Full=Complement C4 beta chain; Contains: RecName: Full=Complement C4-A alpha chain; Contains: RecName: Full=C4a anaphylatoxin; Contains: RecName: Full=C4b-A; Contains: RecName:	1.80E+07

Full=C4d-A; Contains: RecName: Full=Complement C4 gamma chain; Flags: Precursor; [Homo sapiens (Human)] - [CO4A_HUMAN]	
Delta-like protein 4; AltName: Full=Drosophila Delta homolog 4; Short=Delta4; Flags: Precursor; [Homo sapiens (Human)] - [DLL4_HUMAN]	1.80E+07
Mesothelin OS=Homo sapiens GN=MSLN PE=1 SV=2	1.78E+07
Dipeptidyl peptidase 4 OS=Homo sapiens GN=DPP4 PE=1 SV=2	1.64E+07
Actin-related protein 2; AltName: Full=Actin-like protein 2; [Homo sapiens (Human)] - [ARP2_HUMAN]	1.56E+07
Uncharacterized protein KIAA0947; [Homo sapiens (Human)] - [K0947_HUMAN]	1.56E+07
Thyroxine-binding globulin OS=Homo sapiens GN=SERPINA7 PE=1 SV=2	1.56E+07
Complement decay-accelerating factor OS=Homo sapiens GN=CD55 PE=1 SV=4	1.49E+07
Aldo-keto reductase family 1 member C3; EC=1.-.-.-; AltName: Full=17-beta-hydroxysteroid dehydrogenase type 5; Short=17-beta-HSD 5; AltName: Full=3-alpha-HSD type II, brain; AltName: Full=3-alpha-hydroxysteroid dehydrogenase type 2; Short=3-alpha-HSD type 2; EC=1.1.1.213; AltName: Full=Chlordecone reductase homolog HAKRb; AltName: Full=Dihydrodiol dehydrogenase 3; Short=DD-3; Short=DD3; AltName: Full=Dihydrodiol dehydrogenase type I; AltName: Full=HA1753; AltName: Full=Indanol dehydrogenase; EC=1.1.1.112; AltName: Full=Prostaglandin F synthase; Short=PGFS; EC=1.1.1.188; AltName: Full=Testosterone 17-beta-dehydrogenase 5; EC=1.1.1.63; EC=1.1.1.64; AltName: Full=Trans-1,2-dihydrobenzene-1,2-diol dehydrogenase; EC=1.3.1.20; [Homo sapiens (Human)] - [AK1C3_HUMAN]	1.46E+07
Protein kinase-like protein SgK196; AltName: Full=Sugen kinase 196; [Homo sapiens (Human)] - [SG196_HUMAN]	1.39E+07
Mucin-1 OS=Homo sapiens GN=MUC1 PE=1 SV=3	1.31E+07
Thioredoxin; Short=Trx; AltName: Full=ATL-derived factor; Short=ADF; AltName: Full=Surface-associated sulphydryl protein; Short=SASP; [Homo sapiens (Human)] - [THIO_HUMAN]	1.30E+07
Retinoic acid-induced protein 3 OS=Homo sapiens GN=GPRC5A PE=1 SV=2	1.29E+07
Complement C3 OS=Homo sapiens GN=C3 PE=1 SV=2	1.25E+07
Peptidyl-prolyl cis-trans isomerase A OS=Homo sapiens GN=PPIA PE=1 SV=2	1.19E+07
Biotinidase OS=Homo sapiens GN=BTD PE=1 SV=2	1.19E+07
Xaa-Pro dipeptidase; Short=X-Pro dipeptidase; EC=3.4.13.9; AltName: Full=Imidodipeptidase; AltName: Full=Peptidase D; AltName: Full=Proline dipeptidase; Short=Prolidase; [Homo sapiens (Human)] - [PEPD_HUMAN]	1.18E+07
Galectin-3-binding protein OS=Homo sapiens GN=LGALS3BP PE=1 SV=1	1.14E+07
Puromycin-sensitive aminopeptidase; Short=PSA; EC=3.4.11.14; AltName: Full=Cytosol alanyl aminopeptidase; Short=AAP-S; [Homo sapiens (Human)] - [PSA_HUMAN]	1.13E+07
SH3 domain-binding glutamic acid-rich-like protein 3; AltName: Full=SH3 domain-binding protein 1; Short=SH3BP-1; [Homo sapiens (Human)] - [SH3L3_HUMAN]	1.13E+07
Attractin OS=Homo sapiens GN=ATRN PE=1 SV=2	1.13E+07
Histone H3.3C; [Homo sapiens (Human)] - [H3C_HUMAN]	1.08E+07
Apolipoprotein A-IV OS=Homo sapiens GN=APOA4 PE=1 SV=3	1.04E+07
Gelsolin OS=Homo sapiens GN=GSN PE=1 SV=1	9.95E+06
Plasma protease C1 inhibitor OS=Homo sapiens GN=SERPING1 PE=1 SV=2	9.83E+06

Fatty acid-binding protein, adipocyte OS=Homo sapiens GN=FABP4 PE=1 SV=3	9.73E+06
Ig lambda chain V-V region DEL; [Homo sapiens (Human)] - [LV501_HUMAN]	9.50E+06
Carbonic anhydrase 2 OS=Homo sapiens GN=CA2 PE=1 SV=2	9.50E+06
Superoxide dismutase [Cu-Zn] OS=Homo sapiens GN=SOD1 PE=1 SV=2	9.13E+06
Transcriptional adapter 2-beta; AltName: Full=ADA2-like protein beta; Short=ADA2-beta; [Homo sapiens (Human)] - [TAD2B_HUMAN]	8.54E+06
Leukocyte elastase inhibitor OS=Homo sapiens GN=SERPINB1 PE=1 SV=1	8.21E+06
V-set and immunoglobulin domain-containing protein 4; AltName: Full=Protein Z39Ig; Flags: Precursor; [Homo sapiens (Human)] - [VSIG4_HUMAN]	8.17E+06
Protein S100-A11 OS=Homo sapiens GN=S100A11 PE=1 SV=2	7.59E+06
Cystatin-B OS=Homo sapiens GN=CSTB PE=1 SV=2	7.58E+06
Cell adhesion molecule 1; AltName: Full=Immunoglobulin superfamily member 4; Short=IgSF4; AltName: Full=Nectin-like protein 2; Short=NECL-2; AltName: Full=Spermatogenic immunoglobulin superfamily; Short=SgIgSF; AltName: Full=Synaptic cell adhesion molecule; Short=SynCAM; AltName: Full=Tumor suppressor in lung cancer 1; Short=TSLC-1; Flags: Precursor; [Homo sapiens (Human)] - [CADM1_HUMAN]	7.37E+06
Long palate, lung and nasal epithelium carcinoma-associated protein 1; AltName: Full=Von Ebner minor salivary gland protein; Short=VEMSGP; Flags: Precursor; [Homo sapiens (Human)] - [LPLC1_HUMAN]	7.16E+06
Glutathione S-transferase omega-1 OS=Homo sapiens GN=GSTO1 PE=1 SV=2	6.98E+06
Complement C2 OS=Homo sapiens GN=C2 PE=1 SV=2	6.82E+06
Ig delta chain C region; [Homo sapiens (Human)] - [IGHD_HUMAN]	6.39E+06
Dermcidin OS=Homo sapiens GN=DCD PE=1 SV=2	6.20E+06
Peroxiredoxin-5, mitochondrial OS=Homo sapiens GN=PRDX5 PE=1 SV=4	6.12E+06
Vitamin K-dependent protein S; Flags: Precursor; [Homo sapiens (Human)] - [PROS_HUMAN]	6.05E+06
Junctional adhesion molecule A OS=Homo sapiens GN=F11R PE=1 SV=1	5.60E+06
Heme-binding protein 2; AltName: Full=Placental protein 23; Short=PP23; AltName: Full=Protein SOUL; [Homo sapiens (Human)] - [HEBP2_HUMAN]	5.28E+06
Glyoxalase domain-containing protein 4 OS=Homo sapiens GN=GLOD4 PE=1 SV=1	5.28E+06
Kininogen-1 OS=Homo sapiens GN=KNG1 PE=1 SV=2	5.17E+06
Prostaglandin-H2 D-isomerase; EC=5.3.99.2; AltName: Full=Beta-trace protein; AltName: Full=Cerebrin-28; AltName: Full=Glutathione-independent PGD synthase; AltName: Full=Lipocalin-type prostaglandin-D synthase; AltName: Full=Prostaglandin-D2 synthase; Short=PGD2 synthase; Short=PGDS; Short=PGDS2; Flags: Precursor; [Homo sapiens (Human)] - [PTGDS_HUMAN]	4.69E+06
Hornerin OS=Homo sapiens GN=HRNR PE=1 SV=2	4.56E+06
Myoglobin; [Homo sapiens (Human)] - [MYG_HUMAN]	4.44E+06
Putative inactive carboxylesterase 4; AltName: Full=Inactive carboxylesterase 1 pseudogene 1; AltName: Full=Placental carboxylesterase 3; Short=PCE-3; Flags: Precursor; [Homo sapiens (Human)] - [CES1P_HUMAN]	4.34E+06
Neutrophil gelatinase-associated lipocalin; Short=NGAL; AltName: Full=25 kDa alpha-2-microglobulin-related subunit of MMP-9; AltName:	4.22E+06

Full=Lipocalin-2; AltName: Full=Oncogene 24p3; AltName: Full=p25; Flags: Precursor; [Homo sapiens (Human)] - [NGAL_HUMAN]	
Glutathione peroxidase 3 OS=Homo sapiens GN=GPX3 PE=1 SV=2	4.07E+06
CD59 glycoprotein OS=Homo sapiens GN=CD59 PE=1 SV=1	4.04E+06
Phosphatidylethanolamine-binding protein 1; Short=PEBP-1; AltName: Full=HCNPpp; AltName: Full=Neuropolypeptide h3; AltName: Full=Prostatic-binding protein; AltName: Full=Raf kinase inhibitor protein; Short=RKIP; Contains: RecName: Full=Hippocampal cholinergic neurostimulating peptide; Short=HCNP; [Homo sapiens (Human)] - [PEBP1_HUMAN]	4.01E+06
Phosphoglycerate mutase 1 OS=Homo sapiens GN=PGAM1 PE=1 SV=2	3.87E+06
Leucine-rich alpha-2-glycoprotein OS=Homo sapiens GN=LRG1 PE=1 SV=2	3.79E+06
Thioredoxin domain-containing protein 17; AltName: Full=14 kDa thioredoxin-related protein; Short=TRP14; AltName: Full=Protein 42-9-9; AltName: Full=Thioredoxin-like protein 5; [Homo sapiens (Human)] - [TXD17_HUMAN]	3.64E+06
Serpin B6; AltName: Full=Cytoplasmic antiproteinase; Short=CAP; AltName: Full=Peptidase inhibitor 6; Short=PI-6; AltName: Full=Placental thrombin inhibitor; [Homo sapiens (Human)] - [SPB6_HUMAN]	3.30E+06
Eosinophil lysophospholipase; EC=3.1.1.5; AltName: Full=Charcot-Leyden crystal protein; Short=CLC; AltName: Full=Galectin-10; Short=Gal-10; AltName: Full=Lysolecithin acylhydrolase; [Homo sapiens (Human)] - [LPPL_HUMAN]	3.22E+06
Folate receptor alpha OS=Homo sapiens GN=FOLR1 PE=1 SV=3	3.11E+06
Transmembrane protein 200C; AltName: Full=Transmembrane protein TTMA; AltName: Full=Two transmembrane domain-containing family member A; [Homo sapiens (Human)] - [T200C_HUMAN]	2.87E+06
SH3 domain-binding glutamic acid-rich-like protein OS=Homo sapiens GN=SH3BGRL PE=1 SV=1	2.80E+06
Aldose 1-epimerase OS=Homo sapiens GN=GALM PE=1 SV=1	2.77E+06
Lysozyme C OS=Homo sapiens GN=LYZ PE=1 SV=1	2.75E+06
Matrix metalloproteinase-23; Short=MMP-23; EC=3.4.24.-; AltName: Full=Femalysin; AltName: Full=MIFR-1; AltName: Full=Matrix metalloproteinase-21; Short=MMP-21; AltName: Full=Matrix metalloproteinase-22; Short=MMP-22; Contains: RecName: Full=Matrix metalloproteinase-23, soluble form; Flags: Precursor; [Homo sapiens (Human)] - [MMP23_HUMAN]	2.66E+06
Napsin-A OS=Homo sapiens GN=NAPSA PE=1 SV=1	2.37E+06
Peroxiredoxin-6 OS=Homo sapiens GN=PRDX6 PE=1 SV=3	2.13E+06
Protein S100-P; AltName: Full=Protein S100-E; AltName: Full=S100 calcium-binding protein P; [Homo sapiens (Human)] - [S100P_HUMAN]	2.12E+06
Neutrophil defensin 1 OS=Homo sapiens GN=DEFA1 PE=1 SV=1	1.79E+06
Gamma-glutamylcyclotransferase; EC=2.3.2.4; AltName: Full=Cytochrome c-releasing factor 21; [Homo sapiens (Human)] - [GGCT_HUMAN]	1.29E+06
Sodium-dependent phosphate transport protein 2B; Short=Sodium-phosphate transport protein 2B; AltName: Full=Na(+)-dependent phosphate cotransporter 2B; AltName: Full=NaPi3b; AltName: Full=Sodium/phosphate cotransporter 2B; Short=Na(+)/Pi cotransporter 2B; Short=NaPi-2b; AltName: Full=Solute carrier family 34 member 2; [Homo sapiens (Human)] - [NPT2B_HUMAN]	1.14E+06

Table B.2: *All alveolar proteins identified by 1D PAGE and nano LC MS/MS in healthy aged RTLFs. The 163 proteins identified in healthy aged subjects investigated, (n=5), alongside the mean of the three most abundant ion peaks of each respective protein identified. Accession numbers included according to entries in UniProtKB/Swiss-Prot.*

Healthy Aged Control	
14-3-3 protein beta/alpha OS=Homo sapiens GN=YWHAB PE=1 SV=3	1.46E+07
14-3-3 protein epsilon OS=Homo sapiens GN=YWHAE PE=1 SV=1	1.86E+07
14-3-3 protein zeta/delta OS=Homo sapiens GN=YWHAZ PE=1 SV=1	1.57E+07
7-alpha-hydroxycholest-4-en-3-one 12-alpha-hydroxylase; EC=1.14.13.95; AltName: Full=7-alpha-hydroxy-4-cholesten-3-one 12-alpha-hydroxylase; AltName: Full=CYPVIIIB1; AltName: Full=Cytochrome P450 8B1; AltName: Full=Sterol 12-alpha-hydroxylase; [Homo sapiens (Human)] - [CP8B1_HUMAN]	4.20E+07
Actin-related protein 2; AltName: Full=Actin-like protein 2; [Homo sapiens (Human)] - [ARP2_HUMAN]	1.97E+07
Actin, cytoplasmic 1 OS=Homo sapiens GN=ACTB PE=1 SV=1	6.89E+07
Afamin OS=Homo sapiens GN=AFM PE=1 SV=1	2.54E+07
Aldo-keto reductase family 1 member C3; EC=1.-.-.-; AltName: Full=17-beta-hydroxysteroid dehydrogenase type 5; Short=17-beta-HSD 5; AltName: Full=3-alpha-HSD type II, brain; AltName: Full=3-alpha-hydroxysteroid dehydrogenase type 2; Short=3-alpha-HSD type 2; EC=1.1.1.213; AltName: Full=Chlordecone reductase homolog HAKRb; AltName: Full=Dihydrodiol dehydrogenase 3; Short=DD-3; Short=DD3; AltName: Full=Dihydrodiol dehydrogenase type I; AltName: Full=HA1753; AltName: Full=Indanol dehydrogenase; EC=1.1.1.112; AltName: Full=Prostaglandin F synthase; Short=PGFS; EC=1.1.1.188; AltName: Full=Testosterone 17-beta-dehydrogenase 5; EC=1.1.1.63; EC=1.1.1.64; AltName: Full=Trans-1,2-dihydrobenzene-1,2-diol dehydrogenase; EC=1.3.1.20; [Homo sapiens (Human)] - [AK1C3_HUMAN]	3.18E+07
Alpha-1-acid glycoprotein 1 OS=Homo sapiens GN=ORM1 PE=1 SV=1	3.39E+08
Alpha-1-acid glycoprotein 2 OS=Homo sapiens GN=ORM2 PE=1 SV=2	2.40E+08
Alpha-1-antichymotrypsin OS=Homo sapiens GN=SERPINA3 PE=1 SV=2	8.21E+07
Alpha-1-antitrypsin OS=Homo sapiens GN=SERPINA1 PE=1 SV=3	3.20E+09
Alpha-1B-glycoprotein OS=Homo sapiens GN=A1BG PE=1 SV=4	1.33E+08
Alpha-2-HS-glycoprotein OS=Homo sapiens GN=AHSG PE=1 SV=1	1.16E+08
Alpha-2-macroglobulin OS=Homo sapiens GN=A2M PE=1 SV=3	1.66E+08
Alpha-enolase OS=Homo sapiens GN=ENO1 PE=1 SV=2	4.14E+06
Angiotensin-converting enzyme; Short=ACE; EC=3.2.1.-; EC=3.4.15.1; AltName: Full=Dipeptidyl carboxypeptidase I; AltName: Full=Kininase II; AltName: CD_antigen=CD143; Contains: RecName: Full=Angiotensin-converting enzyme, soluble form; Flags: Precursor; [Homo sapiens (Human)] - [ACE_HUMAN]	1.46E+07
Angiotensinogen OS=Homo sapiens GN=AGT PE=1 SV=1	4.94E+07
Annexin A5 OS=Homo sapiens GN=ANXA5 PE=1 SV=2	1.36E+06
Antithrombin-III OS=Homo sapiens GN=SERPINC1 PE=1 SV=1	1.84E+07
Apolipoprotein A-I OS=Homo sapiens GN=APOA1 PE=1 SV=1	1.38E+08
Apolipoprotein A-II OS=Homo sapiens GN=APOA2 PE=1 SV=1	7.40E+07
Apolipoprotein A-IV OS=Homo sapiens GN=APOA4 PE=1 SV=3	2.74E+07
ATP-binding cassette sub-family F member 1; AltName: Full=ATP-binding cassette 50; AltName: Full=TNF-alpha-stimulated ABC protein; [Homo	1.17E+07

sapiens (Human)] - [ABCF1_HUMAN]	
Attractin OS=Homo sapiens GN=ATRN PE=1 SV=2	5.23E+06
Beta-2-microglobulin OS=Homo sapiens GN=B2M PE=1 SV=1	2.59E+07
Biotinidase OS=Homo sapiens GN=BTD PE=1 SV=2	2.84E+06
C2 calcium-dependent domain-containing protein 4B; AltName: Full=Nuclear-localized factor 2; AltName: Full=Protein FAM148B; [Homo sapiens (Human)] - [C2C4B_HUMAN]	8.25E+07
Calmodulin OS=Homo sapiens GN=CALM1 PE=1 SV=2	2.68E+06
Calmodulin-like protein 5; AltName: Full=Calmodulin-like skin protein; [Homo sapiens (Human)] - [CALL5_HUMAN]	2.82E+07
Carbonic anhydrase 1 OS=Homo sapiens GN=CA1 PE=1 SV=2	3.91E+06
CD166 antigen; AltName: Full=Activated leukocyte cell adhesion molecule; AltName: CD_antigen=CD166; Flags: Precursor; [Homo sapiens (Human)] - [CD166_HUMAN]	1.35E+07
CD44 antigen OS=Homo sapiens GN=CD44 PE=1 SV=3	2.73E+07
CD59 glycoprotein; AltName: Full=1F5 antigen; AltName: Full=20 kDa homologous restriction factor; Short=HRF-20; Short=HRF20; AltName: Full=MAC-inhibitory protein; Short=MAC-IP; AltName: Full=MEM43 antigen; AltName: Full=Membrane attack complex inhibition factor; Short=MACIF; AltName: Full=Membrane inhibitor of reactive lysis; Short=MIRL; AltName: Full=Protectin; AltName: CD_antigen=CD59; Flags: Precursor; [Homo sapiens (Human)] - [CD59_HUMAN]	3.54E+06
CD9 antigen; AltName: Full=5H9 antigen; AltName: Full=Cell growth-inhibiting gene 2 protein; AltName: Full=Leukocyte antigen MIC3; AltName: Full=Motility-related protein; Short=MRP-1; AltName: Full=Tetraspanin-29; Short=Tspan-29; AltName: Full=p24; AltName: CD_antigen=CD9; [Homo sapiens (Human)] - [CD9_HUMAN]	9.50E+06
Cell adhesion molecule 2; AltName: Full=Immunoglobulin superfamily member 4D; Short=IgSF4D; AltName: Full=Nectin-like protein 3; Short=NECL-3; Flags: Precursor; [Homo sapiens (Human)] - [CADM2_HUMAN]	2.00E+06
Ceruloplasmin OS=Homo sapiens GN=CP PE=1 SV=1	3.67E+08
Coactosin-like protein OS=Homo sapiens GN=COTL1 PE=1 SV=3	5.15E+06
Complement C2 OS=Homo sapiens GN=C2 PE=1 SV=2	3.41E+07
Complement C3 OS=Homo sapiens GN=C3 PE=1 SV=2	2.66E+06
Complement decay-accelerating factor OS=Homo sapiens GN=CD55 PE=1 SV=4	7.63E+06
Corticosteroid-binding globulin OS=Homo sapiens GN=SERPINA6 PE=1 SV=1	3.95E+07
Deleted in malignant brain tumors 1 protein OS=Homo sapiens GN=DMBT1 PE=1 SV=2	3.69E+07
Delta-like protein 4; AltName: Full=Drosophila Delta homolog 4; Short=Delta4; Flags: Precursor; [Homo sapiens (Human)] - [DLL4_HUMAN]	1.23E+07
Dermcidin OS=Homo sapiens GN=DCD PE=1 SV=2	2.13E+06
Desmoplakin OS=Homo sapiens GN=DSP PE=1 SV=3	1.40E+08
Dipeptidyl peptidase 4 OS=Homo sapiens GN=DPP4 PE=1 SV=2	6.17E+07
Disintegrin and metalloproteinase domain-containing protein 2; Short=ADAM 2; AltName: Full=Cancer/testis antigen 15; Short=CT15; AltName: Full=Fertilin subunit beta; AltName: Full=PH-30; Short=PH30; AltName: Full=PH30-beta; Flags: Precursor; [Homo sapiens (Human)] - [ADAM2_HUMAN]	1.05E+08

Ecto-ADP-ribosyltransferase 4; EC=2.4.2.31; AltName: Full=Dombrock blood group carrier molecule; AltName: Full=Mono(ADP-ribosyl)transferase 4; AltName: Full=NAD(P)(+)--arginine ADP-ribosyltransferase 4; AltName: CD_antigen=CD297; Flags: Precursor; [Homo sapiens (Human)] - [NAR4_HUMAN]	5.81E+07
Elongation factor 1-alpha 1 OS=Homo sapiens GN=EEF1A1 PE=1 SV=1	2.16E+07
Epididymal secretory protein E1 OS=Homo sapiens GN=NPC2 PE=1 SV=1	1.37E+07
FAS-associated factor 1; Short=hFAF1; AltName: Full=UBX domain-containing protein 12; AltName: Full=UBX domain-containing protein 3A; [Homo sapiens (Human)] - [FAF1_HUMAN]	4.89E+08
Ferritin heavy chain; Short=Ferritin H subunit; EC=1.16.3.1; AltName: Full=Cell proliferation-inducing gene 15 protein; [Homo sapiens (Human)] - [FRIH_HUMAN]	2.34E+06
Ferritin light chain; Short=Ferritin L subunit; [Homo sapiens (Human)] - [FRIL_HUMAN]	4.73E+06
Galectin-3-binding protein; AltName: Full=Basement membrane autoantigen p105; AltName: Full=Lectin galactoside-binding soluble 3-binding protein; AltName: Full=Mac-2-binding protein; Short=MAC2BP; Short=Mac-2 BP; AltName: Full=Tumor-associated antigen 90K; Flags: Precursor; [Homo sapiens (Human)] - [LG3BP_HUMAN]	7.88E+06
Galectin-3; Short=Gal-3; AltName: Full=35 kDa lectin; AltName: Full=Carbohydrate-binding protein 35; Short=CBP 35; AltName: Full=Galactose-specific lectin 3; AltName: Full=Galactoside-binding protein; Short=GALBP; AltName: Full=IgE-binding protein; AltName: Full=L-31; AltName: Full=Laminin-binding protein; AltName: Full=Lectin L-29; AltName: Full=Mac-2 antigen; [Homo sapiens (Human)] - [LEG3_HUMAN]	2.03E+06
Glutathione peroxidase 3 OS=Homo sapiens GN=GPX3 PE=1 SV=2	1.19E+06
Glutathione S-transferase A2 OS=Homo sapiens GN=GSTA2 PE=1 SV=4	4.18E+07
Glutathione S-transferase P OS=Homo sapiens GN=GSTP1 PE=1 SV=2	8.51E+06
Haptoglobin OS=Homo sapiens GN=HP PE=1 SV=1	1.26E+08
Heat shock protein beta-1 OS=Homo sapiens GN=HSPB1 PE=1 SV=2	8.93E+06
Hemoglobin subunit alpha OS=Homo sapiens GN=HBA1 PE=1 SV=2	1.49E+08
Hemoglobin subunit beta OS=Homo sapiens GN=HBB PE=1 SV=2	1.28E+08
Hemoglobin subunit delta OS=Homo sapiens GN=HBD PE=1 SV=2	7.65E+07
Hemopexin OS=Homo sapiens GN=HPX PE=1 SV=2	2.71E+08
Histone H3.3C; [Homo sapiens (Human)] - [H3C_HUMAN]	1.79E+07
Histone H4 OS=Homo sapiens GN=HIST1H4A PE=1 SV=2	2.45E+07
HLA class II histocompatibility antigen, DR alpha chain; AltName: Full=MHC class II antigen DRA; Flags: Precursor; [Homo sapiens (Human)] - [DRA_HUMAN]	1.69E+06
HLA class II histocompatibility antigen, DRB1-1 beta chain OS=Homo sapiens GN=HLA-DRB1 PE=1 SV=2	6.88E+06
Homeobox protein Nkx-3.2; AltName: Full=Bagpipe homeobox protein homolog 1; AltName: Full=Homeobox protein NK-3 homolog B; [Homo sapiens (Human)] - [NKX32_HUMAN]	1.75E+07
Ig alpha-1 chain C region OS=Homo sapiens GN=IGHA1 PE=1 SV=2	2.42E+09
Ig alpha-2 chain C region OS=Homo sapiens GN=IGHA2 PE=1 SV=3	1.79E+09
Ig delta chain C region OS=Homo sapiens GN=IGHD PE=1 SV=2	1.10E+07
Ig gamma-1 chain C region OS=Homo sapiens GN=IGHG1 PE=1 SV=1	8,918,000,000
Ig gamma-2 chain C region OS=Homo sapiens GN=IGHG2 PE=1 SV=2	5.60E+09
Ig gamma-3 chain C region OS=Homo sapiens GN=IGHG3 PE=1 SV=2	6.71E+09

Ig gamma-4 chain C region OS=Homo sapiens GN=IGHG4 PE=1 SV=1	5.60E+09
Ig heavy chain V-I region Mot OS=Homo sapiens PE=1 SV=1	2.05E+08
Ig heavy chain V-II region ARH-77; Flags: Precursor; [Homo sapiens (Human)] - [HV209_HUMAN]	4.86E+07
Ig heavy chain V-II region NEWM OS=Homo sapiens PE=1 SV=1	1.47E+08
Ig heavy chain V-II region OU; [Homo sapiens (Human)] - [HV201_HUMAN]	1.44E+08
Ig heavy chain V-III region BRO; [Homo sapiens (Human)] - [HV305_HUMAN]	1.02E+09
Ig heavy chain V-III region BUT; [Homo sapiens (Human)] - [HV306_HUMAN]	1.03E+09
Ig heavy chain V-III region CAM OS=Homo sapiens PE=1 SV=1	1.05E+09
Ig heavy chain V-III region GAL OS=Homo sapiens PE=1 SV=1	1.05E+09
Ig heavy chain V-III region GAR; [Homo sapiens (Human)] - [HV322_HUMAN]	1.05E+08
Ig heavy chain V-III region HIL; [Homo sapiens (Human)] - [HV310_HUMAN]	1.47E+09
Ig heavy chain V-III region TIL OS=Homo sapiens PE=1 SV=1	1.06E+09
Ig kappa chain C region OS=Homo sapiens GN=IGKC PE=1 SV=1	3.47E+09
Ig kappa chain V-I region CAR; [Homo sapiens (Human)] - [KV104_HUMAN]	7.26E+07
Ig kappa chain V-I region DEE; [Homo sapiens (Human)] - [KV105_HUMAN]	2.73E+08
Ig kappa chain V-I region EU OS=Homo sapiens PE=1 SV=1	2.41E+08
Ig kappa chain V-I region Kue OS=Homo sapiens PE=1 SV=1	1.89E+08
Ig kappa chain V-I region Ni; [Homo sapiens (Human)] - [KV121_HUMAN]	1.45E+08
Ig kappa chain V-I region OU; [Homo sapiens (Human)] - [KV114_HUMAN]	3.43E+08
Ig kappa chain V-I region Wes; [Homo sapiens (Human)] - [KV119_HUMAN]	2.71E+08
Ig kappa chain V-II region FR OS=Homo sapiens PE=1 SV=1	8.51E+07
Ig kappa chain V-II region RPMI 6410 OS=Homo sapiens PE=4 SV=1	1.62E+08
Ig kappa chain V-III region B6; [Homo sapiens (Human)] - [KV301_HUMAN]	2.39E+08
Ig kappa chain V-III region POM OS=Homo sapiens PE=1 SV=1	9.77E+07
Ig kappa chain V-III region SIE OS=Homo sapiens PE=1 SV=1	2.40E+08
Ig kappa chain V-III region VG; Flags: Precursor; Fragment; [Homo sapiens (Human)] - [KV309_HUMAN]	1.46E+08
Ig kappa chain V-IV region JI OS=Homo sapiens PE=4 SV=1	3.74E+07
Ig kappa chain V-IV region Len OS=Homo sapiens PE=1 SV=2	9.86E+07
Ig lambda chain V region 4A OS=Homo sapiens PE=4 SV=1	5.01E+07
Ig lambda chain V-I region HA OS=Homo sapiens PE=1 SV=1	1.91E+08
Ig lambda chain V-I region NIG-64 OS=Homo sapiens PE=1 SV=1	7.21E+07
Ig lambda chain V-II region NEI; [Homo sapiens (Human)] - [LV202_HUMAN]	1.91E+07
Ig lambda chain V-III region LOI OS=Homo sapiens PE=1 SV=1	1.57E+08
Ig lambda chain V-III region SH; [Homo sapiens (Human)] - [LV301_HUMAN]	3.09E+07
Ig lambda chain V-IV region Bau; [Homo sapiens (Human)] - [LV401_HUMAN]	1.58E+08
Ig lambda chain V-VI region SUT; [Homo sapiens (Human)] - [LV603_HUMAN]	7.86E+06

Ig lambda-2 chain C regions OS=Homo sapiens GN=IGLC2 PE=1 SV=1	2.31E+09
Ig mu chain C region OS=Homo sapiens GN=IGHM PE=1 SV=3	4.16E+07
Immunoglobulin J chain OS=Homo sapiens GN=IGJ PE=1 SV=4	4.76E+07
Immunoglobulin lambda-like polypeptide 5 OS=Homo sapiens GN=IGLL5 PE=2 SV=2	1.44E+09
Intercellular adhesion molecule 1 OS=Homo sapiens GN=ICAM1 PE=1 SV=2	1.15E+07
Lactotransferrin; Short=Lactoferrin; EC=3.4.21.-; AltName: Full=Talalactoferrin; Contains: RecName: Full=Kaliocin-1; Contains: RecName: Full=Lactoferroxin-A; Contains: RecName: Full=Lactoferroxin-B; Contains: RecName: Full=Lactoferroxin-C; Flags: Precursor; [Homo sapiens (Human)] - [TRFL_HUMAN]	9.47E+08
Leucine-rich alpha-2-glycoprotein OS=Homo sapiens GN=LRG1 PE=1 SV=2	4.46E+07
LIM domain only protein 7; Short=LMO-7; AltName: Full=F-box only protein 20; AltName: Full=LOMP; [Homo sapiens (Human)] - [LMO7_HUMAN]	1.36E+08
Lysosomal alpha-glucosidase; EC=3.2.1.20; AltName: Full=Acid maltase; AltName: Full=Aglucosidase alfa; Contains: RecName: Full=76 kDa lysosomal alpha-glucosidase; Contains: RecName: Full=70 kDa lysosomal alpha-glucosidase; Flags: Precursor; [Homo sapiens (Human)] - [LYAG_HUMAN]	1.40E+06
Lysozyme C; EC=3.2.1.17; AltName: Full=1,4-beta-N-acetylmuramidase C; Flags: Precursor; [Homo sapiens (Human)] - [LYSC_HUMAN]	1.48E+06
Mucin-1 OS=Homo sapiens GN=MUC1 PE=1 SV=3	1.18E+07
Myotubularin-related protein 14; EC=3.1.3.-; AltName: Full=HCV NS5A-transactivated protein 4 splice variant A-binding protein 1; Short=NS5ATP4ABP1; AltName: Full=hJumpy; [Homo sapiens (Human)] - [MTMRE_HUMAN]	3.06E+06
Pancreatic alpha-amylase; Short=PA; EC=3.2.1.1; AltName: Full=1,4-alpha-D-glucan glucanohydrolase; Flags: Precursor; [Homo sapiens (Human)] - [AMYP_HUMAN]	1.35E+07
Peptidyl-prolyl cis-trans isomerase A; Short=PPIase A; EC=5.2.1.8; AltName: Full=Cyclophilin A; AltName: Full=Cyclosporin A-binding protein; AltName: Full=Rotamase A; [Homo sapiens (Human)] - [PPIA_HUMAN]	6.43E+06
Polymeric immunoglobulin receptor OS=Homo sapiens GN=PIGR PE=1 SV=4	1.94E+08
Pre-mRNA cleavage complex 2 protein Pcf11; AltName: Full=Pre-mRNA cleavage complex II protein Pcf11; [Homo sapiens (Human)] - [PCF11_HUMAN]	5.19E+07
Pro-cathepsin H OS=Homo sapiens GN=CTSH PE=1 SV=4	1.06E+07
Proactivator polypeptide OS=Homo sapiens GN=PSAP PE=1 SV=2	2.71E+06
Prostasin; EC=3.4.21.-; AltName: Full=Serine protease 8; Contains: RecName: Full=Prostasin light chain; Contains: RecName: Full=Prostasin heavy chain; Flags: Precursor; [Homo sapiens (Human)] - [PRSS8_HUMAN]	1.22E+06
Protein DJ-1 OS=Homo sapiens GN=PARK7 PE=1 SV=2	1.23E+07
Protein S100-A6 OS=Homo sapiens GN=S100A6 PE=1 SV=1	2.38E+07
Protein S100-A8 OS=Homo sapiens GN=S100A8 PE=1 SV=1	3.59E+07
Protein S100-A9 OS=Homo sapiens GN=S100A9 PE=1 SV=1	1.13E+07
Protein Shroom3; AltName: Full=Shroom-related protein; Short=hShrmL; [Homo sapiens (Human)] - [SHRM3_HUMAN]	9.47E+07
Protein-glutamine gamma-glutamyltransferase E; EC=2.3.2.13; AltName: Full=Transglutaminase E; Short=TG(E); Short=TGE; Short=TGase E; AltName: Full=Transglutaminase-3; Short=TGase-3; Contains: RecName:	3.65E+06

Full=Protein-glutamine gamma-glutamyltransferase E 50 kDa non-catalytic chain; Contains: RecName: Full=Protein-glutamine gamma-glutamyltransferase E 27 kDa catalytic chain; Flags: Precursor; [Homo sapiens (Human)] - [TGM3_HUMAN]	
Pulmonary surfactant-associated protein A2 OS=Homo sapiens GN=SFTPA2 PE=1 SV=1	3.74E+07
Pulmonary surfactant-associated protein B; Short=SP-B; AltName: Full=18 kDa pulmonary-surfactant protein; AltName: Full=6 kDa protein; AltName: Full=Pulmonary surfactant-associated proteolipid SPL(Phe); Flags: Precursor; [Homo sapiens (Human)] - [PSPB_HUMAN]	3.26E+06
Pulmonary surfactant-associated protein D OS=Homo sapiens GN=SFTPD PE=1 SV=3	1.53E+07
Putative V-set and immunoglobulin domain-containing protein 6 OS=Homo sapiens GN=VSIG6 PE=5 SV=2	2.00E+08
Ribonuclease P protein subunit p40; Short=RNaseP protein p40; EC=3.1.26.5; AltName: Full=RNase P subunit 1; [Homo sapiens (Human)] - [RPP40_HUMAN]	5.47E+07
Selenium-binding protein 1 OS=Homo sapiens GN=SELENBP1 PE=1 SV=2	1.67E+07
Serotransferrin OS=Homo sapiens GN=TF PE=1 SV=3	7.62E+09
Serpin B3 OS=Homo sapiens GN=SERPINB3 PE=1 SV=2	2.30E+07
Serum albumin OS=Homo sapiens GN=ALB PE=1 SV=2	2.77E+09
SH3 domain-binding glutamic acid-rich-like protein 3; AltName: Full=SH3 domain-binding protein 1; Short=SH3BP-1; [Homo sapiens (Human)] - [SH3L3_HUMAN]	3.66E+06
Sorting nexin-6; AltName: Full=TRAF4-associated factor 2; [Homo sapiens (Human)] - [SNX6_HUMAN]	2.15E+06
Thioredoxin; Short=Trx; AltName: Full=ATL-derived factor; Short=ADF; AltName: Full=Surface-associated sulphydryl protein; Short=SASP; [Homo sapiens (Human)] - [THIO_HUMAN]	8.21E+06
Thyroxine-binding globulin OS=Homo sapiens GN=SERPINA7 PE=1 SV=2	5.25E+06
Transaldolase OS=Homo sapiens GN=TALDO1 PE=1 SV=2	4.47E+07
Transcriptional adapter 2-beta; AltName: Full=ADA2-like protein beta; Short=ADA2-beta; [Homo sapiens (Human)] - [TAD2B_HUMAN]	2.22E+07
Transmembrane protein 198; [Homo sapiens (Human)] - [TM198_HUMAN]	2.62E+07
Transmembrane protein 200C; AltName: Full=Transmembrane protein TTMA; AltName: Full=Two transmembrane domain-containing family member A; [Homo sapiens (Human)] - [T200C_HUMAN]	3.59E+06
Transthyretin OS=Homo sapiens GN=TTR PE=1 SV=1	2.53E+08
Triosephosphate isomerase OS=Homo sapiens GN=TPI1 PE=1 SV=3	4.37E+07
Uncharacterized protein C3orf38; [Homo sapiens (Human)] - [CC038_HUMAN]	2.73E+09
Uncharacterized protein KIAA0947; [Homo sapiens (Human)] - [K0947_HUMAN]	8.15E+06
Uteroglobin OS=Homo sapiens GN=SCGB1A1 PE=1 SV=1	1.74E+08
Vitamin D-binding protein OS=Homo sapiens GN=GC PE=1 SV=1	4.91E+08
Vitamin K-dependent protein S; Flags: Precursor; [Homo sapiens (Human)] - [PROS_HUMAN]	3.31E+07
Xin actin-binding repeat-containing protein 2 OS=Homo sapiens GN=XIRP2 PE=1 SV=2	2.05E+08
Zinc-alpha-2-glycoprotein OS=Homo sapiens GN=AZGP1 PE=1 SV=2	1.24E+08

Table B.3: *Alveolar proteins identified by 1D PAGE and nano LC MS/MS in healthy young and aged RTLFs. The 124 proteins common to both healthy young and aged subjects investigated n=5 for both subject groups, alongside the mean of the three most abundant ion peaks of each respective protein identified,.Accession numbers included are according to entries in UniProtKB/Swiss-Prot.*

Healthy Control		Healthy Aged Control	
14-3-3 protein beta/alpha OS=Homo sapiens GN=YWHAB PE=1 SV=3	1.07E+08	14-3-3 protein beta/alpha OS=Homo sapiens GN=YWHAB PE=1 SV=3	1.46E+07
14-3-3 protein epsilon OS=Homo sapiens GN=YWHAE PE=1 SV=1	9.02E+07	14-3-3 protein epsilon OS=Homo sapiens GN=YWHAE PE=1 SV=1	1.86E+07
14-3-3 protein zeta/delta OS=Homo sapiens GN=YWHAZ PE=1 SV=1	1.07E+08	14-3-3 protein zeta/delta OS=Homo sapiens GN=YWHAZ PE=1 SV=1	1.57E+07
Actin-related protein 2; AltName: Full=Actin-like protein 2; [Homo sapiens (Human)] - [ARP2_HUMAN]	1.56E+07	Actin-related protein 2; AltName: Full=Actin-like protein 2; [Homo sapiens (Human)] - [ARP2_HUMAN]	1.97E+07
Actin, cytoplasmic 1 OS=Homo sapiens GN=ACTB PE=1 SV=1	5.55E+07	Actin, cytoplasmic 1 OS=Homo sapiens GN=ACTB PE=1 SV=1	6.89E+07
Afamin OS=Homo sapiens GN=AFM PE=1 SV=1	2.55E+07	Afamin OS=Homo sapiens GN=AFM PE=1 SV=1	2.54E+07
Aldo-keto reductase family 1 member C3; EC=1.-.-.-; AltName: Full=17-beta-hydroxysteroid dehydrogenase type 5; Short=17-beta-HSD 5; AltName: Full=3-alpha-HSD type II, brain; AltName: Full=3-alpha-hydroxysteroid dehydrogenase type 2; Short=3-alpha-HSD type 2; EC=1.1.1.213; AltName: Full=Chlordecone reductase homolog HAKRb; AltName: Full=Dihydrodiol dehydrogenase 3; Short=DD-3; Short=DD3; AltName: Full=Dihydrodiol dehydrogenase type I; AltName: Full=HA1753; AltName: Full=Indanol dehydrogenase; EC=1.1.1.112; AltName: Full=Prostaglandin F synthase; Short=PGFS; EC=1.1.1.188; AltName: Full=Testosterone 17-beta-dehydrogenase 5; EC=1.1.1.63; EC=1.1.1.64; AltName: Full=Trans-1,2-dihydrobenzene-1,2-diol dehydrogenase; EC=1.3.1.20;	1.46E+07	Aldo-keto reductase family 1 member C3; EC=1.-.-.-; AltName: Full=17-beta-hydroxysteroid dehydrogenase type 5; Short=17-beta-HSD 5; AltName: Full=3-alpha-HSD type II, brain; AltName: Full=3-alpha-hydroxysteroid dehydrogenase type 2; Short=3-alpha-HSD type 2; EC=1.1.1.213; AltName: Full=Chlordecone reductase homolog HAKRb; AltName: Full=Dihydrodiol dehydrogenase 3; Short=DD-3; Short=DD3; AltName: Full=Dihydrodiol dehydrogenase type I; AltName: Full=HA1753; AltName: Full=Indanol dehydrogenase; EC=1.1.1.112; AltName: Full=Prostaglandin F synthase; Short=PGFS; EC=1.1.1.188; AltName: Full=Testosterone 17-beta-dehydrogenase 5; EC=1.1.1.63; EC=1.1.1.64; AltName: Full=Trans-1,2-dihydrobenzene-1,2-diol dehydrogenase; EC=1.3.1.20;	3.18E+07

[Homo sapiens (Human)] - [AK1C3_HUMAN]		[Homo sapiens (Human)] - [AK1C3_HUMANsapiens (Human)] - [AK1C3_HUMAN]	
Alpha-1-acid glycoprotein 1 OS=Homo sapiens GN=ORM1 PE=1 SV=1	2.04E+08	Alpha-1-acid glycoprotein 1 OS=Homo sapiens GN=ORM1 PE=1 SV=1	3.39E+08
Alpha-1-acid glycoprotein 2 OS=Homo sapiens GN=ORM2 PE=1 SV=2	1.81E+08	Alpha-1-acid glycoprotein 2 OS=Homo sapiens GN=ORM2 PE=1 SV=2	2.40E+08
Alpha-1-antichymotrypsin OS=Homo sapiens GN=SERPINA3 PE=1 SV=2	1.49E+08	Alpha-1-antichymotrypsin OS=Homo sapiens GN=SERPINA3 PE=1 SV=2	8.21E+07
Alpha-1-antitrypsin OS=Homo sapiens GN=SERPINA1 PE=1 SV=3	2.69E+09	Alpha-1-antitrypsin OS=Homo sapiens GN=SERPINA1 PE=1 SV=3	3.20E+09
Alpha-1B-glycoprotein OS=Homo sapiens GN=A1BG PE=1 SV=4	1.36E+08	Alpha-1B-glycoprotein OS=Homo sapiens GN=A1BG PE=1 SV=4	1.33E+08
Alpha-2-HS-glycoprotein OS=Homo sapiens GN=AHSG PE=1 SV=1	7.52E+07	Alpha-2-HS-glycoprotein OS=Homo sapiens GN=AHSG PE=1 SV=1	1.16E+08
Alpha-2-macroglobulin OS=Homo sapiens GN=A2M PE=1 SV=3	6.75E+07	Alpha-2-macroglobulin OS=Homo sapiens GN=A2M PE=1 SV=3	1.66E+08
Angiotensin-converting enzyme OS=Homo sapiens GN=ACE PE=1 SV=1	2.86E+07	Angiotensin-converting enzyme; Short=ACE; EC=3.2.1.-; EC=3.4.15.1; AltName: Full=Dipeptidyl carboxypeptidase I; AltName: Full=Kininase II; AltName: CD_antigen=CD143; Contains: RecName: Full=Angiotensin-converting enzyme, soluble form; Flags: Precursor; [Homo sapiens (Human)] - [ACE_HUMAN]	1.46E+07
Angiotensinogen OS=Homo sapiens GN=AGT PE=1 SV=1	9.61E+07	Angiotensinogen OS=Homo sapiens GN=AGT PE=1 SV=1	4.94E+07
Annexin A5 OS=Homo sapiens GN=ANXA5 PE=1 SV=2	6.60E+07	Annexin A5 OS=Homo sapiens GN=ANXA5 PE=1 SV=2	1.36E+06
Antithrombin-III OS=Homo sapiens GN=SERPINC1 PE=1 SV=1	2.92E+07	Antithrombin-III OS=Homo sapiens GN=SERPINC1 PE=1 SV=1	1.84E+07
Apolipoprotein A-I OS=Homo sapiens GN=APOA1 PE=1 SV=1	9.59E+07	Apolipoprotein A-I OS=Homo sapiens GN=APOA1 PE=1 SV=1	1.38E+08
Apolipoprotein A-II OS=Homo sapiens GN=APOA2 PE=1 SV=1	2.59E+07	Apolipoprotein A-II OS=Homo sapiens GN=APOA2 PE=1 SV=1	7.40E+07
Apolipoprotein A-IV OS=Homo sapiens GN=APOA4 PE=1 SV=3	1.04E+07	Apolipoprotein A-IV OS=Homo sapiens GN=APOA4 PE=1 SV=3	2.74E+07
Attractin OS=Homo sapiens GN=ATRN PE=1 SV=2	1.13E+07	Attractin OS=Homo sapiens GN=ATRN PE=1 SV=2	5.23E+06
Beta-2-microglobulin OS=Homo sapiens GN=B2M PE=1 SV=1	1.20E+08	Beta-2-microglobulin OS=Homo sapiens GN=B2M PE=1 SV=1	2.59E+07

Biotinidase OS=Homo sapiens GN=BTD PE=1 SV=2	1.19E+07	Biotinidase OS=Homo sapiens GN=BTD PE=1 SV=2	2.84E+06
Calmodulin OS=Homo sapiens GN=CALM1 PE=1 SV=2	3.58E+07	Calmodulin OS=Homo sapiens GN=CALM1 PE=1 SV=2	2.68E+06
Carbonic anhydrase 1 OS=Homo sapiens GN=CA1 PE=1 SV=2	2.36E+07	Carbonic anhydrase 1 OS=Homo sapiens GN=CA1 PE=1 SV=2	3.91E+06
CD44 antigen OS=Homo sapiens GN=CD44 PE=1 SV=3	7.78E+07	CD44 antigen OS=Homo sapiens GN=CD44 PE=1 SV=3	2.73E+07
CD59 glycoprotein OS=Homo sapiens GN=CD59 PE=1 SV=1	4.04E+06	CD59 glycoprotein; AltName: Full=1F5 antigen; AltName: Full=20 kDa homologous restriction factor; Short=HRF-20; Short=HRF20; AltName: Full=MAC-inhibitory protein; Short=MAC-IP; AltName: Full=MEM43 antigen; AltName: Full=Membrane attack complex inhibition factor; Short=MACIF; AltName: Full=Membrane inhibitor of reactive lysis; Short=MIRL; AltName: Full=Protectin; AltName: CD_antigen=CD59; Flags: Precursor; [Homo sapiens (Human)] - [CD59_HUMAN]	3.54E+06
CD9 antigen OS=Homo sapiens GN=CD9 PE=1 SV=4	2.20E+07	CD9 antigen; AltName: Full=5H9 antigen; AltName: Full=Cell growth-inhibiting gene 2 protein; AltName: Full=Leukocyte antigen MIC3; AltName: Full=Motility-related protein; Short=MRP-1; AltName: Full=Tetraspanin-29; Short=Tspan-29; AltName: Full=p24; AltName: CD_antigen=CD9; [Homo sapiens (Human)] - [CD9_HUMAN]	9.50E+06
Ceruloplasmin OS=Homo sapiens GN=CP PE=1 SV=1	5.37E+08	Ceruloplasmin OS=Homo sapiens GN=CP PE=1 SV=1	3.67E+08
Coactosin-like protein OS=Homo sapiens GN=COTL1 PE=1 SV=3	3.46E+07	Coactosin-like protein OS=Homo sapiens GN=COTL1 PE=1 SV=3	5.15E+06
Complement C2 OS=Homo sapiens GN=C2 PE=1 SV=2	6.82E+06	Complement C2 OS=Homo sapiens GN=C2 PE=1 SV=2	3.41E+07
Complement C3 OS=Homo sapiens GN=C3 PE=1 SV=2	1.25E+07	Complement C3 OS=Homo sapiens GN=C3 PE=1 SV=2	2.66E+06
Complement decay-accelerating factor OS=Homo sapiens GN=CD55 PE=1 SV=4	1.49E+07	Complement decay-accelerating factor OS=Homo sapiens GN=CD55 PE=1 SV=4	7.63E+06
Corticosteroid-binding globulin OS=Homo sapiens GN=SERPINA6 PE=1 SV=1	5.17E+07	Corticosteroid-binding globulin OS=Homo sapiens GN=SERPINA6 PE=1 SV=1	3.95E+07
Deleted in malignant brain tumors 1 protein OS=Homo sapiens	5.59E+07	Deleted in malignant brain tumors 1 protein OS=Homo sapiens	3.69E+07

GN=DMBT1 PE=1 SV=2		GN=DMBT1 PE=1 SV=2	
Delta-like protein 4; AltName: Full=Drosophila Delta homolog 4; Short=Delta4; Flags: Precursor; [Homo sapiens (Human)] - [DLL4_HUMAN]	1.80E+07	Delta-like protein 4; AltName: Full=Drosophila Delta homolog 4; Short=Delta4; Flags: Precursor; [Homo sapiens (Human)] - [DLL4_HUMAN]	1.23E+07
Dermcidin OS=Homo sapiens GN=DCD PE=1 SV=2	6.20E+06	Dermcidin OS=Homo sapiens GN=DCD PE=1 SV=2	2.13E+06
Desmoplakin OS=Homo sapiens GN=DSP PE=1 SV=3	1.60E+08	Desmoplakin OS=Homo sapiens GN=DSP PE=1 SV=3	1.40E+08
Dipeptidyl peptidase 4 OS=Homo sapiens GN=DPP4 PE=1 SV=2	1.64E+07	Dipeptidyl peptidase 4 OS=Homo sapiens GN=DPP4 PE=1 SV=2	6.17E+07
Epididymal secretory protein E1 OS=Homo sapiens GN=NPC2 PE=1 SV=1	5.26E+07	Epididymal secretory protein E1 OS=Homo sapiens GN=NPC2 PE=1 SV=1	1.37E+07
FAS-associated factor 1; Short=hFAF1; AltName: Full=UBX domain-containing protein 12; AltName: Full=UBX domain-containing protein 3A; [Homo sapiens (Human)] - [FAF1_HUMAN]	2.21E+08	FAS-associated factor 1; Short=hFAF1; AltName: Full=UBX domain-containing protein 12; AltName: Full=UBX domain-containing protein 3A; [Homo sapiens (Human)] - [FAF1_HUMAN]	4.89E+08
Galectin-3-binding protein OS=Homo sapiens GN=LGALS3BP PE=1 SV=1	1.14E+07	Galectin-3-binding protein; AltName: Full=Basement membrane autoantigen p105; AltName: Full=Lectin galactoside-binding soluble 3-binding protein; AltName: Full=Mac-2-binding protein; Short=MAC2BP; Short=Mac-2 BP; AltName: Full=Tumor-associated antigen 90K; Flags: Precursor; [Homo sapiens (Human)] - [LG3BP_HUMAN]	7.88E+06
Glutathione peroxidase 3 OS=Homo sapiens GN=GPX3 PE=1 SV=2	4.07E+06	Glutathione peroxidase 3 OS=Homo sapiens GN=GPX3 PE=1 SV=2	1.19E+06
Glutathione S-transferase A2 OS=Homo sapiens GN=GSTA2 PE=1 SV=4	5.83E+07	Glutathione S-transferase A2 OS=Homo sapiens GN=GSTA2 PE=1 SV=4	4.18E+07
Glutathione S-transferase P OS=Homo sapiens GN=GSTP1 PE=1 SV=2	3.42E+07	Glutathione S-transferase P OS=Homo sapiens GN=GSTP1 PE=1 SV=2	8.51E+06
Haptoglobin OS=Homo sapiens GN=HP PE=1 SV=1	3.82E+08	Haptoglobin OS=Homo sapiens GN=HP PE=1 SV=1	1.26E+08
Hemoglobin subunit alpha; AltName: Full=Alpha-globin; AltName: Full=Hemoglobin alpha chain; [Homo sapiens (Human)] - [HBA_HUMAN]	2.06E+08	Hemoglobin subunit alpha OS=Homo sapiens GN=HBA1 PE=1 SV=2	1.49E+08
Hemoglobin subunit beta OS=Homo sapiens GN=HBB	2.06E+08	Hemoglobin subunit beta OS=Homo sapiens GN=HBB	1.28E+08

PE=1 SV=2		PE=1 SV=2	
Hemoglobin subunit delta OS=Homo sapiens GN=HBD PE=1 SV=2	1.66E+08	Hemoglobin subunit delta OS=Homo sapiens GN=HBD PE=1 SV=2	7.65E+07
Hemopexin OS=Homo sapiens GN=HPX PE=1 SV=2	7.70E+08	Hemopexin OS=Homo sapiens GN=HPX PE=1 SV=2	2.71E+08
Histone H3.3C; [Homo sapiens (Human)] - [H3C_HUMAN]	1.08E+07	Histone H3.3C; [Homo sapiens (Human)] - [H3C_HUMAN]	1.79E+07
Histone H4 OS=Homo sapiens GN=HIST1H4A PE=1 SV=2	4.75E+07	Histone H4 OS=Homo sapiens GN=HIST1H4A PE=1 SV=2	2.45E+07
Ig alpha-1 chain C region OS=Homo sapiens GN=IGHA1 PE=1 SV=2	2.81E+09	Ig alpha-1 chain C region OS=Homo sapiens GN=IGHA1 PE=1 SV=2	2.42E+09
Ig alpha-2 chain C region OS=Homo sapiens GN=IGHA2 PE=1 SV=3	2.05E+09	Ig alpha-2 chain C region OS=Homo sapiens GN=IGHA2 PE=1 SV=3	1.79E+09
Ig gamma-1 chain C region; [Homo sapiens (Human)] - [IGHG1_HUMAN]	1.23E+10	Ig gamma-1 chain C region OS=Homo sapiens GN=IGHG1 PE=1 SV=1	8.92E+09
Ig gamma-2 chain C region OS=Homo sapiens GN=IGHG2 PE=1 SV=2	9.10E+09	Ig gamma-2 chain C region OS=Homo sapiens GN=IGHG2 PE=1 SV=2	5.60E+09
Ig gamma-3 chain C region OS=Homo sapiens GN=IGHG3 PE=1 SV=2	9.36E+09	Ig gamma-3 chain C region OS=Homo sapiens GN=IGHG3 PE=1 SV=2	6.71E+09
Ig gamma-4 chain C region OS=Homo sapiens GN=IGHG4 PE=1 SV=1	9.10E+09	Ig gamma-4 chain C region OS=Homo sapiens GN=IGHG4 PE=1 SV=1	5.60E+09
Ig heavy chain V-II region ARH-77 OS=Homo sapiens PE=4 SV=1	7.57E+07	Ig heavy chain V-II region ARH-77; Flags: Precursor; [Homo sapiens (Human)] - [HV209_HUMAN]	4.86E+07
Ig heavy chain V-II region NEWM; [Homo sapiens (Human)] - [HV207_HUMAN]	1.14E+08	Ig heavy chain V-II region NEWM OS=Homo sapiens PE=1 SV=1	1.47E+08
Ig heavy chain V-II region OU; [Homo sapiens (Human)] - [HV201_HUMAN]	6.80E+07	Ig heavy chain V-II region OU; [Homo sapiens (Human)] - [HV201_HUMAN]	1.44E+08
Ig heavy chain V-III region BRO; [Homo sapiens (Human)] - [HV305_HUMAN]	1.19E+09	Ig heavy chain V-III region BRO; [Homo sapiens (Human)] - [HV305_HUMAN]	1.02E+09
Ig heavy chain V-III region BUT OS=Homo sapiens PE=1 SV=1	1.16E+09	Ig heavy chain V-III region BUT; [Homo sapiens (Human)] - [HV306_HUMAN]	1.03E+09
Ig heavy chain V-III region CAM OS=Homo sapiens PE=1 SV=1	1.22E+09	Ig heavy chain V-III region CAM OS=Homo sapiens PE=1 SV=1	1.05E+09
Ig heavy chain V-III region GAL OS=Homo sapiens PE=1 SV=1	1.17E+09	Ig heavy chain V-III region GAL OS=Homo sapiens PE=1 SV=1	1.05E+09
Ig heavy chain V-III region GAR; [Homo sapiens (Human)] - [HV322_HUMAN]	2.84E+08	Ig heavy chain V-III region GAR; [Homo sapiens (Human)] - [HV322_HUMAN]	1.05E+08
Ig heavy chain V-III region HIL;	1.66E+09	Ig heavy chain V-III region HIL;	1.47E+09

[Homo sapiens (Human)] - [HV310_HUMAN]		[Homo sapiens (Human)] - [HV310_HUMAN]	
Ig kappa chain C region OS=Homo sapiens GN=IGKC PE=1 SV=1	5.90E+09	Ig kappa chain C region OS=Homo sapiens GN=IGKC PE=1 SV=1	3.47E+09
Ig kappa chain V-I region DEE OS=Homo sapiens PE=1 SV=1	4.84E+08	Ig kappa chain V-I region DEE; [Homo sapiens (Human)] - [KV105_HUMAN]	2.73E+08
Ig kappa chain V-I region EU OS=Homo sapiens PE=1 SV=1	4.22E+08	Ig kappa chain V-I region EU OS=Homo sapiens PE=1 SV=1	2.41E+08
Ig kappa chain V-I region Ni; [Homo sapiens (Human)] - [KV121_HUMAN]	1.15E+08	Ig kappa chain V-I region Ni; [Homo sapiens (Human)] - [KV121_HUMAN]	1.45E+08
Ig kappa chain V-I region Wes; [Homo sapiens (Human)] - [KV119_HUMAN]	5.03E+08	Ig kappa chain V-I region Wes; [Homo sapiens (Human)] - [KV119_HUMAN]	2.71E+08
Ig kappa chain V-III region POM OS=Homo sapiens PE=1 SV=1	3.13E+08	Ig kappa chain V-III region POM OS=Homo sapiens PE=1 SV=1	9.77E+07
Ig kappa chain V-III region SIE OS=Homo sapiens PE=1 SV=1	3.17E+08	Ig kappa chain V-III region SIE OS=Homo sapiens PE=1 SV=1	2.40E+08
Ig kappa chain V-III region VG; Flags: Precursor; Fragment; [Homo sapiens (Human)] - [KV309_HUMAN]	3.81E+08	Ig kappa chain V-III region VG; Flags: Precursor; Fragment; [Homo sapiens (Human)] - [KV309_HUMAN]	1.46E+08
Ig kappa chain V-IV region Len OS=Homo sapiens PE=1 SV=2	1.66E+08	Ig kappa chain V-IV region Len OS=Homo sapiens PE=1 SV=2	9.86E+07
Ig lambda chain V region 4A OS=Homo sapiens PE=4 SV=1	1.06E+08	Ig lambda chain V region 4A OS=Homo sapiens PE=4 SV=1	5.01E+07
Ig lambda chain V-I region HA OS=Homo sapiens PE=1 SV=1	2.17E+08	Ig lambda chain V-I region HA OS=Homo sapiens PE=1 SV=1	1.91E+08
Ig lambda chain V-I region NIG-64 OS=Homo sapiens PE=1 SV=1	6.96E+07	Ig lambda chain V-I region NIG-64 OS=Homo sapiens PE=1 SV=1	7.21E+07
Ig lambda chain V-III region LOI; [Homo sapiens (Human)] - [LV302_HUMAN]	2.61E+08	Ig lambda chain V-III region LOI OS=Homo sapiens PE=1 SV=1	1.57E+08
Ig lambda chain V-IV region Bau; [Homo sapiens (Human)] - [LV401_HUMAN]	4.40E+08	Ig lambda chain V-IV region Bau; [Homo sapiens (Human)] - [LV401_HUMAN]	1.58E+08
Ig lambda-2 chain C regions OS=Homo sapiens GN=IGLC2 PE=1 SV=1	3.07E+09	Ig lambda-2 chain C regions OS=Homo sapiens GN=IGLC2 PE=1 SV=1	2.31E+09
Ig mu chain C region OS=Homo sapiens GN=IGHM PE=1 SV=3	6.47E+07	Ig mu chain C region OS=Homo sapiens GN=IGHM PE=1 SV=3	4.16E+07
Immunoglobulin J chain OS=Homo sapiens GN=IGJ PE=1 SV=4	8.29E+07	Immunoglobulin J chain OS=Homo sapiens GN=IGJ PE=1 SV=4	4.76E+07
Immunoglobulin lambda-like polypeptide 5;	1.96E+09	Immunoglobulin lambda-like polypeptide 5 OS=Homo sapiens GN=IGLL5 PE=2 SV=2	1.44E+09
Intercellular adhesion molecule 1 OS=Homo sapiens GN=ICAM1 PE=1 SV=2	4.01E+07	Intercellular adhesion molecule 1 OS=Homo sapiens GN=ICAM1 PE=1 SV=2	1.15E+07

Lactotransferrin OS=Homo sapiens GN=LTF PE=1 SV=6	1.38E+09	Lactotransferrin; Short=Lactoferrin; EC=3.4.21.-; AltName: Full=Talalactoferrin; Contains: RecName: Full=Kaliocin-1; Contains: RecName: Full=Lactoferroxin-A; Contains: RecName: Full=Lactoferroxin-B; Contains: RecName: Full=Lactoferroxin-C; Flags: Precursor; [Homo sapiens (Human)] - [TRFL_HUMAN]	9.47E+08
Leucine-rich alpha-2-glycoprotein; Short=LRG; Flags: Precursor; [Homo sapiens (Human)] - [A2GL_HUMAN]	2.66E+07	Leucine-rich alpha-2-glycoprotein OS=Homo sapiens GN=LRG1 PE=1 SV=2	4.46E+07
LIM domain only protein 7; Short=LMO-7; AltName: Full=F-box only protein 20; AltName: Full=LOMP; [Homo sapiens (Human)] - [LMO7_HUMAN]	1.14E+08	LIM domain only protein 7; Short=LMO-7; AltName: Full=F-box only protein 20; AltName: Full=LOMP; [Homo sapiens (Human)] - [LMO7_HUMAN]	1.36E+08
Lysozyme C OS=Homo sapiens GN=LYZ PE=1 SV=1	2.75E+06	Lysozyme C; EC=3.2.1.17; AltName: Full=1,4-beta-N-acetylmuramidase C; Flags: Precursor; [Homo sapiens (Human)] - [LYSC_HUMAN]	1.48E+06
Mucin-1 OS=Homo sapiens GN=MUC1 PE=1 SV=3	1.31E+07	Mucin-1 OS=Homo sapiens GN=MUC1 PE=1 SV=3	1.18E+07
Peptidyl-prolyl cis-trans isomerase A OS=Homo sapiens GN=PPIA PE=1 SV=2	1.19E+07	Peptidyl-prolyl cis-trans isomerase A; Short=PPIase A; EC=5.2.1.8; AltName: Full=Cyclophilin A; AltName: Full=Cyclosporin A-binding protein; AltName: Full=Rotamase A; [Homo sapiens (Human)] - [PPIA_HUMAN]	6.43E+06
Polymeric immunoglobulin receptor OS=Homo sapiens GN=PIGR PE=1 SV=4	5.24E+08	Polymeric immunoglobulin receptor OS=Homo sapiens GN=PIGR PE=1 SV=4	1.94E+08
Pre-mRNA cleavage complex 2 protein Pcf11; AltName: Full=Pre-mRNA cleavage complex II protein Pcf11; [Homo sapiens (Human)] - [PCF11_HUMAN]	7.88E+07	Pre-mRNA cleavage complex 2 protein Pcf11; AltName: Full=Pre-mRNA cleavage complex II protein Pcf11; [Homo sapiens (Human)] - [PCF11_HUMAN]	5.19E+07
Pro-cathepsin H OS=Homo sapiens GN=CTSH PE=1 SV=4	2.79E+07	Pro-cathepsin H OS=Homo sapiens GN=CTSH PE=1 SV=4	1.06E+07
Protein DJ-1 OS=Homo sapiens GN=PARK7 PE=1 SV=2	3.98E+07	Protein DJ-1 OS=Homo sapiens GN=PARK7 PE=1 SV=2	1.23E+07
Protein S100-A6 OS=Homo sapiens GN=S100A6 PE=1 SV=1	9.49E+07	Protein S100-A6 OS=Homo sapiens GN=S100A6 PE=1 SV=1	2.38E+07
Protein Shroom3; AltName: Full=Shroom-related protein;	8.34E+07	Protein Shroom3; AltName: Full=Shroom-related protein;	9.47E+07

Short=hShrmL; [Homo sapiens (Human)] - [SHRM3_HUMAN]		Short=hShrmL; [Homo sapiens (Human)] - [SHRM3_HUMAN]	
Pulmonary surfactant-associated protein A2 OS=Homo sapiens GN=SFTPA2 PE=1 SV=1	1.95E+08	Pulmonary surfactant-associated protein A2 OS=Homo sapiens GN=SFTPA2 PE=1 SV=1	3.74E+07
Pulmonary surfactant-associated protein B OS=Homo sapiens GN=SFTPB PE=1 SV=3	2.54E+07	Pulmonary surfactant-associated protein B; Short=SP-B; AltName: Full=18 kDa pulmonary-surfactant protein; AltName: Full=6 kDa protein; AltName: Full=Pulmonary surfactant-associated proteolipid SPL(Phe); Flags: Precursor; [Homo sapiens (Human)] - [PSPB_HUMAN]	3.26E+06
Pulmonary surfactant-associated protein D OS=Homo sapiens GN=SFTPD PE=1 SV=3	4.71E+07	Pulmonary surfactant-associated protein D OS=Homo sapiens GN=SFTPD PE=1 SV=3	1.53E+07
Putative V-set and immunoglobulin domain-containing protein 6 OS=Homo sapiens GN=VSIG6 PE=5 SV=2	2.22E+08	Putative V-set and immunoglobulin domain-containing protein 6 OS=Homo sapiens GN=VSIG6 PE=5 SV=2	2.00E+08
Ribonuclease P protein subunit p40; Short=RNaseP protein p40; EC=3.1.26.5; AltName: Full=RNase P subunit 1; [Homo sapiens (Human)] - [RPP40_HUMAN]	1.42E+08	Ribonuclease P protein subunit p40; Short=RNaseP protein p40; EC=3.1.26.5; AltName: Full=RNase P subunit 1; [Homo sapiens (Human)] - [RPP40_HUMAN]	5.47E+07
Selenium-binding protein 1 OS=Homo sapiens GN=SELENBP1 PE=1 SV=2	2.43E+07	Selenium-binding protein 1 OS=Homo sapiens GN=SELENBP1 PE=1 SV=2	1.67E+07
Serotransferrin OS=Homo sapiens GN=TF PE=1 SV=3	1.28E+10	Serotransferrin OS=Homo sapiens GN=TF PE=1 SV=3	7.62E+09
Serpin B3 OS=Homo sapiens GN=SERPINB3 PE=1 SV=2	3.01E+07	Serpin B3 OS=Homo sapiens GN=SERPINB3 PE=1 SV=2	2.30E+07
Serum albumin OS=Homo sapiens GN=ALB PE=1 SV=2	3.97E+09	Serum albumin OS=Homo sapiens GN=ALB PE=1 SV=2	2.77E+09
SH3 domain-binding glutamic acid-rich-like protein 3; AltName: Full=SH3 domain-binding protein 1; Short=SH3BP-1; [Homo sapiens (Human)] - [SH3L3_HUMAN]	1.13E+07	SH3 domain-binding glutamic acid-rich-like protein 3; AltName: Full=SH3 domain-binding protein 1; Short=SH3BP-1; [Homo sapiens (Human)] - [SH3L3_HUMAN]	3.66E+06
Thioredoxin; Short=Trx; AltName: Full=ATL-derived factor; Short=ADF; AltName: Full=Surface-associated sulphydryl protein; Short=SASP; [Homo sapiens (Human)] - [THIO_HUMAN]	1.30E+07	Thioredoxin; Short=Trx; AltName: Full=ATL-derived factor; Short=ADF; AltName: Full=Surface-associated sulphydryl protein; Short=SASP; [Homo sapiens (Human)] - [THIO_HUMAN]	8.21E+06
Thyroxine-binding globulin OS=Homo sapiens GN=SERPINA7 PE=1 SV=2	1.56E+07	Thyroxine-binding globulin OS=Homo sapiens GN=SERPINA7 PE=1 SV=2	5.25E+06

Transaldolase OS=Homo sapiens GN=TALDO1 PE=1 SV=2	2.33E+07	Transaldolase OS=Homo sapiens GN=TALDO1 PE=1 SV=2	4.47E+07
Transcriptional adapter 2-beta; AltName: Full=ADA2-like protein beta; Short=ADA2-beta; [Homo sapiens (Human)] - [TAD2B_HUMAN]	8.54E+06	Transcriptional adapter 2-beta; AltName: Full=ADA2-like protein beta; Short=ADA2-beta; [Homo sapiens (Human)] - [TAD2B_HUMAN]	2.22E+07
Transmembrane protein 198; [Homo sapiens (Human)] - [TM198_HUMAN]	4.77E+07	Transmembrane protein 198; [Homo sapiens (Human)] - [TM198_HUMAN]	2.62E+07
Transmembrane protein 200C; AltName: Full=Transmembrane protein TTMA; AltName: Full=Two transmembrane domain-containing family member A; [Homo sapiens (Human)] - [T200C_HUMAN]	2.87E+06	Transmembrane protein 200C; AltName: Full=Transmembrane protein TTMA; AltName: Full=Two transmembrane domain-containing family member A; [Homo sapiens (Human)] - [T200C_HUMAN]	3.59E+06
Transthyretin OS=Homo sapiens GN=TTR PE=1 SV=1	1.12E+08	Transthyretin OS=Homo sapiens GN=TTR PE=1 SV=1	2.53E+08
Triosephosphate isomerase OS=Homo sapiens GN=TPI1 PE=1 SV=3	3.83E+07	Triosephosphate isomerase OS=Homo sapiens GN=TPI1 PE=1 SV=3	4.37E+07
Uncharacterized protein C3orf38; [Homo sapiens (Human)] - [CC038_HUMAN]	4.10E+09	Uncharacterized protein C3orf38; [Homo sapiens (Human)] - [CC038_HUMAN]	2.73E+09
Uncharacterized protein KIAA0947; [Homo sapiens (Human)] - [K0947_HUMAN]	1.56E+07	Uncharacterized protein KIAA0947; [Homo sapiens (Human)] - [K0947_HUMAN]	8.15E+06
Uteroglobin OS=Homo sapiens GN=SCGB1A1 PE=1 SV=1	6.27E+08	Uteroglobin OS=Homo sapiens GN=SCGB1A1 PE=1 SV=1	1.74E+08
Vitamin D-binding protein OS=Homo sapiens GN=GC PE=1 SV=1	2.19E+08	Vitamin D-binding protein OS=Homo sapiens GN=GC PE=1 SV=1	4.91E+08
Vitamin K-dependent protein S; Flags: Precursor; [Homo sapiens (Human)] - [PROS_HUMAN]	6.05E+06	Vitamin K-dependent protein S; Flags: Precursor; [Homo sapiens (Human)] - [PROS_HUMAN]	3.31E+07
Xin actin-binding repeat-containing protein 2 OS=Homo sapiens GN=XIRP2 PE=1 SV=2	4.22E+08	Xin actin-binding repeat-containing protein 2 OS=Homo sapiens GN=XIRP2 PE=1 SV=2	2.05E+08
Zinc-alpha-2-glycoprotein OS=Homo sapiens GN=AZGP1 PE=1 SV=2	1.16E+08	Zinc-alpha-2-glycoprotein OS=Homo sapiens GN=AZGP1 PE=1 SV=2	1.24E+08

Table B.4: *The biological process classification of Inflammation/immunity according to Gene Ontology annotation of proteins identified. Data shown is a comparison of the mean of the three most abundant ion peaks of each protein identified in Healthy Controls and Healthy Aged Controls respectively, n=5 for both subject groups.*

Inflammation/immunity	Healthy control	Healthy aged control
Alpha-1-acid glycoprotein 1	2.04E+08	3.39E+08
Alpha-1-antichymotrypsin	1.49E+08	8.21E+07
Alpha-1-antichymotrypsin	1.49E+08	8.21E+07
Alpha-2-HS-glycoprotein (fetuin A)	7.52E+07	1.16E+08
Antithrombin-III	2.92E+07	1.84E+07
Beta-2-microglobulin	1.20E+08	2.59E+07
Beta-microseminoprotein	5.82E+07	X
Cell adhesion molecule 1	7.37E+06	X
Complement C2	6.82E+06	3.41E+07
Complement C3	1.25E+07	2.66E+06
Complement C4-A	1.80E+07	X
Complement decay-accelerating factor (CD55)	1.49E+07	X
Complement factor B	X	7.63E+06
Deleted in malignant brain tumors 1 protein	5.59E+07	2.73E+07
Dipeptidyl peptidase 4	1.64E+07	X
Galectin-3 binding protein	1.14E+07	2.34E+06
Haptoglobin	3.82E+08	X
HLA class II histocompatibility antigen, DR alpha chain	X	1.26E+08
HLA class II histocompatibility antigen, DRB1-15 beta chain	7.37E+06	1.69E+06
Ig alpha-1 chain C region	2.81E+09	X
Ig alpha-2 chain C region	2.05E+09	2.42E+09
Ig delta chain C region	6.39E+06	1.79E+09
Ig gamma-1 chain C region	1.23E+10	1.10E+07
Ig gamma-2 chain C region	9.10E+09	8.92E+09
Ig gamma-3 chain C region	9.36E+09	5.60E+09
Ig gamma-4 chain C region	9.10E+09	6.71E+09
Ig heavy chain V-I region HG3	2.14E+08	5.60E+09
Ig heavy chain V-I region V35	6.05E+07	X
Ig heavy chain V-II region ARH-77	7.57E+07	X
Ig heavy chain V-III region CAM	1.22E+09	X
Ig heavy chain V-III region GAL	1.17E+09	1.05E+09
Ig heavy chain V-III region TIL	X	1.05E+09
Ig kappa chain C region	5.90E+09	X
Ig kappa chain V-I region DEE	4.84E+08	3.47E+09
Ig kappa chain V-I region Kue	X	2.73E+08
Ig kappa chain V-II region RPMI 6410	X	1.89E+08
Ig kappa chain V-II region TEW	X	1.62E+08
Ig kappa chain V-III region POM	3.13E+08	9.77E+07
Ig kappa chain V-III region SIE	3.17E+08	2.40E+08
Ig kappa chain V-III region VG	X	1.46E+08

(Fragment)		
Ig kappa chain V-IV region Len	1.66E+08	2.39E+08
Ig lambda chain V region 4A	1.06E+08	9.86E+07
Ig lambda chain V-I region HA	2.17E+08	5.01E+07
Ig lambda chain V-I region NIG-64	6.96E+07	1.91E+08
Ig lambda chain V-III region LOI	2.61E+08	7.21E+07
Ig lambda chain V-III region SH	2.83E+07	1.57E+08
Ig lambda chain V-VI region SUT	2.58E+07	X
Ig lambda-2 chain C regions	3.07E+09	X
Ig mu chain C region	6.47E+07	2.31E+09
IgBF	5.82E+07	4.16E+07
Immunoglobulin J chain	8.29E+07	X
Immunoglobulin lambda-like polypeptide 5	1.96E+09	4.76E+07
Intercellular adhesion molecule 1	4.01E+07	1.44E+09
Junctional adhesion molecule A	5.60E+06	1.15E+07
Lactotransferrin	1.38E+09	9.06E+05
Leukocyte elastase inhibitor	8.21E+06	9.47E+08
Lysozyme C	2.75E+06	3.69E+07
Macrophage Capping Protein	X	1.48E+06
Neutrophil defensin 1	1.79E+06	X
Neutrophil gelatinase-associated lipocalin	4.22E+06	X
Plasma protease C1 inhibitor	9.83E+06	X
Polymeric immunoglobulin receptor	5.24E+08	1.94E+08
Pulmonary surfactant-associated protein A	1.95E+08	3.74E+07
Pulmonary surfactant-associated protein D	4.71E+07	1.53E+07
S100-A8 (Calgranulin A)	X	3.59E+07
Sushi domain-containing protein 2	X	1.63E+06
V-set and immunoglobulin domain-containing protein 6	2.22E+08	X
V-set and immunoglobulin domain-containing protein 8	3.05E+07	2.00E+08
Zinc-alpha-2-glycoprotein	1.16E+08	1.24E+08

Table B.5: *The biological process classification of Protease/antiprotease balance to Gene Ontology annotation of proteins identified. Data shown is a comparison of the mean of the three most abundant ion peaks of each protein identified, in Healthy Controls and Healthy Aged Controls respectively, n=5 for both subject groups.*

Protease/antiprotease balance	Healthy control	Healthy aged control
Alpha-1-antichymotrypsin	1.49E+08	8.21E+07
Alpha-1-antitrypsin	2.69E+09	3.20E+09
Alpha-2-macroglobulin	6.75E+07	1.66E+08
Alpha-N-acetylglucosaminidase	X	X
Angiotensin-converting enzyme; Dipeptidyl carboxypeptidase I	2.86E+07	1.46E+07
Antithrombin-III	2.92E+07	1.84E+07
Cathepsin D	1.10E+09	X

Cathepsin Z	4.01E+06	X
Complement C2	6.82E+06	3.41E+07
Cystatin-B	7.58E+06	4.33E+06
Dermcidin	6.20E+06	2.13E+06
Dipeptidyl peptidase 4	1.64E+07	6.17E+07
Gastricsin	7.66E+06	X
Kininogen-1; Alpha-2-thiol proteinase inhibitor	5.17E+06	X
Latexin	X	X
Leukocyte elastase inhibitor; Monocyte/Neutrophil elastase inhibitor	9.09E+06	3.69E+07
Matrix metalloproteinase-23	2.66E+06	X
Matrix metalloproteinase-28		X
Napsin-A	2.37E+06	X
Pancreatic alpha-amylase	X	1.35E+07
Pro-cathepsin H	2.79E+07	1.06E+07
Probable hydrolase PNKD	1.07E+07	X
Prostasin	2.41E+06	1.22E+06
Proteasome subunit alpha type-1	X	X
Protein DJ-1	3.98E+07	1.23E+07
Serpin B6	X	X
Transmembrane protease serine 13	X	X
Trypsin-3	X	X
Xaa-Pro dipeptidase	1.18E+07	X

Table B.6: *The biological process classification of Oxidant/antioxidant balance to Gene Ontology annotation of proteins identified. Data shown is a comparison of the mean of the three most abundant ion peaks of each protein identified, in Healthy Controls and Healthy Aged Controls respectively, n=5 for both subject groups.*

Oxidant/antioxidant balance	**Healthy control**	**Healthy aged control**
Glutathione peroxidase 3	4.07E+06	1.19E+06
Glutathione S-transferase A2	5.83E+07	4.18E+07
Glutathione S-transferase omega-1	6.98E+06	X
Glutathione S-transferase P	3.42E+07	8.51E+06
Peroxiredoxin-5, mitochondrial	6.12E+06	X
Peroxiredoxin-6	2.13E+06	X
Protein DJ-1	3.98E+07	1.23E+07
Superoxide dismutase [Cu-Zn]	9.13E+06	X
Thioredoxin	1.30E+07	8.21E+06

Table B.7: *The biological process classification of Metal handling according to Gene Ontology annotation of proteins identified. Data shown is a comparison of the mean of the three most abundant ion peaks of each protein identified, in Healthy Controls and Healthy Aged Controls respectively, n=5 for both subject groups.*

Metal handling	Healthy control	Healthy aged control
Annexin A4	2.52E+07	
Annexin A5	6.60E+07	1.36E+06
Calmodulin	3.58E+07	2.68E+06
Carbonic anhydrase 1	2.36E+07	3.91E+06
Carbonic anhydrase 2	9.50E+06	X
Ceruloplasmin	5.37E+08	3.67E+08
Complement decay-accelerating factor	1.49E+07	X
Ferritin heavy chain	X	6.17E+07
Ferritin light chain	X	4.73E+06
Gelsolin	9.95E+06	X
Glutathione peroxidase 3	4.07E+06	1.19E+06
Hemoglobin subunit alpha	2.06E+08	1.49E+08
Hemoglobin subunit beta	2.09E+08	1.28E+08
Hemoglobin subunit delta	1.66E+08	7.65E+07
Hemopexin	7.70E+08	2.71E+08
Hornerin	4.56E+06	X
Kininogen-1	5.17E+06	X
Lactotransferrin	1.38E+09	9.06E+05
Neutrophil gelatinase-associated lipocalin	4.22E+06	X
Probable hydrolase PNKD	1.07E+07	X
Protein S100-A11	7.59E+06	X
Protein S100-A3	1.22E+07	X
Protein S100-A7	X	1.37E+07
Protein S100-A8	X	3.59E+07
Protein S100-A9	X	1.13E+07
Selenium-binding protein 1	2.43E+07	1.67E+07
Serotransferrin	1.28E+10	7.62E+09
Serum albumin	3.97E+09	2.77E+09
Superoxide dismutase [Cu-Zn]	9.13E+06	X
Zinc-alpha-2-glycoprotein	1.16E+08	1.24E+08

Appendix C

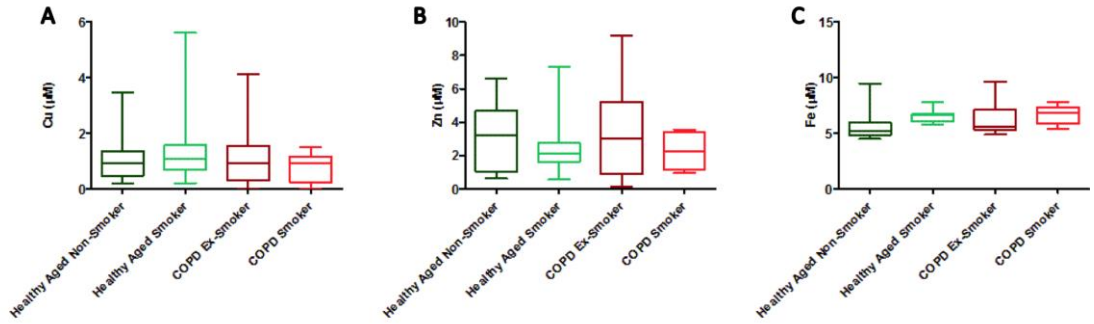

Figure C.1: ***The concentrations of metals: Cu, Zn and Fe, in*** *bronchoalveolar lavage samples as* determined by ICP-MS. Healthy Aged Non-Smoker n=12, Healthy Aged Smoker n=10, COPD Ex-Smoker n = 12, COPD Smoker n = 10 , * denotes a statistical difference where $p<0.05$.

Table C.1: *All alveolar proteins identified by 1D PAGE and nano LC MS/MS in healthy aged RTLFs. The 163 proteins identified in healthy aged subjects investigated, (n=5), alongside the mean of the three most abundant ion peaks of each respective protein identified. Accession numbers included according to entries in UniProtKB/Swiss-Prot.*

Healthy Aged Control	
14-3-3 protein beta/alpha OS=Homo sapiens GN=YWHAB PE=1 SV=3	1.46E+07
14-3-3 protein epsilon OS=Homo sapiens GN=YWHAE PE=1 SV=1	1.86E+07
14-3-3 protein zeta/delta OS=Homo sapiens GN=YWHAZ PE=1 SV=1	1.57E+07
7-alpha-hydroxycholest-4-en-3-one 12-alpha-hydroxylase; EC=1.14.13.95; AltName: Full=7-alpha-hydroxy-4-cholesten-3-one 12-alpha-hydroxylase; AltName: Full=CYPVIIIB1; AltName: Full=Cytochrome P450 8B1; AltName: Full=Sterol 12-alpha-hydroxylase; [Homo sapiens (Human)] - [CP8B1_HUMAN]	4.20E+07
Actin-related protein 2; AltName: Full=Actin-like protein 2; [Homo sapiens (Human)] - [ARP2_HUMAN]	1.97E+07
Actin, cytoplasmic 1 OS=Homo sapiens GN=ACTB PE=1 SV=1	6.89E+07
Afamin OS=Homo sapiens GN=AFM PE=1 SV=1	2.54E+07
Aldo-keto reductase family 1 member C3; EC=1.-.-.-; AltName: Full=17-beta-hydroxysteroid dehydrogenase type 5; Short=17-beta-HSD 5; AltName: Full=3-alpha-HSD type II, brain; AltName: Full=3-alpha-hydroxysteroid dehydrogenase type 2; Short=3-alpha-HSD type 2; EC=1.1.1.213; AltName: Full=Chlordecone reductase homolog HAKRb; AltName: Full=Dihydrodiol dehydrogenase 3; Short=DD-3; Short=DD3; AltName: Full=Dihydrodiol dehydrogenase type I; AltName: Full=HA1753; AltName: Full=Indanol dehydrogenase; EC=1.1.1.112; AltName: Full=Prostaglandin F synthase; Short=PGFS; EC=1.1.1.188; AltName: Full=Testosterone 17-beta-dehydrogenase 5; EC=1.1.1.63; EC=1.1.1.64; AltName: Full=Trans-1,2-dihydrobenzene-1,2-diol dehydrogenase; EC=1.3.1.20; [Homo sapiens (Human)] - [AK1C3_HUMAN]	3.18E+07
Alpha-1-acid glycoprotein 1 OS=Homo sapiens GN=ORM1 PE=1 SV=1	3.39E+08
Alpha-1-acid glycoprotein 2 OS=Homo sapiens GN=ORM2 PE=1 SV=2	2.40E+08

Alpha-1-antichymotrypsin OS=Homo sapiens GN=SERPINA3 PE=1 SV=2	8.21E+07
Alpha-1-antitrypsin OS=Homo sapiens GN=SERPINA1 PE=1 SV=3	3.20E+09
Alpha-1B-glycoprotein OS=Homo sapiens GN=A1BG PE=1 SV=4	1.33E+08
Alpha-2-HS-glycoprotein OS=Homo sapiens GN=AHSG PE=1 SV=1	1.16E+08
Alpha-2-macroglobulin OS=Homo sapiens GN=A2M PE=1 SV=3	1.66E+08
Alpha-enolase OS=Homo sapiens GN=ENO1 PE=1 SV=2	4.14E+06
Angiotensin-converting enzyme; Short=ACE; EC=3.2.1.-; EC=3.4.15.1; AltName: Full=Dipeptidyl carboxypeptidase I; AltName: Full=Kininase II; AltName: CD_antigen=CD143; Contains: RecName: Full=Angiotensin-converting enzyme, soluble form; Flags: Precursor; [Homo sapiens (Human)] - [ACE_HUMAN]	1.46E+07
Angiotensinogen OS=Homo sapiens GN=AGT PE=1 SV=1	4.94E+07
Annexin A5 OS=Homo sapiens GN=ANXA5 PE=1 SV=2	1.36E+06
Antithrombin-III OS=Homo sapiens GN=SERPINC1 PE=1 SV=1	1.84E+07
Apolipoprotein A-I OS=Homo sapiens GN=APOA1 PE=1 SV=1	1.38E+08
Apolipoprotein A-II OS=Homo sapiens GN=APOA2 PE=1 SV=1	7.40E+07
Apolipoprotein A-IV OS=Homo sapiens GN=APOA4 PE=1 SV=3	2.74E+07
ATP-binding cassette sub-family F member 1; AltName: Full=ATP-binding cassette 50; AltName: Full=TNF-alpha-stimulated ABC protein; [Homo sapiens (Human)] - [ABCF1_HUMAN]	1.17E+07
Attractin OS=Homo sapiens GN=ATRN PE=1 SV=2	5.23E+06
Beta-2-microglobulin OS=Homo sapiens GN=B2M PE=1 SV=1	2.59E+07
Biotinidase OS=Homo sapiens GN=BTD PE=1 SV=2	2.84E+06
C2 calcium-dependent domain-containing protein 4B; AltName: Full=Nuclear-localized factor 2; AltName: Full=Protein FAM148B; [Homo sapiens (Human)] - [C2C4B_HUMAN]	8.25E+07
Calmodulin OS=Homo sapiens GN=CALM1 PE=1 SV=2	2.68E+06
Calmodulin-like protein 5; AltName: Full=Calmodulin-like skin protein; [Homo sapiens (Human)] - [CALL5_HUMAN]	2.82E+07
Carbonic anhydrase 1 OS=Homo sapiens GN=CA1 PE=1 SV=2	3.91E+06
CD166 antigen; AltName: Full=Activated leukocyte cell adhesion molecule; AltName: CD_antigen=CD166; Flags: Precursor; [Homo sapiens (Human)] - [CD166_HUMAN]	1.35E+07
CD44 antigen OS=Homo sapiens GN=CD44 PE=1 SV=3	2.73E+07
CD59 glycoprotein; AltName: Full=1F5 antigen; AltName: Full=20 kDa homologous restriction factor; Short=HRF-20; Short=HRF20; AltName: Full=MAC-inhibitory protein; Short=MAC-IP; AltName: Full=MEM43 antigen; AltName: Full=Membrane attack complex inhibition factor; Short=MACIF; AltName: Full=Membrane inhibitor of reactive lysis; Short=MIRL; AltName: Full=Protectin; AltName: CD_antigen=CD59; Flags: Precursor; [Homo sapiens (Human)] - [CD59_HUMAN]	3.54E+06
CD9 antigen; AltName: Full=5H9 antigen; AltName: Full=Cell growth-inhibiting gene 2 protein; AltName: Full=Leukocyte antigen MIC3; AltName: Full=Motility-related protein; Short=MRP-1; AltName: Full=Tetraspanin-29; Short=Tspan-29; AltName: Full=p24; AltName: CD_antigen=CD9; [Homo sapiens (Human)] - [CD9_HUMAN]	9.50E+06
Cell adhesion molecule 2; AltName: Full=Immunoglobulin superfamily member 4D; Short=IgSF4D; AltName: Full=Nectin-like protein 3; Short=NECL-3; Flags: Precursor; [Homo sapiens (Human)] - [CADM2_HUMAN]	2.00E+06
Ceruloplasmin OS=Homo sapiens GN=CP PE=1 SV=1	3.67E+08
Coactosin-like protein OS=Homo sapiens GN=COTL1 PE=1 SV=3	5.15E+06

Complement C2 OS=Homo sapiens GN=C2 PE=1 SV=2	3.41E+07
Complement C3 OS=Homo sapiens GN=C3 PE=1 SV=2	2.66E+06
Complement decay-accelerating factor OS=Homo sapiens GN=CD55 PE=1 SV=4	7.63E+06
Corticosteroid-binding globulin OS=Homo sapiens GN=SERPINA6 PE=1 SV=1	3.95E+07
Deleted in malignant brain tumors 1 protein OS=Homo sapiens GN=DMBT1 PE=1 SV=2	3.69E+07
Delta-like protein 4; AltName: Full=Drosophila Delta homolog 4; Short=Delta4; Flags: Precursor; [Homo sapiens (Human)] - [DLL4_HUMAN]	1.23E+07
Dermcidin OS=Homo sapiens GN=DCD PE=1 SV=2	2.13E+06
Desmoplakin OS=Homo sapiens GN=DSP PE=1 SV=3	1.40E+08
Dipeptidyl peptidase 4 OS=Homo sapiens GN=DPP4 PE=1 SV=2	6.17E+07
Disintegrin and metalloproteinase domain-containing protein 2; Short=ADAM 2; AltName: Full=Cancer/testis antigen 15; Short=CT15; AltName: Full=Fertilin subunit beta; AltName: Full=PH-30; Short=PH30; AltName: Full=PH30-beta; Flags: Precursor; [Homo sapiens (Human)] - [ADAM2_HUMAN]	1.05E+08
Ecto-ADP-ribosyltransferase 4; EC=2.4.2.31; AltName: Full=Dombrock blood group carrier molecule; AltName: Full=Mono(ADP-ribosyl)transferase 4; AltName: Full=NAD(P)(+)--arginine ADP-ribosyltransferase 4; AltName: CD_antigen=CD297; Flags: Precursor; [Homo sapiens (Human)] - [NAR4_HUMAN]	5.81E+07
Elongation factor 1-alpha 1 OS=Homo sapiens GN=EEF1A1 PE=1 SV=1	2.16E+07
Epididymal secretory protein E1 OS=Homo sapiens GN=NPC2 PE=1 SV=1	1.37E+07
FAS-associated factor 1; Short=hFAF1; AltName: Full=UBX domain-containing protein 12; AltName: Full=UBX domain-containing protein 3A; [Homo sapiens (Human)] - [FAF1_HUMAN]	4.89E+08
Ferritin heavy chain; Short=Ferritin H subunit; EC=1.16.3.1; AltName: Full=Cell proliferation-inducing gene 15 protein; [Homo sapiens (Human)] - [FRIH_HUMAN]	2.34E+06
Ferritin light chain; Short=Ferritin L subunit; [Homo sapiens (Human)] - [FRIL_HUMAN]	4.73E+06
Galectin-3-binding protein; AltName: Full=Basement membrane autoantigen p105; AltName: Full=Lectin galactoside-binding soluble 3-binding protein; AltName: Full=Mac-2-binding protein; Short=MAC2BP; Short=Mac-2 BP; AltName: Full=Tumor-associated antigen 90K; Flags: Precursor; [Homo sapiens (Human)] - [LG3BP_HUMAN]	7.88E+06
Galectin-3; Short=Gal-3; AltName: Full=35 kDa lectin; AltName: Full=Carbohydrate-binding protein 35; Short=CBP 35; AltName: Full=Galactose-specific lectin 3; AltName: Full=Galactoside-binding protein; Short=GALBP; AltName: Full=IgE-binding protein; AltName: Full=L-31; AltName: Full=Laminin-binding protein; AltName: Full=Lectin L-29; AltName: Full=Mac-2 antigen; [Homo sapiens (Human)] - [LEG3_HUMAN]	2.03E+06
Glutathione peroxidase 3 OS=Homo sapiens GN=GPX3 PE=1 SV=2	1.19E+06
Glutathione S-transferase A2 OS=Homo sapiens GN=GSTA2 PE=1 SV=4	4.18E+07
Glutathione S-transferase P OS=Homo sapiens GN=GSTP1 PE=1 SV=2	8.51E+06
Haptoglobin OS=Homo sapiens GN=HP PE=1 SV=1	1.26E+08
Heat shock protein beta-1 OS=Homo sapiens GN=HSPB1 PE=1 SV=2	8.93E+06
Hemoglobin subunit alpha OS=Homo sapiens GN=HBA1 PE=1 SV=2	1.49E+08
Hemoglobin subunit beta OS=Homo sapiens GN=HBB PE=1 SV=2	1.28E+08
Hemoglobin subunit delta OS=Homo sapiens GN=HBD PE=1 SV=2	7.65E+07
Hemopexin OS=Homo sapiens GN=HPX PE=1 SV=2	2.71E+08
Histone H3.3C; [Homo sapiens (Human)] - [H3C_HUMAN]	1.79E+07

Histone H4 OS=Homo sapiens GN=HIST1H4A PE=1 SV=2	2.45E+07
HLA class II histocompatibility antigen, DR alpha chain; AltName: Full=MHC class II antigen DRA; Flags: Precursor; [Homo sapiens (Human)] - [DRA_HUMAN]	1.69E+06
HLA class II histocompatibility antigen, DRB1-1 beta chain OS=Homo sapiens GN=HLA-DRB1 PE=1 SV=2	6.88E+06
Homeobox protein Nkx-3.2; AltName: Full=Bagpipe homeobox protein homolog 1; AltName: Full=Homeobox protein NK-3 homolog B; [Homo sapiens (Human)] - [NKX32_HUMAN]	1.75E+07
Ig alpha-1 chain C region OS=Homo sapiens GN=IGHA1 PE=1 SV=2	2.42E+09
Ig alpha-2 chain C region OS=Homo sapiens GN=IGHA2 PE=1 SV=3	1.79E+09
Ig delta chain C region OS=Homo sapiens GN=IGHD PE=1 SV=2	1.10E+07
Ig gamma-1 chain C region OS=Homo sapiens GN=IGHG1 PE=1 SV=1	8,918,000,000
Ig gamma-2 chain C region OS=Homo sapiens GN=IGHG2 PE=1 SV=2	5.60E+09
Ig gamma-3 chain C region OS=Homo sapiens GN=IGHG3 PE=1 SV=2	6.71E+09
Ig gamma-4 chain C region OS=Homo sapiens GN=IGHG4 PE=1 SV=1	5.60E+09
Ig heavy chain V-I region Mot OS=Homo sapiens PE=1 SV=1	2.05E+08
Ig heavy chain V-II region ARH-77; Flags: Precursor; [Homo sapiens (Human)] - [HV209_HUMAN]	4.86E+07
Ig heavy chain V-II region NEWM OS=Homo sapiens PE=1 SV=1	1.47E+08
Ig heavy chain V-II region OU; [Homo sapiens (Human)] - [HV201_HUMAN]	1.44E+08
Ig heavy chain V-III region BRO; [Homo sapiens (Human)] - [HV305_HUMAN]	1.02E+09
Ig heavy chain V-III region BUT; [Homo sapiens (Human)] - [HV306_HUMAN]	1.03E+09
Ig heavy chain V-III region CAM OS=Homo sapiens PE=1 SV=1	1.05E+09
Ig heavy chain V-III region GAL OS=Homo sapiens PE=1 SV=1	1.05E+09
Ig heavy chain V-III region GAR; [Homo sapiens (Human)] - [HV322_HUMAN]	1.05E+08
Ig heavy chain V-III region HIL; [Homo sapiens (Human)] - [HV310_HUMAN]	1.47E+09
Ig heavy chain V-III region TIL OS=Homo sapiens PE=1 SV=1	1.06E+09
Ig kappa chain C region OS=Homo sapiens GN=IGKC PE=1 SV=1	3.47E+09
Ig kappa chain V-I region CAR; [Homo sapiens (Human)] - [KV104_HUMAN]	7.26E+07
Ig kappa chain V-I region DEE; [Homo sapiens (Human)] - [KV105_HUMAN]	2.73E+08
Ig kappa chain V-I region EU OS=Homo sapiens PE=1 SV=1	2.41E+08
Ig kappa chain V-I region Kue OS=Homo sapiens PE=1 SV=1	1.89E+08
Ig kappa chain V-I region Ni; [Homo sapiens (Human)] - [KV121_HUMAN]	1.45E+08
Ig kappa chain V-I region OU; [Homo sapiens (Human)] - [KV114_HUMAN]	3.43E+08
Ig kappa chain V-I region Wes; [Homo sapiens (Human)] - [KV119_HUMAN]	2.71E+08
Ig kappa chain V-II region FR OS=Homo sapiens PE=1 SV=1	8.51E+07
Ig kappa chain V-II region RPMI 6410 OS=Homo sapiens PE=4 SV=1	1.62E+08
Ig kappa chain V-III region B6; [Homo sapiens (Human)] - [KV301_HUMAN]	2.39E+08
Ig kappa chain V-III region POM OS=Homo sapiens PE=1 SV=1	9.77E+07
Ig kappa chain V-III region SIE OS=Homo sapiens PE=1 SV=1	2.40E+08
Ig kappa chain V-III region VG; Flags: Precursor; Fragment; [Homo sapiens (Human)] - [KV309_HUMAN]	1.46E+08
Ig kappa chain V-IV region JI OS=Homo sapiens PE=4 SV=1	3.74E+07
Ig kappa chain V-IV region Len OS=Homo sapiens PE=1 SV=2	9.86E+07
Ig lambda chain V region 4A OS=Homo sapiens PE=4 SV=1	5.01E+07
Ig lambda chain V-I region HA OS=Homo sapiens PE=1 SV=1	1.91E+08
Ig lambda chain V-I region NIG-64 OS=Homo sapiens PE=1 SV=1	7.21E+07
Ig lambda chain V-II region NEI; [Homo sapiens (Human)] - [LV202_HUMAN]	1.91E+07
Ig lambda chain V-III region LOI OS=Homo sapiens PE=1 SV=1	1.57E+08

Ig lambda chain V-III region SH; [Homo sapiens (Human)] - [LV301_HUMAN]	3.09E+07
Ig lambda chain V-IV region Bau; [Homo sapiens (Human)] - [LV401_HUMAN]	1.58E+08
Ig lambda chain V-VI region SUT; [Homo sapiens (Human)] - [LV603_HUMAN]	7.86E+06
Ig lambda-2 chain C regions OS=Homo sapiens GN=IGLC2 PE=1 SV=1	2.31E+09
Ig mu chain C region OS=Homo sapiens GN=IGHM PE=1 SV=3	4.16E+07
Immunoglobulin J chain OS=Homo sapiens GN=IGJ PE=1 SV=4	4.76E+07
Immunoglobulin lambda-like polypeptide 5 OS=Homo sapiens GN=IGLL5 PE=2 SV=2	1.44E+09
Intercellular adhesion molecule 1 OS=Homo sapiens GN=ICAM1 PE=1 SV=2	1.15E+07
Lactotransferrin; Short=Lactoferrin; EC=3.4.21.-; AltName: Full=Talalactoferrin; Contains: RecName: Full=Kaliocin-1; Contains: RecName: Full=Lactoferroxin-A; Contains: RecName: Full=Lactoferroxin-B; Contains: RecName: Full=Lactoferroxin-C; Flags: Precursor; [Homo sapiens (Human)] - [TRFL_HUMAN]	9.47E+08
Leucine-rich alpha-2-glycoprotein OS=Homo sapiens GN=LRG1 PE=1 SV=2	4.46E+07
LIM domain only protein 7; Short=LMO-7; AltName: Full=F-box only protein 20; AltName: Full=LOMP; [Homo sapiens (Human)] - [LMO7_HUMAN]	1.36E+08
Lysosomal alpha-glucosidase; EC=3.2.1.20; AltName: Full=Acid maltase; AltName: Full=Aglucosidase alfa; Contains: RecName: Full=76 kDa lysosomal alpha-glucosidase; Contains: RecName: Full=70 kDa lysosomal alpha-glucosidase; Flags: Precursor; [Homo sapiens (Human)] - [LYAG_HUMAN]	1.40E+06
Lysozyme C; EC=3.2.1.17; AltName: Full=1,4-beta-N-acetylmuramidase C; Flags: Precursor; [Homo sapiens (Human)] - [LYSC_HUMAN]	1.48E+06
Mucin-1 OS=Homo sapiens GN=MUC1 PE=1 SV=3	1.18E+07
Myotubularin-related protein 14; EC=3.1.3.-; AltName: Full=HCV NS5A-transactivated protein 4 splice variant A-binding protein 1; Short=NS5ATP4ABP1; AltName: Full=hJumpy; [Homo sapiens (Human)] - [MTMRE_HUMAN]	3.06E+06
Pancreatic alpha-amylase; Short=PA; EC=3.2.1.1; AltName: Full=1,4-alpha-D-glucan glucanohydrolase; Flags: Precursor; [Homo sapiens (Human)] - [AMYP_HUMAN]	1.35E+07
Peptidyl-prolyl cis-trans isomerase A; Short=PPIase A; EC=5.2.1.8; AltName: Full=Cyclophilin A; AltName: Full=Cyclosporin A-binding protein; AltName: Full=Rotamase A; [Homo sapiens (Human)] - [PPIA_HUMAN]	6.43E+06
Polymeric immunoglobulin receptor OS=Homo sapiens GN=PIGR PE=1 SV=4	1.94E+08
Pre-mRNA cleavage complex 2 protein Pcf11; AltName: Full=Pre-mRNA cleavage complex II protein Pcf11; [Homo sapiens (Human)] - [PCF11_HUMAN]	5.19E+07
Pro-cathepsin H OS=Homo sapiens GN=CTSH PE=1 SV=4	1.06E+07
Proactivator polypeptide OS=Homo sapiens GN=PSAP PE=1 SV=2	2.71E+06
Prostasin; EC=3.4.21.-; AltName: Full=Serine protease 8; Contains: RecName: Full=Prostasin light chain; Contains: RecName: Full=Prostasin heavy chain; Flags: Precursor; [Homo sapiens (Human)] - [PRSS8_HUMAN]	1.22E+06
Protein DJ-1 OS=Homo sapiens GN=PARK7 PE=1 SV=2	1.23E+07
Protein S100-A6 OS=Homo sapiens GN=S100A6 PE=1 SV=1	2.38E+07
Protein S100-A8 OS=Homo sapiens GN=S100A8 PE=1 SV=1	3.59E+07
Protein S100-A9 OS=Homo sapiens GN=S100A9 PE=1 SV=1	1.13E+07
Protein Shroom3; AltName: Full=Shroom-related protein; Short=hShrmL; [Homo sapiens (Human)] - [SHRM3_HUMAN]	9.47E+07
Protein-glutamine gamma-glutamyltransferase E; EC=2.3.2.13; AltName:	3.65E+06

Full=Transglutaminase E; Short=TG(E); Short=TGE; Short=TGase E; AltName: Full=Transglutaminase-3; Short=TGase-3; Contains: RecName: Full=Protein-glutamine gamma-glutamyltransferase E 50 kDa non-catalytic chain; Contains: RecName: Full=Protein-glutamine gamma-glutamyltransferase E 27 kDa catalytic chain; Flags: Precursor; [Homo sapiens (Human)] - [TGM3_HUMAN]	
Pulmonary surfactant-associated protein A2 OS=Homo sapiens GN=SFTPA2 PE=1 SV=1	3.74E+07
Pulmonary surfactant-associated protein B; Short=SP-B; AltName: Full=18 kDa pulmonary-surfactant protein; AltName: Full=6 kDa protein; AltName: Full=Pulmonary surfactant-associated proteolipid SPL(Phe); Flags: Precursor; [Homo sapiens (Human)] - [PSPB_HUMAN]	3.26E+06
Pulmonary surfactant-associated protein D OS=Homo sapiens GN=SFTPD PE=1 SV=3	1.53E+07
Putative V-set and immunoglobulin domain-containing protein 6 OS=Homo sapiens GN=VSIG6 PE=5 SV=2	2.00E+08
Ribonuclease P protein subunit p40; Short=RNaseP protein p40; EC=3.1.26.5; AltName: Full=RNase P subunit 1; [Homo sapiens (Human)] - [RPP40_HUMAN]	5.47E+07
Selenium-binding protein 1 OS=Homo sapiens GN=SELENBP1 PE=1 SV=2	1.67E+07
Serotransferrin OS=Homo sapiens GN=TF PE=1 SV=3	7.62E+09
Serpin B3 OS=Homo sapiens GN=SERPINB3 PE=1 SV=2	2.30E+07
Serum albumin OS=Homo sapiens GN=ALB PE=1 SV=2	2.77E+09
SH3 domain-binding glutamic acid-rich-like protein 3; AltName: Full=SH3 domain-binding protein 1; Short=SH3BP-1; [Homo sapiens (Human)] - [SH3L3_HUMAN]	3.66E+06
Sorting nexin-6; AltName: Full=TRAF4-associated factor 2; [Homo sapiens (Human)] - [SNX6_HUMAN]	2.15E+06
Thioredoxin; Short=Trx; AltName: Full=ATL-derived factor; Short=ADF; AltName: Full=Surface-associated sulphydryl protein; Short=SASP; [Homo sapiens (Human)] - [THIO_HUMAN]	8.21E+06
Thyroxine-binding globulin OS=Homo sapiens GN=SERPINA7 PE=1 SV=2	5.25E+06
Transaldolase OS=Homo sapiens GN=TALDO1 PE=1 SV=2	4.47E+07
Transcriptional adapter 2-beta; AltName: Full=ADA2-like protein beta; Short=ADA2-beta; [Homo sapiens (Human)] - [TAD2B_HUMAN]	2.22E+07
Transmembrane protein 198; [Homo sapiens (Human)] - [TM198_HUMAN]	2.62E+07
Transmembrane protein 200C; AltName: Full=Transmembrane protein TTMA; AltName: Full=Two transmembrane domain-containing family member A; [Homo sapiens (Human)] - [T200C_HUMAN]	3.59E+06
Transthyretin OS=Homo sapiens GN=TTR PE=1 SV=1	2.53E+08
Triosephosphate isomerase OS=Homo sapiens GN=TPI1 PE=1 SV=3	4.37E+07
Uncharacterized protein C3orf38; [Homo sapiens (Human)] - [CC038_HUMAN]	2.73E+09
Uncharacterized protein KIAA0947; [Homo sapiens (Human)] - [K0947_HUMAN]	8.15E+06
Uteroglobin OS=Homo sapiens GN=SCGB1A1 PE=1 SV=1	1.74E+08
Vitamin D-binding protein OS=Homo sapiens GN=GC PE=1 SV=1	4.91E+08
Vitamin K-dependent protein S; Flags: Precursor; [Homo sapiens (Human)] - [PROS_HUMAN]	3.31E+07
Xin actin-binding repeat-containing protein 2 OS=Homo sapiens GN=XIRP2 PE=1 SV=2	2.05E+08
Zinc-alpha-2-glycoprotein OS=Homo sapiens GN=AZGP1 PE=1 SV=2	1.24E+08

Table C.2: *All alveolar proteins identified by 1D PAGE and nano LC MS/MS in healthy smoker RTLFs***.** The 145 proteins identified in healthy smoker subjects investigated, (n=5), alongside the mean of the three most abundant ion peaks of each respective protein identified. Accession numbers included according to entries in UniProtKB/Swiss-Prot

Healthy Smoker	
14-3-3 protein beta/alpha OS=Homo sapiens GN=YWHAB PE=1 SV=3	6.47E+07
14-3-3 protein zeta/delta OS=Homo sapiens GN=YWHAZ PE=1 SV=1	4.51E+07
Actin, cytoplasmic 1 OS=Homo sapiens GN=ACTB PE=1 SV=1	1.38E+08
Afamin OS=Homo sapiens GN=AFM PE=1 SV=1	5.45E+06
Aldo-keto reductase family 1 member B10; EC=1.1.1.-; AltName: Full=ARL-1; AltName: Full=Aldose reductase-like; AltName: Full=Aldose reductase-related protein; Short=ARP; Short=hARP; AltName: Full=Small intestine reductase; Short=SI reductase; [Homo sapiens (Human)] - [AK1BA_HUMAN]	5.19E+05
Aldo-keto reductase family 1 member C1 OS=Homo sapiens GN=AKR1C1 PE=1 SV=1	3.41E+06
Aldose 1-epimerase; EC=5.1.3.3; AltName: Full=Galactose mutarotase; [Homo sapiens (Human)] - [GALM_HUMAN]	2.63E+06
Alpha-1-acid glycoprotein 1 OS=Homo sapiens GN=ORM1 PE=1 SV=1	1.29E+08
Alpha-1-acid glycoprotein 2; Short=AGP 2; AltName: Full=Orosomucoid-2; Short=OMD 2; Flags: Precursor; [Homo sapiens (Human)] - [A1AG2_HUMAN]	1.14E+08
Alpha-1-antichymotrypsin OS=Homo sapiens GN=SERPINA3 PE=1 SV=2	3.72E+07
Alpha-1-antitrypsin OS=Homo sapiens GN=SERPINA1 PE=1 SV=3	2.75E+08
Alpha-1B-glycoprotein OS=Homo sapiens GN=A1BG PE=1 SV=4	2.29E+07
Alpha-2-HS-glycoprotein OS=Homo sapiens GN=AHSG PE=1 SV=1	2.99E+07
Alpha-2-macroglobulin OS=Homo sapiens GN=A2M PE=1 SV=3	4.14E+06
Alpha-enolase OS=Homo sapiens GN=ENO1 PE=1 SV=2	3.19E+07
Angiotensinogen OS=Homo sapiens GN=AGT PE=1 SV=1	1.41E+06
Annexin A3 OS=Homo sapiens GN=ANXA3 PE=1 SV=3	2.81E+06
Annexin A5 OS=Homo sapiens GN=ANXA5 PE=1 SV=2	5.18E+07
Apolipoprotein A-I OS=Homo sapiens GN=APOA1 PE=1 SV=1	7.56E+06
Attractin OS=Homo sapiens GN=ATRN PE=1 SV=2	4.53E+06
Beta-2-microglobulin OS=Homo sapiens GN=B2M PE=1 SV=1	1.03E+07
Beta-microseminoprotein; AltName: Full=Immunoglobulin-binding factor; Short=IGBF; AltName: Full=PN44; AltName: Full=Prostate secreted seminal plasma protein; AltName: Full=Prostate secretory protein of 94 amino acids; Short=PSP-94; Short=PSP94; AltName: Full=Seminal plasma beta-inhibin; Flags: Precursor; [Homo sapiens (Human)] - [MSMB_HUMAN]	1.50E+07
C2 calcium-dependent domain-containing protein 4B; AltName: Full=Nuclear-localized factor 2; AltName: Full=Protein FAM148B; [Homo sapiens (Human)] - [C2C4B_HUMAN]	7.49E+06
Calcyphosin OS=Homo sapiens GN=CAPS PE=1 SV=1	1.44E+07
Calmodulin OS=Homo sapiens GN=CALM1 PE=1 SV=2	2.84E+06
Carbonic anhydrase 2 OS=Homo sapiens GN=CA2 PE=1 SV=2	3.84E+06
Cathepsin B OS=Homo sapiens GN=CTSB PE=1 SV=3	2.14E+06
Cathepsin S OS=Homo sapiens GN=CTSS PE=1 SV=3	3.74E+06
Cathepsin Z OS=Homo sapiens GN=CTSZ PE=1 SV=1	4.21E+06
CD166 antigen; AltName: Full=Activated leukocyte cell adhesion molecule; AltName: CD_antigen=CD166; Flags: Precursor; [Homo sapiens (Human)] - [CD166_HUMAN]	2.77E+06
CD44 antigen OS=Homo sapiens GN=CD44 PE=1 SV=3	3.34E+07

Ceruloplasmin OS=Homo sapiens GN=CP PE=1 SV=1	1.15E+08
Coactosin-like protein OS=Homo sapiens GN=COTL1 PE=1 SV=3	6.78E+06
Corticosteroid-binding globulin OS=Homo sapiens GN=SERPINA6 PE=1 SV=1	5.20E+06
Cystatin-B OS=Homo sapiens GN=CSTB PE=1 SV=2	6.43E+06
Deleted in malignant brain tumors 1 protein OS=Homo sapiens GN=DMBT1 PE=1 SV=2	6.18E+06
Delta-like protein 4; AltName: Full=Drosophila Delta homolog 4; Short=Delta4; Flags: Precursor; [Homo sapiens (Human)] - [DLL4_HUMAN]	1.12E+07
Dermcidin OS=Homo sapiens GN=DCD PE=1 SV=2	4.35E+06
Desmoglein-1; AltName: Full=Cadherin family member 4; AltName: Full=Desmosomal glycoprotein 1; Short=DG1; Short=DGI; AltName: Full=Pemphigus foliaceus antigen; Flags: Precursor; [Homo sapiens (Human)] - [DSG1_HUMAN]	7.80E+06
Desmoplakin OS=Homo sapiens GN=DSP PE=1 SV=3	9.94E+07
Dipeptidyl peptidase 4 OS=Homo sapiens GN=DPP4 PE=1 SV=2	3.08E+06
Dynein heavy chain 10, axonemal; AltName: Full=Axonemal beta dynein heavy chain 10; AltName: Full=Ciliary dynein heavy chain 10; [Homo sapiens (Human)] - [DYH10_HUMAN]	1.25E+08
Ecto-ADP-ribosyltransferase 4; EC=2.4.2.31; AltName: Full=Dombrock blood group carrier molecule; AltName: Full=Mono(ADP-ribosyl)transferase 4; AltName: Full=NAD(P)(+)--arginine ADP-ribosyltransferase 4; AltName: CD_antigen=CD297; Flags: Precursor; [Homo sapiens (Human)] - [NAR4_HUMAN]	2.69E+07
Elongation factor 1-alpha 1 OS=Homo sapiens GN=EEF1A1 PE=1 SV=1	
Epididymal secretory protein E1 OS=Homo sapiens GN=NPC2 PE=1 SV=1	1.32E+07
FAS-associated factor 1; Short=hFAF1; AltName: Full=UBX domain-containing protein 12; AltName: Full=UBX domain-containing protein 3A; [Homo sapiens (Human)] - [FAF1_HUMAN]	4.56E+07
Fatty acid-binding protein, epidermal OS=Homo sapiens GN=FABP5 PE=1 SV=3	8.26E+07
Ferritin heavy chain OS=Homo sapiens GN=FTH1 PE=1 SV=2	5.09E+06
Ferritin light chain OS=Homo sapiens GN=FTL PE=1 SV=2	2.03E+07
Glutathione S-transferase A1 OS=Homo sapiens GN=GSTA1 PE=1 SV=3	1.73E+07
Glutathione S-transferase P OS=Homo sapiens GN=GSTP1 PE=1 SV=2	1.82E+07
Glyceraldehyde-3-phosphate dehydrogenase OS=Homo sapiens GN=GAPDH PE=1 SV=3	4.98E+07
Glyoxalase domain-containing protein 4 OS=Homo sapiens GN=GLOD4 PE=1 SV=1	1.54E+06
Haptoglobin OS=Homo sapiens GN=HP PE=1 SV=1	1.04E+08
Heat shock protein beta-1 OS=Homo sapiens GN=HSPB1 PE=1 SV=2	4.31E+07
Heme-binding protein 2; AltName: Full=Placental protein 23; Short=PP23; AltName: Full=Protein SOUL; [Homo sapiens (Human)] - [HEBP2_HUMAN]	1.49E+06
Hemoglobin subunit alpha OS=Homo sapiens GN=HBA1 PE=1 SV=2	5.40E+07
Hemoglobin subunit beta OS=Homo sapiens GN=HBB PE=1 SV=2	2.04E+07
Hemopexin OS=Homo sapiens GN=HPX PE=1 SV=2	1.89E+08
Histone H3.3C; [Homo sapiens (Human)] - [H3C_HUMAN]	1.36E+07
Histone H4 OS=Homo sapiens GN=HIST1H4A PE=1 SV=2	2.72E+07
Ig alpha-1 chain C region OS=Homo sapiens GN=IGHA1 PE=1 SV=2	6.14E+08
Ig alpha-2 chain C region; [Homo sapiens (Human)] - [IGHA2_HUMAN]	3.06E+08
Ig gamma-1 chain C region OS=Homo sapiens GN=IGHG1 PE=1 SV=1	3.30E+09
Ig gamma-2 chain C region OS=Homo sapiens GN=IGHG2 PE=1 SV=2	2.57E+09

Ig gamma-3 chain C region OS=Homo sapiens GN=IGHG3 PE=1 SV=2	2.87E+09
Ig gamma-4 chain C region OS=Homo sapiens GN=IGHG4 PE=1 SV=1	2.57E+09
Ig heavy chain V-I region HG3; Flags: Precursor; [Homo sapiens (Human)] - [HV102_HUMAN]	3.44E+07
Ig heavy chain V-II region COR; [Homo sapiens (Human)] - [HV202_HUMAN]	2.14E+07
Ig heavy chain V-II region NEWM OS=Homo sapiens PE=1 SV=1	9.45E+07
Ig heavy chain V-III region BRO; [Homo sapiens (Human)] - [HV305_HUMAN]	5.36E+08
Ig heavy chain V-III region BUT; [Homo sapiens (Human)] - [HV306_HUMAN]	4.98E+08
Ig heavy chain V-III region CAM OS=Homo sapiens PE=1 SV=1	
Ig heavy chain V-III region GAL OS=Homo sapiens PE=1 SV=1	4.92E+08
Ig heavy chain V-III region GAR; [Homo sapiens (Human)] - [HV322_HUMAN]	8.76E+07
Ig heavy chain V-III region HIL; [Homo sapiens (Human)] - [HV310_HUMAN]	7.00E+08
Ig heavy chain V-III region VH26 OS=Homo sapiens PE=1 SV=1	4.91E+08
Ig kappa chain C region OS=Homo sapiens GN=IGKC PE=1 SV=1	1.07E+09
Ig kappa chain V-I region DEE; [Homo sapiens (Human)] - [KV105_HUMAN]	1.54E+08
Ig kappa chain V-I region EU OS=Homo sapiens PE=1 SV=1	7.39E+07
Ig kappa chain V-I region WAT OS=Homo sapiens PE=1 SV=1	
Ig kappa chain V-II region RPMI 6410 OS=Homo sapiens PE=4 SV=1	4.64E+07
Ig kappa chain V-III region POM; [Homo sapiens (Human)] - [KV306_HUMAN]	7.29E+07
Ig kappa chain V-III region SIE OS=Homo sapiens PE=1 SV=1	1.24E+08
Ig kappa chain V-III region Ti; [Homo sapiens (Human)] - [KV304_HUMAN]	9.42E+07
Ig kappa chain V-III region VG (Fragment) OS=Homo sapiens PE=1 SV=1	5.54E+07
Ig kappa chain V-IV region B17 OS=Homo sapiens PE=2 SV=1	6.10E+07
Ig kappa chain V-IV region JI; Flags: Precursor; [Homo sapiens (Human)] - [KV403_HUMAN]	6.10E+07
Ig kappa chain V-IV region Len; [Homo sapiens (Human)] - [KV402_HUMAN]	6.10E+07
Ig lambda chain V region 4A; Flags: Precursor; [Homo sapiens (Human)] - [LV001_HUMAN]	1.78E+07
Ig lambda chain V-I region HA; [Homo sapiens (Human)] - [LV102_HUMAN]	5.73E+07
Ig lambda chain V-III region LOI OS=Homo sapiens PE=1 SV=1	6.55E+07
Ig lambda chain V-III region SH OS=Homo sapiens PE=1 SV=1	1.01E+07
Ig lambda chain V-IV region Bau; [Homo sapiens (Human)] - [LV401_HUMAN]	1.05E+07
Ig lambda-2 chain C regions OS=Homo sapiens GN=IGLC2 PE=1 SV=1	7.91E+08
Ig mu chain C region OS=Homo sapiens GN=IGHM PE=1 SV=3	4.18E+07
Immunoglobulin J chain OS=Homo sapiens GN=IGJ PE=1 SV=4	3.90E+07
Immunoglobulin lambda-like polypeptide 5 OS=Homo sapiens GN=IGLL5 PE=2 SV=2	4.43E+08
Intercellular adhesion molecule 1 OS=Homo sapiens GN=ICAM1 PE=1 SV=2	4.60E+06
Leucine-rich alpha-2-glycoprotein OS=Homo sapiens GN=LRG1 PE=1 SV=2	1.76E+07
Leukocyte elastase inhibitor OS=Homo sapiens GN=SERPINB1 PE=1 SV=1	2.61E+06
Lysozyme C; EC=3.2.1.17; AltName: Full=1,4-beta-N-acetylmuramidase C; Flags: Precursor; [Homo sapiens (Human)] - [LYSC_HUMAN]	7.04E+05
Myoglobin; [Homo sapiens (Human)] - [MYG_HUMAN]	1.97E+06
Nicotinamide phosphoribosyltransferase; Short=NAmPRTase; Short=Nampt; EC=2.4.2.12; AltName: Full=Pre-B-cell colony-enhancing factor 1; Short=Pre-B cell-enhancing factor; AltName: Full=Visfatin; [Homo sapiens (Human)] - [NAMPT_HUMAN]	1.55E+07
Olfactory receptor 2A2; AltName: Full=Olfactory receptor 2A17; AltName:	2.70E+08

Full=Olfactory receptor OR7-11; [Homo sapiens (Human)] - [OR2A2_HUMAN]	
Peroxiredoxin-6 OS=Homo sapiens GN=PRDX6 PE=1 SV=3	1.78E+06
Polymeric immunoglobulin receptor OS=Homo sapiens GN=PIGR PE=1 SV=4	1.54E+08
Pro-cathepsin H OS=Homo sapiens GN=CTSH PE=1 SV=4	1.14E+07
Proactivator polypeptide; Contains: RecName: Full=Saposin-A; AltName: Full=Protein A; Contains: RecName: Full=Saposin-B-Val; Contains: RecName: Full=Saposin-B; AltName: Full=Cerebroside sulfate activator; Short=CSAct; AltName: Full=Dispersin; AltName: Full=Sphingolipid activator protein 1; Short=SAP-1; AltName: Full=Sulfatide/GM1 activator; Contains: RecName: Full=Saposin-C; AltName: Full=A1 activator; AltName: Full=Co-beta-glucosidase; AltName: Full=Glucosylceramidase activator; AltName: Full=Sphingolipid activator protein 2; Short=SAP-2; Contains: RecName: Full=Saposin-D; AltName: Full=Component C; AltName: Full=Protein C; Flags: Precursor; [Homo sapiens (Human)] - [SAP_HUMAN]	1.35E+06
Prostasin; EC=3.4.21.-; AltName: Full=Serine protease 8; Contains: RecName: Full=Prostasin light chain; Contains: RecName: Full=Prostasin heavy chain; Flags: Precursor; [Homo sapiens (Human)] - [PRSS8_HUMAN]	1.62E+06
Protein DJ-1 OS=Homo sapiens GN=PARK7 PE=1 SV=2	7.89E+06
Protein S100-A11 OS=Homo sapiens GN=S100A11 PE=1 SV=2	4.08E+06
Protein S100-A6 OS=Homo sapiens GN=S100A6 PE=1 SV=1	4.87E+07
Protein S100-A8 OS=Homo sapiens GN=S100A8 PE=1 SV=1	8.57E+08
Protein S100-A9 OS=Homo sapiens GN=S100A9 PE=1 SV=1	5.29E+08
Protein S100-P; AltName: Full=Protein S100-E; AltName: Full=S100 calcium-binding protein P; [Homo sapiens (Human)] - [S100P_HUMAN]	2.36E+06
Protein Shroom3; AltName: Full=Shroom-related protein; Short=hShrmL; [Homo sapiens (Human)] - [SHRM3_HUMAN]	8.20E+07
Pulmonary surfactant-associated protein A2 OS=Homo sapiens GN=SFTPA2 PE=1 SV=1	2.82E+07
Pulmonary surfactant-associated protein B OS=Homo sapiens GN=SFTPB PE=1 SV=3	
Pulmonary surfactant-associated protein D; Short=PSP-D; Short=SP-D; AltName: Full=Collectin-7; AltName: Full=Lung surfactant protein D; Flags: Precursor; [Homo sapiens (Human)] - [SFTPD_HUMAN]	5.11E+06
Putative V-set and immunoglobulin domain-containing protein 6 OS=Homo sapiens GN=VSIG6 PE=5 SV=2	8.23E+07
Scavenger receptor cysteine-rich type 1 protein M130 OS=Homo sapiens GN=CD163 PE=1 SV=2	1.59E+07
Selenium-binding protein 1 OS=Homo sapiens GN=SELENBP1 PE=1 SV=2	1.15E+07
Serotransferrin OS=Homo sapiens GN=TF PE=1 SV=3	3,420,000,000
Serum albumin OS=Homo sapiens GN=ALB PE=1 SV=2	1.54E+09
SH3 domain-binding glutamic acid-rich-like protein 3; AltName: Full=SH3 domain-binding protein 1; Short=SH3BP-1; [Homo sapiens (Human)] - [SH3L3_HUMAN]	7.49E+06
SH3 domain-binding glutamic acid-rich-like protein OS=Homo sapiens GN=SH3BGRL PE=1 SV=1	1.18E+06
Sorting nexin-6; AltName: Full=TRAF4-associated factor 2; [Homo sapiens (Human)] - [SNX6_HUMAN]	2.48E+06
Superoxide dismutase [Cu-Zn] OS=Homo sapiens GN=SOD1 PE=1 SV=2	7.11E+06
Thioredoxin domain-containing protein 17; AltName: Full=14 kDa thioredoxin-related protein; Short=TRP14; AltName: Full=Protein 42-9-9; AltName:	7.54E+05

Full=Thioredoxin-like protein 5; [Homo sapiens (Human)] - [TXD17_HUMAN]	
Thioredoxin; Short=Trx; AltName: Full=ATL-derived factor; Short=ADF; AltName: Full=Surface-associated sulphydryl protein; Short=SASP; [Homo sapiens (Human)] - [THIO_HUMAN]	1.29E+07
Transaldolase OS=Homo sapiens GN=TALDO1 PE=1 SV=2	2.21E+07
Transcriptional adapter 2-beta; AltName: Full=ADA2-like protein beta; Short=ADA2-beta; [Homo sapiens (Human)] - [TAD2B_HUMAN]	5.10E+07
Transketolase-like protein 2; EC=2.2.1.1; [Homo sapiens (Human)] - [TKTL2_HUMAN]	1.26E+08
Transmembrane protein 198; [Homo sapiens (Human)] - [TM198_HUMAN]	2.08E+07
Transmembrane protein 200C; AltName: Full=Transmembrane protein TTMA; AltName: Full=Two transmembrane domain-containing family member A; [Homo sapiens (Human)] - [T200C_HUMAN]	2.06E+06
Transthyretin OS=Homo sapiens GN=TTR PE=1 SV=1	4.44E+07
Triosephosphate isomerase OS=Homo sapiens GN=TPI1 PE=1 SV=3	1.81E+07
Trypsin-3; EC=3.4.21.4; AltName: Full=Brain trypsinogen; AltName: Full=Mesotrypsinogen; AltName: Full=Serine protease 3; AltName: Full=Serine protease 4; AltName: Full=Trypsin III; AltName: Full=Trypsin IV; Flags: Precursor; [Homo sapiens (Human)] - [TRY3_HUMAN]	1.60E+06
Uncharacterized protein C3orf38; [Homo sapiens (Human)] - [CC038_HUMAN]	1.62E+09
Uteroglobin OS=Homo sapiens GN=SCGB1A1 PE=1 SV=1	8.73E+07
Vitamin D-binding protein OS=Homo sapiens GN=GC PE=1 SV=1	1.16E+08
Voltage-gated potassium channel subunit beta-1; AltName: Full=K(+) channel subunit beta-1; AltName: Full=Kv-beta-1; [Homo sapiens (Human)] - [KCAB1_HUMAN]	6.65E+07
Xin actin-binding repeat-containing protein 2 OS=Homo sapiens GN=XIRP2 PE=1 SV=2	1.77E+08
Zinc-alpha-2-glycoprotein OS=Homo sapiens GN=AZGP1 PE=1 SV=2	5.33E+07

Table C.3: *All alveolar proteins identified by 1D PAGE and nano LC MS/MS in COPD smoker RTLFs. The 234 proteins identified in COPD smoker subjects investigated, (n=5), alongside the mean of the three most abundant ion peaks of each respective protein identified. Accession numbers included according to entries in UniProtKB/Swiss-Prot.*

COPD smoker	
14-3-3 protein beta/alpha OS=Homo sapiens GN=YWHAB PE=1 SV=3	3.26E+07
14-3-3 protein epsilon OS=Homo sapiens GN=YWHAE PE=1 SV=1	3.12E+07
14-3-3 protein eta OS=Homo sapiens GN=YWHAH PE=1 SV=4	3.26E+07
14-3-3 protein gamma OS=Homo sapiens GN=YWHAG PE=1 SV=2	3.26E+07
14-3-3 protein zeta/delta OS=Homo sapiens GN=YWHAZ PE=1 SV=1	3.48E+07
7-alpha-hydroxycholest-4-en-3-one 12-alpha-hydroxylase OS=Homo sapiens GN=CYP8B1 PE=2 SV=2	2.87E+07
Actin-related protein 2; AltName: Full=Actin-like protein 2; [Homo sapiens (Human)] - [ARP2_HUMAN]	1.95E+07
Actin, cytoplasmic 1 OS=Homo sapiens GN=ACTB PE=1 SV=1	5.36E+07
Afamin OS=Homo sapiens GN=AFM PE=1 SV=1	1.76E+07
Aldehyde dehydrogenase, dimeric NADP-preferring OS=Homo sapiens GN=ALDH3A1 PE=1 SV=3	2.75E+06
Aldo-keto reductase family 1 member B10; EC=1.1.1.-; AltName: Full=ARL-1; AltName: Full=Aldose reductase-like; AltName: Full=Aldose reductase-related protein; Short=ARP; Short=hARP; AltName: Full=Small intestine reductase;	7.27E+05

Short=SI reductase; [Homo sapiens (Human)] - [AK1BA_HUMAN]	
Aldo-keto reductase family 1 member C1; EC=1.1.1.-; AltName: Full=20-alpha-hydroxysteroid dehydrogenase; Short=20-alpha-HSD; EC=1.1.1.149; AltName: Full=Chlordecone reductase homolog HAKRC; AltName: Full=Dihydrodiol dehydrogenase 1/2; Short=DD1/DD2; AltName: Full=High-affinity hepatic bile acid-binding protein; Short=HBAB; AltName: Full=Indanol dehydrogenase; EC=1.1.1.112; AltName: Full=Trans-1,2-dihydrobenzene-1,2-diol dehydrogenase; EC=1.3.1.20; [Homo sapiens (Human)] - [AK1C1_HUMAN]	8.87E+06
Aldose 1-epimerase; EC=5.1.3.3; AltName: Full=Galactose mutarotase; [Homo sapiens (Human)] - [GALM_HUMAN]	1.50E+06
Alpha-1-acid glycoprotein 1 OS=Homo sapiens GN=ORM1 PE=1 SV=1	2.76E+08
Alpha-1-acid glycoprotein 2; Short=AGP 2; AltName: Full=Orosomucoid-2; Short=OMD 2; Flags: Precursor; [Homo sapiens (Human)] - [A1AG2_HUMAN]	1.95E+08
Alpha-1-antichymotrypsin OS=Homo sapiens GN=SERPINA3 PE=1 SV=2	1.00E+08
Alpha-1-antitrypsin OS=Homo sapiens GN=SERPINA1 PE=1 SV=3	1.61E+09
Alpha-1B-glycoprotein OS=Homo sapiens GN=A1BG PE=1 SV=4	3.51E+07
Alpha-2-HS-glycoprotein OS=Homo sapiens GN=AHSG PE=1 SV=1	9.30E+07
Alpha-2-macroglobulin OS=Homo sapiens GN=A2M PE=1 SV=3	1.01E+07
Alpha-amylase 1 OS=Homo sapiens GN=AMY1A PE=1 SV=2	3.66E+07
Alpha-enolase OS=Homo sapiens GN=ENO1 PE=1 SV=2	7.37E+06
Angiotensin-converting enzyme OS=Homo sapiens GN=ACE PE=1 SV=1	2.81E+07
Angiotensinogen OS=Homo sapiens GN=AGT PE=1 SV=1	5.39E+07
Ankyrin repeat domain-containing protein 56; [Homo sapiens (Human)] - [ANR56_HUMAN]	4.43E+07
Annexin A3; AltName: Full=35-alpha calcimedin; AltName: Full=Annexin III; AltName: Full=Annexin-3; AltName: Full=Inositol 1,2-cyclic phosphate 2-phosphohydrolase; AltName: Full=Lipocortin III; AltName: Full=Placental anticoagulant protein III; Short=PAP-III; [Homo sapiens (Human)] - [ANXA3_HUMAN]	9.75E+05
Annexin A4; AltName: Full=35-beta calcimedin; AltName: Full=Annexin IV; AltName: Full=Annexin-4; AltName: Full=Carbohydrate-binding protein p33/p41; AltName: Full=Chromobindin-4; AltName: Full=Endonexin I; AltName: Full=Lipocortin IV; AltName: Full=P32.5; AltName: Full=PP4-X; AltName: Full=Placental anticoagulant protein II; Short=PAP-II; AltName: Full=Protein II; [Homo sapiens (Human)] - [ANXA4_HUMAN]	3.12E+07
Annexin A5 OS=Homo sapiens GN=ANXA5 PE=1 SV=2	7.53E+07
Antithrombin-III OS=Homo sapiens GN=SERPINC1 PE=1 SV=1	1.82E+07
Apolipoprotein A-I OS=Homo sapiens GN=APOA1 PE=1 SV=1	5.68E+07
Apolipoprotein A-II OS=Homo sapiens GN=APOA2 PE=1 SV=1	9.64E+06
Apolipoprotein A-IV OS=Homo sapiens GN=APOA4 PE=1 SV=3	1.11E+07
Arginase-1; EC=3.5.3.1; AltName: Full=Liver-type arginase; AltName: Full=Type I arginase; [Homo sapiens (Human)] - [ARGI1_HUMAN]	1.90E+07
Aspartate aminotransferase, cytoplasmic OS=Homo sapiens GN=GOT1 PE=1 SV=3	1.52E+06
ATP-binding cassette sub-family C member 8; AltName: Full=Sulfonylurea receptor 1; [Homo sapiens (Human)] - [ABCC8_HUMAN]	4.40E+07
ATP-binding cassette sub-family F member 1; AltName: Full=ATP-binding cassette 50; AltName: Full=TNF-alpha-stimulated ABC protein; [Homo sapiens (Human)] - [ABCF1_HUMAN]	4.47E+07
Attractin OS=Homo sapiens GN=ATRN PE=1 SV=2	1.08E+07
Beta-2-microglobulin OS=Homo sapiens GN=B2M PE=1 SV=1	3.80E+07

Beta-microseminoprotein; AltName: Full=Immunoglobulin-binding factor; Short=IGBF; AltName: Full=PN44; AltName: Full=Prostate secreted seminal plasma protein; AltName: Full=Prostate secretory protein of 94 amino acids; Short=PSP-94; Short=PSP94; AltName: Full=Seminal plasma beta-inhibin; Flags: Precursor; [Homo sapiens (Human)] - [MSMB_HUMAN]	4.84E+07
Calcineurin-like phosphoesterase domain-containing protein 1 OS=Homo sapiens GN=CPPED1 PE=1 SV=3	3.70E+06
Calcyphosin OS=Homo sapiens GN=CAPS PE=1 SV=1	1.32E+06
Calmodulin OS=Homo sapiens GN=CALM1 PE=1 SV=2	2.48E+07
Carbonic anhydrase 1 OS=Homo sapiens GN=CA1 PE=1 SV=2	5.50E+06
Carbonic anhydrase 2 OS=Homo sapiens GN=CA2 PE=1 SV=2	1.05E+07
Caspase recruitment domain-containing protein 6; [Homo sapiens (Human)] - [CARD6_HUMAN]	1.73E+08
Cathepsin B OS=Homo sapiens GN=CTSB PE=1 SV=3	4.12E+06
Cathepsin D OS=Homo sapiens GN=CTSD PE=1 SV=1	8.45E+08
Cathepsin S OS=Homo sapiens GN=CTSS PE=1 SV=3	3.07E+07
Cathepsin Z OS=Homo sapiens GN=CTSZ PE=1 SV=1	6.46E+06
CD166 antigen OS=Homo sapiens GN=ALCAM PE=1 SV=2	6.34E+06
CD44 antigen OS=Homo sapiens GN=CD44 PE=1 SV=3	3.49E+07
CD59 glycoprotein; AltName: Full=1F5 antigen; AltName: Full=20 kDa homologous restriction factor; Short=HRF-20; Short=HRF20; AltName: Full=MAC-inhibitory protein; Short=MAC-IP; AltName: Full=MEM43 antigen; AltName: Full=Membrane attack complex inhibition factor; Short=MACIF; AltName: Full=Membrane inhibitor of reactive lysis; Short=MIRL; AltName: Full=Protectin; AltName: CD_antigen=CD59; Flags: Precursor; [Homo sapiens (Human)] - [CD59_HUMAN]	2.60E+06
Cell adhesion molecule 2; AltName: Full=Immunoglobulin superfamily member 4D; Short=IgSF4D; AltName: Full=Nectin-like protein 3; Short=NECL-3; Flags: Precursor; [Homo sapiens (Human)] - [CADM2_HUMAN]	1.71E+07
Centromere-associated protein E OS=Homo sapiens GN=CENPE PE=1 SV=2	1.43E+08
Ceruloplasmin OS=Homo sapiens GN=CP PE=1 SV=1	2.38E+08
Chitotriosidase-1 OS=Homo sapiens GN=CHIT1 PE=1 SV=1	2.82E+07
Coactosin-like protein OS=Homo sapiens GN=COTL1 PE=1 SV=3	3.50E+07
Coiled-coil domain-containing protein 37; [Homo sapiens (Human)] - [CCD37_HUMAN]	6.25E+06
Complement C2 OS=Homo sapiens GN=C2 PE=1 SV=2	1.87E+06
Complement C3 OS=Homo sapiens GN=C3 PE=1 SV=2	7.33E+07
Corticosteroid-binding globulin OS=Homo sapiens GN=SERPINA6 PE=1 SV=1	2.38E+07
Cystatin-B OS=Homo sapiens GN=CSTB PE=1 SV=2	1.51E+07
Cytochrome c oxidase subunit 7B2, mitochondrial; AltName: Full=Cytochrome c oxidase polypeptide VIIb2; Flags: Precursor; [Homo sapiens (Human)] - [CX7B2_HUMAN]	6.12E+06
Cytoplasmic aconitate hydratase; Short=Aconitase; EC=4.2.1.3; AltName: Full=Citrate hydro-lyase; AltName: Full=Ferritin repressor protein; AltName: Full=Iron regulatory protein 1; Short=IRP1; AltName: Full=Iron-responsive element-binding protein 1; Short=IRE-BP 1; [Homo sapiens (Human)] - [ACOC_HUMAN]	5.93E+07
Deleted in malignant brain tumors 1 protein OS=Homo sapiens GN=DMBT1 PE=1 SV=2	2.80E+07
Delta-like protein 4; AltName: Full=Drosophila Delta homolog 4; Short=Delta4; Flags: Precursor; [Homo sapiens (Human)] - [DLL4_HUMAN]	5.48E+07

Dermcidin; AltName: Full=Preproteolysin; Contains: RecName: Full=Survival-promoting peptide; Contains: RecName: Full=DCD-1; Flags: Precursor; [Homo sapiens (Human)] - [DCD_HUMAN]	2.94E+06
Desmoglein-1 OS=Homo sapiens GN=DSG1 PE=1 SV=2	5.04E+06
Desmoplakin OS=Homo sapiens GN=DSP PE=1 SV=3	1.06E+08
Dipeptidyl peptidase 4 OS=Homo sapiens GN=DPP4 PE=1 SV=2	1.99E+07
Disintegrin and metalloproteinase domain-containing protein 2; Short=ADAM 2; AltName: Full=Cancer/testis antigen 15; Short=CT15; AltName: Full=Fertilin subunit beta; AltName: Full=PH-30; Short=PH30; AltName: Full=PH30-beta; Flags: Precursor; [Homo sapiens (Human)] - [ADAM2_HUMAN]	1.48E+08
DNA-directed RNA polymerase I subunit RPA34; AltName: Full=A34.5; AltName: Full=Antisense to ERCC-1 protein; Short=ASE-1; AltName: Full=CD3-epsilon-associated protein; Short=CAST; Short=CD3E-associated protein; AltName: Full=RNA polymerase I-associated factor PAF49; [Homo sapiens (Human)] - [RPA34_HUMAN]	2.81E+07
Endonuclease 8-like 1; EC=3.2.2.-; EC=4.2.99.18; AltName: Full=DNA glycosylase/AP lyase Neil1; AltName: Full=DNA-(apurinic or apyrimidinic site) lyase Neil1; AltName: Full=Endonuclease VIII-like 1; AltName: Full=FPG1; AltName: Full=Nei homolog 1; Short=NEH1; AltName: Full=Nei-like protein 1; [Homo sapiens (Human)] - [NEIL1_HUMAN]	6.97E+06
Endothelin-1 receptor; AltName: Full=Endothelin A receptor; Short=ET-A; Short=ETA-R; Short=hET-AR; Flags: Precursor; [Homo sapiens (Human)] - [EDNRA_HUMAN]	1.31E+06
Eosinophil lysophospholipase; EC=3.1.1.5; AltName: Full=Charcot-Leyden crystal protein; Short=CLC; AltName: Full=Galectin-10; Short=Gal-10; AltName: Full=Lysolecithin acylhydrolase; [Homo sapiens (Human)] - [LPPL_HUMAN]	3.02E+06
Epididymal secretory protein E1 OS=Homo sapiens GN=NPC2 PE=1 SV=1	3.19E+07
Ester hydrolase C11orf54; EC=3.1.-.-; [Homo sapiens (Human)] - [CK054_HUMAN]	9.28E+05
Eukaryotic translation initiation factor 2-alpha kinase 1; EC=2.7.11.1; AltName: Full=Heme-controlled repressor; Short=HCR; AltName: Full=Heme-regulated eukaryotic initiation factor eIF-2-alpha kinase; AltName: Full=Heme-regulated inhibitor; AltName: Full=Hemin-sensitive initiation factor 2-alpha kinase; [Homo sapiens (Human)] - [E2AK1_HUMAN]	5.75E+07
FAS-associated factor 1; Short=hFAF1; AltName: Full=UBX domain-containing protein 12; AltName: Full=UBX domain-containing protein 3A; [Homo sapiens (Human)] - [FAF1_HUMAN]	9.69E+07
Fatty acid-binding protein, adipocyte OS=Homo sapiens GN=FABP4 PE=1 SV=3	7.13E+06
Fatty acid-binding protein, epidermal; AltName: Full=Epidermal-type fatty acid-binding protein; Short=E-FABP; AltName: Full=Fatty acid-binding protein 5; AltName: Full=Psoriasis-associated fatty acid-binding protein homolog; Short=PA-FABP; [Homo sapiens (Human)] - [FABP5_HUMAN]	1.88E+06
Fatty acid-binding protein, heart; AltName: Full=Fatty acid-binding protein 3; AltName: Full=Heart-type fatty acid-binding protein; Short=H-FABP; AltName: Full=Mammary-derived growth inhibitor; Short=MDGI; AltName: Full=Muscle fatty acid-binding protein; Short=M-FABP; [Homo sapiens (Human)] - [FABPH_HUMAN]	3.50E+07
Ferritin heavy chain OS=Homo sapiens GN=FTH1 PE=1 SV=2	1.41E+08
Ferritin light chain OS=Homo sapiens GN=FTL PE=1 SV=2	3.93E+08
Filaggrin-2; Short=FLG-2; AltName: Full=Intermediate filament-associated and psoriasis-susceptibility protein; Short=Ifapsoriasin; [Homo sapiens (Human)] -	1.21E+07

[FILA2_HUMAN]	
Folate receptor alpha; Short=FR-alpha; AltName: Full=Adult folate-binding protein; Short=FBP; AltName: Full=Folate receptor 1; AltName: Full=Folate receptor, adult; AltName: Full=KB cells FBP; AltName: Full=Ovarian tumor-associated antigen MOv18; Flags: Precursor; [Homo sapiens (Human)] - [FOLR1_HUMAN]	4.15E+06
Galectin-3-binding protein OS=Homo sapiens GN=LGALS3BP PE=1 SV=1	8.21E+06
Galectin-3; Short=Gal-3; AltName: Full=35 kDa lectin; AltName: Full=Carbohydrate-binding protein 35; Short=CBP 35; AltName: Full=Galactose-specific lectin 3; AltName: Full=Galactoside-binding protein; Short=GALBP; AltName: Full=IgE-binding protein; AltName: Full=L-31; AltName: Full=Laminin-binding protein; AltName: Full=Lectin L-29; AltName: Full=Mac-2 antigen; [Homo sapiens (Human)] - [LEG3_HUMAN]	1.28E+06
Gamma-glutamylcyclotransferase; EC=2.3.2.4; AltName: Full=Cytochrome c-releasing factor 21; [Homo sapiens (Human)] - [GGCT_HUMAN]	2.72E+06
Ganglioside GM2 activator; AltName: Full=Cerebroside sulfate activator protein; AltName: Full=GM2-AP; AltName: Full=Shingolipid activator protein 3; Short=SAP-3; Contains: RecName: Full=Ganglioside GM2 activator isoform short; Flags: Precursor; [Homo sapiens (Human)] - [SAP3_HUMAN]	7.81E+06
Gelsolin OS=Homo sapiens GN=GSN PE=1 SV=1	1.70E+06
Glucosamine--fructose-6-phosphate aminotransferase [isomerizing] 2; EC=2.6.1.16; AltName: Full=D-fructose-6-phosphate amidotransferase 2; AltName: Full=Glutamine:fructose 6 phosphate amidotransferase 2; Short=GFAT 2; Short=GFAT2; AltName: Full=Hexosephosphate aminotransferase 2; [Homo sapiens (Human)] - [GFPT2_HUMAN]	1.11E+08
Glucose-6-phosphate isomerase OS=Homo sapiens GN=GPI PE=1 SV=4	8.09E+06
Glutathione S-transferase A2 OS=Homo sapiens GN=GSTA2 PE=1 SV=4	9.67E+07
Glutathione S-transferase omega-1 OS=Homo sapiens GN=GSTO1 PE=1 SV=2	9.80E+06
Glutathione S-transferase P OS=Homo sapiens GN=GSTP1 PE=1 SV=2	1.74E+07
Glutathione synthetase; Short=GSH synthetase; Short=GSH-S; EC=6.3.2.3; AltName: Full=Glutathione synthase; [Homo sapiens (Human)] - [GSHB_HUMAN]	3.37E+06
Glyceraldehyde-3-phosphate dehydrogenase OS=Homo sapiens GN=GAPDH PE=1 SV=3	4.28E+06
Glyoxalase domain-containing protein 4 OS=Homo sapiens GN=GLOD4 PE=1 SV=1	3.60E+06
Haptoglobin OS=Homo sapiens GN=HP PE=1 SV=1	2.64E+08
Hemicentin-1; AltName: Full=Fibulin-6; Short=FIBL-6; Flags: Precursor; [Homo sapiens (Human)] - [HMCN1_HUMAN]	1.02E+08
Hemoglobin subunit alpha OS=Homo sapiens GN=HBA1 PE=1 SV=2	8.29E+07
Hemoglobin subunit beta OS=Homo sapiens GN=HBB PE=1 SV=2	7.32E+07
Hemopexin OS=Homo sapiens GN=HPX PE=1 SV=2	3.48E+08
HLA class II histocompatibility antigen, DRB1-1 beta chain OS=Homo sapiens GN=HLA-DRB1 PE=1 SV=2	4.64E+06
Hornerin OS=Homo sapiens GN=HRNR PE=1 SV=2	2.68E+07
Ig alpha-1 chain C region OS=Homo sapiens GN=IGHA1 PE=1 SV=2	1.56E+09
Ig alpha-2 chain C region OS=Homo sapiens GN=IGHA2 PE=1 SV=3	8.21E+08
Ig gamma-1 chain C region OS=Homo sapiens GN=IGHG1 PE=1 SV=1	5.79E+09
Ig gamma-2 chain C region OS=Homo sapiens GN=IGHG2 PE=1 SV=2	4.65E+09
Ig gamma-3 chain C region OS=Homo sapiens GN=IGHG3 PE=1 SV=2	5.04E+09
Ig heavy chain V-I region HG3; Flags: Precursor; [Homo sapiens (Human)] -	6.71E+07

[HV102_HUMAN]	
Ig heavy chain V-I region V35; Flags: Precursor; [Homo sapiens (Human)] - [HV103_HUMAN]	3.54E+07
Ig heavy chain V-II region ARH-77 OS=Homo sapiens PE=4 SV=1	7.16E+07
Ig heavy chain V-II region NEWM; [Homo sapiens (Human)] - [HV207_HUMAN]	1.15E+08
Ig heavy chain V-II region OU; [Homo sapiens (Human)] - [HV201_HUMAN]	4.28E+07
Ig heavy chain V-II region WAH; [Homo sapiens (Human)] - [HV206_HUMAN]	1.13E+07
Ig heavy chain V-III region BRO; [Homo sapiens (Human)] - [HV305_HUMAN]	9.27E+08
Ig heavy chain V-III region BUT; [Homo sapiens (Human)] - [HV306_HUMAN]	9.00E+08
Ig heavy chain V-III region CAM OS=Homo sapiens PE=1 SV=1	9.16E+08
Ig heavy chain V-III region GAL OS=Homo sapiens PE=1 SV=1	8.79E+08
Ig heavy chain V-III region GAR; [Homo sapiens (Human)] - [HV322_HUMAN]	2.86E+08
Ig heavy chain V-III region HIL; [Homo sapiens (Human)] - [HV310_HUMAN]	1.24E+09
Ig heavy chain V-III region TUR; [Homo sapiens (Human)] - [HV318_HUMAN]	9.44E+08
Ig heavy chain V-III region VH26; Flags: Precursor; [Homo sapiens (Human)] - [HV303_HUMAN]	9.25E+08
Ig kappa chain C region OS=Homo sapiens GN=IGKC PE=1 SV=1	2.92E+09
Ig kappa chain V-I region CAR OS=Homo sapiens PE=1 SV=1	8.07E+07
Ig kappa chain V-I region EU OS=Homo sapiens PE=1 SV=1	3.10E+08
Ig kappa chain V-I region Kue OS=Homo sapiens PE=1 SV=1	2.80E+08
Ig kappa chain V-I region Roy; [Homo sapiens (Human)] - [KV116_HUMAN]	1.88E+08
Ig kappa chain V-I region Wes; [Homo sapiens (Human)] - [KV119_HUMAN]	3.60E+08
Ig kappa chain V-II region FR OS=Homo sapiens PE=1 SV=1	3.16E+06
Ig kappa chain V-II region TEW OS=Homo sapiens PE=1 SV=1	1.67E+08
Ig kappa chain V-III region NG9; Flags: Precursor; Fragment; [Homo sapiens (Human)] - [KV303_HUMAN]	2.30E+08
Ig kappa chain V-III region POM OS=Homo sapiens PE=1 SV=1	1.58E+08
Ig kappa chain V-III region SIE OS=Homo sapiens PE=1 SV=1	2.67E+08
Ig kappa chain V-III region VG (Fragment) OS=Homo sapiens PE=1 SV=1	6.84E+07
Ig kappa chain V-IV region JI OS=Homo sapiens PE=4 SV=1	1.08E+08
Ig kappa chain V-IV region Len; [Homo sapiens (Human)] - [KV402_HUMAN]	1.49E+08
Ig lambda chain V region 4A OS=Homo sapiens PE=4 SV=1	7.87E+06
Ig lambda chain V-I region HA OS=Homo sapiens PE=1 SV=1	6.98E+07
Ig lambda chain V-I region NIG-64 OS=Homo sapiens PE=1 SV=1	2.25E+07
Ig lambda chain V-III region LOI OS=Homo sapiens PE=1 SV=1	6.09E+07
Ig lambda chain V-III region SH; [Homo sapiens (Human)] - [LV301_HUMAN]	1.31E+07
Ig lambda chain V-IV region Bau; [Homo sapiens (Human)] - [LV401_HUMAN]	5.41E+07
Ig lambda chain V-IV region Hil; [Homo sapiens (Human)] - [LV403_HUMAN]	6.79E+07
Ig lambda-2 chain C regions OS=Homo sapiens GN=IGLC2 PE=1 SV=1	1.09E+09
Ig mu chain C region OS=Homo sapiens GN=IGHM PE=1 SV=3	3.88E+07
Immunoglobulin J chain OS=Homo sapiens GN=IGJ PE=1 SV=4	7.57E+07
Immunoglobulin lambda-like polypeptide 5 OS=Homo sapiens GN=IGLL5 PE=2 SV=2	7.42E+08
Intercellular adhesion molecule 1 OS=Homo sapiens GN=ICAM1 PE=1 SV=2	1.44E+07
IQ domain-containing protein G; [Homo sapiens (Human)] - [IQCG_HUMAN]	6.79E+07
Kazrin; [Homo sapiens (Human)] - [KAZRN_HUMAN]	2.75E+07
Keratan sulfate proteoglycan lumican; Short=KSPG lumican; Flags: Precursor; [Homo sapiens (Human)] - [LUM_HUMAN]	3.26E+06
Keratinocyte proline-rich protein OS=Homo sapiens GN=KPRP PE=1 SV=1	1.15E+07
Kininogen-1; AltName: Full=Alpha-2-thiol proteinase inhibitor; AltName:	1.20E+07

Full=Fitzgerald factor; AltName: Full=High molecular weight kininogen; Short=HMWK; AltName: Full=Williams-Fitzgerald-Flaujeac factor; Contains: RecName: Full=Kininogen-1 heavy chain; Contains: RecName: Full=T-kinin; AltName: Full=Ile-Ser-Bradykinin; Contains: RecName: Full=Bradykinin; AltName: Full=Kallidin I; Contains: RecName: Full=Lysyl-bradykinin; AltName: Full=Kallidin II; Contains: RecName: Full=Kininogen-1 light chain; Contains: RecName: Full=Low molecular weight growth-promoting factor; Flags: Precursor; [Homo sapiens (Human)] - [KNG1_HUMAN]	
Leucine-rich alpha-2-glycoprotein OS=Homo sapiens GN=LRG1 PE=1 SV=2	3.29E+07
Leukocyte elastase inhibitor OS=Homo sapiens GN=SERPINB1 PE=1 SV=1	6.74E+06
Leukotriene A-4 hydrolase OS=Homo sapiens GN=LTA4H PE=1 SV=2	1.50E+07
Liver carboxylesterase 1; EC=3.1.1.1; AltName: Full=Acyl-coenzyme A:cholesterol acyltransferase; Short=ACAT; AltName: Full=Brain carboxylesterase hBr1; AltName: Full=Cocaine carboxylesterase; AltName: Full=Egasyn; AltName: Full=HMSE; AltName: Full=Methylumbelliferyl-acetate deacetylase 1; EC=3.1.1.56; AltName: Full=Monocyte/macrophage serine esterase; AltName: Full=Retinyl ester hydrolase; Short=REH; AltName: Full=Serine esterase 1; AltName: Full=Triacylglycerol hydrolase; Short=TGH; Flags: Precursor; [Homo sapiens (Human)] - [EST1_HUMAN]	1.49E+06
Long palate, lung and nasal epithelium carcinoma-associated protein 1; AltName: Full=Von Ebner minor salivary gland protein; Short=VEMSGP; Flags: Precursor; [Homo sapiens (Human)] - [LPLC1_HUMAN]	5.85E+06
Long-chain fatty acid transport protein 6; Short=FATP-6; Short=Fatty acid transport protein 6; AltName: Full=Fatty-acid-coenzyme A ligase, very long-chain 2; AltName: Full=Solute carrier family 27 member 6; AltName: Full=Very long-chain acyl-CoA synthetase homolog 1; Short=VLCSH1; Short=hVLCS-H1; [Homo sapiens (Human)] - [S27A6_HUMAN]	2.86E+07
Lysosomal alpha-glucosidase OS=Homo sapiens GN=GAA PE=1 SV=4	1.97E+07
Matrix metalloproteinase-28; Short=MMP-28; EC=3.4.24.-; AltName: Full=Epilysin; Flags: Precursor; [Homo sapiens (Human)] - [MMP28_HUMAN]	1.09E+07
Methionyl-tRNA formyltransferase OS=Geobacillus sp. (strain WCH70) GN=fmt PE=3 SV=1	9.01E+07
Mucin-1 OS=Homo sapiens GN=MUC1 PE=1 SV=3	1.02E+07
Myotubularin-related protein 14; EC=3.1.3.-; AltName: Full=HCV NS5A-transactivated protein 4 splice variant A-binding protein 1; Short=NS5ATP4ABP1; AltName: Full=hJumpy; [Homo sapiens (Human)] - [MTMRE_HUMAN]	3.66E+06
N(G),N(G)-dimethylarginine dimethylaminohydrolase 1; Short=DDAH-1; Short=Dimethylarginine dimethylaminohydrolase 1; EC=3.5.3.18; AltName: Full=DDAHI; AltName: Full=Dimethylargininase-1; [Homo sapiens (Human)] - [DDAH1_HUMAN]	1.77E+06
Napsin-A OS=Homo sapiens GN=NAPSA PE=1 SV=1	5.17E+06
Nestin; [Homo sapiens (Human)] - [NEST_HUMAN]	1.23E+06
Neutrophil gelatinase-associated lipocalin OS=Homo sapiens GN=LCN2 PE=1 SV=2	3.72E+06
OTU domain-containing protein 4; AltName: Full=HIV-1-induced protein HIN-1; [Homo sapiens (Human)] - [OTUD4_HUMAN]	1.21E+08
Peptidyl-prolyl cis-trans isomerase A OS=Homo sapiens GN=PPIA PE=1 SV=2	7.32E+06
Phosphatidylethanolamine-binding protein 1 OS=Homo sapiens GN=PEBP1 PE=1 SV=3	2.34E+06
Phosphoglycerate mutase 1; EC=3.1.3.13; EC=5.4.2.1; EC=5.4.2.4; AltName: Full=BPG-dependent PGAM 1; AltName: Full=Phosphoglycerate mutase	2.02E+06

isozyme B; Short=PGAM-B; [Homo sapiens (Human)] - [PGAM1_HUMAN]	
Polymeric immunoglobulin receptor OS=Homo sapiens GN=PIGR PE=1 SV=4	2.83E+08
Pro-cathepsin H OS=Homo sapiens GN=CTSH PE=1 SV=4	1.61E+07
Proactivator polypeptide; Contains: RecName: Full=Saposin-A; AltName: Full=Protein A; Contains: RecName: Full=Saposin-B-Val; Contains: RecName: Full=Saposin-B; AltName: Full=Cerebroside sulfate activator; Short=CSAct; AltName: Full=Dispersin; AltName: Full=Sphingolipid activator protein 1; Short=SAP-1; AltName: Full=Sulfatide/GM1 activator; Contains: RecName: Full=Saposin-C; AltName: Full=A1 activator; AltName: Full=Co-beta-glucosidase; AltName: Full=Glucosylceramidase activator; AltName: Full=Sphingolipid activator protein 2; Short=SAP-2; Contains: RecName: Full=Saposin-D; AltName: Full=Component C; AltName: Full=Protein C; Flags: Precursor; [Homo sapiens (Human)] - [SAP_HUMAN]	6.97E+06
Probable E3 ubiquitin-protein ligase HERC6; EC=6.3.2.-; AltName: Full=HECT domain and RCC1-like domain-containing protein 6; [Homo sapiens (Human)] - [HERC6_HUMAN]	1.12E+09
Probable histone-lysine N-methyltransferase NSD2; EC=2.1.1.43; AltName: Full=Multiple myeloma SET domain-containing protein; AltName: Full=Nuclear SET domain-containing protein 2; AltName: Full=Protein trithorax-5; AltName: Full=Wolf-Hirschhorn syndrome candidate 1 protein; [Homo sapiens (Human)] - [NSD2_HUMAN]	8.55E+07
Profilin-1 OS=Homo sapiens GN=PFN1 PE=1 SV=2	1.94E+08
Prostaglandin-H2 D-isomerase; EC=5.3.99.2; AltName: Full=Beta-trace protein; AltName: Full=Cerebrin-28; AltName: Full=Glutathione-independent PGD synthase; AltName: Full=Lipocalin-type prostaglandin-D synthase; AltName: Full=Prostaglandin-D2 synthase; Short=PGD2 synthase; Short=PGDS; Short=PGDS2; Flags: Precursor; [Homo sapiens (Human)] - [PTGDS_HUMAN]	4.62E+06
Protein AMBP OS=Homo sapiens GN=AMBP PE=1 SV=1	3.11E+06
Protein DJ-1 OS=Homo sapiens GN=PARK7 PE=1 SV=2	1.16E+07
Protein kinase-like protein SgK196; AltName: Full=Sugen kinase 196; [Homo sapiens (Human)] - [SG196_HUMAN]	1.67E+07
Protein S100-A11 OS=Homo sapiens GN=S100A11 PE=1 SV=2	5.82E+06
Protein S100-A6 OS=Homo sapiens GN=S100A6 PE=1 SV=1	1.14E+08
Protein S100-A8 OS=Homo sapiens GN=S100A8 PE=1 SV=1	2.22E+06
Protein S100-P; AltName: Full=Protein S100-E; AltName: Full=S100 calcium-binding protein P; [Homo sapiens (Human)] - [S100P_HUMAN]	2.63E+06
Protein Shroom3; AltName: Full=Shroom-related protein; Short=hShrmL; [Homo sapiens (Human)] - [SHRM3_HUMAN]	2.30E+08
Protein-glutamine gamma-glutamyltransferase E; EC=2.3.2.13; AltName: Full=Transglutaminase E; Short=TG(E); Short=TGE; Short=TGase E; AltName: Full=Transglutaminase-3; Short=TGase-3; Contains: RecName: Full=Protein-glutamine gamma-glutamyltransferase E 50 kDa non-catalytic chain; Contains: RecName: Full=Protein-glutamine gamma-glutamyltransferase E 27 kDa catalytic chain; Flags: Precursor; [Homo sapiens (Human)] - [TGM3_HUMAN]	8.37E+06
Pulmonary surfactant-associated protein A2 OS=Homo sapiens GN=SFTPA2 PE=1 SV=1	2.89E+07
Pulmonary surfactant-associated protein B OS=Homo sapiens GN=SFTPB PE=1 SV=3	9.69E+06
Pulmonary surfactant-associated protein D OS=Homo sapiens GN=SFTPD PE=1 SV=3	2.63E+07
Putative annexin A2-like protein; AltName: Full=Annexin A2 pseudogene 2;	2.21E+07

AltName: Full=Lipocortin II pseudogene; [Homo sapiens (Human)] - [AXA2L_HUMAN]	
Putative golgin subfamily A member 8I; [Homo sapiens (Human)] - [GOG8I_HUMAN]	4.68E+07
Putative methyltransferase NSUN3; EC=2.1.1.-; AltName: Full=NOL1/NOP2/Sun domain family member 3; [Homo sapiens (Human)] - [NSUN3_HUMAN]	1.55E+07
Putative V-set and immunoglobulin domain-containing protein 6; Flags: Precursor; [Homo sapiens (Human)] - [VSIG6_HUMAN]	1.42E+08
Pyridoxal kinase OS=Homo sapiens GN=PDXK PE=1 SV=1	3.73E+06
Retinoic acid-induced protein 3; AltName: Full=G-protein coupled receptor family C group 5 member A; AltName: Full=Orphan G-protein-coupling receptor PEIG-1; AltName: Full=Retinoic acid-induced gene 1 protein; Short=RAIG-1; [Homo sapiens (Human)] - [RAI3_HUMAN]	1.88E+06
Rho GDP-dissociation inhibitor 2 OS=Homo sapiens GN=ARHGDIB PE=1 SV=3	4.51E+06
Ribonuclease P protein subunit p40; Short=RNaseP protein p40; EC=3.1.26.5; AltName: Full=RNase P subunit 1; [Homo sapiens (Human)] - [RPP40_HUMAN]	1.55E+08
Scavenger receptor cysteine-rich type 1 protein M130 OS=Homo sapiens GN=CD163 PE=1 SV=2	5.07E+07
Selenium-binding protein 1 OS=Homo sapiens GN=SELENBP1 PE=1 SV=2	8.65E+06
Serotransferrin OS=Homo sapiens GN=TF PE=1 SV=3	4.56E+09
Serpin B12; [Homo sapiens (Human)] - [SPB12_HUMAN]	1.84E+07
Serpin B6; AltName: Full=Cytoplasmic antiproteinase; Short=CAP; AltName: Full=Peptidase inhibitor 6; Short=PI-6; AltName: Full=Placental thrombin inhibitor; [Homo sapiens (Human)] - [SPB6_HUMAN]	2.74E+06
Serum albumin OS=Homo sapiens GN=ALB PE=1 SV=2	3.86E+09
SH3 domain-binding glutamic acid-rich-like protein 3; AltName: Full=SH3 domain-binding protein 1; Short=SH3BP-1; [Homo sapiens (Human)] - [SH3L3_HUMAN]	1.22E+07
SH3 domain-binding glutamic acid-rich-like protein OS=Homo sapiens GN=SH3BGRL PE=1 SV=1	4.80E+06
Sister chromatid cohesion protein PDS5 homolog B; AltName: Full=Androgen-induced proliferation inhibitor; AltName: Full=Androgen-induced prostate proliferative shutoff-associated protein AS3; [Homo sapiens (Human)] - [PDS5B_HUMAN]	2.25E+07
Sorting nexin-6; AltName: Full=TRAF4-associated factor 2; [Homo sapiens (Human)] - [SNX6_HUMAN]	4.91E+06
Superoxide dismutase [Cu-Zn] OS=Homo sapiens GN=SOD1 PE=1 SV=2	1.08E+07
Thioredoxin domain-containing protein 17; AltName: Full=14 kDa thioredoxin-related protein; Short=TRP14; AltName: Full=Protein 42-9-9; AltName: Full=Thioredoxin-like protein 5; [Homo sapiens (Human)] - [TXD17_HUMAN]	1.84E+06
Thioredoxin; Short=Trx; AltName: Full=ATL-derived factor; Short=ADF; AltName: Full=Surface-associated sulphydryl protein; Short=SASP; [Homo sapiens (Human)] - [THIO_HUMAN]	2.98E+07
Thyroxine-binding globulin OS=Homo sapiens GN=SERPINA7 PE=1 SV=2	1.87E+07
Transaldolase OS=Homo sapiens GN=TALDO1 PE=1 SV=2	3.90E+07
Transcriptional adapter 2-beta; AltName: Full=ADA2-like protein beta; Short=ADA2-beta; [Homo sapiens (Human)] - [TAD2B_HUMAN]	2.68E+07
Transketolase-like protein 2; EC=2.2.1.1; [Homo sapiens (Human)] -	1.32E+08

[TKTL2_HUMAN]	
Transmembrane protein 198; [Homo sapiens (Human)] - [TM198_HUMAN]	4.78E+07
Transmembrane protein 200C; AltName: Full=Transmembrane protein TTMA; AltName: Full=Two transmembrane domain-containing family member A; [Homo sapiens (Human)] - [T200C_HUMAN]	1.94E+06
Transmembrane protein ENSP00000382582; [Homo sapiens (Human)] - [YE031_HUMAN]	3.19E+07
Transthyretin OS=Homo sapiens GN=TTR PE=1 SV=1	1.29E+08
Triosephosphate isomerase OS=Homo sapiens GN=TPI1 PE=1 SV=3	3.25E+07
Trypsin-1 OS=Homo sapiens GN=PRSS1 PE=1 SV=1	7.59E+06
Trypsin-3; EC=3.4.21.4; AltName: Full=Brain trypsinogen; AltName: Full=Mesotrypsinogen; AltName: Full=Serine protease 3; AltName: Full=Serine protease 4; AltName: Full=Trypsin III; AltName: Full=Trypsin IV; Flags: Precursor; [Homo sapiens (Human)] - [TRY3_HUMAN]	2.58E+06
Uncharacterized protein C19orf68; [Homo sapiens (Human)] - [CS068_HUMAN]	2.46E+07
Uncharacterized protein C3orf38; [Homo sapiens (Human)] - [CC038_HUMAN]	1.83E+09
Uteroglobin OS=Homo sapiens GN=SCGB1A1 PE=1 SV=1	1.99E+08
V-set and immunoglobulin domain-containing protein 4; AltName: Full=Protein Z39Ig; Flags: Precursor; [Homo sapiens (Human)] - [VSIG4_HUMAN]	1.28E+06
Vitamin D-binding protein OS=Homo sapiens GN=GC PE=1 SV=1	1.52E+08
Xaa-Pro dipeptidase; Short=X-Pro dipeptidase; EC=3.4.13.9; AltName: Full=Imidodipeptidase; AltName: Full=Peptidase D; AltName: Full=Proline dipeptidase; Short=Prolidase; [Homo sapiens (Human)] - [PEPD_HUMAN]	1.34E+07
Xin actin-binding repeat-containing protein 2 OS=Homo sapiens GN=XIRP2 PE=1 SV=2	1.76E+08
Zinc-alpha-2-glycoprotein OS=Homo sapiens GN=AZGP1 PE=1 SV=2	8.23E+07

Table C.4: *All alveolar proteins identified by 1D PAGE and nano LC MS/MS in COPD ex-smoker RTLFs. The 58 proteins identified in COPD ex-smoker subjects investigated, (n=5), alongside the mean of the three most abundant ion peaks of each respective protein identified. Accession numbers included according to entries in UniProtKB/Swiss-Prot.*

COPD ex-smoker	
Actin, cytoplasmic 1 OS=Homo sapiens GN=ACTB PE=1 SV=1	4.06E+08
Alpha-1-acid glycoprotein 1 OS=Homo sapiens GN=ORM1 PE=1 SV=1	2.88E+06
Alpha-1-acid glycoprotein 2; Short=AGP 2; AltName: Full=Orosomucoid-2; Short=OMD 2; Flags: Precursor; [Homo sapiens (Human)] - [A1AG2_HUMAN]	1.95E+06
Alpha-1-antitrypsin OS=Homo sapiens GN=SERPINA1 PE=1 SV=3	3.86E+07
Alpha-1B-glycoprotein; AltName: Full=Alpha-1-B glycoprotein; Flags: Precursor; [Homo sapiens (Human)] - [A1BG_HUMAN]	1.24E+06
Annexin A5; AltName: Full=Anchorin CII; AltName: Full=Annexin V; AltName: Full=Annexin-5; AltName: Full=Calphobindin I; Short=CBP-I; AltName: Full=Endonexin II; AltName: Full=Lipocortin V; AltName: Full=Placental anticoagulant protein 4; Short=PP4; AltName: Full=Placental anticoagulant protein I; Short=PAP-I; AltName: Full=Thromboplastin inhibitor; AltName: Full=Vascular anticoagulant-alpha; Short=VAC-alpha; [Homo sapiens (Human)] - [ANXA5_HUMAN]	9.47E+07

Arginase-1; EC=3.5.3.1; AltName: Full=Liver-type arginase; AltName: Full=Type I arginase; [Homo sapiens (Human)] - [ARGI1_HUMAN]	1.75E+06
Beta-2-microglobulin OS=Homo sapiens GN=B2M PE=1 SV=1	5.86E+08
Calmodulin-like protein 5; AltName: Full=Calmodulin-like skin protein; [Homo sapiens (Human)] - [CALL5_HUMAN]	6.19E+06
CD44 antigen; AltName: Full=CDw44; AltName: Full=Epican; AltName: Full=Extracellular matrix receptor III; Short=ECMR-III; AltName: Full=GP90 lymphocyte homing/adhesion receptor; AltName: Full=HUTCH-I; AltName: Full=Heparan sulfate proteoglycan; AltName: Full=Hermes antigen; AltName: Full=Hyaluronate receptor; AltName: Full=Phagocytic glycoprotein 1; Short=PGP-1; AltName: Full=Phagocytic glycoprotein I; Short=PGP-I; AltName: CD_antigen=CD44; Flags: Precursor; [Homo sapiens (Human)] - [CD44_HUMAN]	3.87E+07
Ceruloplasmin OS=Homo sapiens GN=CP PE=1 SV=1	2.73E+06
Complement C3 OS=Homo sapiens GN=C3 PE=1 SV=2	2.06E+08
Complement C4-A; AltName: Full=Acidic complement C4; AltName: Full=C3 and PZP-like alpha-2-macroglobulin domain-containing protein 2; Contains: RecName: Full=Complement C4 beta chain; Contains: RecName: Full=Complement C4-A alpha chain; Contains: RecName: Full=C4a anaphylatoxin; Contains: RecName: Full=C4b-A; Contains: RecName: Full=C4d-A; Contains: RecName: Full=Complement C4 gamma chain; Flags: Precursor; [Homo sapiens (Human)] - [CO4A_HUMAN]	5.65E+07
Delta-like protein 4; AltName: Full=Drosophila Delta homolog 4; Short=Delta4; Flags: Precursor; [Homo sapiens (Human)] - [DLL4_HUMAN]	4.85E+07
Dermcidin; AltName: Full=Preproteolysin; Contains: RecName: Full=Survival-promoting peptide; Contains: RecName: Full=DCD-1; Flags: Precursor; [Homo sapiens (Human)] - [DCD_HUMAN]	6.55E+06
Desmoplakin OS=Homo sapiens GN=DSP PE=1 SV=3	3.75E+06
Ferritin light chain OS=Homo sapiens GN=FTL PE=1 SV=2	1.51E+08
G antigen family D member 2; AltName: Full=Cancer/testis antigen 12.1; Short=CT12.1; AltName: Full=Protein XAGE-1; [Homo sapiens (Human)] - [GAGD2_HUMAN]	4.94E+06
Haptoglobin OS=Homo sapiens GN=HP PE=1 SV=1	9.50E+06
Hemoglobin subunit alpha; AltName: Full=Alpha-globin; AltName: Full=Hemoglobin alpha chain; [Homo sapiens (Human)] - [HBA_HUMAN]	5.24E+08
Hemoglobin subunit beta OS=Homo sapiens GN=HBB PE=1 SV=2	1.66E+09
Hemopexin OS=Homo sapiens GN=HPX PE=1 SV=2	4.16E+07
Ig alpha-1 chain C region OS=Homo sapiens GN=IGHA1 PE=1 SV=2	1.89E+07
Ig gamma-1 chain C region OS=Homo sapiens GN=IGHG1 PE=1 SV=1	3.55E+09
Ig gamma-2 chain C region OS=Homo sapiens GN=IGHG2 PE=1 SV=2	5.64E+07
Ig heavy chain V-III region CAM; [Homo sapiens (Human)] - [HV307_HUMAN]	1.68E+07
Ig heavy chain V-III region TIL; [Homo sapiens (Human)] - [HV304_HUMAN]	1.60E+07
Ig kappa chain C region OS=Homo sapiens GN=IGKC PE=1 SV=1	9.25E+09
Ig kappa chain V-II region MIL; [Homo sapiens (Human)] - [KV203_HUMAN]	2.22E+06
Ig kappa chain V-III region B6; [Homo sapiens (Human)] - [KV301_HUMAN]	1.63E+09
Ig kappa chain V-III region SIE; [Homo sapiens (Human)] - [KV302_HUMAN]	1.85E+06

Ig kappa chain V-III region VG (Fragment) OS=Homo sapiens PE=1 SV=1	2.65E+06
Ig lambda chain V-III region LOI; [Homo sapiens (Human)] - [LV302_HUMAN]	4.81E+08
Ig lambda chain V-IV region Bau; [Homo sapiens (Human)] - [LV401_HUMAN]	3.27E+07
Ig lambda-1 chain C regions; [Homo sapiens (Human)] - [LAC1_HUMAN]	3.53E+09
Ig lambda-2 chain C regions OS=Homo sapiens GN=IGLC2 PE=1 SV=1	8.59E+06
Leucine-rich alpha-2-glycoprotein OS=Homo sapiens GN=LRG1 PE=1 SV=2	7.23E+05
Lysozyme C; EC=3.2.1.17; AltName: Full=1,4-beta-N-acetylmuramidase C; Flags: Precursor; [Homo sapiens (Human)] - [LYSC_HUMAN]	5.31E+08
Myoglobin; [Homo sapiens (Human)] - [MYG_HUMAN]	2.39E+06
Myotubularin-related protein 14; EC=3.1.3.-; AltName: Full=HCV NS5A-transactivated protein 4 splice variant A-binding protein 1; Short=NS5ATP4ABP1; AltName: Full=hJumpy; [Homo sapiens (Human)] - [MTMRE_HUMAN]	1.21E+06
Olfactory receptor 2A2; AltName: Full=Olfactory receptor 2A17; AltName: Full=Olfactory receptor OR7-11; [Homo sapiens (Human)] - [OR2A2_HUMAN]	2.34E+07
Peptidyl-prolyl cis-trans isomerase A; Short=PPIase A; EC=5.2.1.8; AltName: Full=Cyclophilin A; AltName: Full=Cyclosporin A-binding protein; AltName: Full=Rotamase A; [Homo sapiens (Human)] - [PPIA_HUMAN]	7.51E+07
Peroxiredoxin-5, mitochondrial OS=Homo sapiens GN=PRDX5 PE=1 SV=4	2.13E+08
Phosphatidylinositol 3,4,5-trisphosphate-dependent Rac exchanger 1 protein; Short=P-Rex1; Short=PtdIns(3,4,5)-dependent Rac exchanger 1; [Homo sapiens (Human)] - [PREX1_HUMAN]	9.18E+06
Polymeric immunoglobulin receptor OS=Homo sapiens GN=PIGR PE=1 SV=4	2.37E+09
Protein kinase-like protein SgK196; AltName: Full=Sugen kinase 196; [Homo sapiens (Human)] - [SG196_HUMAN]	1.36E+07
Protein Shroom3; AltName: Full=Shroom-related protein; Short=hShrmL; [Homo sapiens (Human)] - [SHRM3_HUMAN]	2.29E+07
Pulmonary surfactant-associated protein A2; Short=PSP-A; Short=PSPA; Short=SP-A; Short=SP-A2; AltName: Full=35 kDa pulmonary surfactant-associated protein; AltName: Full=Alveolar proteinosis protein; AltName: Full=Collectin-5; Flags: Precursor; [Homo sapiens (Human)] - [SFPA2_HUMAN]	1.85E+06
Putative annexin A2-like protein; AltName: Full=Annexin A2 pseudogene 2; AltName: Full=Lipocortin II pseudogene; [Homo sapiens (Human)] - [AXA2L_HUMAN]	2.60E+07
Serotransferrin OS=Homo sapiens GN=TF PE=1 SV=3	3.49E+07
Serum albumin OS=Homo sapiens GN=ALB PE=1 SV=2	5.49E+08
Thioredoxin; Short=Trx; AltName: Full=ATL-derived factor; Short=ADF; AltName: Full=Surface-associated sulphydryl protein; Short=SASP; [Homo sapiens (Human)] - [THIO_HUMAN]	1.54E+08
Transcriptional adapter 2-beta; AltName: Full=ADA2-like protein beta; Short=ADA2-beta; [Homo sapiens (Human)] - [TAD2B_HUMAN]	1.11E+06
Transmembrane protein 200C; AltName: Full=Transmembrane protein TTMA; AltName: Full=Two transmembrane domain-containing family member A; [Homo sapiens (Human)] - [T200C_HUMAN]	1.89E+06
Transthyretin OS=Homo sapiens GN=TTR PE=1 SV=1	7.84E+07

Trypsin-3; EC=3.4.21.4; AltName: Full=Brain trypsinogen; AltName: Full=Mesotrypsinogen; AltName: Full=Serine protease 3; AltName: Full=Serine protease 4; AltName: Full=Trypsin III; AltName: Full=Trypsin IV; Flags: Precursor; [Homo sapiens (Human)] - [TRY3_HUMAN]	4.78E+06
Uncharacterized protein C3orf38; [Homo sapiens (Human)] - [CC038_HUMAN]	5.97E+08
Uteroglobin OS=Homo sapiens GN=SCGB1A1 PE=1 SV=1	4.49E+09

Table C.5 *Alveolar proteins identified by 1D PAGE and nano LC MS/MS in healthy smoker and COPD smoker RTLFs. The 119 proteins common to both healthy smoker and COPD smoker subjects investigated n=5 for both subject groups, alongside the mean of the three most abundant ion peaks of each respective protein identified. Accession numbers included according to entries in UniProtKB/Swiss-Prot.*

COPD smoker		**Healthy Smoker**	
14-3-3 protein beta/alpha OS=Homo sapiens GN=YWHAB PE=1 SV=3	3.26E+07	14-3-3 protein beta/alpha OS=Homo sapiens GN=YWHAB PE=1 SV=3	6.47E+07
14-3-3 protein zeta/delta OS=Homo sapiens GN=YWHAZ PE=1 SV=1	3.48E+07	14-3-3 protein zeta/delta OS=Homo sapiens GN=YWHAZ PE=1 SV=1	4.51E+07
Actin, cytoplasmic 1 OS=Homo sapiens GN=ACTB PE=1 SV=1	5.36E+07	Actin, cytoplasmic 1 OS=Homo sapiens GN=ACTB PE=1 SV=1	1.38E+08
Afamin OS=Homo sapiens GN=AFM PE=1 SV=1	1.76E+07	Afamin OS=Homo sapiens GN=AFM PE=1 SV=1	5.45E+06
Aldo-keto reductase family 1 member B10; EC=1.1.1.-; AltName: Full=ARL-1; AltName: Full=Aldose reductase-like; AltName: Full=Aldose reductase-related protein; Short=ARP; Short=hARP; AltName: Full=Small intestine reductase; Short=SI reductase; [Homo sapiens (Human)] - [AK1BA_HUMAN]	7.27E+05	Aldo-keto reductase family 1 member B10; EC=1.1.1.-; AltName: Full=ARL-1; AltName: Full=Aldose reductase-like; AltName: Full=Aldose reductase-related protein; Short=ARP; Short=hARP; AltName: Full=Small intestine reductase; Short=SI reductase; [Homo sapiens (Human)] - [AK1BA_HUMAN]	5.19E+05
Aldo-keto reductase family 1 member C1 OS=Homo sapiens GN=AKR1C1 PE=1 SV=1	8.87E+06	Aldo-keto reductase family 1 member C1 OS=Homo sapiens GN=AKR1C1 PE=1 SV=1	3.41E+06
Aldose 1-epimerase; EC=5.1.3.3; AltName: Full=Galactose mutarotase; [Homo sapiens (Human)] -	1.50E+06	Aldose 1-epimerase; EC=5.1.3.3; AltName: Full=Galactose mutarotase; [Homo sapiens (Human)] -	2.63E+06

[GALM_HUMAN]		[GALM_HUMAN]	
Alpha-1-acid glycoprotein 1 OS=Homo sapiens GN=ORM1 PE=1 SV=1	2.76E+08	Alpha-1-acid glycoprotein 1 OS=Homo sapiens GN=ORM1 PE=1 SV=1	1.29E+08
Alpha-1-acid glycoprotein 2; Short=AGP 2; AltName: Full=Orosomucoid-2; Short=OMD 2; Flags: Precursor; [Homo sapiens (Human)] - [A1AG2_HUMAN]	1.95E+08	Alpha-1-acid glycoprotein 2; Short=AGP 2; AltName: Full=Orosomucoid-2; Short=OMD 2; Flags: Precursor; [Homo sapiens (Human)] - [A1AG2_HUMAN]	1.14E+08
Alpha-1-antichymotrypsin OS=Homo sapiens GN=SERPINA3 PE=1 SV=2	1.00E+08	Alpha-1-antichymotrypsin OS=Homo sapiens GN=SERPINA3 PE=1 SV=2	3.72E+07
Alpha-1-antitrypsin OS=Homo sapiens GN=SERPINA1 PE=1 SV=3	1.61E+09	Alpha-1-antitrypsin OS=Homo sapiens GN=SERPINA1 PE=1 SV=3	2.75E+08
Alpha-1B-glycoprotein OS=Homo sapiens GN=A1BG PE=1 SV=4	3.51E+07	Alpha-1B-glycoprotein OS=Homo sapiens GN=A1BG PE=1 SV=4	2.29E+07
Alpha-2-HS-glycoprotein OS=Homo sapiens GN=AHSG PE=1 SV=1	9.30E+07	Alpha-2-HS-glycoprotein OS=Homo sapiens GN=AHSG PE=1 SV=1	2.99E+07
Alpha-2-macroglobulin OS=Homo sapiens GN=A2M PE=1 SV=3	1.01E+07	Alpha-2-macroglobulin OS=Homo sapiens GN=A2M PE=1 SV=3	4.14E+06
Alpha-enolase OS=Homo sapiens GN=ENO1 PE=1 SV=2	7.37E+06	Alpha-enolase OS=Homo sapiens GN=ENO1 PE=1 SV=2	3.19E+07
Angiotensinogen OS=Homo sapiens GN=AGT PE=1 SV=1	5.39E+07	Angiotensinogen OS=Homo sapiens GN=AGT PE=1 SV=1	1.41E+06
Annexin A3; AltName: Full=35-alpha calcimedin; AltName: Full=Annexin III; AltName: Full=Annexin-3; AltName: Full=Inositol 1,2-cyclic phosphate 2-phosphohydrolase; AltName: Full=Lipocortin III; AltName: Full=Placental anticoagulant protein III; Short=PAP-III; [Homo sapiens (Human)] - [ANXA3_HUMAN]	9.75E+05	Annexin A3 OS=Homo sapiens GN=ANXA3 PE=1 SV=3	2.81E+06
Annexin A5 OS=Homo sapiens GN=ANXA5 PE=1 SV=2	7.53E+07	Annexin A5 OS=Homo sapiens GN=ANXA5 PE=1 SV=2	5.18E+07

Apolipoprotein A-I OS=Homo sapiens GN=APOA1 PE=1 SV=1	5.68E+07	Apolipoprotein A-I OS=Homo sapiens GN=APOA1 PE=1 SV=1	7.56E+06
Attractin OS=Homo sapiens GN=ATRN PE=1 SV=2	1.08E+07	Attractin OS=Homo sapiens GN=ATRN PE=1 SV=2	4.53E+06
Beta-2-microglobulin OS=Homo sapiens GN=B2M PE=1 SV=1	3.80E+07	Beta-2-microglobulin OS=Homo sapiens GN=B2M PE=1 SV=1	1.03E+07
Beta-microseminoprotein; AltName: Full=Immunoglobulin-binding factor; Short=IGBF; AltName: Full=PN44; AltName: Full=Prostate secreted seminal plasma protein; AltName: Full=Prostate secretory protein of 94 amino acids; Short=PSP-94; Short=PSP94; AltName: Full=Seminal plasma beta-inhibin; Flags: Precursor; [Homo sapiens (Human)] - [MSMB_HUMAN]	4.84E+07	Beta-microseminoprotein; AltName: Full=Immunoglobulin-binding factor; Short=IGBF; AltName: Full=PN44; AltName: Full=Prostate secreted seminal plasma protein; AltName: Full=Prostate secretory protein of 94 amino acids; Short=PSP-94; Short=PSP94; AltName: Full=Seminal plasma beta-inhibin; Flags: Precursor; [Homo sapiens (Human)] - [MSMB_HUMAN]	1.50E+07
Calcyphosin OS=Homo sapiens GN=CAPS PE=1 SV=1	1.32E+06	Calcyphosin OS=Homo sapiens GN=CAPS PE=1 SV=1	1.44E+07
Calmodulin OS=Homo sapiens GN=CALM1 PE=1 SV=2	2.48E+07	Calmodulin OS=Homo sapiens GN=CALM1 PE=1 SV=2	2.84E+06
Carbonic anhydrase 2 OS=Homo sapiens GN=CA2 PE=1 SV=2	1.05E+07	Carbonic anhydrase 2 OS=Homo sapiens GN=CA2 PE=1 SV=2	3.84E+06
Cathepsin B OS=Homo sapiens GN=CTSB PE=1 SV=3	4.12E+06	Cathepsin B OS=Homo sapiens GN=CTSB PE=1 SV=3	2.14E+06
Cathepsin S OS=Homo sapiens GN=CTSS PE=1 SV=3	3.07E+07	Cathepsin S OS=Homo sapiens GN=CTSS PE=1 SV=3	3.74E+06
Cathepsin Z OS=Homo sapiens GN=CTSZ PE=1 SV=1	6.46E+06	Cathepsin Z OS=Homo sapiens GN=CTSZ PE=1 SV=1	4.21E+06
CD166 antigen OS=Homo sapiens GN=ALCAM PE=1 SV=2	6.34E+06	CD166 antigen; AltName: Full=Activated leukocyte cell adhesion molecule; AltName: CD_antigen=CD166; Flags: Precursor; [Homo sapiens (Human)] - [CD166_HUMAN]	2.77E+06
CD44 antigen OS=Homo sapiens GN=CD44 PE=1 SV=3	3.49E+07	CD44 antigen OS=Homo sapiens GN=CD44 PE=1 SV=3	3.34E+07

Ceruloplasmin OS=Homo sapiens GN=CP PE=1 SV=1	2.38E+08	Ceruloplasmin OS=Homo sapiens GN=CP PE=1 SV=1	1.15E+08
Coactosin-like protein OS=Homo sapiens GN=COTL1 PE=1 SV=3	3.50E+07	Coactosin-like protein OS=Homo sapiens GN=COTL1 PE=1 SV=3	6.78E+06
Corticosteroid-binding globulin OS=Homo sapiens GN=SERPINA6 PE=1 SV=1	2.38E+07	Corticosteroid-binding globulin OS=Homo sapiens GN=SERPINA6 PE=1 SV=1	5.20E+06
Cystatin-B OS=Homo sapiens GN=CSTB PE=1 SV=2	1.51E+07	Cystatin-B OS=Homo sapiens GN=CSTB PE=1 SV=2	6.43E+06
Deleted in malignant brain tumors 1 protein OS=Homo sapiens GN=DMBT1 PE=1 SV=2	2.80E+07	Deleted in malignant brain tumors 1 protein OS=Homo sapiens GN=DMBT1 PE=1 SV=2	6.18E+06
Delta-like protein 4; AltName: Full=Drosophila Delta homolog 4; Short=Delta4; Flags: Precursor; [Homo sapiens (Human)] - [DLL4_HUMAN]	5.48E+07	Delta-like protein 4; AltName: Full=Drosophila Delta homolog 4; Short=Delta4; Flags: Precursor; [Homo sapiens (Human)] - [DLL4_HUMAN]	1.12E+07
Dermcidin; AltName: Full=Preproteolysin; Contains: RecName: Full=Survival-promoting peptide; Contains: RecName: Full=DCD-1; Flags: Precursor; [Homo sapiens (Human)] - [DCD_HUMAN]	2.94E+06	Dermcidin OS=Homo sapiens GN=DCD PE=1 SV=2	4.35E+06
Desmoglein-1 OS=Homo sapiens GN=DSG1 PE=1 SV=2	5.04E+06	Desmoglein-1; AltName: Full=Cadherin family member 4; AltName: Full=Desmosomal glycoprotein 1; Short=DG1; Short=DGI; AltName: Full=Pemphigus foliaceus antigen; Flags: Precursor; [Homo sapiens (Human)] - [DSG1_HUMAN]	7.80E+06
Desmoplakin OS=Homo sapiens GN=DSP PE=1 SV=3	1.06E+08	Desmoplakin OS=Homo sapiens GN=DSP PE=1 SV=3	9.94E+07
Dipeptidyl peptidase 4 OS=Homo sapiens GN=DPP4 PE=1 SV=2	1.99E+07	Dipeptidyl peptidase 4 OS=Homo sapiens GN=DPP4 PE=1 SV=2	3.08E+06
Epididymal secretory protein E1 OS=Homo sapiens GN=NPC2 PE=1 SV=1	3.19E+07	Epididymal secretory protein E1 OS=Homo sapiens GN=NPC2 PE=1 SV=1	1.32E+07

FAS-associated factor 1; Short=hFAF1; AltName: Full=UBX domain-containing protein 12; AltName: Full=UBX domain-containing protein 3A; [Homo sapiens (Human)] - [FAF1_HUMAN]	9.69E+07	FAS-associated factor 1; Short=hFAF1; AltName: Full=UBX domain-containing protein 12; AltName: Full=UBX domain-containing protein 3A; [Homo sapiens (Human)] - [FAF1_HUMAN]	4.56E+07
Fatty acid-binding protein, epidermal; AltName: Full=Epidermal-type fatty acid-binding protein; Short=E-FABP; AltName: Full=Fatty acid-binding protein 5; AltName: Full=Psoriasis-associated fatty acid-binding protein homolog; Short=PA-FABP; [Homo sapiens (Human)] - [FABP5_HUMAN]	1.88E+06	Fatty acid-binding protein, epidermal OS=Homo sapiens GN=FABP5 PE=1 SV=3	8.26E+07
Ferritin heavy chain OS=Homo sapiens GN=FTH1 PE=1 SV=2	1.41E+08	Ferritin heavy chainOS=Homo sapiens GN=FTH1 PE=1 SV=2	5.09E+06
Ferritin light chain OS=Homo sapiens GN=FTL PE=1 SV=2	3.93E+08	Ferritin light chain OS=Homo sapiens GN=FTL PE=1 SV=2	2.03E+07
Glutathione S-transferase P OS=Homo sapiens GN=GSTP1 PE=1 SV=2	1.74E+07	Glutathione S-transferase P OS=Homo sapiens GN=GSTP1 PE=1 SV=2	1.82E+07
Glyceraldehyde-3-phosphate dehydrogenase OS=Homo sapiens GN=GAPDH PE=1 SV=3	4.28E+06	Glyceraldehyde-3-phosphate dehydrogenase OS=Homo sapiens GN=GAPDH PE=1 SV=3	4.98E+07
Glyoxalase domain-containing protein 4 OS=Homo sapiens GN=GLOD4 PE=1 SV=1	3.60E+06	Glyoxalase domain-containing protein 4 OS=Homo sapiens GN=GLOD4 PE=1 SV=1	1.54E+06
Haptoglobin OS=Homo sapiens GN=HP PE=1 SV=1	2.64E+08	Haptoglobin OS=Homo sapiens GN=HP PE=1 SV=1	1.04E+08
Hemoglobin subunit alpha OS=Homo sapiens GN=HBA1 PE=1 SV=2	8.29E+07	Hemoglobin subunit alpha OS=Homo sapiens GN=HBA1 PE=1 SV=2	5.40E+07
Hemoglobin subunit beta OS=Homo sapiens GN=HBB PE=1 SV=2	7.32E+07	Hemoglobin subunit beta OS=Homo sapiens GN=HBB PE=1 SV=2	2.04E+07
Hemopexin OS=Homo sapiens GN=HPX PE=1 SV=2	3.48E+08	Hemopexin OS=Homo sapiens GN=HPX PE=1 SV=2	1.89E+08
Ig alpha-1 chain C region OS=Homo sapiens GN=IGHA1	1.56E+09	Ig alpha-1 chain C region OS=Homo sapiens GN=IGHA1	6.14E+08

PE=1 SV=2		PE=1 SV=2	
Ig alpha-2 chain C region OS=Homo sapiens GN=IGHA2 PE=1 SV=3	8.21E+08	Ig alpha-2 chain C region; [Homo sapiens (Human)] - [IGHA2_HUMAN]	3.06E+08
Ig gamma-1 chain C region OS=Homo sapiens GN=IGHG1 PE=1 SV=1	5.79E+09	Ig gamma-1 chain C region OS=Homo sapiens GN=IGHG1 PE=1 SV=1	3.30E+09
Ig gamma-2 chain C region OS=Homo sapiens GN=IGHG2 PE=1 SV=2	4.65E+09	Ig gamma-2 chain C region OS=Homo sapiens GN=IGHG2 PE=1 SV=2	2.57E+09
Ig gamma-3 chain C region OS=Homo sapiens GN=IGHG3 PE=1 SV=2	5.04E+09	Ig gamma-3 chain C region OS=Homo sapiens GN=IGHG3 PE=1 SV=2	2.87E+09
Ig heavy chain V-I region HG3; Flags: Precursor; [Homo sapiens (Human)] - [HV102_HUMAN]	6.71E+07	Ig heavy chain V-I region HG3; Flags: Precursor; [Homo sapiens (Human)] - [HV102_HUMAN]	3.44E+07
Ig heavy chain V-II region NEWM; [Homo sapiens (Human)] - [HV207_HUMAN]	1.15E+08	Ig heavy chain V-II region NEWM OS=Homo sapiens PE=1 SV=1	9.45E+07
Ig heavy chain V-III region BRO; [Homo sapiens (Human)] - [HV305_HUMAN]	9.27E+08	Ig heavy chain V-III region BRO; [Homo sapiens (Human)] - [HV305_HUMAN]	5.36E+08
Ig heavy chain V-III region BUT; [Homo sapiens (Human)] - [HV306_HUMAN]	9.00E+08	Ig heavy chain V-III region BUT; [Homo sapiens (Human)] - [HV306_HUMAN]	4.98E+08
Ig heavy chain V-III region CAM OS=Homo sapiens PE=1 SV=1	9.16E+08	Ig heavy chain V-III region CAM OS=Homo sapiens PE=1 SV=1	
Ig heavy chain V-III region GAL OS=Homo sapiens PE=1 SV=1	8.79E+08	Ig heavy chain V-III region GAL OS=Homo sapiens PE=1 SV=1	4.92E+08
Ig heavy chain V-III region GAR; [Homo sapiens (Human)] - [HV322_HUMAN]	2.86E+08	Ig heavy chain V-III region GAR; [Homo sapiens (Human)] - [HV322_HUMAN]	8.76E+07
Ig heavy chain V-III region HIL; [Homo sapiens (Human)] - [HV310_HUMAN]	1.24E+09	Ig heavy chain V-III region HIL; [Homo sapiens (Human)] - [HV310_HUMAN]	7.00E+08
Ig heavy chain V-III region VH26; Flags: Precursor; [Homo sapiens (Human)] -	9.25E+08	Ig heavy chain V-III region VH26 OS=Homo sapiens PE=1 SV=1	4.91E+08

[HV303_HUMAN]			
Ig kappa chain C region OS=Homo sapiens GN=IGKC PE=1 SV=1	2.92E+09	Ig kappa chain C region OS=Homo sapiens GN=IGKC PE=1 SV=1	1.07E+09
Ig kappa chain V-III region POM OS=Homo sapiens PE=1 SV=1	1.58E+08	Ig kappa chain V-III region POM; [Homo sapiens (Human)] - [KV306_HUMAN]	7.29E+07
Ig kappa chain V-III region SIE OS=Homo sapiens PE=1 SV=1	2.67E+08	Ig kappa chain V-III region SIE OS=Homo sapiens PE=1 SV=1	1.24E+08
Ig kappa chain V-III region VG (Fragment) OS=Homo sapiens PE=1 SV=1	6.84E+07	Ig kappa chain V-III region VG (Fragment) OS=Homo sapiens PE=1 SV=1	5.54E+07
Ig kappa chain V-IV region JI OS=Homo sapiens PE=4 SV=1	1.08E+08	Ig kappa chain V-IV region JI; Flags: Precursor; [Homo sapiens (Human)] - [KV403_HUMAN]	6.10E+07
Ig kappa chain V-IV region Len; [Homo sapiens (Human)] - [KV402_HUMAN]	1.49E+08	Ig kappa chain V-IV region Len; [Homo sapiens (Human)] - [KV402_HUMAN]	6.10E+07
Ig lambda chain V region 4A OS=Homo sapiens PE=4 SV=1	7.87E+06	Ig lambda chain V region 4A; Flags: Precursor; [Homo sapiens (Human)] - [LV001_HUMAN]	1.78E+07
Ig lambda chain V-I region HA OS=Homo sapiens PE=1 SV=1	6.98E+07	Ig lambda chain V-I region HA; [Homo sapiens (Human)] - [LV102_HUMAN]	5.73E+07
Ig lambda chain V-III region LOI OS=Homo sapiens PE=1 SV=1	6.09E+07	Ig lambda chain V-III region LOI OS=Homo sapiens PE=1 SV=1	6.55E+07
Ig lambda chain V-III region SH; [Homo sapiens (Human)] - [LV301_HUMAN]	1.31E+07	Ig lambda chain V-III region SH OS=Homo sapiens PE=1 SV=1	1.01E+07
Ig lambda chain V-IV region Bau; [Homo sapiens (Human)] - [LV401_HUMAN]	5.41E+07	Ig lambda chain V-IV region Bau; [Homo sapiens (Human)] - [LV401_HUMAN]	1.05E+07
Ig lambda-2 chain C regions OS=Homo sapiens GN=IGLC2 PE=1 SV=1	1.09E+09	Ig lambda-2 chain C regions OS=Homo sapiens GN=IGLC2 PE=1 SV=1	7.91E+08
Ig mu chain C region OS=Homo sapiens GN=IGHM PE=1 SV=3	3.88E+07	Ig mu chain C region OS=Homo sapiens GN=IGHM PE=1 SV=3	4.18E+07

Immunoglobulin J chain OS=Homo sapiens GN=IGJ PE=1 SV=4	7.57E+07	Immunoglobulin J chain OS=Homo sapiens GN=IGJ PE=1 SV=4	3.90E+07
Immunoglobulin lambda-like polypeptide 5 OS=Homo sapiens GN=IGLL5 PE=2 SV=2	7.42E+08	Immunoglobulin lambda-like polypeptide 5 OS=Homo sapiens GN=IGLL5 PE=2 SV=2	4.43E+08
Intercellular adhesion molecule 1 OS=Homo sapiens GN=ICAM1 PE=1 SV=2	1.44E+07	Intercellular adhesion molecule 1 OS=Homo sapiens GN=ICAM1 PE=1 SV=2	4.60E+06
Leucine-rich alpha-2-glycoprotein OS=Homo sapiens GN=LRG1 PE=1 SV=2	3.29E+07	Leucine-rich alpha-2-glycoprotein OS=Homo sapiens GN=LRG1 PE=1 SV=2	1.76E+07
Leukocyte elastase inhibitor OS=Homo sapiens GN=SERPINB1 PE=1 SV=1	6.74E+06	Leukocyte elastase inhibitor OS=Homo sapiens GN=SERPINB1 PE=1 SV=1	2.61E+06
Polymeric immunoglobulin receptor OS=Homo sapiens GN=PIGR PE=1 SV=4	2.83E+08	Polymeric immunoglobulin receptor OS=Homo sapiens GN=PIGR PE=1 SV=4	1.54E+08
Pro-cathepsin H OS=Homo sapiens GN=CTSH PE=1 SV=4	1.61E+07	Pro-cathepsin H OS=Homo sapiens GN=CTSH PE=1 SV=4	1.14E+07
Proactivator polypeptide; Contains: RecName: Full=Saposin-A; AltName: Full=Protein A; Contains: RecName: Full=Saposin-B-Val; Contains: RecName: Full=Saposin-B; AltName: Full=Cerebroside sulfate activator; Short=CSAct; AltName: Full=Dispersin; AltName: Full=Sphingolipid activator protein 1; Short=SAP-1; AltName: Full=Sulfatide/GM1 activator; Contains: RecName: Full=Saposin-C; AltName: Full=A1 activator; AltName: Full=Co-beta-glucosidase; AltName: Full=Glucosylceramidase activator; AltName: Full=Sphingolipid activator protein 2; Short=SAP-2; Contains: RecName: Full=Saposin-D; AltName: Full=Component C; AltName:	6.97E+06	Proactivator polypeptide; Contains: RecName: Full=Saposin-A; AltName: Full=Protein A; Contains: RecName: Full=Saposin-B-Val; Contains: RecName: Full=Saposin-B; AltName: Full=Cerebroside sulfate activator; Short=CSAct; AltName: Full=Dispersin; AltName: Full=Sphingolipid activator protein 1; Short=SAP-1; AltName: Full=Sulfatide/GM1 activator; Contains: RecName: Full=Saposin-C; AltName: Full=A1 activator; AltName: Full=Co-beta-glucosidase; AltName: Full=Glucosylceramidase activator; AltName: Full=Sphingolipid activator protein 2; Short=SAP-2; Contains: RecName: Full=Saposin-D; AltName: Full=Component C; AltName:	1.35E+06

Full=Protein C; Flags: Precursor; [Homo sapiens (Human)] - [SAP_HUMAN]		Full=Protein C; Flags: Precursor; [Homo sapiens (Human)] - [SAP_HUMAN]	
Protein DJ-1 OS=Homo sapiens GN=PARK7 PE=1 SV=2	1.16E+07	Protein DJ-1 OS=Homo sapiens GN=PARK7 PE=1 SV=2	7.89E+06
Protein S100-A6 OS=Homo sapiens GN=S100A6 PE=1 SV=1	1.14E+08	Protein S100-A6 OS=Homo sapiens GN=S100A6 PE=1 SV=1	4.87E+07
Protein S100-A8 OS=Homo sapiens GN=S100A8 PE=1 SV=1	2.22E+06	Protein S100-A8 OS=Homo sapiens GN=S100A8 PE=1 SV=1	8.57E+08
Protein S100-P; AltName: Full=Protein S100-E; AltName: Full=S100 calcium-binding protein P; [Homo sapiens (Human)] - [S100P_HUMAN]	2.63E+06	Protein S100-P; AltName: Full=Protein S100-E; AltName: Full=S100 calcium-binding protein P; [Homo sapiens (Human)] - [S100P_HUMAN]	2.36E+06
Protein Shroom3; AltName: Full=Shroom-related protein; Short=hShrmL; [Homo sapiens (Human)] - [SHRM3_HUMAN]	2.30E+08	Protein Shroom3; AltName: Full=Shroom-related protein; Short=hShrmL; [Homo sapiens (Human)] - [SHRM3_HUMAN]	8.20E+07
Pulmonary surfactant-associated protein A2 OS=Homo sapiens GN=SFTPA2 PE=1 SV=1	2.89E+07	Pulmonary surfactant-associated protein A2 OS=Homo sapiens GN=SFTPA2 PE=1 SV=1	2.82E+07
Pulmonary surfactant-associated protein B OS=Homo sapiens GN=SFTPB PE=1 SV=3	9.69E+06	Pulmonary surfactant-associated protein B OS=Homo sapiens GN=SFTPB PE=1 SV=3	
Pulmonary surfactant-associated protein D OS=Homo sapiens GN=SFTPD PE=1 SV=3	2.63E+07	Pulmonary surfactant-associated protein D; Short=PSP-D; Short=SP-D; AltName: Full=Collectin-7; AltName: Full=Lung surfactant protein D; Flags: Precursor; [Homo sapiens (Human)] - [SFTPD_HUMAN]	5.11E+06
Putative V-set and immunoglobulin domain-containing protein 6; Flags: Precursor; [Homo sapiens (Human)] - [VSIG6_HUMAN]	1.42E+08	Putative V-set and immunoglobulin domain-containing protein 6 OS=Homo sapiens GN=VSIG6 PE=5 SV=2	8.23E+07
Scavenger receptor cysteine-rich type 1 protein M130 OS=Homo	5.07E+07	Scavenger receptor cysteine-rich type 1 protein M130	1.59E+07

sapiens GN=CD163 PE=1 SV=2		OS=Homo sapiens GN=CD163 PE=1 SV=2	
Selenium-binding protein 1 OS=Homo sapiens GN=SELENBP1 PE=1 SV=2	8.65E+06	Selenium-binding protein 1 OS=Homo sapiens GN=SELENBP1 PE=1 SV=2	1.15E+07
Serotransferrin OS=Homo sapiens GN=TF PE=1 SV=3	4.56E+09	Serotransferrin OS=Homo sapiens GN=TF PE=1 SV=3	3.42E+09
Serum albumin OS=Homo sapiens GN=ALB PE=1 SV=2	3.86E+09	Serum albumin OS=Homo sapiens GN=ALB PE=1 SV=2	1.54E+09
SH3 domain-binding glutamic acid-rich-like protein 3; AltName: Full=SH3 domain-binding protein 1; Short=SH3BP-1; [Homo sapiens (Human)] - [SH3L3_HUMAN]	1.22E+07	SH3 domain-binding glutamic acid-rich-like protein 3; AltName: Full=SH3 domain-binding protein 1; Short=SH3BP-1; [Homo sapiens (Human)] - [SH3L3_HUMAN]	7.49E+06
SH3 domain-binding glutamic acid-rich-like protein OS=Homo sapiens GN=SH3BGRL PE=1 SV=1	4.80E+06	SH3 domain-binding glutamic acid-rich-like protein OS=Homo sapiens GN=SH3BGRL PE=1 SV=1	1.18E+06
Sorting nexin-6; AltName: Full=TRAF4-associated factor 2; [Homo sapiens (Human)] - [SNX6_HUMAN]	4.91E+06	Sorting nexin-6; AltName: Full=TRAF4-associated factor 2; [Homo sapiens (Human)] - [SNX6_HUMAN]	2.48E+06
Superoxide dismutase [Cu-Zn] OS=Homo sapiens GN=SOD1 PE=1 SV=2	1.08E+07	Superoxide dismutase [Cu-Zn] OS=Homo sapiens GN=SOD1 PE=1 SV=2	7.11E+06
Thioredoxin domain-containing protein 17; AltName: Full=14 kDa thioredoxin-related protein; Short=TRP14; AltName: Full=Protein 42-9-9; AltName: Full=Thioredoxin-like protein 5; [Homo sapiens (Human)] - [TXD17_HUMAN]	1.84E+06	Thioredoxin domain-containing protein 17; AltName: Full=14 kDa thioredoxin-related protein; Short=TRP14; AltName: Full=Protein 42-9-9; AltName: Full=Thioredoxin-like protein 5; [Homo sapiens (Human)] - [TXD17_HUMAN]	7.54E+05
Thioredoxin; Short=Trx; AltName: Full=ATL-derived factor; Short=ADF; AltName: Full=Surface-associated sulphydryl protein; Short=SASP; [Homo sapiens (Human)] - [THIO_HUMAN]	2.98E+07	Thioredoxin; Short=Trx; AltName: Full=ATL-derived factor; Short=ADF; AltName: Full=Surface-associated sulphydryl protein; Short=SASP; [Homo sapiens (Human)] - [THIO_HUMAN]	1.29E+07
Transaldolase OS=Homo sapiens GN=TALDO1 PE=1	3.90E+07	Transaldolase OS=Homo sapiens GN=TALDO1 PE=1	2.21E+07

SV=2		SV=2	
Transcriptional adapter 2-beta; AltName: Full=ADA2-like protein beta; Short=ADA2-beta; [Homo sapiens (Human)] - [TAD2B_HUMAN]	2.68E+07	Transcriptional adapter 2-beta; AltName: Full=ADA2-like protein beta; Short=ADA2-beta; [Homo sapiens (Human)] - [TAD2B_HUMAN]	5.10E+07
Transketolase-like protein 2; EC=2.2.1.1; [Homo sapiens (Human)] - [TKTL2_HUMAN]	1.32E+08	Transketolase-like protein 2; EC=2.2.1.1; [Homo sapiens (Human)] - [TKTL2_HUMAN]	1.26E+08
Transmembrane protein 198; [Homo sapiens (Human)] - [TM198_HUMAN]	4.78E+07	Transmembrane protein 198; [Homo sapiens (Human)] - [TM198_HUMAN]	2.08E+07
Transmembrane protein 200C; AltName: Full=Transmembrane protein TTMA; AltName: Full=Two transmembrane domain-containing family member A; [Homo sapiens (Human)] - [T200C_HUMAN]	1.94E+06	Transmembrane protein 200C; AltName: Full=Transmembrane protein TTMA; AltName: Full=Two transmembrane domain-containing family member A; [Homo sapiens (Human)] - [T200C_HUMAN]	2.06E+06
Transthyretin OS=Homo sapiens GN=TTR PE=1 SV=1	1.29E+08	Transthyretin OS=Homo sapiens GN=TTR PE=1 SV=1	4.44E+07
Triosephosphate isomerase OS=Homo sapiens GN=TPI1 PE=1 SV=3	3.25E+07	Triosephosphate isomerase OS=Homo sapiens GN=TPI1 PE=1 SV=3	1.81E+07
Trypsin-3; EC=3.4.21.4; AltName: Full=Brain trypsinogen; AltName: Full=Mesotrypsinogen; AltName: Full=Serine protease 3; AltName: Full=Serine protease 4; AltName: Full=Trypsin III; AltName: Full=Trypsin IV; Flags: Precursor; [Homo sapiens (Human)] - [TRY3_HUMAN]	2.58E+06	Trypsin-3; EC=3.4.21.4; AltName: Full=Brain trypsinogen; AltName: Full=Mesotrypsinogen; AltName: Full=Serine protease 3; AltName: Full=Serine protease 4; AltName: Full=Trypsin III; AltName: Full=Trypsin IV; Flags: Precursor; [Homo sapiens (Human)] - [TRY3_HUMAN]	1.60E+06
Uncharacterized protein C3orf38; [Homo sapiens (Human)] - [CC038_HUMAN]	1.83E+09	Uncharacterized protein C3orf38; [Homo sapiens (Human)] - [CC038_HUMAN]	1.62E+09
Uteroglobin OS=Homo sapiens GN=SCGB1A1 PE=1 SV=1	1.99E+08	Uteroglobin OS=Homo sapiens GN=SCGB1A1 PE=1 SV=1	8.73E+07
Vitamin D-binding protein OS=Homo sapiens GN=GC PE=1 SV=1	1.52E+08	Vitamin D-binding protein OS=Homo sapiens GN=GC PE=1 SV=1	1.16E+08

Xin actin-binding repeat-containing protein 2 OS=Homo sapiens GN=XIRP2 PE=1 SV=2	1.76E+08	Xin actin-binding repeat-containing protein 2 OS=Homo sapiens GN=XIRP2 PE=1 SV=2	1.77E+08
Zinc-alpha-2-glycoprotein OS=Homo sapiens GN=AZGP1 PE=1 SV=2	8.23E+07	Zinc-alpha-2-glycoprotein OS=Homo sapiens GN=AZGP1 PE=1 SV=2	5.33E+07

Table C.6: *Alveolar proteins identified by 1D PAGE and nano LC MS/MS in healthy aged and COPD smoker RTLFs. The 126 proteins common to both healthy aged and COPD smoker subjects investigated n=5 for both subject groups, alongside the mean of the three most abundant ion peaks of each respective protein identified. Accession numbers included according to entries in UniProtKB/Swiss-Prot.*

COPD smoker		**Healthy Aged Control**	
14-3-3 protein beta/alpha OS=Homo sapiens GN=YWHAB PE=1 SV=3	3.26E+07	14-3-3 protein beta/alpha OS=Homo sapiens GN=YWHAB PE=1 SV=3	1.46E+07
14-3-3 protein zeta/delta OS=Homo sapiens GN=YWHAZ PE=1 SV=1	3.48E+07	14-3-3 protein zeta/delta OS=Homo sapiens GN=YWHAZ PE=1 SV=1	1.57E+07
7-alpha-hydroxycholest-4-en-3-one 12-alpha-hydroxylase OS=Homo sapiens GN=CYP8B1 PE=2 SV=2	2.87E+07	7-alpha-hydroxycholest-4-en-3-one 12-alpha-hydroxylase OS=Homo sapiens GN=CYP8B1 PE=2 SV=2	4.20E+07
Actin-related protein 2; AltName: Full=Actin-like protein 2; [Homo sapiens (Human)] - [ARP2_HUMAN]	1.95E+07	Actin-related protein 2; AltName: Full=Actin-like protein 2; [Homo sapiens (Human)] - [ARP2_HUMAN]	1.97E+07
Actin, cytoplasmic 1 OS=Homo sapiens GN=ACTB PE=1 SV=1	5.36E+07	Actin, cytoplasmic 1 OS=Homo sapiens GN=ACTB PE=1 SV=1	6.89E+07
Afamin OS=Homo sapiens GN=AFM PE=1 SV=1	1.76E+07	Afamin OS=Homo sapiens GN=AFM PE=1 SV=1	2.54E+07
Alpha-1-acid glycoprotein 1 OS=Homo sapiens GN=ORM1 PE=1 SV=1	2.76E+08	Alpha-1-acid glycoprotein 1 OS=Homo sapiens GN=ORM1 PE=1 SV=1	3.39E+08
Alpha-1-acid glycoprotein 2; Short=AGP 2; AltName: Full=Orosomucoid-2; Short=OMD 2; Flags: Precursor; [Homo sapiens (Human)] - [A1AG2_HUMAN]	1.95E+08	Alpha-1-acid glycoprotein 2 OS=Homo sapiens GN=ORM2 PE=1 SV=2	2.40E+08
Alpha-1-antichymotrypsin OS=Homo sapiens GN=SERPINA3 PE=1 SV=2	1.00E+08	Alpha-1-antichymotrypsin OS=Homo sapiens GN=SERPINA3 PE=1 SV=2	8.21E+07
Alpha-1-antitrypsin OS=Homo sapiens GN=SERPINA1 PE=1 SV=3	1.61E+09	Alpha-1-antitrypsin OS=Homo sapiens GN=SERPINA1 PE=1 SV=3	3.20E+09

Alpha-1B-glycoprotein OS=Homo sapiens GN=A1BG PE=1 SV=4	3.51E+07	Alpha-1B-glycoprotein OS=Homo sapiens GN=A1BG PE=1 SV=4	1.33E+08
Alpha-2-HS-glycoprotein OS=Homo sapiens GN=AHSG PE=1 SV=1	9.30E+07	Alpha-2-HS-glycoprotein OS=Homo sapiens GN=AHSG PE=1 SV=1	1.16E+08
Alpha-2-macroglobulin OS=Homo sapiens GN=A2M PE=1 SV=3	1.01E+07	Alpha-2-macroglobulin OS=Homo sapiens GN=A2M PE=1 SV=3	1.66E+08
Alpha-enolase OS=Homo sapiens GN=ENO1 PE=1 SV=2	7.37E+06	Alpha-enolase OS=Homo sapiens GN=ENO1 PE=1 SV=2	4.14E+06
Angiotensin-converting enzyme OS=Homo sapiens GN=ACE PE=1 SV=1	2.81E+07	Angiotensin-converting enzyme; Short=ACE; EC=3.2.1.-; EC=3.4.15.1; AltName: Full=Dipeptidyl carboxypeptidase I; AltName: Full=Kininase II; AltName: CD_antigen=CD143; Contains: RecName: Full=Angiotensin-converting enzyme, soluble form; Flags: Precursor; [Homo sapiens (Human)] - [ACE_HUMAN]	1.46E+07
Angiotensinogen OS=Homo sapiens GN=AGT PE=1 SV=1	5.39E+07	Angiotensinogen OS=Homo sapiens GN=AGT PE=1 SV=1	4.94E+07
Annexin A5 OS=Homo sapiens GN=ANXA5 PE=1 SV=2	7.53E+07	Annexin A5 OS=Homo sapiens GN=ANXA5 PE=1 SV=2	1.36E+06
Antithrombin-III OS=Homo sapiens GN=SERPINC1 PE=1 SV=1	1.82E+07	Antithrombin-III OS=Homo sapiens GN=SERPINC1 PE=1 SV=1	1.84E+07
Apolipoprotein A-I OS=Homo sapiens GN=APOA1 PE=1 SV=1	5.68E+07	Apolipoprotein A-I OS=Homo sapiens GN=APOA1 PE=1 SV=1	1.38E+08
Apolipoprotein A-II OS=Homo sapiens GN=APOA2 PE=1 SV=1	9.64E+06	Apolipoprotein A-II OS=Homo sapiens GN=APOA2 PE=1 SV=1	7.40E+07
Apolipoprotein A-IV OS=Homo sapiens GN=APOA4 PE=1 SV=3	1.11E+07	Apolipoprotein A-IV OS=Homo sapiens GN=APOA4 PE=1 SV=3	2.74E+07
ATP-binding cassette sub-family F member 1; AltName: Full=ATP-binding cassette 50; AltName: Full=TNF-alpha-stimulated ABC protein; [Homo sapiens (Human)] - [ABCF1_HUMAN]	4.47E+07	ATP-binding cassette sub-family F member 1; AltName: Full=ATP-binding cassette 50; AltName: Full=TNF-alpha-stimulated ABC protein; [Homo sapiens (Human)] - [ABCF1_HUMAN]	1.17E+07
Attractin OS=Homo sapiens GN=ATRN PE=1 SV=2	1.08E+07	Attractin OS=Homo sapiens GN=ATRN PE=1 SV=2	5.23E+06
Beta-2-microglobulin OS=Homo sapiens GN=B2M	3.80E+07	Beta-2-microglobulin OS=Homo sapiens GN=B2M	2.59E+07

PE=1 SV=1		PE=1 SV=1	
Calmodulin OS=Homo sapiens GN=CALM1 PE=1 SV=2	2.48E+07	Calmodulin OS=Homo sapiens GN=CALM1 PE=1 SV=2	2.68E+06
Carbonic anhydrase 1 OS=Homo sapiens GN=CA1 PE=1 SV=2	5.50E+06	Carbonic anhydrase 1 OS=Homo sapiens GN=CA1 PE=1 SV=2	3.91E+06
CD166 antigen OS=Homo sapiens GN=ALCAM PE=1 SV=2	6.34E+06	CD166 antigen; AltName: Full=Activated leukocyte cell adhesion molecule; AltName: CD_antigen=CD166; Flags: Precursor; [Homo sapiens (Human)] - [CD166_HUMAN]	1.35E+07
CD44 antigen OS=Homo sapiens GN=CD44 PE=1 SV=3	3.49E+07	CD44 antigen OS=Homo sapiens GN=CD44 PE=1 SV=3	2.73E+07
CD59 glycoprotein; AltName: Full=1F5 antigen; AltName: Full=20 kDa homologous restriction factor; Short=HRF-20; Short=HRF20; AltName: Full=MAC-inhibitory protein; Short=MAC-IP; AltName: Full=MEM43 antigen; AltName: Full=Membrane attack complex inhibition factor; Short=MACIF; AltName: Full=Membrane inhibitor of reactive lysis; Short=MIRL; AltName: Full=Protectin; AltName: CD_antigen=CD59; Flags: Precursor; [Homo sapiens (Human)] - [CD59_HUMAN]	2.60E+06	CD59 glycoprotein; AltName: Full=1F5 antigen; AltName: Full=20 kDa homologous restriction factor; Short=HRF-20; Short=HRF20; AltName: Full=MAC-inhibitory protein; Short=MAC-IP; AltName: Full=MEM43 antigen; AltName: Full=Membrane attack complex inhibition factor; Short=MACIF; AltName: Full=Membrane inhibitor of reactive lysis; Short=MIRL; AltName: Full=Protectin; AltName: CD_antigen=CD59; Flags: Precursor; [Homo sapiens (Human)] - [CD59_HUMAN]	3.54E+06
Cell adhesion molecule 2; AltName: Full=Immunoglobulin superfamily member 4D; Short=IgSF4D; AltName: Full=Nectin-like protein 3; Short=NECL-3; Flags: Precursor; [Homo sapiens (Human)] - [CADM2_HUMAN]	1.71E+07	Cell adhesion molecule 2; AltName: Full=Immunoglobulin superfamily member 4D; Short=IgSF4D; AltName: Full=Nectin-like protein 3; Short=NECL-3; Flags: Precursor; [Homo sapiens (Human)] - [CADM2_HUMAN]	2.00E+06
Ceruloplasmin OS=Homo sapiens GN=CP PE=1 SV=1	2.38E+08	Ceruloplasmin OS=Homo sapiens GN=CP PE=1 SV=1	3.67E+08
Coactosin-like protein OS=Homo sapiens GN=COTL1 PE=1 SV=3	3.50E+07	Coactosin-like protein OS=Homo sapiens GN=COTL1 PE=1 SV=3	5.15E+06
Complement C2 OS=Homo sapiens GN=C2 PE=1 SV=2	1.87E+06	Complement C2 OS=Homo sapiens GN=C2 PE=1 SV=2	3.41E+07
Complement C3 OS=Homo sapiens GN=C3 PE=1 SV=2	7.33E+07	Complement C3 OS=Homo sapiens GN=C3 PE=1 SV=2	2.66E+06

Corticosteroid-binding globulin OS=Homo sapiens GN=SERPINA6 PE=1 SV=1	2.38E+07	Corticosteroid-binding globulin OS=Homo sapiens GN=SERPINA6 PE=1 SV=1	3.95E+07
Deleted in malignant brain tumors 1 protein OS=Homo sapiens GN=DMBT1 PE=1 SV=2	2.80E+07	Deleted in malignant brain tumors 1 protein OS=Homo sapiens GN=DMBT1 PE=1 SV=2	3.69E+07
Delta-like protein 4; AltName: Full=Drosophila Delta homolog 4; Short=Delta4; Flags: Precursor; [Homo sapiens (Human)] - [DLL4_HUMAN]	5.48E+07	Delta-like protein 4; AltName: Full=Drosophila Delta homolog 4; Short=Delta4; Flags: Precursor; [Homo sapiens (Human)] - [DLL4_HUMAN]	1.23E+07
Dermcidin; AltName: Full=Preproteolysin; Contains: RecName: Full=Survival-promoting peptide; Contains: RecName: Full=DCD-1; Flags: Precursor; [Homo sapiens (Human)] - [DCD_HUMAN]	2.94E+06	Dermcidin OS=Homo sapiens GN=DCD PE=1 SV=2	2.13E+06
Desmoplakin OS=Homo sapiens GN=DSP PE=1 SV=3	1.06E+08	Desmoplakin OS=Homo sapiens GN=DSP PE=1 SV=3	1.40E+08
Dipeptidyl peptidase 4 OS=Homo sapiens GN=DPP4 PE=1 SV=2	1.99E+07	Dipeptidyl peptidase 4 OS=Homo sapiens GN=DPP4 PE=1 SV=2	6.17E+07
Disintegrin and metalloproteinase domain-containing protein 2; Short=ADAM 2; AltName: Full=Cancer/testis antigen 15; Short=CT15; AltName: Full=Fertilin subunit beta; AltName: Full=PH-30; Short=PH30; AltName: Full=PH30-beta; Flags: Precursor; [Homo sapiens (Human)] - [ADAM2_HUMAN]	1.48E+08	Disintegrin and metalloproteinase domain-containing protein 2; Short=ADAM 2; AltName: Full=Cancer/testis antigen 15; Short=CT15; AltName: Full=Fertilin subunit beta; AltName: Full=PH-30; Short=PH30; AltName: Full=PH30-beta; Flags: Precursor; [Homo sapiens (Human)] - [ADAM2_HUMAN]	1.05E+08
Epididymal secretory protein E1 OS=Homo sapiens GN=NPC2 PE=1 SV=1	3.19E+07	Epididymal secretory protein E1 OS=Homo sapiens GN=NPC2 PE=1 SV=1	1.37E+07
FAS-associated factor 1; Short=hFAF1; AltName: Full=UBX domain-containing protein 12; AltName: Full=UBX domain-containing protein 3A; [Homo sapiens (Human)] - [FAF1_HUMAN]	9.69E+07	FAS-associated factor 1; Short=hFAF1; AltName: Full=UBX domain-containing protein 12; AltName: Full=UBX domain-containing protein 3A; [Homo sapiens (Human)] - [FAF1_HUMAN]	4.89E+08
Ferritin heavy chain OS=Homo sapiens GN=FTH1 PE=1 SV=2	1.41E+08	Ferritin heavy chain; Short=Ferritin H subunit; EC=1.16.3.1; AltName: Full=Cell proliferation-	2.34E+06

		inducing gene 15 protein; [Homo sapiens (Human)] - [FRIH_HUMAN]	
Ferritin light chain OS=Homo sapiens GN=FTL PE=1 SV=2	3.93E+08	Ferritin light chain; Short=Ferritin L subunit; [Homo sapiens (Human)] - [FRIL_HUMAN]	4.73E+06
Galectin-3-binding protein OS=Homo sapiens GN=LGALS3BP PE=1 SV=1	8.21E+06	Galectin-3-binding protein; AltName: Full=Basement membrane autoantigen p105; AltName: Full=Lectin galactoside-binding soluble 3-binding protein; AltName: Full=Mac-2-binding protein; Short=MAC2BP; Short=Mac-2 BP; AltName: Full=Tumor-associated antigen 90K; Flags: Precursor; [Homo sapiens (Human)] - [LG3BP_HUMAN]	7.88E+06
Galectin-3; Short=Gal-3; AltName: Full=35 kDa lectin; AltName: Full=Carbohydrate-binding protein 35; Short=CBP 35; AltName: Full=Galactose-specific lectin 3; AltName: Full=Galactoside-binding protein; Short=GALBP; AltName: Full=IgE-binding protein; AltName: Full=L-31; AltName: Full=Laminin-binding protein; AltName: Full=Lectin L-29; AltName: Full=Mac-2 antigen; [Homo sapiens (Human)] - [LEG3_HUMAN]	1.28E+06	Galectin-3; Short=Gal-3; AltName: Full=35 kDa lectin; AltName: Full=Carbohydrate-binding protein 35; Short=CBP 35; AltName: Full=Galactose-specific lectin 3; AltName: Full=Galactoside-binding protein; Short=GALBP; AltName: Full=IgE-binding protein; AltName: Full=L-31; AltName: Full=Laminin-binding protein; AltName: Full=Lectin L-29; AltName: Full=Mac-2 antigen; [Homo sapiens (Human)] - [LEG3_HUMAN]	2.03E+06
Glutathione S-transferase A2 OS=Homo sapiens GN=GSTA2 PE=1 SV=4	9.67E+07	Glutathione S-transferase A2 OS=Homo sapiens GN=GSTA2 PE=1 SV=4	4.18E+07
Glutathione S-transferase P OS=Homo sapiens GN=GSTP1 PE=1 SV=2	1.74E+07	Glutathione S-transferase P OS=Homo sapiens GN=GSTP1 PE=1 SV=2	8.51E+06
Haptoglobin OS=Homo sapiens GN=HP PE=1 SV=1	2.64E+08	Haptoglobin OS=Homo sapiens GN=HP PE=1 SV=1	1.26E+08
Hemoglobin subunit alpha OS=Homo sapiens GN=HBA1 PE=1 SV=2	8.29E+07	Hemoglobin subunit alpha OS=Homo sapiens GN=HBA1 PE=1 SV=2	1.49E+08
Hemoglobin subunit beta OS=Homo sapiens GN=HBB PE=1 SV=2	7.32E+07	Hemoglobin subunit beta OS=Homo sapiens GN=HBB PE=1 SV=2	1.28E+08
Hemopexin OS=Homo sapiens GN=HPX PE=1 SV=2	3.48E+08	Hemopexin OS=Homo sapiens GN=HPX PE=1 SV=2	2.71E+08

Ig alpha-1 chain C region OS=Homo sapiens GN=IGHA1 PE=1 SV=2	1.56E+09	Ig alpha-1 chain C region OS=Homo sapiens GN=IGHA1 PE=1 SV=2	2.42E+09
Ig alpha-2 chain C region OS=Homo sapiens GN=IGHA2 PE=1 SV=3	8.21E+08	Ig alpha-2 chain C region OS=Homo sapiens GN=IGHA2 PE=1 SV=3	1.79E+09
Ig gamma-1 chain C region OS=Homo sapiens GN=IGHG1 PE=1 SV=1	5.79E+09	Ig gamma-1 chain C region OS=Homo sapiens GN=IGHG1 PE=1 SV=1	8.92E+09
Ig gamma-2 chain C region OS=Homo sapiens GN=IGHG2 PE=1 SV=2	4.65E+09	Ig gamma-2 chain C region OS=Homo sapiens GN=IGHG2 PE=1 SV=2	5.60E+09
Ig gamma-3 chain C region OS=Homo sapiens GN=IGHG3 PE=1 SV=2	5.04E+09	Ig gamma-3 chain C region OS=Homo sapiens GN=IGHG3 PE=1 SV=2	6.71E+09
Ig heavy chain V-II region NEWM; [Homo sapiens (Human)] - [HV207_HUMAN]	1.15E+08	Ig heavy chain V-II region NEWM OS=Homo sapiens PE=1 SV=1	1.47E+08
Ig heavy chain V-II region OU; [Homo sapiens (Human)] - [HV201_HUMAN]	4.28E+07	Ig heavy chain V-II region OU; [Homo sapiens (Human)] - [HV201_HUMAN]	1.44E+08
Ig heavy chain V-III region BRO; [Homo sapiens (Human)] - [HV305_HUMAN]	9.27E+08	Ig heavy chain V-III region BRO; [Homo sapiens (Human)] - [HV305_HUMAN]	1.02E+09
Ig heavy chain V-III region BUT; [Homo sapiens (Human)] - [HV306_HUMAN]	9.00E+08	Ig heavy chain V-III region BUT; [Homo sapiens (Human)] - [HV306_HUMAN]	1.03E+09
Ig heavy chain V-III region CAM OS=Homo sapiens PE=1 SV=1	9.16E+08	Ig heavy chain V-III region CAM OS=Homo sapiens PE=1 SV=1	1.05E+09
Ig heavy chain V-III region GAL OS=Homo sapiens PE=1 SV=1	8.79E+08	Ig heavy chain V-III region GAL OS=Homo sapiens PE=1 SV=1	1.05E+09
Ig heavy chain V-III region GAR; [Homo sapiens (Human)] - [HV322_HUMAN]	2.86E+08	Ig heavy chain V-III region GAR; [Homo sapiens (Human)] - [HV322_HUMAN]	1.05E+08
Ig heavy chain V-III region HIL; [Homo sapiens (Human)] - [HV310_HUMAN]	1.24E+09	Ig heavy chain V-III region HIL; [Homo sapiens (Human)] - [HV310_HUMAN]	1.47E+09
Ig kappa chain C region OS=Homo sapiens GN=IGKC PE=1 SV=1	2.92E+09	Ig kappa chain C region OS=Homo sapiens GN=IGKC PE=1 SV=1	3.47E+09
Ig kappa chain V-I region CAR OS=Homo sapiens PE=1 SV=1	8.07E+07	Ig kappa chain V-I region CAR; [Homo sapiens (Human)] - [KV104_HUMAN]	7.26E+07
Ig kappa chain V-I region EU OS=Homo sapiens PE=1 SV=1	3.10E+08	Ig kappa chain V-I region EU OS=Homo sapiens PE=1 SV=1	2.41E+08
Ig kappa chain V-I region Kue	2.80E+08	Ig kappa chain V-I region Kue	1.89E+08

OS=Homo sapiens PE=1 SV=1		OS=Homo sapiens PE=1 SV=1	
Ig kappa chain V-I region Wes; [Homo sapiens (Human)] - [KV119_HUMAN]	3.60E+08	Ig kappa chain V-I region Wes; [Homo sapiens (Human)] - [KV119_HUMAN]	2.71E+08
Ig kappa chain V-II region FR OS=Homo sapiens PE=1 SV=1	3.16E+06	Ig kappa chain V-II region FR OS=Homo sapiens PE=1 SV=1	8.51E+07
Ig kappa chain V-III region POM OS=Homo sapiens PE=1 SV=1	1.58E+08	Ig kappa chain V-III region POM OS=Homo sapiens PE=1 SV=1	9.77E+07
Ig kappa chain V-III region SIE OS=Homo sapiens PE=1 SV=1	2.67E+08	Ig kappa chain V-III region SIE OS=Homo sapiens PE=1 SV=1	2.40E+08
Ig kappa chain V-III region VG (Fragment) OS=Homo sapiens PE=1 SV=1	6.84E+07	Ig kappa chain V-III region VG; Flags: Precursor; Fragment; [Homo sapiens (Human)] - [KV309_HUMAN]	1.46E+08
Ig kappa chain V-IV region JI OS=Homo sapiens PE=4 SV=1	1.08E+08	Ig kappa chain V-IV region JI OS=Homo sapiens PE=4 SV=1	3.74E+07
Ig kappa chain V-IV region Len; [Homo sapiens (Human)] - [KV402_HUMAN]	1.49E+08	Ig kappa chain V-IV region Len OS=Homo sapiens PE=1 SV=2	9.86E+07
Ig lambda chain V region 4A OS=Homo sapiens PE=4 SV=1	7.87E+06	Ig lambda chain V region 4A OS=Homo sapiens PE=4 SV=1	5.01E+07
Ig lambda chain V-I region HA OS=Homo sapiens PE=1 SV=1	6.98E+07	Ig lambda chain V-I region HA OS=Homo sapiens PE=1 SV=1	1.91E+08
Ig lambda chain V-I region NIG-64 OS=Homo sapiens PE=1 SV=1	2.25E+07	Ig lambda chain V-I region NIG-64 OS=Homo sapiens PE=1 SV=1	7.21E+07
Ig lambda chain V-III region LOI OS=Homo sapiens PE=1 SV=1	6.09E+07	Ig lambda chain V-III region LOI OS=Homo sapiens PE=1 SV=1	1.57E+08
Ig lambda chain V-III region SH; [Homo sapiens (Human)] - [LV301_HUMAN]	1.31E+07	Ig lambda chain V-III region SH; [Homo sapiens (Human)] - [LV301_HUMAN]	3.09E+07
Ig lambda chain V-IV region Bau; [Homo sapiens (Human)] - [LV401_HUMAN]	5.41E+07	Ig lambda chain V-IV region Bau; [Homo sapiens (Human)] - [LV401_HUMAN]	1.58E+08
Ig lambda-2 chain C regions OS=Homo sapiens GN=IGLC2 PE=1 SV=1	1.09E+09	Ig lambda-2 chain C regions OS=Homo sapiens GN=IGLC2 PE=1 SV=1	2.31E+09
Ig mu chain C region OS=Homo sapiens GN=IGHM PE=1 SV=3	3.88E+07	Ig mu chain C region OS=Homo sapiens GN=IGHM PE=1 SV=3	4.16E+07
Immunoglobulin J chain OS=Homo sapiens GN=IGJ PE=1 SV=4	7.57E+07	Immunoglobulin J chain OS=Homo sapiens GN=IGJ PE=1 SV=4	4.76E+07
Immunoglobulin lambda-like polypeptide 5 OS=Homo sapiens GN=IGLL5 PE=2 SV=2	7.42E+08	Immunoglobulin lambda-like polypeptide 5 OS=Homo sapiens GN=IGLL5 PE=2 SV=2	1.44E+09
Intercellular adhesion molecule	1.44E+07	Intercellular adhesion molecule	1.15E+07

1 OS=Homo sapiens GN=ICAM1 PE=1 SV=2		1 OS=Homo sapiens GN=ICAM1 PE=1 SV=2	
Leucine-rich alpha-2-glycoprotein OS=Homo sapiens GN=LRG1 PE=1 SV=2	3.29E+07	Leucine-rich alpha-2-glycoprotein OS=Homo sapiens GN=LRG1 PE=1 SV=2	4.46E+07
Lysosomal alpha-glucosidase OS=Homo sapiens GN=GAA PE=1 SV=4	1.97E+07	Lysosomal alpha-glucosidase; EC=3.2.1.20; AltName: Full=Acid maltase; AltName: Full=Aglucosidase alfa; Contains: RecName: Full=76 kDa lysosomal alpha-glucosidase; Contains: RecName: Full=70 kDa lysosomal alpha-glucosidase; Flags: Precursor; [Homo sapiens (Human)] - [LYAG_HUMAN]	1.40E+06
Mucin-1 OS=Homo sapiens GN=MUC1 PE=1 SV=3	1.02E+07	Mucin-1 OS=Homo sapiens GN=MUC1 PE=1 SV=3	1.18E+07
Myotubularin-related protein 14; EC=3.1.3.-; AltName: Full=HCV NS5A-transactivated protein 4 splice variant A-binding protein 1; Short=NS5ATP4ABP1; AltName: Full=hJumpy; [Homo sapiens (Human)] - [MTMRE_HUMAN]	3.66E+06	Myotubularin-related protein 14; EC=3.1.3.-; AltName: Full=HCV NS5A-transactivated protein 4 splice variant A-binding protein 1; Short=NS5ATP4ABP1; AltName: Full=hJumpy; [Homo sapiens (Human)] - [MTMRE_HUMAN]	3.06E+06
Peptidyl-prolyl cis-trans isomerase A OS=Homo sapiens GN=PPIA PE=1 SV=2	7.32E+06	Peptidyl-prolyl cis-trans isomerase A; Short=PPIase A; EC=5.2.1.8; AltName: Full=Cyclophilin A; AltName: Full=Cyclosporin A-binding protein; AltName: Full=Rotamase A; [Homo sapiens (Human)] - [PPIA_HUMAN]	6.43E+06
Polymeric immunoglobulin receptor OS=Homo sapiens GN=PIGR PE=1 SV=4	2.83E+08	Polymeric immunoglobulin receptor OS=Homo sapiens GN=PIGR PE=1 SV=4	1.94E+08
Pro-cathepsin H OS=Homo sapiens GN=CTSH PE=1 SV=4	1.61E+07	Pro-cathepsin H OS=Homo sapiens GN=CTSH PE=1 SV=4	1.06E+07
Proactivator polypeptide; Contains: RecName: Full=Saposin-A; AltName: Full=Protein A; Contains: RecName: Full=Saposin-B-Val; Contains: RecName: Full=Saposin-B; AltName: Full=Cerebroside sulfate	6.97E+06	Proactivator polypeptide OS=Homo sapiens GN=PSAP PE=1 SV=2	2.71E+06

activator; Short=CSAct; AltName: Full=Dispersin; AltName: Full=Sphingolipid activator protein 1; Short=SAP-1; AltName: Full=Sulfatide/GM1 activator; Contains: RecName: Full=Saposin-C; AltName: Full=A1 activator; AltName: Full=Co-beta-glucosidase; AltName: Full=Glucosylceramidase activator; AltName: Full=Sphingolipid activator protein 2; Short=SAP-2; Contains: RecName: Full=Saposin-D; AltName: Full=Component C; AltName: Full=Protein C; Flags: Precursor; [Homo sapiens (Human)] - [SAP_HUMAN]			
Protein DJ-1 OS=Homo sapiens GN=PARK7 PE=1 SV=2	1.16E+07	Protein DJ-1 OS=Homo sapiens GN=PARK7 PE=1 SV=2	1.23E+07
Protein S100-A6 OS=Homo sapiens GN=S100A6 PE=1 SV=1	1.14E+08	Protein S100-A6 OS=Homo sapiens GN=S100A6 PE=1 SV=1	2.38E+07
Protein S100-A8 OS=Homo sapiens GN=S100A8 PE=1 SV=1	2.22E+06	Protein S100-A8 OS=Homo sapiens GN=S100A8 PE=1 SV=1	3.59E+07
Protein Shroom3; AltName: Full=Shroom-related protein; Short=hShrmL; [Homo sapiens (Human)] - [SHRM3_HUMAN]	2.30E+08	Protein Shroom3; AltName: Full=Shroom-related protein; Short=hShrmL; [Homo sapiens (Human)] - [SHRM3_HUMAN]	9.47E+07
Protein-glutamine gamma-glutamyltransferase E; EC=2.3.2.13; AltName: Full=Transglutaminase E; Short=TG(E); Short=TGE; Short=TGase E; AltName: Full=Transglutaminase-3; Short=TGase-3; Contains: RecName: Full=Protein-glutamine gamma-glutamyltransferase E 50 kDa non-catalytic chain; Contains: RecName: Full=Protein-glutamine gamma-glutamyltransferase E 27 kDa catalytic chain; Flags: Precursor; [Homo sapiens (Human)] -	8.37E+06	Protein-glutamine gamma-glutamyltransferase E; EC=2.3.2.13; AltName: Full=Transglutaminase E; Short=TG(E); Short=TGE; Short=TGase E; AltName: Full=Transglutaminase-3; Short=TGase-3; Contains: RecName: Full=Protein-glutamine gamma-glutamyltransferase E 50 kDa non-catalytic chain; Contains: RecName: Full=Protein-glutamine gamma-glutamyltransferase E 27 kDa catalytic chain; Flags: Precursor; [Homo sapiens	3.65E+06

[TGM3_HUMAN]		(Human)] - [TGM3_HUMAN]	
Pulmonary surfactant-associated protein A2 OS=Homo sapiens GN=SFTPA2 PE=1 SV=1	2.89E+07	Pulmonary surfactant-associated protein A2 OS=Homo sapiens GN=SFTPA2 PE=1 SV=1	3.74E+07
Pulmonary surfactant-associated protein B OS=Homo sapiens GN=SFTPB PE=1 SV=3	9.69E+06	Pulmonary surfactant-associated protein B; Short=SP-B; AltName: Full=18 kDa pulmonary-surfactant protein; AltName: Full=6 kDa protein; AltName: Full=Pulmonary surfactant-associated proteolipid SPL(Phe); Flags: Precursor; [Homo sapiens (Human)] - [PSPB_HUMAN]	3.26E+06
Pulmonary surfactant-associated protein D OS=Homo sapiens GN=SFTPD PE=1 SV=3	2.63E+07	Pulmonary surfactant-associated protein D OS=Homo sapiens GN=SFTPD PE=1 SV=3	1.53E+07
Putative V-set and immunoglobulin domain-containing protein 6; Flags: Precursor; [Homo sapiens (Human)] - [VSIG6_HUMAN]	1.42E+08	Putative V-set and immunoglobulin domain-containing protein 6 OS=Homo sapiens GN=VSIG6 PE=5 SV=2	2.00E+08
Ribonuclease P protein subunit p40; Short=RNaseP protein p40; EC=3.1.26.5; AltName: Full=RNase P subunit 1; [Homo sapiens (Human)] - [RPP40_HUMAN]	1.55E+08	Ribonuclease P protein subunit p40; Short=RNaseP protein p40; EC=3.1.26.5; AltName: Full=RNase P subunit 1; [Homo sapiens (Human)] - [RPP40_HUMAN]	5.47E+07
Selenium-binding protein 1 OS=Homo sapiens GN=SELENBP1 PE=1 SV=2	8.65E+06	Selenium-binding protein 1 OS=Homo sapiens GN=SELENBP1 PE=1 SV=2	1.67E+07
Serotransferrin OS=Homo sapiens GN=TF PE=1 SV=3	4.56E+09	Serotransferrin OS=Homo sapiens GN=TF PE=1 SV=3	7.62E+09
Serum albumin OS=Homo sapiens GN=ALB PE=1 SV=2	3.86E+09	Serum albumin OS=Homo sapiens GN=ALB PE=1 SV=2	2.77E+09
SH3 domain-binding glutamic acid-rich-like protein 3; AltName: Full=SH3 domain-binding protein 1; Short=SH3BP-1; [Homo sapiens (Human)] - [SH3L3_HUMAN]	1.22E+07	SH3 domain-binding glutamic acid-rich-like protein 3; AltName: Full=SH3 domain-binding protein 1; Short=SH3BP-1; [Homo sapiens (Human)] - [SH3L3_HUMAN]	3.66E+06
Sorting nexin-6; AltName: Full=TRAF4-associated factor 2; [Homo sapiens (Human)] - [SNX6_HUMAN]	4.91E+06	Sorting nexin-6; AltName: Full=TRAF4-associated factor 2; [Homo sapiens (Human)] - [SNX6_HUMAN]	2.15E+06
Thioredoxin; Short=Trx; AltName: Full=ATL-derived factor; Short=ADF; AltName:	2.98E+07	Thioredoxin; Short=Trx; AltName: Full=ATL-derived factor; Short=ADF; AltName:	8.21E+06

Full=Surface-associated sulphydryl protein; Short=SASP; [Homo sapiens (Human)] - [THIO_HUMAN]		Full=Surface-associated sulphydryl protein; Short=SASP; [Homo sapiens (Human)] - [THIO_HUMAN]	
Thyroxine-binding globulin OS=Homo sapiens GN=SERPINA7 PE=1 SV=2	1.87E+07	Thyroxine-binding globulin OS=Homo sapiens GN=SERPINA7 PE=1 SV=2	5.25E+06
Transaldolase OS=Homo sapiens GN=TALDO1 PE=1 SV=2	3.90E+07	Transaldolase OS=Homo sapiens GN=TALDO1 PE=1 SV=2	4.47E+07
Transcriptional adapter 2-beta; AltName: Full=ADA2-like protein beta; Short=ADA2-beta; [Homo sapiens (Human)] - [TAD2B_HUMAN]	2.68E+07	Transcriptional adapter 2-beta; AltName: Full=ADA2-like protein beta; Short=ADA2-beta; [Homo sapiens (Human)] - [TAD2B_HUMAN]	2.22E+07
Transmembrane protein 198; [Homo sapiens (Human)] - [TM198_HUMAN]	4.78E+07	Transmembrane protein 198; [Homo sapiens (Human)] - [TM198_HUMAN]	2.62E+07
Transmembrane protein 200C; AltName: Full=Transmembrane protein TTMA; AltName: Full=Two transmembrane domain-containing family member A; [Homo sapiens (Human)] - [T200C_HUMAN]	1.94E+06	Transmembrane protein 200C; AltName: Full=Transmembrane protein TTMA; AltName: Full=Two transmembrane domain-containing family member A; [Homo sapiens (Human)] - [T200C_HUMAN]	3.59E+06
Transthyretin OS=Homo sapiens GN=TTR PE=1 SV=1	1.29E+08	Transthyretin OS=Homo sapiens GN=TTR PE=1 SV=1	2.53E+08
Triosephosphate isomerase OS=Homo sapiens GN=TPI1 PE=1 SV=3	3.25E+07	Triosephosphate isomerase OS=Homo sapiens GN=TPI1 PE=1 SV=3	4.37E+07
Uncharacterized protein C3orf38; [Homo sapiens (Human)] - [CC038_HUMAN]	1.83E+09	Uncharacterized protein C3orf38; [Homo sapiens (Human)] - [CC038_HUMAN]	2.73E+09
Uteroglobin OS=Homo sapiens GN=SCGB1A1 PE=1 SV=1	1.99E+08	Uteroglobin OS=Homo sapiens GN=SCGB1A1 PE=1 SV=1	1.74E+08
Vitamin D-binding protein OS=Homo sapiens GN=GC PE=1 SV=1	1.52E+08	Vitamin D-binding protein OS=Homo sapiens GN=GC PE=1 SV=1	4.91E+08
Xin actin-binding repeat-containing protein 2 OS=Homo sapiens GN=XIRP2 PE=1 SV=2	1.76E+08	Xin actin-binding repeat-containing protein 2 OS=Homo sapiens GN=XIRP2 PE=1 SV=2	2.05E+08
Zinc-alpha-2-glycoprotein OS=Homo sapiens GN=AZGP1 PE=1 SV=2	8.23E+07	Zinc-alpha-2-glycoprotein OS=Homo sapiens GN=AZGP1 PE=1 SV=2	1.24E+08
14-3-3 protein epsilon OS=Homo sapiens GN=YWHAE PE=1 SV=1	3.12E+07	14-3-3 protein epsilon OS=Homo sapiens GN=YWHAE PE=1 SV=1	1.86E+07
HLA class II histocompatibility antigen, DRB1-1 beta chain	4635000	HLA class II histocompatibility antigen,	6.88E+06

OS=Homo sapiens GN=HLA-DRB1 PE=1 SV=2		DRB1-1 beta chain OS=Homo sapiens GN=HLA-DRB1 PE=1 SV=2	

Table C.7 *Alveolar proteins identified by 1D PAGE and nano LC MS/MS in healthy aged and COPD ex-smoker RTLFs***.** The 45 proteins common to both healthy aged (n=5) and COPD ex-smoker (n=10) subjects investigated, alongside the mean of the three most abundant ion peaks of each respective protein identified. Accession numbers included according to entries in UniProtKB/Swiss-Prot.

COPD ex-smoker		**Healthy Aged Control**	
Ig kappa chain C region OS=Homo sapiens GN=IGKC PE=1 SV=1	9.25E+09	Ig kappa chain C region OS=Homo sapiens GN=IGKC PE=1 SV=1	3.47E+09
Ig alpha-1 chain C region OS=Homo sapiens GN=IGHA1 PE=1 SV=2	6.04E+09	Ig alpha-1 chain C region OS=Homo sapiens GN=IGHA1 PE=1 SV=2	2.42E+09
Uteroglobin OS=Homo sapiens GN=SCGB1A1 PE=1 SV=1	4.49E+09	Uteroglobin OS=Homo sapiens GN=SCGB1A1 PE=1 SV=1	1.74E+08
Ig gamma-1 chain C region OS=Homo sapiens GN=IGHG1 PE=1 SV=1	3.55E+09	Ig gamma-1 chain C region OS=Homo sapiens GN=IGHG1 PE=1 SV=1	8.92E+09
Polymeric immunoglobulin receptor OS=Homo sapiens GN=PIGR PE=1 SV=4	2.37E+09	Polymeric immunoglobulin receptor OS=Homo sapiens GN=PIGR PE=1 SV=4	1.94E+08
Hemoglobin subunit beta OS=Homo sapiens GN=HBB PE=1 SV=2	1.66E+09	Hemoglobin subunit beta OS=Homo sapiens GN=HBB PE=1 SV=2	1.28E+08
RecName: Full=Ig kappa chain V-III region B6; [Homo sapiens (Human)] - [KV301_HUMAN]	1.63E+09	Ig kappa chain V-III region B6; [Homo sapiens (Human)] - [KV301_HUMAN]	2.39E+08
Serotransferrin OS=Homo sapiens GN=TF PE=1 SV=3	1.10E+09	Serotransferrin OS=Homo sapiens GN=TF PE=1 SV=3	7.62E+09
Uncharacterized protein C3orf38; [Homo sapiens (Human)] - [CC038_HUMAN]	5.97E+08	Uncharacterized protein C3orf38; [Homo sapiens (Human)] - [CC038_HUMAN]	2.73E+09
Beta-2-microglobulin OS=Homo sapiens GN=B2M PE=1 SV=1	5.86E+08	Beta-2-microglobulin OS=Homo sapiens GN=B2M PE=1 SV=1	2.59E+07
Serum albumin OS=Homo sapiens GN=ALB PE=1 SV=2	5.49E+08	Serum albumin OS=Homo sapiens GN=ALB PE=1 SV=2	2.77E+09
Lysozyme C; EC=3.2.1.17; AltName: Full=1,4-beta-N-acetylmuramidase C; Flags: Precursor; [Homo sapiens (Human)] - [LYSC_HUMAN]	5.31E+08	Lysozyme C; EC=3.2.1.17; AltName: Full=1,4-beta-N-acetylmuramidase C; Flags: Precursor; [Homo sapiens (Human)] - [LYSC_HUMAN]	1.48E+06
Hemoglobin subunit alpha; AltName: Full=Alpha-globin; AltName: Full=Hemoglobin alpha chain; [Homo sapiens (Human)] - [HBA_HUMAN]	5.24E+08	Hemoglobin subunit alpha OS=Homo sapiens GN=HBA1 PE=1 SV=2	1.49E+08

Ig lambda chain V-III region LOI; [Homo sapiens (Human)] - [LV302_HUMAN]	4.81E+08	Ig lambda chain V-III region LOI OS=Homo sapiens PE=1 SV=1	1.57E+08
Actin, cytoplasmic 1 OS=Homo sapiens GN=ACTB PE=1 SV=1	4.06E+08	Actin, cytoplasmic 1 OS=Homo sapiens GN=ACTB PE=1 SV=1	6.89E+07
Complement C3 OS=Homo sapiens GN=C3 PE=1 SV=2	2.06E+08	Complement C3 OS=Homo sapiens GN=C3 PE=1 SV=2	2.66E+06
Hemopexin OS=Homo sapiens GN=HPX PE=1 SV=2	1.75E+08	Hemopexin OS=Homo sapiens GN=HPX PE=1 SV=2	2.71E+08
Thioredoxin; Short=Trx; AltName: Full=ATL-derived factor; Short=ADF; AltName: Full=Surface-associated sulphydryl protein; Short=SASP; [Homo sapiens (Human)] - [THIO_HUMAN]	1.54E+08	Thioredoxin; Short=Trx; AltName: Full=ATL-derived factor; Short=ADF; AltName: Full=Surface-associated sulphydryl protein; Short=SASP; [Homo sapiens (Human)] - [THIO_HUMAN]	8.21E+06
Ferritin light chain OS=Homo sapiens GN=FTL PE=1 SV=2	1.51E+08	Ferritin light chain; Short=Ferritin L subunit; [Homo sapiens (Human)] - [FRIL_HUMAN]	4.73E+06
Annexin A5; AltName: Full=Anchorin CII; AltName: Full=Annexin V; AltName: Full=Annexin-5; AltName: Full=Calphobindin I; Short=CBP-I; AltName: Full=Endonexin II; AltName: Full=Lipocortin V; AltName: Full=Placental anticoagulant protein 4; Short=PP4; AltName: Full=Placental anticoagulant protein I; Short=PAP-I; AltName: Full=Thromboplastin inhibitor; AltName: Full=Vascular anticoagulant-alpha; Short=VAC-alpha; [Homo sapiens (Human)] - [ANXA5_HUMAN]	9.47E+07	Annexin A5 OS=Homo sapiens GN=ANXA5 PE=1 SV=2	1.36E+06
Transthyretin OS=Homo sapiens GN=TTR PE=1 SV=1	7.84E+07	Transthyretin OS=Homo sapiens GN=TTR PE=1 SV=1	2.53E+08
Peptidyl-prolyl cis-trans isomerase A; Short=PPIase A; EC=5.2.1.8; AltName: Full=Cyclophilin A; AltName: Full=Cyclosporin A-binding protein; AltName: Full=Rotamase A; [Homo sapiens (Human)] - [PPIA_HUMAN]	7.51E+07	Peptidyl-prolyl cis-trans isomerase A; Short=PPIase A; EC=5.2.1.8; AltName: Full=Cyclophilin A; AltName: Full=Cyclosporin A-binding protein; AltName: Full=Rotamase A; [Homo sapiens (Human)] - [PPIA_HUMAN]	6.43E+06
Ig gamma-2 chain C region OS=Homo sapiens GN=IGHG2	5.64E+07	Ig gamma-2 chain C region OS=Homo sapiens	5.60E+09

PE=1 SV=2		GN=IGHG2 PE=1 SV=2	
Delta-like protein 4; AltName: Full=Drosophila Delta homolog 4; Short=Delta4; Flags: Precursor; [Homo sapiens (Human)] - [DLL4_HUMAN]	4.85E+07	Delta-like protein 4; AltName: Full=Drosophila Delta homolog 4; Short=Delta4; Flags: Precursor; [Homo sapiens (Human)] - [DLL4_HUMAN]	1.23E+07
RecName: Full=CD44 antigen; AltName: Full=CDw44; AltName: Full=Epican; AltName: Full=Extracellular matrix receptor III; Short=ECMR-III; AltName: Full=GP90 lymphocyte homing/adhesion receptor; AltName: Full=HUTCH-I; AltName: Full=Heparan sulfate proteoglycan; AltName: Full=Hermes antigen; AltName: Full=Hyaluronate receptor; AltName: Full=Phagocytic glycoprotein 1; Short=PGP-1; AltName: Full=Phagocytic glycoprotein I; Short=PGP-I; AltName: CD_antigen=CD44; Flags: Precursor; [Homo sapiens (Human)] - [CD44_HUMAN]	3.87E+07	CD44 antigen OS=Homo sapiens GN=CD44 PE=1 SV=3	2.73E+07
Alpha-1-antitrypsin OS=Homo sapiens GN=SERPINA1 PE=1 SV=3	3.86E+07	Alpha-1-antitrypsin OS=Homo sapiens GN=SERPINA1 PE=1 SV=3	3.20E+09
RecName: Full=Ig lambda chain V-IV region Bau; [Homo sapiens (Human)] - [LV401_HUMAN]	3.27E+07	Ig lambda chain V-IV region Bau; [Homo sapiens (Human)] - [LV401_HUMAN]	1.58E+08
Protein Shroom3; AltName: Full=Shroom-related protein; Short=hShrmL; [Homo sapiens (Human)] - [SHRM3_HUMAN]	2.29E+07	Protein Shroom3; AltName: Full=Shroom-related protein; Short=hShrmL; [Homo sapiens (Human)] - [SHRM3_HUMAN]	9.47E+07
Ig heavy chain V-III region CAM; [Homo sapiens (Human)] - [HV307_HUMAN]	1.68E+07	Ig heavy chain V-III region CAM OS=Homo sapiens PE=1 SV=1	1.05E+09
Ig heavy chain V-III region TIL; [Homo sapiens (Human)] - [HV304_HUMAN]	1.60E+07	Ig heavy chain V-III region TIL OS=Homo sapiens PE=1 SV=1	1.06E+09
Haptoglobin OS=Homo sapiens GN=HP PE=1 SV=1	9.50E+06	Haptoglobin OS=Homo sapiens GN=HP PE=1 SV=1	1.26E+08
Ig lambda-2 chain C regions OS=Homo sapiens GN=IGLC2 PE=1 SV=1	8.59E+06	Ig lambda-2 chain C regions OS=Homo sapiens GN=IGLC2 PE=1 SV=1	2.31E+09
Dermcidin; AltName: Full=Preproteolysin; Contains:	6.55E+06	Dermcidin OS=Homo sapiens GN=DCD PE=1 SV=2	2.13E+06

RecName: Full=Survival-promoting peptide; Contains: RecName: Full=DCD-1; Flags: Precursor; [Homo sapiens (Human)] - [DCD_HUMAN]			
Calmodulin-like protein 5; AltName: Full=Calmodulin-like skin protein; [Homo sapiens (Human)] - [CALL5_HUMAN]	6.19E+06	Calmodulin-like protein 5; AltName: Full=Calmodulin-like skin protein; [Homo sapiens (Human)] - [CALL5_HUMAN]	2.82E+07
Desmoplakin OS=Homo sapiens GN=DSP PE=1 SV=3	3.75E+06	Desmoplakin OS=Homo sapiens GN=DSP PE=1 SV=3	1.40E+08
Alpha-1-acid glycoprotein 1 OS=Homo sapiens GN=ORM1 PE=1 SV=1	2.88E+06	Alpha-1-acid glycoprotein 1 OS=Homo sapiens GN=ORM1 PE=1 SV=1	3.39E+08
Ceruloplasmin OS=Homo sapiens GN=CP PE=1 SV=1	2.73E+06	Ceruloplasmin OS=Homo sapiens GN=CP PE=1 SV=1	3.67E+08
Alpha-1-acid glycoprotein 2; Short=AGP 2; AltName: Full=Orosomucoid-2; Short=OMD 2; Flags: Precursor; [Homo sapiens (Human)] - [A1AG2_HUMAN]	1.95E+06	Alpha-1-acid glycoprotein 2 OS=Homo sapiens GN=ORM2 PE=1 SV=2	2.40E+08
Transmembrane protein 200C; AltName: Full=Transmembrane protein TTMA; AltName: Full=Two transmembrane domain-containing family member A; [Homo sapiens (Human)] - [T200C_HUMAN]	1.89E+06	Transmembrane protein 200C; AltName: Full=Transmembrane protein TTMA; AltName: Full=Two transmembrane domain-containing family member A; [Homo sapiens (Human)] - [T200C_HUMAN]	3.59E+06
Ig kappa chain V-III region SIE; [Homo sapiens (Human)] - [KV302_HUMAN]	1.85E+06	Ig kappa chain V-III region SIE OS=Homo sapiens PE=1 SV=1	2.40E+08
Pulmonary surfactant-associated protein A2; Short=PSP-A; Short=PSPA; Short=SP-A; Short=SP-A2; AltName: Full=35 kDa pulmonary surfactant-associated protein; AltName: Full=Alveolar proteinosis protein; AltName: Full=Collectin-5; Flags: Precursor; [Homo sapiens (Human)] - [SFPA2_HUMAN]	1.85E+06	Pulmonary surfactant-associated protein A2 OS=Homo sapiens GN=SFTPA2 PE=1 SV=1	3.74E+07
Alpha-1B-glycoprotein; AltName: Full=Alpha-1-B glycoprotein; Flags: Precursor; [Homo sapiens (Human)] - [A1BG_HUMAN]	1.24E+06	Alpha-1B-glycoprotein OS=Homo sapiens GN=A1BG PE=1 SV=4	1.33E+08
Myotubularin-related protein 14; EC=3.1.3.-; AltName:	1.21E+06	Myotubularin-related protein 14; EC=3.1.3.-; AltName:	3.06E+06

Full=HCV NS5A-transactivated protein 4 splice variant A-binding protein 1; Short=NS5ATP4ABP1; AltName: Full=hJumpy; [Homo sapiens (Human)] - [MTMRE_HUMAN]		Full=HCV NS5A-transactivated protein 4 splice variant A-binding protein 1; Short=NS5ATP4ABP1; AltName: Full=hJumpy; [Homo sapiens (Human)] - [MTMRE_HUMAN]	
Transcriptional adapter 2-beta; AltName: Full=ADA2-like protein beta; Short=ADA2-beta; [Homo sapiens (Human)] - [TAD2B_HUMAN]	1.11E+06	Transcriptional adapter 2-beta; AltName: Full=ADA2-like protein beta; Short=ADA2-beta; [Homo sapiens (Human)] - [TAD2B_HUMAN]	2.22E+07
Leucine-rich alpha-2-glycoprotein OS=Homo sapiens GN=LRG1 PE=1 SV=2	7.23E+05	Leucine-rich alpha-2-glycoprotein OS=Homo sapiens GN=LRG1 PE=1 SV=2	4.46E+07

Table C.8: *Alveolar proteins identified by 1D PAGE and nano LC MS/MS in healthy smoker and COPD ex-smoker RTLFs. The 40 proteins common to both healthy smoker (n=5) and COPD ex-smoker (n=10) subjects investigated, alongside the mean of the three most abundant ion peaks of each respective protein identified. Accession numbers included according to entries in UniProtKB/Swiss-Prot.*

COPD ex-smoker		**Healthy Smoker**	
Serotransferrin OS=Homo sapiens GN=TF PE=1 SV=3	1.10E+09	Serotransferrin OS=Homo sapiens GN=TF PE=1 SV=3	3.42E+09
Ig gamma-1 chain C region OS=Homo sapiens GN=IGHG1 PE=1 SV=1	3.55E+09	Ig gamma-1 chain C region OS=Homo sapiens GN=IGHG1 PE=1 SV=1	3.30E+09
Ig gamma-2 chain C region OS=Homo sapiens GN=IGHG2 PE=1 SV=2	5.64E+07	Ig gamma-2 chain C region OS=Homo sapiens GN=IGHG2 PE=1 SV=2	2.57E+09
RecName: Full=Uncharacterized protein C3orf38; [Homo sapiens (Human)] - [CC038_HUMAN]	5.97E+08	Uncharacterized protein C3orf38; [Homo sapiens (Human)] - [CC038_HUMAN]	1.62E+09
Serum albumin OS=Homo sapiens GN=ALB PE=1 SV=2	5.49E+08	Serum albumin OS=Homo sapiens GN=ALB PE=1 SV=2	1.54E+09
Ig kappa chain C region OS=Homo sapiens GN=IGKC PE=1 SV=1	9.25E+09	Ig kappa chain C region OS=Homo sapiens GN=IGKC PE=1 SV=1	1.07E+09
Ig lambda-2 chain C regions OS=Homo sapiens GN=IGLC2 PE=1 SV=1	8.59E+06	Ig lambda-2 chain C regions OS=Homo sapiens GN=IGLC2 PE=1 SV=1	7.91E+08
Ig alpha-1 chain C region OS=Homo sapiens GN=IGHA1 PE=1 SV=2	6.04E+09	Ig alpha-1 chain C region OS=Homo sapiens GN=IGHA1 PE=1 SV=2	6.14E+08
Alpha-1-antitrypsin OS=Homo sapiens GN=SERPINA1 PE=1 SV=3	3.86E+07	Alpha-1-antitrypsin OS=Homo sapiens GN=SERPINA1 PE=1 SV=3	2.75E+08
Olfactory receptor 2A2; AltName: Full=Olfactory	2.34E+07	Olfactory receptor 2A2; AltName: Full=Olfactory	2.70E+08

receptor 2A17; AltName: Full=Olfactory receptor OR7-11; [Homo sapiens (Human)] - [OR2A2_HUMAN]		receptor 2A17; AltName: Full=Olfactory receptor OR7-11; [Homo sapiens (Human)] - [OR2A2_HUMAN]	
Hemopexin OS=Homo sapiens GN=HPX PE=1 SV=2	2.83E+08	Hemopexin OS=Homo sapiens GN=HPX PE=1 SV=2	1.89E+08
Polymeric immunoglobulin receptor OS=Homo sapiens GN=PIGR PE=1 SV=4	2.37E+09	Polymeric immunoglobulin receptor OS=Homo sapiens GN=PIGR PE=1 SV=4	1.54E+08
Actin, cytoplasmic 1 OS=Homo sapiens GN=ACTB PE=1 SV=1	4.06E+08	Actin, cytoplasmic 1 OS=Homo sapiens GN=ACTB PE=1 SV=1	1.38E+08
Alpha-1-acid glycoprotein 1 OS=Homo sapiens GN=ORM1 PE=1 SV=1	2.88E+06	Alpha-1-acid glycoprotein 1 OS=Homo sapiens GN=ORM1 PE=1 SV=1	1.29E+08
Ceruloplasmin OS=Homo sapiens GN=CP PE=1 SV=1	2.73E+06	Ceruloplasmin OS=Homo sapiens GN=CP PE=1 SV=1	1.15E+08
Alpha-1-acid glycoprotein 2; Short=AGP 2; AltName: Full=Orosomucoid-2; Short=OMD 2; Flags: Precursor; [Homo sapiens (Human)] - [A1AG2_HUMAN]	1.95E+06	Alpha-1-acid glycoprotein 2; Short=AGP 2; AltName: Full=Orosomucoid-2; Short=OMD 2; Flags: Precursor; [Homo sapiens (Human)] - [A1AG2_HUMAN]	1.14E+08
Haptoglobin OS=Homo sapiens GN=HP PE=1 SV=1	9.50E+06	Haptoglobin OS=Homo sapiens GN=HP PE=1 SV=1	1.04E+08
Uteroglobin OS=Homo sapiens GN=SCGB1A1 PE=1 SV=1	4.49E+09	Uteroglobin OS=Homo sapiens GN=SCGB1A1 PE=1 SV=1	8.73E+07
Protein Shroom3; AltName: Full=Shroom-related protein; Short=hShrmL; [Homo sapiens (Human)] - [SHRM3_HUMAN]	2.29E+07	Protein Shroom3; AltName: Full=Shroom-related protein; Short=hShrmL; [Homo sapiens (Human)] - [SHRM3_HUMAN]	8.20E+07
Ig kappa chain V-III region VG (Fragment) OS=Homo sapiens PE=1 SV=1	2.65E+06	Ig kappa chain V-III region VG (Fragment) OS=Homo sapiens PE=1 SV=1	5.54E+07
RecName: Full=Hemoglobin subunit alpha; AltName: Full=Alpha-globin; AltName: Full=Hemoglobin alpha chain; [Homo sapiens (Human)] - [HBA_HUMAN]	5.24E+08	Hemoglobin subunit alpha OS=Homo sapiens GN=HBA1 PE=1 SV=2	5.40E+07
RecName: Full=Annexin A5; AltName: Full=Anchorin CII; AltName: Full=Annexin V; AltName: Full=Annexin-5; AltName: Full=Calphobindin I; Short=CBP-I; AltName: Full=Endonexin II; AltName: Full=Lipocortin V; AltName: Full=Placental anticoagulant	9.47E+07	Annexin A5 OS=Homo sapiens GN=ANXA5 PE=1 SV=2	5.18E+07

protein 4; Short=PP4; AltName: Full=Placental anticoagulant protein I; Short=PAP-I; AltName: Full=Thromboplastin inhibitor; AltName: Full=Vascular anticoagulant-alpha; Short=VAC-alpha; [Homo sapiens (Human)] - [ANXA5_HUMAN]			
Transcriptional adapter 2-beta; AltName: Full=ADA2-like protein beta; Short=ADA2-beta; [Homo sapiens (Human)] - [TAD2B_HUMAN]	1.11E+06	Transcriptional adapter 2-beta; AltName: Full=ADA2-like protein beta; Short=ADA2-beta; [Homo sapiens (Human)] - [TAD2B_HUMAN]	5.10E+07
Transthyretin OS=Homo sapiens GN=TTR PE=1 SV=1	7.84E+07	Transthyretin OS=Homo sapiens GN=TTR PE=1 SV=1	4.44E+07
RecName: Full=CD44 antigen; AltName: Full=CDw44; AltName: Full=Epican; AltName: Full=Extracellular matrix receptor III; Short=ECMR-III; AltName: Full=GP90 lymphocyte homing/adhesion receptor; AltName: Full=HUTCH-I; AltName: Full=Heparan sulfate proteoglycan; AltName: Full=Hermes antigen; AltName: Full=Hyaluronate receptor; AltName: Full=Phagocytic glycoprotein 1; Short=PGP-1; AltName: Full=Phagocytic glycoprotein I; Short=PGP-I; AltName: CD_antigen=CD44; Flags: Precursor; [Homo sapiens (Human)] - [CD44_HUMAN]	3.87E+07	CD44 antigen OS=Homo sapiens GN=CD44 PE=1 SV=3	3.34E+07
Pulmonary surfactant-associated protein A2; Short=PSP-A; Short=PSPA; Short=SP-A; Short=SP-A2; AltName: Full=35 kDa pulmonary surfactant-associated protein; AltName: Full=Alveolar proteinosis protein; AltName: Full=Collectin-5; Flags: Precursor; [Homo sapiens (Human)] - [SFPA2_HUMAN]	1.85E+06	Pulmonary surfactant-associated protein A2 OS=Homo sapiens GN=SFTPA2 PE=1 SV=1	2.82E+07
Alpha-1B-glycoprotein; AltName: Full=Alpha-1-B	1.24E+06	Alpha-1B-glycoprotein OS=Homo sapiens GN=A1BG	2.29E+07

glycoprotein; Flags: Precursor; [Homo sapiens (Human)] - [A1BG_HUMAN]		PE=1 SV=4	
Hemoglobin subunit beta OS=Homo sapiens GN=HBB PE=1 SV=2	1.66E+09	Transmembrane protein 198; [Homo sapiens (Human)] - [TM198_HUMAN]	2.08E+07
Ferritin light chain OS=Homo sapiens GN=FTL PE=1 SV=2	1.51E+08	Ferritin light chain OS=Homo sapiens GN=FTL PE=1 SV=2	2.03E+07
Leucine-rich alpha-2-glycoprotein OS=Homo sapiens GN=LRG1 PE=1 SV=2	7.23E+05	Leucine-rich alpha-2-glycoprotein OS=Homo sapiens GN=LRG1 PE=1 SV=2	1.76E+07
RecName: Full=Thioredoxin; Short=Trx; AltName: Full=ATL-derived factor; Short=ADF; AltName: Full=Surface-associated sulphydryl protein; Short=SASP; [Homo sapiens (Human)] - [THIO_HUMAN]	1.54E+08	Thioredoxin; Short=Trx; AltName: Full=ATL-derived factor; Short=ADF; AltName: Full=Surface-associated sulphydryl protein; Short=SASP; [Homo sapiens (Human)] - [THIO_HUMAN]	1.29E+07
RecName: Full=Ig lambda chain V-IV region Bau; [Homo sapiens (Human)] - [LV401_HUMAN]	3.27E+07	Ig lambda chain V-IV region Bau; [Homo sapiens (Human)] - [LV401_HUMAN]	1.05E+07
Beta-2-microglobulin OS=Homo sapiens GN=B2M PE=1 SV=1	5.86E+08	Beta-2-microglobulin OS=Homo sapiens GN=B2M PE=1 SV=1	1.03E+07
Dermcidin; AltName: Full=Preproteolysin; Contains: RecName: Full=Survival-promoting peptide; Contains: RecName: Full=DCD-1; Flags: Precursor; [Homo sapiens (Human)] - [DCD_HUMAN]	6.55E+06	Dermcidin OS=Homo sapiens GN=DCD PE=1 SV=2	4.35E+06
Transmembrane protein 200C; AltName: Full=Transmembrane protein TTMA; AltName: Full=Two transmembrane domain-containing family member A; [Homo sapiens (Human)] - [T200C_HUMAN]	1.89E+06	Transmembrane protein 200C; AltName: Full=Transmembrane protein TTMA; AltName: Full=Two transmembrane domain-containing family member A; [Homo sapiens (Human)] - [T200C_HUMAN]	2.06E+06
Myoglobin; [Homo sapiens (Human)] - [MYG_HUMAN]	2.39E+06	Myoglobin; [Homo sapiens (Human)] - [MYG_HUMAN]	1.97E+06
RecName: Full=Trypsin-3; EC=3.4.21.4; AltName: Full=Brain trypsinogen; AltName: Full=Mesotrypsinogen; AltName: Full=Serine protease 3; AltName: Full=Serine protease 4; AltName:	4.78E+06	Trypsin-3; EC=3.4.21.4; AltName: Full=Brain trypsinogen; AltName: Full=Mesotrypsinogen; AltName: Full=Serine protease 3; AltName: Full=Serine protease 4; AltName: Full=Trypsin III; AltName:	1.60E+06

Full=Trypsin III; AltName: Full=Trypsin IV; Flags: Precursor; [Homo sapiens (Human)] - [TRY3_HUMAN]		Full=Trypsin IV; Flags: Precursor; [Homo sapiens (Human)] - [TRY3_HUMAN]	
RecName: Full=Lysozyme C; EC=3.2.1.17; AltName: Full=1,4-beta-N-acetylmuramidase C; Flags: Precursor; [Homo sapiens (Human)] - [LYSC_HUMAN]	5.31E+08	Lysozyme C; EC=3.2.1.17; AltName: Full=1,4-beta-N-acetylmuramidase C; Flags: Precursor; [Homo sapiens (Human)] - [LYSC_HUMAN]	7.04E+05
Ig heavy chain V-III region CAM; [Homo sapiens (Human)] - [HV307_HUMAN]	1.68E+07	Ig heavy chain V-III region CAM OS=Homo sapiens PE=1 SV=1	
Delta-like protein 4; AltName: Full=Drosophila Delta homolog 4; Short=Delta4; Flags: Precursor; [Homo sapiens (Human)] - [DLL4_HUMAN]	4.85E+07	Delta-like protein 4; AltName: Full=Drosophila Delta homolog 4; Short=Delta4; Flags: Precursor; [Homo sapiens (Human)] - [DLL4_HUMAN]	1.12E+07

Table C.9: *Alveolar proteins identified by 1D PAGE and nano LC MS/MS in COPD smoker and COPD ex-smoker RTLFs. The 45 proteins common to both COPD smoker (n=5) and COPD ex-smoker (n=10) subjects investigated, alongside the mean of the three most abundant ion peaks of each respective protein identified. Accession numbers included according to entries in UniProtKB/Swiss-Prot*

COPD smoker		**COPD ex-smoker**	
Ig gamma-1 chain C region OS=Homo sapiens GN=IGHG1 PE=1 SV=1	5.79E+09	Ig gamma-1 chain C region OS=Homo sapiens GN=IGHG1 PE=1 SV=1	3.55E+09
Ig alpha-1 chain C region OS=Homo sapiens GN=IGHA1 PE=1 SV=2	1.56E+09	Ig alpha-1 chain C region OS=Homo sapiens GN=IGHA1 PE=1 SV=2	1.89E+07
Uteroglobin OS=Homo sapiens GN=SCGB1A1 PE=1 SV=1	1.99E+08	Uteroglobin OS=Homo sapiens GN=SCGB1A1 PE=1 SV=1	4.49E+09
Polymeric immunoglobulin receptor OS=Homo sapiens GN=PIGR PE=1 SV=4	2.83E+08	Polymeric immunoglobulin receptor OS=Homo sapiens GN=PIGR PE=1 SV=4	2.37E+09
Hemoglobin subunit beta OS=Homo sapiens GN=HBB PE=1 SV=2	7.32E+07	Hemoglobin subunit beta OS=Homo sapiens GN=HBB PE=1 SV=2	1.66E+09
Ig kappa chain C region OS=Homo sapiens GN=IGKC PE=1 SV=1	2.92E+09	Ig kappa chain C region OS=Homo sapiens GN=IGKC PE=1 SV=1	9.25E+09

Serotransferrin OS=Homo sapiens GN=TF PE=1 SV=3	4.56E+09	Serotransferrin OS=Homo sapiens GN=TF PE=1 SV=3	3.80E+07
Uncharacterized protein C3orf38; [Homo sapiens (Human)] - [CC038_HUMAN]	1.83E+09	RecName: Full=Uncharacterized protein C3orf38; [Homo sapiens (Human)] - [CC038_HUMAN]	5.97E+08
Beta-2-microglobulin OS=Homo sapiens GN=B2M PE=1 SV=1	3.80E+07	Beta-2-microglobulin OS=Homo sapiens GN=B2M PE=1 SV=1	5.86E+08
Serum albumin OS=Homo sapiens GN=ALB PE=1 SV=2	3.86E+09	Serum albumin OS=Homo sapiens GN=ALB PE=1 SV=2	5.49E+08
Hemoglobin subunit alpha OS=Homo sapiens GN=HBA1 PE=1 SV=2	8.29E+07	RecName: Full=Hemoglobin subunit alpha; AltName: Full=Alpha-globin; AltName: Full=Hemoglobin alpha chain; [Homo sapiens (Human)] - [HBA_HUMAN]	5.24E+08
Ig lambda chain V-III region LOI OS=Homo sapiens PE=1 SV=1	6.09E+07	RecName: Full=Ig lambda chain V-III region LOI; [Homo sapiens (Human)] - [LV302_HUMAN]	4.81E+08
Actin, cytoplasmic 1 OS=Homo sapiens GN=ACTB PE=1 SV=1	5.36E+07	Actin, cytoplasmic 1 OS=Homo sapiens GN=ACTB PE=1 SV=1	4.06E+08
Complement C3 OS=Homo sapiens GN=C3 PE=1 SV=2	7.33E+07	Complement C3 OS=Homo sapiens GN=C3 PE=1 SV=2	2.06E+08
Hemopexin OS=Homo sapiens GN=HPX PE=1 SV=2	3.48E+08	Hemopexin OS=Homo sapiens GN=HPX PE=1 SV=2	1.75E+08
Thioredoxin; Short=Trx; AltName: Full=ATL-derived factor; Short=ADF; AltName: Full=Surface-associated sulphydryl protein; Short=SASP; [Homo sapiens (Human)] - [THIO_HUMAN]	2.98E+07	RecName: Full=Thioredoxin; Short=Trx; AltName: Full=ATL-derived factor; Short=ADF; AltName: Full=Surface-associated sulphydryl protein; Short=SASP; [Homo sapiens (Human)] - [THIO_HUMAN]	1.54E+08
Ferritin light chain OS=Homo sapiens GN=FTL PE=1 SV=2	3.93E+08	Ferritin light chain OS=Homo sapiens GN=FTL PE=1 SV=2	1.51E+08
Annexin A5 OS=Homo sapiens GN=ANXA5 PE=1 SV=2	7.53E+07	RecName: Full=Annexin A5; AltName: Full=Anchorin CII; AltName: Full=Annexin V; AltName: Full=Annexin-5; AltName: Full=Calphobindin I; Short=CBP-I; AltName: Full=Endonexin II; AltName: Full=Lipocortin V; AltName: Full=Placental anticoagulant protein 4; Short=PP4; AltName: Full=Placental anticoagulant protein I; Short=PAP-I; AltName:	9.47E+07

		Full=Thromboplastin inhibitor; AltName: Full=Vascular anticoagulant-alpha; Short=VAC-alpha; [Homo sapiens (Human)] - [ANXA5_HUMAN]	
Transthyretin OS=Homo sapiens GN=TTR PE=1 SV=1	1.29E+08	Transthyretin OS=Homo sapiens GN=TTR PE=1 SV=1	7.84E+07
Peptidyl-prolyl cis-trans isomerase A OS=Homo sapiens GN=PPIA PE=1 SV=2	7.32E+06	RecName: Full=Peptidyl-prolyl cis-trans isomerase A; Short=PPIase A; EC=5.2.1.8; AltName: Full=Cyclophilin A; AltName: Full=Cyclosporin A-binding protein; AltName: Full=Rotamase A; [Homo sapiens (Human)] - [PPIA_HUMAN]	7.51E+07
Ig gamma-2 chain C region OS=Homo sapiens GN=IGHG2 PE=1 SV=2	4.65E+09	Ig gamma-2 chain C region OS=Homo sapiens GN=IGHG2 PE=1 SV=2	5.64E+07
Delta-like protein 4; AltName: Full=Drosophila Delta homolog 4; Short=Delta4; Flags: Precursor; [Homo sapiens (Human)] - [DLL4_HUMAN]	5.48E+07	Delta-like protein 4; AltName: Full=Drosophila Delta homolog 4; Short=Delta4; Flags: Precursor; [Homo sapiens (Human)] - [DLL4_HUMAN]	4.85E+07
CD44 antigen OS=Homo sapiens GN=CD44 PE=1 SV=3	3.49E+07	RecName: Full=CD44 antigen; AltName: Full=CDw44; AltName: Full=Epican; AltName: Full=Extracellular matrix receptor III; Short=ECMR-III; AltName: Full=GP90 lymphocyte homing/adhesion receptor; AltName: Full=HUTCH-I; AltName: Full=Heparan sulfate proteoglycan; AltName: Full=Hermes antigen; AltName: Full=Hyaluronate receptor; AltName: Full=Phagocytic glycoprotein 1; Short=PGP-1; AltName: Full=Phagocytic glycoprotein I; Short=PGP-I; AltName: CD_antigen=CD44; Flags: Precursor; [Homo sapiens (Human)] - [CD44_HUMAN]	3.87E+07
Alpha-1-antitrypsin OS=Homo sapiens GN=SERPINA1 PE=1 SV=3	1.61E+09	Alpha-1-antitrypsin OS=Homo sapiens GN=SERPINA1 PE=1 SV=3	3.86E+07
Ig lambda chain V-IV region Bau; [Homo sapiens (Human)]	5.41E+07	RecName: Full=Ig lambda chain V-IV region Bau; [Homo	3.27E+07

- [LV401_HUMAN]		sapiens (Human)] - [LV401_HUMAN]	
Protein Shroom3; AltName: Full=Shroom-related protein; Short=hShrmL; [Homo sapiens (Human)] - [SHRM3_HUMAN]	2.30E+08	Protein Shroom3; AltName: Full=Shroom-related protein; Short=hShrmL; [Homo sapiens (Human)] - [SHRM3_HUMAN]	2.29E+07
Ig heavy chain V-III region CAM OS=Homo sapiens PE=1 SV=1	9.16E+08	Ig heavy chain V-III region CAM; [Homo sapiens (Human)] - [HV307_HUMAN]	1.68E+07
Haptoglobin OS=Homo sapiens GN=HP PE=1 SV=1	2.64E+08	Haptoglobin OS=Homo sapiens GN=HP PE=1 SV=1	9.50E+06
Ig lambda-2 chain C regions OS=Homo sapiens GN=IGLC2 PE=1 SV=1	1.09E+09	Ig lambda-2 chain C regions OS=Homo sapiens GN=IGLC2 PE=1 SV=1	8.59E+06
Dermcidin; AltName: Full=Preproteolysin; Contains: RecName: Full=Survival-promoting peptide; Contains: RecName: Full=DCD-1; Flags: Precursor; [Homo sapiens (Human)] - [DCD_HUMAN]	2.94E+06	Dermcidin; AltName: Full=Preproteolysin; Contains: RecName: Full=Survival-promoting peptide; Contains: RecName: Full=DCD-1; Flags: Precursor; [Homo sapiens (Human)] - [DCD_HUMAN]	6.55E+06
Trypsin-3; EC=3.4.21.4; AltName: Full=Brain trypsinogen; AltName: Full=Mesotrypsinogen; AltName: Full=Serine protease 3; AltName: Full=Serine protease 4; AltName: Full=Trypsin III; AltName: Full=Trypsin IV; Flags: Precursor; [Homo sapiens (Human)] - [TRY3_HUMAN]	2.58E+06	RecName: Full=Trypsin-3; EC=3.4.21.4; AltName: Full=Brain trypsinogen; AltName: Full=Mesotrypsinogen; AltName: Full=Serine protease 3; AltName: Full=Serine protease 4; AltName: Full=Trypsin III; AltName: Full=Trypsin IV; Flags: Precursor; [Homo sapiens (Human)] - [TRY3_HUMAN]	4.78E+06
Desmoplakin OS=Homo sapiens GN=DSP PE=1 SV=3	1.06E+08	Desmoplakin OS=Homo sapiens GN=DSP PE=1 SV=3	3.75E+06
Alpha-1-acid glycoprotein 1 OS=Homo sapiens GN=ORM1 PE=1 SV=1	2.76E+08	Alpha-1-acid glycoprotein 1 OS=Homo sapiens GN=ORM1 PE=1 SV=1	2.88E+06
Ceruloplasmin OS=Homo sapiens GN=CP PE=1 SV=1	2.38E+08	Ceruloplasmin OS=Homo sapiens GN=CP PE=1 SV=1	2.73E+06
Ig kappa chain V-III region VG (Fragment) OS=Homo sapiens PE=1 SV=1	6.84E+07	Ig kappa chain V-III region VG (Fragment) OS=Homo sapiens PE=1 SV=1	2.65E+06

Alpha-1-acid glycoprotein 2; Short=AGP 2; AltName: Full=Orosomucoid-2; Short=OMD 2; Flags: Precursor; [Homo sapiens (Human)] - [A1AG2_HUMAN]	1.95E+08	Alpha-1-acid glycoprotein 2; Short=AGP 2; AltName: Full=Orosomucoid-2; Short=OMD 2; Flags: Precursor; [Homo sapiens (Human)] - [A1AG2_HUMAN]	1.95E+06
Transmembrane protein 200C; AltName: Full=Transmembrane protein TTMA; AltName: Full=Two transmembrane domain-containing family member A; [Homo sapiens (Human)] - [T200C_HUMAN]	1.94E+06	Transmembrane protein 200C; AltName: Full=Transmembrane protein TTMA; AltName: Full=Two transmembrane domain-containing family member A; [Homo sapiens (Human)] - [T200C_HUMAN]	1.89E+06
Ig kappa chain V-III region SIE OS=Homo sapiens PE=1 SV=1	2.67E+08	Ig kappa chain V-III region SIE; [Homo sapiens (Human)] - [KV302_HUMAN]	1.85E+06
Pulmonary surfactant-associated protein A2 OS=Homo sapiens GN=SFTPA2 PE=1 SV=1	2.89E+07	Pulmonary surfactant-associated protein A2; Short=PSP-A; Short=PSPA; Short=SP-A; Short=SP-A2; AltName: Full=35 kDa pulmonary surfactant-associated protein; AltName: Full=Alveolar proteinosis protein; AltName: Full=Collectin-5; Flags: Precursor; [Homo sapiens (Human)] - [SFPA2_HUMAN]	1.85E+06
Arginase-1; EC=3.5.3.1; AltName: Full=Liver-type arginase; AltName: Full=Type I arginase; [Homo sapiens (Human)] - [ARGI1_HUMAN]	1.90E+07	Arginase-1; EC=3.5.3.1; AltName: Full=Liver-type arginase; AltName: Full=Type I arginase; [Homo sapiens (Human)] - [ARGI1_HUMAN]	1.75E+06
Myotubularin-related protein 14; EC=3.1.3.-; AltName: Full=HCV NS5A-transactivated protein 4 splice variant A-binding protein 1; Short=NS5ATP4ABP1; AltName: Full=hJumpy; [Homo sapiens (Human)] - [MTMRE_HUMAN]	3.66E+06	Myotubularin-related protein 14; EC=3.1.3.-; AltName: Full=HCV NS5A-transactivated protein 4 splice variant A-binding protein 1; Short=NS5ATP4ABP1; AltName: Full=hJumpy; [Homo sapiens (Human)] - [MTMRE_HUMAN]	1.21E+06
Transcriptional adapter 2-beta; AltName: Full=ADA2-like protein beta; Short=ADA2-beta; [Homo sapiens (Human)] - [TAD2B_HUMAN]	2.68E+07	Transcriptional adapter 2-beta; AltName: Full=ADA2-like protein beta; Short=ADA2-beta; [Homo sapiens (Human)] - [TAD2B_HUMAN]	1.11E+06

Leucine-rich alpha-2-glycoprotein OS=Homo sapiens GN=LRG1 PE=1 SV=2	3.29E+07	Leucine-rich alpha-2-glycoprotein OS=Homo sapiens GN=LRG1 PE=1 SV=2	7.23E+05
Putative annexin A2-like protein; AltName: Full=Annexin A2 pseudogene 2; AltName: Full=Lipocortin II pseudogene; [Homo sapiens (Human)] - [AXA2L_HUMAN]	2.21E+07	Putative annexin A2-like protein; AltName: Full=Annexin A2 pseudogene 2; AltName: Full=Lipocortin II pseudogene; [Homo sapiens (Human)] - [AXA2L_HUMAN]	2.60E+07
Protein kinase-like protein SgK196; AltName: Full=Sugen kinase 196; [Homo sapiens (Human)] - [SG196_HUMAN]	1.67E+07	Protein kinase-like protein SgK196; AltName: Full=Sugen kinase 196; [Homo sapiens (Human)] - [SG196_HUMAN]	1.36E+07

Table C.10: *Alveolar proteins identified by 1D PAGE and nano LC MS/MS in Healthy smoker and Healthy aged RTLFs. The 105 proteins common to both healthy smoker (n=5) and Healthy aged (n=5) subjects investigated, alongside the mean of the three most abundant ion peaks of each respective protein identified. Accession numbers included according to entries in UniProtKB/Swiss-Prot*

Healthy Smoker		**Healthy Aged Control**	
14-3-3 protein beta/alpha OS=Homo sapiens GN=YWHAB PE=1 SV=3	6.47E+07	14-3-3 protein beta/alpha OS=Homo sapiens GN=YWHAB PE=1 SV=3	1.46E+07
14-3-3 protein zeta/delta OS=Homo sapiens GN=YWHAZ PE=1 SV=1	4.51E+07	14-3-3 protein zeta/delta OS=Homo sapiens GN=YWHAZ PE=1 SV=1	1.57E+07
Actin, cytoplasmic 1 OS=Homo sapiens GN=ACTB PE=1 SV=1	1.38E+08	Actin, cytoplasmic 1 OS=Homo sapiens GN=ACTB PE=1 SV=1	6.89E+07
Afamin OS=Homo sapiens GN=AFM PE=1 SV=1	5.45E+06	Afamin OS=Homo sapiens GN=AFM PE=1 SV=1	2.54E+07
Alpha-1-acid glycoprotein 1 OS=Homo sapiens GN=ORM1 PE=1 SV=1	1.29E+08	Alpha-1-acid glycoprotein 1 OS=Homo sapiens GN=ORM1 PE=1 SV=1	3.39E+08
Alpha-1-acid glycoprotein 2; Short=AGP 2; AltName: Full=Orosomucoid-2; Short=OMD 2; Flags: Precursor; [Homo sapiens (Human)] - [A1AG2_HUMAN]	1.14E+08	Alpha-1-acid glycoprotein 2 OS=Homo sapiens GN=ORM2 PE=1 SV=2	2.40E+08
Alpha-1-antichymotrypsin OS=Homo sapiens GN=SERPINA3 PE=1 SV=2	3.72E+07	Alpha-1-antichymotrypsin OS=Homo sapiens GN=SERPINA3 PE=1 SV=2	8.21E+07
Alpha-1-antitrypsin OS=Homo sapiens GN=SERPINA1 PE=1 SV=3	2.75E+08	Alpha-1-antitrypsin OS=Homo sapiens GN=SERPINA1 PE=1 SV=3	3.20E+09

Alpha-1B-glycoprotein OS=Homo sapiens GN=A1BG PE=1 SV=4	2.29E+07	Alpha-1B-glycoprotein OS=Homo sapiens GN=A1BG PE=1 SV=4	1.33E+08
Alpha-2-HS-glycoprotein OS=Homo sapiens GN=AHSG PE=1 SV=1	2.99E+07	Alpha-2-HS-glycoprotein OS=Homo sapiens GN=AHSG PE=1 SV=1	1.16E+08
Alpha-2-macroglobulin OS=Homo sapiens GN=A2M PE=1 SV=3	4.14E+06	Alpha-2-macroglobulin OS=Homo sapiens GN=A2M PE=1 SV=3	1.66E+08
Alpha-enolase OS=Homo sapiens GN=ENO1 PE=1 SV=2	3.19E+07	Alpha-enolase OS=Homo sapiens GN=ENO1 PE=1 SV=2	4.14E+06
Angiotensinogen OS=Homo sapiens GN=AGT PE=1 SV=1	1.41E+06	Angiotensinogen OS=Homo sapiens GN=AGT PE=1 SV=1	4.94E+07
Annexin A5 OS=Homo sapiens GN=ANXA5 PE=1 SV=2	5.18E+07	Annexin A5 OS=Homo sapiens GN=ANXA5 PE=1 SV=2	1.36E+06
Apolipoprotein A-I OS=Homo sapiens GN=APOA1 PE=1 SV=1	7.56E+06	Apolipoprotein A-I OS=Homo sapiens GN=APOA1 PE=1 SV=1	1.38E+08
Attractin OS=Homo sapiens GN=ATRN PE=1 SV=2	4.53E+06	Attractin OS=Homo sapiens GN=ATRN PE=1 SV=2	5.23E+06
Beta-2-microglobulin OS=Homo sapiens GN=B2M PE=1 SV=1	1.03E+07	Beta-2-microglobulin OS=Homo sapiens GN=B2M PE=1 SV=1	2.59E+07
C2 calcium-dependent domain-containing protein 4B; AltName: Full=Nuclear-localized factor 2; AltName: Full=Protein FAM148B; [Homo sapiens (Human)] - [C2C4B_HUMAN]	7.49E+06	C2 calcium-dependent domain-containing protein 4B; AltName: Full=Nuclear-localized factor 2; AltName: Full=Protein FAM148B; [Homo sapiens (Human)] - [C2C4B_HUMAN]	8.25E+07
Calmodulin OS=Homo sapiens GN=CALM1 PE=1 SV=2	2.84E+06	Calmodulin OS=Homo sapiens GN=CALM1 PE=1 SV=2	2.68E+06
CD166 antigen; AltName: Full=Activated leukocyte cell adhesion molecule; AltName: CD_antigen=CD166; Flags: Precursor; [Homo sapiens (Human)] - [CD166_HUMAN]	2.77E+06	CD166 antigen; AltName: Full=Activated leukocyte cell adhesion molecule; AltName: CD_antigen=CD166; Flags: Precursor; [Homo sapiens (Human)] - [CD166_HUMAN]	1.35E+07
CD44 antigen OS=Homo sapiens GN=CD44 PE=1 SV=3	3.34E+07	CD44 antigen OS=Homo sapiens GN=CD44 PE=1 SV=3	2.73E+07
Ceruloplasmin OS=Homo sapiens GN=CP PE=1 SV=1	1.15E+08	Ceruloplasmin OS=Homo sapiens GN=CP PE=1 SV=1	3.67E+08
Coactosin-like protein OS=Homo sapiens GN=COTL1 PE=1 SV=3	6.78E+06	Coactosin-like protein OS=Homo sapiens GN=COTL1 PE=1 SV=3	5.15E+06
Corticosteroid-binding globulin OS=Homo sapiens GN=SERPINA6 PE=1 SV=1	5.20E+06	Corticosteroid-binding globulin OS=Homo sapiens GN=SERPINA6 PE=1 SV=1	3.95E+07
Deleted in malignant brain	6.18E+06	Deleted in malignant brain	3.69E+07

tumors 1 protein OS=Homo sapiens GN=DMBT1 PE=1 SV=2		tumors 1 protein OS=Homo sapiens GN=DMBT1 PE=1 SV=2	
Delta-like protein 4; AltName: Full=Drosophila Delta homolog 4; Short=Delta4; Flags: Precursor; [Homo sapiens (Human)] - [DLL4_HUMAN]	1.12E+07	Delta-like protein 4; AltName: Full=Drosophila Delta homolog 4; Short=Delta4; Flags: Precursor; [Homo sapiens (Human)] - [DLL4_HUMAN]	1.23E+07
Dermcidin OS=Homo sapiens GN=DCD PE=1 SV=2	4.35E+06	Dermcidin OS=Homo sapiens GN=DCD PE=1 SV=2	2.13E+06
Desmoplakin OS=Homo sapiens GN=DSP PE=1 SV=3	9.94E+07	Desmoplakin OS=Homo sapiens GN=DSP PE=1 SV=3	1.40E+08
Dipeptidyl peptidase 4 OS=Homo sapiens GN=DPP4 PE=1 SV=2	3.08E+06	Dipeptidyl peptidase 4 OS=Homo sapiens GN=DPP4 PE=1 SV=2	6.17E+07
Ecto-ADP-ribosyltransferase 4; EC=2.4.2.31; AltName: Full=Dombrock blood group carrier molecule; AltName: Full=Mono(ADP-ribosyl)transferase 4; AltName: Full=NAD(P)(+)--arginine ADP-ribosyltransferase 4; AltName: CD_antigen=CD297; Flags: Precursor; [Homo sapiens (Human)] - [NAR4_HUMAN]	2.69E+07	Ecto-ADP-ribosyltransferase 4; EC=2.4.2.31; AltName: Full=Dombrock blood group carrier molecule; AltName: Full=Mono(ADP-ribosyl)transferase 4; AltName: Full=NAD(P)(+)--arginine ADP-ribosyltransferase 4; AltName: CD_antigen=CD297; Flags: Precursor; [Homo sapiens (Human)] - [NAR4_HUMAN]	5.81E+07
Elongation factor 1-alpha 1 OS=Homo sapiens GN=EEF1A1 PE=1 SV=1		Elongation factor 1-alpha 1 OS=Homo sapiens GN=EEF1A1 PE=1 SV=1	2.16E+07
Epididymal secretory protein E1 OS=Homo sapiens GN=NPC2 PE=1 SV=1	1.32E+07	Epididymal secretory protein E1 OS=Homo sapiens GN=NPC2 PE=1 SV=1	1.37E+07
FAS-associated factor 1; Short=hFAF1; AltName: Full=UBX domain-containing protein 12; AltName: Full=UBX domain-containing protein 3A; [Homo sapiens (Human)] - [FAF1_HUMAN]	4.56E+07	FAS-associated factor 1; Short=hFAF1; AltName: Full=UBX domain-containing protein 12; AltName: Full=UBX domain-containing protein 3A; [Homo sapiens (Human)] - [FAF1_HUMAN]	4.89E+08
Ferritin heavy chain OS=Homo sapiens GN=FTH1 PE=1 SV=2	5.09E+06	Ferritin heavy chain; Short=Ferritin H subunit; EC=1.16.3.1; AltName: Full=Cell proliferation-inducing gene 15 protein; [Homo sapiens (Human)] - [FRIH_HUMAN]	2.34E+06
Ferritin light chain OS=Homo sapiens GN=FTL PE=1 SV=2	2.03E+07	Ferritin light chain; Short=Ferritin L subunit; [Homo sapiens (Human)] - [FRIL_HUMAN]	4.73E+06

Glutathione S-transferase P OS=Homo sapiens GN=GSTP1 PE=1 SV=2	1.82E+07	Glutathione S-transferase P OS=Homo sapiens GN=GSTP1 PE=1 SV=2	8.51E+06
Haptoglobin OS=Homo sapiens GN=HP PE=1 SV=1	1.04E+08	Haptoglobin OS=Homo sapiens GN=HP PE=1 SV=1	1.26E+08
Heat shock protein beta-1 OS=Homo sapiens GN=HSPB1 PE=1 SV=2	4.31E+07	Heat shock protein beta-1 OS=Homo sapiens GN=HSPB1 PE=1 SV=2	8.93E+06
Hemoglobin subunit alpha OS=Homo sapiens GN=HBA1 PE=1 SV=2	5.40E+07	Hemoglobin subunit alpha OS=Homo sapiens GN=HBA1 PE=1 SV=2	1.49E+08
Hemoglobin subunit beta OS=Homo sapiens GN=HBB PE=1 SV=2	2.04E+07	Hemoglobin subunit beta OS=Homo sapiens GN=HBB PE=1 SV=2	1.28E+08
Hemopexin OS=Homo sapiens GN=HPX PE=1 SV=2	1.89E+08	Hemopexin OS=Homo sapiens GN=HPX PE=1 SV=2	2.71E+08
Histone H3.3C; [Homo sapiens (Human)] - [H3C_HUMAN]	1.36E+07	Histone H3.3C; [Homo sapiens (Human)] - [H3C_HUMAN]	1.79E+07
Histone H4 OS=Homo sapiens GN=HIST1H4A PE=1 SV=2	2.72E+07	Histone H4 OS=Homo sapiens GN=HIST1H4A PE=1 SV=2	2.45E+07
Ig alpha-1 chain C region OS=Homo sapiens GN=IGHA1 PE=1 SV=2	6.14E+08	Ig alpha-1 chain C region OS=Homo sapiens GN=IGHA1 PE=1 SV=2	2.42E+09
Ig gamma-1 chain C region OS=Homo sapiens GN=IGHG1 PE=1 SV=1	3.30E+09	Ig gamma-1 chain C region OS=Homo sapiens GN=IGHG1 PE=1 SV=1	8.92E+09
Ig gamma-2 chain C region OS=Homo sapiens GN=IGHG2 PE=1 SV=2	2.57E+09	Ig gamma-2 chain C region OS=Homo sapiens GN=IGHG2 PE=1 SV=2	5.60E+09
Ig gamma-3 chain C region OS=Homo sapiens GN=IGHG3 PE=1 SV=2	2.87E+09	Ig gamma-3 chain C region OS=Homo sapiens GN=IGHG3 PE=1 SV=2	6.71E+09
Ig gamma-4 chain C region OS=Homo sapiens GN=IGHG4 PE=1 SV=1	2.57E+09	Ig gamma-4 chain C region OS=Homo sapiens GN=IGHG4 PE=1 SV=1	5.60E+09
Ig heavy chain V-II region NEWM OS=Homo sapiens PE=1 SV=1	9.45E+07	Ig heavy chain V-II region NEWM OS=Homo sapiens PE=1 SV=1	1.47E+08
Ig heavy chain V-III region BRO; [Homo sapiens (Human)] - [HV305_HUMAN]	5.36E+08	Ig heavy chain V-III region BRO; [Homo sapiens (Human)] - [HV305_HUMAN]	1.02E+09
Ig heavy chain V-III region BUT; [Homo sapiens (Human)] - [HV306_HUMAN]	4.98E+08	Ig heavy chain V-III region BUT; [Homo sapiens (Human)] - [HV306_HUMAN]	1.03E+09
Ig heavy chain V-III region CAM OS=Homo sapiens PE=1 SV=1		Ig heavy chain V-III region CAM OS=Homo sapiens PE=1 SV=1	1.05E+09
Ig heavy chain V-III region GAL OS=Homo sapiens PE=1 SV=1	4.92E+08	Ig heavy chain V-III region GAL OS=Homo sapiens PE=1 SV=1	1.05E+09

Ig heavy chain V-III region GAR; [Homo sapiens (Human)] - [HV322_HUMAN]	8.76E+07	Ig heavy chain V-III region GAR; [Homo sapiens (Human)] - [HV322_HUMAN]	1.05E+08
Ig heavy chain V-III region HIL; [Homo sapiens (Human)] - [HV310_HUMAN]	7.00E+08	Ig heavy chain V-III region HIL; [Homo sapiens (Human)] - [HV310_HUMAN]	1.47E+09
Ig kappa chain C region OS=Homo sapiens GN=IGKC PE=1 SV=1	1.07E+09	Ig kappa chain C region OS=Homo sapiens GN=IGKC PE=1 SV=1	3.47E+09
Ig kappa chain V-I region DEE; [Homo sapiens (Human)] - [KV105_HUMAN]	1.54E+08	Ig kappa chain V-I region DEE; [Homo sapiens (Human)] - [KV105_HUMAN]	2.73E+08
Ig kappa chain V-I region EU OS=Homo sapiens PE=1 SV=1	7.39E+07	Ig kappa chain V-I region EU OS=Homo sapiens PE=1 SV=1	2.41E+08
Ig kappa chain V-II region RPMI 6410 OS=Homo sapiens PE=4 SV=1	4.64E+07	Ig kappa chain V-II region RPMI 6410 OS=Homo sapiens PE=4 SV=1	1.62E+08
Ig kappa chain V-III region POM; [Homo sapiens (Human)] - [KV306_HUMAN]	7.29E+07	Ig kappa chain V-III region POM OS=Homo sapiens PE=1 SV=1	9.77E+07
Ig kappa chain V-III region SIE OS=Homo sapiens PE=1 SV=1	1.24E+08	Ig kappa chain V-III region SIE OS=Homo sapiens PE=1 SV=1	2.40E+08
Ig kappa chain V-III region VG (Fragment) OS=Homo sapiens PE=1 SV=1	5.54E+07	Ig kappa chain V-III region VG; Flags: Precursor; Fragment; [Homo sapiens (Human)] - [KV309_HUMAN]	1.46E+08
Ig kappa chain V-IV region JI; Flags: Precursor; [Homo sapiens (Human)] - [KV403_HUMAN]	6.10E+07	Ig kappa chain V-IV region JI OS=Homo sapiens PE=4 SV=1	3.74E+07
Ig kappa chain V-IV region Len; [Homo sapiens (Human)] - [KV402_HUMAN]	6.10E+07	Ig kappa chain V-IV region Len OS=Homo sapiens PE=1 SV=2	9.86E+07
Ig lambda chain V region 4A; Flags: Precursor; [Homo sapiens (Human)] - [LV001_HUMAN]	1.78E+07	Ig lambda chain V region 4A OS=Homo sapiens PE=4 SV=1	5.01E+07
Ig lambda chain V-I region HA; [Homo sapiens (Human)] - [LV102_HUMAN]	5.73E+07	Ig lambda chain V-I region HA OS=Homo sapiens PE=1 SV=1	1.91E+08
Ig lambda chain V-III region LOI OS=Homo sapiens PE=1 SV=1	6.55E+07	Ig lambda chain V-III region LOI OS=Homo sapiens PE=1 SV=1	1.57E+08
Ig lambda chain V-III region SH OS=Homo sapiens PE=1 SV=1	1.01E+07	Ig lambda chain V-III region SH; [Homo sapiens (Human)] - [LV301_HUMAN]	3.09E+07
Ig lambda chain V-IV region Bau; [Homo sapiens (Human)]	1.05E+07	Ig lambda chain V-IV region Bau; [Homo sapiens (Human)]	1.58E+08

- [LV401_HUMAN]		- [LV401_HUMAN]	
Ig lambda-2 chain C regions OS=Homo sapiens GN=IGLC2 PE=1 SV=1	7.91E+08	Ig lambda-2 chain C regions OS=Homo sapiens GN=IGLC2 PE=1 SV=1	2.31E+09
Ig mu chain C region OS=Homo sapiens GN=IGHM PE=1 SV=3	4.18E+07	Ig mu chain C region OS=Homo sapiens GN=IGHM PE=1 SV=3	4.16E+07
Immunoglobulin lambda-like polypeptide 5 OS=Homo sapiens GN=IGLL5 PE=2 SV=2	4.43E+08	Immunoglobulin lambda-like polypeptide 5 OS=Homo sapiens GN=IGLL5 PE=2 SV=2	1.44E+09
Intercellular adhesion molecule 1 OS=Homo sapiens GN=ICAM1 PE=1 SV=2	4.60E+06	Intercellular adhesion molecule 1 OS=Homo sapiens GN=ICAM1 PE=1 SV=2	1.15E+07
Leucine-rich alpha-2-glycoprotein OS=Homo sapiens GN=LRG1 PE=1 SV=2	1.76E+07	Leucine-rich alpha-2-glycoprotein OS=Homo sapiens GN=LRG1 PE=1 SV=2	4.46E+07
Lysozyme C; EC=3.2.1.17; AltName: Full=1,4-beta-N-acetylmuramidase C; Flags: Precursor; [Homo sapiens (Human)] - [LYSC_HUMAN]	7.04E+05	Lysozyme C; EC=3.2.1.17; AltName: Full=1,4-beta-N-acetylmuramidase C; Flags: Precursor; [Homo sapiens (Human)] - [LYSC_HUMAN]	1.48E+06
Polymeric immunoglobulin receptor OS=Homo sapiens GN=PIGR PE=1 SV=4	1.54E+08	Polymeric immunoglobulin receptor OS=Homo sapiens GN=PIGR PE=1 SV=4	1.94E+08
Pro-cathepsin H OS=Homo sapiens GN=CTSH PE=1 SV=4	1.14E+07	Pro-cathepsin H OS=Homo sapiens GN=CTSH PE=1 SV=4	1.06E+07
Proactivator polypeptide; Contains: RecName: Full=Saposin-A; AltName: Full=Protein A; Contains: RecName: Full=Saposin-B-Val; Contains: RecName: Full=Saposin-B; AltName: Full=Cerebroside sulfate activator; Short=CSAct; AltName: Full=Dispersin; AltName: Full=Sphingolipid activator protein 1; Short=SAP-1; AltName: Full=Sulfatide/GM1 activator; Contains: RecName: Full=Saposin-C; AltName: Full=A1 activator; AltName: Full=Co-beta-glucosidase; AltName: Full=Glucosylceramidase activator; AltName: Full=Sphingolipid activator protein 2; Short=SAP-2;	1.35E+06	Proactivator polypeptide OS=Homo sapiens GN=PSAP PE=1 SV=2	2.71E+06

Contains: RecName: Full=Saposin-D; AltName: Full=Component C; AltName: Full=Protein C; Flags: Precursor; [Homo sapiens (Human)] - [SAP_HUMAN]			
Prostasin; EC=3.4.21.-; AltName: Full=Serine protease 8; Contains: RecName: Full=Prostasin light chain; Contains: RecName: Full=Prostasin heavy chain; Flags: Precursor; [Homo sapiens (Human)] - [PRSS8_HUMAN]	1.62E+06	Prostasin; EC=3.4.21.-; AltName: Full=Serine protease 8; Contains: RecName: Full=Prostasin light chain; Contains: RecName: Full=Prostasin heavy chain; Flags: Precursor; [Homo sapiens (Human)] - [PRSS8_HUMAN]	1.22E+06
Protein DJ-1 OS=Homo sapiens GN=PARK7 PE=1 SV=2	7.89E+06	Protein DJ-1 OS=Homo sapiens GN=PARK7 PE=1 SV=2	1.23E+07
Protein S100-A6 OS=Homo sapiens GN=S100A6 PE=1 SV=1	4.87E+07	Protein S100-A6 OS=Homo sapiens GN=S100A6 PE=1 SV=1	2.38E+07
Protein S100-A8 OS=Homo sapiens GN=S100A8 PE=1 SV=1	8.57E+08	Protein S100-A8 OS=Homo sapiens GN=S100A8 PE=1 SV=1	3.59E+07
Protein S100-A9 OS=Homo sapiens GN=S100A9 PE=1 SV=1	5.29E+08	Protein S100-A9 OS=Homo sapiens GN=S100A9 PE=1 SV=1	1.13E+07
Protein Shroom3; AltName: Full=Shroom-related protein; Short=hShrmL; [Homo sapiens (Human)] - [SHRM3_HUMAN]	8.20E+07	Protein Shroom3; AltName: Full=Shroom-related protein; Short=hShrmL; [Homo sapiens (Human)] - [SHRM3_HUMAN]	9.47E+07
Pulmonary surfactant-associated protein A2 OS=Homo sapiens GN=SFTPA2 PE=1 SV=1	2.82E+07	Pulmonary surfactant-associated protein A2 OS=Homo sapiens GN=SFTPA2 PE=1 SV=1	3.74E+07
Pulmonary surfactant-associated protein B OS=Homo sapiens GN=SFTPB PE=1 SV=3		Pulmonary surfactant-associated protein B; Short=SP-B; AltName: Full=18 kDa pulmonary-surfactant protein; AltName: Full=6 kDa protein; AltName: Full=Pulmonary surfactant-associated proteolipid SPL(Phe); Flags: Precursor; [Homo sapiens (Human)] - [PSPB_HUMAN]	3.26E+06
Pulmonary surfactant-associated protein D; Short=PSP-D; Short=SP-D; AltName: Full=Collectin-7; AltName: Full=Lung surfactant	5.11E+06	Pulmonary surfactant-associated protein D OS=Homo sapiens GN=SFTPD PE=1 SV=3	1.53E+07

protein D; Flags: Precursor; [Homo sapiens (Human)] - [SFTPD_HUMAN]			
Putative V-set and immunoglobulin domain-containing protein 6 OS=Homo sapiens GN=VSIG6 PE=5 SV=2	8.23E+07	Putative V-set and immunoglobulin domain-containing protein 6 OS=Homo sapiens GN=VSIG6 PE=5 SV=2	2.00E+08
Selenium-binding protein 1 OS=Homo sapiens GN=SELENBP1 PE=1 SV=2	1.15E+07	Selenium-binding protein 1 OS=Homo sapiens GN=SELENBP1 PE=1 SV=2	1.67E+07
Serotransferrin OS=Homo sapiens GN=TF PE=1 SV=3	3.42E+09	Serotransferrin OS=Homo sapiens GN=TF PE=1 SV=3	7.62E+09
Serum albumin OS=Homo sapiens GN=ALB PE=1 SV=2	1.54E+09	Serum albumin OS=Homo sapiens GN=ALB PE=1 SV=2	2.77E+09
SH3 domain-binding glutamic acid-rich-like protein 3; AltName: Full=SH3 domain-binding protein 1; Short=SH3BP-1; [Homo sapiens (Human)] - [SH3L3_HUMAN]	7.49E+06	SH3 domain-binding glutamic acid-rich-like protein 3; AltName: Full=SH3 domain-binding protein 1; Short=SH3BP-1; [Homo sapiens (Human)] - [SH3L3_HUMAN]	3.66E+06
Sorting nexin-6; AltName: Full=TRAF4-associated factor 2; [Homo sapiens (Human)] - [SNX6_HUMAN]	2.48E+06	Sorting nexin-6; AltName: Full=TRAF4-associated factor 2; [Homo sapiens (Human)] - [SNX6_HUMAN]	2.15E+06
Thioredoxin; Short=Trx; AltName: Full=ATL-derived factor; Short=ADF; AltName: Full=Surface-associated sulphydryl protein; Short=SASP; [Homo sapiens (Human)] - [THIO_HUMAN]	1.29E+07	Thioredoxin; Short=Trx; AltName: Full=ATL-derived factor; Short=ADF; AltName: Full=Surface-associated sulphydryl protein; Short=SASP; [Homo sapiens (Human)] - [THIO_HUMAN]	8.21E+06
Transaldolase OS=Homo sapiens GN=TALDO1 PE=1 SV=2	2.21E+07	Transaldolase OS=Homo sapiens GN=TALDO1 PE=1 SV=2	4.47E+07
Transcriptional adapter 2-beta; AltName: Full=ADA2-like protein beta; Short=ADA2-beta; [Homo sapiens (Human)] - [TAD2B_HUMAN]	5.10E+07	Transcriptional adapter 2-beta; AltName: Full=ADA2-like protein beta; Short=ADA2-beta; [Homo sapiens (Human)] - [TAD2B_HUMAN]	2.22E+07
Transmembrane protein 198; [Homo sapiens (Human)] - [TM198_HUMAN]	2.08E+07	Transmembrane protein 198; [Homo sapiens (Human)] - [TM198_HUMAN]	2.62E+07
Transmembrane protein 200C; AltName: Full=Transmembrane protein TTMA; AltName: Full=Two transmembrane domain-containing family member A; [Homo sapiens (Human)] - [T200C_HUMAN]	2.06E+06	Transmembrane protein 200C; AltName: Full=Transmembrane protein TTMA; AltName: Full=Two transmembrane domain-containing family member A; [Homo sapiens (Human)] - [T200C_HUMAN]	3.59E+06

Transthyretin OS=Homo sapiens GN=TTR PE=1 SV=1	4.44E+07	Transthyretin OS=Homo sapiens GN=TTR PE=1 SV=1	2.53E+08
Triosephosphate isomerase OS=Homo sapiens GN=TPI1 PE=1 SV=3	1.81E+07	Triosephosphate isomerase OS=Homo sapiens GN=TPI1 PE=1 SV=3	4.37E+07
Uncharacterized protein C3orf38; [Homo sapiens (Human)] - [CC038_HUMAN]	1.62E+09	Uncharacterized protein C3orf38; [Homo sapiens (Human)] - [CC038_HUMAN]	2.73E+09
Uteroglobin OS=Homo sapiens GN=SCGB1A1 PE=1 SV=1	8.73E+07	Uteroglobin OS=Homo sapiens GN=SCGB1A1 PE=1 SV=1	1.74E+08
Vitamin D-binding protein OS=Homo sapiens GN=GC PE=1 SV=1	1.16E+08	Vitamin D-binding protein OS=Homo sapiens GN=GC PE=1 SV=1	4.91E+08
Xin actin-binding repeat-containing protein 2 OS=Homo sapiens GN=XIRP2 PE=1 SV=2	1.77E+08	Xin actin-binding repeat-containing protein 2 OS=Homo sapiens GN=XIRP2 PE=1 SV=2	2.05E+08
Zinc-alpha-2-glycoprotein OS=Homo sapiens GN=AZGP1 PE=1 SV=2	5.33E+07	Zinc-alpha-2-glycoprotein OS=Homo sapiens GN=AZGP1 PE=1 SV=2	1.24E+08

Table. C.11: *The 32 common alveolar proteins identified by 1D PAGE and nano LC MS/MS in Healthy Aged, Healthy Smoker, COPD smoker, smoker and COPD ex-smoking RTLFs. The 32 proteins common across all groups are listed for Healthy Aged (n=5) , Healthy Smoker (n=5), COPD smoker (n=5), smoker and COPD ex-smoker (n=10), subjects investigated, alongside the mean of the three most abundant ion peaks of each respective protein identified. Accession numbers included according to entries in UniProtKB/Swiss-Prot*

Healthy Aged Control		**Healthy Smoker**		**COPD smoker**		**COPD ex-smoker**	
Actin, cytoplasmic 1 OS=Homo sapiens GN=ACTB PE=1 SV=1	6.89E+07	Actin, cytoplasmic 1 OS=Homo sapiens GN=ACTB PE=1 SV=1	1.38E+08	Actin, cytoplasmic 1 OS=Homo sapiens GN=ACTB PE=1 SV=1	5.36E+07	Actin, cytoplasmic 1 OS=Homo sapiens GN=ACTB PE=1 SV=1	4.06E+08
Alpha-1-acid glycoprotein 1 OS=Homo sapiens GN=ORM1 PE=1 SV=1	3.39E+08	Alpha-1-acid glycoprotein 1 OS=Homo sapiens GN=ORM1 PE=1 SV=1	1.29E+08	Alpha-1-acid glycoprotein 1 OS=Homo sapiens GN=ORM1 PE=1 SV=1	2.76E+08	Alpha-1-acid glycoprotein 1 OS=Homo sapiens GN=ORM1 PE=1 SV=1	2.88E+06
Alpha-1-acid glycoprotein 2 OS=Homo sapiens GN=ORM2 PE=1 SV=2	2.40E+08	Alpha-1-acid glycoprotein 2; Short=AGP 2; AltName: Full=Orosomucoid-2; Short=OMD 2; Flags:	1.14E+08	Alpha-1-acid glycoprotein 2; Short=AGP 2; AltName: Full=Orosomucoid-2; Short=OMD 2; Flags:	1.95E+08	Alpha-1-acid glycoprotein 2; Short=AGP 2; AltName: Full=Orosomucoid-2; Short=OMD 2; Flags:	1.95E+06

		Precursor; [Homo sapiens (Human)] - [A1AG2_HUMAN]		Precursor; [Homo sapiens (Human)] - [A1AG2_HUMAN]		Precursor; [Homo sapiens (Human)] - [A1AG2_HUMAN]	
Alpha-1-antitrypsin OS=Homo sapiens GN=SERPINA1 PE=1 SV=3	3.20E+09	Alpha-1-antitrypsin OS=Homo sapiens GN=SERPINA1 PE=1 SV=3	2.75E+08	Alpha-1-antitrypsin OS=Homo sapiens GN=SERPINA1 PE=1 SV=3	1.61E+09	Alpha-1-antitrypsin OS=Homo sapiens GN=SERPINA1 PE=1 SV=3	3.86E+07
Alpha-1B-glycoprotein OS=Homo sapiens GN=A1BG PE=1 SV=4	1.33E+08	Alpha-1B-glycoprotein OS=Homo sapiens GN=A1BG PE=1 SV=4	2.29E+07	Alpha-1B-glycoprotein OS=Homo sapiens GN=A1BG PE=1 SV=4	3.51E+07	Alpha-1B-glycoprotein; AltName: Full=Alpha-1-B glycoprotein; Flags: Precursor; [Homo sapiens (Human)] - [A1BG_HUMAN]	1.24E+06
Annexin A5 OS=Homo sapiens GN=ANXA5 PE=1 SV=2	1.36E+06	Annexin A5 OS=Homo sapiens GN=ANXA5 PE=1 SV=2	5.18E+07	Annexin A5 OS=Homo sapiens GN=ANXA5 PE=1 SV=2	7.53E+07	Annexin A5 OS=Homo sapiens GN=ANXA5 PE=1 SV=2	9.47E+07
Beta-2-microglobulin OS=Homo sapiens GN=B2M PE=1 SV=1	2.59E+07	Beta-2-microglobulin OS=Homo sapiens GN=B2M PE=1 SV=1	1.03E+07	Beta-2-microglobulin OS=Homo sapiens GN=B2M PE=1 SV=1	3.80E+07	Beta-2-microglobulin OS=Homo sapiens GN=B2M PE=1 SV=1	5.86E+08
CD44 antigen OS=Homo sapiens GN=CD44 PE=1 SV=3	2.73E+07	CD44 antigen OS=Homo sapiens GN=CD44 PE=1 SV=3	3.34E+07	CD44 antigen OS=Homo sapiens GN=CD44 PE=1 SV=3	3.49E+07	CD44 antigen OS=Homo sapiens GN=CD44 PE=1 SV=3	3.87E+07
Ceruloplasmin OS=Homo sapiens GN=CP PE=1 SV=1	3.67E+08	Ceruloplasmin OS=Homo sapiens GN=CP PE=1 SV=1	1.15E+08	Ceruloplasmin OS=Homo sapiens GN=CP PE=1 SV=1	2.38E+08	Ceruloplasmin OS=Homo sapiens GN=CP PE=1 SV=1	2.73E+06
Delta-like protein 4; AltName: Full=Drosophila Delta	1.23E+07	Delta-like protein 4; AltName: Full=Drosophila Delta	1.12E+07	Delta-like protein 4; AltName: Full=Drosophila Delta	5.48E+07	Delta-like protein 4; AltName: Full=Drosophila Delta	4.85E+07

homolog 4; Short=Delta4; Flags: Precursor; [Homo sapiens (Human)] - [DLL4_HUMAN]		homolog 4; Short=Delta4; Flags: Precursor; [Homo sapiens (Human)] - [DLL4_HUMAN]		homolog 4; Short=Delta4; Flags: Precursor; [Homo sapiens (Human)] - [DLL4_HUMAN]		homolog 4; Short=Delta4; Flags: Precursor; [Homo sapiens (Human)] - [DLL4_HUMAN]	
Ferritin light chain; Short=Ferritin L subunit; [Homo sapiens (Human)] - [FRIL_HUMAN]	4.73E+06	Ferritin light chain OS=Homo sapiens GN=FTL PE=1 SV=2	2.03E+07	Ferritin light chain OS=Homo sapiens GN=FTL PE=1 SV=2	3.93E+08	Ferritin light chain OS=Homo sapiens GN=FTL PE=1 SV=2	1.51E+08
Haptoglobin OS=Homo sapiens GN=HP PE=1 SV=1	1.26E+08	Haptoglobin OS=Homo sapiens GN=HP PE=1 SV=1	1.04E+08	Haptoglobin OS=Homo sapiens GN=HP PE=1 SV=1	2.64E+08	Haptoglobin OS=Homo sapiens GN=HP PE=1 SV=1	9.50E+06
Hemoglobin subunit alpha OS=Homo sapiens GN=HBA1 PE=1 SV=2	1.49E+08	Hemoglobin subunit alpha OS=Homo sapiens GN=HBA1 PE=1 SV=2	5.40E+07	Hemoglobin subunit alpha OS=Homo sapiens GN=HBA1 PE=1 SV=2	8.29E+07	Hemoglobin subunit alpha; AltName: Full=Alpha-globin; AltName: Full=Hemoglobin alpha chain; [Homo sapiens (Human)] - [HBA_HUMAN]	5.24E+08
Hemopexin OS=Homo sapiens GN=HPX PE=1 SV=2	2.71E+08	Hemopexin OS=Homo sapiens GN=HPX PE=1 SV=2	1.89E+08	Hemopexin OS=Homo sapiens GN=HPX PE=1 SV=2	3.48E+08	Hemopexin OS=Homo sapiens GN=HPX PE=1 SV=2	1.75E+08
Ig alpha-1 chain C region OS=Homo sapiens GN=IGHA1 PE=1 SV=2	2.42E+09	Ig alpha-1 chain C region OS=Homo sapiens GN=IGHA1 PE=1 SV=2	6.14E+08	Ig alpha-1 chain C region OS=Homo sapiens GN=IGHA1 PE=1 SV=2	1.56E+09	Ig alpha-1 chain C region OS=Homo sapiens GN=IGHA1 PE=1 SV=2	6.04E+09
Ig gamma-1 chain C region OS=Homo sapiens	8.92E+09	Ig gamma-1 chain C region OS=Homo	3.30E+09	Ig gamma-1 chain C region OS=Homo	5.79E+09	Ig gamma-1 chain C region OS=Homo	3.55E+09

GN=IGHG1 PE=1 SV=1		sapiens GN=IGHG1 PE=1 SV=1		sapiens GN=IGHG1 PE=1 SV=1		sapiens GN=IGHG1 PE=1 SV=1	
Ig gamma-2 chain C region OS=Homo sapiens GN=IGHG2 PE=1 SV=2	5.60E+09	Ig gamma-2 chain C region OS=Homo sapiens GN=IGHG2 PE=1 SV=2	2.57E+09	Ig gamma-2 chain C region OS=Homo sapiens GN=IGHG2 PE=1 SV=2	4.65E+09	Ig gamma-2 chain C region OS=Homo sapiens GN=IGHG2 PE=1 SV=2	5.64E+07
Ig kappa chain C region OS=Homo sapiens GN=IGKC PE=1 SV=1	3.47E+09	Ig kappa chain C region OS=Homo sapiens GN=IGKC PE=1 SV=1	1.07E+09	Ig kappa chain C region OS=Homo sapiens GN=IGKC PE=1 SV=1	2.92E+09	Ig kappa chain C region OS=Homo sapiens GN=IGKC PE=1 SV=1	9.25E+09
Ig lambda chain V-IV region Bau; [Homo sapiens (Human)] - [LV401_HUMAN]	1.58E+08	Ig lambda chain V-IV region Bau; [Homo sapiens (Human)] - [LV401_HUMAN]	1.05E+07	Ig lambda chain V-IV region Bau; [Homo sapiens (Human)] - [LV401_HUMAN]	5.41E+07	Ig lambda chain V-IV region Bau; [Homo sapiens (Human)] - [LV401_HUMAN]	3.27E+07
Ig lambda-2 chain C regions OS=Homo sapiens GN=IGLC2 PE=1 SV=1	2.31E+09	Ig lambda-2 chain C regions OS=Homo sapiens GN=IGLC2 PE=1 SV=1	7.91E+08	Ig lambda-2 chain C regions OS=Homo sapiens GN=IGLC2 PE=1 SV=1	1.09E+09	Ig lambda-2 chain C regions OS=Homo sapiens GN=IGLC2 PE=1 SV=1	8.59E+06
Leucine-rich alpha-2-glycoprotein OS=Homo sapiens GN=LRG1 PE=1 SV=2	4.46E+07	Leucine-rich alpha-2-glycoprotein OS=Homo sapiens GN=LRG1 PE=1 SV=2	1.76E+07	Leucine-rich alpha-2-glycoprotein OS=Homo sapiens GN=LRG1 PE=1 SV=2	3.29E+07	Leucine-rich alpha-2-glycoprotein OS=Homo sapiens GN=LRG1 PE=1 SV=2	7.23E+05
Polymeric immunoglobulin receptor OS=Homo sapiens GN=PIGR PE=1 SV=4	1.94E+08	Polymeric immunoglobulin receptor OS=Homo sapiens GN=PIGR PE=1 SV=4	1.54E+08	Polymeric immunoglobulin receptor OS=Homo sapiens GN=PIGR PE=1 SV=4	2.83E+08	Polymeric immunoglobulin receptor OS=Homo sapiens GN=PIGR PE=1 SV=4	2.37E+09
Protein Shroom3; AltName: Full=Shroom-related protein;	9.47E+07	Protein Shroom3; AltName: Full=Shroom-related protein;	8.20E+07	Protein Shroom3; AltName: Full=Shroom-related protein;	2.30E+08	Protein Shroom3; AltName: Full=Shroom-related protein;	2.29E+07

Short=hShrmL; [Homo sapiens (Human)] - [SHRM3_HUMAN]		Short=hShrmL; [Homo sapiens (Human)] - [SHRM3_HUMAN]		Short=hShrmL; [Homo sapiens (Human)] - [SHRM3_HUMAN]		Short=hShrmL; [Homo sapiens (Human)] - [SHRM3_HUMAN]	
Pulmonary surfactant-associated protein A2 OS=Homo sapiens GN=SFTPA2 PE=1 SV=1	3.74E+07	Pulmonary surfactant-associated protein A2 OS=Homo sapiens GN=SFTPA2 PE=1 SV=1	2.82E+07	Pulmonary surfactant-associated protein A2 OS=Homo sapiens GN=SFTPA2 PE=1 SV=1	2.89E+07	Pulmonary surfactant-associated protein A2 OS=Homo sapiens GN=SFTPA2 PE=1 SV=1	1.85E+06
Serotransferrin OS=Homo sapiens GN=TF PE=1 SV=3	7.62E+09	Serotransferrin OS=Homo sapiens GN=TF PE=1 SV=3	3.42E+09	Serotransferrin OS=Homo sapiens GN=TF PE=1 SV=3	4.56E+09	Serotransferrin OS=Homo sapiens GN=TF PE=1 SV=3	1.10E+09
Serum albumin OS=Homo sapiens GN=ALB PE=1 SV=2	2.77E+09	Serum albumin OS=Homo sapiens GN=ALB PE=1 SV=2	1.54E+09	Serum albumin OS=Homo sapiens GN=ALB PE=1 SV=2	3.86E+09	Serum albumin OS=Homo sapiens GN=ALB PE=1 SV=2	5.49E+08
Thioredoxin; Short=Trx; AltName: Full=ATL-derived factor; Short=ADF; AltName: Full=Surface-associated sulphydryl protein; Short=SASP; [Homo sapiens (Human)] - [THIO_HUMAN]	8.21E+06	Thioredoxin; Short=Trx; AltName: Full=ATL-derived factor; Short=ADF; AltName: Full=Surface-associated sulphydryl protein; Short=SASP; [Homo sapiens (Human)] - [THIO_HUMAN]	1.29E+07	Thioredoxin; Short=Trx; AltName: Full=ATL-derived factor; Short=ADF; AltName: Full=Surface-associated sulphydryl protein; Short=SASP; [Homo sapiens (Human)] - [THIO_HUMAN]	2.98E+07	Thioredoxin; Short=Trx; AltName: Full=ATL-derived factor; Short=ADF; AltName: Full=Surface-associated sulphydryl protein; Short=SASP; [Homo sapiens (Human)] - [THIO_HUMAN]	1.54E+08
Transcriptional adapter 2-beta; AltName: Full=ADA2-like protein beta; Short=ADA2-beta; [Homo	2.22E+07	Transcriptional adapter 2-beta; AltName: Full=ADA2-like protein beta; Short=ADA2-beta; [Homo	5.10E+07	Transcriptional adapter 2-beta; AltName: Full=ADA2-like protein beta; Short=ADA2-beta; [Homo	2.68E+07	Transcriptional adapter 2-beta; AltName: Full=ADA2-like protein beta; Short=ADA2-beta; [Homo	1.11E+06

sapiens (Human)] - [TAD2B_HUMAN]		sapiens (Human)] - [TAD2B_HUMAN]		sapiens (Human)] - [TAD2B_HUMAN]		sapiens (Human)] - [TAD2B_HUMAN]	
Transmembrane protein 200C; AltName: Full=Transmembrane protein TTMA; AltName: Full=Two transmembrane domain-containing family member A; [Homo sapiens (Human)] - [T200C_HUMAN]	3.59E+06	Transmembrane protein 200C; AltName: Full=Transmembrane protein TTMA; AltName: Full=Two transmembrane domain-containing family member A; [Homo sapiens (Human)] - [T200C_HUMAN]	2.06E+06	Transmembrane protein 200C; AltName: Full=Transmembrane protein TTMA; AltName: Full=Two transmembrane domain-containing family member A; [Homo sapiens (Human)] - [T200C_HUMAN]	1.94E+06	Transmembrane protein 200C; AltName: Full=Transmembrane protein TTMA; AltName: Full=Two transmembrane domain-containing family member A; [Homo sapiens (Human)] - [T200C_HUMAN]	1.89E+06
Transthyretin OS=Homo sapiens GN=TTR PE=1 SV=1	2.53E+08	Transthyretin OS=Homo sapiens GN=TTR PE=1 SV=1	4.44E+07	Transthyretin OS=Homo sapiens GN=TTR PE=1 SV=1	1.29E+08	Transthyretin OS=Homo sapiens GN=TTR PE=1 SV=1	7.84E+07
Uncharacterized protein C3orf38; [Homo sapiens (Human)] - [CC038_HUMAN]	2.73E+09	Uncharacterized protein C3orf38; [Homo sapiens (Human)] - [CC038_HUMAN]	1.62E+09	Uncharacterized protein C3orf38; [Homo sapiens (Human)] - [CC038_HUMAN]	1.83E+09	Uncharacterized protein C3orf38; [Homo sapiens (Human)] - [CC038_HUMAN]	5.97E+08
Uteroglobin OS=Homo sapiens GN=SCGB1A1 PE=1 SV=1	1.74E+08	Uteroglobin OS=Homo sapiens GN=SCGB1A1 PE=1 SV=1	8.73E+07	Uteroglobin OS=Homo sapiens GN=SCGB1A1 PE=1 SV=1	1.99E+08	Uteroglobin OS=Homo sapiens GN=SCGB1A1 PE=1 SV=1	4.49E+09

Table C.12: *The biological process classification of Inflammation/immunity according to Gene Ontology annotation of proteins identified. Data shown is a comparison of the mean of the three most abundant ion peaks of each protein identified, in Healthy Aged Non-Smokers, n=5, Healthy Aged Smokers, n=5, COPD Ex-Smokers, n = 10 , and COPD Smokers, n = 5, respectively.*

Inflammation/immunity	Healthy aged control	Healthy Smoker	COPD Ex-Smoker	COPD Smoker
Alpha-1-acid glycoprotein 1	3.39E+08	1.29E+08	X	2.76E+08
Alpha-1-antichymotrypsin	8.21E+07	3.72E+07	X	1.00E+08
Alpha-1-antichymotrypsin	8.21E+07	3.72E+07	X	1.00E+08
Alpha-2-HS-glycoprotein (fetuin A)	1.16E+08	2.99E+07	X	9.30E+07
Annexin A3	X	2.81E+06	X	9.75E+05
Antithrombin-III	1.84E+07	X	X	1.82E+07
Beta-2-microglobulin	2.59E+07	1.03E+07	5.86E+08	3.80E+07
Beta-microseminoprotein	X	1.50E+07	X	4.84E+07
Cell adhesion molecule 2	X	X	X	1.71E+07
Complement C2	3.41E+07	X		1.87E+06
Complement C3	2.66E+06	X	2.06E+08	7.33E+07
Complement C4-A	X	X	7.09E+07	X
Complement decay-accelerating factor (CD55)	X	X	5.65E+07	X
Complement factor B	7.63E+06	X	X	X
Deleted in malignant brain tumors 1 protein	2.73E+07	3.34E+07	1.13E+06	3.49E+07
Dipeptidyl peptidase 4	X	X	X	1.99E+07
Galectin-3 binding protein	2.34E+06	5.09E+06	X	1.41E+08
Haptoglobin	X	X	X	8.21E+06
HLA class II histocompatibility antigen, DR alpha chain	1.26E+08	1.04E+08	9.50E+06	2.64E+08
HLA class II histocompatibility antigen, DRB1-15 beta chain	1.69E+06	X	X	X
Ig alpha-1 chain C region	X	X	X	4.64E+06
Ig alpha-2 chain C region	2.42E+09	6.14E+08	6.04E+09	1.56E+09
Ig delta chain C region	1.79E+09	3.06E+08	X	8.21E+08
Ig gamma-1 chain C region	1.10E+07	X	X	X
Ig gamma-2 chain C region	8.92E+09	3.30E+09	3.55E+09	5.79E+09
Ig gamma-3 chain C region	5.60E+09	2.57E+09	5.64E+07	4.65E+09
Ig gamma-4 chain C region	6.71E+09	2.87E+09	Present-not quantified	5.04E+09
Ig heavy chain V-I region HG3	5.60E+09	2.57E+09	X	X
Ig heavy chain V-I region V35	X	3.44E+07	X	6.71E+07
Ig heavy chain V-II region ARH-77	X	X	X	3.54E+07
Ig heavy chain V-III region CAM	X	X	X	7.16E+07
Ig heavy chain V-III region GAL	1.05E+09	X	1.68E+07	9.16E+08

Ig heavy chain V-III region TIL	1.05E+09	4.92E+08	X	8.79E+08
Ig kappa chain C region	X	X	1.60E+07	X
Ig kappa chain V-I region DEE	3.47E+09	1.07E+09	9.25E+09	2.92E+09
Ig kappa chain V-I region Kue	2.73E+08	1.54E+08	X	X
Ig kappa chain V-II region RPMI 6410	1.89E+08	X	X	2.80E+08
Ig kappa chain V-II region TEW	1.62E+08	4.64E+07	X	X
Ig kappa chain V-III region B6	X	X	X	1.67E+08
Ig kappa chain V-III region POM	9.77E+07	7.29E+07	X	1.58E+08
Ig kappa chain V-III region SIE	2.40E+08	1.24E+08	X	2.67E+08
Ig kappa chain V-III region VG (Fragment)	1.46E+08	5.54E+07	2.65E+06	6.84E+07
Ig kappa chain V-IV region Len	2.39E+08	X	1.63E+09	X
Ig lambda chain V region 4A	9.86E+07	6.10E+07	X	1.49E+08
Ig lambda chain V-I region HA	5.01E+07	1.78E+07	X	7.87E+06
Ig lambda chain V-I region NIG-64	1.91E+08	5.73E+07	X	6.98E+07
Ig lambda chain V-III region LOI	7.21E+07	X	X	2.25E+07
Ig lambda chain V-III region SH	1.57E+08	6.55E+07	4.81E+08	6.09E+07
Ig lambda chain V-VI region SUT	X	1.01E+07	X	1.31E+07
Ig lambda-2 chain C regions	X	X	3.53E+09	X
Ig mu chain C region	2.31E+09	7.91E+08	8.59E+06	1.09E+09
IgBF	4.16E+07	4.18E+07	X	3.88E+07
IgGFc-binding protein	X	1.50E+07	X	4.84E+07
Immunoglobulin lambda-like polypeptide 5	4.76E+07	3.90E+07	X	7.57E+07
Intercellular adhesion molecule 1	1.44E+09	4.43E+08	X	7.42E+08
Junctional adhesion molecule A	1.15E+07	4.60E+06	X	1.44E+07
Lactotransferrin	9.06E+05	X	X	X
Leukocyte elastase inhibitor	9.47E+08	X	X	X
Lysozyme C	3.69E+07	2.61E+06	X	6.74E+06
Neutrophil defensin 1	X	X	1.54E+08	X
Plasma protease C1 inhibitor	X	X	7.51E+07	7.32E+06
Polymeric immunoglobulin receptor	1.94E+08	1.54E+08	2.37E+09	2.83E+08
Pulmonary surfactant-associated protein A	3.74E+07	2.82E+07	9.75E+08	2.89E+07
Pulmonary surfactant-associated protein D	1.53E+07	5.11E+06	X	2.63E+07
S100-A8 (Calgranulin A)	3.59E+07	8.57E+08	2.33E+07	2.22E+06

Sushi domain-containing protein 2	1.63E+06	X	X	X
V-set and immunoglobulin domain-containing protein 6	X	1.16E+08	X	1.52E+08
V-set and immunoglobulin domain-containing protein 8	2.00E+08	8.23E+07	X	1.42E+08
Zinc-alpha-2-glycoprotein	1.24E+08	5.33E+07	2.87E+06	8.23E+07

Table C.12: *The biological process classification of Oxidant/antioxidant balance according to Gene Ontology annotation of proteins identified. Data shown is a comparison of the mean of the three most abundant ion peaks of each protein identified, in Healthy Aged Non-Smokers, n=5, Healthy Aged Smokers, n=5, COPD Ex-Smokers, n = 10 , and COPD Smokers, n = 5, respectively.*

Oxidant/antioxidant balance	**Healthy aged control**	**Healthy Smoker**	**COPD Ex-Smoker**	**COPD Smoker**
Glutathione peroxidase 3	1.19E+06	X	X	X
Glutathione S-transferase A1	X	1.73E+07	X	X
Glutathione S-transferase A2	4.18E+07	X	X	9.67E+07
Glutathione S-transferase omega-1	X	X	X	9.80E+06
Glutathione S-transferase P	8.51E+06	1.82E+07	3.52E+08	1.74E+07
Peroxiredoxin-5, mitochondrial	X	X	2.13E+08	2.13E+08
Peroxiredoxin-6	X	1.78E+06	X	X
Protein DJ-1	1.23E+07	7.89E+06	X	1.16E+07
Superoxide dismutase [Cu-Zn]	X	7.11E+06	X	1.08E+07
Thioredoxin	8.21E+06	1.29E+07	1.54E+08	2.98E+07

Table C.13: *The biological process classification of Protease/antiprotease balance according to Gene Ontology annotation of proteins identified. Data shown is a comparison of the mean of the three most abundant ion peaks of each protein identified, , in Healthy Aged Non-Smokers, n=5, Healthy Aged Smokers, n=5, COPD Ex-Smokers, n = 10 , and COPD Smokers, n = 5, respectively.*

Protease/antiprotease balance	**Healthy aged control**	**Healthy Smoker**	**COPD Ex-Smoker**	**COPD Smoker**
Alpha-1-antichymotrypsin	8.21E+07	3.72E+07	X	1.00E+08
Alpha-1-antitrypsin	3.20E+09	2.75E+08	2.31E+09	1.61E+09
Alpha-2-macroglobulin	1.66E+08	4.14E+06	X	1.01E+07
Alpha-amylase 1	X	X	X	3.66E+07
Angiotensin-converting enzyme; Dipeptidyl carboxypeptidase I	1.46E+07	X	X	2.81E+07
Antithrombin-III	1.84E+07	X	X	1.82E+07
Cathepsin D	X	4.68E+08	X	8.45E+08

Cathepsin Z	X	4.21E+06	X	6.46E+06
Complement C2	3.41E+07	X	X	1.87E+06
Cystatin-B	4.33E+06	6.43E+06	X	1.51E+07
Dermcidin	2.13E+06	4.35E+06	6.19E+06	2.94E+06
Dipeptidyl peptidase 1	X	X	X	1.99E+07
Dipeptidyl peptidase 4	6.17E+07	3.08E+06	X	1.99E+07
Haptoglobin	1.26E+08	1.04E+08	9.50E+06	2.64E+08
Kininogen-1; Alpha-2-thiol proteinase inhibitor	X	X	X	1.20E+07
Lactotransferrin	9.47E+08	X	X	X
Leukocyte elastase inhibitor; Monocyte/Neutrophil elastase inhibitor	3.69E+07	2.61E+06	X	6.74E+06
Leukotriene A-4 hydrolase	X	X	X	1.50E+07
Matrix metalloproteinase-28	X	X	X	1.09E+07
Napsin-A	X	X	X	5.17E+06
Pancreatic alpha-amylase	1.35E+07	X	X	X
Pro-cathepsin H	1.06E+07	1.14E+07	X	1.61E+07
Prostasin	1.22E+06	1.62E+06	X	X
Protein DJ-1	1.23E+07	7.89E+06	X	1.16E+07
Serpin B6	X	X	X	2.74E+06
Trypsin-3	X	1.60E+06	X	2.58E+06
Xaa-Pro dipeptidase	X	X	X	1.34E+07

Table C.14: *The biological process classification of Metal handling according to Gene Ontology annotation of proteins identified. Data shown is a comparison of the mean of the three most abundant ion peaks of each protein identified, in Healthy Aged Non-Smokers, n=5, Healthy Aged Smokers, n=5, COPD Ex-Smokers, n = 10 , and COPD Smokers, n = 5, respectively*

Metal handling	Healthy aged control	Healthy Smoker	COPD Ex-Smoker	COPD Smoker
7-alpha-hydroxycholest-4-en-3-one 12-alpha-hydroxylase	X	X	X	2.87E+07
Annexin A3 OS=Homo sapiens	X	2.81E+06	X	X
Annexin A5	1.36E+06	5.18E+07	X	7.53E+07
Calcineurin-like phosphoesterase domain-containing protein 1	X	X	X	3.70E+06
Calcyphosin	X	1.44E+07	X	1.32E+06
Calmodulin	2.68E+06	2.84E+06	X	2.48E+07
Calmodulin-like protein 3	X	1.93E+07	X	X
Calmodulin-like protein 5	X	2.40E+07	X	X
Carbonic anhydrase 1	3.91E+06	X	X	5.50E+06
Carbonic anhydrase 2	X	3.84E+06	X	1.05E+07
Ceruloplasmin	3.67E+08	1.15E+08	2.73E+06	2.38E+08
Complement decay-accelerating factor	X	X	5.65E+07	X
Ferritin heavy chain	6.17E+07	3.08E+06	X	1.99E+07
Ferritin light chain	4.73E+06	2.03E+07	1.51E+08	3.93E+08
Gelsolin	X	X	X	1.70E+06
Glutathione peroxidase 3	1.19E+06	X	X	X
Glutathione synthetase	X	8.00E+06	X	3.37E+06
Hemoglobin subunit alpha	1.49E+08	5.40E+07	5.24E+08	8.29E+07
Hemoglobin subunit beta	1.28E+08	2.04E+07	1.66E+09	7.32E+07
Hemoglobin subunit delta	7.65E+07		X	X
Hemopexin	2.71E+08	1.89E+08	X	3.48E+08
Hornerin	X	X	X	2.68E+07
Lactotransferrin	9.06E+05	X	X	
Leukotriene A-4 hydrolase	X	X	X	1.50E+07
Protein S100-A11	X	4.08E+06	X	5.82E+06
Protein S100-A6	X	X	X	1.14E+08
Protein S100-A7	1.37E+07	8.42E+07	X	X
Protein S100-A8	3.59E+07	8.57E+08	2.33E+07	2.22E+06
Protein S100-A9	1.13E+07	X	X	X
Pyridoxal kinase	X	X	X	3.73E+06
Selenium-binding protein 1	1.67E+07	1.15E+07	X	8.65E+06
Serotransferrin	7.62E+09	3.42E+09	1.10E+09	4.56E+09
Serum albumin	2.77E+09	1.54E+09	2.62E+10	3.86E+09
Superoxide dismutase [Cu-Zn]	X	7.11E+06	X	1.08E+07
Zinc-alpha-2-glycoprotein	1.24E+08	5.33E+07	2.87E+06	8.23E+07

Appendix D

a

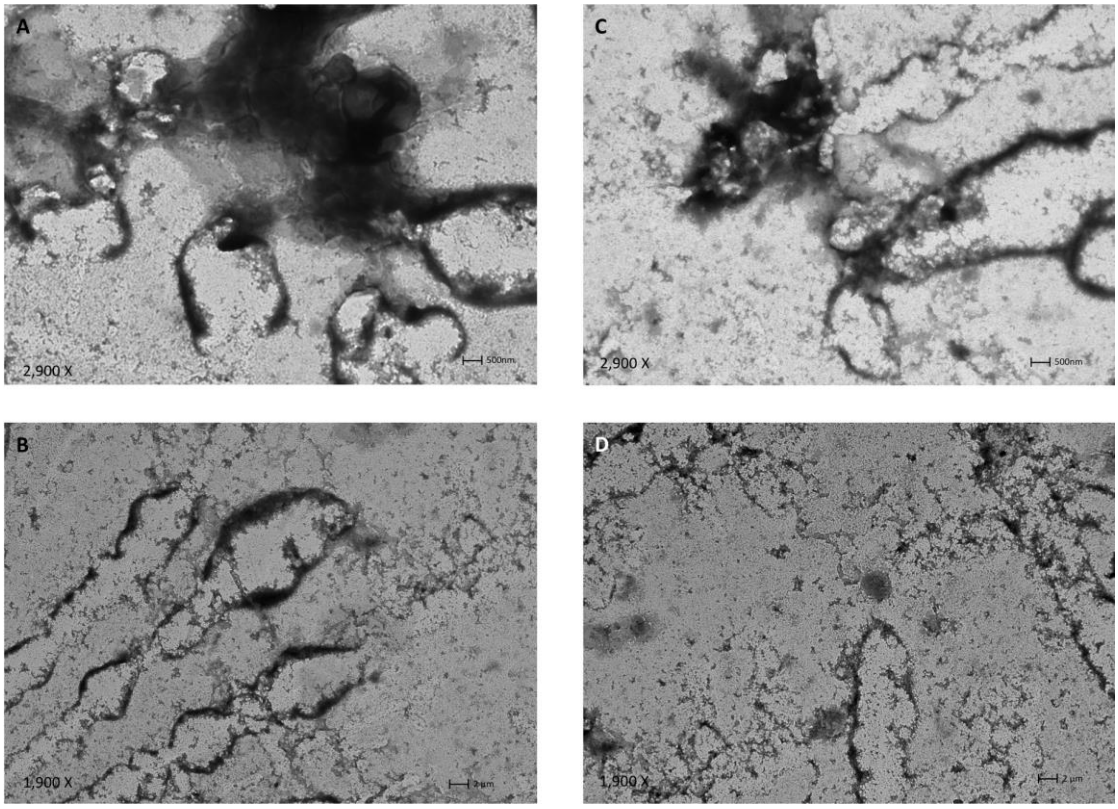

Figure D.1: *TEM images acquired for concentrated BAL fluids investigated. Representative TEM images of Concentrated BAL, respectively. TEM images were acquired with an AMT 16000M camera using a FEI Tecnai 12 transmission microscope operated at 120 kV, Negative staining of liposomes with 2% PTA pH 6.5 and 0.1% trehalose was employed.*

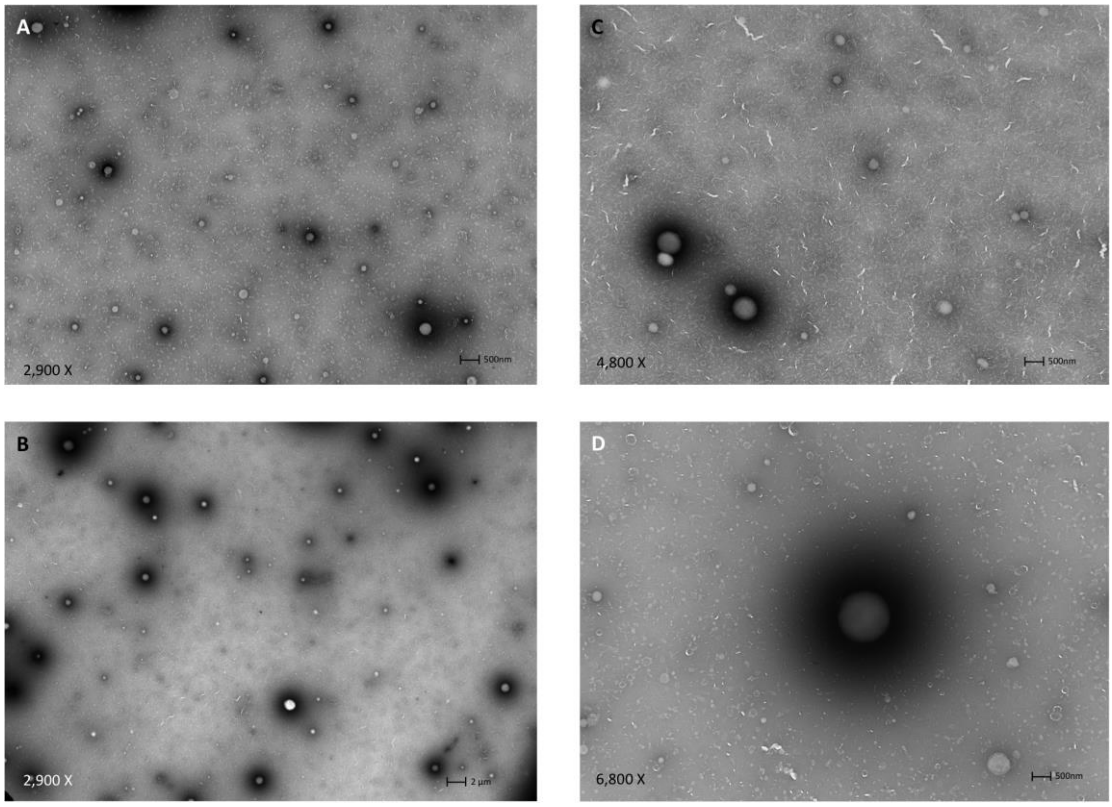

Figure D.2: *TEM images acquired for simulant: Protein and DPPC in HEPES investigated. Representative TEM images of Concentrated BAL, respectively. TEM images were acquired with an AMT 16000M camera using a FEI Tecnai 12 transmission microscope operated at 120 kV, Negative staining of liposomes with 2% PTA pH 6.5 and 0.1% trehalose was employed.*

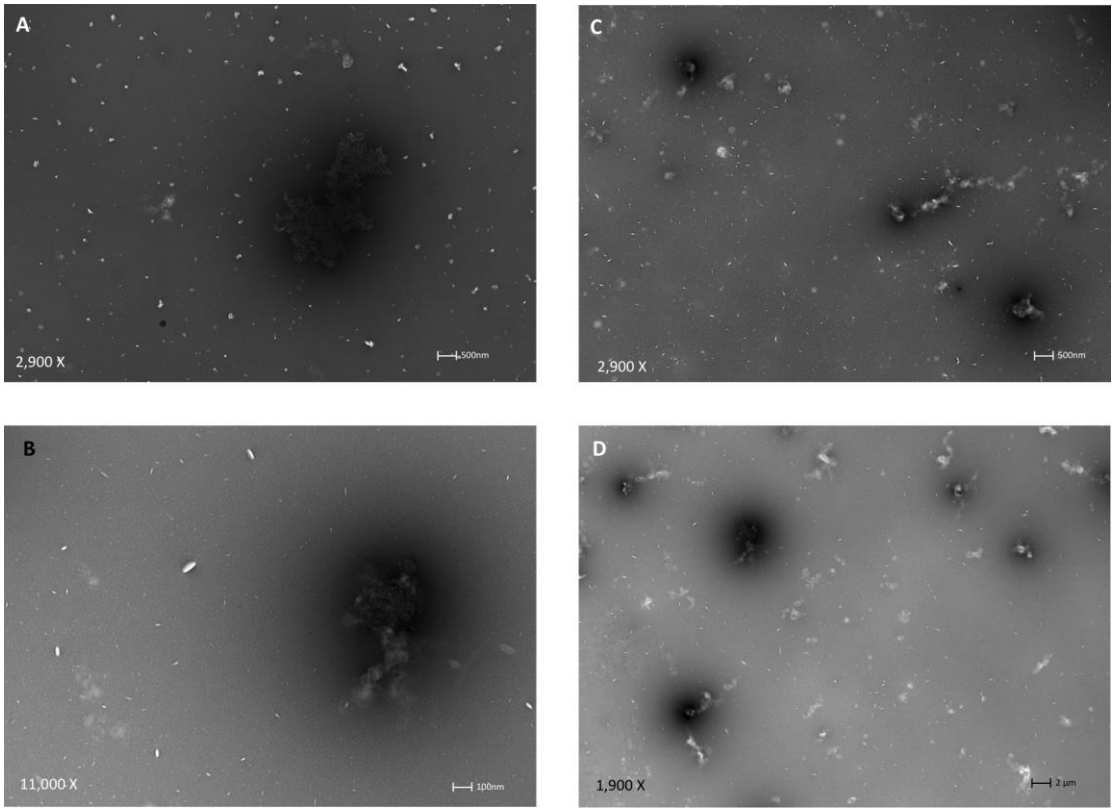

Figure D.3: *TEM images acquired for simulant: Protein and DPPC, PG, Chol in HEPES investigated. Representative TEM images of Concentrated BAL, respectively. TEM images were acquired with an AMT 16000M camera using a FEI Tecnai 12 transmission microscope operated at 120 kV, Negative staining of liposomes with 2% PTA pH 6.5 and 0.1% trehalose was employed.*

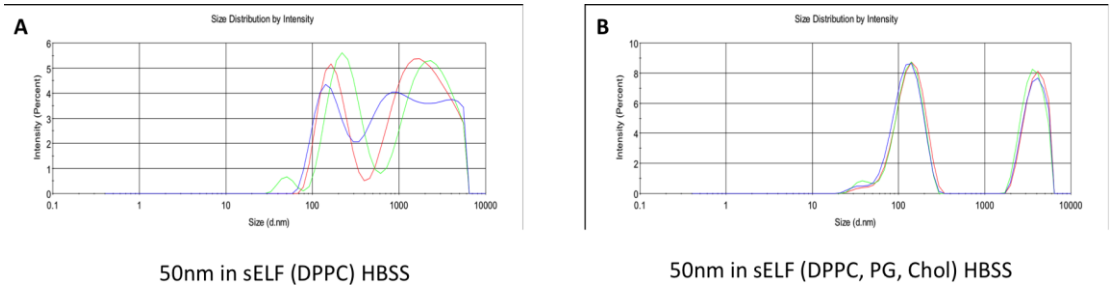

Figure D.4: *The average intensity distribution measurements for 50nm polystyrene particles in simulant variants (A) simulant: Protein and DPPC in HEPES; (B) simulant: Protein and DPPC, PG, Chol in HEPES respectively. All distribution curves as measured by DLS are representative of at n = 3 at 37 °C at t=0 h,.*

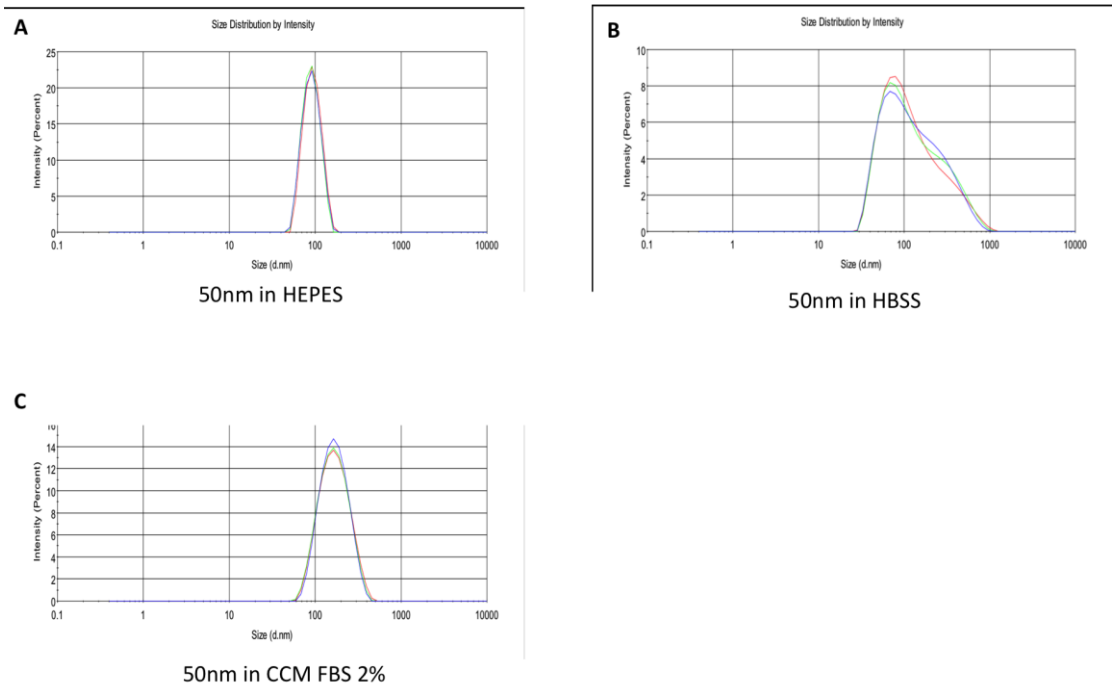

Figure D.5: *The average intensity distribution measurements for 50nm polystyrene particles in (A) Hepes (B) HBSS and (C) CCM FBS 2% respectively. All distribution curves as measured by DLS are representative of at n = 3 at 37 °C at t=0 h.*

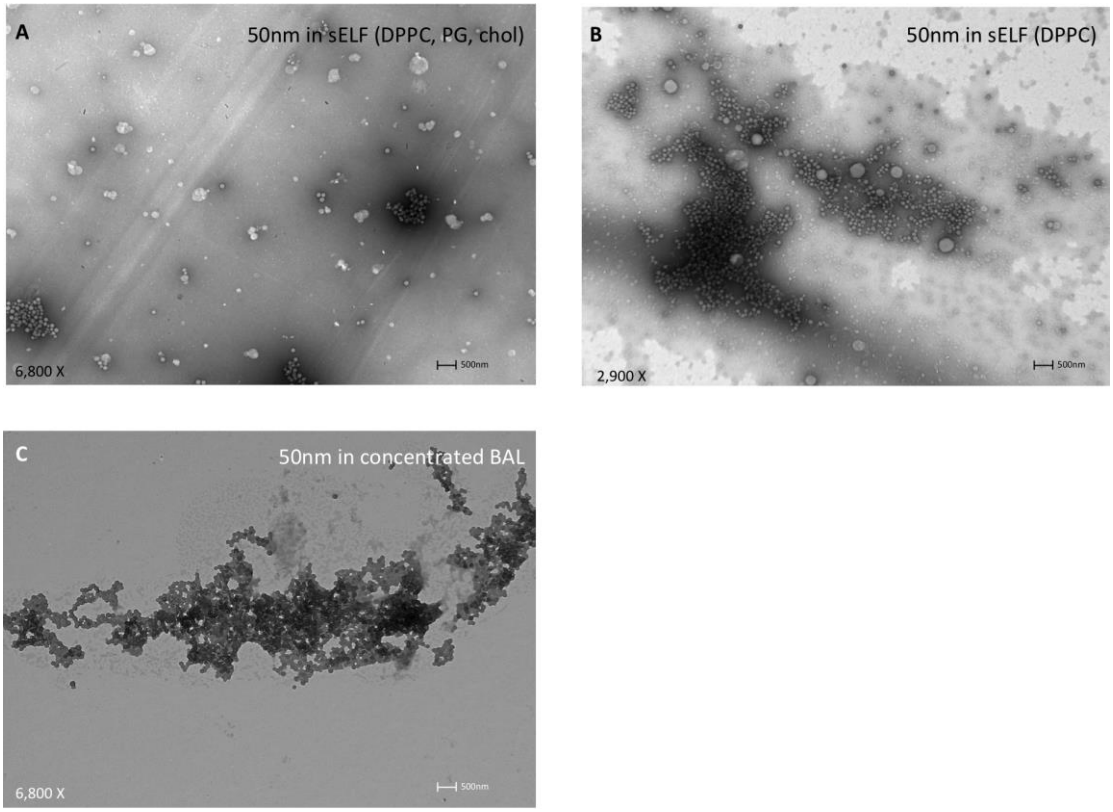

Figure D.6: *The average intensity distribution measurements and respective TEM images acquired for 50nm polystyrene particles in simulant variants and concentrated BAL fluids investigated. (A) simulant: Protein and DPPC, PG, Chol; (B) simulant: Protein and DPPC in HEPES and (C) Concentrated BAL, respectively. TEM images were acquired with an AMT 16000M camera using a FEI Tecnai 12 transmission microscope operated at 120 kV, Negative staining of liposomes with 2% PTA pH 6.5 and 0.1% trehalose was employed.*

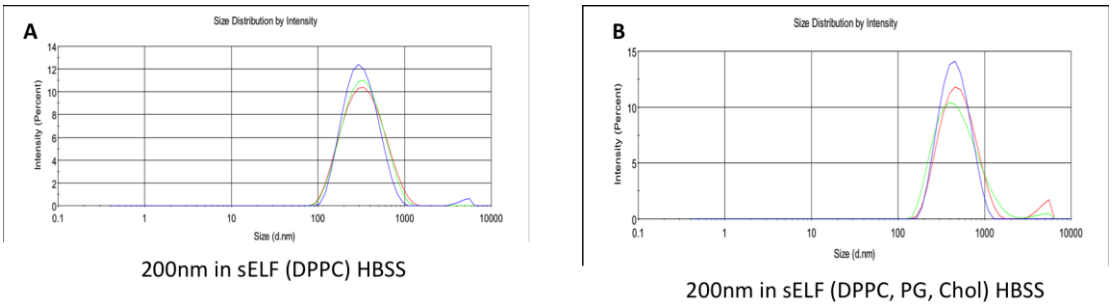

Figure D.7: *The average intensity distribution measurements for 200nm polystyrene particles in simulant variants (A) simulant: Protein and DPPC in HEPES; (B) simulant: Protein and DPPC, PG, Chol in HEPES respectively.* All distribution curves as measured by DLS are representative of at n = 3 at 37 °C at t=0 h.

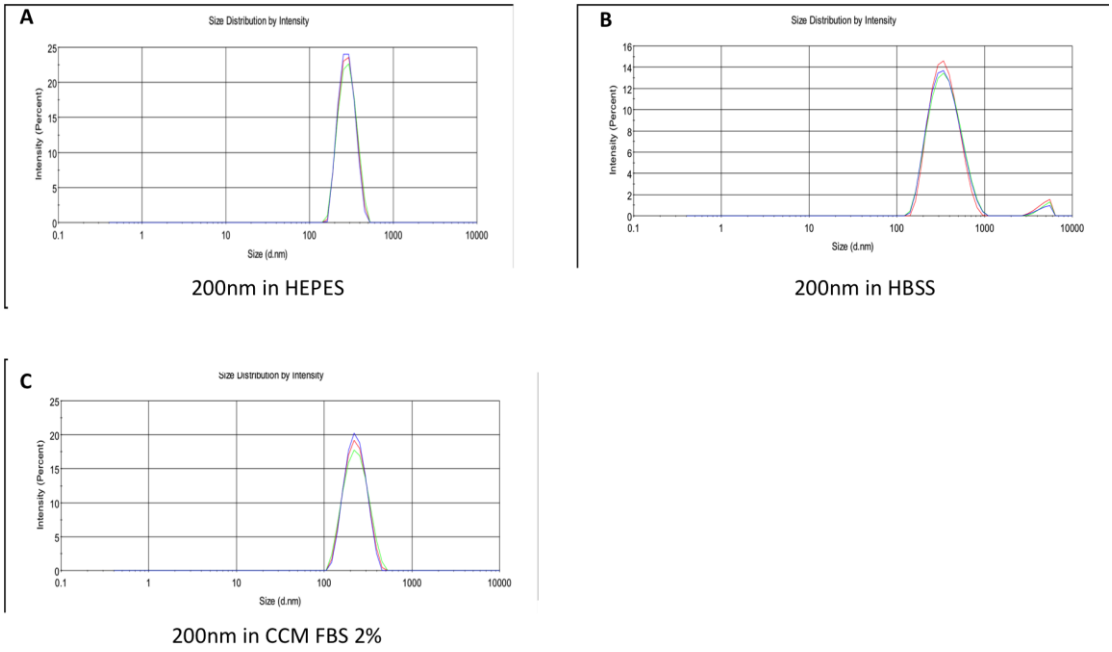

Figure D.8: *The average intensity distribution measurements for 200nm polystyrene particles in (A) HEPES (B) HBSS and (C) CCM FBS 2% respectively. All distribution curves as measured by DLS are representative of at n = 3 at 37 °C at t=0 h.*

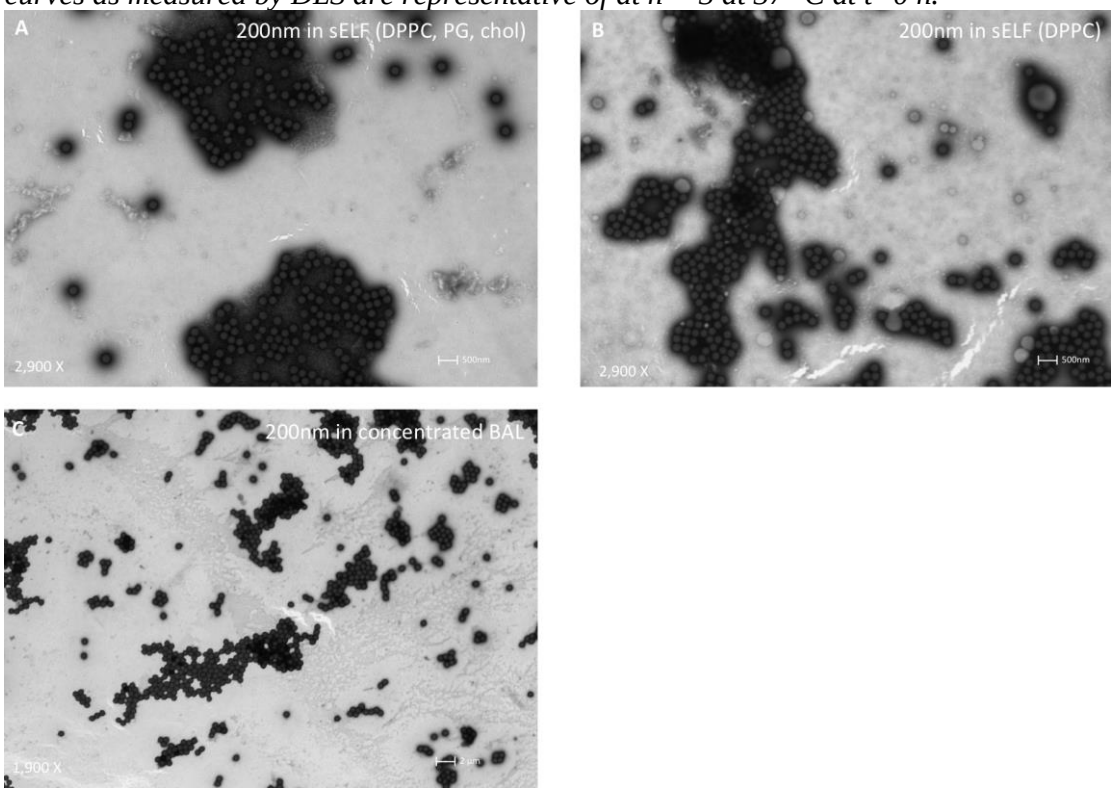

Figure D.9: *The average intensity distribution measurements and respective TEM images acquired for 200nm polystyrene particles in simulant variants and concentrated BAL fluids investigated. (A) simulant: Protein and DPPC, PG, Chol; (B) simulant: Protein and DPPC in HEPES and (C) Concentrated BAL, respectively. TEM images were acquired with an AMT 16000M camera using a FEI Tecnai 12 transmission microscope operated at 120 kV, Negative staining of liposomes with 2% PTA pH 6.5 and 0.1% trehalose was employed.*

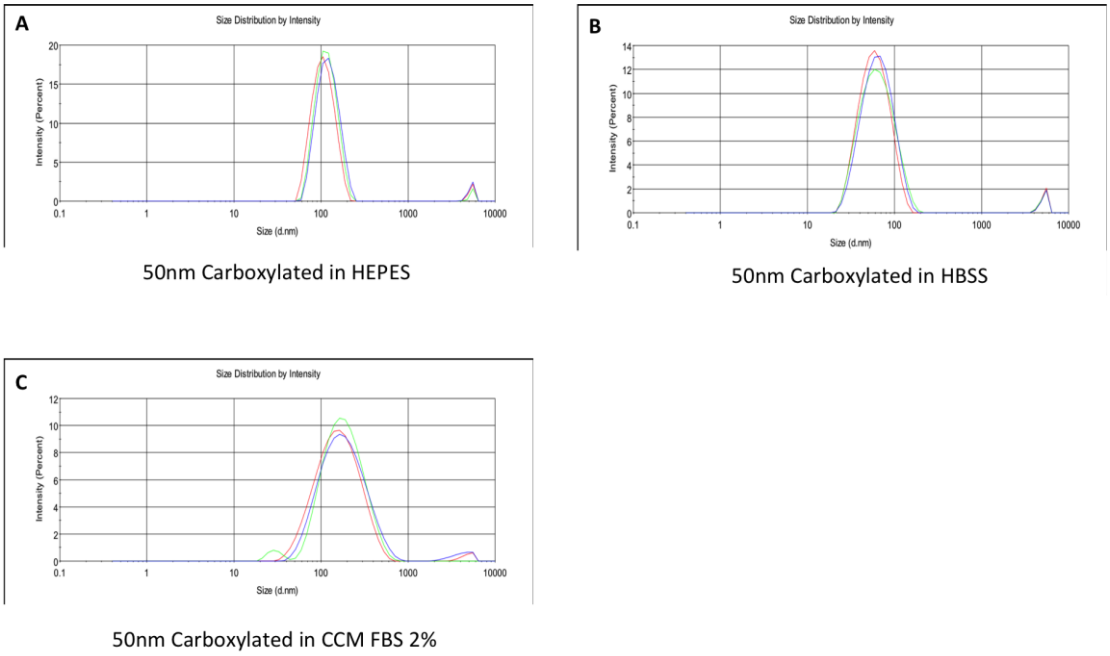

Figure D.10: *The average intensity distribution measurements for 50nm carboxylated polystyrene particles in (A) HEPES (B) HBSS and (C) CCM FBS 2% respectively. All distribution curves as measured by DLS are representative of at n = 3 at 37 °C at t=0 h.*

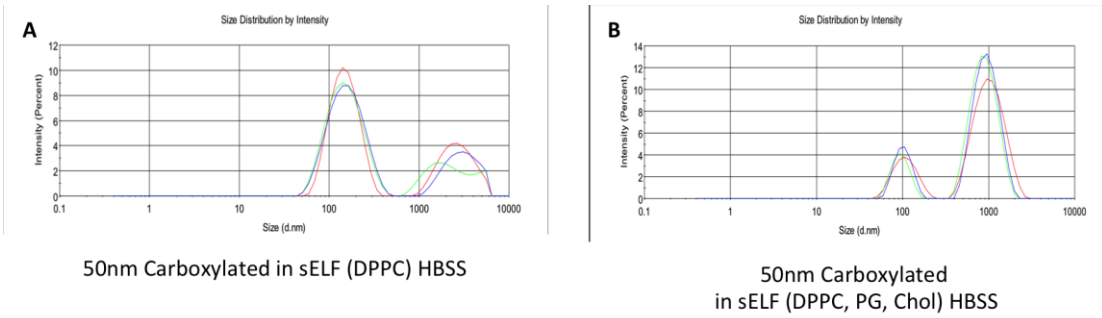

Figure D.11: *The average intensity distribution measurements for 50nm carboxylated polystyrene particles in simulant variants (A) simulant: Protein and DPPC in HEPES; (B) simulant: Protein and DPPC, PG, Chol in HEPES respectively. All distribution curves as measured by DLS are representative of at n = 3 at 37 °C at t=0 h,.*

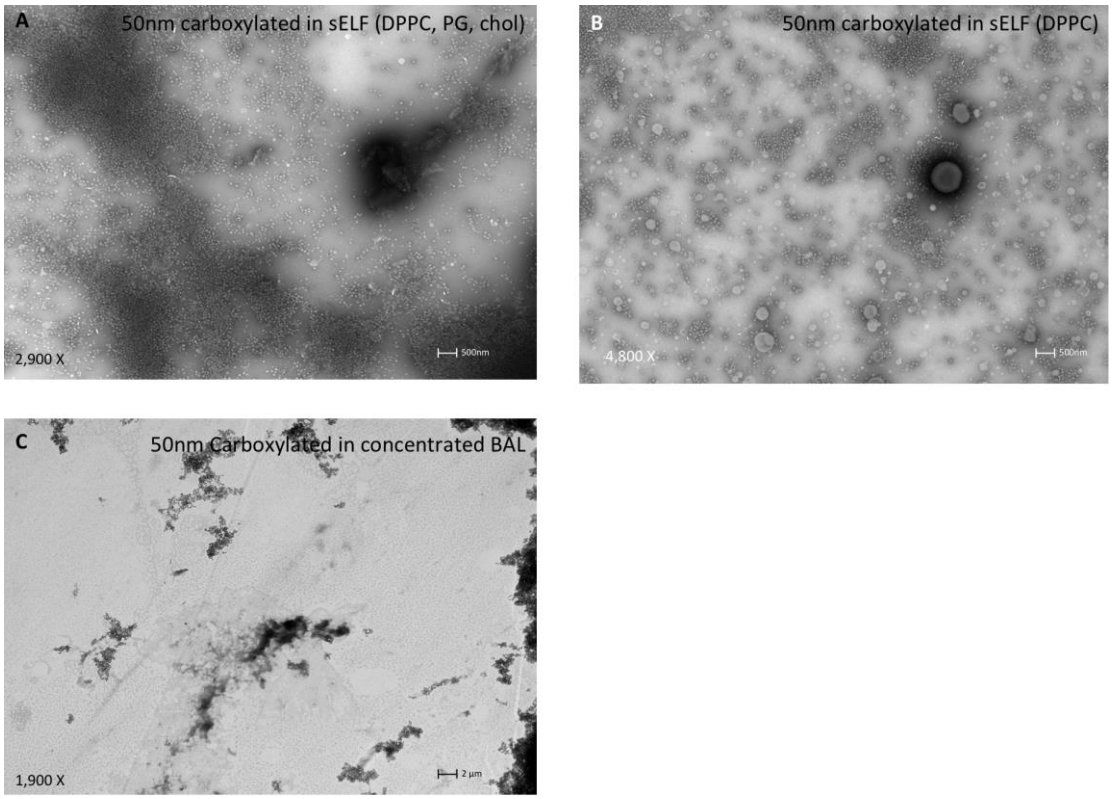

Figure D.12: *The average intensity distribution measurements and respective TEM images acquired for 50nm carboxylated polystyrene particles in simulant variants and concentrated BAL fluids investigated* (A) simulant: Protein and DPPC, PG, Chol; (B) simulant: Protein and DPPC in HEPES and (C) Concentrated BAL, respectively. *TEM images were acquired with an AMT 16000M camera using a FEI Tecnai 12 transmission microscope operated at 120 kV, Negative staining of liposomes with 2% PTA pH 6.5 and 0.1% trehalose was employed.*

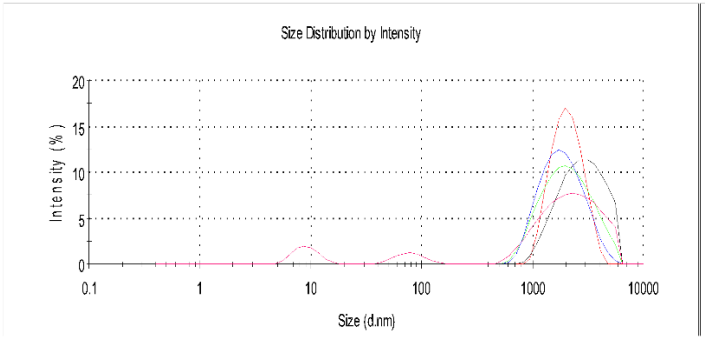

50nm in sELF (DPPC) HBSS

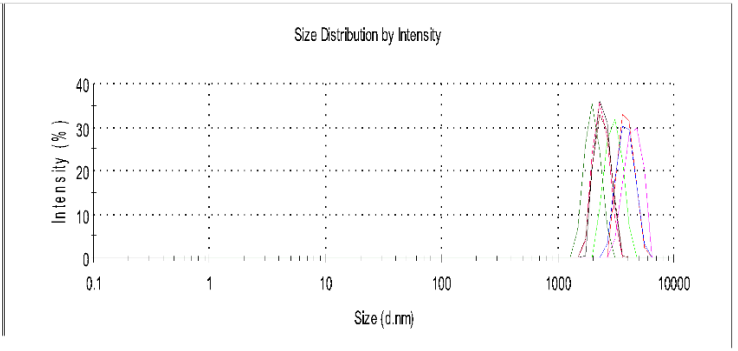

200nm in sELF (DPPC) HBSS

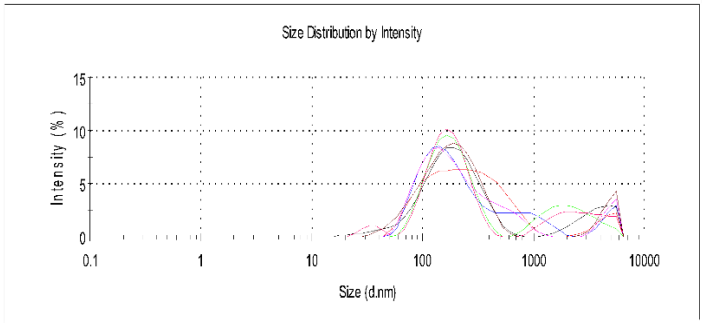

50nm Carboxylated in sELF (DPPC) HBSS

Figure D.13: *The average intensity distribution measurements for 50nm , 200nm and 50nm carboxylated polystyrene particles in simulant: Protein and DPPC in HEPES. All distribution curves as measured by DLS are representative of n=3 measurements taken over a 4 hour period at 37 °C.*

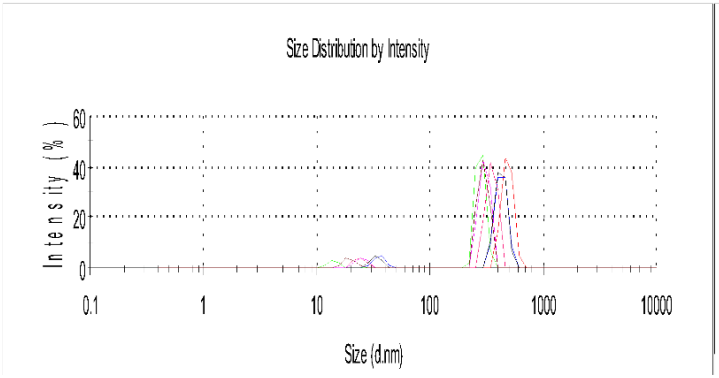

50nm in sELF (DPPC, PG, Chol) HBSS

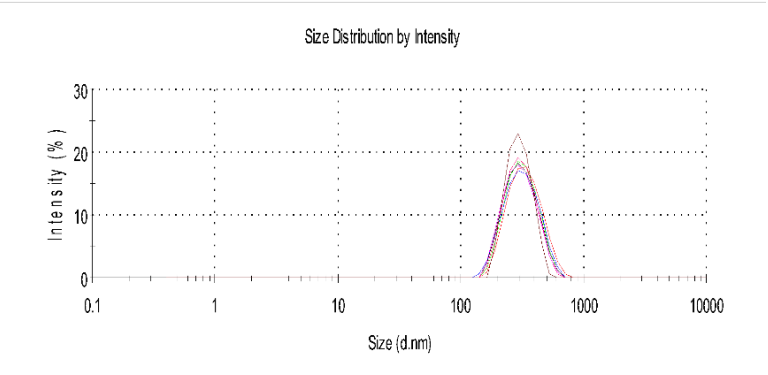

200nm in sELF (DPPC, PG, Chol) HBSS

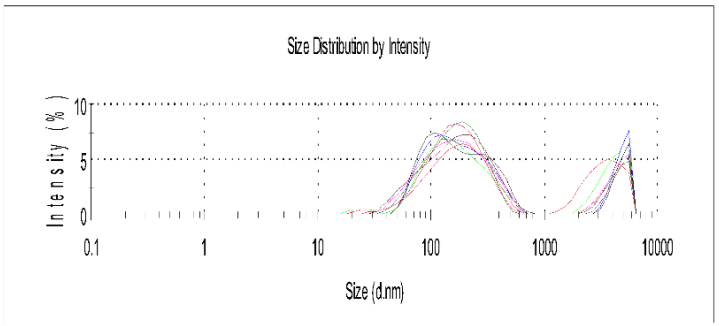

50nm Carboxylated in sELF (DPPC, PG, Chol) HBSS

Figure D.14: *The average intensity distribution measurements for 50nm , 200nm and 50nm carboxylated polystyrene particles in simulant: Protein and DPPC, PG ,chol in HEPES. All distribution curves as measured by DLS are representative of n=3 measurements taken over a 4 hour period at 37 °C.*

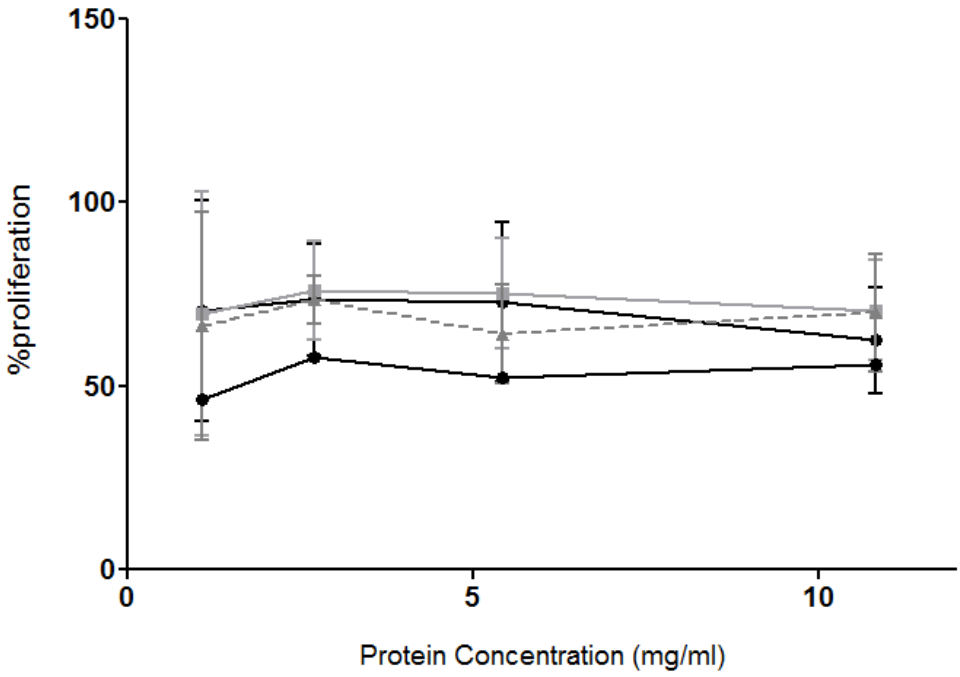

Figure D. 15*: The effect of simulant (Protein and DPPC) on the proliferation of J774 cell monolayers. The influence of simulant on cell proliferation was calculated as a percentage of the control (CCM 2%) versus simulant. The effect of a series of dilutions of simulant (concentrations of 1.1, 2.2, 4.3, 6.5, 8.7, 10.8 mg/ml protein respectively) was assessed over a 12 hour periodsof incubation with cells respectively. Cellular metabolic activity was measured spectrophotometrically at 570nm, data represents the mean±SD, , n = 3 experiments, four replicates per experiment at each dilution*

Table D.1: *Hanks' Balanced Salt Solution incorporated with simulant: HBSS Modified, with calcium, with magnesium, without phenol red (CATALOG NO. 55037C).*

Ionic constituent	Concentration (mg/L)
Inorganic salts	
Calcium chloride dihydrate	185.4
Magnesium sulfate heptahydrate	200
Potassium chloride	400
Potassium phosphate monobasic anhydrous	60
Sodium bicarbonate	350
Sodium chloride	8000
Sodium phosphate dibasic heptahydrate	90
OTHER	Concentration (mg/L)
D-Glucose (Dextrose)	1000
pH	7-7.4

References

Abdulamir, A., Hafidh, R.R. & Abubakar, F. 2009, "Different inflammatory mechanisms in lungs of severe and mild asthma: crosstalk of NF-kappa-B, TGFβ1, Bax, Bcl-2, IL-4 and IgE", *Scandinavian Journal of Clinical & Laboratory Investigation,* vol. 69, no. 4, pp. 487-495.

Ageuk.org.uk, (2014). *Key stats | Age UK London*. [online] Available at: http://www.ageuk.org.uk/london/about-age-uk-london/media-centre/key-stats/ [Accessed 8 Sep. 2014].

Agius, A.M., Smallman, L.A. & Pahor, A.L. 1998, "Age, smoking and nasal ciliary beat frequency", *Clinical otolaryngology and allied sciences,* vol. 23, no. 3, pp. 227-230.

Agu, R.U. & Ugwoke, M.I. 2011, "In vitro and in vivo testing methods for respiratory drug delivery", *Expert opinion on drug delivery,* vol. 8, no. 1, pp. 57-69.

Agusti, A., MacNee, W., Donaldson, K. & Cosio, M. 2003, "Hypothesis: does COPD have an autoimmune component?", *Thorax,* vol. 58, no. 10, pp. 832-834.

Ahsan, F., Rivas, I.P., Khan, M.A. & Torres Suárez, A.I. 2002, "Targeting to macrophages: role of physicochemical properties of particulate carriers--liposomes and microspheres--on the phagocytosis by macrophages", *Journal of Controlled Release,* vol. 79, no. 1-3, pp. 29-40.

Aldridge, R.E., Chan, T., van Dalen, C.J., Senthilmohan, R., Winn, M., Venge, P., Town, G.I. & Kettle, A.J. 2002, "Eosinophil peroxidase produces hypobromous acid in the airways of stable asthmatics", *Free Radical Biology and Medicine,* vol. 33, no. 6, pp. 847-856.

Allen, A. 1983, "Mucus--a protective secretion of complexity", *Trends in biochemical sciences,* vol. 8, no. 5, pp. 169-173.

Ansoborlo, E., Chalabreysse, J., Escallon, S. & Henge-Napoli, M. 1990, "In vitro solubility of uranium tetrafluoride with oxidizing medium compared with in vivo solubility in rats", *International journal of radiation biology,* vol. 58, no. 4, pp. 681-689.

Anthonisen, N.R., Connett, J.E., Kiley, J.P., Altose, M.D., Bailey, W.C., Buist, A.S., Conway, W.A., Enright, P.L., Kanner, R.E. & O'Hara, P. 1994, "Effects of smoking intervention and the use of an inhaled anticholinergic bronchodilator on the rate of decline of FEV1: the Lung Health Study", *Jama,* vol. 272, no. 19, pp. 1497-1505.

Anthonisen, N.R., Wright, E.C. & Hodgkin, J.E. 1986, "Prognosis in chronic obstructive pulmonary disease", *The American Review of Respiratory Disease,* vol. 133, no. 1, pp. 14-20.

Armstrong, P.B. & Quigley, J.P. 2001, "A role for protease inhibitors in immunity of long-lived animals" in *Phylogenetic Perspectives on the Vertebrate Immune System* Springer, , pp. 141-160.

Aulton, M.E. 2007, *Aulton's pharmaceutics: the design and manufacture of medicines*, Churchill Livingstone.

Babusyte, A., Stravinskaite, K., Jeroch, J., Lotvall, J., Sakalauskas, R. & Sitkauskiene, B. 2007, "Patterns of airway inflammation and MMP-12 expression in smokers and ex-smokers with COPD", *Respir Res*, vol. 8, no. 1, pp. 81-89.

Bader, N. & Grune, T. 2006, "Protein oxidation and proteolysis", *Biological chemistry*, vol. 387, no. 10/11, pp. 1351-1355.

Baker, M.A., Cerniglia, G.J. & Zaman, A. 1990, "Microtiter plate assay for the measurement of glutathione and glutathione disulfide in large numbers of biological samples", *Analytical Biochemistry*, vol. 190, no. 2, pp. 360-365.

BAL Cooperative Group Steering Committee 1990, "Bronchoalveolar lavage constituents in healthy individuals, idiopathic pulmonary fibrosis, and selected comparison groups", *Am Rev Respir Dis*, vol. 141, pp. s169-s202.

Baldwin, D.R., Wise, R., Andrews, J.M. & Honeybourne, D. 1991, "Microlavage: a technique for determining the volume of epithelial lining fluid", *Thorax*, vol. 46, no. 9, pp. 658-662.

Bals, R. & Hiemstra, P.S. 2004, "Innate immunity in the lung: how epithelial cells fight against respiratory pathogens", *The European respiratory journal*, vol. 23, no. 2, pp. 327-333.

Balzar, S., Strand, M., Nakano, T. & Wenzel, S.E. 2006, "Subtle immunodeficiency in severe asthma: IgA and IgG2 correlate with lung function and symptoms", *International archives of allergy and immunology*, vol. 140, no. 2, pp. 96-102.

Bao, D. & Zhao, Y. 2010, "Building membrane emulsification into pulmonary drug delivery and targeting", *Pharmaceutical research*, vol. 27, no. 11, pp. 2505-2508.

Baraibar, M.A., Ladouce, R. & Friguet, B. 2013, "Proteomic quantification and identification of carbonylated proteins upon oxidative stress and during cellular aging", *Journal of proteomics*, vol. 92, pp. 63-70.

Barcelo, B., Pons, J., Ferrer, J.M., Sauleda, J., Fuster, A. & Agusti, A.G. 2008, "Phenotypic characterisation of T-lymphocytes in COPD: abnormal CD4+CD25+ regulatory T-lymphocyte response to tobacco smoking", *The European respiratory journal*, vol. 31, no. 3, pp. 555-562.

Bargagli, E., Olivieri, C., Prasse, A., Bianchi, N., Magi, B., Cianti, R., Bini, L. & Rottoli, P. 2008, "Calgranulin B (S100A9) levels in bronchoalveolar lavage fluid of patients with interstitial lung diseases", *Inflammation*, vol. 31, no. 5, pp. 351-354.

Barnes, P.J. & Liew, F. 1995, "Nitric oxide and asthmatic inflammation", *Immunology today*, vol. 16, no. 3, pp. 128-130.

Barnes, P.J. 2004, "Alveolar macrophages as orchestrators of COPD", *COPD: Journal of Chronic Obstructive Pulmonary Disease,* vol. 1, no. 1, pp. 59-70.

Barnes, P.J., Shapiro, S.D. & Pauwels, R.A. 2003, "Chronic obstructive pulmonary disease: molecular and cellular mechanisms", *The European respiratory journal,* vol. 22, no. 4, pp. 672-688.

Barreiro, E. 2014, "Protein carbonylation and muscle function in COPD and other conditions", *Mass spectrometry reviews,* vol. 33, no. 3, pp. 219-236.

Barreiro, E., De La Puente, B., Minguella, J., Corominas, J.M., Serrano, S., Hussain, S.N. & Gea, J. 2005, "Oxidative stress and respiratory muscle dysfunction in severe chronic obstructive pulmonary disease", *American journal of respiratory and critical care medicine,* vol. 171, no. 10, pp. 1116-1124.

Bauer, W., Gorny, M., Baumann, H. & Morell, A. 1985, "T-lymphocyte subsets and immunoglobulin concentrations in bronchoalveolar lavage of patients with sarcoidosis and high and low intensity alveolitis.", *The American Review of Respiratory Disease,* vol. 132, no. 5, pp. 1060.

Baughman, R. 1997, "The uncertainties of bronchoalveolar lavage", *European Respiratory Journal,* vol. 10, no. 9, pp. 1940.

Baveye, S., Elass, E., Mazurier, J., Spik, G. & Legrand, D. 1999, "Lactoferrin: a multifunctional glycoprotein involved in the modulation of the inflammatory process", *Clinical chemistry and laboratory medicine,* vol. 37, no. 3, pp. 281-286.

Beatty, K., Bieth, J. & Travis, J. 1980, "Kinetics of association of serine proteinases with native and oxidized alpha-1-proteinase inhibitor and alpha-1-antichymotrypsin", *The Journal of biological chemistry,* vol. 255, no. 9, pp. 3931-3934.

Beck, J.M., Young, V.B. & Huffnagle, G.B. 2012, "The microbiome of the lung", *Translational Research,* vol. 160, no. 4, pp. 258-266.

Beeh, K.M., Beier, J., Koppenhoefer, N. & Buhl, R. 2004, "Increased glutathione disulfide and nitrosothiols in sputum supernatant of patients with stable COPD", *CHEST Journal,* vol. 126, no. 4, pp. 1116-1122.

Behera, D., Balamugesh, T., Venkateswarlu, D., Gupta, A. & Majumdar, S. 2005, "Serum surfactant protein-A levels in chronic bronchitis and its relation to smoking", *Indian J Chest Dis Allied Sci,* vol. 47, no. 1, pp. 13-17.

Behndig, A.F., Blomberg, A., Helleday, R., Kelly, F.J. & Mudway, I.S. 2009, "Augmentation of respiratory tract lining fluid ascorbate concentrations through supplementation with vitamin C", *Inhalation toxicology,* vol. 21, no. 3, pp. 250-258.

Behndig, A., Blomberg, A., Roos-Engstrand, E. & Mudway, I. 2009, "Intracellular antioxidant enzyme differency in COPD reflects age-related declines in function, rather than disease state", *Respiratory medicine,* vol. 103, pp. S4.

Behndig, A.F., Blomberg, A., Helleday, R., Duggan, S.T., Kelly, F.J. & Mudway, I.S. 2009, "Antioxidant responses to acute ozone challenge in the healthy human airway", *Inhalation toxicology*, vol. 21, no. 11, pp. 933-942.

Bell, D., Haseman, J., Spock, A., McLennan, G. & Hook, G. 1981, "Plasma proteins of the bronchoalveolar surface of the lungs of smokers and nonsmokers.", *The American Review of Respiratory Disease*, vol. 124, no. 1, pp. 72.

Bell, D.Y. & Hook, G.E. 1979, "Pulmonary alveolar proteinosis: analysis of airway and alveolar proteins", *The American Review of Respiratory Disease*, vol. 119, no. 6, pp. 979-990.

Benlloch-Navarro, S., Franco, I., Sánchez-Vallejo, V., Silvestre, D., Romero, F.J. & Miranda, M. 2013, "Lipid peroxidation is increased in tears from the elderly", *Experimental eye research*, vol. 115, pp. 199-205.

Berlett, B.S. & Stadtman, E.R. 1997, "Protein oxidation in aging, disease, and oxidative stress", *The Journal of biological chemistry*, vol. 272, no. 33, pp. 20313-20316.

Bernard, A., Marchandise, F., Depelchin, S., Lauwerys, R. & Sibille, Y. 1992, "Clara cell protein in serum and bronchoalveolar lavage", *European Respiratory Journal*, vol. 5, no. 10, pp. 1231.

Bernard, A., Hermans, C. & Van Houte, G. 1997, "Transient increase of serum Clara cell protein (CC16) after exposure to smoke", *Occupational and environmental medicine*, vol. 54, no. 1, pp. 63-65.

Bernhard, W., Haslam, P.L. & Floros, J. 2004, "From birds to humans: new concepts on airways relative to alveolar surfactant", *American journal of respiratory cell and molecular biology*, vol. 30, no. 1, pp. 6-11.

Bertini, I. & Cavallaro, G. 2008, "Metals in the “omics” world: copper homeostasis and cytochrome c oxidase assembly in a new light", *JBIC Journal of Biological Inorganic Chemistry*, vol. 13, no. 1, pp. 3-14.

Betsuyaku, T., Nishimura, M., Takeyabu, K., Tanino, M., Venge, P., Xu, S. & Kawakami, Y. 2000, "Evidence for neutrophil involvement in the development of subclinical emphysema", *CHEST Journal*, vol. 117, no. 5_suppl_1, pp. 302S-303S.

Betsuyaku, T., Kuroki, Y., Nagai, K., Nasuhara, Y. & Nishimura, M. 2004, "Effects of ageing and smoking on SP-A and SP-D levels in bronchoalveolar lavage fluid", *The European respiratory journal*, vol. 24, no. 6, pp. 964-970.

Bihari, P., Vippola, M., Schultes, S., Praetner, M., Khandoga, A.G., Reichel, C.A., Coester, C., Tuomi, T., Rehberg, M. & Krombach, F. 2008, "Optimized dispersion of nanoparticles for biological in vitro and in vivo studies", *Particle and Fibre Toxicology*, vol. 5, no. 1, pp. 14.

Bito, R., Hino, S., Baba, A., Tanaka, M., Watabe, H. & Kawabata, H. 2005, "Degradation of oxidative stress-induced denatured albumin in rat liver endothelial cells", *American journal of physiology.Cell physiology*, vol. 289, no. 3, pp. C531-42.

Blacker, D., Wilcox, M.A., Laird, N.M., Rodes, L., Horvath, S.M., Go, R.C., Perry, R., Watson, B., Bassett, S.S. & McInnis, M.G. 1998, "Alpha-2 macroglobulin is genetically associated with Alzheimer disease", *Nature genetics*, vol. 19, no. 4, pp. 357-360.

Blanc, P.D., Iribarren, C., Trupin, L., Earnest, G., Katz, P.P., Balmes, J., Sidney, S. & Eisner, M.D. 2009, "Occupational exposures and the risk of COPD: dusty trades revisited", *Thorax*, vol. 64, no. 1, pp. 6-12.

Blomberg, A., Mudway, I., Nordenhäll, C., Hedenström, H., Kelly, F., Frew, A., Holgate, S. & Sandström, T. 1999, "Ozone- induced lung function decrements do not correlate with early airway inflammatory or antioxidant responses", *European respiratory journal*, vol. 13, no. 6, pp. 1418-1428.

Blomberg, A., Sainsbury, C., Rudell, B., Frew, A., Holgate, S., Sandströw, T. & Kelly, F. 1998, "Nasal cavity lining fluid ascorbic acid concentration increases in healthy human volunteers following short term exposure to diesel exhaust", *Free radical research*, vol. 28, no. 1, pp. 59-67.

Blomberg, A., Mudway, I., Svensson, M., Hagenbjork-Gustafsson, A., Thomasson, L., Helleday, R., Dumont, X., Forsberg, B., Nordberg, G. & Bernard, A. 2003, "Clara cell protein as a biomarker for ozone-induced lung injury in humans", *The European respiratory journal*, vol. 22, no. 6, pp. 883-888.

Bloom, B.T. & Clark, R.H. 2005, "Comparison of Infasurf (calfactant) and Survanta (beractant) in the prevention and treatment of respiratory distress syndrome", *Pediatrics*, vol. 116, no. 2, pp. 392-399.

Bloom, B.T., Kattwinkel, J., Hall, R.T., Delmore, P.M., Egan, E.A., Trout, J.R., Malloy, M.H., Brown, D.R., Holzman, I.R., Coghill, C.H., Carlo, W.A., Pramanik, A.K., McCaffree, M.A., Toubas, P.L., Laudert, S., Gratny, L.L., Weatherstone, K.B., Seguin, J.H., Willett, L.D., Gutcher, G.R., Mueller, D.H. & Topper, W.H. 1997, "Comparison of Infasurf (calf lung surfactant extract) to Survanta (Beractant) in the treatment and prevention of respiratory distress syndrome", *Pediatrics*, vol. 100, no. 1, pp. 31-38.

Bondarenko, P.V., Chelius, D. & Shaler, T.A. 2002, "Identification and Relative Quantitation of Protein Mixtures by Enzymatic Digestion Followed by Capillary Reversed-Phase Liquid Chromatography− Tandem Mass Spectrometry", *Anal.Chem*, vol. 74, no. 18, pp. 4741-4749.

Bonomo, L. & D'Addabbo, A. 1964, "Albumin turnover and loss of protein into the sputum in chronic bronchitis", *Clinica Chimica Acta*, vol. 10, no. 3, pp. 214-222.

Borm, P.J.A., Robbins, D., Haubold, S., Kuhlbusch, T., Fissan, H., Donaldson, K., Schins, R., Stone, V., Kreyling, W. & Lademann, J. 2006, "The potential risks of nanomaterials: a review carried out for ECETOC", *Particle and fibre toxicology*, vol. 3, no. 1, pp. 11.

Borm, P., Klaessig, F.C., Landry, T.D., Moudgil, B., Pauluhn, J., Thomas, K., Trottier, R. & Wood, S. 2006, "Research strategies for safety evaluation of nanomaterials, part V:

role of dissolution in biological fate and effects of nanoscale particles", *Toxicological sciences : an official journal of the Society of Toxicology,* vol. 90, no. 1, pp. 23-32.

Boutten, A., Venembre, P., Seta, N., Hamelin, J., Aubier, M., Durand, G. & Dehoux, M.S. 1998, "Oncostatin M is a potent stimulator of alpha1-antitrypsin secretion in lung epithelial cells: modulation by transforming growth factor-beta and interferon-gamma", *American journal of respiratory cell and molecular biology,* vol. 18, no. 4, pp. 511-520.

Braeckmans, K., Buyens, K., Bouquet, W., Vervaet, C., Joye, P., Vos, F.D., Plawinski, L., Doeuvre, L., Angles-Cano, E. & Sanders, N.N. 2010, "Sizing nanomatter in biological fluids by fluorescence single particle tracking", *Nano letters,* vol. 10, no. 11, pp. 4435-4442.

Braido, F., Riccio, A.M., Guerra, L., Gamalero, C., Zolezzi, A., Tarantini, F., Giovanni, B.D., Folli, C., Descalzi, D. & Canonica, G.W. 2007, "Clara cell 16 protein in COPD sputum: a marker of small airways damage?", *Respiratory medicine,* vol. 101, no. 10, pp. 2119-2124.

Brandli, O., Schindler, C., Kunzli, N., Keller, R. & Perruchoud, A.P. 1996, "Lung function in healthy never smoking adults: reference values and lower limits of normal of a Swiss population", *Thorax,* vol. 51, no. 3, pp. 277-283.

Brandsma, C.A., Kerstjens, H.A., van Geffen, W.H., Geerlings, M., Postma, D.S., Hylkema, M.N. & Timens, W. 2012, "Differential switching to IgG and IgA in active smoking COPD patients and healthy controls", *The European respiratory journal,* vol. 40, no. 2, pp. 313-321.

Brewer, G.J. 2007, "Iron and copper toxicity in diseases of aging, particularly atherosclerosis and Alzheimer's disease", *Experimental biology and medicine (Maywood, N.J.),* vol. 232, no. 2, pp. 323-335.

Broeckaert, F., Clippe, A., Knoops, B., Hermans, C. & Bernard, A. 2000, "Clara cell secretory protein (CC16): features as a peripheral lung biomarker", *Annals of the New York Academy of Sciences,* vol. 923, no. 1, pp. 68-77.

Brown, D.M., Wilson, M.R., MacNee, W., Stone, V. & Donaldson, K. 2001, "Size-dependent proinflammatory effects of ultrafine polystyrene particles: a role for surface area and oxidative stress in the enhanced activity of ultrafines", *Toxicology and applied pharmacology,* vol. 175, no. 3, pp. 191-199.

Brown, D., Roberts, N. & Donaldson, K. 1997, "Effect of coating with lung lining fluid on the ability of fibres to produce a respiratory burst in rat alveolar macrophages", *Toxicology in vitro,* vol. 12, no. 1, pp. 15-24.

Brugha, R.E., Mushtaq, N., Round, T., Gadhvi, D.H., Dundas, I., Gaillard, E., Koh, L., Fleming, L.J., Lewis, D.J., Sanak, M., Wood, H.E., Barratt, B., Mudway, I.S., Kelly, F.J., Griffiths, C.J. & Grigg, J. 2014, "Carbon in airway macrophages from children with asthma", *Thorax,* vol. 69, no. 7, pp. 654-659.

Brunk, U.T. & Terman, A. 2002, "The mitochondrial- lysosomal axis theory of aging", *European Journal of Biochemistry,* vol. 269, no. 8, pp. 1996-2002.

Buch, P., Langguth, P., Kataoka, M. & Yamashita, S. 2009, "IVIVC in oral absorption for fenofibrate immediate release tablets using a dissolution/permeation system", *Journal of pharmaceutical sciences,* vol. 98, no. 6, pp. 2001-2009.

Bur, M., Rothen-Rutishauser, B., Huwer, H. & Lehr, C. 2009, "A novel cell compatible impingement system to study in vitro drug absorption from dry powder aerosol formulations", *European Journal of Pharmaceutics and Biopharmaceutics,* vol. 72, no. 2, pp. 350-357.

Burgel, P.R., Paillasseur, J.L., Caillaud, D., Tillie-Leblond, I., Chanez, P., Escamilla, R., Court-Fortune, I., Perez, T., Carre, P., Roche, N. & Initiatives BPCO Scientific Committee 2010, "Clinical COPD phenotypes: a novel approach using principal component and cluster analyses", *The European respiratory journal,* vol. 36, no. 3, pp. 531-539.

Burnett, D. 1986, "Immunoglobulins in the lung.", *Thorax,* vol. 41, no. 5, pp. 337.

Burnett, D., Hill, S., Chamba, A. & Stockley, R. 1987, "Neutrophils from subjects with chronic obstructive lung disease show enhanced chemotaxis and extracellular proteolysis", *The Lancet,* vol. 330, no. 8567, pp. 1043-1046.

Burton, G.W., Joyce, A. & Ingold, K.U. 1983, "Is vitamin E the only lipid-soluble, chain-breaking antioxidant in human blood plasma and erythrocyte membranes?* 1", *Archives of Biochemistry and Biophysics,* vol. 221, no. 1, pp. 281-290.

Buttini, F., Grainger, C., Jones, S., Royall, P., Martin, P. & Forbes, B. 2008, "Characterization of particles emitted from two formulations of beclomethasone dipropionate solutoin metered dose inhalers", *RDD,* vol. 2, pp. 581-584.

Byers, D.E. & Holtzman, M.J. 2011, "Alternatively Activated Macrophages and Airway DiseaseMacrophages and Airway Disease", *CHEST Journal,* vol. 140, no. 3, pp. 768-774.

Campion, E.W., deLabry, L.O. & Glynn, R.J. 1988, "The effect of age on serum albumin in healthy males: report from the Normative Aging Study", *Journal of gerontology,* vol. 43, no. 1, pp. M18-20.

Campisi, J. 2005, "Senescent cells, tumor suppression, and organismal aging: good citizens, bad neighbors", *Cell,* vol. 120, no. 4, pp. 513-522.

Campisi, J. 2003, "Cellular senescence and apoptosis: how cellular responses might influence aging phenotypes", *Experimental gerontology,* vol. 38, no. 1, pp. 5-11.

Cantin, A., North, S., Hubbard, R. & Crystal, R. 1987, "Normal alveolar epithelial lining fluid contains high levels of glutathione", *Journal of applied physiology,* vol. 63, no. 1, pp. 152.

Cantin, A.M., Hubbard, R.C. & Crystal, R.G. 1989, "Glutathione deficiency in the epithelial lining fluid of the lower respiratory tract in idiopathic pulmonary fibrosis", *The American Review of Respiratory Disease,* vol. 139, no. 2, pp. 370-372.

Carlens, E. 1942, "Studies of Immunity in Cases of Pneumococcus Type 3 Otitis.: A Preliminary Report", *Acta Oto-Laryngologica,* vol. 30, no. 4, pp. 291-297.

Carney, J.M., Smith, C.D., Carney, A.M. & BUTTERFIELD, D. 1994, "Aging- and Oxygen- induced Modifications in Brain Biochemistry and Behaviora", *Annals of the New York Academy of Sciences,* vol. 738, no. 1, pp. 44-53.

Casals, C., Miguel, E. & Perez-Gil, J. 1993, "Tryptophan fluorescence study on the interaction of pulmonary surfactant protein A with phospholipid vesicles.", *Biochemical Journal,* vol. 296, no. Pt 3, pp. 585.

Casals, C. 2001, "Role of surfactant protein A (SP-A)/lipid interactions for SP-A functions in the lung", *Fetal & Pediatric Pathology,* vol. 20, no. 4, pp. 249-268.

Castellan, R.M., Olenchock, S.A., Kinsley, K.B. & Hankinson, J.L. 1987, "Inhaled endotoxin and decreased spirometric values", *New England Journal of Medicine,* vol. 317, no. 10, pp. 605-610.

Cecarini, V., Ding, Q. & Keller, J.N. 2007, "Oxidative inactivation of the proteasome in Alzheimer's disease", *Free radical research,* vol. 41, no. 6, pp. 673-680.

Chanez, P., Dent, G. and Yukawa, T. (1988). Increased eosinophil responsiveness to platelet-activating factor in asthma. *Clinical Science*, 74, pp.5P-5P.

Charrier, J.G. & Anastasio, C. 2010, "Impacts of antioxidants on hydroxyl radical production from individual and mixed transition metals in a surrogate lung fluid", *Atmospheric Environment,* .

Chelius, D., Zhang, T., Wang, G. & Shen, R. 2003, "Global protein identification and quantification technology using two-dimensional liquid chromatography nanospray mass spectrometry", *Analytical Chemistry,* vol. 75, no. 23, pp. 6658-6665.

Chen, J., Chen, Z., Narasaraju, T., Jin, N. & Liu, L. 2004, "Isolation of highly pure alveolar epithelial type I and type II cells from rat lungs", *Laboratory investigation,* vol. 84, no. 6, pp. 727-735.

Cheng, Z. & Li, Y. 2007, "What is responsible for the initiating chemistry of iron-mediated lipid peroxidation: an update", *Chemical reviews,* vol. 107, no. 3, pp. 748-766.

Cheng, G., Ueda, T., Numao, T., Kuroki, Y., Nakajima, H., Fukushima, Y., Motojima, S. & Fukuda, T. 2000, "Increased levels of surfactant protein A and D in bronchoalveolar lavage fluids in patients with bronchial asthma", *The European respiratory journal,* vol. 16, no. 5, pp. 831-835.

Cheng, K.C., Cahill, D.S., Kasai, H., Nishimura, S. & Loeb, L.A. 1992, "8-Hydroxyguanine, an abundant form of oxidative DNA damage, causes G----T and A----C substitutions", *The Journal of biological chemistry,* vol. 267, no. 1, pp. 166-172.

Chhabra, S.K. & Gupta, M. 2012, "Exhaled breath condensate analysis in chronic obstructive pulmonary disease.", .

Chithrani, B.D., Ghazani, A.A. & Chan, W.C. 2006, "Determining the size and shape dependence of gold nanoparticle uptake into mammalian cells", *Nano letters,* vol. 6, no. 4, pp. 662-668.

Choi, H.S., Liu, W., Misra, P., Tanaka, E., Zimmer, J.P., Ipe, B.I., Bawendi, M.G. & Frangioni, J.V. 2007, "Renal clearance of quantum dots", *Nature biotechnology,* vol. 25, no. 10, pp. 1165-1170.

Chuman, Y., Bergman, A., Ueno, T., Saito, S., Sakaguchi, K., Alaiya, A.A., Franzen, B., Bergman, T., Arnott, D., Auer, G., Appella, E., Jornvall, H. & Linder, S. 1999, "Napsin A, a member of the aspartic protease family, is abundantly expressed in normal lung and kidney tissue and is expressed in lung adenocarcinomas", *FEBS letters,* vol. 462, no. 1-2, pp. 129-134.

Chung, K.F. 2005, "Inflammatory mediators in chronic obstructive pulmonary disease", *Current Drug Targets-Inflammation & Allergy,* vol. 4, no. 6, pp. 619-625.

Churg, A. & Wright, J.L. 2005, "Proteases and emphysema", *Current opinion in pulmonary medicine,* vol. 11, no. 2, pp. 153-159.

Clements, J.A., Platzker, A.C.G., Tierney, D.F., Hobel, C.J., Creasy, R.K., Margolis, A.J., Thibeault, D.W., Tooley, W.H. & Oh, W. 1972, "Assessment of the risk of the respiratory-distress syndrome by a rapid test for surfactant in amniotic fluid", *New England Journal of Medicine,* vol. 286, no. 20, pp. 1077-1081.

Cluzel, M., Damon, M., Chanez, P., Bousquet, J., De Paulet, A.C., Michel, F. & Godard, P. 1987, "Enhanced alveolar cell luminol-dependent chemiluminescence in asthma* 1", *Journal of allergy and clinical immunology,* vol. 80, no. 2, pp. 195-201.

Comhair, S.A., Bhathena, P.R., Dweik, R.A., Kavuru, M. & Erzurum, S.C. 2000, "Rapid loss of superoxide dismutase activity during antigen-induced asthmatic response", *The Lancet,* vol. 355, no. 9204, pp. 624.

Comhair, S.A., Xu, W., Ghosh, S., Thunnissen, F.B., Almasan, A., Calhoun, W.J., Janocha, A.J., Zheng, L., Hazen, S.L. & Erzurum, S.C. 2005, "Superoxide dismutase inactivation in pathophysiology of asthmatic airway remodeling and reactivity", *The American journal of pathology,* vol. 166, no. 3, pp. 663-674.

Conrad, C.C., Choi, J., Malakowsky, C.A., Talent, J.M., Dai, R., Marshall, P. & Gracy, R.W. 2001, "Identification of protein carbonyls after two- dimensional electrophoresis", *Proteomics,* vol. 1, no. 7, pp. 829-834.

Cook, C.I. & Yu, B.P. 1998, "Iron accumulation in aging: modulation by dietary restriction", *Mechanisms of ageing and development,* vol. 102, no. 1, pp. 1-13.

Cooney, D., Kazantseva, M. & Hickey, A.J. 2004, "Development of a size-dependent aerosol deposition model utilising human airway epithelial cells for evaluating aerosol drug delivery", *Alternatives to Laboratory Animals : ATLA,* vol. 32, no. 6, pp. 581-590.

Corcoran, J.D., Berggren, P., Sun, B., Halliday, H.L., Robertson, B. & Curstedt, T. 1994, "Comparison of surface properties and physiological effects of a synthetic and a

natural surfactant in preterm rabbits", *Archives of disease in childhood.Fetal and neonatal edition*, vol. 71, no. 3, pp. F165-9.

Corhay, J., Henket, M., Nguyen, D., Duysinx, B., Sele, J. & Louis, R. 2009, "Leukotriene B4 contributes to exhaled breath condensate and sputum neutrophil chemotaxis in COPD", *CHEST Journal*, vol. 136, no. 4, pp. 1047-1054.

Crapo, J.D., Young, S.L., Fram, E.K., Pinkerton, K.E., Barry, B.E. & Crapo, R.O. 1983, "Morphometric characteristics of cells in the alveolar region of mammalian lungs", *The American Review of Respiratory Disease*, vol. 128, no. 2 Pt 2, pp. S42-6.

Creuwels, L., Van Golde, L. & Haagsman, H. 1997, "The pulmonary surfactant system: biochemical and clinical aspects", *Lung*, vol. 175, no. 1, pp. 1-39.

Cross, C.E., Motchnik, P.A., Bruener, B.A., Jones, D.A., Kaur, H., Ames, B.N. & Halliwell, B. 1992, "Oxidative damage to plasma constituents by ozone", *FEBS letters*, vol. 298, no. 2-3, pp. 269-272.

Cross, C.E., van der Vliet, A., Louie, S., Thiele, J.J. & Halliwell, B. 1998, "Oxidative stress and antioxidants at biosurfaces: plants, skin, and respiratory tract surfaces.", *Environmental health perspectives*, vol. 106, no. Suppl 5, pp. 1241.

Cross, C.E., van der Vliet, A., O'Neill, C.A., Louie, S. & Halliwell, B. 1994, "Oxidants, antioxidants, and respiratory tract lining fluids.", *Environmental health perspectives*, vol. 102, no. Suppl 10, pp. 185.

Crouch, E. & Wright, J.R. 2001, "Surfactant proteins A and D and pulmonary host defense", *Annual Review of Physiology*, vol. 63, no. 1, pp. 521-554.

Crouch, E.C. 1998, "Collectins and pulmonary host defense", *American journal of respiratory cell and molecular biology*, vol. 19, no. 2, pp. 177-201.

Cruz, M., Sánchez-Vidaurre, S., Romero, P., Morell, F. & Munoz, X. 2009, "Impact of age on pH, 8-isoprostane, and nitrogen oxides in exhaled breath condensate", *CHEST Journal*, vol. 135, no. 2, pp. 462-467.

Cucullo, L., Marchi, N., Marroni, M., Fazio, V., Namura, S. & Janigro, D. 2003, "Blood-brain barrier damage induces release of alpha2-macroglobulin", *Molecular & cellular proteomics : MCP*, vol. 2, no. 4, pp. 234-241.

Cuervo, A.M. & Dice, J.F. 2000, "Age-related decline in chaperone-mediated autophagy", *The Journal of biological chemistry*, vol. 275, no. 40, pp. 31505-31513.

Currais, A. & Maher, P. 2013, "Functional consequences of age-dependent changes in glutathione status in the brain", *Antioxidants & redox signaling*, vol. 19, no. 8, pp. 813-822.

Curstedt, T. & Johansson, J. 2006, "New synthetic surfactant - how and when?", *Biology of the neonate*, vol. 89, no. 4, pp. 336-339.

Curtis, J.L., Freeman, C.M. & Hogg, J.C. 2007, "The immunopathogenesis of chronic obstructive pulmonary disease: insights from recent research", *Proceedings of the American Thoracic Society,* vol. 4, no. 7, pp. 512-521.

Dalhamn, T. 1958, "The influence of some expectorants on the rate of ciliary beat in the trachea of living rats", *AMA archives of otolaryngology,* vol. 68, no. 1, pp. 20-21.

Dalle-Donne, I., Rossi, R., Giustarini, D., Milzani, A. & Colombo, R. 2003, "Protein carbonyl groups as biomarkers of oxidative stress", *Clinica Chimica Acta,* vol. 329, no. 1, pp. 23-38.

Daniele, R. 1990, "Immunoglobulin secretion in the airways", *Annual Review of Physiology,* vol. 52, no. 1, pp. 177-195.

Dargaville, P.A., South, M., Vervaart, P. & McDougall, P.N. 1999, "Validity of markers of dilution in small volume lung lavage", *American journal of respiratory and critical care medicine,* vol. 160, no. 3, pp. 778.

Darquenne, C., Harrington, L. & Prisk, G. 2009, "Alveolar duct expansion greatly enhances aerosol deposition: a three-dimensional computational fluid dynamics study", *Philosophical Transactions of the Royal Society A: Mathematical, Physical and Engineering Sciences,* vol. 367, no. 1896, pp. 2333.

Davies, N.M. & Feddah, M.R. 2003, "A novel method for assessing dissolution of aerosol inhaler products", *International journal of pharmaceutics,* vol. 255, no. 1, pp. 175-187.

Davis, W. & Pacht, E. 1991, "Extracellular antioxidant defenses", *The Lung: Sciencetific Foundations,* , pp. 2271-2278.

Daviskas, E., Anderson, S.D., Gomes, K., Briffa, P., Cochrane, B., Chan, H., Young, I.H. & Rubin, B.K. 2005, "Inhaled mannitol for the treatment of mucociliary dysfunction in patients with bronchiectasis: effect on lung function, health status and sputum", *Respirology,* vol. 10, no. 1, pp. 46-56.

De Jong, J., Van der Belt-Gritter, B., Koeter, G. & Postma, D. 1997, "Peripheral blood lymphocyte cell subsets in subjects with chronic obstructive pulmonary disease: association with smoking, IgE and lung function", *Respiratory medicine,* vol. 91, no. 2, pp. 67-76.

De Meringo, A., Morscheidt, C., Thélohan, S. & Tiesler, H. 1994, "In vitro assessment of biodurability: acellular systems.", *Environmental health perspectives,* vol. 102, no. Suppl 5, pp. 47.

Degen, W.G., van Kempen, L.C., Gijzen, E.G., van Groningen, J.J., van Kooyk, Y., Bloemers, H.P. & Swart, G.W. 1998, "MEMD, a new cell adhesion molecule in metastasizing human melanoma cell lines, is identical to ALCAM (activated leukocyte cell adhesion molecule)", *The American journal of pathology,* vol. 152, no. 3, pp. 805-813.

Dehner, C., Morales-Soto, N., Behera, R.K., Shrout, J., Theil, E.C., Maurice, P.A. & Dubois, J.L. 2013, "Ferritin and ferrihydrite nanoparticles as iron sources for

Pseudomonas aeruginosa", *JBIC Journal of Biological Inorganic Chemistry,* vol. 18, no. 3, pp. 371-381.

Dekhuijzen, P.N., Aben, K.K., Dekker, I., Aarts, L.P., Wielders, P.L., van Herwaarden, C.L. & Bast, A. 1996, "Increased exhalation of hydrogen peroxide in patients with stable and unstable chronic obstructive pulmonary disease", *American journal of respiratory and critical care medicine,* vol. 154, no. 3 Pt 1, pp. 813-816.

Demedts, I.K., Demoor, T., Bracke, K.R., Joos, G.F. & Brusselle, G.G. 2006, "Role of apoptosis in the pathogenesis of COPD and pulmonary emphysema", *Respir Res,* vol. 7, no. 1, pp. 53.

Di Stefano, A., Capelli, A., Lusuardi, M., Balbo, P., Vecchio, C., Maestrelli, P., Mapp, C.E., Fabbri, L.M., Donner, C.F. & Saetta, M. 1998, "Severity of airflow limitation is associated with severity of airway inflammation in smokers", *American journal of respiratory and critical care medicine,* vol. 158, no. 4, pp. 1277-1285.

Di Stefano, A., Caramori, G., Oates, T., Capelli, A., Lusuardi, M., Gnemmi, I., Ioli, F., Chung, K.F., Donner, C.F., Barnes, P.J. & Adcock, I.M. 2002, "Increased expression of nuclear factor-kappaB in bronchial biopsies from smokers and patients with COPD", *The European respiratory journal,* vol. 20, no. 3, pp. 556-563.

Di Stefano, A., Turato, G., Maestrelli, P., Mapp, C.E., Ruggieri, M.P., Roggeri, A., Boschetto, P., Fabbri, L.M. & Saetta, M. 1996, "Airflow limitation in chronic bronchitis is associated with T-lymphocyte and macrophage infiltration of the bronchial mucosa", *American journal of respiratory and critical care medicine,* vol. 153, no. 2, pp. 629-632.

Do, T., Chiang, S., Ward, R., Heldt, G., Fujii, G. & Ernst, W. 2014, "Evaluation Of A Synthetic Lung Surfactant For Neonatal Respiratory Distress Syndrome", *Am J Respir Crit Care Med,* vol. 189, pp. A6656.

Doll, R., Peto, R., Boreham, J. & Sutherland, I. 2004, "Mortality in relation to smoking: 50 years' observations on male British doctors", *BMJ (Clinical research ed.),* vol. 328, no. 7455, pp. 1519.

Dolovich, M. 1989, "Physical principles underlying aerosol therapy", *Journal of aerosol medicine,* vol. 2, no. 2, pp. 171-186.

Doshi, N. & Mitragotri, S. 2010, "Macrophages recognize size and shape of their targets", *PLoS One,* vol. 5, no. 4, pp. e10051.

Doyle, I.R., Bersten, A.D. & Nicholas, T.E. 1997, "Surfactant proteins-A and-B are elevated in plasma of patients with acute respiratory failure", *American journal of respiratory and critical care medicine,* vol. 156, no. 4, pp. 1217.

Dozor, A.J. 2010, "The role of oxidative stress in the pathogenesis and treatment of asthma", *Annals of the New York Academy of Sciences,* vol. 1203, no. 1, pp. 133-137.

Dressman, J.B., Amidon, G.L., Reppas, C. & Shah, V.P. 1998, "Dissolution testing as a prognostic tool for oral drug absorption: immediate release dosage forms", *Pharmaceutical research,* vol. 15, no. 1, pp. 11-22.

Dubin, W., Martin, T.R., Swoueland, P., Leturcq, D.J., Moriarty, A.M., Tobias, P.S., Bleecker, E.R., Goldblum, S.E. & Hasday, J.D. 1996, "Asthma and endotoxin: lipopolysaccharide-binding protein and soluble CD14 in bronchoalveolar compartment", *American Journal of Physiology-Lung Cellular and Molecular Physiology*, vol. 14, no. 5, pp. L736.

Duddridge, M., Kelly, C., Fenwick, J., Hendrick, D. & Walters, E. 1988, "Assessment of mixing between sequential aliquots during bronchoalveolar lavage", *Thorax*, vol. 43, pp. 822–823.

Dwyer, T. 2003, "Urea: an estimate of airway surface liquid (ASL) dilution in expired breath condensate (EBC)", *Am J Respir Crit Care Med*, vol. 167, pp. A425.

Dyer, C. 2012, "The interaction of ageing and lung disease", *Chronic respiratory disease*, vol. 9, no. 1, pp. 63-67.

Effros, R.M. 2010, "Exhaled Breath Condensate", *Chest*, vol. 138, no. 3, pp. 471.

Effros, R.M., Biller, J., Foss, B., Hoagland, K., Dunning, M.B., Castillo, D., Bosbous, M., Sun, F. & Shaker, R. 2003, "A simple method for estimating respiratory solute dilution in exhaled breath condensates", *American journal of respiratory and critical care medicine*, vol. 168, no. 12, pp. 1500.

Effros, R.M., Feng, N., Mason, G., Sietsema, K., Silverman, P. & Hukkanen, J. 1990, "Solute concentrations of the pulmonary epithelial lining fluid of anesthetized rats", *Journal of applied physiology*, vol. 68, no. 1, pp. 275.

Effros, R.M., Hoagland, K.W., Bosbous, M., Castillo, D., Foss, B., Dunning, M., Gare, M., Lin, W. & Sun, F. 2002, "Dilution of respiratory solutes in exhaled condensates", *American journal of respiratory and critical care medicine*, vol. 165, no. 5, pp. 663.

Eggleton, P. & Reid, K. 1999, "Lung surfactant proteins involved in innate immunity", *Current opinion in immunology*, vol. 11, no. 1, pp. 28-33.

Eixarch, H., Haltner-Ukomadu, E., Beisswenger, C. & Bock, U. 2010, "Drug delivery to the lung: permeability and physicochemical characteristics of drugs as the basis for a pulmonary biopharmaceutical classification system (pBCS)", *Journal of Epithelial Biology and Pharmacology*, vol. 3, pp. 1-14.

el-Kholy, M.S., Gas Allah, M.A., el-Shimi, S., el-Baz, F., el-Tayeb, H. & Abdel-Hamid, M.S. 1990, "Zinc and copper status in children with bronchial asthma and atopic dermatitis", *The Journal of the Egyptian Public Health Association*, vol. 65, no. 5-6, pp. 657-668.

Ellison, R.T.,3rd & Giehl, T.J. 1991, "Killing of gram-negative bacteria by lactoferrin and lysozyme", *The Journal of clinical investigation*, vol. 88, no. 4, pp. 1080-1091.

El-Sherbiny, I.M. 2010, "Enhanced pH-responsive carrier system based on alginate and chemically modified carboxymethyl chitosan for oral delivery of protein drugs: Preparation and in-vitro assessment", *Carbohydrate Polymers*, vol. 80, no. 4, pp. 1125-1136.

Epithelix.com, (2014). *Epithelix Sarl – MucilAir™*. [online] Available at: http://www.epithelix.com/content/view/6/5/lang,en/ [Accessed 8 Sep. 2014].

Erbaycu, A.E., Ucar, H., Gulpek, M., Tuksavul, F., Kalenci, D. & Guclu, S. 2007, "The contribution of serum ferritin, iron, iron binding capacity and bronchoalveolar lavage ferritin levels in differential diagnosis of lung cancer from benign pulmonary diseases", *ULUSLARARASI HEMATOLOJI VE ONKOLOJI DERGISI*, vol. 17, no. 3, pp. 129.

Eriksson, S. 1965, "Studies in alpha 1-antitrypsin deficiency", *Acta medica Scandinavica.Supplementum*, vol. 432, pp. 1-85.

Ermis, B., Armutcu, F., Gurel, A., Kart, L., Demircan, N., Altin, R. & Demirel, F. 2004, "Trace elements status in children with bronchial asthma", .

Erzurum, S.C., Danel, C., Gillissen, A., Chu, C., Trapnell, B.C. & Crystal, R.G. 1993, "In vivo antioxidant gene expression in human airway epithelium of normal individuals exposed to 100% O~ 2", *Journal of applied physiology*, vol. 75, pp. 1256-1256.

Esmailpour, N., Hogger, P., Rabe, K., Heitmann, U., Nakashima, M. & Rohdewald, P. 1997, "Distribution of inhaled fluticasone propionate between human lung tissue and serum in vivo", *European Respiratory Journal*, vol. 10, no. 7, pp. 1496.

Esther, C.R., Boysen, G., Olsen, B.M., Collins, L.B., Ghio, A.J., Swenberg, J.W. & Boucher, R.C. 2009, "Mass spectrometric analysis of biomarkers and dilution markers in exhaled breath condensate reveals elevated purines in asthma and cystic fibrosis", *American Journal of Physiology-Lung Cellular and Molecular Physiology*, vol. 296, no. 6, pp. L987.

Evans, M., Cabral-Anderson, L. and Freeman, G. (1978). Role of the Clara cell in the renewal of the terminal bronchiolar epithelium in the rat. *Laboratory Investigation*, 38, p.648455.

Evans, M.D. & Cooke, M.S. 2004, "Factors contributing to the outcome of oxidative damage to nucleic acids", *Bioessays*, vol. 26, no. 5, pp. 533-542.

Fahy, J.V. 2009, "Eosinophilic and neutrophilic inflammation in asthma: insights from clinical studies", *Proceedings of the American Thoracic Society*, vol. 6, no. 3, pp. 256-259.

Fahy, J.V. & Dickey, B.F. 2010, "Airway mucus function and dysfunction", *New England Journal of Medicine*, vol. 363, no. 23, pp. 2233-2247.

Feng, N., Hacker, A. & Effros, R.M. 1992, "Solute exchange between the plasma and epithelial lining fluid of rat lungs", *Journal of applied physiology*, vol. 72, no. 3, pp. 1081.

Fernandez-Real, J. & Pickup, J. 2012, "Innate immunity, insulin resistance and type 2 diabetes", *Diabetologia*, vol. 55, no. 2, pp. 273-278.

Fiegel, J., Ehrhardt, C., Schaefer, U.F., Lehr, C. & Hanes, J. 2003, "Large porous particle impingement on lung epithelial cell monolayers—toward improved particle characterization in the lung", *Pharmaceutical research,* vol. 20, no. 5, pp. 788-796.

Finkbeiner, W.E. 1999, "Physiology and pathology of tracheobronchial glands", *Respiration physiology,* vol. 118, no. 2, pp. 77-83.

Finkelstein, R., Fraser, R.S., Ghezzo, H. & Cosio, M.G. 1995, "Alveolar inflammation and its relation to emphysema in smokers", *American journal of respiratory and critical care medicine,* vol. 152, no. 5 Pt 1, pp. 1666-1672.

Finkelstein, R., Fraser, R.S., Ghezzo, H. & Cosio, M.G. 1995, "Alveolar inflammation and its relation to emphysema in smokers", *American journal of respiratory and critical care medicine,* vol. 152, no. 5 Pt 1, pp. 1666-1672.

Fischer, A.J., Goss, K.L., Scheetz, T.E., Wohlford-Lenane, C.L., Snyder, J.M. & McCray Jr, P.B. 2009, "Differential gene expression in human conducting airway surface epithelia and submucosal glands", *American journal of respiratory cell and molecular biology,* vol. 40, no. 2, pp. 189.

Fischer, B.M., Pavlisko, E. & Voynow, J.A. 2011, "Pathogenic triad in COPD: oxidative stress, protease-antiprotease imbalance, and inflammation", *International journal of chronic obstructive pulmonary disease,* vol. 6, pp. 413-421.

Fitzpatrick, A.M., Teague, W.G., Burwell, L., Brown, M.S. & Brown, L.A.S. 2011, "Glutathione oxidation is associated with airway macrophage functional impairment in children with severe asthma", *Pediatric research,* vol. 69, no. 2, pp. 154-159.

Fitzpatrick, A.M., Teague, W.G., Holguin, F., Yeh, M. & Brown, L.A.S. 2009, "Airway glutathione homeostasis is altered in children with severe asthma: evidence for oxidant stress", *Journal of Allergy and Clinical Immunology,* vol. 123, no. 1, pp. 146-152. e8.

Flatt, A., Pearce, N., Thomson, C.D., Sears, M.R., Robinson, M.F. & Beasley, R. 1990, "Reduced selenium in asthmatic subjects in New Zealand", *Thorax,* vol. 45, no. 2, pp. 95-99.

Fleming, A. & Allison, V. 1922, "Observations on a bacteriolytic substance (“lysozyme”) found in secretions and tissues", *British journal of experimental pathology,* vol. 3, no. 5, pp. 252.

Fletcher, C. & Peto, R. 1977, "The natural history of chronic airflow obstruction", *British medical journal,* vol. 1, no. 6077, pp. 1645-1648.

Folkerts, G., Busse, W.W., Nijkamp, F.P., Sorkness, R. & Gern, J.E. 1998, "Virus-induced airway hyperresponsiveness and asthma", *American journal of respiratory and critical care medicine,* vol. 157, no. 6, pp. 1708-1720.

Folkesson, H., Matthay, M., Westrom, B., Kim, K., Karlsson, B. & Hastings, R. 1996, *Journal of applied physiology,* vol. 80, no. 5, pp. 1431.

Forbes, B. 2000, "Human airway epithelial cell lines for in vitro drug transport and metabolism studies", *Pharmaceutical science & technology today*, vol. 3, no. 1, pp. 18-27.

Forbes, B., Asgharian, B., Dailey, L.A., Ferguson, D., Gerde, P., Gumbleton, M., Gustavsson, L., Hardy, C., Hassall, D. & Jones, R. 2010, "Challenges in inhaled product development and opportunities for open innovation", *Advanced Drug Delivery Reviews*, .

Forbes, B. & Ehrhardt, C. 2005, "Human respiratory epithelial cell culture for drug delivery applications", *European journal of pharmaceutics and biopharmaceutics*, vol. 60, no. 2, pp. 193-205.

Forbes, B., Shah, A., Martin, G.P. & Lansley, A.B. 2003, "The human bronchial epithelial cell line 16HBE14o− as a model system of the airways for studying drug transport", *International journal of pharmaceutics*, vol. 257, no. 1, pp. 161-167.

Forster, M.J., Dubey, A., Dawson, K.M., Stutts, W.A., Lal, H. & Sohal, R.S. 1996, "Age-related losses of cognitive function and motor skills in mice are associated with oxidative protein damage in the brain", *Proceedings of the National Academy of Sciences of the United States of America*, vol. 93, no. 10, pp. 4765-4769.

Foster, K.A., Oster, C.G., Mayer, M.M., Avery, M.L. & Audus, K.L. 1998, "Characterization of the A549 cell line as a type II pulmonary epithelial cell model for drug metabolism", *Experimental cell research*, vol. 243, no. 2, pp. 359-366.

Foucaud, L., Wilson, M., Brown, D. & Stone, V. 2007, "Measurement of reactive species production by nanoparticles prepared in biologically relevant media", *Toxicology letters*, vol. 174, no. 1, pp. 1-9.

Frei, B., Stocker, R. & Ames, B. 1992, "Small molecule antioxidant defenses in human extracellular fluids", *Molecular biology of free radical scavenging systems*, , pp. 23-45.

Friend, D.S., Papahadjopoulos, D. & Debs, R.J. 1996, "Endocytosis and intracellular processing accompanying transfection mediated by cationic liposomes", *Biochimica et Biophysica Acta (BBA)-Biomembranes*, vol. 1278, no. 1, pp. 41-50.

Fruth, K., Best, N., Amro, M., Ingel, K., Gosepath, J., Mann, W.J. & Brieger, J. 2011, "No evidence for a correlation of glutathione S-tranferase polymorphisms and chronic rhinosinusitis", *Rhinology*, vol. 49, no. 2, pp. 180-184.

Furumoto, K., Ogawara, K., Yoshida, M., Takakura, Y., Hashida, M., Higaki, K. & Kimura, T. 2001, "Biliary excretion of polystyrene microspheres depends on the type of receptor-mediated uptake in rat liver", *Biochimica et Biophysica Acta (BBA)-General Subjects*, vol. 1526, no. 2, pp. 221-226.

Gabazza, E., Taguchi, O., Tamaki, S., Takeya, H., Kobayashi, H., Yasui, H., Kobayashi, T., Hataji, O., Urano, H. & Zhou, H. 1999, "Thrombin in the airways of asthmatic patients", *Lung*, vol. 177, no. 4, pp. 253-262.

Gadek, J., Fells, G., Zimmerman, R., Rennard, S. & Crystal, R. 1981, "Antielastases of the human alveolar structures. Implications for the protease-antiprotease theory of emphysema.", *Journal of Clinical Investigation,* vol. 68, no. 4, pp. 889.

Gerson, C., Sabater, J., Scuri, M., Torbati, A., Coffey, R., Abraham, J.W., Lauredo, I., Forteza, R., Wanner, A. & Salathe, M. 2000, "The lactoperoxidase system functions in bacterial clearance of airways", *American journal of respiratory cell and molecular biology,* vol. 22, no. 6, pp. 665-671.

Ghafouri, B., Irander, K., Lindbom, J., Tagesson, C. & Lindahl, M. 2006, "Comparative proteomics of nasal fluid in seasonal allergic rhinitis", *Journal of proteome research,* vol. 5, no. 2, pp. 330-338.

Ghio, A.J. 2009, "Disruption of iron homeostasis and lung disease", *Biochimica et Biophysica Acta (BBA)-General Subjects,* vol. 1790, no. 7, pp. 731-739.

Ghio, A.J., Hilborn, E.D., Stonehuerner, J.G., Dailey, L.A., Carter, J.D., Richards, J.H., Crissman, K.M., Foronjy, R.F., Uyeminami, D.L. & Pinkerton, K.E. 2008, "Particulate matter in cigarette smoke alters iron homeostasis to produce a biological effect", *American journal of respiratory and critical care medicine,* vol. 178, no. 11, pp. 1130-1138.

Ghio, A.J., Pritchard, R.J., Dittrich, K.L. & Samet, J.M. 1997, "Non-heme (Fe< sup> 3 </sup>) in the lung increases with age in both humans and rats", *Journal of Laboratory and Clinical Medicine,* vol. 129, no. 1, pp. 53-61.

Ghio, A.J., Turi, J.L., Madden, M.C., Dailey, L.A., Richards, J.D., Stonehuerner, J.G., Morgan, D.L., Singleton, S., Garrick, L.M. & Garrick, M.D. 2007, "Lung injury after ozone exposure is iron dependent", *American journal of physiology.Lung cellular and molecular physiology,* vol. 292, no. 1, pp. L134-43.

Giard, D.J., Aaronson, S.A., Todaro, G.J., Arnstein, P., Kersey, J.H., Dosik, H. & Parks, W.P. 1973, "In vitro cultivation of human tumors: establishment of cell lines derived from a series of solid tumors", *Journal of the National Cancer Institute,* vol. 51, no. 5, pp. 1417-1423.

Ginasthma.org, (2014). *2006 Revision: GINA Report, Global Strategy for Asthma Management and Prevention | Variants | GINA*. [online] Available at: http://www.ginasthma.org/documents/5/documents_variants/31 [Accessed 28 Sep. 2014].

Gillooly, M. & Lamb, D. 1993, "Airspace size in lungs of lifelong non-smokers: effect of age and sex", *Thorax,* vol. 48, no. 1, pp. 39-43.

Goerke, J. 1998, "Pulmonary surfactant: functions and molecular composition", *Biochimica et Biophysica Acta (BBA)-Molecular Basis of Disease,* vol. 1408, no. 2-3, pp. 79-89.

Goodman, R.M., Yergin, B.M., Landa, J.F., Golivanux, M.H. & Sackner, M.A. 1978, "Relationship of smoking history and pulmonary function tests to tracheal mucous

velocity in nonsmokers, young smokers, ex-smokers, and patients with chronic bronchitis", *The American Review of Respiratory Disease,* vol. 117, no. 2, pp. 205-214.

Gorska, K., Krenke, R., Domagala-Kulawik, J., Korczynski, P., Nejman-Gryz, P., Kosciuch, J., Hildebrand, K. & Chazan, R. 2008, "Comparison of cellular and biochemical markers of airway inflammation in patients with mild-to-moderate asthma and chronic obstructive pulmonary disease: an induced sputum and bronchoalveolar lavage fluid study", *J Physiol Pharmacol,* vol. 59, no. Suppl 6, pp. 271-283.

Grainger, C., Greenwell, L., Martin, G. & Forbes, B. 2009, "The permeability of large molecular weight solutes following particle delivery to air-interfaced cells that model the respiratory mucosa", *European Journal of Pharmaceutics and Biopharmaceutics,* vol. 71, no. 2, pp. 318-324.

Gratton, S.E., Ropp, P.A., Pohlhaus, P.D., Luft, J.C., Madden, V.J., Napier, M.E. & DeSimone, J.M. 2008, "The effect of particle design on cellular internalization pathways", *Proceedings of the National Academy of Sciences of the United States of America,* vol. 105, no. 33, pp. 11613-11618.

Gray, V., Hickey, A., Balmer, P., Davies, N., Dunbar, C., Foster, T., Olsson, B., Sakagami, M., Shah, V. & Smurthwaite, M. 2008, "The inhalation ad hoc advisory panel for the USP performance tests of inhalation dosage forms", *Pharmacopeial Forum,* pp. 1068.

Griffith, O.W. & Meister, A. 1979, "Translocation of intracellular glutathione to membrane-bound gamma-glutamyl transpeptidase as a discrete step in the gamma-glutamyl cycle: glutathionuria after inhibition of transpeptidase", *Proceedings of the National Academy of Sciences of the United States of America,* vol. 76, no. 1, pp. 268-272.

Gross, N.J., Barnes, E. & Narine, K. 1988, "Recycling of surfactant in black and beige mice: pool sizes and kinetics", *Journal of applied physiology,* vol. 64, no. 5, pp. 2017.

Gutteridge, J., Mumby, S., Quinlan, G., Chung, K. & Evans, T. 1996, "Pro-oxidant iron is present in human pulmonary epithelial lining fluid: implications for oxidative stress in the lung", *Biochemical and biophysical research communications,* vol. 220, no. 3, pp. 1024-1027.

Gyetko, M.R. & Toews, G.B. 1993, "Immunology of the aging lung", *Clinics in chest medicine,* vol. 14, no. 3, pp. 379-391.

Haagsman, H.P. 2002, "Structural and functional aspects of the collectin SP-A", *Immunobiology,* vol. 205, no. 4, pp. 476-489.

Halliwell, B. & Chirico, S. 1993, "Lipid peroxidation: its mechanism, measurement, and significance", *The American Journal of Clinical Nutrition,* vol. 57, no. 5 Suppl, pp. 715S-724S; discussion 724S-725S.

Hamm, H., Lührs, J., y Rotaeche, J.G., Costabel, U., Fabel, H. & Bartsch, W. 1994, "Elevated surfactant protein A in bronchoalveolar lavage fluids from sarcoidosis and

hypersensitivity pneumonitis patients", *CHEST Journal*, vol. 106, no. 6, pp. 1766-1770.

Hansel, T.T., Johnston, S.L. & Openshaw, P.J. 2013, "Microbes and mucosal immune responses in asthma", *The Lancet*, vol. 381, no. 9869, pp. 861-873.

Harman, D. 1956, "Aging: a theory based on free radical and radiation chemistry", *Journal of gerontology*, vol. 11, no. 3, pp. 298-300.

Harrington, A.D., Hylton, S. & Schoonen, M.A. 2012, "Pyrite-driven reactive oxygen species formation in simulated lung fluid: implications for coal workers' pneumoconiosis", *Environmental Geochemistry and Health*, vol. 34, no. 4, pp. 527-538.

Haslam, P. & Baughman, R. 1999, "Report of ERS Task Force: guidelines for measurement of acellular components and standardization of BAL", *European Respiratory Journal*, vol. 14, no. 2, pp. 245.

Hastings, R.H., Grady, M., Sakuma, T. & Matthay, M.A. 1992, "Clearance of different-sized proteins from the alveolar space in humans and rabbits", *Journal of applied physiology*, vol. 73, no. 4, pp. 1310.

Hatch, G. 1992, "Comparative biochemistry of airway lining fluid", *Treatise on pulmonary toxicology*, vol. 1, pp. 617-632.

Hawgood, S. & Poulain, F.R. 2001, "The pulmonary collectins and surfactant metabolism", *Annual Review of Physiology*, vol. 63, no. 1, pp. 495-519.

Hayflick, L. 1987, "Origins of longevity", *Modern biological theories of aging.Raven, New York, ,* pp. 21-34.

Heeley, E.L., Hohlfeld, J.M., Krug, N. & Postle, A.D. 2000, "Phospholipid molecular species of bronchoalveolar lavage fluid after local allergen challenge in asthma", *American journal of physiology.Lung cellular and molecular physiology*, vol. 278, no. 2, pp. L305-11.

Hein, S., Bur, M., Schaefer, U.F. & Lehr, C. 2011, "A new pharmaceutical aerosol deposition device on cell cultures (PADDOCC) to evaluate pulmonary drug absorption for metered dose dry powder formulations", *European Journal of Pharmaceutics and Biopharmaceutics*, vol. 77, no. 1, pp. 132-138.

Heinrich, S., Hartl, D. & Griese, M. 2006, "Surfactant protein A-from genes to human lung diseases", *Current medicinal chemistry*, vol. 13, no. 27, pp. 3239-3252.

Heizmann, C.W. & Cox, J.A. 1998, "New perspectives on S100 proteins: a multi-functional Ca 2 -, Zn 2 -and Cu 2 -binding protein family", *Biometals*, vol. 11, no. 4, pp. 383-397.

Hermans, C., Aly, O., Nyberg, B.I., Peterson, C. & Bernard, A. 1998, "Determinants of Clara cell protein (CC16) concentration in serum: a reassessment with two different immunoassays", *Clinica chimica acta*, vol. 272, no. 2, pp. 101-110.

Hermans, C. & Bernard, A. 1996, "Clara cell protein (CC16): characteristics and potential applications as biomarker of lung toxicity", *Biomarkers,* vol. 1, no. 1, pp. 3-8.

Hermans, C., Knoops, B., Wiedig, M., Arsalane, K., Toubeau, G., Falmagne, P. & Bernard, A. 1999, "Clara cell protein as a marker of Clara cell damage and bronchoalveolar blood barrier permeability", *European Respiratory Journal,* vol. 13, no. 5, pp. 1014-1021.

Hermans, C. & Bernard, A. 1999, "Lung epithelium–specific proteins: characteristics and potential applications as markers", *American Journal of Respiratory and Critical Care Medicine,* vol. 159, no. 2, pp. 646-678.

Hernandez, M., Zhou, H., Zhou, B., Robinette, C., Crissman, K., Hatch, G., Alexis, N.E. & Peden, D. 2009, "Combination treatment with high-dose vitamin C and alpha-tocopherol does not enhance respiratory-tract lining fluid vitamin C levels in asthmatics", *Inhalation toxicology,* vol. 21, no. 3, pp. 173-181.

Herting, G., Odnevall Wallinder, I. & Leygraf, C. 2006, "Factors that influence the release of metals from stainless steels exposed to physiological media", *Corrosion Science,* vol. 48, no. 8, pp. 2120-2132.

Heyder, J. 2004, "Deposition of inhaled particles in the human respiratory tract and consequences for regional targeting in respiratory drug delivery", *Proceedings of the American Thoraic Society*Am Thoracic Soc, , pp. 315.

Hills, B.A. 1988, *The biology of surfactant,* Cambridge Univ Pr.

Hilty, M., Burke, C., Pedro, H., Cardenas, P., Bush, A., Bossley, C., Davies, J., Ervine, A., Poulter, L. & Pachter, L. 2010, "Disordered microbial communities in asthmatic airways", *PloS one,* vol. 5, no. 1, pp. e8578.

Hoffmann, P. 2008, "Selenium and asthma: a complex relationship", *Allergy,* vol. 63, no. 7, pp. 854-856.

Hogg, J.C., Chu, F., Utokaparch, S., Woods, R., Elliott, W.M., Buzatu, L., Cherniack, R.M., Rogers, R.M., Sciurba, F.C. & Coxson, H.O. 2004, "The nature of small-airway obstruction in chronic obstructive pulmonary disease", *New England Journal of Medicine,* vol. 350, no. 26, pp. 2645-2653.

Hogg, J.C. & Timens, W. 2009, "The pathology of chronic obstructive pulmonary disease", *Annual Review of Pathological Mechanical Disease,* vol. 4, pp. 435-459.

Höhn, A., König, J. & Grune, T. 2013, "Protein oxidation in aging and the removal of oxidized proteins", *Journal of proteomics,* vol. 92, pp. 132-159.

Holgate, S.T. 2012, "Innate and adaptive immune responses in asthma", *Nature medicine,* vol. 18, no. 5, pp. 673-683.

Holter, J.F., Weiland, J.E., Pacht, E.R., Gadek, J.E. & Davis, W.B. 1986, "Protein permeability in the adult respiratory distress syndrome. Loss of size selectivity of the alveolar epithelium.", *Journal of Clinical Investigation,* vol. 78, no. 6, pp. 1513.

Honda, Y., Takahashi, H., Kuroki, Y., Akino, T. & Abe, S. 1996, "Decreased contents of surfactant proteins A and D in BAL fluids of healthy smokers", *CHEST Journal,* vol. 109, no. 4, pp. 1006-1009.

Hoskins, A., Wu, P., Reiss, S. & Dworski, R. 2013, "Glutathione S- transferase P1 Ile105Val polymorphism modulates allergen- induced airway inflammation in human atopic asthmatics in vivo", *Clinical & Experimental Allergy,* vol. 43, no. 5, pp. 527-534.

Housley, D.G., Mudway, I., Kelly, F.J., Eccles, R. & Richards, R.J. 1995, "Depletion of urate in human nasal lavage following in vitro ozone exposure", *The international journal of biochemistry & cell biology,* vol. 27, no. 11, pp. 1153-1159.

Huang, Y.J. 2013, "Asthma microbiome studies and the potential for new therapeutic strategies", *Current allergy and asthma reports,* vol. 13, no. 5, pp. 453-461.

Huang, Y.J., Nelson, C.E., Brodie, E.L., DeSantis, T.Z., Baek, M.S., Liu, J., Woyke, T., Allgaier, M., Bristow, J. & Wiener-Kronish, J.P. 2011, "Airway microbiota and bronchial hyperresponsiveness in patients with suboptimally controlled asthma", *Journal of Allergy and Clinical Immunology,* vol. 127, no. 2, pp. 372-381. e3.

Hye, A., Lynham, S., Thambisetty, M., Causevic, M., Campbell, J., Byers, H.L., Hooper, C., Rijsdijk, F., Tabrizi, S.J., Banner, S., Shaw, C.E., Foy, C., Poppe, M., Archer, N., Hamilton, G., Powell, J., Brown, R.G., Sham, P., Ward, M. & Lovestone, S. 2006, "Proteome-based plasma biomarkers for Alzheimer's disease", *Brain : a journal of neurology,* vol. 129, no. Pt 11, pp. 3042-3050.

Ikeda, S. 1968, "YanaiN", *IshikanaS.: Flexible bronchofiberscope.Keio JMed,* vol. 17, pp. 1-16.

Ingels, F., Deferme, S., Destexhe, E., Oth, M., Van den Mooter, G. & Augustijns, P. 2002, "Simulated intestinal fluid as transport medium in the Caco-2 cell culture model", *International journal of pharmaceutics,* vol. 232, no. 1, pp. 183-192.

Iriyama, K., Yoshiura, M., Iwamoto, T. & Ozaki, Y. 1984, "Simultaneous determination of uric and ascorbic acids in human serum by reversed-phase high-performance liquid chromatography with electrochemical detection", *Analytical Biochemistry,* vol. 141, no. 1, pp. 238-243.

Ishikawa, N., Ohlmeier, S., Salmenkivi, K., Myllärniemi, M., Rahman, I., Mazur, W. & Kinnula, V.L. 2010, "Hemoglobin a and b are ubiquitous in the human lung, decline in idiopathic pulmonary fibrosis but not in COPD", *Respir Res,* vol. 11, no. 1, pp. 123-124.

Ishikawa, N., Hattori, N., Tanaka, S., Horimasu, Y., Haruta, Y., Yokoyama, A., Kohno, N. & Kinnula, V.L. 2011, "Levels of surfactant proteins A and D and KL-6 are elevated in the induced sputum of chronic obstructive pulmonary disease patients: a sequential sputum analysis", *Respiration; international review of thoracic diseases,* vol. 82, no. 1, pp. 10-18.

Ishizaka, A., Watanabe, M., Yamashita, T., Ogawa, Y., Koh, H., Hasegawa, N., Nakamura, H., Asano, K., Yamaguchi, K. & Kotani, M. 2001, "New bronchoscopic

microsample probe to measure the biochemical constituents in epithelial lining fluid of patients with acute respiratory distress syndrome", *Critical Care Medicine*, vol. 29, no. 4, pp. 896.

Ito, K. & Barnes, P.J. 2009, "COPD as a disease of accelerated lung aging", *CHEST Journal*, vol. 135, no. 1, pp. 173-180.

Ito, N., Hirota, K., Momoeda, K. & Iwamori, M. 2006, "Change in the concentration of neutrophil elastase in bronchoalveolar lavage fluid during anesthesia and its inhibition by cholesterol sulfate", *Translational Research*, vol. 148, no. 2, pp. 96-102.

Ito, T., Kitamura, H., Inayama, Y., Nozawa, A. & Kanisawa, M. 1992, "Uptake and intracellular transport of cationic ferritin in the bronchiolar and alveolar epithelia of the rat", *Cell and tissue research*, vol. 268, no. 2, pp. 335-340.

Iwao, Y., Anraku, M., Hiraike, M., Kawai, K., Nakajou, K., Kai, T., Suenaga, A. & Otagiri, M. 2006, "The structural and pharmacokinetic properties of oxidized human serum albumin, advanced oxidation protein products (AOPP)", *Drug metabolism and pharmacokinetics*, vol. 21, no. 2, pp. 140-146.

Jackson, A.S., Sandrini, A., Campbell, C., Chow, S., Thomas, P.S. & Yates, D.H. 2007, "Comparison of biomarkers in exhaled breath condensate and bronchoalveolar lavage", *American journal of respiratory and critical care medicine*, vol. 175, no. 3, pp. 222.

Jackson, C. 1904, "Primary malignant disease of the larynx", *The Laryngoscope*, vol. 14, no. 8, pp. 590-618.

Jacob, K.D., Noren Hooten, N., Trzeciak, A.R. & Evans, M.K. 2013, "Markers of oxidant stress that are clinically relevant in aging and age-related disease", *Mechanisms of ageing and development*, vol. 134, no. 3, pp. 139-157.

Jacobson, G., Yee, K. & Ng, C. 2007, "Elevated plasma glutathione peroxidase concentration in acute severe asthma: comparison with plasma glutathione peroxidase activity, selenium and malondialdehyde", *Scandinavian Journal of Clinical & Laboratory Investigation*, vol. 67, no. 4, pp. 423-430.

Jaffar, Z., Ferrini, M.E., Herritt, L.A. & Roberts, K. 2009, "Cutting edge: lung mucosal Th17-mediated responses induce polymeric Ig receptor expression by the airway epithelium and elevate secretory IgA levels", *Journal of immunology (Baltimore, Md.: 1950)*, vol. 182, no. 8, pp. 4507-4511.

James, K. 1990, "Interactions between cytokines and α< sub> 2</sub>-macroglobulin", *Immunology today*, vol. 11, pp. 163-166.

Janssens, J., Pache, J. & Nicod, L. 1999, "Physiological changes in respiratory function associated with ageing", *European Respiratory Journal*, vol. 13, no. 1, pp. 197-205.

Jantratid, E., De Maio, V., Ronda, E., Mattavelli, V., Vertzoni, M. & Dressman, J.B. 2009, "Application of biorelevant dissolution tests to the prediction of< i> in vivo</i> performance of diclofenac sodium from an oral modified-release pellet dosage form", *European Journal of Pharmaceutical Sciences*, vol. 37, no. 3, pp. 434-441.

Jeong, H., Rhim, T., Ahn, M.H., Yoon, P.O., Kim, S.H., Chung, I.Y., Uh, S., Kim, S.I. & Park, C.S. 2005, "Proteomic analysis of differently expressed proteins in a mouse model for allergic asthma", *Journal of Korean medical science,* vol. 20, no. 4, pp. 579-585.

Jobe, A.H., Mitchell, B.R. & Harry Gunkel, J. 1993, "Beneficial effects of the combined use of prenatal corticosteroids and postnatal surfactant on preterm infants", *American Journal of Obstetrics and Gynecology,* vol. 168, no. 2, pp. 508-513.

John, R. & Thomas, J. 1972, "Chemical compositions of elastins isolated from aortas and pulmonary tissues of humans of different ages", *Biochem.J,* vol. 127, pp. 261-269.

Johnston, C.J., Mango, G.W., Finkelstein, J.N. & Stripp, B.R. 1997, "Altered pulmonary response to hyperoxia in Clara cell secretory protein deficient mice", *American journal of respiratory cell and molecular biology,* vol. 17, no. 2, pp. 147-155.

Johnston, H.J., Semmler-Behnke, M., Brown, D.M., Kreyling, W., Tran, L. & Stone, V. 2010, "Evaluating the uptake and intracellular fate of polystyrene nanoparticles by primary and hepatocyte cell lines< i> in vitro</i>", *Toxicology and applied pharmacology,* vol. 242, no. 1, pp. 66-78.

Jomova, K. & Valko, M. 2011, "Advances in metal-induced oxidative stress and human disease", *Toxicology,* vol. 283, no. 2, pp. 65-87.

Jones, C.F. & Grainger, D.W. 2009, "< i> In vitro</i> assessments of nanomaterial toxicity", *Advanced Drug Delivery Reviews,* vol. 61, no. 6, pp. 438-456.

Jones, M., Jones, S.A., Riffo-Vasquez, Y., Spina, D., Hoffman, E., Morgan, A., Patel, A., Page, C., Forbes, B. & Dailey, L.A. 2014, "Quantitative assessment of nanoparticle surface hydrophobicity and its influence on pulmonary biocompatibility", *Journal of Controlled Release,* vol. 183, pp. 94-104.

Jorens, P.G., Sibille, Y., Goulding, N.J., van Overveld, F.J., Herman, A.G., Bossaert, L., De Backer, W.A., Lauwerys, R., Flower, R.J. & Bernard, A. 1995, "Potential role of Clara cell protein, an endogenous phospholipase A2 inhibitor, in acute lung injury", *The European respiratory journal,* vol. 8, no. 10, pp. 1647-1653.

Jung, T., Bader, N. & Grune, T. 2007, "Lipofuscin", *Annals of the New York Academy of Sciences,* vol. 1119, no. 1, pp. 97-111.

Juniper, E., Cockcroft, D. & Hargreave, F. 1994, "Histamine and methacholine inhalation tests: a laboratory tidal breathing protocol", *Astra Draco AB,* , pp. 1-49.

Kadrabova, J., Mad'Arić, A., Podivinsky, F., Gazdik, F. & Ginter, E. 1996, "Plasma zinc, copper and copper/zinc ratio in intrinsic asthma", *Journal of Trace Elements in Medicine and Biology,* vol. 10, no. 1, pp. 50-53.

Kahn, M.C., Anderson, G.J., Anyan, W.R. & Hall, S.B. 1995, "Phosphatidylcholine molecular species of calf lung surfactant", *American Journal of Physiology-Lung Cellular and Molecular Physiology,* vol. 269, no. 5, pp. L567.

Kalina, M., Blau, H., Riklis, S. & Kravtsov, V. 1995, "Interaction of surfactant protein A with bacterial lipopolysaccharide may affect some biological functions", *American Journal of Physiology-Lung Cellular and Molecular Physiology*, vol. 268, no. 1, pp. L144.

Kaliner, M.A. 1991, "Human nasal respiratory secretions and host defense", *The American Review of Respiratory Disease*, vol. 144, no. 3 Pt 2, pp. S52-6.

Kang, S., Sung, H., Ahn, J., Park, J., Lee, S., Park, C. & Cho, J. 2011, "The Haptoglobin β chain as a supportive biomarker for human lung cancers", *Molecular BioSystems*, vol. 7, no. 4, pp. 1167-1175.

Kanno, S., Furuyama, A. & Hirano, S. 2007, "A murine scavenger receptor MARCO recognizes polystyrene nanoparticles", *Toxicological sciences : an official journal of the Society of Toxicology*, vol. 97, no. 2, pp. 398-406.

Kataoka, M., Masaoka, Y., Sakuma, S. & Yamashita, S. 2006, "Effect of food intake on the oral absorption of poorly water- soluble drugs: In vitro assessment of drug dissolution and permeation assay system", *Journal of pharmaceutical sciences*, vol. 95, no. 9, pp. 2051-2061.

Kato, T., Yashiro, T., Murata, Y., Herbert, D.C., Oshikawa, K., Bando, M., Ohno, S. & Sugiyama, Y. 2003, "Evidence that exogenous substances can be phagocytized by alveolar epithelial cells and transported into blood capillaries", *Cell and tissue research*, vol. 311, no. 1, pp. 47-51.

Kaulbach, H.C., White, M.V., Igarashi, Y., Hahn, B.K. & Kaliner, M.A. 1993, "Estimation of nasal epithelial lining fluid using urea as a marker", *Journal of allergy and clinical immunology*, vol. 92, no. 3, pp. 457-465.

Kawada, H., Katsura, H., Kamimura, M., Toyoda, E. & Kudo, K. 2003, "Coagulation activity in the airways of asthmatic patients", *Nihon Kokyuki Gakkai zasshi = the journal of the Japanese Respiratory Society*, vol. 41, no. 9, pp. 620-625.

Kawasaki, S., Takizawa, H., Takami, K., Desaki, M., Okazaki, H., Kasama, T., Kobayashi, K., Yamamoto, K., Nakahara, K. & Tanaka, M. 2001, "Benzene-extracted components are important for the major activity of diesel exhaust particles: effect on interleukin-8 gene expression in human bronchial epithelial cells", *American journal of respiratory cell and molecular biology*, vol. 24, no. 4, pp. 419-426.

Keane, M., Xing, S., Harrison, J., Ong, T. & Wallace, W. 1991, "Genotoxicity of diesel-exhaust particles dispersed in simulated pulmonary surfactant", *Mutation Research/Genetic Toxicology*, vol. 260, no. 3, pp. 233-238.

Keatings, V.M. & Barnes, P.J. 1997, "Granulocyte activation markers in induced sputum: comparison between chronic obstructive pulmonary disease, asthma, and normal subjects", *American journal of respiratory and critical care medicine*, vol. 155, no. 2, pp. 449-453.

Keatings, V.M., Collins, P.D., Scott, D.M. & Barnes, P.J. 1996, "Differences in interleukin-8 and tumor necrosis factor-alpha in induced sputum from patients with

chronic obstructive pulmonary disease or asthma", *American journal of respiratory and critical care medicine,* vol. 153, no. 2, pp. 530-534.

Keller, A., Nesvizhskii, A.I., Kolker, E. & Aebersold, R. 2002, "Empirical statistical model to estimate the accuracy of peptide identifications made by MS/MS and database search", *Analytical Chemistry,* vol. 74, no. 20, pp. 5383-5392.

Kelly, C., Kotre, C., Ward, C., Hendrick, D. & Walters, E. 1987, "Anatomical distribution of bronchoalveolar lavage fluid as assessed by digital subtraction radiography.", *Thorax,* vol. 42, no. 8, pp. 624.

Kelly, F.J., Mudway, I., Blomberg, A., Frew, A. & Sandström, T. 1999, "Altered lung antioxidant status in patients with mild asthma", *The Lancet,* vol. 354, no. 9177, pp. 482-483.

Kelly, F. & Mudway, I. 2003, "Protein oxidation at the air-lung interface", *Amino acids,* vol. 25, no. 3, pp. 375-396.

Kelly, F.J., Blomberg, A., Frew, A., Holgate, S.T. & Sandstrom, T. 1996, "Antioxidant kinetics in lung lavage fluid following exposure of humans to nitrogen dioxide", *American journal of respiratory and critical care medicine,* vol. 154, no. 6 Pt 1, pp. 1700-1705.

Kendall, M., Brown, L. & Trought, K. 2004, "Molecular adsorption at particle surfaces: a PM toxicity mediation mechanism", *Inhalation toxicology,* vol. 16, no. s1, pp. 99-105.

Ketterer, B. 1982, "The role of nonenzymatic reactions of glutathione in xenobiotic metabolism", *Drug metabolism reviews,* vol. 13, no. 1, pp. 161-187.

Khoor, A., Gray, M., Hull, W., Whitsett, J. & Stahlman, M. 1993, "Developmental expression of SP-A and SP-A mRNA in the proximal and distal respiratory epithelium in the human fetus and newborn.", *Journal of Histochemistry & Cytochemistry,* vol. 41, no. 9, pp. 1311.

Kim, J.N. & Shim, E.J. 2013, "Comparison of Curosurf® versus Surfacten® in the Treatment of Respiratory Distress Syndrome", *Neonatal Medicine,* vol. 20, no. 2, pp. 207-213.

Kim, W., Kim, W., Koh, Y., Lee, S., Lim, C., Kim, D. & Cho, Y. 2002, "Abnormal peripheral blood T-lymphocyte subsets in a subgroup of patients with COPD", *CHEST Journal,* vol. 122, no. 2, pp. 437-444.

Kim, S., Shim, J.J., Burgel, P.R., Ueki, I.F., Dao-Pick, T., Tam, D.C. & Nadel, J.A. 2002, "IL-13-induced Clara cell secretory protein expression in airway epithelium: role of EGFR signaling pathway", *American journal of physiology.Lung cellular and molecular physiology,* vol. 283, no. 1, pp. L67-75.

King, R.J., Klass, D.J., Gikas, E.G. & Clements, J. 1973, "Isolation of apoproteins from canine surface active material", *American Journal of Physiology--Legacy Content,* vol. 224, no. 4, pp. 788.

Kırkıl, G., Hamdi Muz, M., Seçkin, D., Şahin, K. & Küçük, Ö. 2008, "Antioxidant effect of zinc picolinate in patients with chronic obstructive pulmonary disease", *Respiratory medicine,* vol. 102, no. 6, pp. 840-844.

Kirkwood, T.B. 2005, "Understanding the odd science of aging", *Cell,* vol. 120, no. 4, pp. 437-447.

Kleberg, K., Jacobsen, J. & Müllertz, A. 2010, "Characterising the behaviour of poorly water soluble drugs in the intestine: application of biorelevant media for solubility, dissolution and transport studies", *Journal of Pharmacy and Pharmacology,* vol. 62, no. 11, pp. 1656-1668.

Ko, F.W., Diba, C., Roth, M., McKay, K., Johnson, P.R., Salome, C. & King, G.G. 2005, "A comparison of airway and serum matrix metalloproteinase-9 activity among normal subjects, asthmatic patients, and patients with asthmatic mucus hypersecretion", *CHEST Journal,* vol. 127, no. 6, pp. 1919-1927.

Kobzik, L., Godleski, J.J. & Brain, J.D. 1990, "Selective down-regulation of alveolar macrophage oxidative response to opsonin-independent phagocytosis", *Journal of immunology (Baltimore, Md.: 1950),* vol. 144, no. 11, pp. 4312-4319.

Kocyigit, A., Armutcu, F., Gurel, A. & Ermis, B. 2004, "Alterations in plasma essential trace elements selenium, manganese, zinc, copper, and iron concentrations and the possible role of these elements on oxidative status in patients with childhood asthma", *Biological trace element research,* vol. 97, no. 1, pp. 31-41.

Kodama, T., Kanazawa, H., Tochino, Y., Kyoh, S., Asai, K. & Hirata, K. 2009, "A technological advance comparing epithelial lining fluid from different regions of the lung in smokers", *Respiratory medicine,* vol. 103, no. 1, pp. 35-40.

Kongerud, J., Crissman, K., Hatch, G. & Alexis, N. 2003, "Ascorbic acid is decreased in induced sputum of mild asthmatics", *Inhalation toxicology,* vol. 15, no. 2, pp. 101-110.

Kramer, H.J., Schmidt, R., Gunther, A., Becker, G., Suzuki, Y. & Seeger, W. 1995, "ELISA technique for quantification of surfactant protein B (SP-B) in bronchoalveolar lavage fluid", *American journal of respiratory and critical care medicine,* vol. 152, no. 5 Pt 1, pp. 1540-1544.

Kreyling, W., Semmler, M., Erbe, F., Mayer, P., Takenaka, S., Schulz, H., Oberdörster, G. & Ziesenis, A. 2002, "Translocation of ultrafine insoluble iridium particles from lung epithelium to extrapulmonary organs is size dependent but very low", *Journal of Toxicology and Environmental Health Part A,* vol. 65, no. 20, pp. 1513-1530.

Kronenberg, R.S., Drage, C.W., Ponto, R.A. & Williams, L.E. 1973, "The effect of age on the distribution of ventilation and perfusion in the lung", *The American Review of Respiratory Disease,* vol. 108, no. 3, pp. 576-586.

Kuan, S.F., Rust, K. & Crouch, E. 1992, "Interactions of surfactant protein D with bacterial lipopolysaccharides. Surfactant protein D is an Escherichia coli-binding protein in bronchoalveolar lavage.", *Journal of Clinical Investigation,* vol. 90, no. 1, pp. 97.

Kueppers, F. & Black, L.F. 1974, "Alpha1-antitrypsin and its deficiency", *The American Review of Respiratory Disease,* vol. 110, no. 2, pp. 176-194.

Kuhn, L.C. & Kraehenbuhl, J.P. 1981, "The membrane receptor for polymeric immunoglobulin is structurally related to secretory component. Isolation and characterization of membrane secretory component from rabbit liver and mammary gland", *The Journal of biological chemistry,* vol. 256, no. 23, pp. 12490-12495.

Kuilman, T., Michaloglou, C., Mooi, W.J. & Peeper, D.S. 2010, "The essence of senescence", *Genes & development,* vol. 24, no. 22, pp. 2463-2479.

Kumawat, M., Sharma, T.K., Singh, I., Singh, N., Singh, S.K., Ghalaut, V.S., Shankar, V. & Vardey, S.K. 2012, "Decrease in antioxidant status of plasma and erythrocytes from geriatric population", *Disease markers,* vol. 33, no. 6, pp. 303-308.

Kurashima, K., Fujimura, M., Tsujiura, M. & Matsuda, T. 1997, "Effect of surfactant inhalation on allergic bronchoconstriction in guinea pigs", *Clinical & Experimental Allergy,* vol. 27, no. 3, pp. 337-342.

Kurdowska, A., Alden, S.M., Noble, J.M., Stevens, M.D. & Carr, F.K. 2000, "Involvement of alpha-2-macroglobulin receptor in clearance of interleukin 8-alpha-2-macroglobulin complexes by human alveolar macrophages", *Cytokine,* vol. 12, no. 7, pp. 1046-1053.

Kuroki, Y. & Akino, T. 1991, "Pulmonary surfactant protein A (SP-A) specifically binds dipalmitoylphosphatidylcholine.", *Journal of Biological Chemistry,* vol. 266, no. 5, pp. 3068.

Kuroki, Y., Tsutahara, S., Shijubo, N., Takahashi, H., Shiratori, M., Hattori, A., Honda, Y., Abe, S. & Akino, T. 1993, "Elevated levels of lung surfactant protein A in sera from patients with idiopathic pulmonary fibrosis and pulmonary alveolar proteinosis", *American Review of Respiratory Disease,* vol. 147, no. 3, pp. 723-729.

Laan, M., Bozinovski, S. & Anderson, G.P. 2004, "Cigarette smoke inhibits lipopolysaccharide-induced production of inflammatory cytokines by suppressing the activation of activator protein-1 in bronchial epithelial cells", *Journal of immunology (Baltimore, Md.: 1950),* vol. 173, no. 6, pp. 4164-4170.

Lacoste, J., Bousquet, J., Chanez, P., Van Vyve, T., Simony-Lafontaine, J., Lequeu, N., Vic, P., Enander, I., Godard, P. & Michel, F. 1993, "Eosinophilic and neutrophilic inflammation in asthma, chronic bronchitis, and chronic obstructive pulmonary disease", *Journal of allergy and clinical immunology,* vol. 92, no. 4, pp. 537-548.

Lal, M.K. & Sinha, S.K. 2008, "Surfactant respiratory therapy using Surfaxin/sinapultide", *Therapeutic advances in respiratory disease,* vol. 2, no. 5, pp. 339-344.

Lawson, P.R. & Reid, K. 2000, "The roles of surfactant proteins A and D in innate immunity", *Immunological reviews,* vol. 173, no. 1, pp. 66-78.

Lenz, A.G., Meyer, B., Costabel, U. & Maier, K. 1993, "Bronchoalveolar lavage fluid proteins in human lung disease: Analysis by two- dimensional electrophoresis", *Electrophoresis,* vol. 14, no. 1, pp. 242-244.

Lesur, O., Bernard, A., Arsalane, K., Lauwerys, R., Begin, R., Cantin, A. & Lane, D. 1995, "Clara cell protein (CC-16) induces a phospholipase A2-mediated inhibition of fibroblast migration in vitro", *American journal of respiratory and critical care medicine,* vol. 152, no. 1, pp. 290-297.

Levin, S.W., Butler, J.D., Schumacher, U.K., Wightman, P.D. & Mukherjee, A.B. 1986, "Uteroglobin inhibits phospholipase A2 activity", *Life Sciences,* vol. 38, no. 20, pp. 1813-1819.

Levine, R.L. 2002, "Carbonyl modified proteins in cellular regulation, aging, and disease< sup> 2, 3</sup>", *Free Radical Biology and Medicine,* vol. 32, no. 9, pp. 790-796.

Levine, R.L. & Stadtman, E.R. 2006, "Carbonylated proteins and their implication in physiology and pathology", *Redox proteomics: from protein modification to cellular dysfunction and disease,* , pp. 563-603.

Levine, R.L. 2002, "Carbonyl modified proteins in cellular regulation, aging, and disease", *Free radical biology & medicine,* vol. 32, no. 9, pp. 790-796.

Liao, H., Wu, J., Kuhn, E., Chin, W., Chang, B., Jones, M.D., O'Neil, S., Clauser, K.R., Karl, J. & Hasler, F. 2004, "Use of mass spectrometry to identify protein biomarkers of disease severity in the synovial fluid and serum of patients with rheumatoid arthritis", *Arthritis & Rheumatism,* vol. 50, no. 12, pp. 3792-3803.

Liao, X. & Wiedmann, T.S. 2003, "Solubilization of cationic drugs in lung surfactant", *Pharmaceutical research,* vol. 20, no. 11, pp. 1858-1863.

Lim, B.L., Wang, J.Y., Holmskov, U., Hoppe, H.J. & Reid, K.B.M. 1994, "Expression of the carbohydrate recognition domain of lung surfactant protein D and demonstration of its binding to lipopolysaccharides of gram-negative bacteria", *Biochemical and biophysical research communications,* vol. 202, no. 3, pp. 1674-1680.

Lim, S., Roche, N., Oliver, B.G., Mattos, W., Barnes, P.J. & Fan Chung, K. 2000, "Balance of matrix metalloprotease-9 and tissue inhibitor of metalloprotease-1 from alveolar macrophages in cigarette smokers: regulation by interleukin-10", *American journal of respiratory and critical care medicine,* vol. 162, no. 4, pp. 1355-1360.

Lin, T.Y., Poon, A.H. & Hamid, Q. 2013, "Asthma phenotypes and endotypes", *Current opinion in pulmonary medicine,* vol. 19, no. 1, pp. 18-23.

Lind, M.L., Jacobsen, J., Holm, R. & Müllertz, A. 2007, "Development of simulated intestinal fluids containing nutrients as transport media in the Caco-2 cell culture model: assessment of cell viability, monolayer integrity and transport of a poorly aqueous soluble drug and a substrate of efflux mechanisms", *European Journal of Pharmaceutical Sciences,* vol. 32, no. 4, pp. 261-270.

Lindahl, M., Ståhlbom, B., Svartz, J. & Tagesson, C. 1998, "Protein patterns of human nasal and bronchoalveolar lavage fluids analyzed with two- dimensional gel electrophoresis", *Electrophoresis,* vol. 19, no. 18, pp. 3222-3229.

Lindahl, M., Ståhlbom, B. & Tagesson, C. 2001, "Identification of a new potential airway irritation marker, palate lung nasal epithelial clone protein, in human nasal lavage

fluid with two- dimensional electrophoresis and matrix- assisted laser desorption/ionization- time of flight", *Electrophoresis,* vol. 22, no. 9, pp. 1795-1800.

Lindahl, M., Ståhlbom, B. & Tagesson, C. 1995, "Two- dimensional gel electrophoresis of nasal and bronchoalveolar lavage fluids after occupational exposure", *Electrophoresis,* vol. 16, no. 1, pp. 1199-1204.

Linden, M., Rasmussen, J.B., Piitulainen, E., Tunek, A., Larson, M., Tegner, H., Venge, P., Laitinen, L.A. & Brattsand, R. 1993, "Airway inflammation in smokers with nonobstructive and obstructive chronic bronchitis", *American Review of Respiratory Disease,* vol. 148, no. 5, pp. 1226-1230.

Lindmark, B.E., Arborelius Jr, M. & Eriksson, S.G. 1990, "Pulmonary function in middle-aged women with heterozygous deficiency of the serine protease inhibitor alpha1-antichymotrypsin", *American Review of Respiratory Disease,* vol. 141, no. 4_pt_1, pp. 884-888.

Lippmann, M., Yeates, D.B. & Albert, R.E. 1980, "Deposition, retention, and clearance of inhaled particles", *British journal of industrial medicine,* vol. 37, no. 4, pp. 337-362.

Liu, F., Shao, Z., Kildsig, D.O. & Mitra, A.K. 1993, "Pulmonary delivery of free and liposomal insulin", *Pharmaceutical research,* vol. 10, no. 2, pp. 228-232.

Liu, F., Shao, Z., Kildsig, D.O. & Mitra, A.K. 1993, "Pulmonary delivery of free and liposomal insulin", *Pharmaceutical research,* vol. 10, no. 2, pp. 228-232.

Lopez, E., Gascoin, G., Flamant, C., Merhi, M., Tourneux, P. & Baud, O. 2013, "Exogenous surfactant therapy in 2013: what is next? who, when and how should we treat newborn infants in the future?", *BMC pediatrics,* vol. 13, no. 1, pp. 165.

Lötvall, J., Akdis, C.A., Bacharier, L.B., Bjermer, L., Casale, T.B., Custovic, A., Lemanske Jr, R.F., Wardlaw, A.J., Wenzel, S.E. & Greenberger, P.A. 2011, "Asthma endotypes: a new approach to classification of disease entities within the asthma syndrome", *Journal of Allergy and Clinical Immunology,* vol. 127, no. 2, pp. 355-360.

Louhelainen, N., Rytilä, P., Haahtela, T., Kinnula, V.L. & Djukanović, R. 2009, "Persistence of oxidant and protease burden in the airways after smoking cessation", *BMC pulmonary medicine,* vol. 9, no. 1, pp. 25.

Lue, B., Nielsen, F.S., Magnussen, T., Schou, H.M., Kristensen, K., Jacobsen, L.O. & Müllertz, A. 2008, "Using biorelevant dissolution to obtain IVIVC of solid dosage forms containing a poorly-soluble model compound", *European Journal of Pharmaceutics and Biopharmaceutics,* vol. 69, no. 2, pp. 648-657.

Lykkesfeldt, J. 2007, "Ascorbate and dehydroascorbic acid as reliable biomarkers of oxidative stress: analytical reproducibility and long-term stability of plasma samples subjected to acidic deproteinization", *Cancer epidemiology, biomarkers & prevention : a publication of the American Association for Cancer Research, cosponsored by the American Society of Preventive Oncology,* vol. 16, no. 11, pp. 2513-2516.

Ma, Y., Wu, S., Lee, W., Cheng, J. & Wei, Y. 2009, "Response to the increase of oxidative stress and mutation of mitochondrial DNA in aging", *Biochimica et Biophysica Acta (BBA)-General Subjects,* vol. 1790, no. 10, pp. 1021-1029.

Macklin, C.C. 1955, "Pulmonary sumps, dust accumulations, alveolar fluid and lymph vessels", *Cells Tissues Organs,* vol. 23, no. 1, pp. 1-33.

Macklin, C.C. 1954, "The pulmonary alveolar mucoid film and the pneumonocytes", *Lancet,* vol. 266, no. 6822, pp. 1099-1104.

MacNee, W. 2001, "Oxidative stress and lung inflammation in airways disease", *European journal of pharmacology,* vol. 429, no. 1, pp. 195-207.

MacNee, W. 2000, "Oxidants/antioxidants and COPD", *CHEST Journal,* vol. 117, no. 5_suppl_1, pp. 303S-317S.

MacNee, W., Wiggs, B., Belzberg, A.S. & Hogg, J.C. 1989, "The effect of cigarette smoking on neutrophil kinetics in human lungs", *New England Journal of Medicine,* vol. 321, no. 14, pp. 924-928.

Magi, B., Bargagli, E., Bini, L. & Rottoli, P. 2006, "Proteome analysis of bronchoalveolar lavage in lung diseases", *Proteomics,* vol. 6, no. 23, pp. 6354-6369.

Mahbub, S., Brubaker, A.L. & Kovacs, E.J. 2011, "Aging of the Innate Immune System: An Update", *Current immunology reviews,* vol. 7, no. 1, pp. 104-115.

Majo, J., Ghezzo, H. & Cosio, M.G. 2001, "Lymphocyte population and apoptosis in the lungs of smokers and their relation to emphysema", *The European respiratory journal,* vol. 17, no. 5, pp. 946-953.

Makino, K., Yamamoto, N., Higuchi, K., Harada, N., Ohshima, H. & Terada, H. 2003, "Phagocytic uptake of polystyrene microspheres by alveolar macrophages: effects of the size and surface properties of the microspheres", *Colloids and Surfaces B: Biointerfaces,* vol. 27, no. 1, pp. 33-39.

Mamolen, M., Lewis, D.M., Blanchet, M.A., Satink, F.J. & Vogt, R.L. 1993, "Investigation of an outbreak of “humidifier fever” in a print shop", *American Journal of Industrial Medicine,* vol. 23, no. 3, pp. 483-490.

Mango, G.W., Johnston, C.J., Reynolds, S.D., Finkelstein, J.N., Plopper, C.G. & Stripp, B.R. 1998, "Clara cell secretory protein deficiency increases oxidant stress response in conducting airways", *The American Journal of Physiology,* vol. 275, no. 2 Pt 1, pp. L348-56.

Manuyakorn, W., Howarth, P.H. & Holgate, S.T. 2013, "Airway remodelling in asthma and novel therapy", *Asian Pacific Journal of Allergy and Immunology,* vol. 31, no. 1, pp. 3-10.

Marchandise, F.X., Mathieu, B., Francis, C. & Sibille, Y. 1989, "Local increase of antiprotease and neutrophil elastase-alpha 1-proteinase inhibitor complexes in lung cancer", *The European respiratory journal,* vol. 2, no. 7, pp. 623-629.

Marcy, T., Merrill, W., Rankin, J. & Reynolds, H. 1987, "Limitations of using urea to quantify epithelial lining fluid recovered by bronchoalveolar lavage.", *The American Review of Respiratory Disease,* vol. 135, no. 6, pp. 1276.

Marques, M.R., Loebenberg, R. & Almukainzi, M. 2011, "Simulated biological fluids with possible application in dissolution testing", *Dissolution Technol,* vol. 18, no. 3, pp. 15-28.

Martin, T.R. & Frevert, C.W. 2005, "Innate immunity in the lungs", *Proceedings of the American Thoracic Society,* vol. 2, no. 5, pp. 403-411.

Martinez-Vicente, M., Sovak, G. & Cuervo, A.M. 2005, "Protein degradation and aging", *Experimental gerontology,* vol. 40, no. 8, pp. 622-633.

Mateos, F., Brock, J.H. & Pérez-Arellano, J.L. 1998, "Iron metabolism in the lower respiratory tract", *Thorax,* vol. 53, no. 7, pp. 594.

Mathias, N.R., Timoszyk, J., Stetsko, P.I., Megill, J.R., Smith, R.L. & Wall, D.A. 2002, "Permeability characteristics of calu-3 human bronchial epithelial cells: in vitro-in vivo correlation to predict lung absorption in rats", *Journal of drug targeting,* vol. 10, no. 1, pp. 31-40.

Matthay, M.A., Folkesson, H.G. & Verkman, A. 1996, "Salt and water transport across alveolar and distal airway epithelia in the adult lung", *American Journal of Physiology-Lung Cellular and Molecular Physiology,* vol. 270, no. 4, pp. L487.

Mazur, W., Toljamo, T., Ohlmeier, S., Vuopala, K., Nieminen, P., Kobayashi, H. & Kinnula, V.L. 2011, "Elevation of surfactant protein A in plasma and sputum in cigarette smokers", *The European respiratory journal,* vol. 38, no. 2, pp. 277-284.

McCormack, F.X., King, T.E.,Jr, Voelker, D.R., Robinson, P.C. & Mason, R.J. 1991, "Idiopathic pulmonary fibrosis. Abnormalities in the bronchoalveolar lavage content of surfactant protein A", *The American Review of Respiratory Disease,* vol. 144, no. 1, pp. 160-166.

McGowan, S.E. & Henley, S.A. 1988, "Iron and ferritin contents and distribution in human alveolar macrophages", *J Lab Clin Med,* vol. 111, no. 6, pp. 611-617.

McGrath, L.T., Mallon, P., Dowey, L., Silke, B., McClean, E., McDonnell, M., Devine, A., Copeland, S. & Elborn, S. 1999, "Oxidative stress during acute respiratory exacerbations in cystic fibrosis", *Thorax,* vol. 54, no. 6, pp. 518-523.

McNeil, S.E. 2009, "Nanoparticle therapeutics: a personal perspective", *Wiley Interdisciplinary Reviews: Nanomedicine and Nanobiotechnology,* vol. 1, no. 3, pp. 264-271.

Meadows, J. & Smith, R.C. 1986, "Uric acid protection of nucleobases from ozone-induced degradation* 1", *Archives of Biochemistry and Biophysics,* vol. 246, no. 2, pp. 838-845.

Medina, C., Santos- Martinez, M., Radomski, A., Corrigan, O. & Radomski, M. 2007, "Nanoparticles: pharmacological and toxicological significance", *British journal of pharmacology*, vol. 150, no. 5, pp. 552-558.

Medvedev, Z.A. 1990, "An attempt at a rational classification of theories of ageing", *Biological Reviews*, vol. 65, no. 3, pp. 375-398.

Meister, A. & Anderson, M.E. 1983, "Glutathione", *Annual Review of Biochemistry*, vol. 52, no. 1, pp. 711-760.

Merali, S., Barrero, C.A., Bowler, R.P., Chen, D.E., Criner, G., Braverman, A., Litwin, S., Yeung, A. & Kelsen, S.G. 2014, "Analysis of the Plasma Proteome in COPD: Novel Low Abundance Proteins Reflect the Severity of Lung Remodeling", *COPD: Journal of Chronic Obstructive Pulmonary Disease*, vol. 11, no. 2, pp. 177-189.

Mercer, R., Russell, M. & Crapo, J. 1992, "Mucous lining layers in human and rat airways", *Annrew Resp Dis*, vol. 145, pp. 355.

Merkel, D., Rist, W., Seither, P., Weith, A. & Lenter, M.C. 2005, "Proteomic study of human bronchoalveolar lavage fluids from smokers with chronic obstructive pulmonary disease by combining surface- enhanced laser desorption/ionization- mass spectrometry profiling with mass spectrometric protein identification", *Proteomics*, vol. 5, no. 11, pp. 2972-2980.

Merrill, W., O'Hearn, E., Rankin, J., Naegel, G., Matthay, R. & Reynolds, H. 1982, "Kinetic analysis of respiratory tract proteins recovered during a sequential lavage protocol.", *The American Review of Respiratory Disease*, vol. 126, no. 4, pp. 617.

Meyer, K.C. 2004, "Lung infections and aging", *Ageing research reviews*, vol. 3, no. 1, pp. 55-67.

Meyer, K.C. 2001, "The role of immunity in susceptibility to respiratory infection in the aging lung", *Respiration physiology*, vol. 128, no. 1, pp. 23-31.

Meyer, K.C., Rosenthal, N.S., Soergel, P. & Peterson, K. 1998, "Neutrophils and low-grade inflammation in the seemingly normal aging human lung", *Mechanisms of ageing and development*, vol. 104, no. 2, pp. 169-181.

Meyer, K.C., Sharma, A., Brown, R., Weatherly, M., Moya, F.R., Lewandoski, J. & Zimmerman, J.J. 2000, "Function and composition of pulmonary surfactant and surfactant-derived fatty acid profiles are altered in young adults with cystic fibrosis", *CHEST Journal*, vol. 118, no. 1, pp. 164-174.

Meyer, K.C., Ershler, W., Rosenthal, N.S., Lu, X.G. & Peterson, K. 1996, "Immune dysregulation in the aging human lung", *American journal of respiratory and critical care medicine*, vol. 153, no. 3, pp. 1072-1079.

Michel, O., Ginanni, R., Duchateau, J., Vertongen, F., Bon, B. & Sergysels, R. 1991, "Domestic endotoxin exposure and clinical severity of asthma", *Clinical & Experimental Allergy*, vol. 21, no. 4, pp. 441-448.

Michel, O., Murdoch, R. & Bernard, A. 2005, "Inhaled LPS induces blood release of Clara cell specific protein (CC16) in human beings", *Journal of allergy and clinical immunology*, vol. 115, no. 6, pp. 1143-1147.

Michel, O. 2003, "Role of lipopolysaccharide (LPS) in asthma and other pulmonary conditions", *Journal of endotoxin research*, vol. 9, no. 5, pp. 293-300.

Midander, K., Wallinder, I.O. & Leygraf, C. 2007, "In vitro studies of copper release from powder particles in synthetic biological media", *Environmental Pollution*, vol. 145, no. 1, pp. 51-59.

Milic-Emili, J. 2004, "Does mechanical injury of the peripheral airways play a role in the genesis of COPD in smokers?", *COPD: Journal of Chronic Obstructive Pulmonary Disease*, vol. 1, no. 1, pp. 85-92.

Misso, N., Powers, K., Gillon, R., Stewart, G. & Thompson, P. 1996, "Reduced platelet glutathione peroxidase activity and serum selenium concentration in atopic asthmatic patients", *Clinical & Experimental Allergy*, vol. 26, no. 7, pp. 838-847.

Moestrup, S.K., Holtet, T.L., Etzerodt, M., Thøgersen, H.C., Nykjær, A., Andreasen, P., Rasmussen, H., Sottrup-Jensen, L. & Gliemann, J. 1993, "Alpha 2-macroglobulin-proteinase complexes, plasminogen activator inhibitor type-1-plasminogen activator complexes, and receptor-associated protein bind to a region of the alpha 2-macroglobulin receptor containing a cluster of eight complement-type repeats.", *Journal of Biological Chemistry*, vol. 268, no. 18, pp. 13691.

Montuschi, P., Collins, J.V., Ciabattoni, G., Lazzeri, N., Corradi, M., Kharitonov, S.A. & Barnes, P.J. 2000, "Exhaled 8-isoprostane as an in vivo biomarker of lung oxidative stress in patients with COPD and healthy smokers", *American journal of respiratory and critical care medicine*, vol. 162, no. 3, pp. 1175-1177.

Montuschi, P., Barnes, P.J. & Roberts, L.J.,2nd 2004, "Isoprostanes: markers and mediators of oxidative stress", *FASEB journal : official publication of the Federation of American Societies for Experimental Biology*, vol. 18, no. 15, pp. 1791-1800.

Mudway, I.S., Stenfors, N., Duggan, S.T., Roxborough, H., Zielinski, H., Marklund, S.L., Blomberg, A., Frew, A.J., Sandström, T. & Kelly, F.J. 2004, "An in vitro and in vivo investigation of the effects of diesel exhaust on human airway lining fluid antioxidants* 1", *Archives of Biochemistry and Biophysics*, vol. 423, no. 1, pp. 200-212.

Mudway, I.S., Behndig, A.F., Helleday, R., Pourazar, J., Frew, A.J., Kelly, F.J. & Blomberg, A. 2006, "Vitamin supplementation does not protect against symptoms in ozone-responsive subjects", *Free Radical Biology and Medicine*, vol. 40, no. 10, pp. 1702-1712.

Mudway, I.S., Stenfors, N., Blomberg, A., Helleday, R., Dunster, C., Marklund, S., Frew, A.J., Sandström, T. & Kelly, F.J. 2001, "Differences in basal airway antioxidant concentrations are not predictive of individual responsiveness to ozone: a comparison of healthy and mild asthmatic subjects", *Free Radical Biology and Medicine*, vol. 31, no. 8, pp. 962-974.

Mudway, I., Blomberg, A., Frew, A., Holgate, S., Sandstrom, T. & Kelly, F. 1999, "Antioxidant consumption and repletion kinetics in nasal lavage fluid following exposure of healthy human volunteers to ozone", *European Respiratory Journal,* vol. 13, no. 6, pp. 1429.

Mudway, I. & Kelly, F. 2000, "Ozone and the lung: a sensitive issue", *Molecular aspects of medicine,* vol. 21, no. 1-2, pp. 1-48.

Muhlfeld, C., Rothen-Rutishauser, B., Blank, F., Vanhecke, D., Ochs, M. & Gehr, P. 2008, "Interactions of nanoparticles with pulmonary structures and cellular responses", *American journal of physiology.Lung cellular and molecular physiology,* vol. 294, no. 5, pp. L817-29.

Munro, H.N. & Linder, M.C. 1978, "Ferritin: structure, biosynthesis, and role in iron metabolism", *Physiol Rev,* vol. 58, no. 2, pp. 317-396.

Murata, K., Fujimoto, K., Kitaguchi, Y., Horiuchi, T., Kubo, K. & Honda, T. 2014, "Hydrogen Peroxide Content and pH of Expired Breath Condensate from Patients with Asthma and COPD", *COPD: Journal of Chronic Obstructive Pulmonary Disease,* vol. 11, no. 1, pp. 81-87.

Mutlu, G.M., Garey, K.W., Robbins, R.A., Danziger, L.H. & Rubinstein, I. 2001, "Collection and analysis of exhaled breath condensate in humans", *American journal of respiratory and critical care medicine,* vol. 164, no. 5, pp. 731.

Nagai, K., Betsuyaku, T., Kondo, T., Nasuhara, Y. & Nishimura, M. 2006, "Long term smoking with age builds up excessive oxidative stress in bronchoalveolar lavage fluid", *Thorax,* vol. 61, no. 6, pp. 496-502.

Nel, A., Xia, T., Mädler, L. & Li, N. 2006, "Toxic potential of materials at the nanolevel", *Science,* vol. 311, no. 5761, pp. 622.

Nesvizhskii, A.I., Keller, A., Kolker, E. & Aebersold, R. 2003, "A statistical model for identifying proteins by tandem mass spectrometry", *Analytical Chemistry,* vol. 75, no. 17, pp. 4646-4658.

Newman, S.P., Weisz, A.W., Talaee, N. & Clarke, S.W. 1991, "Improvement of drug delivery with a breath actuated pressurised aerosol for patients with poor inhaler technique", *Thorax,* vol. 46, no. 10, pp. 712-716.

Nguyen, T.N., Cunsolo, S.M., Gal, P. & Ransom, J.L. 2003, "Infasurf and Curosurf: Theoretical and practical considerations with new surfactants", *The Journal of Pediatric Pharmacology and Therapeutics,* vol. 8, no. 2, pp. 97-114.

Nicholas, B.L., Skipp, P., Barton, S., Singh, D., Bagmane, D., Mould, R., Angco, G., Ward, J., Guha-Niyogi, B. & Wilson, S. 2010, "Identification of lipocalin and apolipoprotein A1 as biomarkers of chronic obstructive pulmonary disease", *American journal of respiratory and critical care medicine,* vol. 181, no. 10, pp. 1049-1060.

Nijhuis-Heddes, J., Lindeman, J., Otto, A., Snieders, M., Kievit-Tyson, P. & Dijkman, J. 1982, "Distribution of immunoglobulin-containing cells in the bronchial mucosa of

patients with chronic respiratory disease.", *European journal of respiratory diseases,* vol. 63, no. 3, pp. 249.

Nikota, J.K. & Stämpfli, M.R. 2012, "Cigarette smoke-induced inflammation and respiratory host defense: Insights from animal models", *Pulmonary pharmacology & therapeutics,* vol. 25, no. 4, pp. 257-262.

Nishimura, M., Makita, H., Nagai, K., Konno, S., Nasuhara, Y., Hasegawa, M., Shimizu, K., Betsuyaku, T., Ito, Y.M. & Fuke, S. 2012, "Annual change in pulmonary function and clinical phenotype in chronic obstructive pulmonary disease", *American journal of respiratory and critical care medicine,* vol. 185, no. 1, pp. 44-52.

Niven, R.M., Fletcher, A.M., Pickering, C.A., Fishwick, D., Warburton, C.J., Simpson, J.C., Francis, H. & Oldham, L.A. 1997, "Chronic bronchitis in textile workers", *Thorax,* vol. 52, no. 1, pp. 22-27.

Nocker, R.E.T., van der Zee, J.S., Weller, F.R., van Overveld, F.J., Jansen, H.M. & Out, T.A. 1999, "Segmental allergen challenge induces plasma protein leakage into the airways of asthmatic subjects at 4 hours but not at 5 minutes after challenge* 1", *Journal of Laboratory and Clinical Medicine,* vol. 134, no. 1, pp. 74-82.

Noel-Georis, I., Bernard, A., Falmagne, P. & Wattiez, R. 2002, "Database of bronchoalveolar lavage fluid proteins", *Journal of Chromatography B: Analytical Technologies in the Biomedical and Life Sciences,* vol. 771, no. 1-2, pp. 221-236.

Noël-Georis, I., Bernard, A., Falmagne, P. & Wattiez, R. 2001, "Proteomics as the tool to search for lung disease markers in bronchoalveolar lavage", *Disease markers,* vol. 17, no. 4, pp. 271-284.

Nowak, D., Kasielski, M., Antczak, A., Pietras, T. & Bialasiewicz, P. 1999, "Increased content of thiobarbituric acid-reactive substances and hydrogen peroxide in the expired breath condensate of patients with stable chronic obstructive pulmonary disease: no significant effect of cigarette smoking", *Respiratory medicine,* vol. 93, no. 6, pp. 389-396.

Oberdörster, G., Oberdörster, E. & Oberdörster, J. 2005, "Nanotoxicology: an emerging discipline evolving from studies of ultrafine particles", *Environmental health perspectives,* , pp. 823-839.

Oberdörster, G., Oberdörster, E. & Oberdörster, J. 2005, "Nanotoxicology: an emerging discipline evolving from studies of ultrafine particles", *Environmental health perspectives,* , pp. 823-839.

Oberdorster, G., Ferin, J. & Lehnert, B.E. 1994, "Correlation between particle size, in vivo particle persistence, and lung injury", *Environmental health perspectives,* vol. 102 Suppl 5, pp. 173-179.

Oettl, K. & Stauber, R. 2007, "Physiological and pathological changes in the redox state of human serum albumin critically influence its binding properties", *British journal of pharmacology,* vol. 151, no. 5, pp. 580-590.

Ohlmeier, S., Toljamo, T., Linja-Aho, A., Nieminen, P., Ronty, M., Kinnula, V. & Mazur, W. 2012, "Elevation Of Polymeric Immunoglobulin Receptor In Smokers And Patients With COPD", *Am J Respir Crit Care Med*, vol. 185, pp. A4554.

Ohlmeier, S., Mazur, W., Salmenkivi, K., Myllärniemi, M., Bergmann, U. & Kinnula, V.L. 2010, "Proteomic studies on receptor for advanced glycation end product variants in idiopathic pulmonary fibrosis and chronic obstructive pulmonary disease", *PROTEOMICS-Clinical Applications*, vol. 4, no. 1, pp. 97-105.

Ohlmeier, S., Vuolanto, M., Toljamo, T., Vuopala, K., Salmenkivi, K., Myllärniemi, M. & Kinnula, V.L. 2008, "Proteomics of human lung tissue identifies surfactant protein A as a marker of chronic obstructive pulmonary disease", *Journal of proteome research*, vol. 7, no. 12, pp. 5125-5132.

Ohnishi, K., Takagi, M., Kurokawa, Y., Satomi, S. & Konttinen, Y.T. 1998, "Matrix metalloproteinase-mediated extracellular matrix protein degradation in human pulmonary emphysema", *Laboratory investigation; a journal of technical methods and pathology*, vol. 78, no. 9, pp. 1077-1087.

Ohtani, N. & Hara, E. 2013, "Roles and mechanisms of cellular senescence in regulation of tissue homeostasis", *Cancer science*, vol. 104, no. 5, pp. 525-530.

Okamoto, T., Miyazaki, Y., Shirahama, R., Tamaoka, M. & Inase, N. 2012, "Proteome analysis of bronchoalveolar lavage fluid in chronic hypersensitivity pneumonitis", *Allergol Int*, vol. 61, no. 1, pp. 83-92.

Okumu, A., DiMaso, M. & Löbenberg, R. 2008, "Dynamic dissolution testing to establish in vitro/in vivo correlations for montelukast sodium, a poorly soluble drug", *Pharmaceutical research*, vol. 25, no. 12, pp. 2778-2785.

Olusi, S., Ojutiku, O., Jessop, W. & Iboko, M. 1979, "Plasma and white blood cell ascorbic acid concentrations in patients with bronchial asthma", *Clinica chimica acta*, vol. 92, no. 2, pp. 161-166.

O'Neil, S.E., Lundbäck, B. & Lötvall, J. 2011, "Proteomics in asthma and COPD phenotypes and endotypes for biomarker discovery and improved understanding of disease entities", *Journal of proteomics*, vol. 75, no. 1, pp. 192-201.

Ong, W.Y. & Halliwell, B. 2004, "Iron, atherosclerosis, and neurodegeneration: a key role for cholesterol in promoting iron-dependent oxidative damage?", *Annals of the New York Academy of Sciences*, vol. 1012, pp. 51-64.

O'Shaughnessy, T.C., Ansari, T.W., Barnes, N.C. & Jeffery, P.K. 1997, "Inflammation in bronchial biopsies of subjects with chronic bronchitis: inverse relationship of CD8+ T lymphocytes with FEV1", *American journal of respiratory and critical care medicine*, vol. 155, no. 3, pp. 852-857.

Out, T.A., Jansen, H.M., van Steenwijk, R.P., de Nooijer, M.J., van de Graaf, E.A. & Zuijderhoudt, F.M. 1987, "ELISA of ceruloplasmin and alpha-2-macroglobulin in paired bronchoalveolar lavage fluid and serum samples", *Clinica chimica acta; international journal of clinical chemistry*, vol. 165, no. 2-3, pp. 277-288.

Pacht, E.R. & Davis, W.B. 1988, "Role of transferrin and ceruloplasmin in antioxidant activity of lung epithelial lining fluid", *Journal of applied physiology*, vol. 64, no. 5, pp. 2092.

Pacht, E.R., Kaseki, H., Mohammed, J.R., Cornwell, D.G. & Davis, W.B. 1986, "Deficiency of vitamin E in the alveolar fluid of cigarette smokers. Influence on alveolar macrophage cytotoxicity", *The Journal of clinical investigation*, vol. 77, no. 3, pp. 789-796.

Pal, T.M., de Monchy, J.G., Groothoff, J.W. & Post, D. 1997, "The clinical spectrum of humidifier disease in synthetic fiber plants", *American Journal of Industrial Medicine*, vol. 31, no. 6, pp. 682-692.

Palaniyar, N., Ikegami, M., Korfhagen, T., Whitsett, J. & McCormack, F.X. 2001, "Domains of surfactant protein A that affect protein oligomerization, lipid structure and surface tension", *Comparative Biochemistry and Physiology Part A: Molecular & Integrative Physiology*, vol. 129, no. 1, pp. 109-127.

Palaniyar, N., Ridsdale, R.A., Holterman, C.E., Inchley, K., Possmayer, F. & Harauz, G. 1998, "Structural changes of surfactant protein A induced by cations reorient the protein on lipid bilayers", *Journal of structural biology*, vol. 122, no. 3, pp. 297-310.

Papadopoulos, N., Christodoulou, I., Rohde, G., Agache, I., Almqvist, C., Bruno, A., Bonini, S., Bont, L., Bossios, A. & Bousquet, J. 2011, "Viruses and bacteria in acute asthma exacerbations–A GA2LEN- DARE* systematic review", *Allergy*, vol. 66, no. 4, pp. 458-468.

Papassotiropoulos, A., Bagli, M., Kurz, A., Kornhuber, J., Forstl, H., Maier, W., Pauls, J., Lautenschlager, N. & Heun, R. 2000, "A genetic variation of cathepsin D is a major risk factor for Alzheimer's disease", *Annals of Neurology*, vol. 47, no. 3, pp. 399-403.

Paredi, P., Kharitonov, S.A., Leak, D., Ward, S., Cramer, D. & Barnes, P.J. 2000, "Exhaled ethane, a marker of lipid peroxidation, is elevated in chronic obstructive pulmonary disease", *American journal of respiratory and critical care medicine*, vol. 162, no. 2 Pt 1, pp. 369-373.

Pastor, M., Nogal, A., Molina-Pinelo, S., Meléndez, R., Salinas, A., González De la Peña, M, Martín-Juan, J., Corral, J., García-Carbonero, R. & Carnero, A. 2013, "Identification of proteomic signatures associated with lung cancer and COPD", *Journal of proteomics*, vol. 89, pp. 227-237.

Patel, N., Forbes, B., Eskola, S. & Murray, J. 2006, "Use of simulated intestinal fluids with Caco-2 cells and rat ileum", *Drug development and industrial pharmacy*, vol. 32, no. 2, pp. 151-161.

Pattle, R. 1955, "Properties, function and origin of the alveolar lining layer", .

Patton, J.S. 1996, "Mechanisms of macromolecule absorption by the lungs", *Advanced Drug Delivery Reviews*, vol. 19, no. 1, pp. 3-36.

Pauwels, R. 2001, "Global initiative for chronic obstructive lung diseases (GOLD): time to act", *The European respiratory journal*, vol. 18, no. 6, pp. 901-902.

Peden, D.B., Hohman, R., Brown, M.E., Mason, R.T., Berkebile, C., Fales, H.M. & Kaliner, M.A. 1990, "Uric acid is a major antioxidant in human nasal airway secretions", *Proceedings of the National Academy of Sciences,* vol. 87, no. 19, pp. 7638.

Peden, D.B., Swiersz, M., Ohkubo, K., Hahn, B., Emery, B. & Kaliner, M.A. 1993, "Nasal secretion of the ozone scavenger uric acid", *American Review of Respiratory Disease,* vol. 148, pp. 455-455.

Peleman, R., Rytilä, P.H., Kips, J., Joos, G. & Pauwels, R. 1999, "The cellular composition of induced sputum in chronic obstructive pulmonary disease", *European Respiratory Journal,* vol. 13, no. 4, pp. 839-843.

Perez-Arellano, J., Barrios, M., Martin, T., Sanchez, M., Jimenez, A. & Gonzalez-Buitrago, J. 1996, "Hydrolytic enzyme of the alveolar macrophage in diffuse pulmonary interstitial disease", *Respiratory medicine,* vol. 90, no. 3, pp. 159-166.

Pérez-Gil, J. 2008, "Structure of pulmonary surfactant membranes and films: the role of proteins and lipid-protein interactions", *Biochimica et Biophysica acta (BBA)-Biomembranes,* vol. 1778, no. 7-8, pp. 1676-1695.

Perez-Gil, J., Nag, K., Taneva, S. & Keough, K. 1992, "Pulmonary surfactant protein SP-C causes packing rearrangements of dipalmitoylphosphatidylcholine in spread monolayers", *Biophysical journal,* vol. 63, no. 1, pp. 197-204.

Perez-Gil, J. & Keough, K.M. 1998, "Interfacial properties of surfactant proteins", *Biochimica et biophysica acta,* vol. 1408, no. 2-3, pp. 203-217.

Persson, Carl G., and Lena Uller. "Review Resolution of cell-mediated airways diseases." *Respir Res* 11 (2010): 75.

Pesci, A., Balbi, B., Majori, M., Cacciani, G., Bertacco, S., Alciato, P. & Donner, C.F. 1998, "Inflammatory cells and mediators in bronchial lavage of patients with chronic obstructive pulmonary disease", *The European respiratory journal,* vol. 12, no. 2, pp. 380-386.

Peterson, B.T., Griffith, D.E., Tate, R.W. & Clancy, S.J. 1993, "Single-cycle bronchoalveolar lavage to determine solute concentrations in epithelial lining fluid", *The American Review of Respiratory Disease,* vol. 147, no. 5, pp. 1216-1222.

Pham, S. & Wiedmann, T.S. 2001, "Note: Dissolution of aerosol particles of budesonide in Survanta™, a model lung surfactant", *Journal of pharmaceutical sciences,* vol. 90, no. 1, pp. 98-104.

Phipps, R. & Richardson, P. 1976, "The effects of irritation at various levels of the airway upon tracheal mucus secretion in the cat.", *The Journal of physiology,* vol. 261, no. 3, pp. 563.

Pinamonti, S., Leis, M., Barbieri, A., Leoni, D., Muzzoli, M., Sostero, S., Chicca, M.C., Carrieri, A., Ravenna, F. & Fabbri, L.M. 1998, "Detection of xanthine oxidase activity products by EPR and HPLC in bronchoalveolar lavage fluid from patients

with chronic obstructive pulmonary disease", *Free Radical Biology and Medicine,* vol. 25, no. 7, pp. 771-779.

Plopper, C., Nishio, S., Alley, J., Kass, P. & Hyde, D. 1992, "The role of the nonciliated bronchiolar epithelial (Clara) cell as the progenitor cell during bronchiolar epithelial differentiation in the perinatal rabbit lung", *American journal of respiratory cell and molecular biology,* vol. 7, no. 6, pp. 606-613.

Plumlee, G.S., Morman, S.A. & Ziegler, T.L. 2006, "The toxicological geochemistry of earth materials: An overview of processes and the interdisciplinary methods used to understand them", *Reviews in Mineralogy and Geochemistry,* vol. 64, no. 1, pp. 5-57.

Polin, R.A., Carlo, W.A., Committee on Fetus and Newborn & American Academy of Pediatrics 2014, "Surfactant replacement therapy for preterm and term neonates with respiratory distress", *Pediatrics,* vol. 133, no. 1, pp. 156-163.

Powers, K.W., Palazuelos, M., Moudgil, B.M. & Roberts, S.M. 2007, "Characterization of the size, shape, and state of dispersion of nanoparticles for toxicological studies", *Nanotoxicology,* vol. 1, no. 1, pp. 42-51.

Powers, K.W., Brown, S.C., Krishna, V.B., Wasdo, S.C., Moudgil, B.M. & Roberts, S.M. 2006, "Research strategies for safety evaluation of nanomaterials. Part VI. Characterization of nanoscale particles for toxicological evaluation", *Toxicological sciences : an official journal of the Society of Toxicology,* vol. 90, no. 2, pp. 296-303.

Profita, M., Giorgi, R.D., Sala, A., Bonanno, A., Riccobono, L., Mirabella, F., Gjomarkaj, M., Bonsignore, G., Bousquet, J. & Vignola, A. 2005, "Muscarinic receptors, leukotriene B4 production and neutrophilic inflammation in COPD patients", *Allergy,* vol. 60, no. 11, pp. 1361-1369.

Pryor, W.A. 1991, "Can vitamin E protect humans against the pathological effects of ozone in smog?", *The American Journal of Clinical Nutrition,* vol. 53, no. 3, pp. 702-722.

Putman, E., Creuwels, L., Van Golde, L. & Haagsman, H.P. 1996, "Surface properties, morphology and protein composition of pulmonary surfactant subtypes.", *Biochemical Journal,* vol. 320, no. Pt 2, pp. 599.

Quinton, P.M. 1979, "Composition and control of secretions from tracheal bronchial submucosal glands", .

Raeve, H.D., Thunnissen, F., Kaneko, F., Guo, F., Lewis, M., Kavuru, M., Secic, M., Thomassen, M. & Erzurum, S. 1997, "Decreased Cu, Zn-SOD activity in asthmatic airway epithelium: correction by inhaled corticosteroid in vivo", *American Journal of Physiology-Lung Cellular and Molecular Physiology,* vol. 16, no. 1, pp. L148.

Rahman, I. & MacNee, W. 2000, "Oxidative stress and regulation of glutathione in lung inflammation", *European Respiratory Journal,* vol. 16, no. 3, pp. 534.

Rahman, I. & MacNee, W. 1996, "Role of oxidants/antioxidants in smoking-induced lung diseases", *Free Radical Biology and Medicine,* vol. 21, no. 5, pp. 669-681.

Rahman, I. & MacNee, W. 1996, "Role of oxidants/antioxidants in smoking-induced lung diseases", *Free Radical Biology and Medicine,* vol. 21, no. 5, pp. 669-681.

Rahman, I., van Schadewijk, A.A., Crowther, A.J., Hiemstra, P.S., Stolk, J., MacNee, W. & De Boer, W.I. 2002, "4-Hydroxy-2-nonenal, a specific lipid peroxidation product, is elevated in lungs of patients with chronic obstructive pulmonary disease", *American journal of respiratory and critical care medicine,* vol. 166, no. 4, pp. 490-495.

Rahman, I. & Adcock, I.M. 2006, "Oxidative stress and redox regulation of lung inflammation in COPD", *The European respiratory journal,* vol. 28, no. 1, pp. 219-242.

Rahman, I., Morrison, D., Donaldson, K. & MacNee, W. 1996, "Systemic oxidative stress in asthma, COPD, and smokers", *American journal of respiratory and critical care medicine,* vol. 154, no. 4 Pt 1, pp. 1055-1060.

Ramanathan, R., Rasmussen, M.R., Gerstmann, D.R., Finer, N., Sekar, K. & North American Study Group 2004, "A randomized, multicenter masked comparison trial of poractant alfa (Curosurf) versus beractant (Survanta) in the treatment of respiratory distress syndrome in preterm infants", *American Journal of Perinatology,* vol. 21, no. 03, pp. 109-119.

Rana, G.S., York, T.P., Edmiston, J.S., Zedler, B.K., Pounds, J.G., Adkins, J.N., Smith, R.D., Liu, Z., Li, G. & Webb, B.T. 2010, "Proteomic biomarkers in plasma that differentiate rapid and slow decline in lung function in adult cigarette smokers with chronic obstructive pulmonary disease (COPD)", *Analytical and bioanalytical chemistry,* vol. 397, no. 5, pp. 1809-1819.

Ranguelova, K., Rice, A.B., Khajo, A., Triquigneaux, M., Garantziotis, S., Magliozzo, R.S. & Mason, R.P. 2012, "Formation of reactive sulfite-derived free radicals by the activation of human neutrophils: an ESR study", *Free Radical Biology and Medicine,* vol. 52, no. 8, pp. 1264-1271.

Rankin, J., Naegel, G., Schrader, C., Matthay, R. & Reynolds, H. 1983, "Air-space immunoglobulin production and levels in bronchoalveolar lavage fluid of normal subjects and patients with sarcoidosis.", *The American Review of Respiratory Disease,* vol. 127, no. 4, pp. 442.

Raphael, G.D., Jeney, E.V., Baraniuk, J.N., Kim, I., Meredith, S.D. & Kaliner, M.A. 1989, "Pathophysiology of rhinitis. Lactoferrin and lysozyme in nasal secretions.", *Journal of Clinical Investigation,* vol. 84, no. 5, pp. 1528.

Raphael, G.D., Druce, H.M., Baraniuk, J.N. & Kaliner, M.A. 1988, "Pathophysiology of Rhinitis: 1. Assessment of the Sources of Protein in Methacholine-induced Nasal Secretions", *American Review of Respiratory Disease,* vol. 138, no. 2, pp. 413-420.

Rattan, S.I. 1996, "Synthesis, modifications, and turnover of proteins during aging", *Experimental gerontology,* vol. 31, no. 1, pp. 33-47.

Ratto, J., Wong, H., Liu, J., Fahy, J., Boushey, H., Solomon, C. & Balmes, J. 2006, *Environmental health perspectives,* vol. 114, no. 2, pp. 209.

Reid, L. 1960, "Measurement of the bronchial mucous gland layer: a diagnostic yardstick in chronic bronchitis", *Thorax,* vol. 15, no. 2, pp. 132.

Reid, L. & Clamp, J. 1978, "The biochemical and histochemical nomenclature of mucus", *British medical bulletin,* vol. 34, no. 1, pp. 5.

Rejman, J., Oberle, V., Zuhorn, I. & Hoekstra, D. 2004, "Size-dependent internalization of particles via the pathways of clathrin-and caveolae-mediated endocytosis", *Biochem.J,* vol. 377, pp. 159-169.

Rennard, S., Basset, G., Lecossier, D., O'donnell, K., Pinkston, P., Martin, P. & Crystal, R. 1986, "Estimation of volume of epithelial lining fluid recovered by lavage using urea as marker of dilution", *Journal of applied physiology,* vol. 60, no. 2, pp. 532.

Rennard, S., Ghafouri, M., Thompson, A., Linder, J., Vaughan, W., Jones, K., Ertl, R., Christensen, K., Prince, A. & Stahl, M. 1990, "Fractional processing of sequential bronchoalveolar lavage to separate bronchial and alveolar samples.", *The American Review of Respiratory Disease,* vol. 141, no. 1, pp. 208.

Renwick, L., Donaldson, K. & Clouter, A. 2001, "Impairment of alveolar macrophage phagocytosis by ultrafine particles", *Toxicology and applied pharmacology,* vol. 172, no. 2, pp. 119-127.

Repine, J.E., Bast, A. & Lankhorst, I. 1997, "Oxidative stress in chronic obstructive pulmonary disease", *American Journal of Respiratory and Critical Care Medicine,* vol. 156, no. 2, pp. 341-357.

Retamales, I., Elliott, W.M., Meshi, B., Coxson, H.O., Pare, P.D., Sciurba, F.C., Rogers, R.M., Hayashi, S. & Hogg, J.C. 2001, "Amplification of inflammation in emphysema and its association with latent adenoviral infection", *American journal of respiratory and critical care medicine,* vol. 164, no. 3, pp. 469-473.

Revak, S.D., Merritt, T.A., Degryse, E., Stefani, L., Courtney, M., Hallman, M. & Cochrane, C.G. 1988, "Use of human surfactant low molecular weight apoproteins in the reconstitution of surfactant biologic activity", *The Journal of clinical investigation,* vol. 81, no. 3, pp. 826-833.

Revenis, M.E. & Kaliner, M.A. 1992, "Lactoferrin and lysozyme deficiency in airway secretions: association with the development of bronchopulmonary dysplasia", *The Journal of pediatrics,* vol. 121, no. 2, pp. 262-270.

Reynaert, N.L. 2011, "Glutathione biochemistry in asthma", *Biochimica et Biophysica Acta (BBA)-General Subjects,* .

Reynolds, H.Y. 2011, "Bronchoalveolar Lavage and Other Methods to Define the Human Respiratory Tract Milieu in Health and Disease", *Lung,* , pp. 1-13.

Reynolds, H.Y., Fulmer, J.D., Kazmierowski, J., Roberts, W.C., Frank, M.M. & Crystal, R.G. 1977, "Analysis of cellular and protein content of broncho-alveolar lavage fluid from patients with idiopathic pulmonary fibrosis and chronic hypersensitivity pneumonitis.", *Journal of Clinical Investigation,* vol. 59, no. 1, pp. 165.

Reynolds, H. 2008, "Bronchoalveolar lavage: obtaining biologic specimens from the respiratory tract surface", *Sarcoidosis Vasc Diffuse Lung Dis*, vol. 25, pp. 5-9.

Reynolds, H. 2000, "Use of bronchoalveolar lavage in humans—past necessity and future imperative", *Lung*, vol. 178, no. 5, pp. 271-293.

Reynolds, H.Y. & Newball, H.H. 1974, "Analysis of proteins and respiratory cells obtained from human lungs by bronchial lavage", *The Journal of laboratory and clinical medicine*, vol. 84, no. 4, pp. 559-573.

Ricciardolo, F.L., Caramori, G., Ito, K., Capelli, A., Brun, P., Abatangelo, G., Papi, A., Chung, K.F., Adcock, I. & Barnes, P.J. 2005, "Nitrosative stress in the bronchial mucosa of severe chronic obstructive pulmonary disease", *Journal of allergy and clinical immunology*, vol. 116, no. 5, pp. 1028-1035.

Rode, A. & Shephard, R.J. 1994, "The ageing of lung function: cross-sectional and longitudinal studies of an Inuit community", *The European respiratory journal*, vol. 7, no. 9, pp. 1653-1659.

Rodier, F. & Campisi, J. 2011, "Four faces of cellular senescence", *The Journal of cell biology*, vol. 192, no. 4, pp. 547-556.

Rogan, M.P., Geraghty, P., Greene, C.M., O'Neill, S.J., Taggart, C.C. & McElvaney, N.G. 2006, "Antimicrobial proteins and polypeptides in pulmonary innate defence", *Respir Res*, vol. 7, no. 29, pp. 1-11.

Rogers, R.M., Braunstein, M.S. & Shuman, J.F. 1972, "Role of Bronchopulmonary Lavage in the Treatment of Respiratory Failure", *Chest*, vol. 62, no. 5 Supplement, pp. 95S.

Romero, A., PÉREZ- ARELLANO, J., GONZÁLEZ- VILLARÓN, L., Brock, J., Bellido, J.L.M. & CASTRO, S. 1993, "Effect of transferrin concentration on bacterial growth in human ascitic fluid from cirrhotic and neoplastic patients", *European journal of clinical investigation*, vol. 23, no. 11, pp. 699-705.

Rosenthal, L.A., Avila, P.C., Heymann, P.W., Martin, R.J., Miller, E.K., Papadopoulos, N.G., Peebles Jr, R.S. & Gern, J.E. 2010, "Viral respiratory tract infections and asthma: the course ahead", *Journal of Allergy and Clinical Immunology*, vol. 125, no. 6, pp. 1212-1217.

Roth, M. & Black, J. 2006, "Transcription factors in asthma: are transcription factors a new target for asthma therapy?", *Current Drug Targets*, vol. 7, no. 5, pp. 589-595.

Rothen-Rutishauser, B.M., Kiama, S.G. & Gehr, P. 2005, "A three-dimensional cellular model of the human respiratory tract to study the interaction with particles", *American journal of respiratory cell and molecular biology*, vol. 32, no. 4, pp. 281-289.

Roum, J., Buhl, R., McElvaney, N., Borok, Z. & Crystal, R. 1993, "Systemic deficiency of glutathione in cystic fibrosis", *Journal of applied physiology*, vol. 75, no. 6, pp. 2419.

Roy, Michelle G., et al. "Muc5b is required for airway defence." *Nature*505.7483 (2014): 412-416.

Ruano, M., Miguel, E., Perez-Gil, J. & Casals, C. 1996, "Comparison of lipid aggregation and self-aggregation activities of pulmonary surfactant-associated protein A.", *Biochem.J*, vol. 313, pp. 683-689.

Ruano, M.L., García-Verdugo, I., Miguel, E., Pérez-Gil, J. & Casals, C. 2000, "Self-aggregation of surfactant protein A", *Biochemistry*, vol. 39, no. 21, pp. 6529-6537.

Ruge, C.A., Schaefer, U.F., Herrmann, J., Kirch, J., Canadas, O., Echaide, M., Pérez-Gil, J., Casals, C., Müller, R. & Lehr, C. 2012, "The interplay of lung surfactant proteins and lipids assimilates the macrophage clearance of nanoparticles", *PloS one*, vol. 7, no. 7, pp. e40775.

Russell, R.E., Culpitt, S.V., DeMatos, C., Donnelly, L., Smith, M., Wiggins, J. & Barnes, P.J. 2002, "Release and activity of matrix metalloproteinase-9 and tissue inhibitor of metalloproteinase-1 by alveolar macrophages from patients with chronic obstructive pulmonary disease", *American journal of respiratory cell and molecular biology*, vol. 26, no. 5, pp. 602-609.

Rustow, B., Haupt, R., Stevens, P. & Kunze, D. 1993, "Type II pneumocytes secrete vitamin E together with surfactant lipids", *American Journal of Physiology-Lung Cellular and Molecular Physiology*, vol. 265, no. 2, pp. L133.

Rutgers, S.R., Postma, D.S., ten Hacken, N.H., Kauffman, H.F., van Der Mark, T.W., Koeter, G.H. & Timens, W. 2000, "Ongoing airway inflammation in patients with COPD who do not currently smoke", *Thorax*, vol. 55, no. 1, pp. 12-18.

Ryan, R.M., Mineo-Kuhn, M.M., Kramer, C.M. & Finkelstein, J.N. 1994, "Growth factors alter neonatal type II alveolar epithelial cell proliferation", *American Journal of Physiology-Lung Cellular and Molecular Physiology*, vol. 10, no. 1, pp. L17.

Rylander, R. & Haglind, P. 1984, "Airborne endotoxins and humidifier disease", *Clinical & Experimental Allergy*, vol. 14, no. 1, pp. 109-112.

Sadler, R., Prime, D., Burnell, P., Martin, G. & Forbes, B. 2011, "Integrated in vitro experimental modelling of inhaled drug delivery: deposition, dissolution and absorption", *Journal of drug delivery science and technology*, vol. 21, no. 4, pp. 331-338.

Saetta, M. 1999, "Airway inflammation in chronic obstructive pulmonary disease", *American journal of respiratory and critical care medicine*, vol. 160, no. supplement_1, pp. S17-S20.

Saetta, M., Di Stefano, A., Maestrelli, P., Ferraresso, A., Drigo, R., Potena, A., Ciaccia, A. & Fabbri, L.M. 1993, "Activated T-lymphocytes and macrophages in bronchial mucosa of subjects with chronic bronchitis", *American review of respiratory disease*, vol. 147, no. 2, pp. 301-306.

Saetta, M., Turato, G., Facchini, F.M., Corbino, L., Lucchini, R.E., Casoni, G., Maestrelli, P., Mapp, C.E., Ciaccia, A. & Fabbri, L.M. 1997, "Inflammatory cells in the bronchial glands of smokers with chronic bronchitis", *American journal of respiratory and critical care medicine*, vol. 156, no. 5, pp. 1633-1639.

Salive, M.E., Cornoni-Huntley, J., Phillips, C.L., Guralnik, J.M., Cohen, H.J., Ostfeld, A.M. & Wallace, R.B. 1992, "Serum albumin in older persons: relationship with age and health status", *Journal of clinical epidemiology*, vol. 45, no. 3, pp. 213-221.

Sánchez-Barbero, F., Rivas, G., Steinhilber, W. & Casals, C. 2007, "Structural and functional differences among human surfactant proteins SP-A1, SP-A2 and co-expressed SP-A1/SP-A2: role of supratrimeric oligomerization", *Biochem.J*, vol. 406, pp. 479-489.

Sánchez-Barbero, F., Rivas, G., Steinhilber, W. & Casals, C. 2007, "Structural and functional differences among human surfactant proteins SP-A1, SP-A2 and co-expressed SP-A1/SP-A2: role of supratrimeric oligomerization", *Biochem.J*, vol. 406, pp. 479-489.

Sanchez-Barbero, F., Strassner, J., Garcia-Canero, R., Steinhilber, W. & Casals, C. 2005, "Role of the degree of oligomerization in the structure and function of human surfactant protein A", *The Journal of biological chemistry*, vol. 280, no. 9, pp. 7659-7670.

Sanders, R.L., Hassett, R.J. & Vatter, A.E. 1980, "Isolation of lung lamellar bodies and their conversion to tubular myelin figures in vitro", *The Anatomical Record*, vol. 198, no. 3, pp. 485-501.

Schalk, B.W., Visser, M., Deeg, D.J. & Bouter, L.M. 2004, "Lower levels of serum albumin and total cholesterol and future decline in functional performance in older persons: the Longitudinal Aging Study Amsterdam", *Age and Ageing*, vol. 33, no. 3, pp. 266-272.

Schleh, C., Kreyling, W.G. & Lehr, C. 2013, "Pulmonary surfactant is indispensable in order to simulate the in vivo situation", *Part Fibre Toxicol*, vol. 10, pp. 1-6.

Schleh, C., Muhlfeld, C., Pulskamp, K., Schmiedl, A., Nassimi, M., Lauenstein, H.D., Braun, A., Krug, N., Erpenbeck, V.J. & Hohlfeld, J.M. 2009, "The effect of titanium dioxide nanoparticles on pulmonary surfactant function and ultrastructure", *Respir Res*, vol. 10, pp. 90.

Schmidt, R., Steinhilber, W., Ruppert, C., Daum, C., Grimminger, F., Seeger, W. & Gunther, A. 2002, "An ELISA technique for quantification of surfactant apoprotein (SP)-C in bronchoalveolar lavage fluid", *American journal of respiratory and critical care medicine*, vol. 165, no. 4, pp. 470-474.

Schock, B.C., Koostra, J., Kwack, S., Hackman, R.M., van der Vliet, A. & Cross, C.E. 2004, "Ascorbic acid in nasal and tracheobronchial airway lining fluids", *Free Radical Biology and Medicine*, vol. 37, no. 9, pp. 1393-1401.

Schock, B.C., Young, I.S., Brown, V., Fitch, P.S., Shields, M.D. & Ennis, M. 2003, "Antioxidants and oxidative stress in BAL fluid of atopic asthmatic children", *Pediatric research*, vol. 53, no. 3, pp. 375-381.

Schoonbrood, D.F., Lutter, R., Habets, F.J., Roos, C.M., Jansen, H.M. & Out, T.A. 1994, "Analysis of plasma-protein leakage and local secretion in sputum from patients with

asthma and chronic obstructive pulmonary disease", *American journal of respiratory and critical care medicine,* vol. 150, no. 6 Pt 1, pp. 1519-1527.

Schroer, K.T. 2010, *The role of glutathione S-transferase Pi (GSTPi) in asthma,* .

Schwartz, D.A., Thorne, P.S., Yagla, S.J., Burmeister, L.F., Olenchock, S.A., Watt, J.L. & Quinn, T.J. 1995, "The role of endotoxin in grain dust-induced lung disease", *American journal of respiratory and critical care medicine,* vol. 152, no. 2, pp. 603-608.

Schwartz, J. & Weiss, S.T. 1990, "Dietary factors and their relation to respiratory symptoms. The Second National Health and Nutrition Examination Survey", *American Journal of Epidemiology,* vol. 132, no. 1, pp. 67-76.

ScienceDaily, (2014). *Asthma tied to bacterial communities in the airway*. [online] Available at: http://www.sciencedaily.com/releases/2011/02/110217151457.htm [Accessed 8 Sep. 2014].

Sdraulig, S., Franich, R., Tinker, R., Solomon, S., O'Brien, R. & Johnston, P. 2008, "In vitro dissolution studies of uranium bearing material in simulated lung fluid", *Journal of environmental radioactivity,* vol. 99, no. 3, pp. 527-538.

Sebastien, P., Begin, R. & Masse, S. 1990, "Mass, number and size of lung fibres in the pathogenesis of asbestosis in sheep", *Journal of experimental pathology (Oxford, England),* vol. 71, no. 1, pp. 1-10.

Serrano, A.G. & Perez-Gil, J. 2006, "Protein-lipid interactions and surface activity in the pulmonary surfactant system", *Chemistry and physics of lipids,* vol. 141, no. 1-2, pp. 105-118.

Shacter, E. 2000, "Quantification and significance of protein oxidation in biological samples 1*", *Drug metabolism reviews,* vol. 32, no. 3-4, pp. 307-326.

Shapiro, S.D. 1999, "The macrophage in chronic obstructive pulmonary disease", *American Journal of Respiratory and Critical Care Medicine,* vol. 160, no. supplement_1, pp. S29-S32.

Shapiro, S.D. 2002, "Proteinases in chronic obstructive pulmonary disease", *Biochemical Society transactions,* vol. 30, no. 2, pp. 98-102.

Shargel, L. & Yu, A. "Applied Biopharmaceutics & Pharmacokinetics. 1999", *Appleton & Lange, Stamford, CT,* .

Sharma, G. & Goodwin, J. 2006, "Effect of aging on respiratory system physiology and immunology", *Clinical interventions in aging,* vol. 1, no. 3, pp. 253-260.

Shaw, A.C., Goldstein, D.R. & Montgomery, R.R. 2013, "Age-dependent dysregulation of innate immunity", *Nature Reviews Immunology,* .

Shevchenko, A., Wilm, M., Vorm, O. & Mann, M. 1996, "Mass spectrometric sequencing of proteins from silver-stained polyacrylamide gels", *Analytical Chemistry,* vol. 68, no. 5, pp. 850-858.

Shields, M.D. & Riedler, J. 2000, "Bronchoalveolar lavage and tracheal aspirate for assessing airway inflammation in children", *American journal of respiratory and critical care medicine,* vol. 162, no. 2, pp. S15.

Shock, N.W. 1962, "The physiology of aging", *Scientific American,* vol. 206, pp. 100-110.

Shono, Y., Jantratid, E., Janssen, N., Kesisoglou, F., Mao, Y., Vertzoni, M., Reppas, C. & Dressman, J.B. 2009, "Prediction of food effects on the absorption of celecoxib based on biorelevant dissolution testing coupled with physiologically based pharmacokinetic modeling", *European Journal of Pharmaceutics and Biopharmaceutics,* vol. 73, no. 1, pp. 107-114.

Sibille, Y. & Reynolds, H.Y. 1990, "Macrophages and polymorphonuclear neutrophils in lung defense and injury", *American Review of Respiratory Disease,* vol. 141, no. 2, pp. 471-501.

Simm, A. 2013, "Protein glycation during aging and in cardiovascular disease", *Journal of proteomics,* vol. 92, pp. 248-259.

Simpson, J., Gibson, P., Yang, I., Upham, J., James, A., Reynolds, P. & Hodge, S. 2013, "Impaired macrophage phagocytosis in non- eosinophilic asthma", *Clinical & Experimental Allergy,* vol. 43, no. 1, pp. 29-35.

Sinden, N.J. & Stockley, R.A. 2010, "Systemic inflammation and comorbidity in COPD: a result of 'overspill' of inflammatory mediators from the lungs? Review of the evidence", *Thorax,* vol. 65, no. 10, pp. 930-936.

Singh, G., Singh, J., Katyal, S.L., Brown, W.E., Kramps, J.A., Paradis, I.L., Dauber, J.H., Macpherson, T.A. & Squeglia, N. 1988, "Identification, cellular localization, isolation, and characterization of human Clara cell-specific 10 KD protein", *The journal of histochemistry and cytochemistry : official journal of the Histochemistry Society,* vol. 36, no. 1, pp. 73-80.

Singh, P.K., Tack, B.F., McCray, P.B.,Jr & Welsh, M.J. 2000, "Synergistic and additive killing by antimicrobial factors found in human airway surface liquid", *American journal of physiology.Lung cellular and molecular physiology,* vol. 279, no. 5, pp. L799-805.

Sinswat, P., Overhoff, K.A., McConville, J.T., Johnston, K.P. & Williams III, R.O. 2008, "Nebulization of nanoparticulate amorphous or crystalline tacrolimus-Single-dose pharmacokinetics study in mice", *European Journal of Pharmaceutics and Biopharmaceutics,* vol. 69, no. 3, pp. 1057-1066.

Siomek, A., Gackowski, D., Rozalski, R., Dziaman, T., Szpila, A., Guz, J. & Olinski, R. 2007, "Higher leukocyte 8-oxo-7, 8-dihydro-2'-deoxyguanosine and lower plasma ascorbate in aging humans?", *Antioxidants & redox signaling,* vol. 9, no. 1, pp. 143-150.

Skoza, L., Snyder, A. & Kikkawa, Y. 1983, "Ascorbic acid in bronchoalveolar wash", *Lung*, vol. 161, no. 1, pp. 99-109.

Slade, R., Crissman, K., Norwood, J. & Hatch, G. 1993, "Comparison of antioxidant substances in bronchoalveolar lavage cells and fluid from humans, guinea pigs, and rats", *Experimental lung research*, vol. 19, no. 4, pp. 469-484.

Sleigh, M.A., Blake, J.R. & Liron, N. 1988, "The propulsion of mucus by cilia", *The American Review of Respiratory Disease*, vol. 137, no. 3, pp. 726-741.

Smith, L.J., Shamsuddin, M., Sporn, P.H., Denenberg, M. & Anderson, J. 1997, "Reduced superoxide dismutase in lung cells of patients with asthma", *Free Radical Biology and Medicine*, vol. 22, no. 7, pp. 1301-1307.

Smith, P., Krohn, R., Hermanson, G., Mallia, A., Gartner, F., Provenzano, M.D., Fujimoto, E., Goeke, N., Olson, B. & Klenk, D. 1985, "Measurement of protein using bicinchoninic acid", *Analytical Biochemistry*, vol. 150, no. 1, pp. 76-85.

Smith, L.J., Houston, M. & Anderson, J. 1993, "Increased levels of glutathione in bronchoalveolar lavage fluid from patients with asthma", *The American Review of Respiratory Disease*, vol. 147, no. 6 Pt 1, pp. 1461-1464.

Snider, G.L. 1989, "Chronic obstructive pulmonary disease: risk factors, pathophysiology and pathogenesis", *Annual Review of Medicine*, vol. 40, no. 1, pp. 411-429.

Snipes, M.B. 1989, "Long-term retention and clearance of particles inhaled by mammalian species", *CRC critical reviews in toxicology*, vol. 20, no. 3, pp. 175-211.

Sobin, S., Fung, Y. & Tremer, H. 1988, "Collagen and elastin fibers in human pulmonary alveolar walls", *J.Appl.Physiol*, vol. 64, no. 4, pp. 1659-1675.

Solana, R., Tarazona, R., Gayoso, I., Lesur, O., Dupuis, G. & Fulop, T. 2012, "Innate immunosenescence: effect of aging on cells and receptors of the innate immune system in humans", *Seminars in immunology*Elsevier, , pp. 331.

Soll, R. & Blanco, F. 2001, "Natural surfactant extract versus synthetic surfactant for neonatal respiratory distress syndrome", *Cochrane Database Syst Rev*, vol. 2, no. 2.

Son, Y.J. & McConville, J.T. 2009, "Development of a standardized dissolution test method for inhaled pharmaceutical formulations", *International journal of pharmaceutics*, vol. 382, no. 1-2, pp. 15-22.

Soutar, C. 1977, "Distribution of plasma cells and other cells containing immunoglobulin in the respiratory tract in chronic bronchitis", *Thorax*, vol. 32, no. 4, pp. 387.

Soutar, A., Seaton, A. & Brown, K. 1997, "Bronchial reactivity and dietary antioxidants", *Thorax*, vol. 52, no. 2, pp. 166-170.

Sparrow, D., Glynn, R., Cohen, M. & Weiss, S. 1984, "The relationship of the peripheral leukocyte count and cigarette smoking to pulmonary function among adult men.", *CHEST Journal*, vol. 86, no. 3, pp. 383-386.

Sporty, J.L., Horálková, L. & Ehrhardt, C. 2008, "In vitro cell culture models for the assessment of pulmonary drug disposition", .

Stadtman, E.R., Van Remmen, H., Richardson, A., Wehr, N.B. & Levine, R.L. 2005, "Methionine oxidation and aging", *Biochimica et Biophysica Acta (BBA)-Proteins and Proteomics*, vol. 1703, no. 2, pp. 135-140.

Standardization of Spirometry 1995, "1994 update: American Thoracic Society", *Am J Respir Crit Care Med*, vol. 152, pp. 1107-1136.

Starkey, P.M. & Barrett, A. 1977, "α 2-Macroglobulin, a physiological regulator of proteinase activity", *Proteinases in mammalian cells and tissues*, , pp. 663-696.

Stearns, R.C., Paulauskis, J.D. & Godleski, J.J. 2001, "Endocytosis of ultrafine particles by A549 cells", *American Journal of Respiratory Cell and Molecular Biology*, vol. 24, no. 2, pp. 108-115.

Steinfeld, R., Reinhardt, K., Schreiber, K., Hillebrand, M., Kraetzner, R., Bruck, W., Saftig, P. & Gartner, J. 2006, "Cathepsin D deficiency is associated with a human neurodegenerative disorder", *American Journal of Human Genetics*, vol. 78, no. 6, pp. 988-998.

Stemcell.com, (2014). *PneumaCult™-ALI: Air-Liquid Interface Culture of Human Bronchial Epithelial Cells | STEMCELL Technologies*. [online] Available at: http://www.stemcell.com/en/Products/Popular-Product-Lines/PneumaCult.aspx [Accessed 8 Sep. 2014].

Stites, S.W., Nelson, M.E. & Wesselius, L.J. 1995, "Transferrin concentrations in serum and lower respiratory tract fluid of mechanically ventilated patients with COPD or ARDS", *CHEST Journal*, vol. 107, no. 6, pp. 1681-1685.

Stockley, R. 1984, "Measurement of soluble proteins in lung secretions.", *Thorax*, vol. 39, no. 4, pp. 241.

Stockley, R. & Burnett, D. 1980, "Local IgA production in patients with chronic bronchitis: effect of acute respiratory infection.", *Thorax*, vol. 35, no. 3, pp. 202.

Stockley, R., Mistry, M., Bradwell, A. & Burnett, D. 1979, "A study of plasma proteins in the sol phase of sputum from patients with chronic bronchitis.", *Thorax*, vol. 34, no. 6, pp. 777.

Stone, V. & Donaldson, K. 2006, "Nanotoxicology: Signs of stress", *Nature Nanotechnology*, vol. 1, no. 1, pp. 23-24.

Strauss, S., Bauer, J., Ganter, U., Jonas, U., Berger, M. & Volk, B. 1992, "Detection of interleukin-6 and alpha 2-macroglobulin immunoreactivity in cortex and hippocampus of Alzheimer's disease patients", *Laboratory investigation; a journal of technical methods and pathology*, vol. 66, no. 2, pp. 223-230.

Subramaniam, S., Whitsett, J., Hull, W. & Gairola, C. 1996, "Alteration of pulmonary surfactant proteins in rats chronically exposed to cigarette smoke", *Toxicology and applied pharmacology*, vol. 140, no. 2, pp. 274-280.

Sun, W., Xie, C., Wang, H. & Hu, Y. 2004, "Specific role of polysorbate 80 coating on the targeting of nanoparticles to the brain", *Biomaterials*, vol. 25, no. 15, pp. 3065-3071.

Sun, B., Curstedt, T., Lindgren, G., Franzen, B., Alaiya, A.A., Calkovska, A. & Robertson, B. 1997, "Biophysical and physiological properties of a modified porcine surfactant enriched with surfactant protein A", *The European respiratory journal*, vol. 10, no. 9, pp. 1967-1974.

Sun, G., Crissman, K., Norwood, J., Richards, J., Slade, R. & Hatch, G.E. 2001, "Oxidative interactions of synthetic lung epithelial lining fluid with metal-containing particulate matter", *American journal of physiology.Lung cellular and molecular physiology*, vol. 281, no. 4, pp. L807-15.

Sunesen, V.H., Pedersen, B.L., Kristensen, H.G. & Müllertz, A. 2005, "In vivo in vitro correlations for a poorly soluble drug, danazol, using the flow-through dissolution method with biorelevant dissolution media", *European journal of pharmaceutical sciences*, vol. 24, no. 4, pp. 305-313.

Sung, J.C., Pulliam, B.L. & Edwards, D.A. 2007, "Nanoparticles for drug delivery to the lungs", *Trends in biotechnology*, vol. 25, no. 12, pp. 563-570.

Sung, J.C., Pulliam, B.L. & Edwards, D.A. 2007, "Nanoparticles for drug delivery to the lungs", *Trends in biotechnology*, vol. 25, no. 12, pp. 563-570.

Sutinen, S., Riska, H., Backman, R., Sutinen, S. & Fröseth, B. 1995, "Alveolar lavage fluid (ALF) of normal volunteer subjects: cytologic, immunocytochemical, and biochemical reference values", *Respiratory medicine*, vol. 89, no. 2, pp. 85-92.

Suzuki, Y., Fujita, Y. & Kogishi, K. 1989, "Reconstitution of tubular myelin from synthetic lipids and proteins associated with pig pulmonary surfactant", *American Review of Respiratory Disease*, vol. 140, no. 1, pp. 75-81.

Svardal, A.M., Mansoor, M.A. & Ueland, P.M. 1990, "Determination of reduced, oxidized, and protein-bound glutathione in human plasma with precolumn derivatization with monobromobimane and liquid chromatography", *Analytical Biochemistry*, vol. 184, no. 2, pp. 338-346.

Szweda, P.A., Camouse, M., Lundberg, K.C., Oberley, T.D. & Szweda, L.I. 2003, "Aging, lipofuscin formation, and free radical-mediated inhibition of cellular proteolytic systems", *Ageing research reviews*, vol. 2, no. 4, pp. 383-405.

Tager, I.B., Segal, M.R., Speizer, F.E. & Weiss, S.T. 1988, "The natural history of forced expiratory volumes: effect of cigarette smoking and respiratory symptoms", *American Review of Respiratory Disease*, vol. 138, no. 4, pp. 837-849.

Taggart, C., Cervantes-Laurean, D., Kim, G., McElvaney, N.G., Wehr, N., Moss, J. & Levine, R.L. 2000, "Oxidation of either methionine 351 or methionine 358 in alpha 1-

antitrypsin causes loss of anti-neutrophil elastase activity", *The Journal of biological chemistry*, vol. 275, no. 35, pp. 27258-27265.

Takaya, M., Shinohara, Y., Serita, F., Ono-Ogasawara, M., Otaki, N., Toya, T., Takata, A., Yoshida, K. & Kohyama, N. 2006, "Dissolution of functional materials and rare earth oxides into pseudo alveolar fluid", *Industrial health*, vol. 44, no. 4, pp. 639-644.

Takeda, T., Hosokawa, M., Takeshita, S., Irino, M., Higuchi, K., Matsushita, T., Tomita, Y., Yasuhira, K., Hamamoto, H. & Shimizu, K. 1981, "A new murine model of accelerated senescence", *Mechanisms of ageing and development*, vol. 17, no. 2, pp. 183-194.

Takemura, S., Rossing, T. & Perlmutter, D. 1986, "A lymphokine regulates expression of alpha-1-proteinase inhibitor in human monocytes and macrophages.", *Journal of Clinical Investigation*, vol. 77, no. 4, pp. 1207.

Takizawa, H. 2009, "Recent development of drug delivery systems for the treatment of asthma and related disorders", *Recent Patents on Inflammation &# 38; Allergy Drug Discovery*, vol. 3, no. 3, pp. 232-239.

Taunton, A.E., Gunter, M.E., Druschel, G.K. & Wood, S.A. 2010, "Geochemistry in the lung: Reaction-path modeling and experimental examination of rock-forming minerals under physiologic conditions", *American Mineralogist*, vol. 95, no. 11-12, pp. 1624.

Tee, S., Forbes, B., Larhrib, H., Marriott, C. & Martin, G. 2001, "Development of an in vitro dissolution–absorption model to evaluate the delivery of aerosolised drug from dry powder inhaler formulations", *Drug Deliv.Lung*, vol. 12, pp. 115-118.

Tenner, A.J., Robinson, S.L., Borchelt, J. & Wright, J.R. 1989, "Human pulmonary surfactant protein (SP-A), a protein structurally homologous to C1q, can enhance FcR- and CR1-mediated phagocytosis", *The Journal of biological chemistry*, vol. 264, no. 23, pp. 13923-13928.

Teramoto, S., Fukuchi, Y., Uejima, Y., Teramoto, K., Ito, H. & Orimo, H. 1994, "Age-related changes in the antioxidant screen of the distal lung in mice", *Lung*, vol. 172, no. 4, pp. 223-230.

Terashima, T., Wiggs, B., English, D., Hogg, J.C. & van Eeden, S.F. 1997, "Phagocytosis of small carbon particles (PM10) by alveolar macrophages stimulates the release of polymorphonuclear leukocytes from bone marrow", *American journal of respiratory and critical care medicine*, vol. 155, no. 4, pp. 1441-1447.

Terman, A. & Brunk, U.T. 2004, "Aging as a catabolic malfunction", *The international journal of biochemistry & cell biology*, vol. 36, no. 12, pp. 2365-2375.

Thelohan, S., De Meringo, A., Furtak, H. & Holstein, W. 1993, *Mineral fibers decomposable in a physiological medium*, .

Thompson, A., Bohling, T., Payvandi, F. & Rennard, S. 1990, "Lower respiratory tract lactoferrin and lysozyme arise primarily in the airways and are elevated in association

with chronic bronchitis.", *The Journal of laboratory and clinical medicine,* vol. 115, no. 2, pp. 148.

Thompson, A.B., Daughton, D., Robbins, R.A., Ghafouri, M.A., Oehlerking, M. & Rennard, S.I. 1989, "Intraluminal airway inflammation in chronic bronchitis: characterization and correlation with clinical parameters", *American Review of Respiratory Disease,* vol. 140, no. 6, pp. 1527-1537.

Thompson, A.B., Scholer, S.G., Daughton, D.M., Potter, J.F. & Rennard, S.I. 1992, "Altered epithelial lining fluid parameters in old normal individuals", *Journal of gerontology,* vol. 47, no. 5, pp. M171-6.

Thurlbeck, W.M. 1967, "The internal surface area of nonemphysematous lungs", *The American Review of Respiratory Disease,* vol. 95, no. 5, pp. 765-773.

Titanian, A.S., Selitskaia, R.P. & Kim, A.C. 1987, "Determination of the concentration of immunoglobulins and other proteins in bronchoalveolar fluid of patients with various types of pulmonary pathology", *Terapevticheskii arkhiv,* vol. 59, no. 12, pp. 48-51.

Toews, G. 2005, "Impact of bacterial infections on airway diseases", *European Respiratory Review,* vol. 14, no. 95, pp. 62-68.

Tony, R. & Knight, D.A. 2005, "Structural changes in the airways in asthma: observations and consequences", *Clinical science,* vol. 108, pp. 463-477.

Travis, S.M., Conway, B.D., Zabner, J., Smith, J.J., Anderson, N.N., Singh, P.K., Peter Greenberg, E. & Welsh, M.J. 1999, "Activity of abundant antimicrobials of the human airway", *American journal of respiratory cell and molecular biology,* vol. 20, no. 5, pp. 872-879.

Tu, C., Mammen, M.J., Li, J., Shen, X., Jiang, X., Hu, Q., Wang, J., Sethi, S. & Qu, J. 2013, "Large-Scale, Ion-Current-Based Proteomics Investigation of Bronchoalveolar Lavage Fluid in Chronic Obstructive Pulmonary Disease Patients", *Journal of proteome research,* vol. 13, no. 2, pp. 627-639.

Tuder, R.M., Janciauskiene, S.M. & Petrache, I. 2010, "Lung Disease Associated with α1-Antitrypsin Deficiency", *Proceedings of the American Thoracic Society,* vol. 7, no. 6, pp. 381-386.

Turato, G., Zuin, R., Miniati, M., Baraldo, S., Rea, F., Beghé, B., Monti, S., Formichi, B., Boschetto, P. & Harari, S. 2002, "Airway inflammation in severe chronic obstructive pulmonary disease: relationship with lung function and radiologic emphysema", *American journal of respiratory and critical care medicine,* vol. 166, no. 1, pp. 105-110.

Umstead, T.M., Freeman, W.M., Chinchilli, V.M. & Phelps, D.S. 2009, "Age-related changes in the expression and oxidation of bronchoalveolar lavage proteins in the rat", *American journal of physiology.Lung cellular and molecular physiology,* vol. 296, no. 1, pp. L14-29.

van de Graaf, E.A., Jansen, H.M., Weber, J.A., Koolen, M.G.J. & Out, T.A. 1991, "Influx of urea during bronchoalveolar lavage depends on the permeability of the respiratory membrane", *Clinica chimica acta*, vol. 196, no. 1, pp. 27-39.

van den Dobbelsteen, D.J., Nobel, C.S., Schlegel, J., Cotgreave, I.A., Orrenius, S. & Slater, A.F. 1996, "Rapid and specific efflux of reduced glutathione during apoptosis induced by anti-Fas/APO-1 antibody", *The Journal of biological chemistry*, vol. 271, no. 26, pp. 15420-15427.

van der Vliet, A., O'Neill, C.A., Cross, C.E., Koostra, J.M., Volz, W.G., Halliwell, B. & Louie, S. 1999, "Determination of low-molecular-mass antioxidant concentrations in human respiratory tract lining fluids", *American Journal of Physiology-Lung Cellular and Molecular Physiology*, vol. 276, no. 2, pp. L289.

van der Vliet, A. & Cross, C.E. 2001, "Innate antioxidant defense systems in the respiratory tract", *Biofactors*, vol. 15, no. 2, pp. 83-86.

van Gaal, E., Spierenburg, G., Hennink, W., Crommelin, D. & Mastrobattista, E. 2010, "Flow cytometry for rapid size determination and sorting of nucleic acid containing nanoparticles in biological fluids", *Journal of Controlled Release*, vol. 141, no. 3, pp. 328-338.

van Iwaarden, F., Welmers, B., Verhoef, J., Haagsman, H.P. & van Golde, L.M. 1990, "Pulmonary surfactant protein A enhances the host-defense mechanism of rat alveolar macrophages", *American journal of respiratory cell and molecular biology*, vol. 2, no. 1, pp. 91-98.

Van Iwaarden, J., Pikaar, J., Storm, J., Brouwer, E., Verhoef, J., Oosting, R., Van Golde, L. & Van Strijp, J. 1994, "Binding of surfactant protein A to the lipid A moiety of bacterial lipopolysaccharides.", *Biochemical Journal*, vol. 303, no. Pt 2, pp. 407.

Van Iwaarden, J., Shimizu, H., Van Golde, P., Voelker, D. & Van Golde, L. 1992, "Rat surfactant protein D enhances the production of oxygen radicals by rat alveolar macrophages.", *Biochemical Journal*, vol. 286, no. Pt 1, pp. 5.

Vasanthakumar, G., Manjunath, R., Mukherjee, A.B., Warabi, H. & Schiffmann, E. 1988, "Inhibition of phagocyte chemotaxis by uteroglobin, an inhibitor of blastocyst rejection", *Biochemical pharmacology*, vol. 37, no. 3, pp. 389-394.

Veldhuizen, R., Marcou, J., Yao, L., McCaig, L., Ito, Y. & Lewis, J. 1996, "Alveolar surfactant aggregate conversion in ventilated normal and injured rabbits", *American Journal of Physiology-Lung Cellular and Molecular Physiology*, vol. 270, no. 1, pp. L152.

Verrills, N.M., Irwin, J.A., Yan He, X., Wood, L.G., Powell, H., Simpson, J.L., McDonald, V.M., Sim, A. & Gibson, P.G. 2011, "Identification of novel diagnostic biomarkers for asthma and chronic obstructive pulmonary disease", *American journal of respiratory and critical care medicine*, vol. 183, no. 12, pp. 1633-1643.

Vestbo, J., Edwards, L.D., Scanlon, P.D., Yates, J.C., Agusti, A., Bakke, P., Calverley, P.M., Celli, B., Coxson, H.O. & Crim, C. 2011, "Changes in forced expiratory

volume in 1 second over time in COPD", *New England Journal of Medicine,* vol. 365, no. 13, pp. 1184-1192.

Vestbo, J. & Lange, P. 2002, "Can GOLD Stage 0 provide information of prognostic value in chronic obstructive pulmonary disease?", *American journal of respiratory and critical care medicine,* vol. 166, no. 3, pp. 329-332.

Vestbo, J., Prescott, E. & Lange, P. 1996, "Association of chronic mucus hypersecretion with FEV1 decline and chronic obstructive pulmonary disease morbidity. Copenhagen City Heart Study Group", *American journal of respiratory and critical care medicine,* vol. 153, no. 5, pp. 1530-1535.

Vida, C., Corpas, I., De la Fuente, M. & González, E.M. 2011, "Age-related changes in xanthine oxidase activity and lipid peroxidation, as well as in the correlation between both parameters, in plasma and several organs from female mice", *Journal of physiology and biochemistry,* vol. 67, no. 4, pp. 551-558.

Vitale, G., Salvioli, S. & Franceschi, C. 2013, "Oxidative stress and the ageing endocrine system", *Nature Reviews Endocrinology,* vol. 9, no. 4, pp. 228-240.

Vlachaki, E.M., Koutsopoulos, A.V., Tzanakis, N., Neofytou, E., Siganaki, M., Drositis, I., Moniakis, A., Schiza, S., Siafakas, N.M. & Tzortzaki, E.G. 2010, "Altered surfactant protein-A expression in type II pneumocytes in COPD", *CHEST Journal,* vol. 137, no. 1, pp. 37-45.

Von Neergaard, K. 1929, "New notions on a fundamental principle of respiratory mechanics: the retractile force of the lung, dependent on the surface tension in the alveoli", *Z.Gesamte Exp.Med,* vol. 66, pp. 373-394.

Voynow, J.A. & Kummarapurugu, A. 2011, "Isoprostanes and asthma", *Biochimica et Biophysica Acta (BBA)-General Subjects,* vol. 1810, no. 11, pp. 1091-1095.

Vranic, S., Garcia-Verdugo, I., Darnis, C., Sallenave, J., Boggetto, N., Marano, F., Boland, S. & Baeza-Squiban, A. 2013, "Internalization of SiO2 nanoparticles by alveolar macrophages and lung epithelial cells and its modulation by the lung surfactant substitute Curosurf®", *Environmental Science and Pollution Research,* vol. 20, no. 5, pp. 2761-2770.

Vural, H., Uzun, K., Uz, E., Kocyigit, A., Cigli, A. & Akyol, Ö. 2000, "Concentrations of copper, zinc and various elements in serum of patients with bronchial asthma", *Journal of trace elements in medicine and biology,* vol. 14, no. 2, pp. 88-91.

Walford, R.L. 1969, "The immunologic theory of aging", *Immunological reviews,* vol. 2, no. 1, pp. 171-171.

Wallace, W.A., Gillooly, M. & Lamb, D. 1992, "Intra-alveolar macrophage numbers in current smokers and non-smokers: a morphometric study of tissue sections", *Thorax,* vol. 47, no. 6, pp. 437-440.

Walters, E. & Gardiner, P. 1991, "Bronchoalveolar lavage as a research tool.", *Thorax,* vol. 46, no. 9, pp. 613.

Wang, J., Kishore, U., Lim, B., Strong, P. & Reid, K. 1996, "Interaction of human lung surfactant proteins A and D with mite (Dermatophagoides pteronyssinus) allergens", *Clinical and experimental immunology*, vol. 106, no. 2, pp. 367.

Wang, L., Castranova, V., Mishra, A., Chen, B., Mercer, R.R., Schwegler-Berry, D. & Rojanasakul, Y. 2010, "Dispersion of single-walled carbon nanotubes by a natural lung surfactant for pulmonary in vitro and in vivo toxicity studies", *Particle and fibre toxicology*, vol. 7, no. 1, pp. 31.

Wang, W., Zhou, H., Lin, H., Roy, S., Shaler, T.A., Hill, L.R., Norton, S., Kumar, P., Anderle, M. & Becker, C.H. 2003, "Quantification of proteins and metabolites by mass spectrometry without isotopic labeling or spiked standards", *Analytical Chemistry*, vol. 75, no. 18, pp. 4818-4826.

Wang, C.H., Wu, S.B., Wu, Y.T. & Wei, Y.H. 2013, "Oxidative stress response elicited by mitochondrial dysfunction: implication in the pathophysiology of aging", *Experimental biology and medicine (Maywood, N.J.)*, vol. 238, no. 5, pp. 450-460.

Wanner, A. 1994, "Possible control of airway hypersecretion", *Lung biology in health and disease*, vol. 72, pp. 629-646.

Ward, C., Duddridge, M., Fenwick, J., Gardiner, P., Fleetwood, A., Hendrick, D. & Walters, E. 1993, "Evaluation of albumin as a reference marker of dilution in bronchoalveolar lavage fluid from asthmatic and control subjects.", *Thorax*, vol. 48, no. 5, pp. 518.

Ward, W.F. 2002, "Protein degradation in the aging organism" in *Protein Degradation in Health and Disease* Springer, , pp. 35-42.

Warfvinge, L. 1955, "Paper Electrophoresis of Sputum in Bronchiolar Carcinoma (Pulmonary Adenomatosis) 1", *Acta Medica Scandinavica*, vol. 153, no. 1, pp. 49-52.

Watanabe, M., Ishizaka, A., Ikeda, E., Ohashi, A. & Kobayashi, K. 2003, "Contributions of bronchoscopic microsampling in the supplemental diagnosis of small peripheral lung carcinoma", *The Annals of Thoracic Surgery*, vol. 76, no. 5, pp. 1668-1672.

Wattiez, R., Hermans, C., Bernard, A., Lesur, O. & Falmagne, P. 1999, "Human bronchoalveolar lavage fluid: Two- dimensional gel electrophoresis, amino acid microsequencing and identification of major proteins", *Electrophoresis*, vol. 20, no. 7, pp. 1634-1645.

Wattiez, R., Hermans, C., Cruyt, C., Bernard, A. & Falmagne, P. 2000, "Human bronchoalveolar lavage fluid protein two- dimensional database: Study of interstitial lung diseases", *Electrophoresis*, vol. 21, no. 13, pp. 2703-2712.

Weaver, T.E. & Conkright, J.J. 2001, "Function of surfactant proteins B and C", *Annual Review of Physiology*, vol. 63, no. 1, pp. 555-578.

Weaver, T.E. & Whitsett, J.A. 1991, "Function and regulation of expression of pulmonary surfactant-associated proteins.", *Biochemical journal*, vol. 273, no. Pt 2, pp. 249.

Webber, S. & Widdicombe, J. 1989, "The transport of albumin across the ferret in vitro whole trachea.", *The Journal of physiology*, vol. 408, no. 1, pp. 457.

Wei, H. & Löbenberg, R. 2006, "Biorelevant dissolution media as a predictive tool for glyburide a class II drug", *European journal of pharmaceutical sciences*, vol. 29, no. 1, pp. 45-52.

Weibel, E. 1963, "Morphometry of the human lung", .

Weibel, E.R. 1973, "Morphological basis of alveolar-capillary gas exchange", *Physiol Rev*, vol. 53, no. 2, pp. 419-495.

Wenzel, S.E. 2013, "Complex phenotypes in asthma: current definitions", *Pulmonary pharmacology & therapeutics*, vol. 26, no. 6, pp. 710-715.

Wesselius, L.J., Nelson, M.E. & Skikne, B.S. 1994, "Increased release of ferritin and iron by iron-loaded alveolar macrophages in cigarette smokers", *American journal of respiratory and critical care medicine*, vol. 150, no. 3, pp. 690.

Wesselius, L.J., Flowers, C.H. & Skikne, B.S. 1992, "Alveolar macrophage content of isoferritins and transferrin: comparison of nonsmokers and smokers with and without chronic airflow obstruction", *American Review of Respiratory Disease*, vol. 145, no. 2_pt_1, pp. 311-316.

White, R., Janoff, A. & Godfrey, H. 1980, "Secretion of alpha-2-macroglobulin by human alveolar macrophages", *Lung*, vol. 158, no. 1, pp. 9-14.

White, R.T., Damm, D., Miller, J., Spratt, K., Schilling, J., Hawgood, S., Benson, B. & Cordell, B. 1985, "Isolation and characterization of the human pulmonary surfactant apoprotein gene", .

Widdicombe, J. & Widdicombe, J. 1995, "Regulation of human airway surface liquid", *Respiration physiology*, vol. 99, no. 1, pp. 3-12.

Widdicombe, J.G. 1997, "Airway liquid: a barrier to drug diffusion?", *The European respiratory journal*, vol. 10, no. 10, pp. 2194-2197.

Wiedmann, T., Bhatia, R. & Wattenberg, L. 2000, "Drug solubilization in lung surfactant", *Journal of Controlled Release*, vol. 65, no. 1, pp. 43-47.

Wijkstrom-Frei, C., El-Chemaly, S., Ali-Rachedi, R., Gerson, C., Cobas, M.A., Forteza, R., Salathe, M. & Conner, G.E. 2003, "Lactoperoxidase and human airway host defense", *American journal of respiratory cell and molecular biology*, vol. 29, no. 2, pp. 206-212.

Williams, M.C., Hawgood, S. & Hamilton, R.L. 1991, "Changes in lipid structure produced by surfactant proteins SP-A, SP-B, and SP-C", *Am J Respir Cell Mol Biol*, vol. 5, no. 1, pp. 41-50.

Wilson, M.R., Stone, V., Cullen, R.T., Searl, A., Maynard, R.L. & Donaldson, K. 2000, "In vitro toxicology of respirable Montserrat volcanic ash", *Occupational and environmental medicine,* vol. 57, no. 11, pp. 727-733.

Woischnik, M., Bauer, A., Aboutaam, R., Pamir, A., Stanzel, F., de Blic, J. & Griese, M. 2008, "Cathepsin H and napsin A are active in the alveoli and increased in alveolar proteinosis", *The European respiratory journal,* vol. 31, no. 6, pp. 1197-1204.

Worthman, L.D., Nag, K., Rich, N., Ruano, M.L., Casals, C., Pérez-Gil, J. & Keough, K.M. 2000, "Pulmonary surfactant protein A interacts with gel-like regions in monolayers of pulmonary surfactant lipid extract", *Biophysical journal,* vol. 79, no. 5, pp. 2657-2666.

Worwood, M. 1982, "Ferritin in human tissues and serum", *Clinics in haematology,* vol. 11, no. 2, pp. 275-307.

Wright, J.R. 2005, "Immunoregulatory functions of surfactant proteins", *Nature Reviews Immunology,* vol. 5, no. 1, pp. 58-68.

Wright, J.L. & Churg, A. 2008, "Animal models of COPD: barriers, successes, and challenges", *Pulmonary pharmacology & therapeutics,* vol. 21, no. 5, pp. 696-698.

Wright, J. 1990, "Clearance and recycling of pulmonary surfactant", *Am J Physiol,* vol. 259, no. 2 Pt 1, pp. L1-12.

Wright, J., Benson, B., Williams, M., Georke, J. & Clements, J. 1984, "Protein composition of rabbit alveolar surfactant subfractions", *Biochimica et Biophysica Acta (BBA)-Protein Structure and Molecular Enzymology,* vol. 791, no. 3, pp. 320-332.

Wright, J.R. 1997, "Immunomodulatory functions of surfactant", *Physiological Reviews,* vol. 77, no. 4, pp. 931-962.

Wright, J.R. & Clements, J.A. 1987, "Metabolism and turnover of lung surfactant", *The American Review of Respiratory Disease,* vol. 136, no. 2, pp. 426-444.

Wright, S.M., Hockey, P.M., Enhorning, G., Strong, P., Reid, K.B., Holgate, S.T., Djukanovic, R. & Postle, A.D. 2000, "Altered airway surfactant phospholipid composition and reduced lung function in asthma", *Journal of applied physiology (Bethesda, Md.: 1985),* vol. 89, no. 4, pp. 1283-1292.

Wrobel, S. 2004, "Bubbles, babies and biology: the story of surfactant", *The FASEB Journal,* vol. 18, no. 13, pp. 1624e-1624e.

Wu, J., Kobayashi, M., Sousa, E.A., Liu, W., Cai, J., Goldman, S.J., Dorner, A.J., Projan, S.J., Kavuru, M.S. & Qiu, Y. 2005, "Differential proteomic analysis of bronchoalveolar lavage fluid in asthmatics following segmental antigen challenge", *Molecular & Cellular Proteomics,* vol. 4, no. 9, pp. 1251.

Xia, T., Kovochich, M., Liong, M., Zink, J.I. & Nel, A.E. 2007, "Cationic polystyrene nanosphere toxicity depends on cell-specific endocytic and mitochondrial injury pathways", *ACS nano,* vol. 2, no. 1, pp. 85-96.

Yamamoto, C., Yoneda, T., Yoshikawa, M., Fu, A., Tokuyama, T., Tsukaguchi, K. & Narita, N. 1997, "Airway inflammation in COPD assessed by sputum levels of interleukin-8", *CHEST Journal*, vol. 112, no. 2, pp. 505-510.

Yamazaki, K., Ogura, S., Ishizaka, A., Oh-hara, T. & Nishimura, M. 2003, "Bronchoscopic microsampling method for measuring drug concentration in epithelial lining fluid", *American journal of respiratory and critical care medicine*, vol. 168, no. 11, pp. 1304.

Yang, W., Peters, J.I. & Williams III, R.O. 2008, "Inhaled nanoparticles—a current review", *International journal of pharmaceutics*, vol. 356, no. 1, pp. 239-247.

Yang, F., Friedrichs, W.E., Navarijo-Ashbaugh, A.L., deGraffenried, L.A., Bowman, B.H. & Coalson, J.J. 1995, "Cell type-specific and inflammatory-induced expression of haptoglobin gene in lung", *Laboratory investigation; a journal of technical methods and pathology*, vol. 73, no. 3, pp. 433-440.

Yokoyama, M. 2005, "Drug targeting with nano-sized carrier systems", *Journal of Artificial Organs*, vol. 8, no. 2, pp. 77-84.

Yoneda, K. 1976, "Mucous blanket of rat bronchus: an ultrastructural study", *The American Review of Respiratory Disease*, vol. 114, no. 5, pp. 837-842.

York, T.P., van den Oord, Edwin JCG, Langston, T.B., Edmiston, J.S., McKinney, W., Webb, B.T., Murrelle, E.L., Zedler, B.K. & Flora, J.W. 2010, "High-resolution mass spectrometry proteomics for the identification of candidate plasma protein biomarkers for chronic obstructive pulmonary disease", *Biomarkers*, vol. 15, no. 4, pp. 367-377.

Yoshioka, A., Betsuyaku, T., Nishimura, M., Miyamoto, K., Kondo, T. & Kawakami, Y. 1995, "Excessive neutrophil elastase in bronchoalveolar lavage fluid in subclinical emphysema", *American journal of respiratory and critical care medicine*, vol. 152, no. 6 Pt 1, pp. 2127-2132.

Young, I.S. & Woodside, J.V. 2001, "Antioxidants in health and disease", *Journal of clinical pathology*, vol. 54, no. 3, pp. 176-186.

Zauner, W., Farrow, N.A. & Haines, A.M. 2001, "In vitro uptake of polystyrene microspheres: effect of particle size, cell line and cell density", *Journal of Controlled Release*, vol. 71, no. 1, pp. 39-51.